

# GEOLOGICAL FIELDWORK 2008

A SUMMARY OF FIELD ACTIVITIES AND CURRENT RESEARCH





# **GEOLOGICAL FIELDWORK 2008**

*A Summary of Field Activities and Current Research*

**Ministry of Energy, Mines  
and Petroleum Resources**  
British Columbia Geological Survey

**Paper 2009-1**

# Ministry of Energy, Mines and Petroleum Resources

## Mining and Minerals Division

### British Columbia Geological Survey

Parts of this publication may be quoted or reproduced if source and authorship are acknowledged.  
The following is the recommended format for referencing individual works contained in this publication:

**Diakow, L.J. and Barrios, A.** (2009): Geology and mineral occurrences of the mid-Cretaceous Spences Bridge Group near Merritt, southern British Columbia (parts of NTS 092H/14, 15, 092I/02, 03); in *Geological Fieldwork 2008, BC Ministry of Energy Mines and Petroleum Resources*, Paper 2009-1, pages 63–80.

**COVER PHOTO:** *Mitch Mihalynuk examines bedrock in the Chilanko Forks area of central British Columbia during fieldwork in 2008. The British Columbia Geological Survey has had many of its mapping and mineral deposit studies in the Beetle-Impacted Zone during the past 3 years. Mitch and his field crews have identified several new mineral occurrences during field mapping in areas largely ignored by prospectors and exploration companies. Photo by Jennifer Wardle, 2008 Geoscience Assistant.*

This publication is also available, free of charge, as colour digital files, in Adobe Acrobat PDF format, from the BC Ministry of Energy, Mines and Petroleum Resources website at:

<http://www.empr.gov.bc.ca/Mining/Geoscience/PublicationsCatalogue/Fieldwork/Pages/default.aspx>

#### British Columbia Cataloguing in Publication Data

Main entry under title:

Geological Fieldwork: - 1974 -

Annual.

Issuing body varies

Vols. For 1978-1996 issued in series: Paper / British Columbia. Ministry of Energy, Mines and Petroleum Resources; vols for 1997- 1998, Paper / British Columbia. Ministry of Employment and Investment; vols for 1999-2004, Paper / British Columbia Ministry of Energy and Mines; vols for 2005- , Paper / British Columbia Ministry of Energy, Mines and Petroleum Resources.

Includes Bibliographical references.

ISSN 0381-243X=Geological Fieldwork

1. Geology - British Columbia - Periodicals. 2. Mines and mineral resources - British Columbia - Periodicals. 3. Geology - Fieldwork - Periodicals. 4. Geology, Economic - British Columbia - Periodicals. 5. British Columbia. Geological Survey Branch - Periodicals. I. British Columbia. Geological Division. II. British Columbia. Geological Survey Branch. III. British Columbia. Geological Survey Branch. IV. British Columbia. Dept. of Mines and Petroleum Resources. V. British Columbia. Ministry of Energy, Mines and Petroleum Resources. VI. British Columbia. Ministry of Employment and Investment. VII. British Columbia Ministry of Energy and Mines. VIII. Series: Paper (British Columbia. Ministry of Energy, Mines and Petroleum Resources). IX. Series: Paper (British Columbia. Ministry of Employment and Investment). X. Series: Paper (British Columbia Ministry of Energy and Mines). XI. Series: Paper (British Columbia Ministry of Energy, Mines and Petroleum Resources).

QE187.46 622.1'09711 C76-083084-3 (Rev.)

VICTORIA  
BRITISH COLUMBIA  
CANADA

JANUARY 2009

## FOREWORD

### ***Geological Fieldwork 2008***

The provision of new geoscience data about British Columbia is aimed primarily at increasing mineral tenure acquisition and mineral exploration activity in the Province. The **British Columbia Geological Survey** (BCGS) presents here the results of 2008 field surveys and geoscience research in a 34<sup>th</sup> edition of *Geological Fieldwork*. Most articles are contributions by Survey staff to the understanding of the geology, geochemistry and mineral deposits of the Province. The volume also includes contributions about collaborative research with other organizations and projects completed by other professional geoscientists.

### ***British Columbia Geological Survey Successes***

New mineralization was discovered during mapping programs in the Chezacut, Princeton, Quesnel and 100 Mile House areas, which raises significantly the mineral potential of several underexplored areas in the Province.

The Survey has developed a new client-friendly database called 'Property File' to provide access to more than 100 000 documents. These unique reports, maps and notes span more than 100 years of exploration. Currently available online are 5200 documents, including the Falconbridge collection and 3000 mine plans.

The BCGS completed its first surficial geology and till sampling program in more than a decade, in the region west of Williams Lake that has been impacted by the mountain pine beetle.

Our online interface MapPlace and its supporting site now exceed 11 000 web pages. This interface is used 24 hours a day, 7 days a week by the exploration community worldwide and plays an essential and growing role in attracting investment to the Province.

Geological mapping near Kitimat confirmed the presence of a 30 km long volcanic belt with new potential to host massive sulphide deposits.

The Survey has started work towards producing value-added database products that use customized algorithms and computer software to automate interpretations. Work is currently focusing on defining catchment basins for provincial regional geochemical samples.

In a year of unprecedentedly rapid market developments across the industry, Survey staff, including those in the Vancouver and regional offices, contributed up-to-date expertise to decisions at all levels of government, responded to client inquiries in confidence, and reported on industry activity in the Province.

The Survey released data for the Terrace region in an interactive digital format with files formatted for MapPlace, Google Earth<sup>®</sup> and GIS programs.

The Survey continued its Geoscience Student Training Program for mentoring geology students. In fiscal year 2008–09, we hired more than 30 geoscience trainees, many of whom will go on to professional careers in industry.

Survey geologists were organizers and presenters at workshops on the pine beetle affected region and till sampling, and led a field trip on Vancouver Island for industry participants.

*D.V. Lefebure  
Chief Geologist  
British Columbia Geological Survey*



## CONTENTS

<b>Lefebure, D.V., Demchuk, T., Erdmer, P., Fredericks, J. and Jones, L.:</b> British Columbia Geological Survey activities in 2008 . . . . .	1
<b>NORTHERN BRITISH COLUMBIA</b>	
<b>Nelson, J.L.:</b> Terrace Regional Mapping Project, Year 4: Extension of Paleozoic volcanic belt and indicators of volcanogenic massive sulphide– style mineralization near Kitimat, British Columbia (NTS 103I/02, 07). . . . .	7
<b>Angen, J.J.:</b> Geospatial structural analysis of the Terrace area, west-central British Columbia (NTS 103I/08, 09, 10, 16) . . . . .	21
<b>Venable, M.E and Wojdak, P.J.:</b> Shan deposit, east-central British Columbia (NTS 103I/09): an emerging deposit model. . . . .	35
<b>MacIntyre, D.G. and Kilby, W.E.:</b> Atlin-Taku Mineral Resource Assessment, northwestern British Columbia (parts of NTS 104F, J, K, L, M, N): methodology and results . . . . .	45
<b>Legun, A.S.:</b> Bedrock and coal geology of the Wolverine River area, northeastern British Columbia (parts of NTS 093P/03, 093I/14) . . . . .	55
<b>CENTRAL BRITISH COLUMBIA: BEETLE-IMPACTED ZONE</b>	
<b>Diakow, L.J. and Barrios, A.:</b> Geology and mineral occurrences of the mid-Cretaceous Spences Bridge Group near Merritt, southern British Columbia (parts of NTS 092H/14, 15, 092I/02, 03). . . . .	63
<b>Mihalynuk, M.G., Orovan, E.A., Larocque, J.P., Friedman, R.M. and Bachiu, T.:</b> Geology, geochronology and mineralization of the Chilanko Forks to southern Clusko River area, British Columbia (NTS 93C/01, 08, 09S). . . . .	81
<b>Mihalynuk, M.G. and Friedman, R.M.:</b> First isotopic age constraints for the Dean River Metamorphic belt, Anahim Lake area: implications for crustal extension and resource evaluation in west-central British Columbia . . . . .	101
<b>Larocque, J.P. and Mihalynuk, M.G.:</b> Geochemical character of Neogene volcanic rocks of the central beetle-infested zone, south-central British Columbia (NTS 093B, C). . . . .	109
<b>Ferbey, T. Vickers, K.J., Hietava, T.J.O. and Nicholson, S.C.:</b> Quaternary geology and till geochemistry of the Redstone and Loomis Lake map areas, central British Columbia (NTS 93B/04, 05) . . . . .	117
<b>Logan, J.M. and Moynihan, D.P.:</b> Geology and mineral occurrences of the Quesnel River map area, central British Columbia (NTS 093B/16). . . . .	127
<b>Moynihan, D.P. and Logan J.M.:</b> Geological relationships on the western margin of the Naver pluton, central British Columbia (NTS 093G/08). . . . .	153
<b>Paterson, K., Lett, R.E. and Telmer, K.:</b> Litho-geochemistry of the Spanish Mountain gold deposit, east-central British Columbia (NTS 093A/11W) . . . . .	163
<b>Schiarizza, P., Bell, K. and Bayliss, S.:</b> Geology and mineral occurrences of the Murphy Lake area, south-central British Columbia (NTS 093A/03) . . . . .	169
<b>SOUTHERN BRITISH COLUMBIA</b>	
<b>Massey, N.W.D., Vineham, J.M.S. and Oliver, S.L.:</b> Southern Nicola Project: Whipsaw Creek–Eastgate–Wolfe Creek area, southern British Columbia (NTS 092H/01W, 02E, 07E, 08W). . . . .	189
<b>Simandl, G.J. and Paradis, S.:</b> Carbonate-hosted, nonsulphide, zinc-lead deposits in the southern Kootenay Arc, British Columbia (NTS 082F/03) . . . . .	205
<b>PROVINCE-WIDE</b>	
<b>Lett, R.E. and Doyle, J.:</b> Geochemistry projects of the British Columbia Geological Survey . . . . .	219
<b>Cui, Y., Eckstrand, H. and Lett, R.E.:</b> Regional geochemical survey: delineation of catchment basins for sample sites in British Columbia . . . . .	231



# British Columbia Geological Survey Activities in 2008

by D.V. Lefebure, T. Demchuk, P. Erdmer, J. Fredericks and L. Jones

*KEYWORDS: Geological Fieldwork, MapPlace, marketing, Mineral Development Office, geoscience assistants, partnerships, British Columbia Geological Survey, geoscience activities, mountain pine beetle*

## INTRODUCTION

This report is an overview of the operations of the British Columbia Geological Survey (BCGS) in 2008, prepared by the Chief Geologist and management team. The BCGS is committed to supporting a thriving, safe and responsible mining industry for the benefit of all British Columbians. We accomplish this by providing globally competitive geoscience expertise and data to attract mineral industry investment, advice to government on land-use decisions and geoscience information to the public.

The BCGS had another active year with 11 separate crews in the field; ongoing progress in delivering geoscience data to industry, government and other clients; and significant collaboration and interaction with other agencies. We completed aggregate and geoscience database projects with the Resource Development and Geoscience Branch, Ministry of Energy, Mines and Petroleum Resources (MEMPR). Many of our programs involve co-operative partnerships with universities, other government agencies, First Nations, local communities and industry.

Geoscience BC, a key partner of the BCGS, has become an increasingly active organization that is generating abundant new geophysical, geochemical and other geoscience data. Specific projects involving both Geoscience BC and the BCGS in partnership during 2008 are till sample reanalysis near Babine Lake, regional geochemical sample reanalysis in the Terrace area and uploading all Geoscience BC data on MapPlace.

The BCGS continued its long collaboration with the Geological Survey of Canada (GSC) in a number of field programs, including technical assistance to the Targeted Geoscience Initiative in southern and central B.C. The BCGS also continued its active support of the National Geological Surveys Committee and the Committee of Provincial Geologists.

## 2008 GEOLOGICAL FIELDWORK VOLUME

The locations of field projects in the province are shown in Figure 1. In addition to the continuing multiyear projects, new projects initiated in 2008 include surficial mapping in the Chilcotin region (Ferbey et al., 2009)<sup>1</sup> bedrock mapping near Princeton (Massey et al., 2009) and studies related to geochemistry (Lett and Doyle, 2009; Patterson et al., 2009) and industrial minerals (Simandl and Paradis, 2009).

The BCGS continues to address the impact of the mountain pine beetle infestation in the central interior of the province by expanding its 2006–2008 map coverage in this region. Despite its untested mineral potential, B.C.'s central interior has been underexplored in part due to widespread glacial deposits and young volcanic cover rocks blanketing the area. Our objective is to help diversify local economies by attracting mineral exploration activity, which can lead to potential new mines. In other parts of the province, both mineral exploration and mining are essential drivers of local employment and tax revenue, and directly support the development of regional infrastructure.

## MAPPLACE AND DATABASE ACTIVITIES

### MapPlace

MapPlace, our internet portal and one of the most effective geoscience online map systems globally, continues to improve with the addition of new data layers and improved interface tools. Data themes and applications available on MapPlace include mineral potential, bedrock and surficial geology, publications, mineral and petroleum tenure, MINFILE, assessment reports, geochemical and geophysical surveys, among others.

New maps and data layers on MapPlace include Nechako NATMAP Project digital geoscience information for central B.C. in the following NTS map areas: Manson River (093N), Fort Fraser (093K), Nechako River (093F), Prince George (093G/W), Smithers (093L/09, 16) and Hazelton (093M/01, 02, 07, 08). The data are from the GSC (Open File 5623), the BCGS (Open File 2007-10), universities and industry. The thematic MapPlace map related to this project can be found at <http://www.empr.gov.bc.ca/Mining/Geoscience/MapPlace/thematicmaps/Pages/nechakoNATMAP.aspx>; and

a Terrace geology and metallogeny compilation map, released as GeoFile 2008-11, which includes ESRI shape files, original Manifold map files and KML files for display in Google Earth. The interactive map for

<sup>1</sup> All reference citations are to other papers in this volume.

This publication is also available, free of charge, as colour digital files in Adobe Acrobat® PDF format from the BC Ministry of Energy, Mines and Petroleum Resources website at <http://www.empr.gov.bc.ca/Mining/Geoscience/PublicationsCatalogue/Fieldwork/Pages/default.aspx>.

GeoFile 2008-11 can be found at <http://www.empr.gov.bc.ca/Mining/Geoscience/MapPlace/hematicmaps/Pages/Terrace.aspx>.

Geoscience BC data added to MapPlace in 2008 include

- QUEST and QUEST-West airborne gravity data;
- a reanalysis of 2253 stream sediment pulps from a 1978 BCGS survey of the Terrace and Prince Rupert map areas (NTS 103I and part of 103J);
- stream sediment and water geochemical data for 906 samples from the Pine Pass map area (NTS 093O);
- infill lake sediment and water survey data from more than 1800 sites in NTS map areas 093G, J, N and O, and part of 093K;
- a reanalysis of 3976 stream sediment pulps from NTS map areas 093A, B, G, H, N and K;
- rock property data for 11 582 sites, displaying magnetic susceptibility, density and electrical conductivity measurements; and
- SpecTIR hyperspectral imagery and new tools for the Image Analysis Toolbox, which can be found at <http://www.empr.gov.bc.ca/Mining/Geoscience/MapPlace/MainMaps/Exploration/Pages/IAT.aspx>.

## Databases

In 2007 and 2008, considerable progress was made in populating the Property File database, which includes doc-

uments donated to the MEMPR by individuals and companies that span more than 150 years. There are about 100 000 documents available in hard copy and many of these are the only copy in existence. Approximately 25 000 of these have now been indexed and scanned. Documents currently available on the Property File search application (<http://propertyfile.gov.bc.ca>) include 400 items from the Falconbridge collection, 1800 from the Library collection and 3000 mine plans.

Users can now access 100% of company mineral assessment reports using the Assessment Report Indexing System (ARIS) database over the web. The number of off-confidentiality assessment reports for 2008 was 796.

## Mineral Resource Evaluations

The Integrated Land Management Bureau of the Ministry of Agriculture and Lands asked the BCGS to undertake a Level 2 Mineral Resource Assessment of the Atlin-Taku land-use planning area in 2008. This area encompasses approximately 4 million hectares in northwest B.C. The resource assessment was carried out by experts in September 2008 (Figure 2) and final results were presented at a land-use planning workshop held in Atlin in November 2008.

Over the past year, BCGS staff provided assessments of the mineral resource potential of different areas of B.C. for the Ministry of Aboriginal Relations and Reconciliation to assist with treaty negotiations.

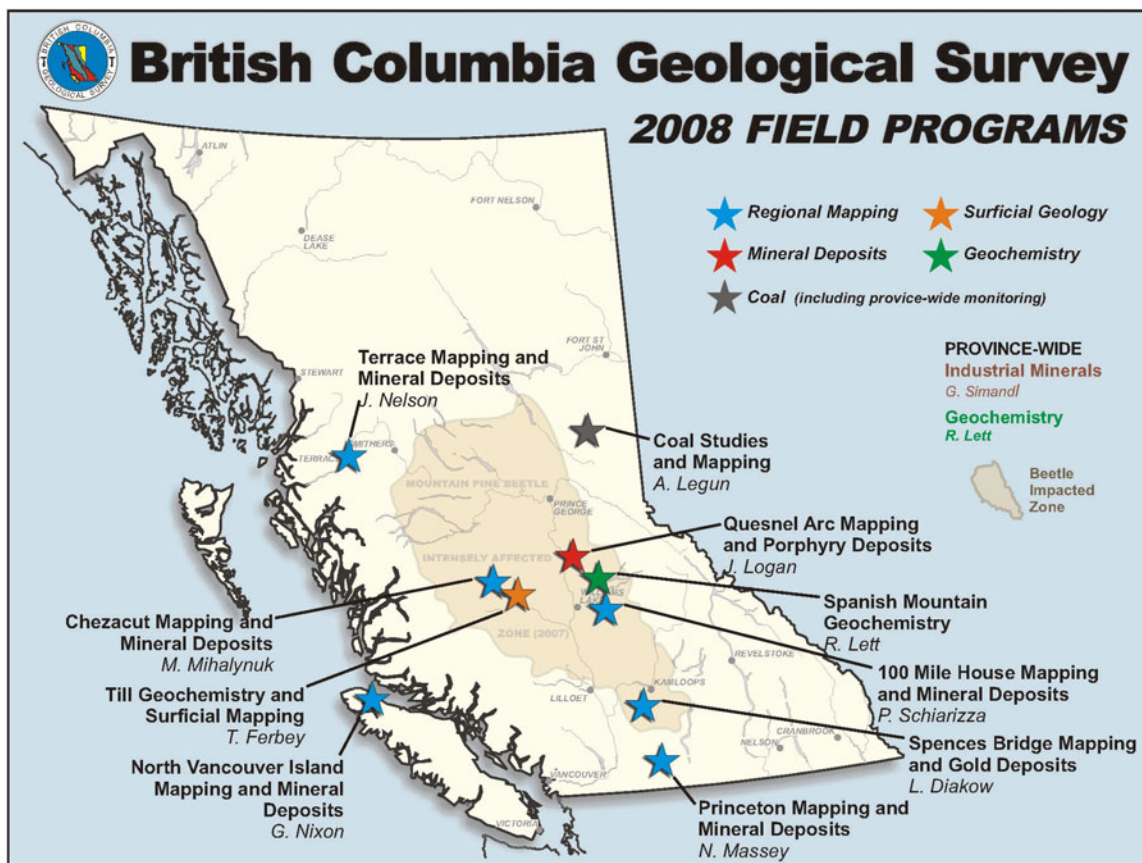


Figure 1. British Columbia Geological Survey 2008 field program areas.

## TECHNICAL MARKETING AND THE BC MINERAL DEVELOPMENT OFFICE

The staff of the BCGS played active roles as presenters and organizers at conferences and events showcasing B.C.'s mineral potential. This included presentations, posters and booths at the Mineral Exploration Roundup, the Kamloops Exploration Group Conference, and the Minerals North and Minerals South conferences. The BCGS staff played key technical and organizational roles for the Ministry-led Asia trade mission in November. The BCGS staff also contributed to the organizing and presentations at a mountain pine beetle Geoscience Workshop in Kamloops and a till prospecting workshop in Smithers (Figure 3). A field trip across northern Vancouver Island was organized as part of the 2008 Goldschmidt Geochemistry Conference in Vancouver.

The role of the BC Mineral Development Office (MDO) in Vancouver is to promote investment in the province's mineral exploration and mining, both domestically and internationally. This includes delivering a multifaceted technical campaign to highlight the province's superior mineral potential and user-friendly geoscience databases. The MDO interacts with decision-makers in industry, including executive management, geologists and prospectors, and forms part of the wider marketing efforts of the MEMPR. The MDO also hosts incoming national and international companies and government representatives and provides leadership in government-mineral-industry trade missions.

## PUBLICATIONS

Over the past year, the BCGS published *Geological Fieldwork 2007*, 10 Open File maps and reports, 1 Geoscience Map, 13 GeoFile maps, reports and data files and 2 Information Circulars. Staff also published articles in external journals. The BCGS processed more than 600 assessment reports for tenure maintenance.

With the Regional Geologists as principal authors, the BCGS published *Exploration and Mining in British Columbia 2007* and *British Columbia Mines and Mineral Exploration Overview 2007* and co-ordinated articles on provincial industry activities in the Canadian Institute of Mining, the Mineral Exploration Review and The Northern Miner.

All geoscience publications are available online at the BCGS website: <http://www.empr.gov.bc.ca/Mining/Geoscience>.

## STAFF UPDATE

In 2008, three professional staff with long careers at the BCGS left to pursue other opportunities. Dani Alldrick retired after more than 24 years as a regional mapper and mineral deposits senior geologist. The Director of Geoscience Initiatives, Brian Grant, became President of Goldbrook Ventures Inc. The Director of Resource Information, Gib McArthur, retired after making numerous contributions to the provincial geoscience database and related tools.

New staff members hired for the BCGS in late 2007 and in 2008 are



**Figure 2:** Experts discussing the mineral resource potential of a tract in the Atlin-Taku land-use planning area.

Tania Demchuk, who is taking on the new position of Manager, Geoscience Marketing and Partnerships; Philippe Erdmer, who joined us as interim Director, Geoscience Initiatives Section; Travis Ferbey, who joined us as Quaternary Geologist; Jay Fredericks, who is the new Director, BC Mineral Development Office in Vancouver; and Tasneem Pirani, who works as Finance and Management Administrative Assistant.

Staff promotions were

Larry Jones, who is now Director, Resource Information; and

Kirk Hancock, who became MapPlace Resource Geoscientist.

## GEOSCIENCE ASSISTANT PROGRAM

The MEMPR has partnered with universities and colleges since the 1940s to educate and inspire geoscience students and recent graduates. With its 23 permanent staff as professional mentors, the BCGS hired a total of 61 students and recent graduates over the past two years (Figure 4). These professionals in training have allowed us to deliver a



**Figure 3.** Field trip stop for the Smithers till prospecting workshop led by BCGS and GSC staff.

considerably enhanced geoscience program. The MEMPR geologists play a key role in helping the students develop awareness of their profession, workplace and expected standard of excellence.

As in past years, some students use geoscience data collected during fieldwork to complete a bachelor's or master's thesis. This maintains the ongoing partnership among BCGS staff, students and university researchers, which positively impacts the training and mentorship experience for the students.

The MEMPR offers one of the best career-oriented student employment programs in the province in any field. It incorporates a full circle of learning in which leading geoscientists share their passion, dedication and commitment with junior colleagues in the service of British Columbians. Previous generations of government geologists similarly helped today's mentors train for their own careers.

## MOVING FORWARD: HIGHLIGHTS

The BCGS will continue field and database projects in the coming year, including an emphasis on progressing with Property File and continuing to support MEMPR's Asia-Pacific initiative. New projects are being started with partner organizations to collect and distribute geoscience information about the province, including the EDGES project and an updated geology map for the Beetle-Impacted Zone in central B.C. between Williams Lake and Mackenzie.

### Property File

The Property File documents and database will be a priority for the BCGS Resource Information Section for the next several years, with all documents planned to be indexed, scanned and posted to the Internet. The documents will be linked to MINFILE through the MINFILE bibliography. The MEMPR library holdings will be included, as well as the following collections (year acquired, number of items where known are shown in parentheses): Starr (1999, 159), Placer Dome (1999, 1433), Prospector's Pit (1994–2001, 406), Chevron (2001, 1107), Cyprus-Anvil (2004, 1100), Sherwin Kelly (2004), Rimfire (2006, 2500),



**Figure 4.** Geoscience assistant, April Barrios, from field crews working in the Beetle-Impacted Zone (BIZ) near Merritt.

Samatosum mine (2008, 400), Eskay Creek mine (2008, 520) and J. Cam Stephen (2008, 50 uncatalogued office boxes). When completed, this project will place approximately 100 000 documents online for free access by users such as prospectors, exploration geologists, researchers, geoscientists and others.

### Marketing Coal and Minerals to the Asia-Pacific Region

The MEMPR implemented an active Asia-Pacific marketing strategy to attract direct investment from Asian investors to exploration and mining projects in B.C. Key selling points are B.C.'s rich geology, expert geoscience information, user-friendly online databases, continuing demand for commodities such as copper and coal, a Pacific Rim gateway, modern infrastructure and a skilled workforce. The BCGS provides the MEMPR with most of the technical expertise and professional delegates for international presentations and meetings with Asian companies. It is the point of contact for incoming international investors through the BC Mineral Development Office in Vancouver.

Asian countries are leading consumers of the province's coal and metal ores and have a record of investment in B.C.'s mineral industry. The BCGS is a continuing part of the MEMPR Asia-Pacific initiative. Against the backdrop of current global financial volatility, countries such as the People's Republic of China, Korea and Japan are more important than ever as business partners.

### EDGES: Modelling the Evolution of the Northern Cordillera Resource Environment from the Edges of Exotic Terranes

The Geoscience for Energy and Minerals (GEM) EDGES project is a highly focused, multiyear geological mapping initiative involving formal collaboration at the working level between the Government of Canada, the Province of British Columbia, the Yukon Territory, Geoscience BC, the United States Geological Survey and the Alaska Department Geological and Geophysical Surveys. It began field operations in 2008 in the Yukon, it will last until 2013, and it is partially funded by the federal GEM program. Support is being contributed by all participating agencies.

The goal is to improve the effectiveness of resource exploration and discovery in the northern Cordillera by outlining resource-rich environments in B.C., the Yukon and Alaska. The geological targets are the exotic outer terranes with their enclosed preaccretionary syngenetic and epigenetic deposits and the metal-rich Triassic through Paleogene magmatic arcs and associated accretion zones that resulted from interaction of the terranes with the western margin of ancient North America.

The target areas include parts of northern and central B.C. where the geological map base is either several decades out of date or at a large scale that is insufficient to evaluate mineral potential using modern tectonic interpretations. The BCGS will start its field programs in conjunction with the GSC and Geoscience BC in 2009.

## **Beetle-Impacted Zone BC GeoMap Update**

Geologists from the BCGS (Jim Logan, Mitch Mihalynuk, JoAnne Nelson and Paul Schiarizza) and Fil Ferri (Resource Development and Geoscience Branch of MEMPR) will update the provincial digital geological map coverage at 1:100 000 scale for the Quesnel Trough area in 2009. They will collaborate with the Geological Survey of Canada (Bert Struik and others) to integrate all bedrock mapping and geophysical and geochemical data to interpret bedrock geology in areas with significant glacial overburden.

The Quesnel Trough has been heavily impacted by the mountain pine beetle infestation and is part of the Beetle-Impacted Zone (BIZ) that has been targeted by the BCGS with field programs for the last three years. The province's digital geology map (BC GeoMap) is used by numerous industry and government clients.

Geoscience BC is an active partner on this project. Their new databases for the QUEST project will play a key role in updating the BC GeoMap, as will their staff and contractors.

## **NEED MORE INFORMATION? WANT TO COMMENT?**

The BCGS staff has considerable expertise and welcome the chance to share it. Our contact list is online at: <http://www.empr.gov.bc.ca/Mining/Geoscience/Staff/Pages/default.aspx>.

We always appreciate your input regarding our many programs and activities. Please email us at [Geological.Survey@gov.bc.ca](mailto:Geological.Survey@gov.bc.ca) or call us at (250) 952-0429.



# Terrace Regional Mapping Project, Year 4: Extension of Paleozoic Volcanic Belt and Indicators of Volcanogenic Massive Sulphide–style Mineralization near Kitimat, British Columbia (NTS 103I/02, 07)

by J.L. Nelson

**KEYWORDS:** Terrace, Kitimat, Stikinia, regional geology, VMS, Paleozoic, Telkwa, Coast Mountains, Skeena River

## INTRODUCTION

This paper reports on results from the fourth and final year of the Terrace regional mapping and mineral potential evaluation project. Mapping in the vicinity of Williams and Chist creeks in 2007 led to the discovery of previously unrecognized Paleozoic volcanic rocks, the Mt. Attree volcanic complex, which contains broad zones of syngenetic alteration (quartz-sericite schist) and local occurrences of volcanogenic sulphides (McKeown et al., 2008; Nelson et al., 2008a). Given the northeast-trending structural grain of the area, it seemed possible that both the Paleozoic hosts and the belt of volcanogenic massive sulphide–related mineralization could extend beneath the glacial deposits of the Terrace-Kitimat valley and into the eastern Coast Mountains. Thus, it was decided to conclude the project with reconnaissance mapping in this area, focused on metavolcanic units identified in earlier regional coverage (Woodsworth et al., 1985; Heah, 1991).

Geological mapping in July and August of 2008 covered the Terrace-Kitimat valley between the Skeena River and Kitimat, and adjacent mountainous areas and the Skeena River valley to the west. Lowland traverses were done by truck and by foot; in general, logging operations in these areas date from the 1970s through to the early 1990s, and roads are reverting to dense linear stands of small alders. An A-Star helicopter was used to access the more remote ridges; from a base at the Terrace airport typical set-out times were around 25 minutes round trip.

The most important new geological and exploration-related observations include

- the Paleozoic metavolcanic unit and its stratigraphically overlying, discontinuous Lower Permian limestone both extend west and southwest into the Coast Mountains in the core of a broad, regional, northeast-trending anticline;

- the anticlinal structure predates northwest-striking, northeast-side-down normal faults such as the Shames River and Amesbury Creek faults, which in turn are truncated by more northerly faults of the Kitsumkalum-Kitimat graben (Figure 2);

- the three base-metal sulphide mineral showings northwest of Kitimat show characteristics of volcanogenic massive sulphide (VMS) feeder zone systems; one contains abundant barite (Billy Barite, MINFILE 103I 217; MINFILE, 2008), and all have associated prekinematic quartz-sericite alteration; and

- the local northeasterly foliation-parallel orientations of these zones, as well as the continuity of trend with the Gazelle mineralization identified in 2007, which suggest that they form a single belt of VMS-style mineralization, probably controlled by a penecontemporaneous seafloor structure.

## PREVIOUS WORK

The area covered in 2008 was previously mapped at 1:125 000 scale by Woodsworth et al. (1985). The Skeena River valley west of Terrace was mapped at 1:50 000 scale in the course of M.Sc. thesis work by Heah (1991). Assessment report mapping at 1:20 000 scale by Belik (1987) in the Paleozoic belt northwest of Kitimat was of great aid in locating overgrown showings and key outcrops.

## GEOLOGY

### Overview

The Terrace-Kitimat area lies within the central western Stikine terrane (Wheeler et al., 1991), which consists of superimposed island arc buildups of mid-Paleozoic through mid-Jurassic age, overlain by postcollisional clastic strata of the Bowser Basin. Regional geology of the area, compiled from 1:20 000 scale mapping in 2005–2008, shows Paleozoic to Lower Jurassic volcanic and related units intruded by the Early Jurassic Kleanza pluton, all of them overlain to the north and east by the mid-Jurassic Smithers Formation and Troy Ridge facies, and Upper Jurassic and younger Bowser siliciclastic units (Figure 2). The southern margin of the Bowser Basin is defined by the Skeena arch, which formed a topographic high in Jurassic–Cretaceous time and shed detritus northwards into the basin (Tipper and Richards, 1976; Nelson and Kennedy, 2007). Abundant Cretaceous and younger plutons in the area represent the eastern part of the Coast Plutonic Complex.

In the mountains southeast of Terrace, volcanic, volcanoclastic and overlying carbonate strata of the Permian and older Zymoetz Group are overlain by extensive exposures of the Early Jurassic Telkwa Formation (Figure 2). The sequence is deformed into a broad, regional northeasterly anticline cored by the pre-Permian Mt. Attree volcanic complex. This regional structural culmination plunges to

---

*This publication is also available, free of charge, as colour digital files in Adobe Acrobat® PDF format from the BC Ministry of Energy, Mines and Petroleum Resources website at <http://www.empr.gov.bc.ca/Mining/Geoscience/PublicationsCatalogue/Fieldwork/Pages/default.aspx>.*

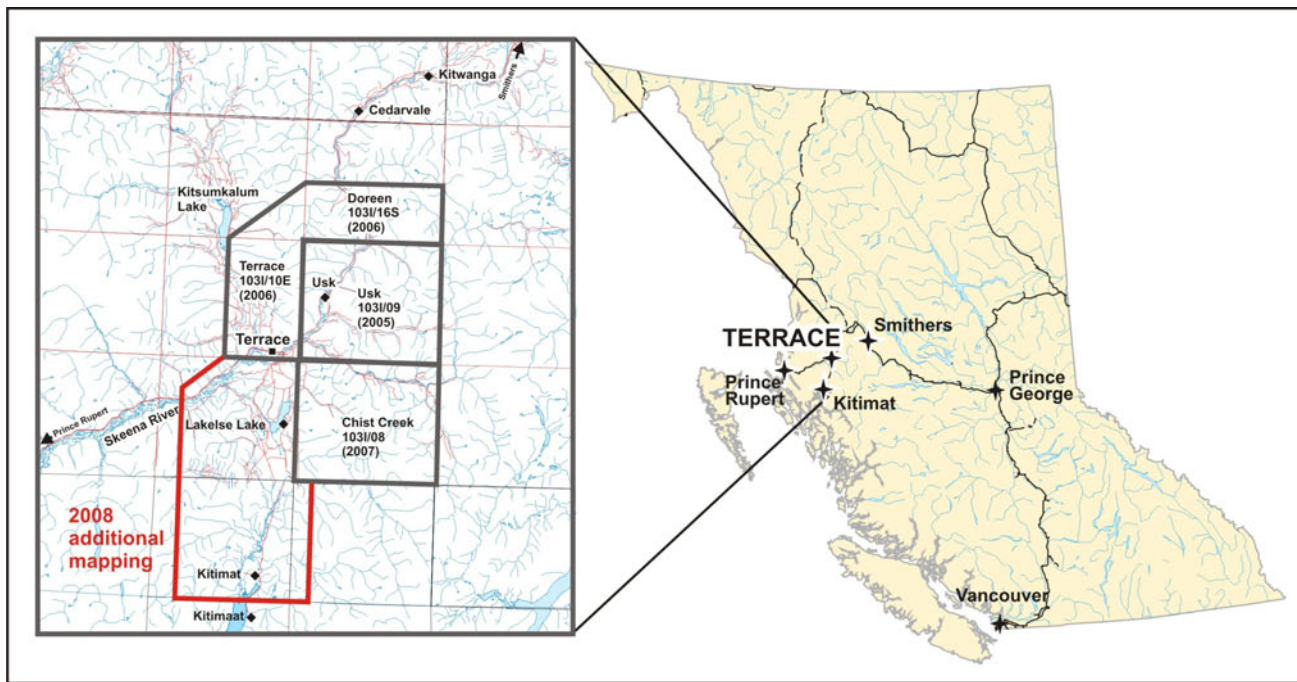


Figure 1. Location of 2005–2008 geological mapping near Terrace, BC.

the northeast; thus the deepest structural levels are exposed on peaks that flank the deep valley between Terrace and Kitimat (Angen, 2009). The valley itself is occupied by a complex graben structure, the Kitsumkalum–Kitimat graben (Figure 2). Farther west, pre-Permian volcanic units are found on the eastern slopes of Mt. Clague near Kitimat and on Nash Ridge west of the Terrace airport. These western Paleozoic volcanic rocks are dominated by opaline quartz-phyric dacite and fine-grained greenstone; they are unlike the andesite-dominated, plagioclase- and clinopyroxene-phyric volcanic sequences near Williams and Chist creeks. It is likely that they were the products of separate but coeval volcanic centres.

## Stratified Units

### ZYMOETZ GROUP

The name Zymoetz Group was proposed by Nelson et al. (2006a) for a section of Paleozoic volcanogenic and marine sedimentary strata overlain by Permian limestone, which outcrops between the lower Zymoetz River valley northeast of Terrace and the lower reaches of Chist Creek. The Zymoetz Group is divided into two units: a lower, volcanogenic unit, the Mt. Attree volcanic complex, overlain by Lower Permian limestone that is age equivalent to, and correlative with, the Ambition Formation of Gunning et al. (1994). In 2008, both of these units were traced west and south across the broad glacial valley between Terrace and Kitimat, to exposures along the Skeena River and south into the eastern Coast Mountains (Figures 2, 3).

#### Mt. Attree Volcanic Complex

This unit was named for Mt. Attree, a prominent summit on the ridge between the Zymoetz River and Williams Creek (Nelson et al., 2008a). The dominant composition on the ridge is andesitic, as flows and pyroclastic and epiclastic beds. Farther south from the height of land be-

tween Williams and Chist Creek, it also contains rhyolite and dacite and a thin interval of volcanic-derived sedimentary strata.

Greenschist-facies metavolcanic rocks probably equivalent to the previously defined Mt. Attree volcanic complex occur near the Skeena River west of Terrace, extending southwards onto Nash Ridge, near the Wedene River and on Mt. Clague near Kitimat (Figure 3). Typically in these exposures, opaline quartz-phyric dacite (Figure 4a, b) is interlayered with metabasaltic (?) greenstone. The dacite represents both tuff (Figure 4a) and related high-level porphyritic intrusions (Figure 4b). In some instances, well-preserved primary volcanoclastic textures allow identification of pyroclastic andesite and rhyolite-dacite breccia (Figure 4c). More commonly, the quartz-phyric dacite appears as chlorite-actinolite schist with round relict quartz phenocrysts. Pyritic quartz-sericite schist occurs on Nash Ridge and near Bowbyes Lake north of Kitimat.

The dating of these rocks as Paleozoic is based on preliminary evidence. They lie on structural trend with the Mt. Attree volcanic complex as previously defined; they share characteristic lithological features, metamorphic grade and northeasterly structural orientations. Heah (1991) reported a ca. 331–317 Ma U-Pb age from metatonalite within the unit north of the Skeena River, and there are unpublished U-Pb data indicating possible Mississippian age from northwest of Kitimat (G. Woodsworth, pers comm, January 2008). Several samples were collected this year for new U-Pb dating.

#### Ambition Formation

Fossiliferous Permian limestone outcrops in an east-striking belt between the Old Remo Road and the Skeena River. Farther south near Lakelse Lake, marble forms part of several roof pendants less than 1 km in scale. It is correlated with the Ambition Formation as defined locally (Nelson et al., 2008a). Its stratigraphic context is seen clearly

along a logging cut west of Mt. Herman, where it is overlain by a sequence typical of the Triassic sedimentary unit and Jurassic Telkwa volcanoclastic rocks. Ovoid, centimetre-scale wollastonite patches in the marble resemble chert blobs in unmetamorphosed Permian limestone east of Mt. Remo.

On the lower slopes of the mountain east of Shames River, well-bedded, pure to impure, siliceous marble intervenes between Paleozoic, mainly intrusive rocks and the Telkwa Formation (Heah, 1991). This is also regarded as correlative with the Ambition Formation.

Duffell and Souther (1964) showed a broad, kilometre-scale band of marble on the western side of Fire Mountain northeast of Kitimat. In traversing this area, we found only a very small marble pod apparently surrounded by diorite and gabbro. Nearby chlorite schist and greenstone are correlated with the Mt. Attree volcanic complex.

### TRIASSIC SEDIMENTARY STRATA

A thin unit of dark, thin-bedded, fine-grained sedimentary strata occurs between the Permian limestone and overlying andesitic volcanoclastic rocks at two localities within the valley south of Terrace, one along a logging spur west of Mt. Herman and another on a low hill east of Old Remo (Figure 2). The Mt. Herman locality is part of a roof pendant surrounded by diorite and gabbro of probable Early Jurassic age. Northeast-striking, thick-bedded pure marble is overlain on a sharp contact by 200 m of thin-bedded black siliceous hornfels. The beds are pyritic and coated with rusty iron-oxide weathering products. Their protoliths included chert, siliceous siltstone and lesser calcareous siltstone. They are overlain on a sharp contact by green tuff of the basal Jurassic Telkwa Formation. Although no fossils were found at this locality, the sequence of limestone, thin-bedded dark sedimentary strata and green volcanoclastic beds is identical to well-exposed and well-dated sequences along the Zymoetz River (Nelson et al., 2008a). As is the case there, the chert-argillite unit represents a thin, basinal Triassic facies that contrasts strongly with thick volcanic sequences in the Stuhini Group farther north and east within the Stikine terrane.

The Old Remo locality has been described previously by Mihalynuk (1987). It is atypical of the Triassic section seen elsewhere near Terrace. A small quarry pit near Kozar Road exposes monolithologic basalt breccia with entrained irregular, contorted inclusions of thin-bedded, black siliceous and calcareous argillite (Figure 5a, b). The basalt breccia is generally finely comminuted, with most clasts in the centimetre range. Basalt clasts within it contain well-formed, abundant augite phenocrysts in a glassy matrix. Both matrix and clasts are flooded by carbonate. The sedimentary inclusions range in size from subcentimetre wisps to decimetre blocks. The large inclusions are chaotically folded (Figure 5a). Their margins are irregular and wavy, with fine-scale penetration of the basalt matrix into laminated argillite (Figure 5b). As noted by Mihalynuk (1987), the textures at this outcrop are consistent with volcanism in a marine environment, incorporating wet, unlithified sediment into a pyroclastic breccia. The strong carbonate alteration of the basalt and the wispy basalt-sediment contacts are typical of peperite texture.

The depositional relationship between Triassic basalt and sedimentary strata at the Old Remo pit is unique within the Terrace area. In every other exposure, the Triassic unit contains no volcanic material, and is overlain unconform-

ably by basal conglomerate and andesite breccia of the Telkwa Formation (Nelson et al., 2006a, 2008). North of the Zymoetz River, angular chert clasts in the conglomerate record incorporation after lithification (Figure 5c). Moreover, the basal unconformity of the Telkwa Formation cuts through the Triassic unit, across the Permian limestone and down into the upper part of the Mt. Attree volcanic complex (Nelson et al., 2008a). Therefore, it is most likely that the basalt east of Old Remo represents a unique occurrence within the Triassic section, rather than a precursor of Telkwa volcanism.

### TELKWA FORMATION (HAZELTON GROUP)

The Lower Jurassic Telkwa Formation is exposed in several localities in the valley south of Terrace (Figure 3). On the logging spur west of Mt. Herman, basal Telkwa beds are mainly fine-grained green tuff and tuffaceous greywacke, with a few instances of andesitic lapilli tuff. On hills and in roadcuts southeast of Old Remo, coherent dacite and dacite breccia occur. They differ from Paleozoic dacite in that they have aphyric to small plagioclase-phyric texture, identical to those in the main Telkwa exposures farther east (Figure 6). They do not contain quartz eyes, nor are they associated with greenstone. They are similar to Telkwa dacite exposed along Highway 17 at the southern end of Kitsumkalum Mountain and on the west bank of the Zymagotitz River.

The westernmost outcrop along Highway 17 that is comparable to other Telkwa exposures lies east of the Amesbury Creek fault (Figure 3; 08JN27-03; UTM Zone 9, 514933E, 6036012N, NAD83). It consists of large-clast andesite breccia in which clasts contain millimetre-scale plagioclase phenocrysts, and augite-phyric basalt. Epidote patches and vein networks are prominent. Outcrops west of Amesbury Creek consist of greenstone and metadiorite of unknown age and possible subvolcanic origin, as well as abundant coarser plutonic rock types. No evidence was found to extend the Telkwa Formation west of the Amesbury Creek fault.

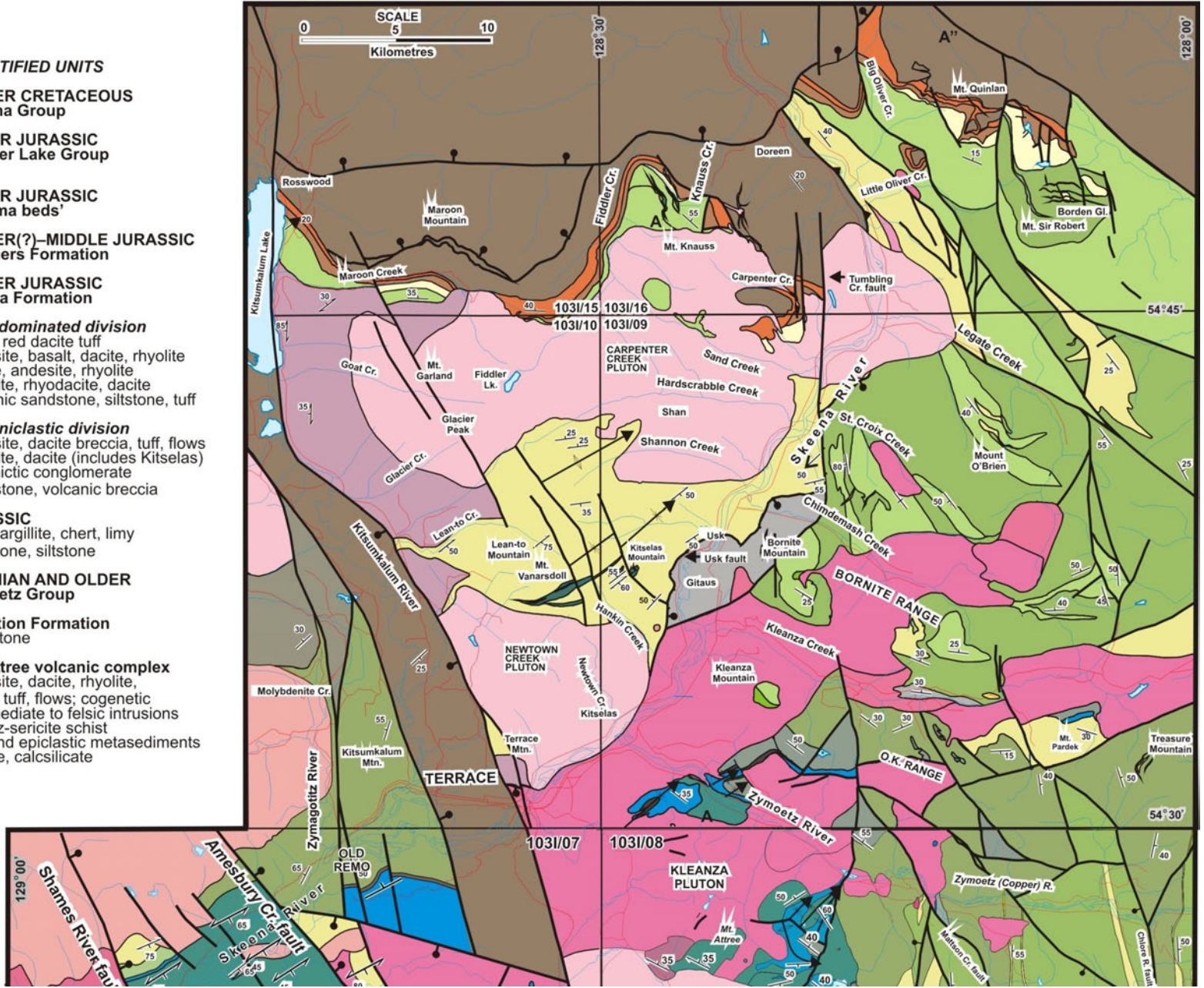
### Intrusive Rocks

The region between Terrace and Kitimat is mainly underlain by plutonic bodies (Figure 3). They vary from gabbro and local ultramafite to true granite; their inferred ages range from possibly Paleozoic, through Early Jurassic, to Eocene. As there are few published U-Pb dates from the area, the very tentative age assignments that are offered here are based on lithological correlation and in some cases similarity of metamorphic grade and state of strain with dated bodies (including R. Friedman, pers comm, September 2008). There is clear opportunity in this area for a more detailed study of these intrusions than was possible within the scope of this project, which focused on stratified rocks and their enclosed deposits.

### PALEOZOIC INTRUSIONS

Deformed plutonic rocks outcrop extensively on the north side of the Skeena River, east of the Shames River fault. They include tonalite, diorite and minor gabbro. At least some units are of Paleozoic age, as is shown by a Late Mississippian U-Pb zircon date of 331–317 Ma on a foliated metatonalite reported by Heah (1991). Foliated tonalite and granite on the north side of Williams Creek southeast of Terrace, described by Nelson et al. (2008a), are

- STRATIFIED UNITS**
- LOWER CRETACEOUS  
Skeena Group
  - UPPER JURASSIC  
Bowser Lake Group
  - UPPER JURASSIC  
'Pyjama beds'
  - LOWER(?)–MIDDLE JURASSIC  
Smithers Formation
  - LOWER JURASSIC  
Telkwa Formation
  - Flow-dominated division**  
Bright red dacite tuff  
Andesite, basalt, dacite, rhyolite  
Dacite, andesite, rhyolite  
Rhyolite, rhyodacite, dacite  
Volcanic sandstone, siltstone, tuff
  - Volcaniclastic division**  
Andesite, dacite breccia, tuff, flows  
Rhyolite, dacite (includes Kitselas)  
Polymictic conglomerate  
Sandstone, volcanic breccia
  - TRIASSIC**  
Black argillite, chert, limy  
mudstone, siltstone
  - PERMIAN AND OLDER**  
Zymoetz Group
  - Ambition Formation**  
Limestone
  - Mt. Attree volcanic complex**  
Andesite, dacite, rhyolite,  
basalt tuff, flows; cogenetic  
intermediate to felsic intrusions  
Quartz-sericite schist  
Tuff and epiclastic metasediments  
Marble, calcsilicate



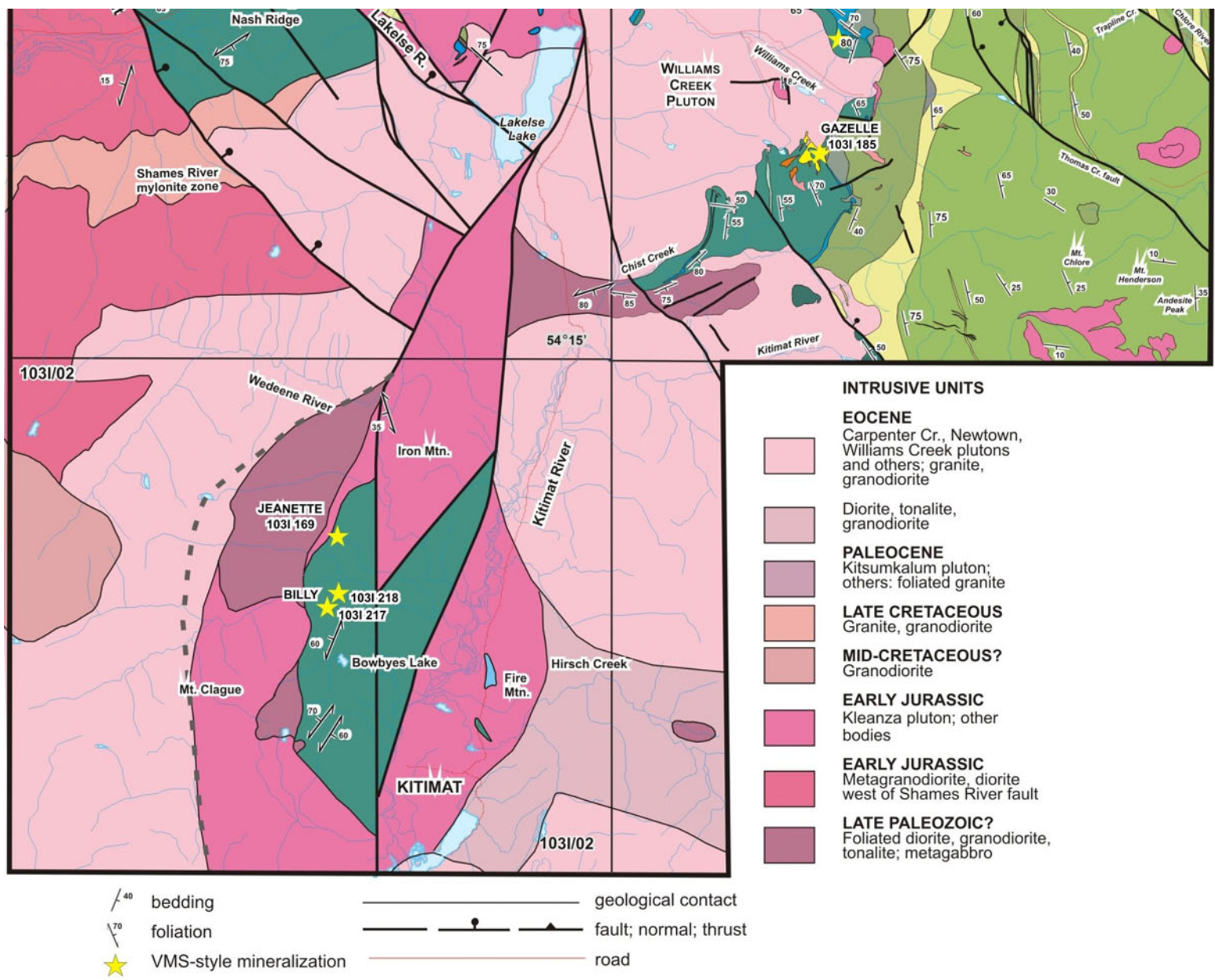


**Figure 2.** Geology of the Terrace area, compiled from field mapping at 1:20 000 scale in 2005–2008 (Nelson et al., 2006b, 2007, 2008b), with additional data from Woodsworth et al. (1985) and Heah (1991).

also Late Mississippian (R. Friedman, U-Pb zircon data, pers comm, September 2008), suggesting that they are part of the same suite. In contrast to younger plutonic bodies northeast of the Shames River fault, these Paleozoic intrusions are dynamically metamorphosed. Metamorphic grades are upper greenschist to lower amphibolite. Syn- and postkinematic hornblende, indicative of relatively higher-temperature, amphibolite-grade conditions, occurs in a few localities within their westernmost extent.

West of Kitimat, foliated quartz-eye dacite and greenstone of probable Paleozoic age (see description above) are interlayered with foliated quartz-eye tonalite and diorite. They probably represent a suite of cogenetic intrusions and extrusive rocks. Opaline quartz phenocrysts are identical in volcanic and plutonic rocks, and lithologic contacts are transposed into the foliation. A sample of metatonalite has been collected for U-Pb dating. As this volcanic-intrusive unit is traced west onto Mt. Clague, the extrusive component disappears and coarser metagabbro and metapyroxenite become prominent together with tonalite and diorite. Along strike to the north, between Raley and Dahl creeks, is a metamorphosed mafic complex of diorite, gabbro, plagioclase and augite porphyry, and plagiogranite. It is characterized by extreme compositional and textural variations on a small scale, but an overall large-scale homogeneity. Contacts between phases are highly ir-

regular and nonplanar, suggesting coeval emplacement in a subvolcanic environment. A Paleozoic age is suggested based on its continuity with volcanic-intrusive rocks near Kitimat, and on the characteristic irregular shape of plagioclase phenocrysts in andesitic phases, which closely resemble those in porphyritic andesite of the Mt. Attree volcanic complex near Williams Creek (Figure 7).

Metamorphosed layered gabbro, peridotite and clinopyroxenite occur in a 500 m wide inlier surrounded by younger intrusive rocks on the north side of Hirsch Creek near the southeastern corner of the map area (Figure 3). Augite is pseudomorphed by coarse crystalline actinolite, and olivine has been converted to serpentine and talc. This body is tentatively assigned a Paleozoic age by correlation with the mafic complex described above, and from its pervasive greenschist metamorphism, which is not seen to affect the known Early Jurassic and younger intrusive bodies.

### EARLY JURASSIC INTRUSIVE ROCKS

Unmetamorphosed diorite, microdiorite, granodiorite, gabbro and minor hornblendite underlie large parts of the valley between Terrace and Kitimat. They occur on the hill southeast of the confluence of the Kitimat and Skeena rivers, on Mt. Herman, along the Wedeene River, at the base of Iron Mountain, on Fire Mountain and in road outcrops within the town of Kitimat. Except for the microdiorite, this

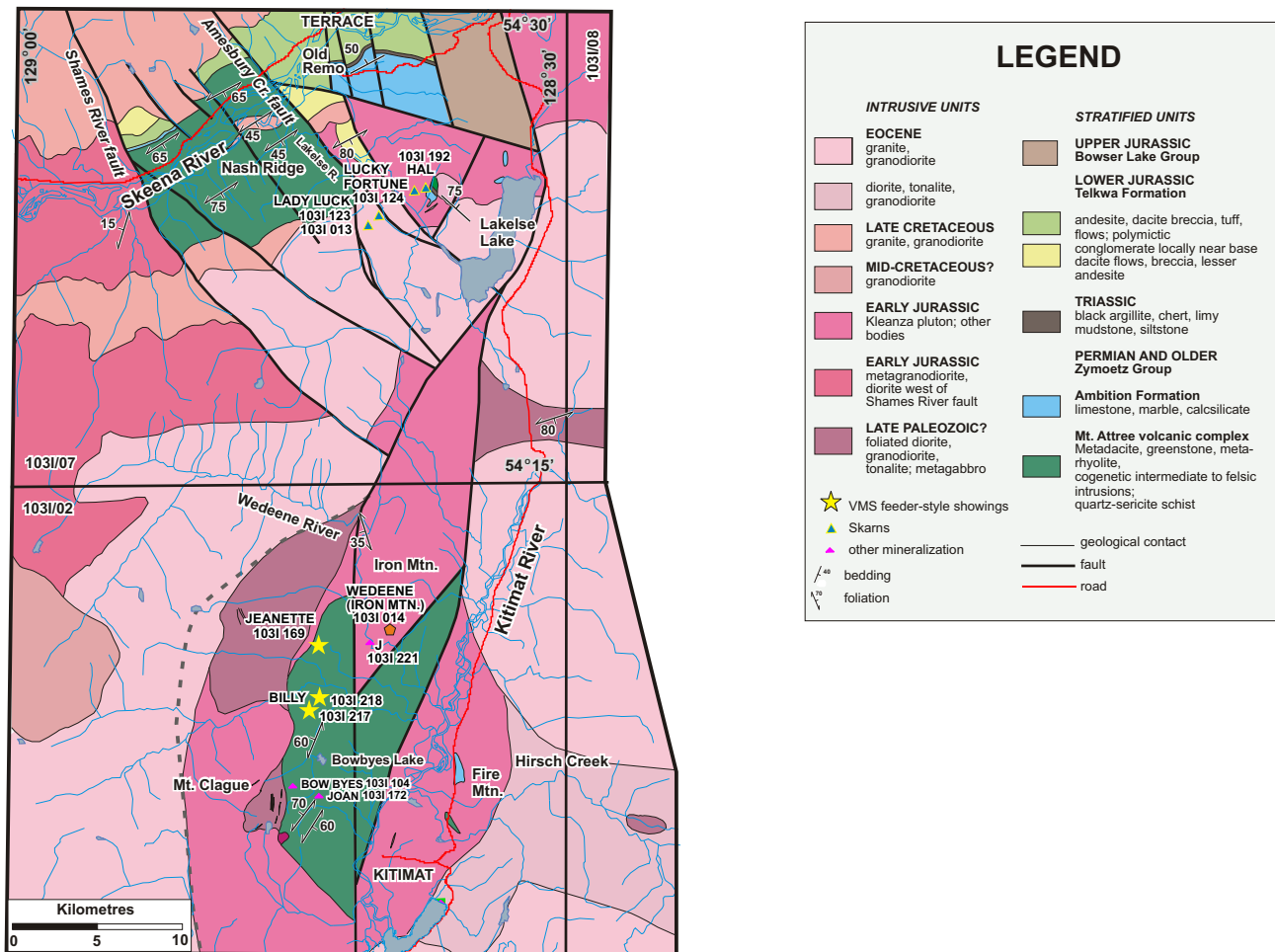


Figure 3. Geology of the Terrace-Kitimat valley and adjacent Coast Mountains, compiled from 1:20 000 field maps completed in 2008 and data from Woodsworth et al. (1985) and Heah (1991).

suite is coarse grained and equigranular to somewhat inequigranular. Transitional contacts between coarse-grained phases indicate that this suite probably forms a single large pluton that cooled at significant depth. In one instance of possible subvolcanic character, intrusive breccia textures are well developed along the logging road on the west side of the hill near the Kitimat-Skeena confluence, near an assumed intrusive contact with the Telkwa dacite. Hornblendes in all phases of the suite are fresh. Augite, where present, appears actinolized. For the most part, these rocks are undeformed, except for brittle shearing in outcrops in Kitimat, possibly due to local faulting. Textural and compositional variability characterize this suite, although not to the same degree as in the Raley-Dahl mafic complex (*see above*). Individual phases occur on hundred metre to kilometre scales. The compositional range from gabbro to granodiorite, as well as the overall textures and presence of characteristic phases like microdiorite and coarse hornblendite, all support correlation with the Early Jurassic Kleanza pluton, exposed north and east of the current area (Figure 2).

A body of fresh, coarse-grained, weakly foliated hornblende-biotite tonalite and diorite intrudes the Paleozoic (?) metaintrusive complex near the summit of Mt. Clague. It contains decimetre-scale rafts of strongly foliated greenstone. It was emplaced, therefore, after the development of the transposition foliation in older rocks, but was affected by regional northeasterly deformation. It may be Early Jurassic, or even Cretaceous in age. A sample has been collected for U-Pb dating.

Large areas west of the Shames River fault are underlain by gneissic granodiorite and diorite, dated at ca. 188 Ma by U-Pb in zircon (Heah, 1991). This is somewhat younger than dates obtained from the Telkwa Formation and Kleanza pluton, ca. 200–195 Ma (Gareau et al., 1997; Nelson et al., 2008a).

### LATE CRETACEOUS INTRUSIONS

Late Cretaceous, ca. 70 Ma granodiorite underlies high ridges north of the Skeena River west of Terrace (Heah, 1991). A small body of quartz-rich granodiorite, tonalite and diorite, also assumed to be Late Cretaceous (Heah, 1991), outcrops along the road south of the Skeena River, west of the Lakelse River crossing (Figure 2). This body is weakly metamorphosed in the lower greenschist facies. It shows both local ductile and more prevalent brittle, northeasterly foliations that are congruent with the stronger fabrics in Paleozoic metadacite that it intrudes.

Slightly metamorphosed and foliated granodiorite outcrops on a hill located 2.5 km east of the Lakelse River outlet, opposite from the body described above. It is inferred to represent a fault offset in the down-faulted valley bottom (Figure 3). It intrudes weakly foliated Telkwa dacite, and diorite and intrusive breccia of probable Early Jurassic age.

A body of variably foliated quartz-rich granodiorite and granite occurs on Nash Ridge, where it intrudes Paleozoic metavolcanic rocks. Heah (1991) considered it to be Late Cretaceous, a correlation that is consistent with its compositional and textural resemblance to intrusions farther north.

### EOCENE INTRUSIONS

White granite and granodiorite outcrop both east and west of Lakelse Lake and extend farther west into the Coast Mountains. Compared to the intrusions of inferred Jurassic age, these exhibit much more homogeneous, more felsic



**Figure 4.** Representative felsic textures, Mt. Attree volcanic complex: **a**) opaline quartz-eye porphyry dacite (metatuff), east slope of Mt. Clague, 08JN05-08, UTM Zone 9, 517824E, 5993220N, NAD83; hammer head for scale; **b**) ovoid quartz-eye porphyry from small, subvolcanic intrusion, Nash Ridge; 08JN21-04, UTM 514517E, 6026691N, pen for scale; **c**) dacite breccia with white rhyolite clast, near Bowbyes Lake, 08JN01-02, UTM 578403E, 5998115N, pencil for scale.

and more quartz-rich compositions. This broad area of felsic plutonic exposure is apparently continuous with the Eocene Williams Creek pluton to the east (Figure 2; R. Friedman, U-Pb date, pers comm, September 2008). Planar pink pegmatite and aplite dikes are present in places (Figure 9b). Biotite is more abundant than hornblende, and both are unaltered and fresh. A key identifying characteristic is the presence of millimetre-scale, clear, euhedral, amber-coloured titanite grains. The rocks are massive and are interpreted to postdate the penetrative deformation that affects Late Cretaceous and older units.

Massive, medium-grained equigranular diorite, tonalite and granodiorite occur together east of Fire Mountain in the lower Hirsch Creek drainage in the southeastern corner of the map area. Tonalite dike complexes in diorite and intrusive breccia of diorite in tonalite show curvilinear phase contacts suggestive of magma mixing. The age of this body is unknown; it is unlike the Early Jurassic suite, and may be a relatively mafic Eocene intrusion.

## Structure and Metamorphism

### NORTHEASTERLY FOLDING

Fieldwork in 2007 (Nelson et al., 2008a, b) identified a northeast-trending, regional anticline outlined by the curved outcrop pattern of the Permian limestone, which strikes north-northeast near Chist Creek, changing to north-northwest on the ridge south of Williams Creek, west-northwest on the ridge east of Mt. Attree and is deformed into a series of northeasterly folds in the hinge area in the Zymoetz River valley and on Copper Mountain (Figure 2). Rocks of the pre-Permian Mt. Attree volcanic complex occupy the anticlinal core. Mapping in 2008 extends the north limb of the regional culmination across the valley south of Terrace and into the Coast Mountains as far west as the Shames River fault. A band of east-striking, north-dipping Permian limestone extends across the valley near Old Remo; farther west, marble separates Paleozoic from Telkwa exposures in a northwesterly overturned section north of the Skeena River and east of the Shames River (Figures 2, 3). Structural continuity is indicated across the normal faults that bound the valley. South and downsection from the westernmost limestone, metavolcanic and metaintrusive rocks correlated with the Mt. Attree volcanic complex outcrop in the eastern Coast Mountains as far south as Kitimat, on trend with the anticlinal core, as defined farther northeast (Figure 2). Texturally identical, opaline quartz-phyric volcanic units occur on Nash Ridge in the north and on Mt. Clague to the south, on opposite sides of the projection of the Shames River fault. A possible explanation for the implied structural anomaly is outlined below.

Northeasterly foliations are only locally developed in the Telkwa Formation in the valley south of Terrace. In contrast, northeasterly foliations are strongly developed in Paleozoic greenschist-facies dacite and tonalite west of the Amesbury Creek fault. The schistosity and transposition in these rocks are similar to those in metavolcanic schist at lower topographic elevations near the mouth of Chist Creek (see Nelson et al., 2008a). Intrusive rocks as young as Late Cretaceous show development of northeasterly fabrics, which are axial planar to the anticline. Fabrics in Late Cretaceous granitoid rocks are not as penetrative as in the host metavolcanic and metaplutonic rocks, suggesting that the plutons were emplaced during deformation and metamor-



**Figure 5.** Contrasting relationships between the Triassic sedimentary unit and volcanoclastic units: **a)** folded Triassic sedimentary unit (basalt breccia) in a quarry east of Old Remo, 07JA11-3, UTM Zone 9, 520025E, 6036282N, NAD83; fold development appears to have been penecontemporaneous, probably related to inclusion within pyroclastic flow, pen for scale; **b)** contact between basalt breccia and inclusion of Triassic sedimentary strata, quarry east of Old Remo, 07JA11-3, pen for scale; note wispy, soft-sediment contact; **c)** highly angular, lithified Triassic chert clasts in basal Telkwa conglomerate from Kleanza Mountain north of Zymoetz River, 05NB13-01, UTM 542849E, 6043341N, pencil for scale.

phic cooling. Strongly foliated, garnet-bearing granitoid rocks in Williams Creek are not Paleocene, as suggested by Nelson et al. (2008a, b), but likely Mississippian (R. Friedman, pers comm, September 2008); their age does not date the deformation as Paleogene. An upper limit on deformation is established by Eocene bodies, including the dated Williams Creek pluton as well as its inferred correlatives farther west, which cut these fabrics. This constrains the folding event to Late Cretaceous age.

Besides age, three factors influence the degree of northeasterly fabric development associated with the regional folding event: stratigraphic level, location and rock composition. First, stratigraphic level is considered the most important. Foliation in Telkwa volcanic units is weak, sporadic and widely spaced. The same is generally true of the Permian limestone and Triassic sedimentary unit. In continuous exposures, for instance near Chist Creek, foliation becomes increasingly penetrative, and metamorphic grade increases downsection in the Mt. Attree volcanic complex. The highest metamorphic grades occur at the lowest exposed stratigraphic levels: east of the Kitsumkalum-Kitimat valley near the mouth of Chist Creek and along the Kitimat River, where knotted green biotite schist contains cordierite with relict garnet cores, and west of the valley in the eastern Coast Mountains, where schist is common.

Second, in any given unit, intensity of foliation development increases along with metamorphic grade in a northeast direction. East of and within the valley near Terrace, Telkwa volcanic rocks are at incipient greenschist grade (first growth of actinolite) or lower; only in the far west do greenschist minerals, actinolite and chlorite, define a foliation. Permian fossiliferous limestone near Old Remo is equivalent to highly foliated marble near the Shames River.

Last, rock type exerts an influence: Early Jurassic gabbro and diorite show only rare weak foliation, as do mafic complexes of inferred Paleozoic age, for instance, the one between Raley and Dahl creeks. Even within the Paleozoic volcanic-intrusive unit, highly foliated metadacite and tonalite is interlayered with apparently unfoliated greenstone and diorite. All of these features are characteristic of a folding event that affected upper crustal rocks in greenschist conditions, in which temperature increased with depth and towards the west.

## NORMAL FAULTS

The northwest-striking Shames River fault (Figures 2, 3) is a listric, down-to-the-northeast normal fault. This fault has accommodated an estimated total of 6–9 km, based on contrasting pressure-temperature conditions across it (Heah, 1991; Andronicos et al., 2003). All of the stratified rocks and the regional northeasterly fold, described above, with the exception of those near Kitimat, lie in its hangingwall. Its footwall to the west near the Skeena River is occupied by the low-angle Shames River mylonite zone (SRMZ), which also shows a top-to-the-northeast, normal sense of displacement involving Early Jurassic orthogneiss, Late Cretaceous and Eocene granite, and older gneiss (Figure 8a). Both mylonitic deformation in the SRMZ and normal faulting are constrained as Eocene, ca. 54 to ca. 47 Ma (Andronicos et al., 2003; Heah, 1991). They have been interpreted to record progressive tectonic denudation of the core of the Coast Mountains during regional transtension.



**Figure 6.** Small plagioclase-phyric dacite from Telkwa Formation, 08JN15-03, UTM Zone 9, 520701E, 6032249N, NAD83, quarry on Thunderbird Main logging road, rock hammer for scale.

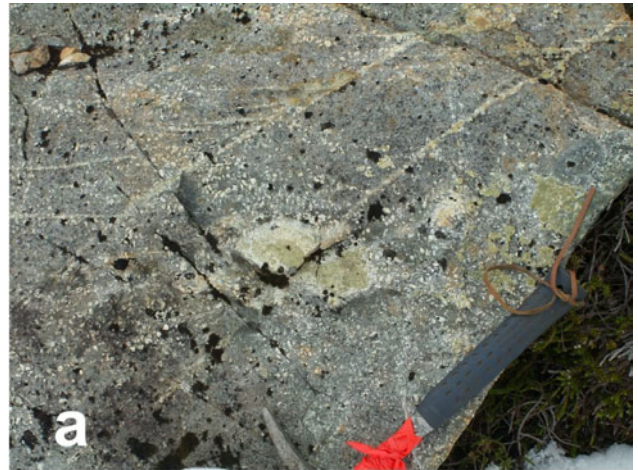


**Figure 7. a)** Raggedly terminated plagioclase phenocrysts in andesite, mafic intrusive complex on ridge between Raley and Dahl creeks, 08JN13-04; UTM Zone 9, 512470E, 6003608N, NAD83, rock hammer for scale. **b)** Typical Mt. Attree andesite, north of Williams Creek, pen for scale. Note identical plagioclase morphologies in a) and b).

The Amesbury Creek fault is a northeasterly analogue of the Shames River fault, similarly northwest striking, with the northeast block down. The displacement on it is perhaps 600–800 m of vertical offset, based on the outcrop elevations of the Permian limestone to the east and west (Figures 3, 8b). It separates mainly Paleozoic volcanic and intrusive rocks to the west from Permian limestone, Triassic sedimentary beds and Telkwa Formation within the valley south of Terrace.

The Kitsumkalum-Kitimat graben coincides with the deep intermontane valley that extends from New Aiyansh along the Nass River to Kitimat. Stratigraphic throw on its bounding faults can be estimated from offset of the Permian limestone, which lies at elevations of 1 000 m east of the valley and 100–200 m within the valley, and would crop out above present erosion levels to the west where underlying volcanic units are exposed. No Paleozoic volcanic units are found within the graben; they are presumed to underlie the younger rocks.

The sense of motion on its eastern bounding fault is indicated in outcrops east of Kitsumkalum Lake, where minor synthetic structures show ductile and brittle down-to-the-west and dextral sense of motion (Nelson and Kennedy, 2007). It juxtaposes greenschist-facies Kitselas metavolcanic rocks to the east with unmetamorphosed Bowser Lake Group (shale or siltstone?) along the Kitsumkalum River. Between Terrace and Lakelse Lake, the southern extension of this fault is not exposed. Geological interpretations favour an anastomosing fault system between Lakelse Lake and Kitimat, but there are no exposures of high stratigraphic levels in that part of the valley, suggesting that it is not floored by a graben there. South of the Wedeene River, a quarry in mylonitized granodiorite (Figure 8c) shows thrust-sense, top-to-the-northeast motion on north-northwest striking, west-dipping surfaces and low-plunge ( $173^{\circ}/05^{\circ}\text{N}$ ) slickensides indicative of transcurrent motion. The outcrop is near the projected location of one of the important fault strands.

Inferences from geological mapping in 2008, along with compilation from mapping by Woodsworth et al. (1985) and Heah (1991), show that the main Kitsumkalum fault is deflected into a gentle eastward arc near Lakelse Lake (Figure 2). The Shames River and Amesbury Creek faults can be projected eastward as far as this fault; however, further extensions are incompatible with mapped geological relationships farther east, and for this reason they are interpreted to terminate against the main fault near Lakelse Lake. The fault geometry would form a complex flower structure within a releasing bend in a dextral fault system. It explains the prevalence of tilted fault blocks south of Terrace and the graben-within-graben, downropped panel of Bowser Lake Group farther north.

In this view, the normal-dextral fault east of Kitsumkalum Lake and in fact the entire Kitsumkalum-Kitimat graben were coupled to Eocene normal motion on the Shames River and Amesbury Creek faults, as parts of a transtensional, partitioned system. Dating of fabrics in the Kitsumkalum pluton would provide a test of the suggested geometry.

A major unsolved structural problem associated with the map compilation of Figure 2 concerns the distribution of Paleozoic metavolcanic rocks west of the valley. Opaline quartz-phyric dacite on the south side of the Skeena River and on Nash Ridge is identical to that near Kitimat. Not only are these outcrops located across nearly 30 km of

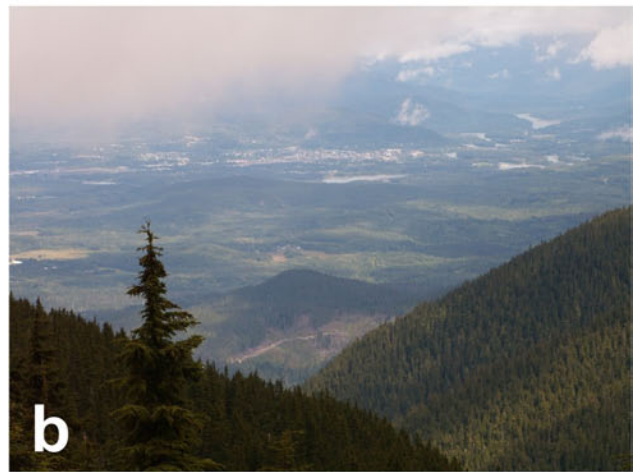


**Figure 8.** a) Top-to-the-east (left in photograph) mylonitic fabric developed in Early Jurassic orthogneiss, Shames River mylonite zone south of the Skeena River; 08JN25-01, UTM Zone 9, 506916E, 6026292N, NAD83. b) Looking from Paleozoic volcanic exposures on Nash Ridge, northeast across the concealed Amesbury Creek fault into the Kitsumkalum-Kitimat graben. The low hill in the middle distance is underlain by Late Cretaceous granite, Early Jurassic diorite and dacite of the Telkwa Formation. c) Less-deformed plagioclase porphyry intruding mylonitized granodiorite south of Wedeene River, 08JN26-03; UTM 520590E, 6009325N, pen magnet for scale.

**Table 1.** Geochemical and assay results from 2008 for the NTS 1031/02 and 07 map areas. Elevated values indicating higher mineral potential are highlighted in yellow.

Field No.	UTM E	UTM N	Description	Element	Cu	Pb	Zn	Ag	Au	Mo	Cd	As	Sb	W	Hg	Ba	
				Unit	ppm	ppm	ppm	ppb	ppb	ppm	ppm	ppm	ppm	ppm	ppm	ppb	PPM
Method				ARMS	ARMS	ARMS	ARMS	ARMS	ARMS	ARMS	ARMS	ARMS	ARMS	ARMS	ARMS	ARMS	ARES
Lab				ACM	ACM	ACM	ACM	ACM	ACM	ACM	ACM	ACM	ACM	ACM	ACM	ACM	acm
Detection Limit				0.01	0.01	0.1	2	0.2	0.01	0.01	0.1	0.02	0.1	0.02	0.1	5	1
08JN01-04	517335	5996907	Billy; strongly silicified zone with wispy pyrite, possible barite		12.93	1.26	36.4	59	8.4	1.69	0.02	2.2	-0.02	-0.1	14		
08JN02-01	518036	5997674	Billy (Gold zone?): representative grab, 5% pyrite in silicified dacite		79.13	11.5	23.9	1727	22.7	2.08	0.04	112	1.61	0.7	50		
08JN02-04	518140	5998299	Billy Barite showing; barite, silicification; pyrite, trace galena, mt, cpy		108.45	42.58	28.9	2178	92.1	75.66	0.07	12.3	0.34	1	15	>50000	
08JN04-01	517659	6001837	Jeannette showing, high grade chalcocopyrite-rich grab from 25 cm thick zone		4.75%	2.87	165.5	15403	4710.1	25.75	1.14	4.6	0.02	-0.1	20		
08JN07-02	516392	6030797	silicified, pyritic quartz-eye phyrlic metadacite		49.79	0.51	16.1	41	3.3	0.85	0.01	0.8	0.04	-0.1	-5		
08JN07-05	512928	6031122	zone of rich pyrite, magnetite in quartz-phyric metadacite, south Skeena		64.49	0.37	66.2	162	7.7	0.27	0.02	0.4	0.02	-0.1	-5		
08JN11-05	537933	6014644	silicified, pyritic zone in ductile shear cutting fine grained greenstone		961.5	2.12	8.2	1613	46.5	22.47	0.11	3.9	0.03	0.4	-5		
08JN13-03	512419	6003594	1 m thick greisen near edge of Eocene pluton; contains pyrite, maybe trace chalcocopyrite		69.35	0.83	29.3	58	3.1	1.22	-0.01	1.9	0.06	-0.1	-5		
08JN14-01	528972	6031008	pods of pyrite, pyrrhotite skarn in metamorphosed Permian limestone		24.44	10.56	49.5	79	0.9	0.69	0.45	3.3	0.22	0.1	-5		
08JN14-05-1	528582	6029456	skarn pod in Permian marble northwest end Lakelse Lake - sphalerite - rich high-grade grab sample		268.94	21.02	12.44%	2284	42	1.49	859.13	11.4	0.06	7.8	517		
08JN14-05-2	528582	6029456	skarn pod in Permian marble northwest end Lakelse Lake - contains sphalerite, stibnite, chalcocopyrite		414.89	7.78	94.7	1106	7.6	10.62	0.5	36.5	0.44	0.1	-5		
08JN14-06	528460	6029329	skarn in limestone, minor sphalerite		7.84	1.11	148.6	66	0.6	1.69	0.63	17.9	0.23	0.8	-5		
08JN14-13	524718	6028703	pyrrhotite-rich skarn in Permian limestone		148.94	2.69	54.2	352	3.1	28.12	0.27	2.1	0.14	0.3	-5		
08JN21-04	514517	6026691	quartz-sericite schist with pyrite, Nash Ridge		20.43	2.05	55.3	299	26.9	4.24	0.08	1	0.03	-0.1	-5		
08JN22-06	515710	6027083	quartz-sericite schist with pyrite, Nash Ridge		9.18	1.14	39.7	86	16.1	3.31	0.01	0.5	0.02	-0.1	70		
08JN24-03	514853	6026880	quartz-sericite schist with pyrite, Nash Ridge		362.06	1.54	64.5	216	6.8	2.2	0.11	1.5	-0.02	-0.1	-5		
08JN26-01	522440	6001971	J showing - pyritic shear in greenstone		77.01	0.57	302.7	86	23.5	8.68	0.06	0.4	-0.02	-0.1	-5		

Analysis of steel milled crushed rock prepared by ACME Analytical. Duplicate on crushed rock

ARMS = Aqua regia digestion - ICPMS. 15 g sample

ARES = Aqua regia digestion - ICPES

ACM = ACME Analytical, Vancouver

% Difference =  $ABS((x1-x2)/(x1+x2)/2) \times 100$

Acme report VAN08009445

structural (and assumed stratigraphic) strike, they are on opposite sides of the Shames River fault, interpreted to have a vertical offset of 6–9 km where it crosses the Skeena River (Heah, 1991; Andronicos et al., 2003). This geometry could be accommodated by a western splay of the main valley fault, shown as the dashed grey line on Figure 3. Restoration of >20 km of dextral motion across such a fault could restore the Nash Ridge Paleozoic sequence close to the Mt. Clague rocks. This fault, part of the Shames River–Kitsumkalum–Kitimat system, would have to offset rock bodies as young as 52–47 Ma. A traverse in 2008 across the eastern edge of the Eocene (?) granite on the ridge between Raley and Dahl creeks discovered a clearly intrusive contact, with extensive local pegmatite development, greisen and hornfelsing. On the other hand, the pluton has not been precisely dated and may be composite, and shear zones may lie farther west within it.

## MINERAL OCCURRENCES AND MINERAL POTENTIAL

### *Southwestern Extension of Paleozoic VMS Belt*

In 2007, the recognition of indicators of significant volcanogenic massive sulphide potential within the Paleozoic Mt. Attree volcanic complex added new mineral potential to the Terrace area (McKeown et al., 2008). The most significant zones of quartz-sericite-pyrite schist with associated small base-metal showings were on and near the Gazelle property at the height of land between Chist Creek and Williams Creek. Projection of the mainly northeasterly trending zones and their hostrocks to the southwest led to the hypothesis that the belt could be exposed in the eastern Coast Mountains northwest of Kitimat. Review of geological data in an assessment report support this, as showings of inferred VMS style had previously been documented in the Wedeene River area (Belik, 1987). The report was accompanied by a 1:20 000 scale outcrop-based geological map of high quality that became of great value in guiding our work in the area, through dense bush and overgrown logging roads.

Belik (1987) reported three main showings of possible volcanogenic character in metavolcanic hostrocks: Billy (MINFILE 103I 218), Billy Barite (MINFILE 103I 217) and Jeannette (MINFILE 103I 169; Figures 2, 3). We confirmed these locations and evaluated and sampled the showings. All are of feeder style, alteration and vein systems transposed into the dominant northeasterly foliation. They are associated with quartz-rich dacite, rhyolite and minor rhyolite-clast breccia. Quartz-sericite-pyrite schist occurs at the Billy showings, in foliation-parallel pods distributed along 2 km of strike length. Belik (1987) reported assay results from a chip sample of the Billy ‘gold’ showing to be 2.4 g/t Au over 5 m, and a grab sample near the base of the zone that assayed 5.18 g/t Au, 32.9 g/t Ag, 0.7% Pb and 0.2% Zn. Our geochemical analysis of altered dacite at the Billy showing yielded unremarkable levels of base and precious metals (Table 1). The Billy barite showing (Figure 9a) is located on a logging landing north of the other showings. It is dominated by highly deformed, massive, coarse-grained barite, similar to the barite at the Sub showing, described by McKeown et al. (2008). High contents of barium in the assay analysis confirmed handsample mineral identification (Table 1). The barite is coarse grained and strongly

deformed. It was emplaced as a vein or veins within the volcanic pile prior to folding and probably in a penecontemporaneous seafloor structure. Traces of visible sulphides—chalcopyrite, galena and sphalerite—are confirmed by slightly elevated values of Cu, Pb, Zn and Ag.

The Jeannette showing (MINFILE 103I 169) is in an overgrown trench next to a logging cut north of the Wedeene River (Figure 3). It is a silicified, northeast-striking shear zone that contains a zone 20–30 cm wide of semimassive pyrite and chalcopyrite. Assay results confirm the tenor of the mineralization: 4.75% Cu and 15.4 g/t Ag. Both the Jeannette and Billy showings are of epigenetic character. Their host metadacite and metarhyolite, however, match the typical hosts of volcanogenic deposits. Moreover, associated quartz-sericite-pyrite schist indicates that alteration occurred relatively early in the history, possibly near the time of their eruption on the seafloor. These showings are roughly on strike with the volcanogenic belt defined at the head of Chist Creek, and are considered to represent an extension. In 2007 and 2008, we identified a 30 km long belt of Paleozoic feeder-zone style, volcanogenic-associated mineralization. Preliminary geochronological results from Paleozoic rocks in the Terrace area are



**Figure 9.** a) Billy barite showing; rusty massive barite with pyrite and traces of base-metal sulphides; 08JN02-04; UTM Zone 9, 518140E, 5998299N, NAD83, pen for scale; b) rusty quartz-sericite schist, Nash Ridge; 08JN 22-06; UTM 515710E, 6027083N, rock hammer for scale.

ca. 330–320 Ma (Heah, 1991; R. Friedman, pers comm, September 2008). These are compatible with a Late Mississippian age for the Chist Creek–Wedeeene River volcanogenic belt, contemporaneous with the orebody at the Tulsequah Chief mine of far northwestern British Columbia, similarly hosted by Paleozoic volcanic strata of the Stikine terrane.

Quartz-sericite schist occurs regionally within the Mt. Attree volcanic complex west of the Terrace-Kitimat valley, for instance, on Nash Ridge (Figure 9b), and on the logging road south of the Skeena River, where very rusty quartz-sericite-chlorite schist hosts abundant pyrite and up to 10% magnetite (08JN07-05, Table 1).

Other showings on Mt. Clague and near the Wedeeene River are minor shear-zone hosted or intrusion-related in character, and are of limited extent. This includes the 'J' showing (MINFILE 1031 221), a rusty shear zone on the bank of the Wedeeene River opposite Iron Mountain (08JN26-01, Table 1), the Joan (MINFILE 1031 172), a zone of scheelite, magnetite and chalcopyrite and the Bowbys (MINFILE 1031 114), a small zone of shear-hosted copper mineralization on the eastern slope of Mt. Clague.

West of Lakelse Lake, a number of contact skarn deposits are developed involving marbles of the Permian Ambition Formation, and Early Jurassic and Eocene intrusive bodies. Known showings of this type include the Lady Luck (MINFILE 1031 013, 1031 123), Lucky Fortune (MINFILE 1031 124) and Hal (MINFILE 1031 192). Mineralization comprises sphalerite, magnetite, molybdenite and chalcopyrite associated with epidote and garnet. In 2008, a previously undocumented skarn occurrence was discovered in a burrow pit near the northwestern shore of Lakelse Lake (08JN14-05-1, -2; Table 1). It contains at least one 30 cm wide zone of sphalerite-rich material, from which a sample returned over 12% Zn.

## SUMMARY AND CONCLUSIONS

Field mapping in 2008 documented the continuation of a belt of Paleozoic volcanic rocks and enclosed VMS feeder-style mineralization from the Zymoetz River to the eastern Coast Mountains between Terrace and Kitimat. The Paleozoic volcanic unit, the Mt. Attree volcanic complex, forms the core of an unusually oriented, northeast-trending anticline that formed in latest Cretaceous to earliest Paleogene time. Its enclosed belt of VMS-related mineralization comprises zones of quartz-sericite-pyrite schist and local occurrences of deformed early epigenetic barite and rare base-metal sulphides. All of these are characteristic of feeder zones rather than seafloor exhalative deposits. The trend of the mineralized belt parallel to the regional northeasterly foliation and anticlinal hinge zone suggest that early northeasterly structures may have played a role in later crustal deformation.

The regional northeasterly folding event that controls distribution of the Mt. Attree volcanic complex is probably Late Cretaceous in age, as it affects ca. 69 Ma intrusive bodies near the Skeena River but not Eocene plutons. Northeasterly folding affected Paleozoic and younger strata both in the hangingwall of the Skeena River fault zone northeast of Terrace, and the Kitselas facies in its footwall (Nelson et al., 2008a; Angen, 2009). The deflection of the fault zone from north-northeast-striking to west-northwest-striking north of Legate Creek (Figure 2) may also result from

northeasterly folding, a further indication that the folding event postdates the fault. The Skeena River fault zone has been interpreted as a mid-Cretaceous top-to-the-east thrust fault (Nelson et al., 2008a), that developed as part of the Skeena fold-and-thrust belt (Evenchick, 2001). Although northeast-trending folds are prominent in the Skeena fold-and-thrust belt, the folds near Terrace formed later, after the Skeena River fault zone, and cannot be ascribed to a mid-Cretaceous sinistral-transpressive event. They arose during an episode of orogen-parallel compression, possibly localized by a crustal-scale discontinuity that had earlier found surface expression in the Skeena arch.

## ACKNOWLEDGMENTS

The safe, skilful service of Craig Kendell and his staff at Canadian Helicopters in Terrace was greatly appreciated. Field visits with Tony Barresi, Margaret Venable, Peter Shorts, Farshad Shirvani, Ray Cook, J-F Gagnon of the University of Alberta, and Brian Mahoney and Geoff Pignotta of the University of Wisconsin enlivened the summer's work and provided fresh perspectives on local geology and mineralization. Cordula Thielke is acknowledged for assistance in the field. Once more, long-standing and valued friendships of Terrace residents Lael and Dave McKeown, Bill and Helene McRae, Doug McRae and Andrea Komlos and her family continued to sustain this project.

## REFERENCES

- Andronicos, C.L., Chardon, D. Hollister, L.S., Gehrels, G. and Woodsworth, G.J. (2003): Strain partitioning in an obliquely convergent orogen, plutonism, and synorogenic collapse: Coast Mountains batholith, British Columbia, Canada; *Tectonics*, Volume 22, Number 2, doi: 10.1029/2001TC001312, 2003, pages 7-1-7-24.
- Angen, J.J. (2009): Geospatial structural analysis of the Terrace area, west-central British Columbia (NTS 1031/08, 09, 10, 16); in *Geological Fieldwork 2008, BC Ministry of Energy, Mines and Petroleum Resources*, Paper 2009-1, pages 21-34.
- Belik, G., 1987, Geological and geochemical report on the Billy property, Skeena Mining Division, NTS 1031/2E, *BC Ministry of Energy, Mines and Petroleum Resources Assessment Report 15 528*, 51 pages.
- Duffell, S. and Souther, J.G. (1964): Geology of Terrace map area, British Columbia; *Geological Survey of Canada*, Memoir 329, 117 pages.
- Evenchick, C.A. (2001): Northeast-trending folds in the western Skeena fold belt, northern Canadian Cordillera: a record of Early Cretaceous sinistral plate convergence; *Journal of Structural Geology*, Volume 23, pages 1123-1140.
- Gareau, S.A., Friedman, R.M., Woodsworth, G.J. and Childe, F. (1997a): U-Pb ages from the northeastern quadrant of Terrace map area, west-central British Columbia; in *Current Research, Geological Survey of Canada*, Paper 1997-A/B, pages 31-40.
- Gunning, M.H., Bamber, E.W., Brown, D.A., Rui, L., Mamet, B.L. and Orchard, M.J. (1994): The Permian Ambition Formation of northwestern Stikinia, British Columbia, in *Pangea: Global Environments and Resources*, Embry, A.F., Beauchamp, B. and Glass, D.J., (Editors), *Canadian Society of Petroleum Geologists*, Memoir 17, pages 589-619.
- Heah, T.S.T. (1991): Mesozoic ductile shear and Paleogene extension along the eastern margin of the Central Gneiss Complex, Coast Belt, Shames River area, near Terrace, British

- Columbia; M.Sc. thesis, *The University of British Columbia*, 155 pages.
- McKeown, M., Nelson, J.L. and Friedman, R. (2008): Newly discovered VHMS potential within Paleozoic volcanics of the Stikine assemblage, Terrace area, northwestern B.C.; in *Geological Fieldwork 2007, BC Ministry of Energy, Mines and Petroleum Resources*, Paper 2008-1, pages 103–116.
- Mihalynuk, M.G. (1987): Metamorphic, structural and stratigraphic evolution of the Telkwa Formation, Zymoetz River area (NTS 103I/08 and 93L/05), near Terrace, British Columbia; M.Sc. thesis, *University of Calgary*, 128 pages.
- MINFILE (2008): MINFILE BC mineral deposits database; *BC Ministry of Energy, Mines and Petroleum Resources*, URL <<http://www.minfile.ca>> [December 2008].
- Nelson, J.L., Barresi, T., Knight, E. and Boudreau, N. (2006a): Geology and mineral potential of the Usk map area (103I/09) near Terrace, British Columbia; in *Geological Fieldwork 2005, BC Ministry of Energy, Mines and Petroleum Resources*, Paper 2006-1, pages 117–134.
- Nelson, J.L., Barresi, T., Knight, E. and Boudreau, N. (2006b): Geology of the Usk map area (193I/09); *BC Ministry of Energy, Mines and Petroleum Resources*, Open-File 2006-3, 1:50 000 scale.
- Nelson, J.L. and Kennedy, R. (2007): Terrace regional mapping project Year 2: New geological insights and exploration targets (NTS 103I/16S, 10W), west-central British Columbia; in *Geological Fieldwork 2006, BC Ministry of Energy, Mines and Petroleum Resources*, Paper 2007-1, pages 149–162.
- Nelson, J.L., Kennedy, R., Angen, J. and Newman, S. (2007): Geology of the Doreen south half (103I/16S) and Terrace east half (103I/10E) map areas, near Terrace, British Columbia; *BC Ministry of Energy, Mines and Petroleum Resources*, Open-File 2007-4, 1:50 000 scale.
- Nelson, J.L., Kyba, J., McKeown, M. and Angen, J. (2008a): Terrace regional mapping project, Year 3: contributions to stratigraphic, structural and exploration concepts, Zymoetz River to Kitimat River, east-central British Columbia; in *Geological Fieldwork 2006, BC Ministry of Energy, Mines and Petroleum Resources*, Paper 2007-1, pages 159–174.
- Nelson, J.L., Kyba, J., McKeown, M. and Angen, J. (2007b): Geology of the Chist Creek map area (103I/08); *B.C. Ministry of Energy, Mines and Petroleum Resources*, Open-File 2008-3, 1:50 000 scale.
- Tipper, H.W. and Richards, T.A. (1976): Jurassic stratigraphy and history of north-central British Columbia; *Geological Survey of Canada*, Bulletin 270, 73 pages.
- Wheeler, J.O., Brookfield, A.J., Gabrielse, H., Monger, J.W.H., Tipper, H.W. and Woodsworth, G.J. (1991): Terrane map of the Canadian Cordillera: *Geological Survey of Canada*, Map 1713A, scale 1:2 000 000.
- Woodsworth, G., van der Heyden, P. and Hill, M.L. (1985): Terrace East map area; *Geological Survey of Canada*, Open File 1136, 1:125 000 scale.

# Geospatial Structural Analysis of the Terrace Area, West-Central British Columbia (NTS 103I/08, 09, 10, 16)

by J.J. Angen<sup>1</sup>

**KEYWORDS:** Stikinia, Terrace, structure, geospatial analysis, down-plunge projection

## INTRODUCTION

In this study, geographic information system (GIS)-based geospatial analysis is used to assist in the interpretation of a large database of georeferenced structural measurements, in order to reconstruct the structural history of the Terrace area in west-central British Columbia (Figure 1). This area has been the target of a multiyear regional geological mapping and mineral potential evaluation project conducted by the BC Geological Survey from 2005 through 2008.

Field structural measurements were taken in NTS 1:50 000 scale map areas 103I/08, 09, 10 and 16 during the course of regional mapping in the summers of 2005 through 2007. In this study, the structural data were sorted into domains in a GIS program and then plotted by structure type using stereonet. One of the key findings of this study is a series of folds with northeast-trending hinge lines. This implies a northwest-southeast compressional event. Northeasterly fabrics associated with this event affect latest Cretaceous granitoid plutons along the Skeena River west of the map area (Heah, 1991). They are cut by Eocene intrusions. There are no structures yet documented regionally that correspond to a compressional event of this orientation and age; therefore, its cause and extent are somewhat enigmatic.

Northeasterly-trending folds occur in both the footwall and hangingwall of the Skeena River fault zone, a postulated northeasterly-vergent thrust fault that places Paleozoic and younger strata southeast of the Skeena River on top of Jurassic and younger, more metamorphosed strata to the northwest. The Skeena River fault zone was possibly reactivated as a top-to-the-northeast detachment during early stages of Eocene extension. The later stages of this extensional regime are recorded by steep, north-northwest-striking normal faults. The local expression of this high-angle brittle regime is the Kitsumkalum-Kitimat graben, which underlies a broad valley in which the towns of Terrace and Kitimat are situated (Figure 1). The graben is bounded to the east along Kitsumkalum Lake by a well-exposed normal fault. Brittle and ductile deformation are re-

corded along the extent of this fault, showing down-to-the-southwest motion.

## OVERVIEW OF GEOLOGICAL UNITS

The Terrace area is located near the western margin of Stikinia (as defined by Colpron et al., 2007), along the eastern margin of the Coast Plutonic Complex and the southern margin of the Bowser Lake Group. Stikinia is the largest intermontane terrane, formed dominantly by island-arc volcanism, along with clastic and calcareous sedimentation, through Paleozoic and into Mesozoic time (Nelson et al., 2006). The Coast Plutonic Complex is a belt of granitoid and metamorphic rocks formed by continental-arc magmatism along western North America from mid-Jurassic to Eocene time. The Bowser Lake Group is a sequence of Late Jurassic–Early Cretaceous siliciclastic sedimentary rocks deposited in a broad successor basin, the Bowser Basin, in central Stikinia.

This section presents an overview of the rock units in the Terrace area, whose distribution is shown in Figure 2. More detailed descriptions can be found in Nelson et al. (2006), Nelson and Kennedy (2007) and Nelson et al. (2008).

### Stratified Units

#### ZYMOETZ GROUP

The oldest rocks in the region belong to the Permian and older Zymoetz Group. It consists of a lower volcanic-clastic-dominated unit, the Mount Attree volcanic complex, overlain by a limestone unit that has been correlated with the Permian Ambition Formation, as defined by Gunning et al. (1994). The Mount Attree volcanic complex comprises dark green andesite flows, tuff and volcanic breccia, along with minor siliceous and calcareous sedimentary strata. A U-Pb zircon date of ca. 285 Ma for tuff within the upper extent of this unit by Gareau et al. (1997a) is interpreted as the age of deposition. The Mt. Attree volcanic complex is metamorphosed in greenschist and lower amphibolite facies.

Where unmetamorphosed, the Ambition Formation limestone consists of thinly to thickly bedded fossiliferous limestone. Bedding-controlled hematite and silica replacement has led to the development of highly fossiliferous, pink beds that are exceptionally well preserved (Figure 3). In other areas, it consists of coarsely recrystallized marble. An Early Permian age was reported by Duffell and Souther (1964) on the basis of macrofossil assemblages.

<sup>1</sup>School of Earth and Ocean Sciences, University of Victoria, Victoria, BC, jangen@uvic.ca

This publication is also available, free of charge, as colour digital files in Adobe Acrobat® PDF format from the BC Ministry of Energy, Mines and Petroleum Resources website at <http://www.empr.gov.bc.ca/Mining/Geoscience/PublicationsCatalogue/Fieldwork/Pages/default.aspx>.

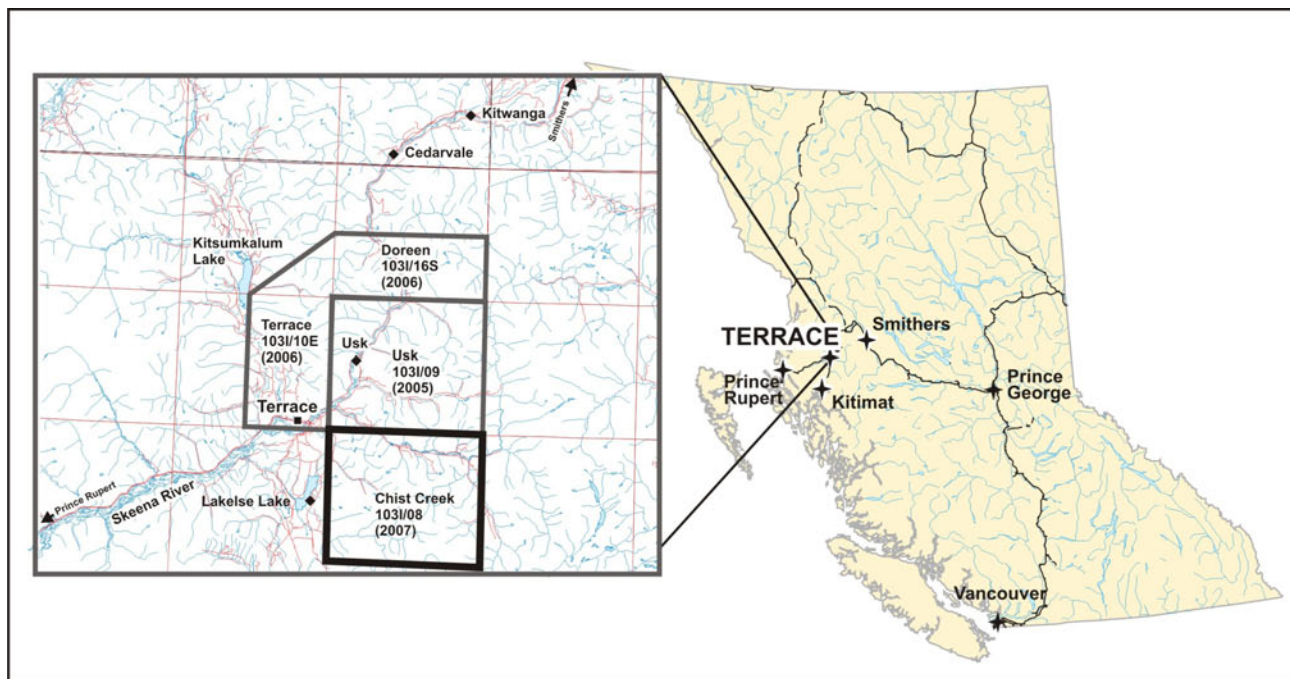


**Figure 1:** Location of the Terrace map area within British Columbia. The mapping completed in the summers of 2005, 2006 and 2007 is outlined.

## TELKWA FORMATION

The Early Jurassic Telkwa Formation is the lowest unit of the Hazelton Group. It unconformably overlies the Zymoetz Group. It consists of dominantly andesitic and dacitic subaerial volcanic units with minor associated, volcanic-derived sedimentary beds. Where thinly bedded units were observed within the lower Telkwa, they are parallel to bedding in the underlying limestone. The base of the Telkwa Formation is a disconformity because, in some areas, the Telkwa is depositionally on top of the Mount Attree volcanic complex and the limestone is absent. In most areas, this relationship is obscured by the irregular topography and abrupt facies changes inherent in volcanic provinces and high-energy sedimentary environments. The basal unit of the Telkwa Formation is a highly variable polymictic conglomerate, containing clasts derived from the underlying Paleozoic strata as well as from Telkwa volcanic rocks. Above this, the lower Telkwa consists dominantly of volcanoclastic units; andesite breccia and crystal lithic lapilli tuff are common constituents. The upper Telkwa is dominated by amygdaloidal andesite and dacite flows, with lesser volcanoclastic and sedimentary components. Regionally, faunal assemblages of sedimentary layers within the Telkwa Formation indicate a Sinemurian (Early Jurassic) age (Tipper and Richards, 1976). The Telkwa Formation has undergone regional zeolite to lowest greenschist facies metamorphism.

## KITSELAS FACIES

The Kitselas facies is a dominantly felsic volcanic unit restricted to the footwall of the Skeena River fault system. Its bounding faults are poorly exposed, obscured both by Eocene intrusions and by recent fluvial deposits along the Skeena River. The unit is dominated by well-bedded volcanoclastic rhyolite that shows eutaxitic, strongly welded textures in places. Andesite flows in the Kitselas resemble those in the Telkwa. The Kitselas has been interpreted

as a local felsic centre within the Telkwa Formation. A U-Pb zircon date of ca. 195 Ma is documented as the age of deposition, reinforcing the interpretation of the Kitselas facies as a metamorphosed equivalent to the Telkwa Formation (Gareau et al., 1997a). The Kitselas rocks have been metamorphosed in the greenschist to lower amphibolite facies.

## SMITHERS FORMATION

The Middle Jurassic Smithers Formation paraconformably overlies the upper Telkwa and is composed of uniform, thinly bedded, tuffaceous greywacke. Macrofossils and trace fossils are common. An Aalenian (Middle Jurassic) age has been established on the basis of macrofossil assemblages (G. Woodsworth and H. Tipper, unpublished data, 1985, as a pers comm from J. Nelson, 2008).

## TROY RIDGE FACIES

The Smithers Formation is overlain by the 'pyjama beds', which derive their name from their striped appearance. This unit is composed of thinly bedded black chert and siliceous argillite, commonly with interbeds of white to pink siliceous tuff. These strata are correlative with the Troy Ridge facies in the Iskut region, which has been dated as Bajocian (Middle Jurassic; K. Simpson and V. McNicoll, unpublished data, 1994, as a pers comm from J. Nelson, 2008). Together with the underlying Smithers Formation, the pyjama beds form a distinctive marker unit between the volcanic Telkwa Formation and the Bowser Lake Group, and can be used to trace regional folds and faults.

## BOWSER LAKE GROUP

Bowser Lake Group sedimentary strata crop out in the northern part of the map area. They conformably overlie the 'pyjama beds'. Regionally, the Bowser Lake Group is characterized by siltstone to cobble conglomerate of domi-

nantly chert clasts derived from the Cache Creek Terrane to the northeast. In its southern exposures near Terrace and Smithers, there is significant input of volcanic-derived clasts from the uplifted Skeena arch. These volcanic-protolith sedimentary beds cause the Bowser Lake Group to weather an off-white colour (leading to the field name of 'white Bowser'). Deposition of the Bowser Lake Group occurred between the Late Jurassic and Early Cretaceous (Tipper and Richards, 1976).

## **Intrusive Rocks**

### **EARLY JURASSIC PLUTONIC SUITE**

These are the oldest intrusions large enough to be mapped at 1:50 000 scale. The largest of these is the Kleanza pluton, which typifies this suite in its significant heterogeneity, varying from gabbro to quartz-rich granitoid. A sample from the Kleanza pluton yielded a U-Pb zircon date of ca. 200 Ma (Gareau et al., 1997a). This date, interpreted as the age of crystallization, along with similar lithological characteristics between this intrusive suite and the Telkwa volcanic rocks, suggests that it forms the middle to upper crustal roots of the Telkwa arc.

### **EARLY TERTIARY GRANITOID ROCKS**

The Kitsumkalum suite occurs within one plutonic body that consists of granite with lesser granodiorite and diorite. It is variably to strongly foliated. Gareau et al. (1997a) dated it as ca. 59 Ma by U-Pb methods on zircon. The Eocene Carpenter Creek suite includes the Carpenter Creek, Newtown and Williams Creek plutons, and an unnamed pluton that is exposed along the Kitimat River. They are composed predominantly of granite and granodiorite, compositionally similar to the Kitsumkalum suite. Like it, they commonly contain small, clear, euhedral titanite grains. They are interpreted as postkinematic to the ductile deformation event that affected the Kitsumkalum suite, due to their lack of a penetrative foliation. The Carpenter Creek pluton provided a U-Pb zircon date of ca. 53 Ma (Gareau et al., 1997a).

## **STRUCTURAL GEOLOGY**

Stratified rocks at deeper levels in the Terrace area are deformed into regional-scale northeasterly-trending folds (Figure 2). Most prominent among these is an anticline cored by Mount Attree volcanic complex and Ambition Formation limestone in the area between the Skeena River, the lower Zymoetz (Copper) River and the Kitimat River. Northeasterly folds are also well developed within the Kitselas volcanic rocks. At higher stratigraphic levels in the Hazelton and Bowser Lake groups, strata form homoclinal, fault-bounded panels. These may represent a more brittle expression of the folds, or they may have formed as a response to unrelated fault activity.

## **Methods**

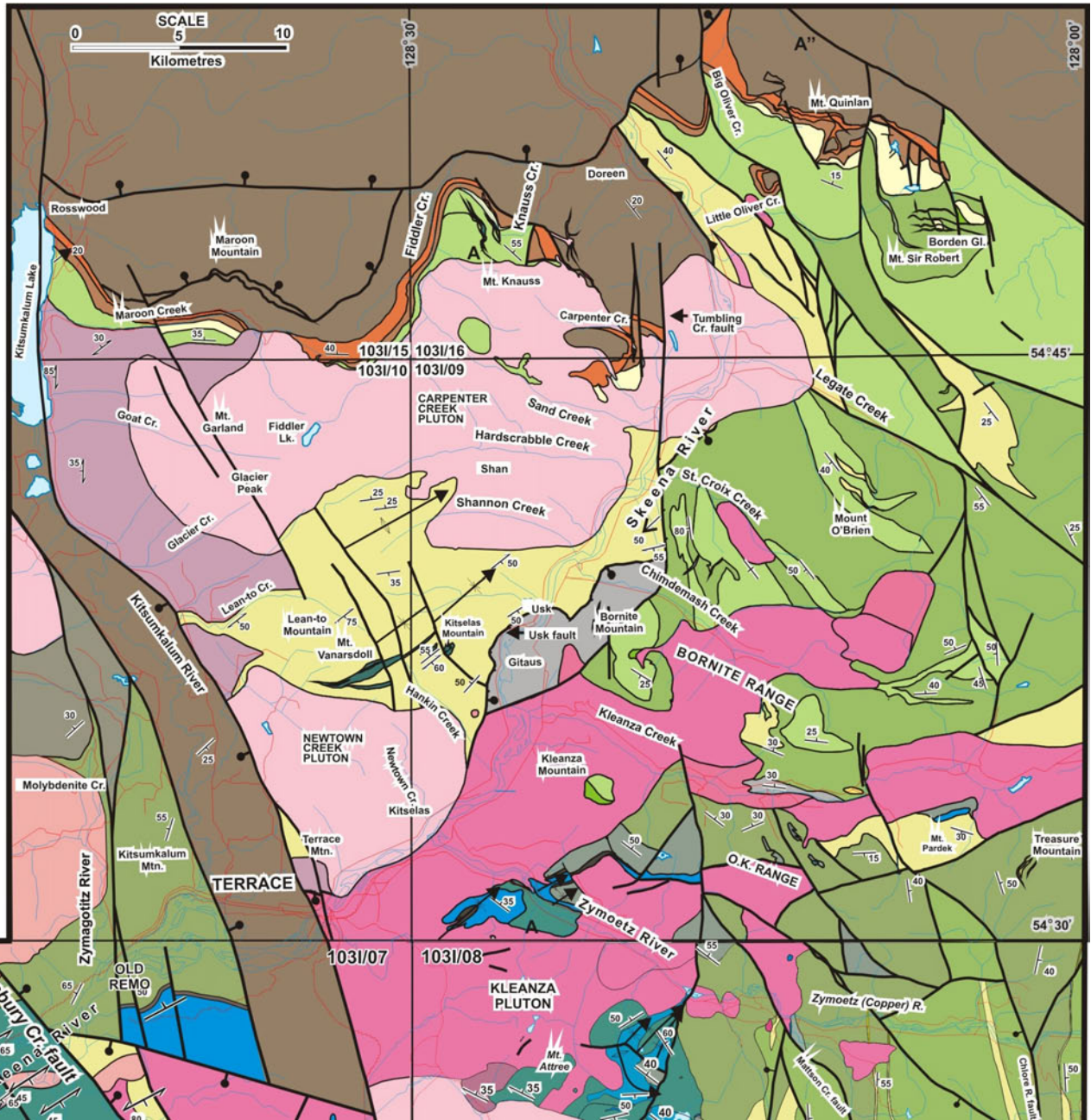
A geospatial structural analysis of the Terrace area was conducted by digitally partitioning the Terrace regional map (Figure 2) into structurally coherent domains and plotting the structures for each domain on separate stereonet projections. The result is a structural history that constrains models of the geological evolution of the region. The structural domains, shown in Figure 4, were defined visually as

sets of geological polygons in a GIS (Manifold<sup>®</sup>) file that showed consistent structural characteristics. A simplified map was created that includes layers for only the linework, geology polygons and structures. Then all of the polygons in a given domain were selected and a query was done to select all structural data within the indicated area. In Manifold, this task is done using the selector function at bottom of the window (All objects in Structures Select Contained within All objects in Polygons Apply). The structures table was then opened with the selected structural data already highlighted. A 'Domain name' column was added to the table and all of the selected structures were labelled by typing the name in one of the highlighted rows. That name is automatically applied to all of the other highlighted structures. Once all of the domains had been selected and labelled, the entire table was exported as an Excel<sup>®</sup> file. This file was simplified to contain only the domain name, structure type and structural measurement. A separate file was created for each structure type represented within each domain (S0, layering; Sn, foliation; Ln, lineation; Bs, brittle shear; Bl, brittle lineation; Lf, fold hinge). These were then saved as tab-delimited text files and imported into Spheristat<sup>™</sup> 2.2 to produce lower-hemisphere stereonet projections.

Once all of the first draft stereonets had been produced, they were assessed and modifications to the domains were made to refine insights into specific deformational events. The process was repeated to produce a final set of stereonets for analysis. A Gaussian density distribution was applied to each stereonet to give the average orientation of that structure type; where folds were suspected, an eigenvector principal direction analysis was also applied. Both of these analysis methods are found under the analysis menu in SpheriStat<sup>™</sup> 2.2. An eigenvector analysis is represented as three mutually perpendicular planes. The stereonets with poles to bedding and foliation plotted are presented in the context of regional geology in Figures 5 and 6, respectively. Other structure types, such as fold axes and slickensides, are not well enough represented regionally to be of statistical significance and so were not presented in the same way. Note that, in some areas, there were two observed foliations but insufficient data were available to plot them separately.

## **Results**

The bedding measurements within the map area, compiled in Figure 5, show several common themes. There is a broad east-dipping homocline defined by the Telkwa bedding attitudes in the southeastern part of the map area. The dip of bedding varies from shallow (5°) to vertical, and strike is consistently northerly. The average poles to bedding plunge between 26° and 41° towards 270°, leading to an average bedding plane of 000/57°. This homocline can also be observed within the underlying Zymoetz Group in the Gazelle domain, although it is possible that this is a coincidental feature. Bedding measurements within the Telkwa Formation farther to the north are highly variable, possibly due to control by local rhyolitic centres, which would have generated irregular paleotopography. The mid-Jurassic to Cretaceous strata that crop out along the northern boundary of the map area define a broad homocline that dips northeast. This domain is characterized by a pole to bedding of orientation 214/65°, with an average bedding orientation of 294/35°.



**STRATIFIED UNITS**



**LOWER CRETACEOUS**  
Skeena Group



**UPPER JURASSIC**  
Bowser Lake Group



**UPPER JURASSIC**  
'Pyjama beds'

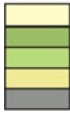


**LOWER(?)–MIDDLE JURASSIC**  
Smithers Formation



**LOWER JURASSIC**  
Telkwa Formation

**Flow-dominated division**



Bright red dacite tuff  
Andesite, basalt, dacite, rhyolite  
Dacite, andesite, rhyolite  
Rhyolite, rhyodacite, dacite  
Volcanic sandstone, siltstone, tuff

**Volcaniclastic division**



Andesite, dacite breccia, tuff, flows  
Rhyolite, dacite (includes Kitselas)  
Polymictic conglomerate  
Sandstone, volcanic breccia

**TRIASSIC**



Black argillite, chert, limy mudstone, siltstone

**PERMIAN AND OLDER**  
Zymoetz Group



**Ambition Formation**  
Limestone



**Mt. Attree volcanic complex**  
Andesite, dacite, rhyolite, basalt tuff, flows; cogenetic intermediate to felsic intrusions  
Quartz-sericite schist  
Tuff and epiclastic metasediments  
Marble, calcisilicate



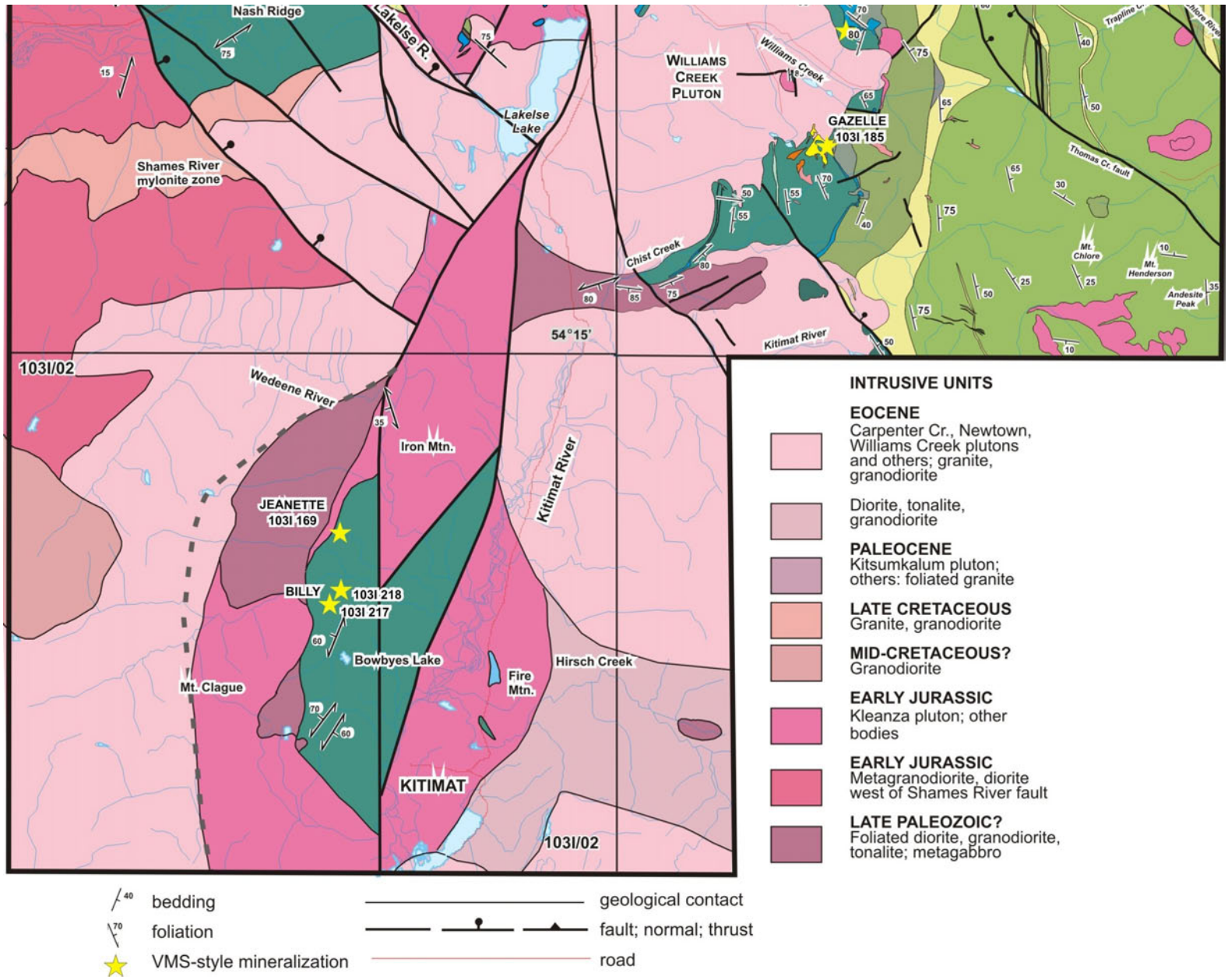


Figure 2. Geology of the Terrace area, compiled from the Terrace regional mapping project (from Nelson, 2009).

Folds are evident within the Zymoetz Group and lower Telkwa Formation, particularly in the Kitselas facies. The four stereonet with eigenvectors shown highlight folds with hinge lines plunging shallowly to moderately northeast. The hinge lines described by each domain vary somewhat: Antiform, 038 /10 ; Sausage, 052 /52 ; Kitselas, 074 /07 ; Zymoetz, 054°/31°. The two remaining domains for which layering data were collected, Chist Creek and Camp 1, seem to define two limbs of an overturned fold with a hinge line plunging southeast. This feature is not discussed in detail here, as limited data prevented a proper analysis.

Foliation data are presented in Figure 6. Foliation, in the form of mineral and clast flattening, is developed only locally within the upper Telkwa and younger stratigraphy. Where it is observed, it is parallel to layering and poorly developed. The Kitselas facies of the Telkwa is well foliated and, in areas, two phases of foliation were observed. One phase, described by mineral flattening, is dominantly bedding parallel and developed prior to the deformation of layering described above. There is another foliation developed parallel to the axial plane of northeasterly-plunging folds at an orientation of 240 /85 (one measurement documented as axial planar in the field). This foliation shows mineral flattening, as well as weak cleavage development. The northeasterly hinge lines lie within this plane. The Gitaus domain also shows a well-developed foliation for the Telkwa Formation. The poles to foliation lie on a great circle similar to what is seen in the Kitselas domain, suggesting this is likely the same bedding-parallel foliation. The Kitsumkalum pluton has a well-developed foliation defined by biotite aggregates and stretching lineations. Analysis of the data collected shows a strong clustering of foliation data, with an average pole orientation of 010 /55 . The mineral lineations, mainly stretched quartz crystals on foliation-parallel surfaces, show an almost perfect down-dip orientation of 259 /44 (Figure 7a). The brittle shear and brittle lineation orientation pairs show the same down-dip sense of motion, with an average orientation of 259 /45 (Figure 7b). Shear-sense indicators, both tails on mineral grains and steps on brittle shear surfaces, show top-down-to-the-west motion.

## DOWN-PLUNGE PROJECTION

### Methods

A semiquantitative axial-plunge projection that proxies as a crustal cross-section can be developed using a graphics program, such as CorelDraw®, by using a command to ‘squeeze’ the geological map image in a direction parallel to the trend of the hinge line (Johnston, 1999). The orientation of the down-plunge projection was determined by taking a weighted average of hinge-line orientations for each domain that contains a known fold. This was done in Spheristat by plotting the four different hinge lines on the same stereonet. Each hinge line was duplicated to the number of data points represented by it, and the average orientation of this plot was used. The resulting average hinge-line orientation is 057 /29 . The Terrace regional map (Figure 2) was rotated by 57° and compressed in the vertical direction by a factor of 0.48. This value was calculated by taking the sine of 29°, which gives the ratio of the cross-



**Figure 3.** Silica- and hematite-replaced crinoid fossil within the Ambition Formation. Note the exceptional preservation of the calyx on the right side of the photo.

section height over the map height. The resulting down-plunge projection is presented in Figure 8.

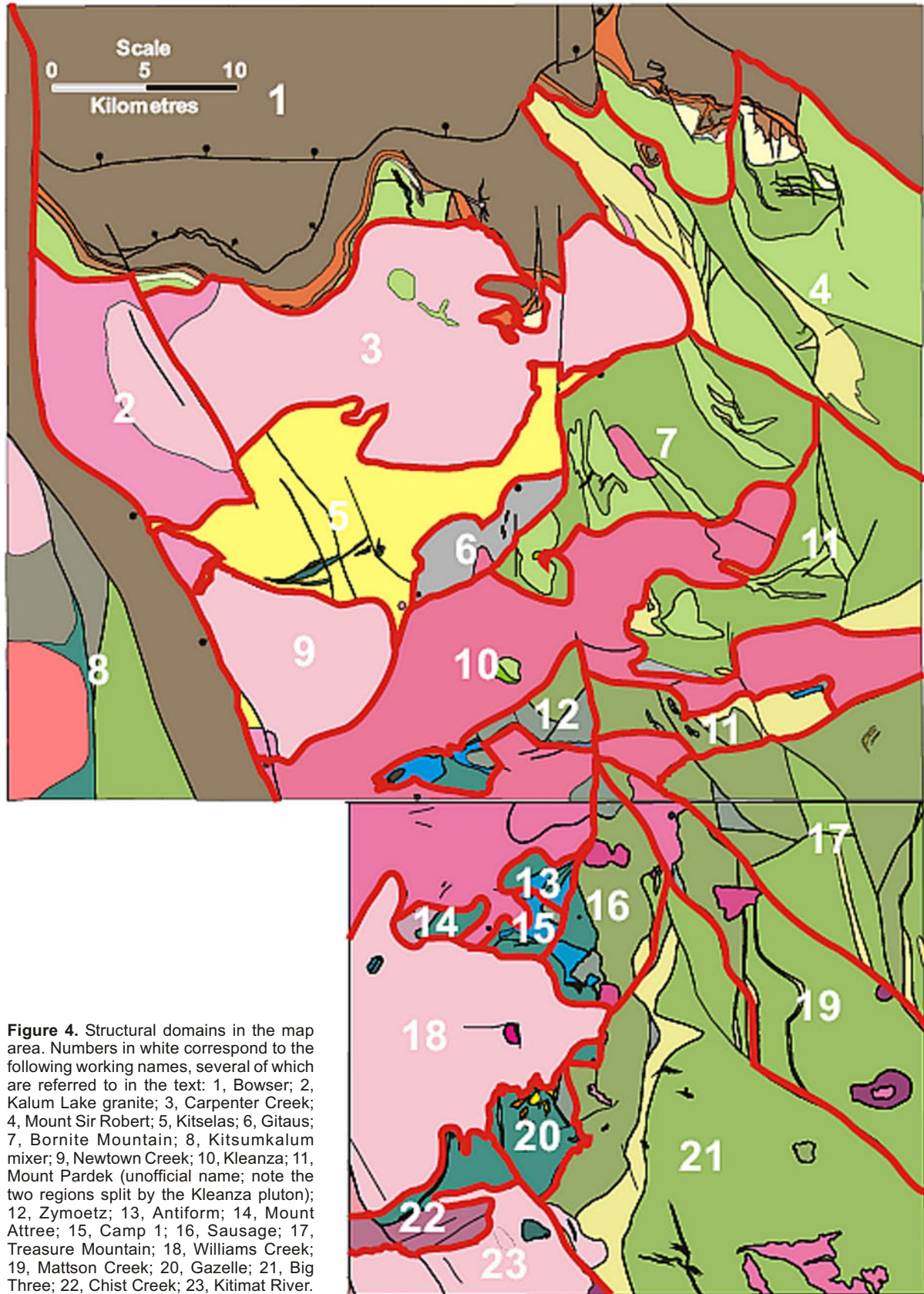
## Results

The down-plunge projection provides an approximate cross-section through the upper crust (Figure 8). The section shows a nearly 10 km thick sequence of Telkwa volcanic rocks. Part of the thickness is probably due to repetition across reverse faults, such as those that bound the Treasure Mountain, Mattson Creek and Big Three domains. The upper sedimentary stratigraphy does not project well in this cross-section because it dips shallowly to the north, but it is worth noting that the sequence from Telkwa Formation to Bowser Lake Group is repeated across a fault running along the Skeena River, the Skeena River fault zone (Nelson and Kennedy, 2007). The base of the section is dominated by laterally extensive and bulbous plutons of varying age. The most interesting of these is the Kleanza pluton, which cuts through the entire Telkwa Formation; it is interpreted as the feeder for Telkwa. Another feature highlighted on the section is that the Ambition Formation, which dips to the northeast, resurfaces southeast of the Kleanza pluton. Further discussion is provided with the structural interpretations.

## DISCUSSION

### Folding

Northeasterly folds were likely formed with a horizontal hinge line (discussed later), in response to a principal compressive stress oriented northeast-southwest and vertical minimum compressive stress. It is plausible that the east- and northeast-dipping homoclines are two limbs of a large, regional-scale fold with the same orientation as the smaller folds. The folds in the Kitselas facies rocks restrict the age of this northwest-southeast compression to post-Early Jurassic. West of the study area, Heah (1991) and Nelson (2009) reported strong northeasterly fabrics within Late Cretaceous granitoid bodies, as well as in metamorphosed volcanic rocks likely correlative with the Mount Atree volcanic complex and Telkwa Formation. Massive



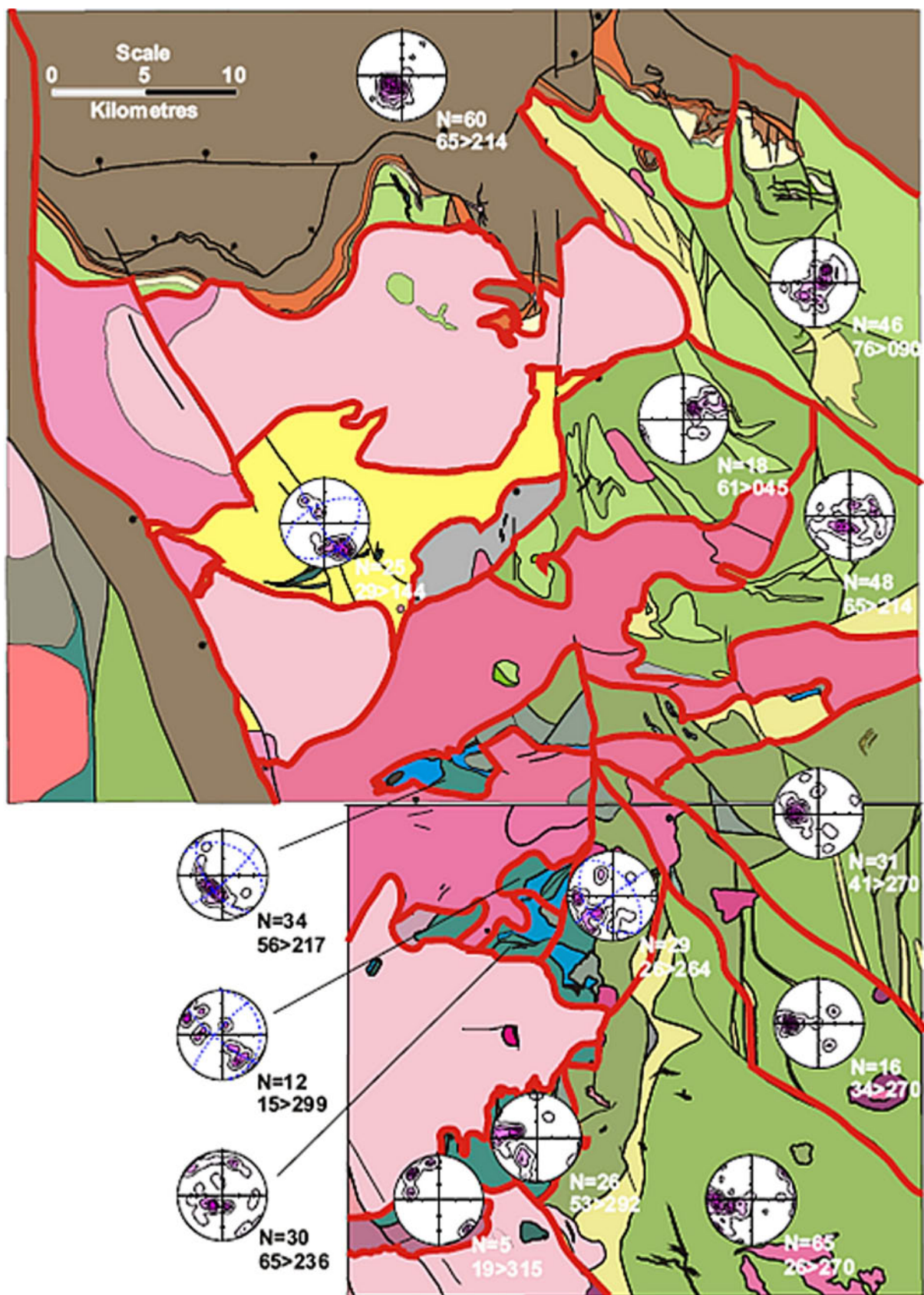


**Figure 5.** Stereonet projections of poles to bedding (N is the number of data points included). The average trend and plunge of each stereonet is included. A principal direction analysis was done for the domains with observable folds. The intersection of the two blue planes that does not lie within the data concentration indicates the hinge line of the fold.

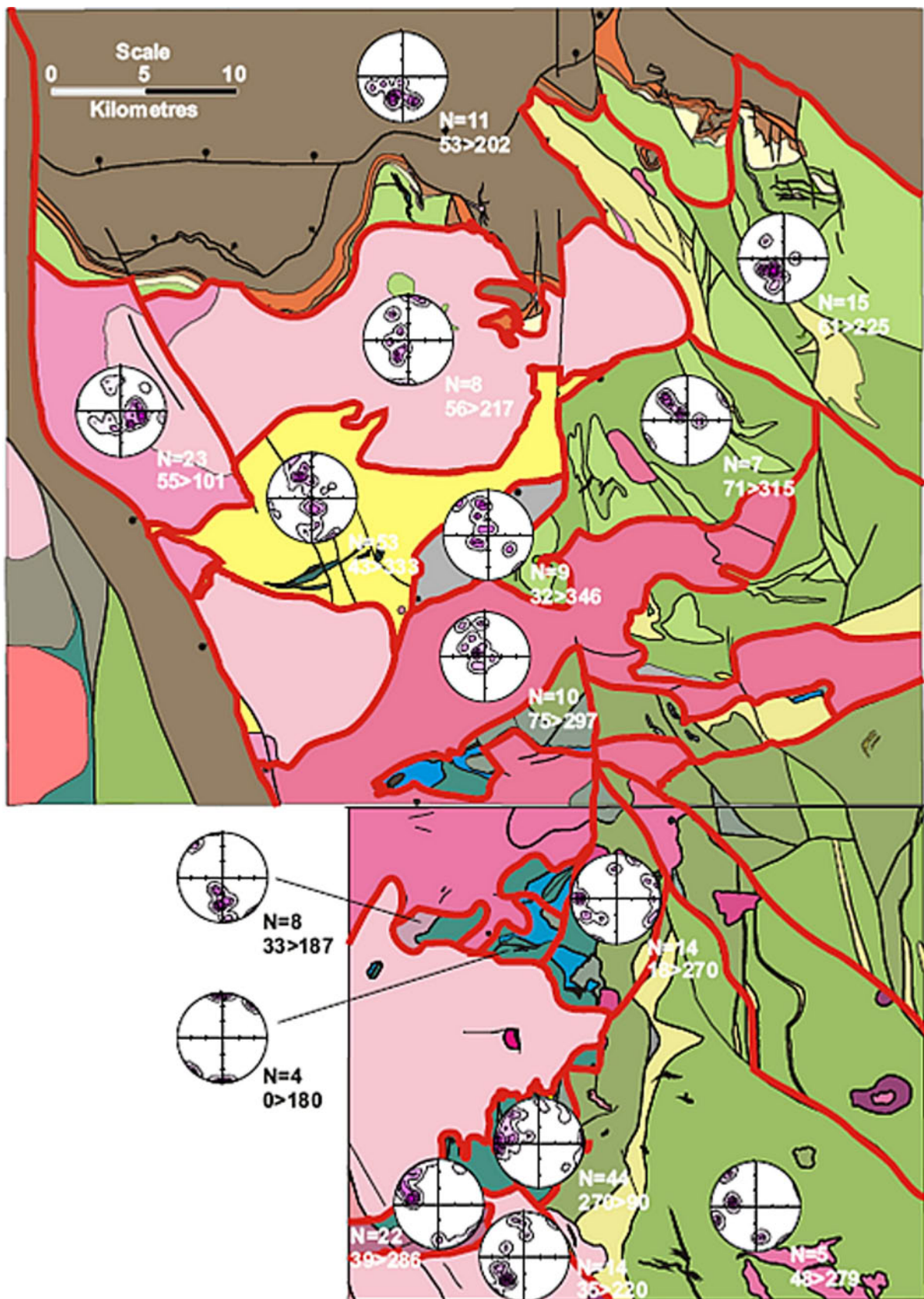


Figure 6. Stereonet projections of poles to foliation (N is the number of data points included). The average trend and plunge of each stereonet is included.

plutons of the Carpenter Creek suite cut across folds and foliations in both the Kitselas block and the Williams Creek–Kitimat River area. Thus, the main age of northeasterly folding is constrained to between 70 and 53 Ma, or earliest Tertiary.

Northeast-trending folds of regional magnitude are uncommon in the Cordillera; they are orthogonal to the dominant northwesterly structural trend, which may be controlled by the margin of ancestral North America as well as the present plate margin. Hinge lines in the Terrace area are parallel to the trend of the Skeena arch. Little is known about the mechanics of how the Skeena arch actually formed. It was a prominent feature by Late Jurassic time, as it forms the southern boundary of the Bowser Basin. Tipper and Richards (1976) interpreted it as a simple uplift with no associated compression. A detailed analysis of the folds here could provide insight into potential reactivation of the Skeena arch during Early Tertiary orogen-parallel compression. The two homoclines could be two limbs of a large fold. The presence of large folds affecting all of the stratigraphy present in the map area is permissible, as the Telkwa Formation is involved in the deformation event and there is a near-continuous stratigraphy starting with the Telkwa in the early Jurassic through to the Cretaceous Bowser Lake Group. The only significant unconformity lies between the top of the Telkwa and the Smithers Formation. This interpreted paraconformity would imply that the Telkwa was not folded prior to deposition of the Smithers Formation.

The lower Telkwa and underlying stratigraphic units were near the brittle-ductile boundary for crustal rocks (10 km depth) in Middle Jurassic time, when Telkwa volcanism was coming to an end, and much deeper with deposition of the Bowser Lake Group. These burial depths are supported by regional zeolite to lowest greenschist facies metamorphic grade within the Telkwa, and greenschist to lower amphibolite grade in the stratigraphically and struc-

turally underlying rocks of the Zymoetz Group and Kitselas facies. This model would explain the prevalence of brittle rather than ductile features within the upper Telkwa and higher stratigraphy associated with this event, compared to folding and development of cleavage at deeper crustal levels.

### Metamorphism of the Kitselas Facies

The Kitselas facies has been metamorphosed to greenschist to lower amphibolite facies, whereas the coeval Telkwa Formation is only metamorphosed to zeolite or lowest greenschist facies. The difference in metamorphic grade has been explained by a thrust fault along the Skeena River fault zone, placing Telkwa on top of Kitselas and younger strata, as seen in Figure 8 (Gareau et al., 1997b; Nelson and Kennedy, 2007). Gareau et al. (1997b) interpreted this fault as a top-to-the-northeast detachment. The structural data show limited evidence of these low-angle structures. Four elongation lineations with values of approximately 0.35 / 10 were measured within the Gitaus domain. If these are stretching fabrics, then foliation observed within this domain could be a tectonic fabric along a curvilinear detachment surface. Given the parallelism of these lineations with the hinge-line orientation and the similar attitudes of foliations between the Gitaus and Kitselas domains, it is likely that these lineations are associated with northeast-southwest compression, not extension. However, the duplication of the stratigraphy noted at the northwest edge of the down-plunge projection associated with the Skeena River fault zone still supports the possibility of top-to-the-northeast thrust imbrication. This thrust is restricted to post–Early Cretaceous, as it affects the Bowser Lake Group, and pre-Eocene as it is crosscut by Eocene intrusions. In terms of style, timing and the observed orientation of the thrust (cutting up-section towards the northeast),

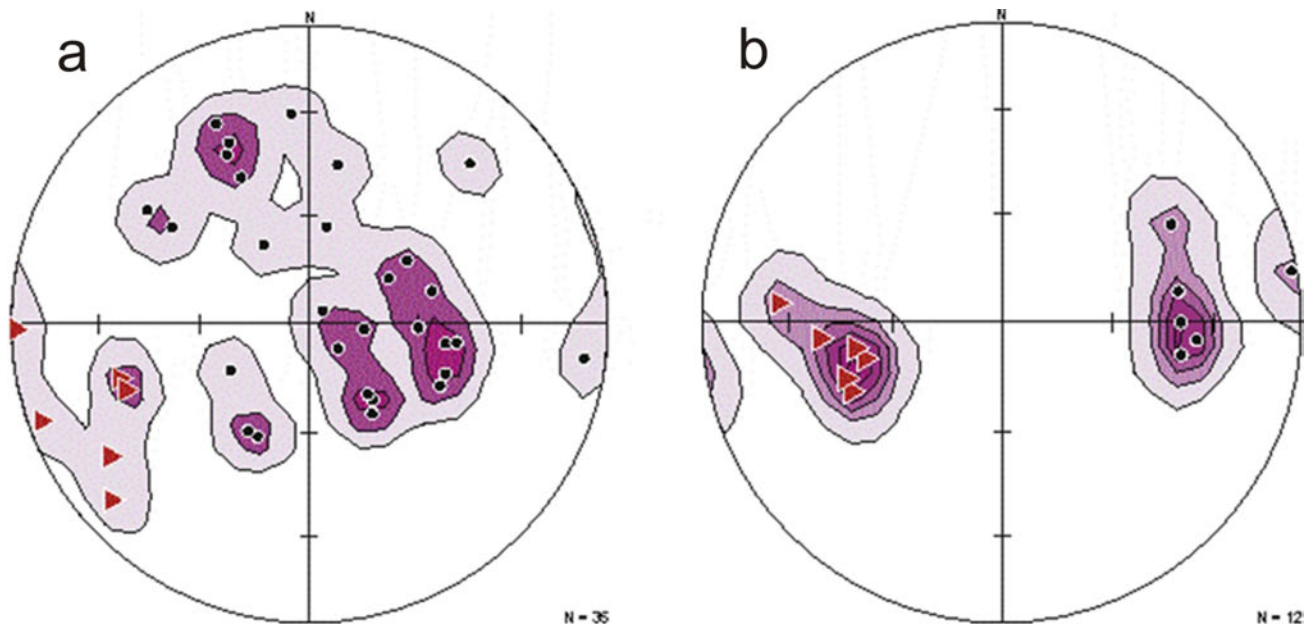


**Figure 7.** Stereonets describing deformation associated with the formation of the Kitsumkalum-Kitimat graben: **a)** poles to foliation (black dots) and elongation lineations (red triangles); **b)** poles to brittle shear surfaces (black dots) and slickenlines (red triangles). These represent the ductile and brittle phases of the normal fault defining the eastern edge of the Kitsumkalum-Kitimat graben. The motion, described by ductile and brittle lineations, is at an orientation of 259 / 45 .

NNW

ESE

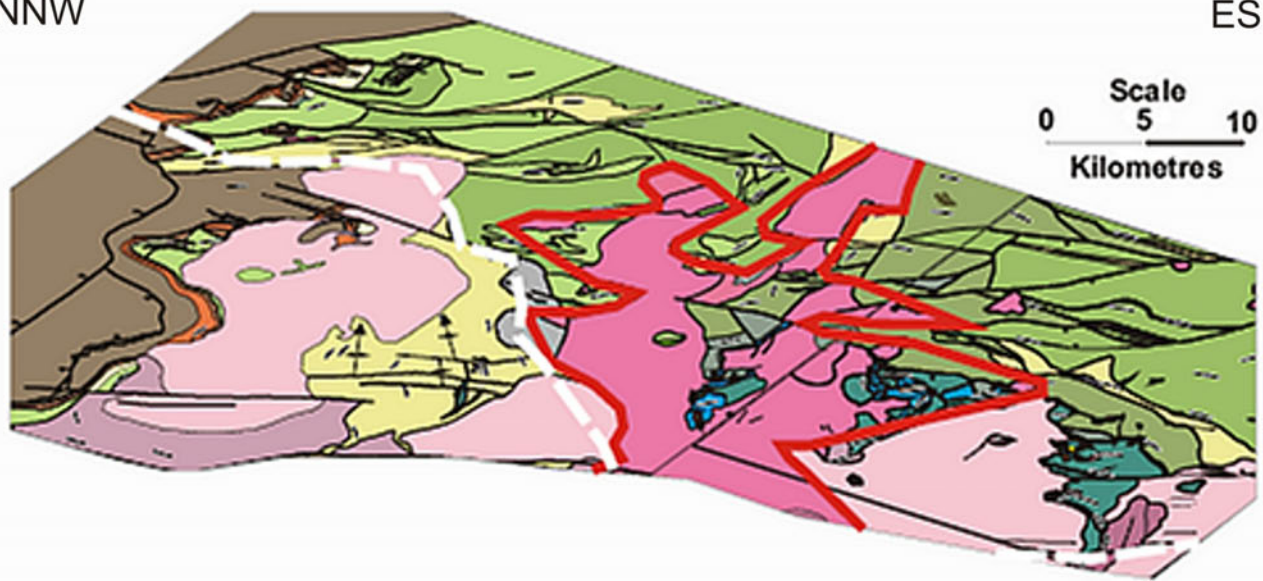


**Figure 8.** Down-plunge projection (without vertical exaggeration). The base of the projection follows the trace of the Kitsumkalum-Kitimat graben. The red lines highlight the approximate extent of the Kleanza pluton, indicating its 'Christmas tree' form. The white line traces the approximate orientation of the Skeena River fault zone.

the Skeena River fault zone matches other structures attributed to the Skeena fold-and-thrust belt by Evenchick (1991).

Two sets of southwest-verging thrust faults active between 87 and 59 Ma have been documented in the region west of the map area (Andronicus et al., 2003). Neither mapped relations in the Terrace area nor the structural data set in this study can be linked to this faulting. Northeastward detachment along the Skeena River fault zone, although not well documented in this study, may have occurred contemporaneous with the Shames River mylonite zone and other northeastward-directed shearing at approximately 54–47 Ma (Heah, 1991; Andronicus et al., 2003).

**Kitsumkalum-Kitimat Graben**

The most recent major structural event in the Terrace area is extension associated with the Kitsumkalum-Kitimat graben. The Kitsumkalum pluton is cut by a normal fault along which both brittle and ductile deformation are apparent. The fault strikes south-southeast and dips moderately southwest, perpendicular to axes of northeast-plunging folds, leading to the interpretation that the a-c joint plane of the folds was an initial weakness along which the fault developed. Top-down-to-the-west motion on a fault of this orientation would lead to rotation of the footwall block, giving the regional east-northeast plunge of the hinge lines and dip of the layering.

There are numerous smaller faults to the east of the main normal fault that are parallel to it. Some of these are cut by apophyses of the Kleanza pluton, whereas others offset them. Their sense of motion is also variable: some are top-down-to-the-west, others are top-up-to-the-east. Thus, they cannot be simply coeval with the eastern fault of the Kitsumkalum-Kitimat graben. The younger (post-

Kleanza) faults can be explained by local stress being accommodated by the same a-c joint plane in folds.

The age of the Kitsumkalum-Kitimat graben is Eocene or younger because it truncates both the deformed Kitsumkalum pluton and plutons of the undeformed 53 Ma Carpenter Creek suite. This age is consistent with steeper normal faulting succeeding the shallow detachments of the Skeena River fault zone and the Shames River mylonite

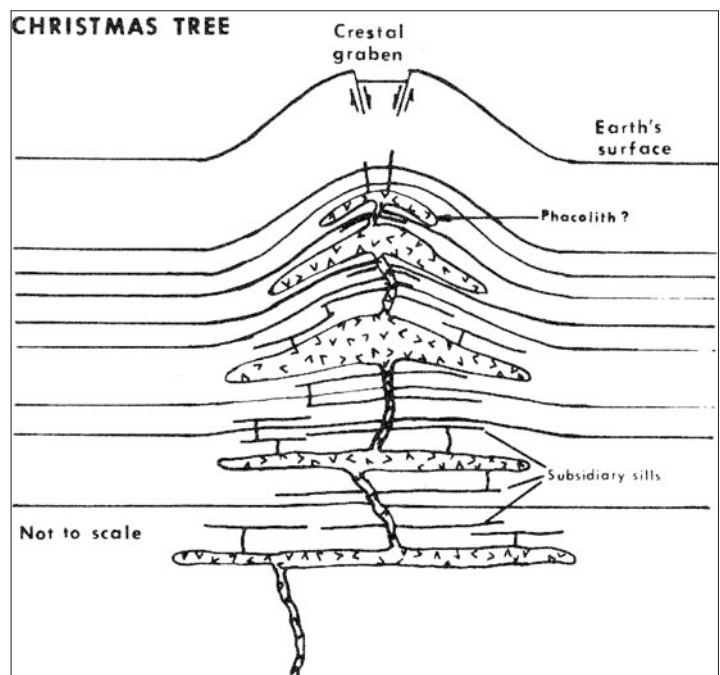


**Figure 9.** Schematic diagram of a 'Christmas tree' laccolith, representing the extreme end-member case. The Kleanza pluton shows some of the characteristics of a Christmas tree laccolith but differs from this model because it is actually feeding a volcanic vent above (Corry, 1988).

zone, but being a result of the same extensional event (Heah, 1991).

### **Kleanza Pluton**

The shape of the Kleanza pluton in the down-plunge projection (Figure 8) is similar to that of ‘Christmas tree’ laccoliths (Corry, 1988). A Christmas tree laccolith (Figure 9) forms when parts of an intrusion spread out parallel to layering at various depths. For all intrusions, rising magma becomes neutrally buoyant and stops when the density of the magma equals that of the surrounding country rock. The Kleanza pluton seems to be ordered into several (paleo-) horizontally extensive layers, as outlined on Figure 8. Since the pluton is interpreted as the dominant local feeder for the Telkwa volcanic rocks, each layer would have led to a thickening of the overlying volcanic package, resulting in increased pressure inside the magma chamber. This would have made the magma positively buoyant, leading to the formation of a shallower magma chamber. Emplacement of the Kleanza suite could have led to the irregular layering of the domains that lie above it, in cross-section, both through paleoslopes of the volcanic edifice(s) and through doming over the intrusion.

### **Implications for Geological History**

Analysis of structural data collected during the Terrace regional mapping project has contributed to an understanding of the local geological history in the area. The sequence of events recorded by these rocks is as outlined below. Volcanic and associated intrusive units of the Mount Attree volcanic complex developed in an island-arc setting during late Paleozoic time. This arc became dormant, allowing for the prolific biological activity that gave rise to Ambition Formation limestone in Permian time, followed by deep-water, starved basinal conditions in the Triassic. The magmatic arc was reactivated in the Early Jurassic. A nearly 10 km thick succession of Telkwa volcanic rocks was deposited, together with intrusion of the Kleanza pluton. In mid-Jurassic time, volcanism was succeeded by subaqueous deposition of the Smithers Formation. The shift from subaerial to subaqueous conditions suggests subsidence associated with the cooling of the island-arc root. Continued subsidence would allow deposition of the fine-grained Troy Ridge facies, possibly accompanied by regional extension (J-F. Gagnon, pers comm to J. Nelson, 2008). Clastic influx began in the Late Jurassic (Oxfordian) and deposition into the Bowser Basin continued up to Early Cretaceous time.

Northeast-vergent thrusting along the Skeena River fault zone buried the Kitselas facies of the Telkwa Formation under a hangingwall of Paleozoic and younger strata during the mid-Cretaceous. The Paleocene Kitsumkalum pluton intruded this assemblage and was later deformed with it. Similarly, latest Cretaceous granitoid rocks intruded the hangingwall and were folded along with it into gently northeast-plunging folds with steep axial planes.

Megascopic northeasterly folds lie in the hangingwall of the Shames River fault zone, a listric, northwest-striking, down-to-the-east Eocene normal fault exposed 20 km west of Terrace. West of the Shames River fault, mylonitized deeper crustal rocks were exposed by a shallowly dipping, top-to-the-northeast detachment zone. The Shames River fault is regarded as a late-stage expression of the same

crustal extension event, which overall occurred between 54 and 47 Ma (Andronicos et al., 2003). This mid-crustal extension was coeval with postkinematic plutons of the Carpenter Lake suite, which cut northeasterly-trending folds east of the Shames River fault. Therefore, the folding, which is post 69 Ma, predated Eocene top-to-the-northeast extension.

Tertiary northeasterly folds along the Skeena arch allow the hypothesis that it could have been reactivated as an orogen-normal compressional structure. Late Cretaceous to Eocene dextral strike-slip motion was widespread in the Cordillera. The Skeena arch may have acted as a restraining bend, with transcurrent motion stepping west from the Cordilleran interior into the Coast Plutonic Complex and farther outboard.

In the Terrace area, continued east-northeast-directed extension during the early Eocene reactivated the Skeena River fault zone and gave rise to the Kitsumkalum-Kitimat graben. Originally horizontal, northeasterly-trending folds to the east of the graben were rotated into their current northeast-plunging orientation.

## **CONCLUSIONS**

Three deformation events were identified in the Terrace area. The first produced the northeast-vergent Skeena fold-and-thrust belt in mid-Cretaceous time. The second involved northwest-southeast compression, which gave rise to folds that affected the Paleozoic to Early Cretaceous succession and plutons as young as Late Cretaceous. Folds trend parallel to the Skeena arch, suggesting this compressional event involved structural reactivation of the arch. This was succeeded by extension and the formation of steep, west-southwest- and east-northeast-dipping normal faults that define the eastern and western edges of the Kitsumkalum-Kitimat graben, respectively. The eastern bounding fault is interpreted to have formed along the a-c joint set of the earlier folds, and was likely responsible for rotating the footwall block to the east, giving rise to the northeast plunge of hinge lines and eastward dip of layering. This block rotation affected an approximately 10 km thick section through the upper crust, exposing the relationships between the local strata and the underlying intrusions.

The most prominent unanswered question resulting from the analysis presented here is the nature of regional compression leading to the northeast-trending folds. A more detailed study can also provide insight into the nature of the Skeena arch.

## **ACKNOWLEDGMENTS**

I would like to thank Stephen Johnston for helpful discussions and guidance, as well as acting as a constant reminder that things don’t change unless you stir the pot. I would also like to thank Jeff Kyba and Reid Kennedy for their friendship and assistance over my first two field seasons. Philippe Erdmer provided a helpful review of this manuscript. A special thanks goes out to JoAnne Nelson who has done everything to inspire and promote the budding geologist in me.

## REFERENCES

- Andronicos, C.L., Chardon, D.H., Hollister, L.S., Gehrels, G.E. and Woodsworth, G.J. (2003): Strain partitioning in an obliquely convergent orogen, plutonism, and synorogenic collapse: Coast Mountains Batholith, British Columbia, Canada; *Tectonics*, Volume 22, Number 2, pages 7.1–7.24.
- Colpron, M., Nelson, J.L. and Murphy, D.C. (2007): Northern Cordilleran terranes and their interactions through time; *GSA Today*, Volume 17, Numbers 4–5, pages 4–10.
- Corry, C.E. (1988): Laccoliths: mechanics of emplacement and growth; *Geological Society of America*, Special Paper 220, 110 pages.
- Duffell, S. and Souther, J.G. (1964): Geology of Terrace map area, British Columbia; *Geological Survey of Canada*, Memoir 329, 117 pages.
- Evenchick, C. (1991): Structural relationships of the Skeena Fold Belt west of the Bowser Basin; *Canadian Journal of Earth Sciences*, Volume 28, pages 973–983.
- Gareau, S.A., Friedman, R.M., Woodsworth, G.J. and Childe, F. (1997a): U-Pb ages from the north-eastern quadrant of Terrace map area, west-central British Columbia; in Current Research 1997-A/B, *Geological Survey of Canada*, pages 31–40.
- Gareau, S.A., Woodsworth, G.J., Rickli, M. (1997b): Regional geology of the northeastern quadrant of Terrace map area, west-central British Columbia; in Current Research 1997-A/B, *Geological Survey of Canada*, pages 47–55.
- Gunning, M.H., Bamber, E.W., Brown, D.A., Rui, L., Mamet, B.L. and Orchard, M.J. (1994): The Permian Ambition Formation of northwestern Stikinia, British Columbia; in Pangea: Global Environments and Resources, Embry, A.F., Beauchamp, B. and Glass, D.J., Editors, *Canadian Society of Petroleum Geologists*, Memoir 17, pages 589–619.
- Heah, T.S.T. (1991): Mesozoic ductile shear and Palaeogene extension along the eastern margin of the Central Gneiss Complex, Coast Belt, Shames River area, near Terrace, British Columbia; unpublished MSc thesis, *University of British Columbia*, 155 pages.
- Johnston, S.T. (1999): Squeezing down plunge projections out of graphics packages; *Computers & Geosciences*, Volume 25, pages 197–200.
- Nelson, J.L. (2009): Terrace Regional Mapping Project, Year 4: extension of Paleozoic volcanic belt and indicators of volcanogenic massive sulphide-style mineralization near Kitimat, British Columbia (NTS 1031/02, 07); in Geological Fieldwork 2008, *BC Ministry of Energy, Mines and Petroleum Resources*, Paper 2009-1, pages 7–20.
- Nelson, J.L. and Kennedy, R. (2007): Terrace Regional Mapping Project, Year 2: new geological insights and exploration targets (NTS 1031/16S, 10W), west-central British Columbia; in Geological Fieldwork 2006, *BC Ministry of Energy, Mines and Petroleum Resources*, Paper 2007-1 and *Geoscience BC*, Report 2007-1, pages 149–162.
- Nelson, J.L., Barresi, T., Knight, E., and Boudreau, N. (2006): Geology and mineral potential of the Usk map area (NTS 1031/09), Terrace, British Columbia; in Geological Fieldwork 2005, *BC Ministry of Energy, Mines and Petroleum Resources*, Paper 2006-1 and *Geoscience BC*, Report 2006-1, pages 117–134.
- Nelson, J.L., Kyba, J., McKeown, M. and Angen, J. (2008): Terrace Regional Mapping Project, Year 3: contributions to stratigraphic, structural and exploration concepts, Zymoetz River to Kitimat River, west-central British Columbia (NTS 1031/08); in Geological Fieldwork 2007, *BC Ministry of Energy, Mines, and Petroleum Resources*, Paper 2008-1, pages 159–173.
- Tipper, H.W. and Richards, T.A. (1976): Jurassic stratigraphy and history of north-central British Columbia; *Geological Survey of Canada*, Bulletin 270, 73 pages.



# Shan Deposit, East-Central British Columbia (NTS 103I/09): An Emerging Deposit Model

by M.E. Venable<sup>1</sup> and P.J. Wojdak

**KEYWORDS:** exploration, molybdenum, South Shan

## INTRODUCTION

While no mineral deposit looks exactly like another, and none entirely follows the classic textbook models, molybdenum deposits seem to be even more individualistic. Likewise, true exploration case histories are rarely tidy. Our work to date at Shan is a work in progress, in terms of both finding a model for it and determining the exploration techniques most suited to investigating it. The following history may serve as an example of what worked and what did not, and will concentrate on the Shan South part of the property, where the Las Margaritas zone is substantially mineralized and largely intact.

## GENERAL

The Shan property is located 20 km north-northeast of Terrace, British Columbia and is close to existing road, rail, power and port infrastructure. Logging roads enter the central part of the property along the north sides of Shannon Creek and Hardscrabble Creek. BCM Resources Corp. obtained a 100% interest in the property, then comprising six claims (112 hectares), from N.C. Carter in June 2005. It has since been expanded to 7604.5 hectares (Figure 1).

The topography of the Shan North and South prospects includes two ridges featuring relatively gentle terrain on ridge tops that are bounded by steep flanks, and more rugged terrain on the north side of Hardscrabble Creek in the area referred to as the McRea claims. A series of four creeks drains eastward into the Skeena River. Bedrock exposures occur principally in drainages and as scattered outcrops on ridge crests, although outcrop is more abundant north of Hardscrabble Creek in the McRea sector.

Molybdenum mineralization identified to date is located in three zones at Shan South (Las Margaritas zone, Camp zone and Triangle zone) and in the Banana Lake corridor at Shan North.

## GEOLOGICAL SETTING

### *Regional Geology*

The Shan property is underlain largely by granite to granodiorite of the Eocene Carpenter Creek pluton, an eastern lobe of the Coast plutonic complex. The Carpenter Creek pluton, with a U-Pb date of 53 Ma on a zircon, underlies an area of >1000 km<sup>2</sup> and includes large areas of homogeneous granodiorite, tonalite and granite (Nelson et al., 2006). These granitic rocks intrude the Kitselas facies of the Lower Jurassic Telkwa Formation, the lowest unit of the Jurassic Hazelton Group. Kitselas rocks consist of a lower coherent rhyolite unit and an overlying volcanoclastic unit, as well as some thin (60–220 m) basalt horizons. All units are cut by later intermediate to mafic dikes and narrow (generally <1 m), pink, fine-grained aplitic dikes.

### *Property Geology*

Molybdenum mineralization is hosted mainly by the intrusive rocks (hereafter referred to as ‘granodiorite’), generally near the contact with the Hazelton volcanic rocks (Figure 2). Blocks of altered volcanic rock of intermediate composition, thought to be roof pendants or large xenoliths, also host significant mineralization locally, but most of the volcanic rocks appear to be only weakly mineralized and may mask underlying mineralization.

The Carpenter Creek pluton, as exposed on surface and in drillcore, is generally a medium-grained granodiorite with biotite as the major mafic mineral. The rock is generally hydrothermally altered and details of its original composition are obscured, making delineation of phases difficult. A somewhat coarser and possibly more potassic phase was drilled at depth in some holes. Given the extensive potassic alteration of the coarser phase where it was drilled, it is uncertain whether the original composition differed from that of the rest of the pluton.

The volcanic rocks are generally found as float on the surface and are best seen in drillcore. Textures vary from aphanitic to porphyritic, with plagioclase crystals up to a centimetre in length. The rocks are commonly altered, but the original composition is interpreted to have been intermediate to mafic. The volcanic rocks are commonly found in one drillhole but not in adjacent ones, and may occur as roof pendants or large xenoliths. In some instances, these rocks may be shallow intrusions. Rhyolitic rocks with textures typical of the upper Kitselas facies are found in some drillholes and surface exposures, but they generally occur in marginal areas away from significant mineralization. Contact metamorphic effects are not apparent.

Structural features include a north-northwest-striking strike-slip fault, along which a postmineralization dis-

<sup>1</sup>BCM Resources Corp., Vancouver, BC, [mevenable@fastmail.fm](mailto:mevenable@fastmail.fm)

This publication is also available, free of charge, as colour digital files in Adobe Acrobat® PDF format from the BC Ministry of Energy, Mines and Petroleum Resources website at <http://www.empr.gov.bc.ca/Mining/Geoscience/PublicationsCatalogue/Fieldwork/Pages/default.aspx>.

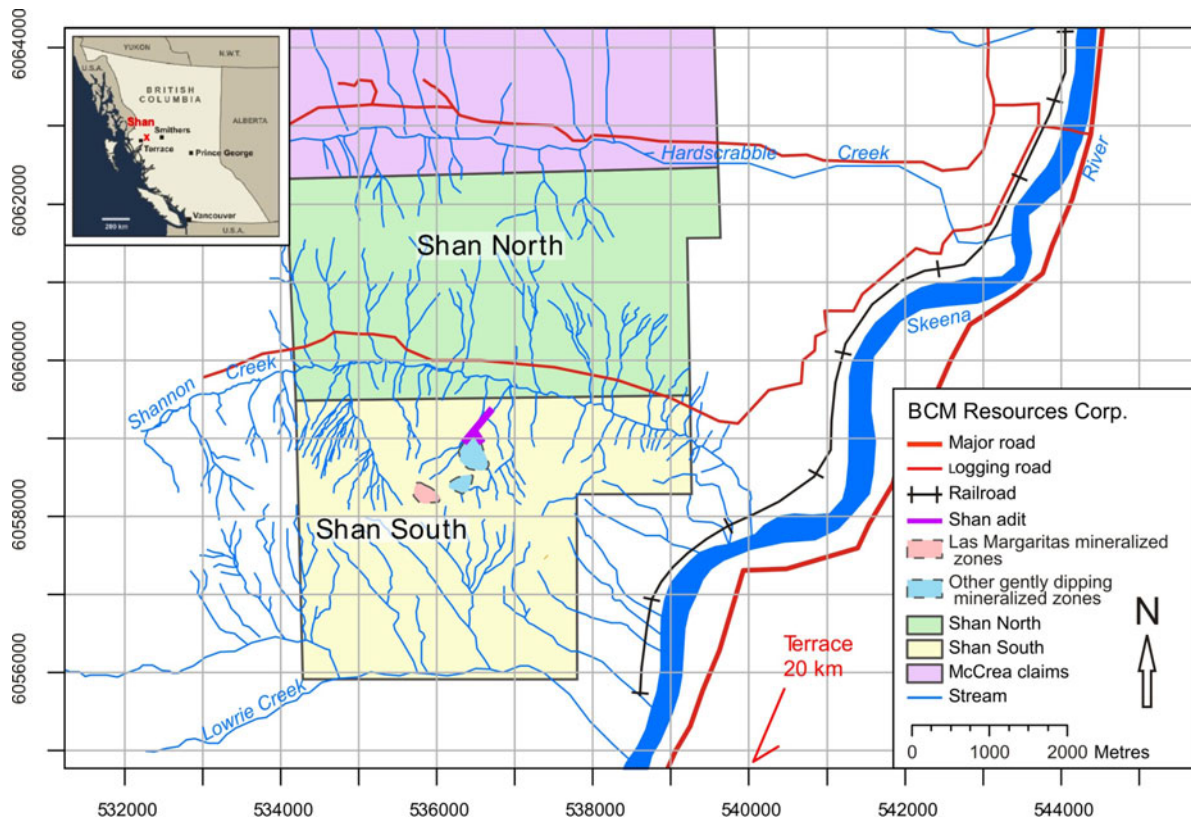


Figure 1. Location of the Shan South part of the BCM Resources Corp. property.

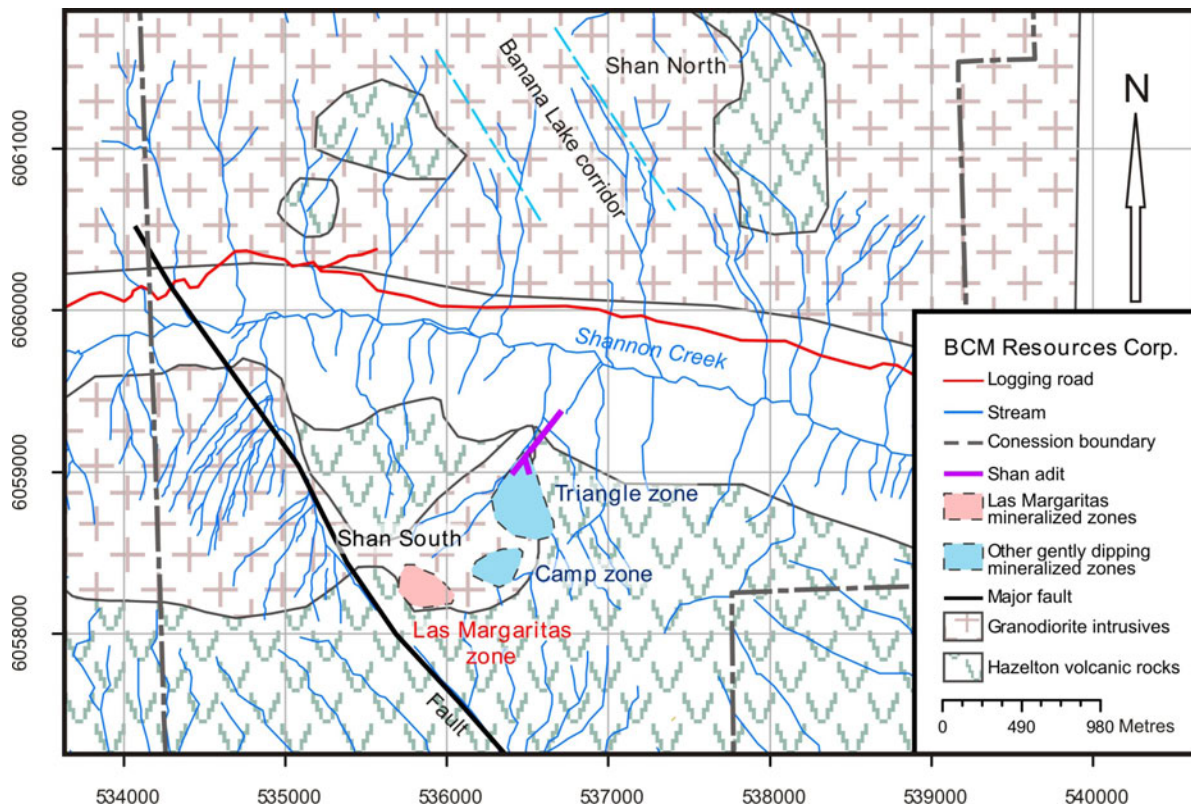


Figure 2. Geology of the Shan South property. Adapted from Nelson et al. (2006) and Riocanex 1:10 000 scale geological map, with modifications based on recent mapping.

placement of ~1 km is suggested from offset of modelled aeromagnetic data patterns. There may also be other faults featuring lesser displacement, such as a possible north-northeast-striking fault along Molybdenum Creek (unofficial name), the site of the historical Shan adit (Figure 2). This and other possible structures have been inferred from topographic breaks and linear depressions, and from observations of some drillholes and bedrock exposures. Both steeply dipping, brecciated, north-northeast- and north-northwest-striking veins and gently northeast-dipping sheeted veins have been observed on the property.

Several faults were intersected in drillholes. Some of these host Mo mineralization, while others appear to truncate mineralized zones. These generally occur as zones of fault gouge ranging up to several metres in width, but the sense and magnitude of displacement cannot be determined.

### **Molybdenum Mineralization**

Molybdenum mineralization is principally in the form of molybdenite and is commonly found associated with quartz veins, generally in sheeted veins with densities of up to several veins per metre of core length. Veins range in width from a few millimetres to several metres, but most are no more than a few centimetres in width, and veins of greater widths are generally more weakly mineralized. Molybdenite also occurs as fracture coatings up to 1 cm thick without quartz, and locally as low-grade disseminations. Quartz-molybdenite veins may also contain pyrite, magnetite and hematite, in any combination of the three, and locally chalcopyrite as well.

A petrographic study of polished thin sections by Vancouver GeoTech Labs from a sample chosen for its variety of mineral phases reported the following (Vancouver GeoTech Labs, 2006):

*“An early stage euhedral pyrite is now largely replaced by later hematite. This euhedral pyrite is followed by a later phase of more abundant anhedral pyrite lenses. The anhedral pyrite is cut by veinlets and fracture fillings of later chalcopyrite with bornite inclusions and calcite. The molybdenite appears to be late stage associated with sericite and spatially associated with the hematite replacement. Some of the hematite could be primary. The molybdenite is not associated with chalcopyrite and anhedral pyrite. Magnetite is only observed associated with chlorite development.”*

Of the 2795 drillcore samples collected and analyzed by BCM Resources during its drill programs, 327 were at or above 0.06% Mo (maximum value of 2.80%), 56 contained 0.1% Cu or greater (maximum value of 1.74%), 39 contained 0.1% or more Zn (maximum value of 2%), 5 contained 0.1% or more Pb (maximum value of 0.27%), and 26 contained >10 ppm Ag (high of 299 ppm). There is little correlation between any of these elements, although Pb, Zn and Ag mineralization generally tend to occur together. Copper does not correlate with Mo, and high Mo assay values commonly occur in areas of low Cu, and vice versa. As can be seen in Table 1, high Cu values are more likely to occur in samples with Mo mineralization, but Cu can be nearly as abundant in low-grade Mo samples as high-grade ones, which is reflected in a decrease of the Mo:Cu ratio

with increasing Mo grade. All mineralization appears to occur in the same general area, but the paragenesis is unclear, and the distribution of various elements may result from a number of factors. Notwithstanding this uncertainty, Mo is the most prevalent metal.

In 2008, a limited number of samples were assayed for Re content. Results indicate an average of 1 ppm Re for every 10 000 ppm Mo (i.e., sufficient to add economic value to the deposit). The Re content of the molybdenite is on the high end for Mo porphyry systems; in general, the higher the Re:Mo ratio, the more abundant the Cu (K. Krahulec, pers comm, 2008).

Anhydrite was observed in mineralized zones in several drillholes, and was initially misidentified as fluorite; three fluorine analyses were undertaken on previously submitted drill samples thought to contain fluorite and returned values of between 0.02 and 0.04% F. RioCanex reported values of up to nearly 0.5% F from their drillholes (Haynes and Knight, 1980).

### **Alteration**

The typical alteration in the Las Margaritas zone is a mix of sericitic and potassic (K-feldspar), with local argillic. Potassic alteration is common along fractures and, in some cases, may overprint sericitic alteration, which is more pervasive. The strongest mineralization is commonly associated with sericitic alteration with or without a potassic overprint. Marginal to zones of better mineralization, molybdenite occurs in fractures and veins with potassic selvages, or in quartz veins and fractures in relatively unaltered hostrocks. Potassic and sericitic alteration are also present in areas devoid of molybdenite, although they are not commonly found together except in mineralized areas. Volcanic and related high-level intrusive rocks are commonly propylitized, although potassic alteration along fractures and argillic alteration within fault zones have been noted. Some late mafic dikes are essentially unaltered. An effort was made to identify a pattern in the various styles of alteration but none was found.

### **PREVIOUS EXPLORATION**

First known as the Nicholson Creek and later as the Sak showings, quartz veins with pyrite and molybdenite were discovered south of Shannon Creek (formerly known as Nicholson Creek) prior to 1928. Exploration work completed by the Nicholson Creek Mining Company between 1934 and 1940 included an adit at an elevation of about 470 m, which was driven ~500 m in a south-southwesterly direction beneath a tributary of Shannon Creek known locally as Molybdenum Creek. The adit was excavated to explore for Au and Ag, which were not encountered, but Mo assays up to 0.42% were reported from small quartz veins (Kindle, 1937).

In the late 1960s, Kokanee Resources Ltd. blasted shallow trenches in the area of Shan South now referred to as the Camp zone, and subsequently completed 1650 m of diamond-drilling in 11 holes. This drilling program recovered small diameter (EX) core from shallowly inclined holes (N.C. Carter, pers comm, 2006). These holes encountered scattered Mo mineralization in all except one hole; modest intercepts in six holes included 50 m grading 0.065% Mo and 15 m grading 0.151% Mo.

**Table 1.** Comparison of Mo and Cu mineralization on the Shan South property.

Category	No. of Samples	Avg. Mo Grade (%)	Av Cu Grade (%)	Mo:Cu Ratio	High Cu Value (%)	Percentage of Samples >0.1% Cu	Correlation Coefficient Mo:Cu
0.1–2.8%	166	0.24	0.08	1:3	1.739	16	0.24
0.06–0.099%	161	0.07	0.035	1:2	0.596	4	0.02
0.01–0.059%	1253	0.02	0.02	1:1	0.794	1	0.15
<0.01%	1215	NA	NA	NA	0.363	1	NA

In 1971, New Gold Star Mines carried out soil sampling in the Shan South area, consisting of samples collected at 30 m intervals along lines spaced 125 m apart over 8.7 line-km of grid (Venkataramani, 1972). Soil samples were obtained using an auger and yielded up to 700 ppm Mo.

In 1975, International Shasta Resources Ltd completed a small program that included geological reconnaissance, stream sediment sampling and a fracture analysis study using aerial photos (Blanchet, 1975). Work was focused on the south side of the Shan South ridge, extending eastward nearly to the Skeena River. In addition to examining the Camp zone workings, the work identified two areas interpreted as having potential for Mo mineralization in granodiorite at shallow depth below relatively unmineralized volcanic rocks.

In 1979, Rio Tinto Canadian Exploration Ltd. (Riocanex) mapped and sampled Molybdenum Creek and its tributary, Calhoun Creek (unofficial name), and carried out 1:10 000 scale geological mapping over a broader area that included both the current Shan North and Shan South zones. A 60 line-km soil sampling survey was also completed over the mapped area and an experimental IP line was completed at Shan South (Haynes and Knight, 1980). The soil survey had a sample spacing of about 100 m along lines spaced 150 m apart over Shan South, and was a bit tighter over Shan North. This work was followed by 969 m of diamond-drilling in two inclined holes trending roughly east and west from the same collar on the north slope of the Shan South zone, immediately west of Molybdenum Creek. Reports indicate that the drillholes encountered narrow but occasionally high-grade intercepts of Mo mineralization. In 1980, Riocanex completed four additional IP lines around and to the north of the 1979 drillholes. The IP survey was hampered by steep terrain and, although it identified some anomalous areas, these were dismissed as having been tested by prior drillholes.

## EXPLORATION BY BCM RESOURCES CORP.

### Initial Work

BCM Resources Corp. commenced its exploration program with an aeromagnetic survey in November 2005, covering a 4.4 km<sup>2</sup> area about 2 km west and south of the Shan adit. The first fieldwork involved surface sampling and mapping on the Shan South ridge in the summer of 2006. Both the 1971 soil survey and the 1:10 000 scale geological and geochemical maps prepared by Riocanex in 1980 were used to identify potentially mineralized areas

that were subsequently located and examined. While it was apparent early on that there was a correlation between anomalous Mo values in the 1971 soil survey and underlying mineralization, detailed prospecting and stripping of moss to find small mineralized outcrops was required. The limited bedrock exposure rarely allowed a clear determination of vein attitude. A series of steeply dipping mineralized zones was inferred, however, and initial drillholes were located to test the intersection of two major structures.

Several conclusions were drawn from this fieldwork. First, the 1971 soil sampling, which was done using an auger, proved to be far more effective in locating mineralization than the 1979 survey done with a mattock, possibly because the auger could collect samples at a greater depth. The earlier survey yielded Mo values in the hundreds of parts per million in mineralized areas, whereas the 1979 survey returned values in the tens of parts per million. Second, the 1979 geological mapping identified mainly the relatively fresh and barren bedrock that resists erosion. Detailed prospecting guided by the 1971 soil survey was more effective at locating better mineralized areas, which are generally recessive due to associated alteration and differential weathering. This suggests that it is more effective to do follow-up mapping to check geochemical anomalies than to map simultaneously with geochemical sampling. Our observations in this regard also led to targeting the low-lying swampy areas on the ridge top that might mask significant mineralization. Third, it was recognized that the 'spurious' pyrite observed in some areas could produce an IP response unrelated to molybdenum mineralization. Fourth, the highest-grade Mo mineralization seemed to coincide with areas of low magnetic intensity adjacent to magnetic highs. It was hypothesized that the magnetic highs might represent a causative intrusion.

### Phase 1 and Phase 2 Drilling

Diamond-drilling began in the fall of 2006 (Figure 3). Initial holes intersected substantial mineralization and work continued until heavy snowfall ended the program in late November at a total of 20 holes (3496 m of BTW core). The new molybdenite zone, located 500 m west-northwest of the previously known Camp zone, was named 'Las Margaritas'. Thirteen holes contained significant molybdenite intercepts, most notably in drillholes 1, 3 and 7. However, some apparently good mineralization in surface outcrops was found not to extend to depth. Interpretation of the Las Margaritas zone was revised to include several steeply dipping mineralized structures or, alternatively, one gently dipping zone. Based on sparse surface data, a steep orientation for the mineralized zone was modelled to plan the next series of drillholes.

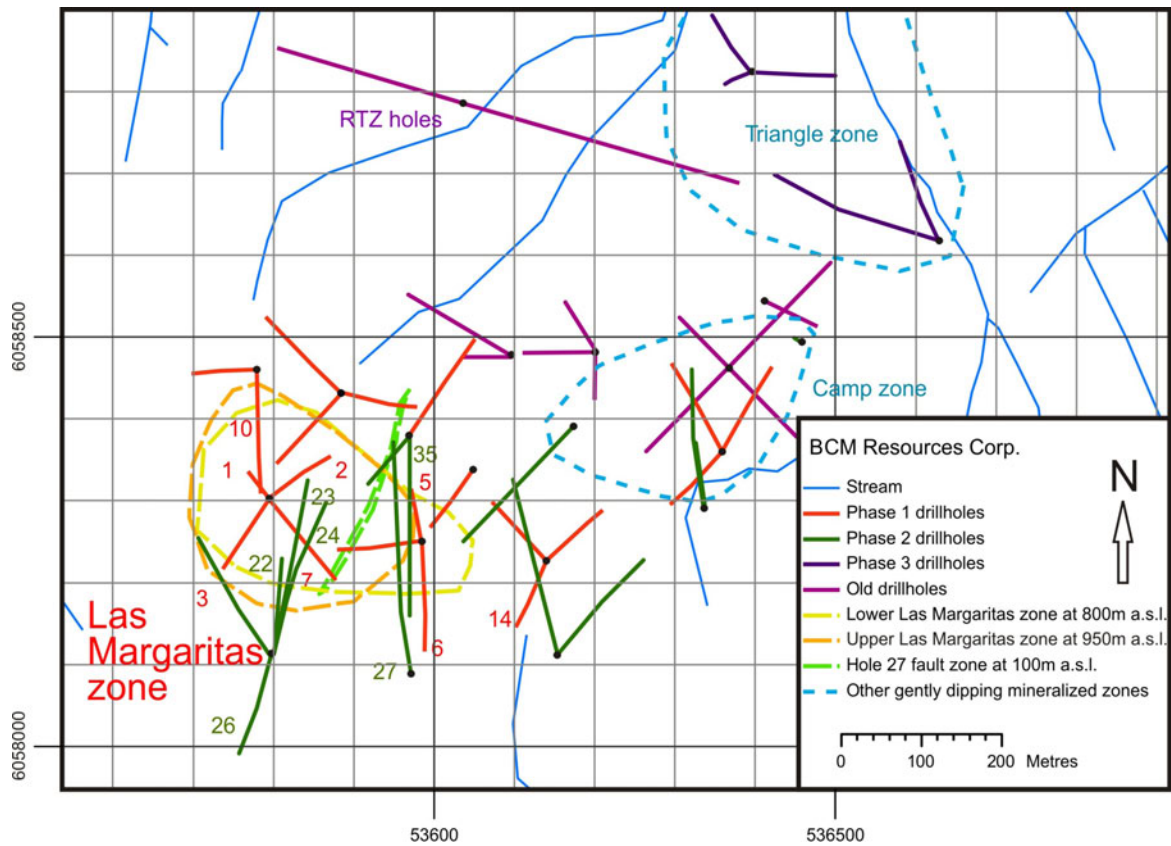


Figure 3. Locations of diamond-drill holes, Shan South property.

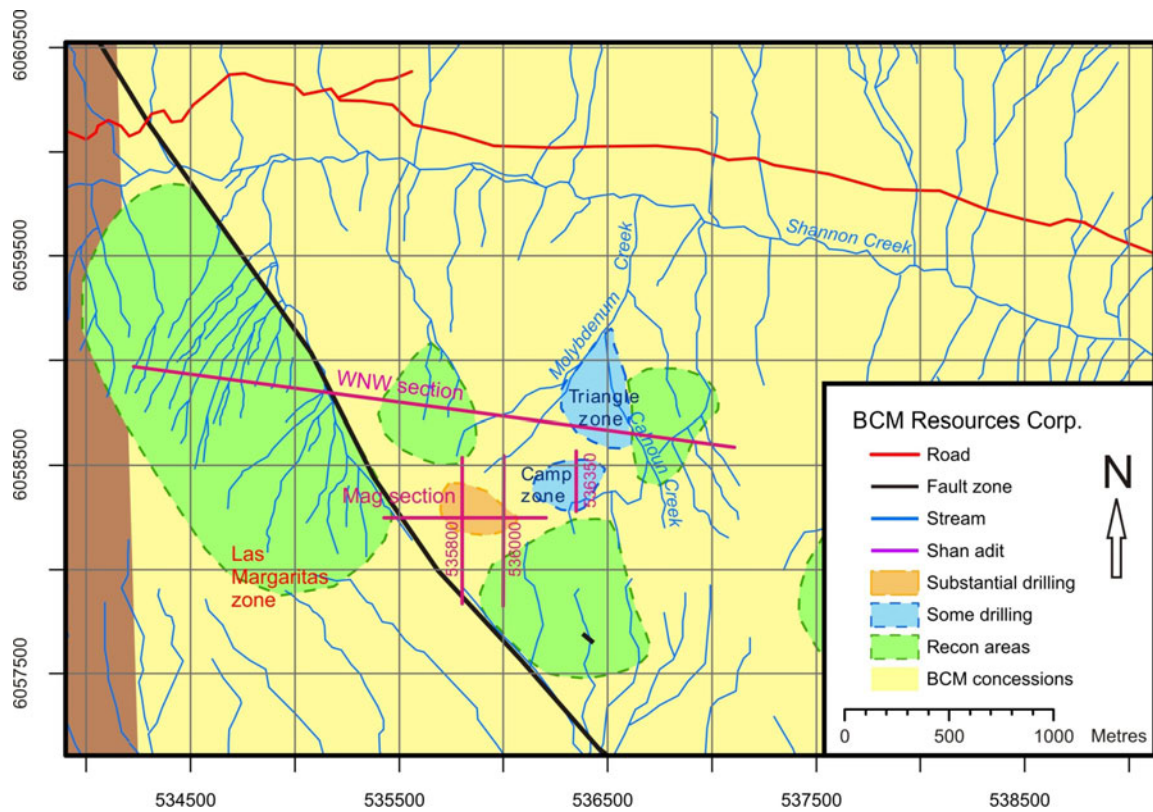
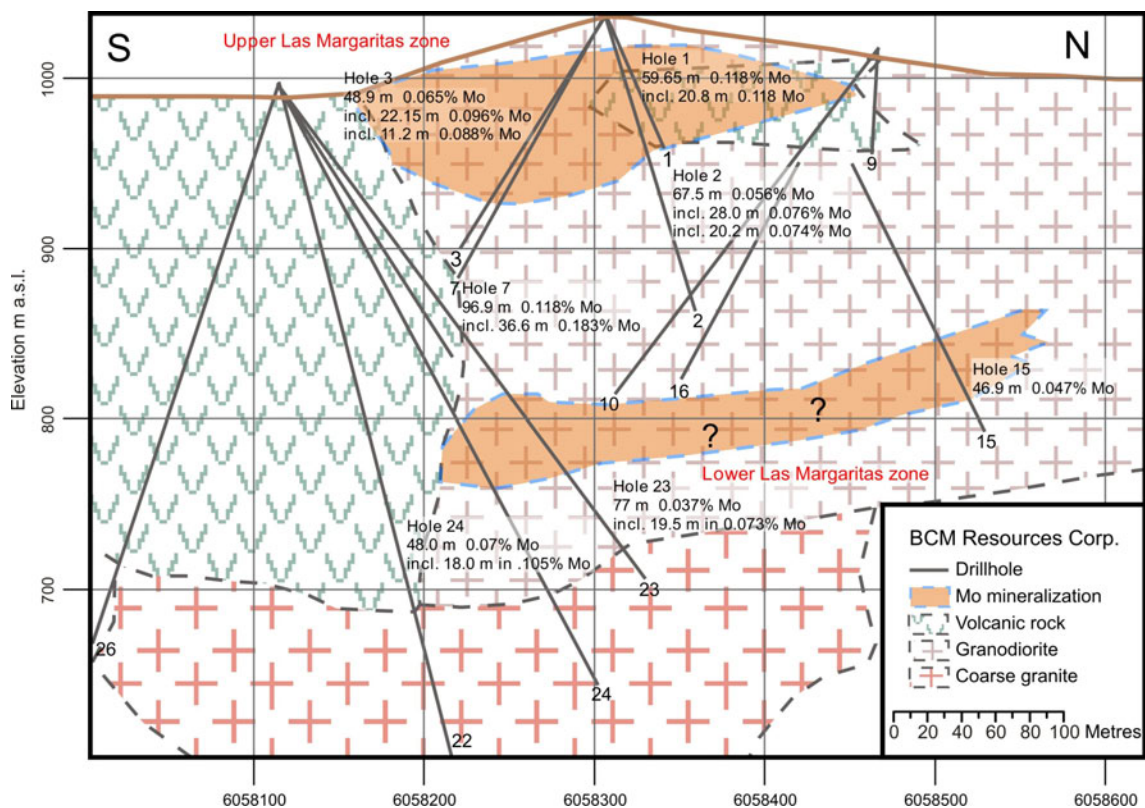


Figure 4. Locations of mineralized zones and sections, Shan South property.



**Figure 5.** Section 535800 E through the Upper and Lower Las Margaritas zones, Shan South property (see Figure 4 for location). Note that zones of Mo mineralization are zones with significant visible Mo mineralization that should be tested with additional drillholes, and include intercepts with 0.06% Mo cutoff, as quoted in press releases (BCM Resources Corp., 2007).

Phase 2 drilling, consisting of 5682 m of HQ drilling in 16 holes, was carried out in the spring of 2007. The first fan of holes was drilled under the best phase 1 intercepts, to intersect what was hypothesized to be the principal structure, striking east and dipping steeply south. Although mineralization was intercepted at depth, it did not match the pattern that was expected in a steeply south-dipping mineralized body; in fact, holes 23 and 24 appeared to have intersected a shallowly north-dipping mineralized zone (see Figures 4, 5). A secondary drill target was the edge of a magnetic high interpreted to correspond to the contact between the granodiorite and the volcanic hostrocks, where mineralization and stronger alteration were encountered in phase 1 drilling. One of these holes, hole 27, encountered strong mineralization and has the longest and most highly mineralized drill intercept to date, beginning in granodiorite near the contact with the volcanic hostrocks and remaining in mineralized and altered rock throughout most of its length (Figure 6). Quartz-molybdenite veins in the hole are subparallel and intersect drillcore at a smaller angle than predicted for a steeply south-dipping zone. Gently dipping mineralized zones are a likely alternative, a conclusion supported by gently dipping veining encountered in several vertical holes drilled as part of the phase 2 program. Granodiorite above and between these tabular zones is generally less altered and contains only sporadic mineralization. Surface mineralization in the Camp zone is thought to be the eroded remnant of a gently dipping mineralized zone like those at Las Margaritas (Figure 7).

A zone of mineralized fault gouge encountered at the end of hole 27 (referred to hereafter as the hole 27 FZ) was

not found in adjacent holes 36 and 37, which suggests that it might represent a steeply dipping structure; this could be a feeder zone (see Figure 3). Intervals of fault gouge, such as the one intersected at the end of hole 27 FZ, commonly contain Ag values ranging from 10 ppm to nearly 300 ppm, plus trace amounts of Pb and Zn. These are thought to be steeply dipping fault zones with multiple episodes of movement and mineralization. The current interpretation is that Mo was introduced along these conduits and spread out into a series of gently dipping fractures at shallow depth.

### Summer 2007

In the summer of 2007, additional mapping and sampling were completed at Shan South, including rock, soil and stream sediments; similar mapping and sampling were started on Shan North. A gently dipping zone of mineralization, found in Calhoun Creek 400 m northeast of the Camp zone, was determined to be associated with strongly anomalous soils identified in both the 1971 and 1979 soil surveys. This was named the Triangle zone and was tested by phase 3 drilling.

In addition, an aeromagnetic survey was flown in July 2007 with 100 m line spacing and a 100 m drape over the greater Shan area (136 km<sup>2</sup>). Subsequent 3-D modelling of the results of this survey was used to better define areas of magnetite destruction/alteration. The area of hole 27 FZ appeared as a magnetic low, and the two gently dipping zones now thought to form the Las Margaritas mineralized body also coincide with zones of low magnetic susceptibility

(Figure 8). A hand-held magnetic susceptibility meter gave readings of 0.01–0.02 SI units of magnetic susceptibility for unaltered intrusive rock, compared to less than 0.001 SI units for altered intrusive rock. It must be noted, however, that these low susceptibility zones are only permissive, and can be altered but not mineralized. The 3-D modelling also suggested a northwest-striking, steeply dipping fault zone immediately south of the Las Margaritas zone. Subsequent mapping encountered evidence of this fault in several drainages, and it was originally noted as a major structure in the 1975 airphoto interpretation work. Although the sense of movement along this fault is not known, faults of this orientation in the region commonly have right-lateral dis-

placements of hundreds of metres (J. Nelson, pers comm, 2008). The magnetic data for this area can be interpreted to show 800 m of fault displacement. Such an offset would displace potentially mineralized rocks originally located to the southwest of Las Margaritas. Mapping and sampling in summer 2008, however, found only weak alteration and mineralization in the hypothesized, displaced southwestern Las Margaritas block.

### Phase 3 Drilling

Phase 3 drilling in the fall of 2007 was limited and tested the Triangle zone on the north slope of Shan South

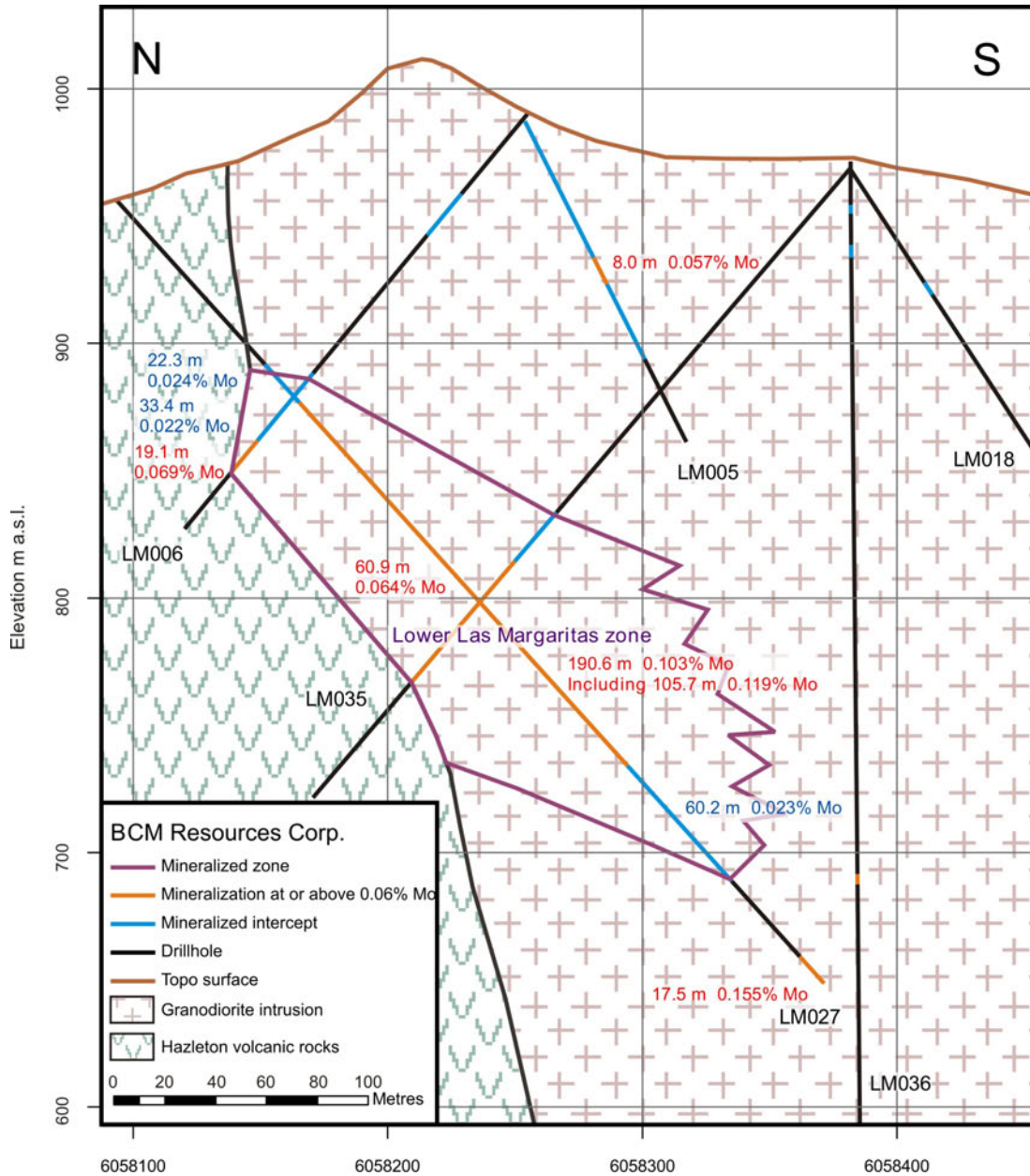


**Figure 6.** Section 536000 E through the Lower Las Margaritas zone, Shan South property (see Figure 4 for location). Note that zones of Mo mineralization are zones with significant visible Mo mineralization that should be tested with additional drillholes, and include intercepts with 0.06% Mo cutoff, as quoted in press releases (BCM Resources Corp., 2007).

and the Banana Lake corridor on Shan North. Holes in the Triangle zone were drilled beneath areas of good surface outcrop and intense Mo anomalies identified in both the 1971 and 1979 soil surveys, but encountered only scattered narrow zones of mineralization (generally <1 m). It was concluded that the mineralized zone dipped moderately north rather than being horizontal, as first thought, and that the holes drilled were entirely in the footwall of the mineralized zone. The zone may extend beneath volcanic cover east of Calhoun Creek and west of Molybdenum Creek (Figure 9).

### Summer 2008

Additional mapping and sampling in the summer of 2008 identified five potential satellite zones of mineralization largely concealed beneath the less favourable volcanic

strata (see Figure 4). The principal technique was soil sampling and moss-mat sampling in streams to detect zones of leakage through the volcanic strata, plus prospecting and sampling in stream drainages, which commonly form along fault and fracture zones. Moss-mat samples were collected because most streams contained little or no sediment suitable for sieved samples. Two satellite zones lie in the area covered by the 1975 reconnaissance work (Blanchet, 1975), and roughly coincide with the previously identified areas of high fracture density and anomalous stream-sediment geochemistry.

### ECONOMIC POTENTIAL

Each of the two mineralized zones at Las Margaritas is about 350 m by 200 m in area and about 60 m thick, which represents between 10 and 12 million tonnes of Mo-miner-

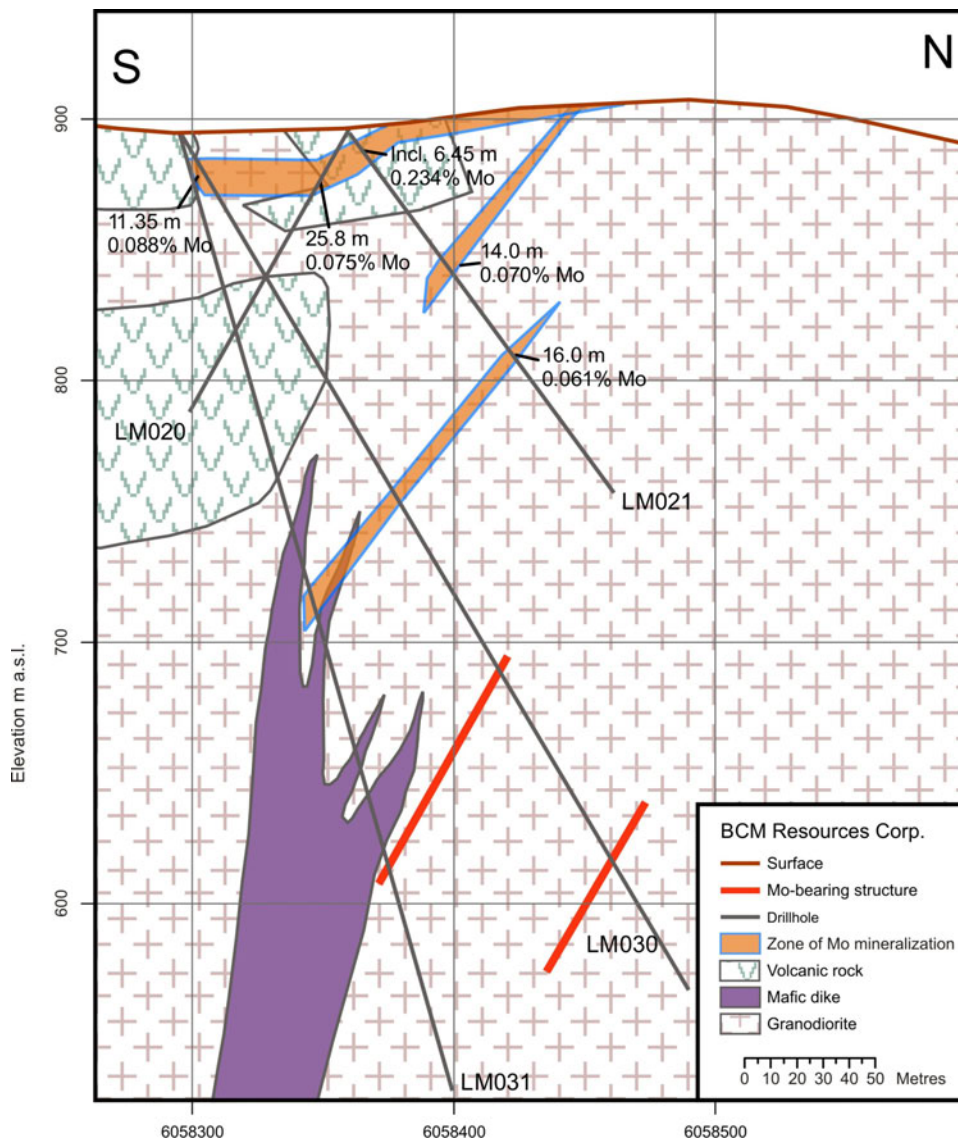


**Figure 7.** Section 536350 E, Shan South property (see Figure 4 for location). Note that zones of Mo mineralization are zones with significant visible Mo mineralization that should be tested with additional drillholes, and include intercepts with 0.06% Mo cutoff, as quoted in press releases (BCM Resources Corp., 2007).

alized rock in each. The upper zone is open to the west and the lower zone is open to the east. Average grades may be ~0.1% Mo throughout most of these two zones, although this is largely speculative and more drilling is required to delineate the mineralization. Additional zones may be present beneath volcanic cover and overburden, and exploration is ongoing.

## DISCUSSION AND CONCLUSIONS

The understanding of the Las Margaritas mineralized zone and the exploration for similar satellite zones is a work in progress. Both the exploration techniques used to date and the model for the Mo mineralization are evolving with each stage of exploration. It now appears that the bulk of

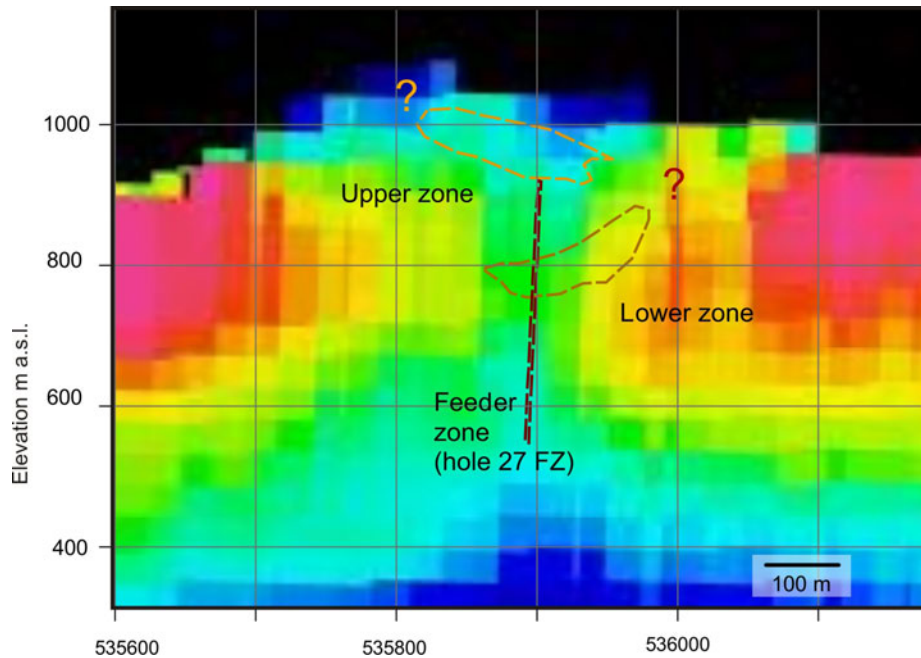


**Figure 8.** Magnetic susceptibility section (6058250 N) through the Las Margaritas zone, Shan South property (see Figure 4 for location).

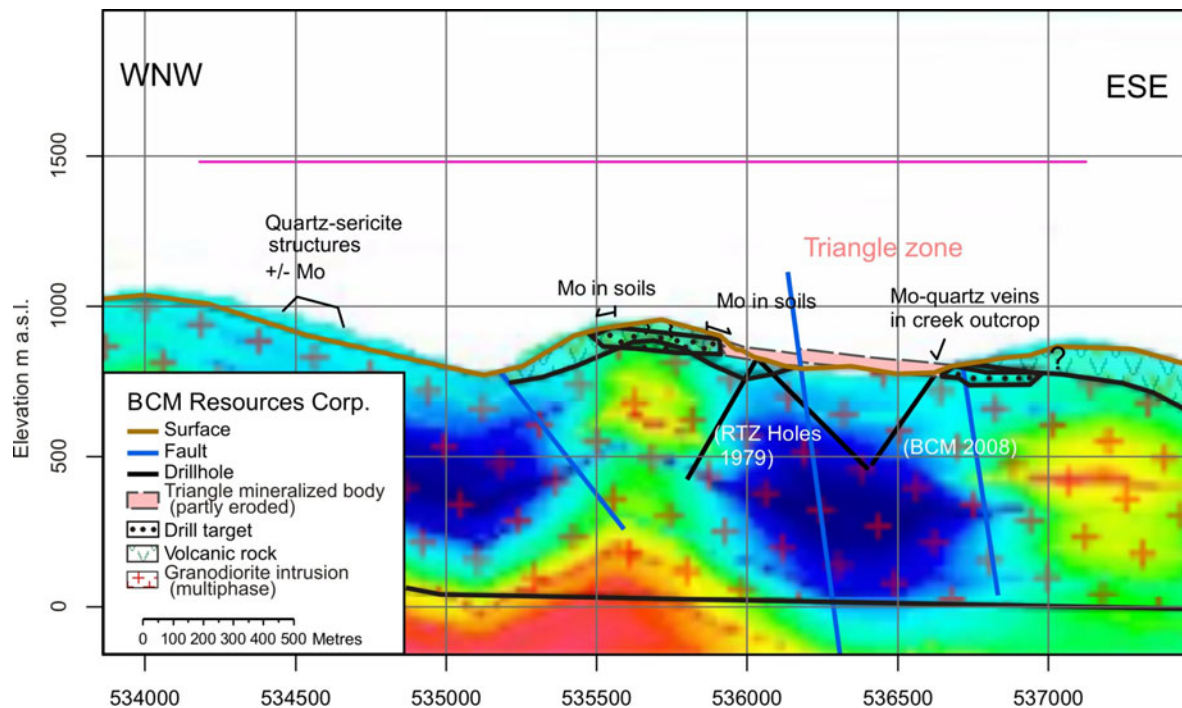


**Figure 9.** West-northwest-trending section through the Triangle zone superimposed on aeromagnetic modelling results, Shan South property (see Figure 4 for location).

mineralization is found in gently dipping tabular zones in the upper part of the granodiorite intrusive, and is associated with steep feeder zones along faults that underwent multiple episodes of movement and mineralization. There are at least three such zones and the possibility of several more.

Soil sampling has been an effective exploration technique, particularly if an auger is used for sample collection at 25–30 m intervals along lines spaced no more than 100 m apart. Detailed geological mapping can then be focused in areas of anomalous Mo values in soil to find alteration and mineralization.

Moss-mat results indicate that the technique may be highly effective for detecting mineralization beneath the less favourable volcanic cover. In the area of the hypothesized western extension of the Triangle zone (Figures 4, 9), moss-mat samples returned strongly anomalous Mo values (up to 658 ppm) in areas of weak to negligible soil anomalies. It is believed that this represents Mo brought up by circulating groundwater from mineralization at depth along structures responsible for the localization of the streams. Background values for samples from structurally controlled streams away from mineralization are less than 10 ppm Mo.

When drilling, it is advisable to drill at least one vertical hole in a strategic location fairly early on to gain a better understanding of the dip of mineralized structures; alternatively, techniques for recovering oriented drillcore might be used.

Molybdenum mineralization at Shan occurs in subhorizontal tabular zones near the roof of the Carpenter Lake granodiorite batholith. Location of the Mo zones is governed by a steep north-northeast-striking fault from which mineralizing fluids are interpreted to have spread laterally into gently dipping fractures, possibly developed in the case of the lower Las Margaritas zone near a subhorizontal contact between an upper medium-grained and lower coarse-grained phase of the pluton.

Although Cu is locally present, Shan belongs clearly to the stockwork Mo group of deposits; it is not a porphyry Cu-Mo deposit. Copper and molybdenum minerals have a different paragenesis and distribution and do not correlate. Rhenium content is comparable to stockwork Mo deposits

and below the range commonly found in porphyry Cu-Mo deposits.

An ongoing study of stockwork Mo deposits in north-western BC by the second author shows a clear separation into two groups. Shan is comparable to the Endako, Storie and Ruby Creek deposits. Molybdenite occurs in a subhorizontal zone near the margin or top of a batholith, commonly near a phase boundary that is characterized by a change in grain size rather than composition. A subvertical feeder zone may be present but is not (as yet) an economic component of the ore zone. Batholith-associated systems are passive (brecciation is rarely evident) and the amount of introduced quartz is low.

## REFERENCES

- BCM Resources Corp. (2007): Shan drill results: 112.7 m of 0.107% molybdenum; *BCM Resources Corp.*, press release, January 5, 2007, URL <[http://www.bcmresources.com/s/NewsReleases.asp?ReportID=165285&Type=NewsReleases&\\_Title=Shan-Drill-Results-112.7m-of-0.107-Molybdenum](http://www.bcmresources.com/s/NewsReleases.asp?ReportID=165285&Type=NewsReleases&_Title=Shan-Drill-Results-112.7m-of-0.107-Molybdenum)> [December 2008].
- Blanchet, P.H. (1975): Geological, geochemical and photogeological progress report on the Paula group in the Usk-Terrace area, BC; unpublished company report, *International Shasta Resources Ltd.*, 11 pages.
- Haynes, L. and Knight, D. (1980): Sak and Shan claims: geochemistry, geology, geophysics, and diamond drilling; *BC Ministry of Energy, Mines and Petroleum Resources*, Assessment Report 7932, 26 pages.
- Kindle, E.A. (1937): Mineral resources of Terrace area, coastal district, British Columbia; *Geological Survey of Canada*, Memoir 205, pages 53–56.
- Nelson, J.L., Barresi, T., Knight, E. and Boudreau, N. (2006): Geology and mineral potential of the Usk map area (1031/09) near Terrace, British Columbia; in *Geological Fieldwork 2005*, *BC Ministry of Energy, Mines and Petroleum Resources*, Paper 2006-1, pages 117–134.
- Vancouver GeoTech Labs (2006): Petrographic report, Shan molybdenum deposit (?), 20 km northeast of Terrace, BC; unpublished report prepared by Vancouver GeoTech Labs for *BCM Resources Corp.*, 5 pages.
- Venkataramani, S. (1972): Report on the “J” group of claims, Omineca Mining Division, British Columbia; unpublished company report, *New Gold Star Mines Ltd.*, 6 pages.

# Atlin-Taku Mineral Resource Assessment, Northwestern British Columbia (Parts of NTS 104F, J, K, L, M, N): Methodology and Results

by D.G. MacIntyre<sup>1</sup> and W.E. Kilby<sup>2</sup>

**KEYWORDS:** Atlin-Taku, mineral resource assessment, methodology, results, Mark 3B simulator, ordinal ranking, expert workshops, sub-tracts

## INTRODUCTION

The wise use of renewable and nonrenewable resources is an important issue for British Columbians. Government agencies and other groups in the province are committed to land-use processes that lead to the best possible decisions.

A common element in planning the administration of the land surface—or base—is to collect information that summarizes current and potential uses of an area under consideration for a change of use. This information should encompass all measures of value of the land, such as cultural, economic, environmental or wildlife. British Columbia has a well-established procedure for land-use assessment, which includes mineral potential assessment to consider both known and potential subsurface mineral resources. The province-wide **Level 1 Mineral Resource Assessment (MRA1)** was completed in the 1990s by the British Columbia Geological Survey (BCGS) of the Ministry of Energy, Mines and Petroleum Resources. Several additional regional assessments, such as North Coast, Central Coast and Lillooet, have been undertaken since then (MacIntyre et al., 2003). These **Level 2 Mineral Resource Assessments (MRA2)** generally involved subdivision of existing tracts and redistribution of the Level 1 values to these new tracts or, in the case of Atlin-Taku, new assessments. The methodologies employed in the Level 1 and 2 assessments were described by MacIntyre et al. (2003).

The BCGS was asked by the Integrated Land Management Bureau of the Ministry of Agriculture and Lands to undertake a Level 2 Mineral Resource Assessment of the Atlin-Taku land-use planning area, which encompasses approximately 4 million hectares in northwestern BC (Figure 2). The primary purpose was to provide detailed up-to-date information on metallic and industrial mineral resource potential. Resource assessment was carried out by BCGS professionals and contractors in September 2008. Final results will be presented at a land-use planning workshop in late November 2008. This report summarizes the



**Figure 1.** Experts discussing the mineral resource potential of a tract in the Atlin-Taku study area.

methodology used in the assessment and provides an initial review of the results, which are also available on the BCGS MapPlace website (<http://www.mapplace.ca>).

## MINERAL POTENTIAL PROJECT

Early in 1992, the BCGS launched the Mineral Potential Project (Kilby, 1992; Kilby, 1996). Its purpose was to provide mineral potential information to the Commission on Resources and the Environment (CORE). The BCGS dedicated significant staff resources to the project, which resulted in the MRA1.

The first task of the Mineral Potential Project was to determine what information was needed in land-use negotiations and then develop a methodology to produce this information. A two-day workshop of participants with experience in producing and using a Mineral Resource Assessment (MRA) determined that MRA products must be quantitative rather than qualitative, provide a ranking of the land base, have expert input from the mining and exploration industries, be compatible with a geographic information system (GIS) and be available on the Web.

Quantitative, easily understood results were necessary because the Land Resource Management Plan (LRMP) process includes users with nontechnical backgrounds in the decision-making process; quantitative information is a preferred tool in socioeconomic analysis. Ranking of the land base was necessary because the new provincial Protected Areas Strategy required a protection target of 12% of the land area in every region, double the previous level. A major objective of the Mineral Potential Project was therefore to rank the relative mineral potential so that planners

<sup>1</sup> D.G. MacIntyre and Associates Ltd., Victoria, BC,  
Don.Macintyre@shaw.ca

<sup>2</sup> CalData Ltd., Kelowna, BC

This publication is also available, free of charge, as colour digital files in Adobe Acrobat® PDF format from the BC Ministry of Energy, Mines and Petroleum Resources website at <http://www.empr.gov.bc.ca/Mining/Geoscience/PublicationsCatalogue/Fieldwork/Pages/default.aspx>.

could identify areas with the lowest relative mineral potential.

The mining and exploration industries in BC have built an enormous knowledge base that is not public. Industry co-operation gave the BCGS access to some of this knowledge and allowed familiarization of the public-sector stakeholders with the strengths and limitations of MRAs. The provincial government required that all information for land-use planning be in GIS-compatible digital format. This ensured that information could be easily incorporated into the systems used by planners. In addition, storage in digital format provides for easy upgrades in the future. All data and map products referred to in this report are available through the MapPlace website.

## MINERAL RESOURCE ASSESSMENT METHODOLOGY

### Deposit Models

Descriptive models were developed as part of the Level 1 MRA for mineral deposits known and believed to exist in BC. This built on the work by the United States Geological Survey and others (Cox and Singer, 1986), and updated the models and refined the list of characteristics expected in BC deposits. Along with the descriptive models, a classification framework was established in which deposit types were ordered according to their genetic characteristics (Lefebure and Ray, 1995; Lefebure et al., 1995; Lefebure and Höy, 1996; Simandl et al., 1999).

Descriptive deposit models are essential to mineral resource assessment. They provide the standardization required to understand a given deposit type, with examples. The deposit descriptions identify geological, geochemical, geophysical, alteration and weathering features.

### Geology Compilation

Mineral resource assessments rely on accurate, up-to-date geological information about the distribution of mineral resources in the Earth's crust. A major task during the 1990s was for the BCGS to compile the geology of the province at a scale of 1:250 000 (Kilby, 1994, 1995). All available information was compiled and digitized to form the final map product. More than 30 person-years were dedicated to the project. Compilations were produced in GIS digital format and are available over the Internet (<http://www.mapplace.ca>). The BCGS ensures that new geology from its field programs and other sources is updated for future mineral resource assessments.

### Mineral Resource Assessment Tracts

Upon completion of the compilation, the area of the province was divided into mineral assessment tracts. These are based on common geological features; their boundaries correspond to existing geological contacts, such as faults or intrusive contacts. Tracts become the base unit areas for the assessments. The Level 1 Mineral Resource Assessment

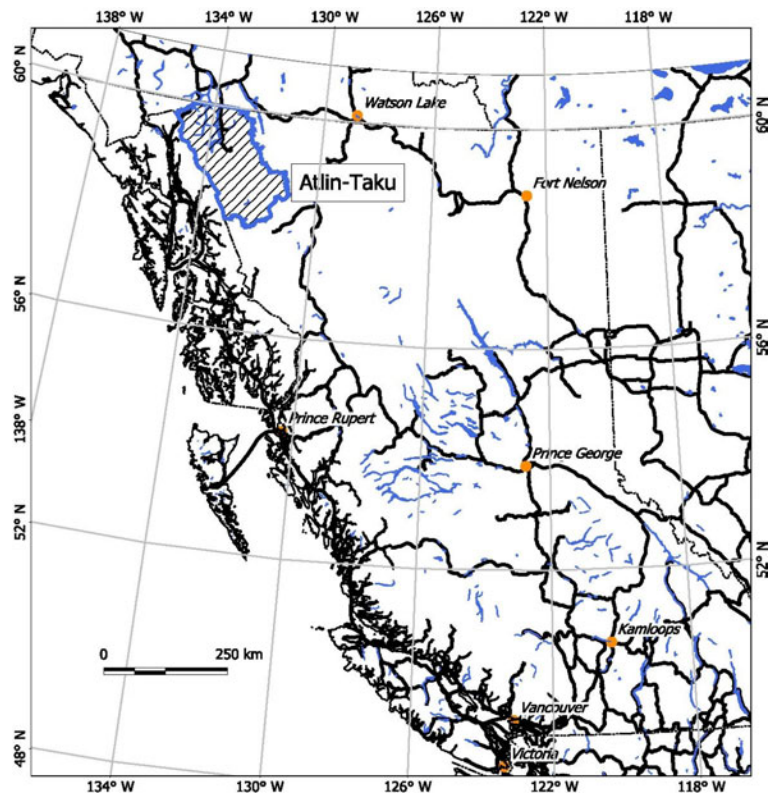


Figure 2. Location of the Atlin-Taku land-use planning area.

defined 794 tracts across the province. The size of tracts varies but they are intended for consideration at a regional scale (e.g., 1:250 000). The average size of tracts in the MRA1 assessment is about 100 000 ha. For each tract, permissible deposit types were determined and an estimate for the probability of their existence was made independently by several geologists.

### Mineral Resource Estimation Process

Staff of the BCGS developed a Mineral Development Assessment process based on the United States Geological Survey's *Three Part Mineral Assessment Methodology* (Brew, 1992; Cox, 1993). The methodology used for Atlin-Taku was generally the same as earlier assessments, with minor differences that are described in this report. The Atlin-Taku assessment followed the Level 2 methodology described in MacIntyre et al. (2003). This methodology has been used since 2003 for area-specific assessments, such as the North Coast, Central Coast and Lillooet Land Resource Management Plan (LRMP) areas.

A six-step process is used for metallic mineral resource assessments:

- 1) compile geology
- 2) select mineral assessment tracts
- 3) tabulate discovered resources and construct deposit models
- 4) use a team of industry and government geological experts to estimate the number of undiscovered deposits by deposit type and tract
- 5) estimate quantities of metallic commodities remaining to be discovered using the Mark3B resource simula-

tion computer program developed by the United States Geological Survey (Root et al., 1992)

- 6) estimate the in-place value of each tract based on the undiscovered and known commodities it contains

For industrial mineral assessments, the first four steps are the same. However, due to their higher dependence than metallic minerals on low-cost infrastructure and access to markets, a relative ranking of industrial mineral deposit types was employed. Industrial mineral deposit types are given a relative ranking score from 1 to 100 based on their value and viability. This relative deposit value score is used to determine the importance of each tract with respect to undiscovered deposits. The estimates are then blended with the value of discovered industrial mineral deposits to produce the overall industrial mineral tract assessment ranking.

### **Deposit Model Data Preparation**

The two inputs required for the computer simulation are

- the estimates of the potential for new discoveries; and
- the digital deposit models describing the grade and tonnage distribution of each deposit type.

The digital deposit model contains a list of realistic deposit grades and tonnages for the model types that might be found in the area being assessed (Grunsky, 1995).

### **Known Mineral Resources**

In the Level 1 Mineral Resource Assessment, the final resource assessment value for each tract incorporated both the known and yet-to-be-discovered resources. For Level 2 assessments, such as Atlin-Taku, known resources were presented as a separate data layer and not used to rank tracts for their undiscovered resources potential.

### **Commodity Values**

A dollar value was established for each commodity to allow the calculation of gross in-place values for each tract. In the Level 1 Mineral Resource Assessment, the dollar value used for each commodity was the average market value of that commodity for the 10-year period from 1981 to 1990. The dollar values used for the Level 2 Atlin-Taku Mineral Resource Assessment described in this report are based on September 2008 commodity prices.

### **Estimation Workshops**

For all mineral resource assessments, government and industry experts are invited to workshops to contribute their knowledge of the area being assessed, based on their familiarity with specific deposit types.

Geological data form the basis of all discussions during the expert workshops. At the workshops, this basic information was provided both as paper maps at various scales and as online access to the MapPlace website. Other spatial geoscience datasets, such as geochemistry, mineral occurrences and tract outlines, were superimposed on the geology as overlays or plotted directly on the printed maps. For some datasets, such as geophysical information, it proved to be more important to have the supporting information available in its original format.

In addition to the information presented in map format, a compendium of the following information was provided to each group of estimators:

- descriptive deposit models
- graphs of the digital deposit models
- a list of deposit types with their median tonnages and grades
- a map displaying all tracts in the study area
- a list of tracts and their areas
- a list of resource-bearing deposits by tract
- a list of all MINFILE occurrences by tract with information on deposit type
- a tracking sheet for the group facilitator to log estimates made
- the PC-based MINFILE/pc database system

Six estimators participated in the Atlin-Taku expert estimation workshop—four from industry and two from government. This allowed the creation of two groups of experts, with each group doing estimates for specific deposit types on a tract-by-tract basis. All of these individuals had extensive knowledge of the Atlin-Taku area through years of exploration and geological mapping work in the area. This provided the basis for estimating the number of undiscovered deposits of each deposit type.

The Atlin-Taku assessment followed the methodology used in other land-use studies, such as those for Lillooet and Central Coast. When reviewing the results of the assessment, the user needs to remember the following points:

- The assessment only considered tracts that were within or intersected the Atlin-Taku boundary. Even if only a small part of the tract was actually within the study area, estimates were made for the entire tract, not just the area within the boundary.

- The per-hectare values used to rank the tracts were based on the entire tract, not just that portion within the Atlin-Taku boundary.

- The resource assessment ranked tracts according to their potential for the discovery of new resources. The assessment did not consider economic viability of these resources.

### **Tract Ranking**

Final ranking of tracts for both the metallic and industrial minerals assessment were performed in the same way once the valued estimation information was merged with the area information. In the calculations, each tract was ranked using each of the six confidence interval values, and then the six rankings were weighted according to probability and combined to produce the final rank value. This was done to isolate the estimates at the various confidence levels so they would not bias the final ranking score. This practice prevents a high ranking at a low confidence level from overshadowing a lower ranking with a high confidence level.

For each of the variables (confidence interval levels), the tract was assigned a rank based on that variable normalized for the size of the tract (its area). The rank numbers ranged from 1, for the lowest ranking, to the total number of tracts for the highest ranked tract for that variable. In the case of Atlin-Taku, 67 tracts formed the assessment, so 67 was the highest ranking. The rank numbers for each variable were then weighted by their confidence value and summed to give a total score for each tract. For the final

ranking, scores for each of the tracts were sorted from lowest to highest and assigned ordinal numbers from 1 to the total number of tracts, to give the final ranking.

The weightings assigned to the variables were 0.9 for the 90% confidence value, 0.5 for 50%, 0.1 for 10%, 0.05 for 5% and 0.01 for 1%.

## ATLIN-TAKU MINERAL RESOURCE ASSESSMENT RESULTS

A new mineral resource assessment of the Atlin-Taku land-use planning area was initiated in September 2008, under a contract awarded to D.G. MacIntyre and Associates Ltd. Prior to the expert workshops, tract boundaries from the previous assessment were adjusted to reflect new geological knowledge. Some larger tracts were subdivided to make assessment more manageable and to better reflect the distribution of known mineral resources; these were CCPJ, CCPJ2, STTR3, STTR4 and OLLJ1 (Table 1).

### Metallic Mineral Assessment

A metallic minerals expert workshop was convened at Smithers on September 11. This workshop involved six experts with specific knowledge of the geology and mineral resources of the study area and two facilitators, D. MacIntyre and W. Kilby. P. Desjardins of the BCGS assisted with organizing the workshops. It was not possible to complete a new assessment in the time allotted for the Smithers meeting, so a follow-up meeting was convened in Victoria on September 17

**Table 1.** Metallic mineral deposit types considered to be present in the Atlin-Taku land-use planning area.

Model Code	Model Name
C1	Placer Au
E4	Carbonate-hosted Au (Carlin type)
E7	Sandstone-hosted Pb-Zn
EC	Eskay Creek-type
H2	Sandstone/sedex Pb-Zn
H4-6	VMS merged
I	Epithermal Au-Ag veins
I4	Hot springs Au-Ag veins
J2	Stibnite veins and disseminations (combined)
J4	Gold-quartz / greenstone Au / turbidite-hosted Au veins
J5	Iron formation Au
K5	Polymetallic vein
M2	Replacement
N1	Cu skarn
N3	Zn-Pb skarn
N4	Fe skarn
N5	Au skarn
N6	W skarn
N7	Sn skarn
N8	Mo skarn
NICK	Serpentinite Ni
O1	Epithermal quartz-alunite Au
O2	Cu-Mo-Au porphyry
O4	Alkalic Cu-Au porphyry
O5	Intrusion-related Au
O8	Mo porphyry
O11	W porphyry
P3	Podiform chromite
P5	Alaskan PGE

At the workshops, estimators were asked initially to review a table of median grade and tonnage for a range of metallic deposit models. When estimating the number of undiscovered deposits, they were asked to use these median values for a typical deposit. A list of metallic deposit models is given in Table 1.

During the estimation process, experts had access to all available geophysical, geochemical and geological data. Online access to MINFILE and assessment reports by exploration companies was also made available. Each group reviewed the geology and mineral resource endowment of the study area on a tract-by-tract basis, providing estimates for the number of undiscovered deposits for each deposit model at confidence levels between 1 and 100%. Individual estimates included confidence ratings from other people at the assessment table. These ratings were used to weight the final combined estimate of undiscovered deposits of each deposit type.

The predicted number of undiscovered deposits was recast to the 90, 50, 10, 5 and 1% confidence levels. This provided input for the Mark3B resource simulation program developed by the United States Geological Survey (Root et al., 1992). Output from the program is in the form of predicted tonnes of metal at the 90, 50, 10, 5 and 1% confidence levels for each deposit type. The probability analysis is based on grade and tonnage data from BC deposits and, where appropriate, deposits elsewhere in the world.

**Table 2.** Metallic mineral potential tract rankings. Tract IDs with -1 and -2 extensions have been subdivided.

Rank	Tract ID	Area (ha)	Rank	Tract ID	Area (ha)
1	YTPZ4	17,141	35	STTR17	16,277
2	OIMJ3	72,260	36	OVPT1	5,140
3	OVN3	253,752	37	OLV1	30,422
4	OVEE1	50,205	38	STTR18	33,475
5	CCPZ5	24,048	39	CCPZ8	53,487
6	OIMJ2	10,391	40	CPPJ2-2	86,003
7	OVN2	24,850	41	STTR19	27,701
8	OVN5	7,999	42	STRPZ4	105,377
9	OSLJ1	115,680	43	STTR3-1	196,788
10	OVE3	28,792	44	OSJ2	19,494
11	CCPZ2	143,780	45	OIET2	120,458
12	OL1	31,096	46	STTR4-1	13,449
13	OSTR1	6,836	47	YTPZ6	9,691
14	CPPZ7	51,932	48	YTPZ5	51,222
15	OIK1	58,367	49	OIK2	70,141
16	CCPJ-2	116,686	50	STPZ11	46,298
17	OVE2	33,027	51	CCPZ9	66,911
18	OSLJ2	131,578	52	STPZ12	16,013
19	OIE3	29,833	53	STTR1	59,810
20	CPPZ1	90,667	54	YTPR1	61,579
21	STTR4-2	66,904	55	OS1	6,454
22	OSMZ1	53,413	56	STTR15	42,883
23	OIEK3	27,312	57	OLLJ1-1	74,076
24	CCPZ11	43,525	58	OIE5	10,601
25	OIMJ1	112,560	59	STTR16	23,464
26	OIE2	48,987	60	CCPJ-1	62,771
27	OIK3	51,890	61	SPTZ13	35,861
28	CCPZ4	63,993	62	OSJ1	31,191
29	CCPZ1	431,408	63	YTPZ2	48,163
30	OLLJ1-2	71,344	64	YTPR3	19,944
31	YTPZ7	13,855	65	CPPJ2-1	86,050
32	CCPZ10	40,656	66	STTR14	72,173
33	OIJE1	136,163	67	OIE4	4,653
34	OIKT1	20,460			

The predicted tonnages at the five different confidence levels were then given values using current commodity prices and totalled.

The tract value at the five confidence levels was then converted to a dollar value per hectare by dividing the predicted value of undiscovered resources by the tract area in hectares. The per-hectare values were used to rank the

tracts from 1 (lowest) to 67 (highest) at the 90, 50, 10, 5 and 1% confidence levels. These rankings were weighted using the confidence level. This score was used to produce the final ranking (Table 2). This methodology was the same as in previous assessments. Tract rankings were divided into five groups on the basis of each group representing 20% of the total area (Figure 3). This was also consistent with previous assessments. The location of known resources is

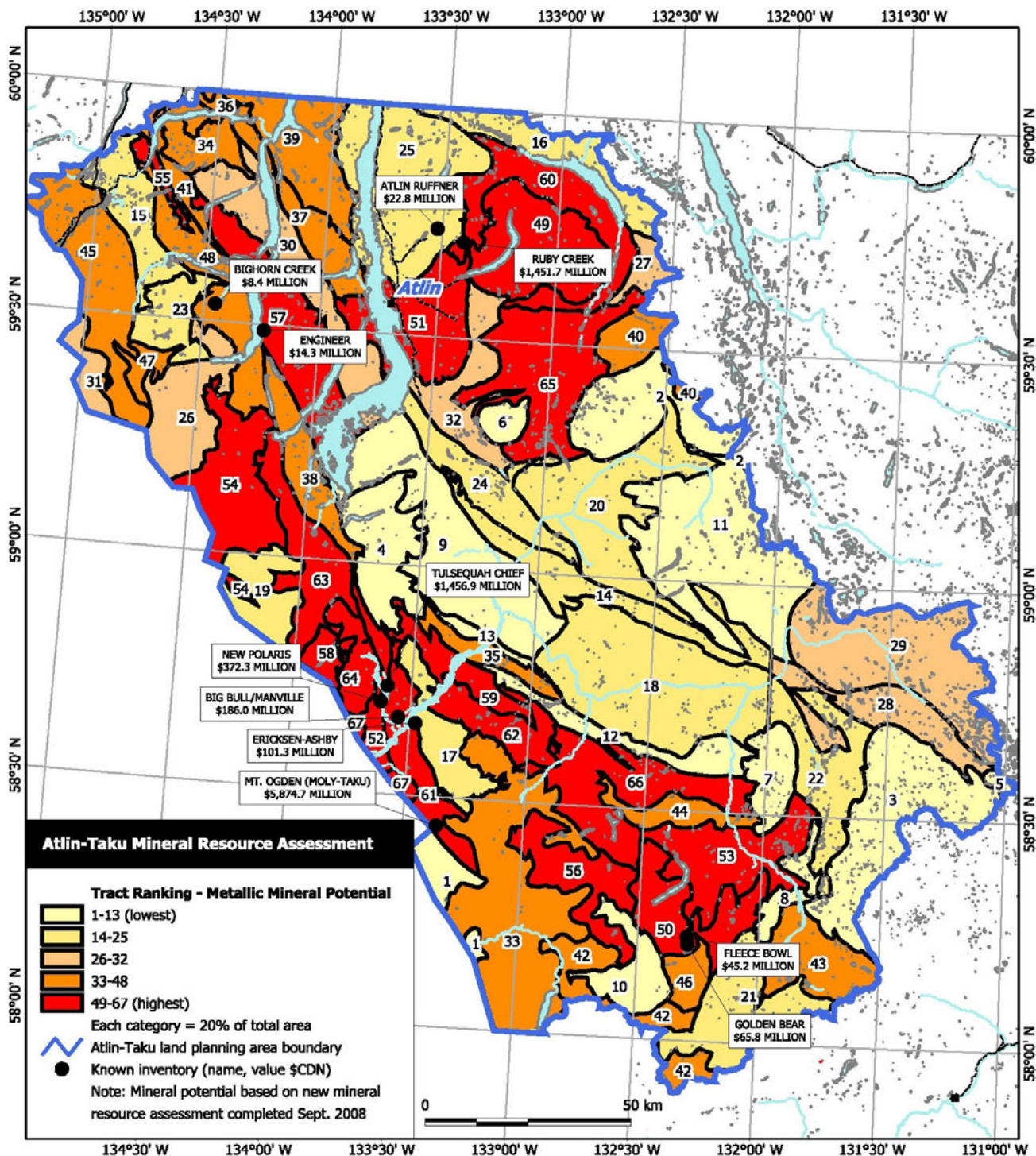


Figure 3. Metallic mineral potential and location of known resources in the Atlin-Taku land-use planning area See Table 2 for list of tracts and their ranking. Note that tracts included in the assessment have been clipped at the study area boundary for presentation clarity.

Table 3. Known metallic mineral inventory, Atlin-Taku land-use planning area.

MINFILE No.	UTM		Name	Commodities	Tonnes	Value (Million C\$)	Year	Comment	Reference
	Easting	Northing							
104K 002	580980	6511483	Tulsequah Chief	Zn Cu Pb Ag Au	7,910,000	\$1,456.92	2006	An initial mineable reserve, which is part of the overall geological reserve of 8.9 million tonnes	Schroeter (1998)
104K 003	579630	6507525	New Polaris	Au	1,670,000	\$372.32	2007	Combined measured and Indicated reserves, based on 2 g/t cut-off grade	Schroeter et al. (2007)
104K 009	588477	6502983	Ericksen-Ashby	Ag Pb Zn	907,100	\$101.27	1964	Year of reserves is questionable	MINFILE 104K 009
104K 013	595697	6478679	Mt Ogden (Moly-Taku)	Mo	217,704,000	\$5,874.65	1981	Grade given was 0.3% MoS <sub>2</sub> ; conversion to Mo using the factor 1.6681	MINFILE 104K 013
104K 079	659005	6455376	Golden Bear (Grizzly)	Au	152,900	\$65.80	1999	Combined resource	MINFILE 104K 013
104K 087	658767	6457224	Fleece Bowl (Kodiak C)	Au	276,000	\$45.19	1999	Combined resource	MINFILE 104K 013
104M 006	530995	6600002	Bighorn Creek (Lawson)	Au	69,000	\$8.44	1991	Rough estimate.	Baldys (1991)
104M 014	543328	6594556	Engineer (Total)	Au	20,000	\$14.28	1993	Estimated reserves	Schroeter (1994)
104N 011	583110	6622918	Atlin Ruffner	Ag Pb	113,638	\$22.76	1988	Reserves from the two zones from which underground development and production have taken place	Mclvor (1989)
104N 052	589738	6620163	Ruby Creek	Mo	157,685,000	\$1,451.73	2007	Combined proven and probable reserves using a 0.04% MoS <sub>2</sub> mining grade cut-off	Adanac Molybdenum Corporation (2007)
104K 008	584181	6504063	Big Bull (Main/60-62)	Cu Zn Pb Ag Au	888,000	\$185.99	2006	Inferred and Indicated resource using cut-off NSR C\$86	Redcorp Ventures Ltd. (2007)

Abbreviation: NSR, net smelter return

shown on Figure 3 and listed in Table 3. The calculated gross in-place value of known resources shown in Table 3 is based on commodity prices current as of the end of November 2008.

### Industrial Mineral Assessment

A separate expert workshop was convened at Victoria on October 8, 2008 to reassess the 1996 industrial mineral estimates for the Atlin-Taku land-use planning area. This involved four experts from the BCGS, with D. MacIntyre as facilitator. New estimates were done for a number of deposit models not considered in the original 1996 assessment. These included rhodonite (Q02), schist-hosted emerald (Q07) and jade (Q01). The deposit models considered in the assessment are listed in Table 4.

For subdivided tracts, the existing 1996 estimates were redistributed following the methodology described in MacIntyre et al. (2003). The results of the industrial mineral assessment are presented in Table 5. Note that 15 tracts did not have any estimates for industrial mineral deposits and are given a rank of 0. Tract rankings, colour-coded by ranking group (each group representing 20% of the tract area), are shown on Figure 4.

### Comparison to the Provincial Resource Assessment

In comparing the results of the 1996 mineral resource assessment with the Atlin-Taku assessment, the following observations can be made:

Tract rankings are relative to the Atlin-Taku land-use planning area only and are not provincial rankings. Tracts within the study area are ranked from 1 to 67, whereas the provincial ranking (MRA1) was from 1 to 794.

**Table 4.** Industrial mineral deposit types considered to be present in the Atlin-Taku land-use planning area and associated relative deposit value scores (RDVS) used to

Model Code	Model Name	RDVS
D6	Zeolites	22.5
E10	Sedimentary kaolin	42.5
E6a	Sparry magnesite	22.5
I13	U-Th pegmatite	50
J8	Vein barite	22.5
J9	Barite-flourite vein	22.5
L1	Pegmatite lithium-cesium-tantalum LCT	50
P6	Asbestos	10
P7	Serpentinite-hosted magnesite-talc	22.5
Q01	Jade	55
Q02	Rhodonite	75
Q07	Schist-hosted emerald	95
R2	Kyanite family	25
R6	Crystalline flake graphite	65
T1	Cement shale	15
T10	Pumice	40
T11	Perlite	22.5
T2	Expanding shale	25
T3	Dimension-stone granite	15
T4	Dimension-stone marble	17.5
T9	Limestone/dolostone	40
T9a	Limestone/dolostone (White)	25

The new assessment had the advantage of an additional 12 years of data collection (mineral exploration and BCGS mapping) since the last assessment.

Six new deposit models (E4, E7, EC, I4, J2 and O1; Table 2) were considered, and estimates made for these models were not part of the MRA1. This increase reflects increased knowledge of the mineral resource endowment of the area since 1996.

Unlike the earlier Level 1 assessment, the Level 2 assessment did not factor in the known resources in the tract ranking scheme. As shown in Figure 2, known resources are treated as a separate point layer in the assessment. This is consistent with other Level 2 assessments, such as the one carried out for the Lillooet Land Resource Management Plan (LRMP).

The assessment used current commodity prices to determine per-hectare values. The previous assessment used a 10-year average price. For some commodities, current prices are significantly higher than their historical range. Depending on the deposit model being considered, higher commodity prices can have a significant impact on tract rankings, again making comparison with the previous assessment difficult.

### CONCLUSION

A new Level 2 mineral resource assessment of the Atlin-Taku land-use planning area was completed in September 2008. The new assessment follows an assessment

**Table 5.** Industrial mineral potential tract rankings. Tract IDs with -1 and -2 extensions have been subdivided.

Rank	Tract ID	Hectares	Rank	Tract ID	Hectares
0	CCPZ5	24,048	35	OIE3	29,833
0	OIE4	4,653	36	OLLJ1-2	71,344
0	OIEK3	27,312	37	OLLJ1-1	74,076
0	OIET2	120,458	38	OIK2	70,141
0	OIKT1	20,460	39	YTPZ2	48,163
0	OL1	31,096	40	OSLJ1	115,680
0	OLV1	30,422	41	OVEE1	50,205
0	OS1	6,454	42	CCPJ11	43,525
0	OSJ1	31,191	43	CCPJ-1	62,771
0	OVN2	24,850	44	CCPJ-2	116,686
0	OVN3	253,752	45	SPTZ13	35,861
0	OVPT1	5,140	46	YTPZ5	51,222
0	STTR16	23,464	47	CCPJ10	40,656
0	STTR18	33,475	48	CPPZ1	90,667
15	OIMJ3	72,260	49	OVE3	28,792
16	STTR1	59,810	50	STPJ11	46,298
17	OSMZ1	53,413	51	STTR17	16,277
18	STTR15	42,883	52	OVE2	33,027
19	CCPZ2	143,780	53	CCPZ4	63,993
20	STTR3-1	196,788	54	CCPZ8	53,487
21	OIMJ2	10,391	55	YTPZ7	13,855
22	STTR4-1	13,449	56	STRPZ4	105,377
23	STTR4-2	66,904	57	YTPR1	61,579
24	OSLJ2	131,578	58	STTR19	27,701
25	STTR14	72,173	59	STPJ12	16,013
26	OIE5	10,601	60	OSJ2	19,494
27	OIJE1	136,163	61	YTPZ4	17,141
28	CCPJ2-2	86,003	62	YTPZ6	9,691
29	CCPJ2-1	86,050	63	YTPR3	19,944
30	OIK3	51,890	64	OVN5	7,999
31	CCPJ1	431,408	65	OSTR1	6,836
32	OIE2	48,987	66	CCPJ9	66,911
33	OIK1	58,367	67	CCPJ7	51,932
34	OIMJ1	112,560			

completed in 1996 and includes new estimates for an expanded list of mineral deposit types. Sixty-seven tracts within the study area were given relative ranks that reflect their potential for the discovery of new resources in the future. Highest ranked tracts for metallic mineral potential are those where the geological framework is favourable for the presence of large-tonnage, low-grade porphyry Cu, Mo, W and Au deposits. Such deposits have a high value be-

cause of their relatively large size compared to, for example, smaller vein deposits

Users are cautioned, however, that mineral resource assessments use only currently available geological knowledge and expert views. These are, therefore, a snapshot in time that can change subject to additional information. They are also among the most challenging land-use assessments to complete, as they estimate a hidden subsurface re-

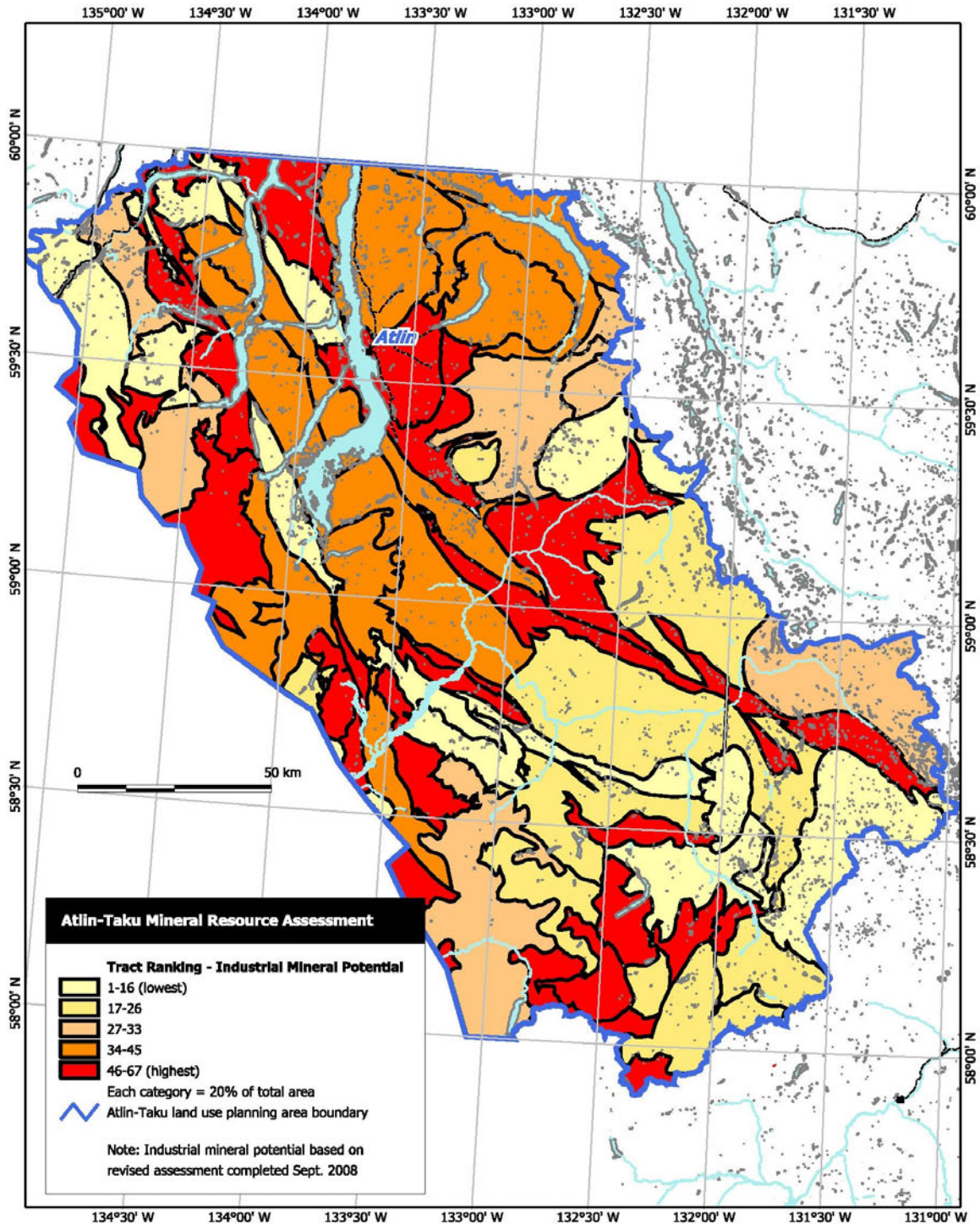


**Figure 4.** Atlin-Taku industrial mineral potential. See Table 5 for list of tracts and rankings. Note that tracts included in the assessment have been clipped at the study area boundary for presentation clarity.

source. The caution applies to both negative and positive uncertainty: the sudden discovery of diamonds in the Northwest Territories in the 1990s demonstrates the difficulty of predicting future resource discoveries. Areas currently considered to have low mineral potential may simply reflect lack of understanding of the geology and associated mineral resources.

## REFERENCES

- Adanac Molybdenum Corporation (2007): Adanac confirms positive economics on its Ruby Creek project; *Adanac Molybdenum Corporation*, press release, December 6, 2007.
- Baldys, C. (1991): Rock geochemistry surveys on Lawson vein, Sephil and Norm claims, ATlin Mining Division; submitted by Karl Gruber, Sr., *BC Ministry of Energy, Mines and Petroleum Resources*, Assessment Report 21816, 25 pages.
- Brew, D.A. (1992): Decision points and strategies in quantitative probabilistic assessment of undiscovered mineral resources; *United States Geological Survey*, Open File 92-308, 23 pages.
- Cox, D.P. and Singer, D.A., Editors (1986): Mineral deposit models; *United States Geological Survey*, Bulletin 1693, 379 pages.
- Cox, D.P. (1993): Estimation of undiscovered deposits in quantitative mineral resource assessments—examples from Venezuela and Puerto Rico; *Nonrenewable Resources*, Volume 2, number 2, pages 82–91.
- Grunsky, E.C. (1995): Grade and tonnage data for British Columbia mineral deposit models; in *Geological Fieldwork 1994*, *BC Ministry of Energy, Mines and Petroleum Resources*, Paper 1995-1, pages 417–423.
- Kilby, W.E. (1992): Mineral Potential Workshop, report of proceedings, April 22–23, 1992, Victoria, British Columbia; *BC Ministry of Energy, Mines and Petroleum Resources*, Information Circular 1992-22, 50 pages.
- Kilby, W.E. (1995): Mineral Potential Project—overview; in *Geological Fieldwork 1994*, *BC Ministry of Energy, Mines and Petroleum Resources*, Paper 1995-1, pages 411–416.
- Kilby, W.E. (1996): Mineral Potential Project—an update; in *Geological Fieldwork 1995*, *BC Ministry of Energy, Mines and Petroleum Resources*, Paper 1996-1.
- Lefebure, D.V. and Hoy, T. (1996): Selected British Columbia mineral deposit profiles, Volume II—more metallic deposits; *BC Ministry of Employment and Investment*, Open File 1996-13, 172 pages.
- Lefebure, D.V. and Ray, G.E. (1995): Selected British Columbia mineral deposit profiles, Volume I—metallics and coal; *BC Ministry of Energy, Mines and Petroleum Resources*, Open File 1995-20, 136 pages.
- Lefebure, D.V., Alldrick, G.J., Simandl, G.J. and Ray, G. (1995): British Columbia mineral deposit profiles; in *Geological Fieldwork 1994*, *BC Ministry of Energy, Mines and Petroleum Resources*, Paper 1995-1, pages 469–490.
- MacIntyre, D.G., Massey, N.W.D. and Kilby, W.E. (2003): The BC Mineral Potential Project—new Level 2 Mineral Resource Assessment methodology and results; in *Geological Fieldwork 2003*, *BC Ministry of Energy, Mines and Petroleum Resources*, Paper 2004-1, pages 125–140.
- McIvor, D.F. (1989): Geological, geophysical and geochemical report on the Mount Vaughan property; submitted by Homestake Canada Inc, *BC Ministry of Energy, Mines and Petroleum Resources*, Assessment Report 18646, 373 pages.
- MINFILE (2008): MINFILE BC mineral deposits database; *BC Ministry of Energy, Mines and Petroleum Resources*, URL <<http://www.empr.gov.bc.ca/Mining/Geoscience/MINFILE/Pages/default.aspx>> [December 18, 2008].
- Redcorp Ventures Ltd (2007): New resource estimate for Big Bull expands Tulsequah project resources; *Redcorp Ventures Ltd*, press release, April 3, 2007.
- Root, D.H., Menzie, W.D. and Scott, W.A. (1992): Computer Monte Carlo simulation in quantitative resource assessment; *Nonrenewable Resources*, Volume 1, number 2, pages 125–138.
- Schroeter, T.G. (1998): British Columbia 1997 mineral exploration review; in *British Columbia Mineral Exploration Review 1998*, *BC Ministry of Energy, Mines and Petroleum Resources*, Information Circular 1998-1, pages 17 and 20.
- Schroeter, T.G. (1994): British Columbia mining, development and exploration 1993 highlights; in *British Columbia Mineral Exploration Review 1994*, *BC Ministry of Energy, Mines and Petroleum Resources*, Information Circular 1994-1, page 19.
- Schroeter T.G., Grieve, D., Madu, B., Northcote, B. and Wojdak, P. (2007): British Columbia mining and mineral exploration overview 2006; in *Exploration and Mining in British Columbia 2006*, *BC Ministry of Energy, Mines and Petroleum Resources*, page 25.
- Simandl, G.J., Hora, Z.D. and Lefebure, D.V. (1999): Selected British Columbia mineral deposit profiles, Volume 3—industrial minerals and gemstones, *BC Ministry of Energy, Mines and Petroleum Resources*, Open File 1999-10, 136 pages.
- Singer, D.A. (1993): Basic concepts in three-part quantitative assessments of undiscovered mineral resources; *Nonrenewable Resources*, Volume 2, number 2, pages 69–81.



# Bedrock and Coal Geology of the Wolverine River Area, Northeastern British Columbia (Parts of NTS 093P/03, 093I/14)

by A.S. Legun

**KEYWORDS:** Peace River coalfield, coal exploration, geological mapping, Gates Formation, coal seam traces, J seam, E seam, Falher D, Gething Formation, Chamberlain Member, Bird seam, Bullmoose thrust fault, Transfer fault coalbed gas

## INTRODUCTION

This report updates the coal geology of the area between Bullmoose Creek and the Murray River in the Peace River coalfield, northeastern British Columbia (Figure 1).

The study area covers approximately 300 km<sup>2</sup> and is located southwest of Tumbler Ridge in northeastern British Columbia. It spans parts of NTS map areas 093P/03 and 093I/14. It was chosen to cover the main trend of outcropping coal measures of the Early Cretaceous. The Gates and Gething formations are the principal coal-bearing stratigraphic units of economic interest. The stratigraphic interval that was mapped ranges from the Cadomin Formation to the Boulder Creek Formation.

This is an area of coal mines and proposed coal developments, with developed infrastructure including rail, power and loadout facilities. The Bullmoose and Quintette mines opened in the early 1980s and closed earlier in this decade. Quintette Coal Ltd. extracted metallurgical coal from the Wolverine, Mesa and Shikano pits. Teck Cominco Limited mined the South Fork pit, Bullmoose mine. After a lull due to low coal prices, the Perry Creek mine (facing the Mesa pit across the Wolverine River) was opened in 2006 by Western Canada Coal Corp. (WCCC). In 2008, exploration is at an advanced stage in several portions of the study area, including the Hermann and EB areas.

A variety of property-scale maps, included in assessment reports of the 1970s and 1980s, cover parts of the area. Kilby and Wrightson (1987) and Kilby and Johnston (1988) provided a 1:50 000 scale compilation map of the general geology.

## CURRENT MAPPING

This study revises the basal contact of the Gates Formation to be the base of the lowest sandstone bed in the thickly bedded to massive Quintette sandstone. This is in accord with the original definition of the Gates Formation lower contact as the base of the first thick sandstone bed

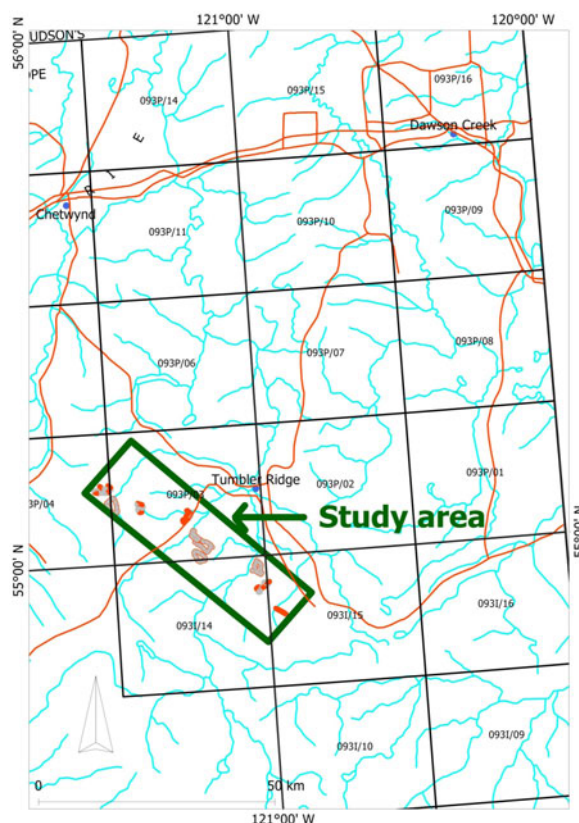


**Figure 1.** Location of study area in northeastern British Columbia.

above which few, or no, mudstone beds occur (McLean 1982, page 12). Previous maps included a “transitional facies” of interbedded sandstone and shale below the Quintette sandstone as part of the Gates Formation. The revised contact is more useful in identifying the area mapped as Gates Formation with potential for coal resources. Many coal boreholes in the area terminate in the Quintette sandstone.

A new geological map (Figure 2) shows the surface trace of major Gates Formation coals that bound the economic interval of the middle Gates Formation. These are the J seam at base of the middle Gates Formation and the D seam at the top. In the areas of Mount Spieker, South Fork, West Fork and Bullmoose Creek, the A seam of the A/B pair is traced as equivalent to the J seam. Where the D seam is absent or thin (areas north of Wolverine River), the E seam is traced as the upper seam.

Bedrock mapping was facilitated by the use of light detection and ranging (LIDAR) imagery, orthophotography

---

*This publication is also available, free of charge, as colour digital files in Adobe Acrobat® PDF format from the BC Ministry of Energy, Mines and Petroleum Resources website at <http://www.empr.gov.bc.ca/Mining/Geoscience/PublicationsCatalogue/Fieldwork/Pages/default.aspx>.*

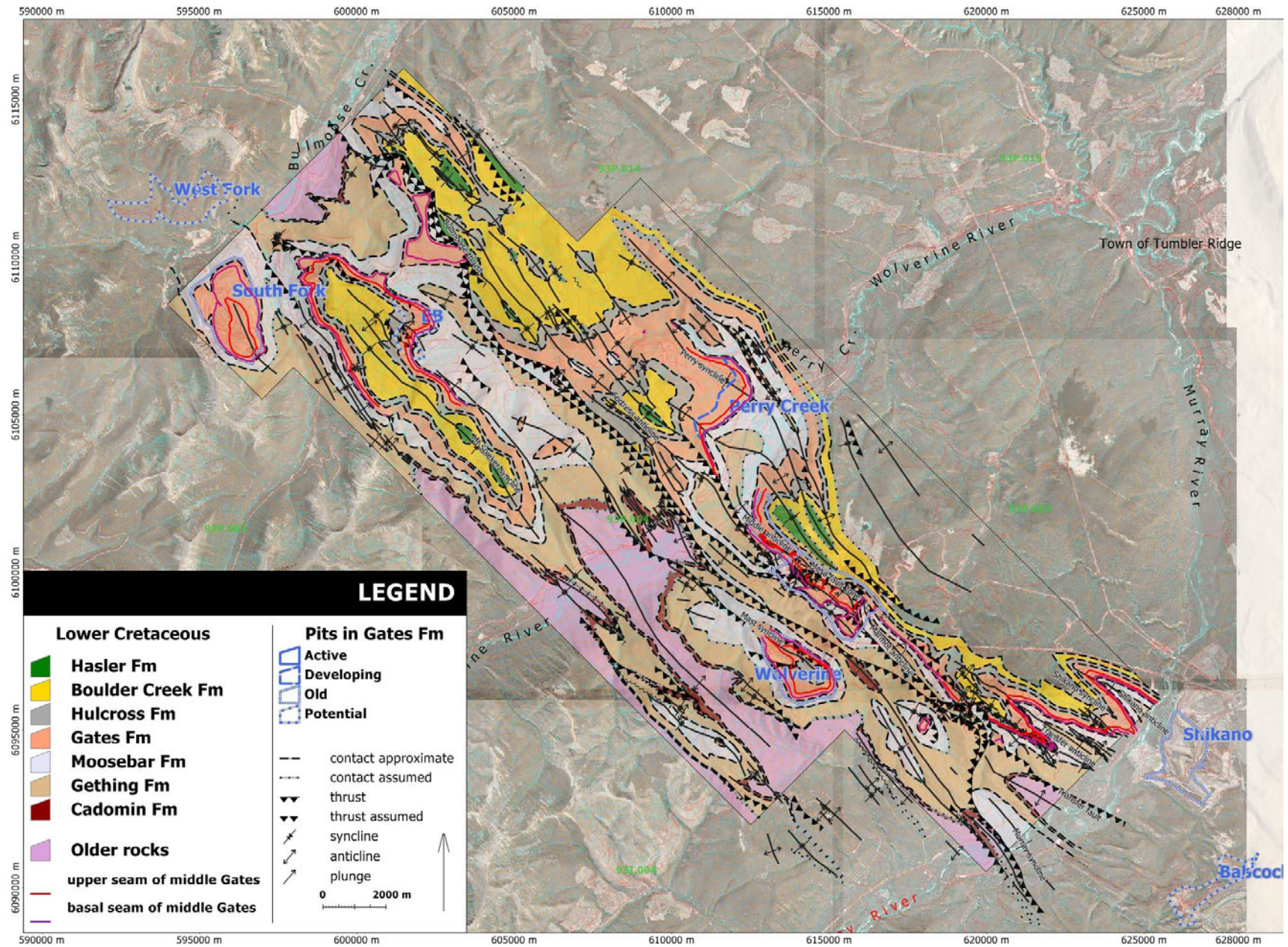


Figure 2. Bedrock geology of the Wolverine River area, northeastern British Columbia.

and GPS navigation. Map images from assessment reports were georeferenced and imported into the Manifold® System GIS package. LIDAR imagery is useful in outlining macroscopic fold structures and fold axes in areas of tree cover. Orthophotographs and GPS data provided location precision. In some areas where surface exposure was poor, subsurface data were projected up-dip to constrain surface contacts.

Results of earlier work were reported by Legun (2007). In 2007 and 2008, approximately five weeks in total were spent mapping in the field, mostly at lower elevations.

This bedrock map supplements a previous stratigraphic study of Gates Formation coal measures in the area (Legun, 2008).

### Stratigraphic Framework

The stratigraphic framework is correlated with the gamma ray and formation density log of a recent well (well authorization number 20207; BC Oil and Gas Commission, 2008) located immediately east of the coalfield near Wolverine River and Perry Creek (Figure 3). The descriptions below focus on the two main coal-bearing formations.

### GETHING FORMATION

The Gething Formation has upper and lower coal measures of calcareous sandstone, shale, siltstone and coal separated by a sequence of marine shale. It is approximately 245 m thick in the Mount Spieker area. Borehole data at Perry Creek indicates a 207 m thickness and 200 m is indicated near Hermann Gething (well authorization number 5099). The writer follows Gibson (1992) in dividing the formation into three members.

#### Gaylard Member (Lower Gething Formation)

The Gaylard Member consists of sandstone, coal, black and carbonaceous shale, and rippled siltstone. This sequence is interpreted to represent channel, overbank and flood basin deposits. The top of the Gaylard Member is marked by a pebble lag, indicating a marine transgression. The upper 20 m of the Gaylard Member may include clean quartzitic sandstone and is often devoid of coal. The first significant coal, about 45 m below the top of the member, is represented by seams GT1 and GT2 in the Hermann Gething resource area (near UTM Zone 10, 6095200N, 619000E, NAD 83).

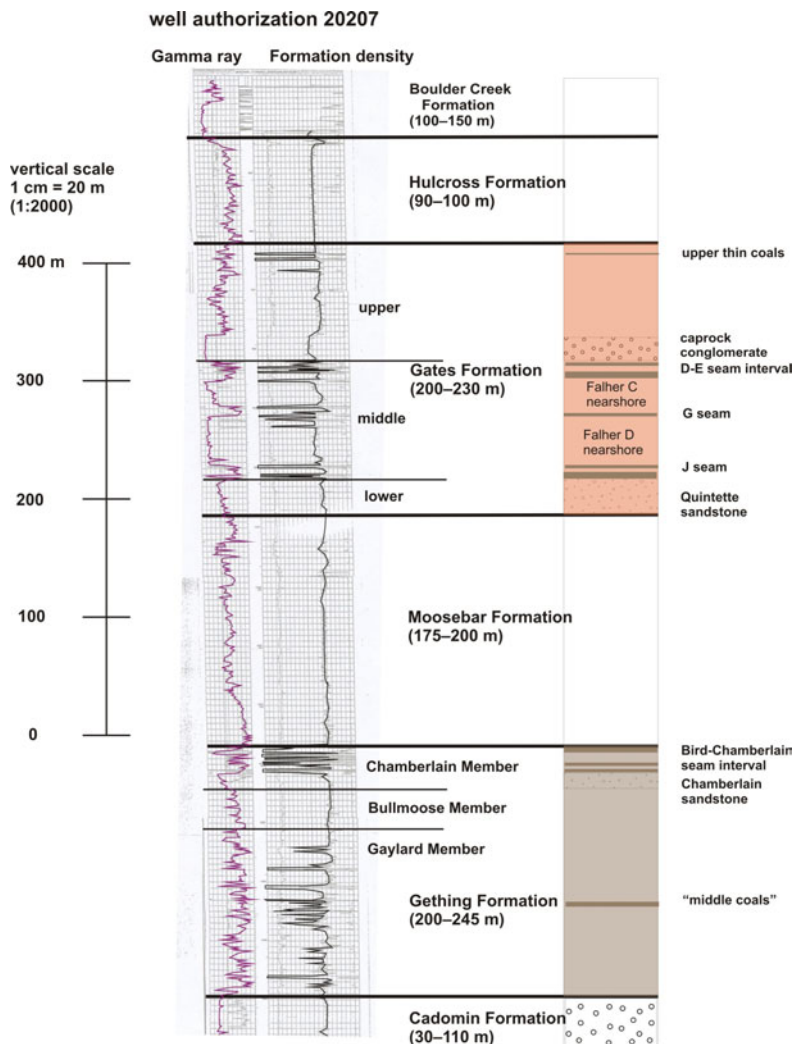


Figure 3: Stratigraphic column, Wolverine River area, northeastern British Columbia (log from well authorization number 20207; BC Oil and Gas Commission, 2008).

Units of clast-supported conglomerate outcrop here and in areas immediately to the west. These units, in the absence of drill data, may be easily misidentified as Cadomin Formation conglomerate. One bed, characterized by well-packed siliceous cobbles, forms a flat ridge in the Hermann Gething resource area and caps the GT1 seam. Another conglomerate bed underlies the GT2 seam.

### ***Bullmoose Member***

Overlying the Gaylard Member are shale beds of a marine tongue named the Bullmoose Member. The sand content of these beds increases upward in the sequence. This noncoal bearing interval extends to the base of the Chamberlain Member. This member thins from 45 m thick at Mount Spieker to 15 m at Hermann Gething in the south. The regional southeast thinning of the marine tongue was recorded by Legun (1990, Figure 7).

### ***Chamberlain Member***

The basal unit of the Chamberlain Member is a massive clean sandstone unit. The Chamberlain, Skeeter and Bird coal seams occur in the overlying sedimentary rocks. These seams are variably developed within the map area (see 'Economic Geology' below). They are well developed to the north in the Sukunka area. In some areas, a few metres of clean sandstone with herringbone crossbeds lie above the Bird seam. Clean sandstone locally forms a prominent ledge against the overlying recessive Moosebar Formation mudstone. Up to 8 m of carbonaceous sandstone, siltstone and glauconitic beds may lie between the Bird seam and Moosebar Formation mudstone. This is included within the Gething Formation.

The areal distribution of coal facies in the Chamberlain Member is discussed in Legun (1990).

## **GATES FORMATION**

### ***Lower Gates Formation***

The lower Gates Formation or Quintette sandstone unit forms the floor of the major economic J coal seam in the area. The sandstone averages 25 m in thickness and ranges from 5 to 50 m thick. The sandstone is locally not well developed. It is dominated by sheet sandstone with trace fossils indicative of shoreface conditions. To the north, the lower Gates Formation is conglomeratic in a wide east-trending tract near Mount Spieker and Bullmoose Mountain, suggesting a western source. In areas where the Quintette sandstone is thin, the intersection of the J seam in nearby drillholes constrains the position of the basal contact of the Gates Formation.

### ***Middle Gates Formation***

The middle Gates Formation carries the coal beds of most economic interest in the map area. In Quintette Coal Ltd.'s nomenclature, this encompasses the base of the J seam to the top of the D seam. The thickness of the middle Gates Formation varies from 60 to >135 m. It is thicker in the north due to two coarsening-upward wedges of marine sandstone and conglomerate. These are locally known as the Falher C and D. In the Mesa pit area, south of the limit of the two marine tongues, there is a maximum development of coal in section. From 18 to >60 m of coal was mined in Quintette Coal Ltd.'s Mesa pit.

### ***Upper Gates Formation***

The upper Gates Formation corresponds to the interval from the base of the cap-rock conglomerate (overlying D seam) to the top of carbonaceous shale in contact with marine shale and siltstone of the Hulcross Formation. The upper Gates Formation is known as the Notikewan Member in the subsurface. It includes a major coarsening-upward marine interval.

South of the Wolverine River, a conglomerate bed lies at the base of the Notikewan Formation and underpins the coarsening-upward interval. This body has a linear trend interpreted to represent deposition within an estuary (Carmichael, 1988). Its extent is confirmed by recent well data (e.g., a thickness of 20 m was recognized in well authorization number 20207). It has potential as a reservoir for coalbed natural gas.

The stratigraphically highest beds of the upper Gates Formation are regionally dominated by shale and include several thin coals. In the area of Fortress Mountain and the Mount Spieker syncline, however, thick sandstone are present and identified as a distinct unit (Armand sandstone) by WCCC.

## **General Structure**

Macroscopic folds vary from concentric (rounded) to kink band (chevron) geometry. They are open to tight and occasionally asymmetric with overturned east limbs, indicating northeast vergence. Shallow, northwest- or southeast-plunging folds are dominant. Faulting varies from westward-dipping, low-angle, thrust faults to steep, reverse faults. There is a zone of east-dipping faults at the east margin of the coalfield near the Transfer and Hermann areas, parallel to the Bullmoose thrust zone to the west.

The major faulting in the area is in the Bullmoose thrust zone (see 'Bullmoose Thrust Zone' below).

## **MAPPING RESULTS**

### ***Structural Revisions***

#### **BULLMOOSE THRUST ZONE**

The Bullmoose thrust zone can be traced south to the Murray River. It consists of the Transfer fault to the east and the Murray fault to the west. The Transfer fault bounds the western limit of the Gates Formation resource area in the Shikano and Transfer folds. The Murray fault appears to overlap this fault with panels of Moosebar and Gething formations strata. The most eastern segment of the Murray fault juxtaposes Moosebar Formation over Gates Formation strata near the southern end of the proposed Hermann pit area. Southward, a single fault is shown to continue to the Murray River where the Cadomin Formation is juxtaposed against the Moosebar Formation on the west side of the Murray syncline. The Murray fault also lies immediately east of the Hermann syncline and is parallel to the macroscopic fold axis near the Murray River. This suggests that a shallow-dipping fault underlies that fold at depth.

Near the Wolverine River, the Bullmoose thrust zone comprises three splays bounding two fold structures. The eastern fold is the Fortress Mountain anticline; it is overturned toward Mesa and is underpinned by the Fortress

thrust fault. The zone is about 1.5 km wide and consists of two duplexes.

The relationship of the Fortress thrust fault and the Mesa thrust fault near the Mesa North pit is unclear; exposure is presently obscured by dump material. The Mesa North pit, now mined out below the level of the Mesa thrust fault, exposes steep to overturned limbs of the Marmot anticline in the footwall. The Marmot anticline may correlate with the Fortress Mountain anticline.

### Geological Contact Revisions

The interpreted bedrock geology has been revised for the area between the Mount Spieker syncline ridge and Perry Creek, southeast of the EB pit area. This is an area of broad open macroscopic folds with limited exposure on the slopes draining toward Perry Creek. Kilby and Wrightson (1987) suggested that the contact trace between the Gates and Moosebar formations is oriented downslope. The strata have been reassigned to the Moosebar Formation in this study following redefinition of the Gates Formation contact (see 'Current Mapping' above). Only one east-trending ridge opposite Fortress Mountain preserves lower Gates Formation strata in a shallow syncline.

The lowest slopes near Perry Creek are underlain by the Gething Formation, which outcrops near the west and

north forks of Perry Creek. It is also exposed on the slopes of the east-trending ridge facing Fortress Mountain and along some recent access roads built by Peace River Coal Inc. In this area, a shallow syncline east of drillhole EB4 (UTM 6106906N, 603142E) probably preserves the Bird seam at shallow depth (see 'Economic Geology' below). The syncline may be a continuation of the open syncline in the pit area at a deeper structural level.

The Gething Formation–Moosebar Formation contact has been reinterpreted in a number of other areas. This includes the Mast syncline, the Bullmoose Creek area southeast of South Fork pit, and the Wolverine Valley near the junction of Perry Creek.

The Moosebar Formation underlies a larger area in the Mast syncline than initially mapped by Quintette Coal Ltd. The trace of the J seam in the Wolverine pit suggests that reserves remain in the northwest portion of the syncline, although they may not be amenable to open pit extraction.

Detailed mapping east of the Perry Creek bridge and immediately north of the Perry pit indicates that the lower to middle Gates Formation is exposed over several kilometres of gently folded strata along Perry Creek. A thin J2 seam lies a few metres above the valley floor and massive sandstone of the Falher D marine tongue are exposed in the north valley wall (Figure 4).

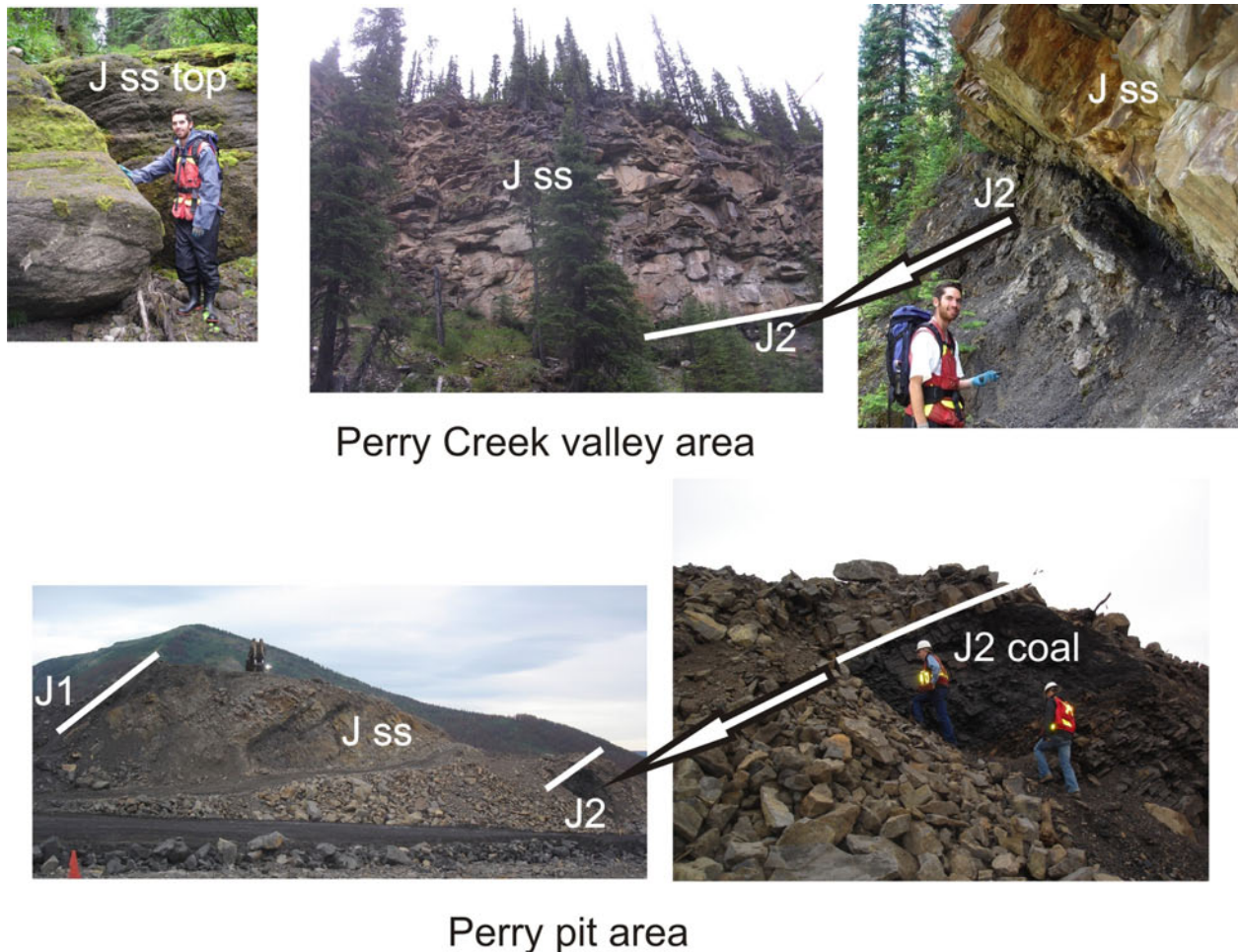


**Figure 4.** Split of J seam exposed at Perry pit (lower panel) and same interval preserved in valley walls of Perry Creek about 3 km to northwest (upper panel), northeastern British Columbia. Jss refers to Falher D sandstone.

West of the bridge, Perry Creek has eroded the cores of two anticlines and exposed two small areas of Moosebar Formation strata.

West of the Wolverine pit, a canoe-shaped, synclinal basin preserves Gething and Moosebar formations strata. Only a few metres of coarse carbonaceous sandstone exposed in a small area underlying the high ground can be correlated with the basal Gates Formation. The syncline has been the target of recent drilling. While Peace River Coal Inc. (COALFILE 899; COALFILE, 2008) suggests intercepts of both Gates Formation coal and Gething Formation coal, mapping clearly indicates only Gething Formation coal measures are preserved in the syncline. The syncline is well outlined by ridge-forming Cadomin Formation strata. These are affected by secondary folds at the south margin of the structure.

## ECONOMIC GEOLOGY

### *Gething Formation Coals*

Within the study area, the exploration for coal has focused largely on seams within the Gates Formation. There are coal seams hosted within the Gething Formation that warrant consideration.

Most historical drilling in the Gething Formation has been in the north part of the map area pursuing Chamberlain Member coal seams. Drilling in the south has focused on Gaylard Member coal seams on the Hermann Gething property. Older assessment reports document outcrops of coal of the Gething Formation but there is no indication that exposures were trenched. Some earlier bedding data for the Gething Formation were not included in later maps, possibly due to a focus on Gates Formation exploration.

### **CHAMBERLAIN MEMBER COALS (BIRD, SKEETER, CHAMBERLAIN SEAMS)**

A number of correlation charts outline Chamberlain coals in the northern part of the map area near Bullmoose Creek and Mount Spieker (COALFILE 474, 555, 559). The Chamberlain and Skeeter seams are thinner to the north. Exploration focused on the thickness and quality of the upper and lower Bird seams.

The upper and lower Bird seams generally comprise 5 m of coal in gently dipping beds exposed around Mount Spieker and interpreted to underlie it at depth. The stratigraphic separation between the plies is commonly around 5 m in the area but expands to 13 m in drillhole EB-4. Part of the seam is partially exposed in a roadcut to well authorization number 16824 on the northwest flank of Mount Spieker (Figure 5).

A postulated shallow resource of metallurgical quality coal with acceptable sulphur content was tested by drilling in the valley of the south fork of Bullmoose Creek, as a possible supplement to Gates Formation coal at the Bullmoose mine. Results were disappointing. The seam is locally faulted and varies in thickness (COALFILE 559). A stratigraphic fence diagram (COALFILE 474) allows an interpretation that the entire seam interval splits and stratigraphically separates southwest of Bullmoose Creek.

An area of untested shallow resource also lies southeast of the proposed EB pit area. The area is underlain by a shallow syncline between drillhole EB4 and Gething Formation outcrops and subcrop near Perry Creek (UTM



**Figure 5.** Exposure of the Bird seam, northwest flank of Mount Spieker, northeastern British Columbia, along the access road to well authorization number 16824 (BC Oil and Gas Commission, 2008).

6107276N, 604119E; COALFILE 555, Figure 77-07-03). The upper Bird seam is fault duplicated in EB4 and 2.3 m thick (its duplicate is 3.2 m) with 9% raw ash with 20% volatile matter, fracture spacing index (FSI) of 8 and 1.68% sulphur (COALFILE 555, Table 7). The sulphur content of the Bird seam varies from moderate to high in the area, at least in part due to pyrite (<1 to >2%). Blending with Gates Formation coal at the proposed EB pit is an option.

Further southeast, a poorly developed Bird seam appears to have been intersected in drillhole R001 by Peace River Coal Inc. (COALFILE 901). Drillhole R002 is probably in Gething Formation coal but the stratigraphic level is uncertain.

The Chamberlain–Skeeter interval is developed in the Perry pit area and is cumulatively 4 m thick. It has been drilled as a coalbed gas target (well authorization number 16367). The interval is near surface at drillhole WDH #1 in the Perry Creek anticline where the seams are approximately 1.4 m apart and comprise 5.6 m of coal over 7 m. The seams were described as Gates Formation coal in an early assessment report (COALFILE 597) but amended to upper Gething Formation (Chamberlain Member) based on subsequent drilling and a correlation chart (COALFILE 606).

Quintette Coal Ltd. drilled Chamberlain coals at the edge of the Mesa and Wolverine pits. At the Mesa pit, seams averaged 2 m in thickness, and reached 3 m, but were reported to be ashy (COALFILE 826). This indicates potential that needs further testing. Coals in this interval are also exposed in creeks draining the axial area of the Mast syncline near the Wolverine River.

### *Gates Formation Coals*

The following is an update on the split of the J seam at the Perry pit of WCCC. The reader is referred to Legun (2008) for additional information.

This is an area of dramatic change in the middle Gates Formation. Two marine tongues are near their southern limit. The lower tongue locally splits the J seam and the upper tongue separates the G seam from the E seam. Isopachs and zero-edge position for each tongue were compiled by Legun (2006b).

Stripping at the Perry pit has exposed the substantial rock split of J seam coal (Figure 4). J1 and J2 have maintained thickness even though they are separated by ~20 m of sandstone. The interval includes granule beds near the base, inclined carbonaceous lenses in sandstone and an upper clean sandstone. The basal contact is sharp and the seam is not elevated in sulphur. To the north at Perry Creek, the J seam is overlain by a pebbly mudstone lag and followed by fluted and load-cast sandstone suggesting rapid deposition and loading. Overlying beds show little internal structure. They are succeeded upward by crossbedded pebbly sandstone (Figure 4).

Generally sandy nearshore deposits at Perry Creek contrast with thick conglomerate that directly overlies basal coal at Mount Spieker. Further stripping at the Perry pit is predicted to reveal more complexities in the transition from coastal peat swamp (J seam) to a wave-dominated paleoshore in this area.

## ACKNOWLEDGMENTS

The field assistance provided by David Lilly in 2007 and Doug Wells in 2008 is much appreciated. Dan McNeil of Western Canada Coal Corp. is thanked for providing a tour of the Perry pit. This article benefited from edits by Philippe Erdmer and David Lefebure.

## REFERENCES

- BC Oil and Gas Commission (2006): Public internet site; *BC Ministry of Energy, Mines and Petroleum Resources*, URL <<http://www.ogc.gov.bc.ca>> [December 2008].
- Carmichael, S.M. (1988): Linear estuarine conglomerate bodies formed during a mid-Albian marine transgression; "upper Gates" Formation, Rocky Mountain foothills of northeastern British Columbia; in *Sequences, Stratigraphy, Sedimentology: Surface and Subsurface*, James, D.P. and Leckie, D.A., Editors, *Canadian Society of Petroleum Geologists*, Memoir 15, pages 49–62.
- COALFILE (2008): COALFILE BC coal data and reports; *BC Ministry of Energy, Mines and Petroleum Resources*, URL <<http://www.empr.gov.bc.ca/Mining/Geoscience/PublicationsCatalogue/Pages/CoalinBC.aspx>> [December 16, 2008].
- Gibson, D.W. (1992): Stratigraphy, sedimentology, coal geology and depositional environments of the Lower Cretaceous Gething Formation, northeastern British Columbia and west-central Alberta; *Geological Survey of Canada*, Bulletin 431, 127 pages.
- Kilby, W. and Johnston, S.T. (1988): Bedrock geology of the Kinuseo Creek area, northeast British Columbia (93I/15); *BC Ministry of Energy, Mines and Petroleum Resources*, Open File 88-22.
- Kilby, W. and Wrightson, C.B. (1987): Bedrock geology of the Bullmoose Creek area (93P/3); *BC Ministry of Energy, Mines and Petroleum Resources*, Open File 87-6.
- Legun, A. (1990): Stratigraphic trends in the Gething Formation; *BC Ministry of Energy, Mines and Petroleum Resources*, Open File 1990-33.
- Legun, A.S. (2006a): The Gates Formation in the Wolverine River area, northeastern BC; in *Geological Fieldwork 2005*, *BC Ministry of Energy, Mines and Petroleum Resources*, Paper 2006-1, pages 73–82.
- Legun, A.S. (2006b): Manifold map files, Peace River coalfield, northeast British Columbia (NTS 93P, I, O, 094B), *BC Ministry of Energy, Mines and Petroleum Resources*, Open File 2006-13.
- Legun, A.S. (2007): Mapping and review of coal geology in the Wolverine River area, Peace River coalfield (NTS 093P/03), northeastern British Columbia; in *Geological Fieldwork 2006*, *BC Ministry of Energy, Mines and Petroleum Resources*, Paper 2007-1, pages 67–76.
- Legun, A.S. (2008): Thickness trends of J seam and its split at the Falher D shoreline, Wolverine River area, Peace River coalfield, northeastern British Columbia (parts of NTS 093I, P); in *Geological Fieldwork 2007*, *BC Ministry of Energy, Mines and Petroleum Resources*, Paper 2008-1, pages 39–48.
- McLean, J.R. (1982): Lithostratigraphy of the Lower Cretaceous coal-bearing sequence, Foothills of Alberta; *Geological Survey of Canada*, Paper 80-29, 46 pages.



# Geology and Mineral Occurrences of the Mid-Cretaceous Spences Bridge Group near Merritt, Southern British Columbia (Parts of NTS 092H/14, 15, 092I/02, 03)

by L.J. Diakow and A. Barrios

**KEYWORDS:** Spences Bridge Group, Nicola Group, Castillion Creek, Gillis Lake, Shovelnose Mountain, epithermal quartz veins, exhalite, sinter, gold mineralization

## INTRODUCTION

The Spences Bridge Project is a bedrock mapping program with objectives to refine stratigraphy of the Cretaceous Spences Bridge Group, determine the geological setting and characteristics of gold-bearing epithermal vein systems, and assess the regional economic potential of Cretaceous volcanic stratigraphy in southern British Columbia. The program focuses on two major rock successions: island-arc rocks of the Late Triassic Nicola Group, specifically the western belt (facies) mapped locally around Merritt in 2007 (Diakow, 2008); and a superimposed Early Cretaceous continent-margin arc succession, the Spences Bridge Group. The paper describes a new exhalite and sinter discovered in Late Triassic felsic stratigraphy, as well as low-sulphidation epithermal veins in the Cretaceous Spences Bridge Group.

## PREVIOUS WORK AND CURRENT STUDY

Early Cretaceous volcanic rocks of the Spences Bridge Group form a narrow, northwest-trending belt regionally covering nearly 3200 km<sup>2</sup> east of the Fraser fault in southern British Columbia (Figure 1). They unconformably overlie both the oceanic Cache Creek terrane and, at the latitude of the study area, the more broadly distributed magmatic arc making up the Quesnel terrane. The Quesnel terrane in the study area consists primarily of mafic volcanic and interstratified sedimentary rocks of the Late Triassic Nicola Group and contemporaneous intrusive rocks of the Mount Lytton Plutonic Complex (Monger and McMillan, 1989; Monger, 1989). Together with the Late Jurassic Eagle Plutonic Complex (Greig, 1991), these tectonic elements define part of the southwestern margin of the Quesnel terrane.

Thorkelson (1986) studied a segment of the mid-Cretaceous belt south of Merritt and, after integrating relationships documented in previous regional mapping studies, proposed revisions to the confusing stratigraphic nomen-

clature for mid-Cretaceous rocks in southwestern BC. Consequently, Thorkelson and Rouse (1989) proposed that the Spences Bridge Group, with further subdivision into two formations, be formally adopted. The lower of these, the Pimainus Formation, is a lithologically diverse subaerial volcanic sequence composed largely of flows and fragmental deposits of andesitic and rhyolitic compositions, interspersed with terrestrial sedimentary rocks. The overlying Spius Formation differs significantly and is composed mainly of brownish-weathering amygdaloidal andesite flows. Palynomorphs from sedimentary rocks and K-Ar dates from volcanic rocks aided in assigning a somewhat broad, Early to Late Cretaceous time of deposition for these two formations (Thorkelson and Rouse, 1989).

Epithermal gold-bearing veins of the low sulphidation type were discovered within subaerial volcanic rocks of the Spences Bridge Group in 2002, and a bedrock–mineral deposit study was initiated in 2007 by the BC Geological Survey in order to evaluate the economic mineral potential of this succession. In the first year, 1:20 000 scale bedrock mapping focused on older, Triassic ‘basement’ rocks between Iron and Selish mountains, and a study of the Spences Bridge Group stratigraphy was started at a reference section exposed in the vicinity of Gillis Lake (Thorkelson, 1986; Diakow, 2008). During 2008, the mapping program extended beyond the Gillis Lake area, expanding the study of Spences Bridge stratigraphy laterally, northwest towards Prospect Creek and south to the Shovelnose Mountain area. This bedrock mapping has been published at 1:50 000 scale (Diakow and Barrios, 2008).

## LITHOLOGICAL UNITS

The study area (Figure 2) lies near the western margin of the Quesnel terrane, which is dominated by Late Triassic volcanic and sedimentary rocks of the Nicola Group and associated intrusions of diorite to granodiorite composition, which have been divided into four regional facies belts (Preto, 1979). In the study area, the Nicola Group consists mainly of mafic volcanic rocks, although a unique felsic volcano-sedimentary facies is mapped between Iron and Selish mountains (McMillan, 1981; Diakow and Barrios, 2008). Triassic stratigraphy at this locality has been described in Diakow (2008), and several U-Pb isotopic dates obtained from felsic volcanic rocks are reported in this paper. The Nicola Group is unconformably overlain by Cretaceous sedimentary and volcanic units. The sedimentary rocks, characterized by chert-bearing conglomerate, are thought to be older and constitute a poorly exposed, recessive unit upon which volcanic and lesser sedimentary rocks of the mid-Cretaceous Spences Bridge Group were depos-

---

*This publication is also available, free of charge, as colour digital files in Adobe Acrobat® PDF format from the BC Ministry of Energy, Mines and Petroleum Resources website at <http://www.empr.gov.bc.ca/Mining/Geoscience/PublicationsCatalogue/Fieldwork/Pages/default.aspx>.*

ited. Throughout most of the study area, however, the chert-rich clastic unit is missing, and Spences Bridge rocks apparently rest nonconformably on intrusive rocks of the Late Triassic Coldwater pluton, the Triassic–Jurassic Mount Lytton Plutonic Complex and the Late Jurassic–Cretaceous Eagle Plutonic Complex (Monger, 1989; Monger and McMillan, 1989; Greig, 1991). The Eocene Princeton Group is the youngest succession mapped. Composed largely of hornblende-phyric dacite flows, it is a relatively flat-lying succession unconformably overlying Cretaceous strata. Thick deposits of conglomerate, marking a period of Eocene tectonic instability, are confined to the Fig Lake graben. Unconsolidated glacial deposits are relatively thin throughout most of the study area but have been reworked and redeposited in broad fluvial terraces that completely conceal bedrock in several major valleys, such as that occupied by the Coldwater River.

### Geochronology and Paleontology Results from Iron and Selish Mountains

Stratigraphy on Iron Mountain and the lower west slope of Selish Mountain were remapped in 2007 (Diakow, 2008; Diakow and Barrios, 2008). Significant felsic volcanic strata in these areas overlie a mafic succession resembling rocks more typical of the Late Triassic Nicola Group. Previous workers collected fossils from the Iron Mountain section, but none provided definitive age constraints. Two new U-Pb dates have been obtained from stratified felsic

volcano-sedimentary sequences at Iron Mountain and Selish Mountain.

Stratigraphy mapped between Iron Mountain and Selish Mountain, south-southwest of Merritt, consists generally of a thick basaltic sequence conformably overlain by intervals characterized by felsic volcanic rocks interlayered with shallow marine limestone and sandstone (Diakow, 2008). With the exception of the Ashcroft map area, significant felsic volcanic accumulations are absent from within Late Triassic magmatic-arc successions elsewhere in BC. Two samples for U-Pb isotopic dating were collected from felsic rocks at widely spaced localities in order to determine their temporal relationship with the Nicola Group: one at Iron Mountain and the other from a Coquihalla Highway exposure at Castillion Creek (*see* ‘Castillion Creek Exhalite-Sinter’ section). Sample preparation and analytical work for U-Pb isotopic ages was conducted by R. Friedman at the Pacific Centre for Isotopic and Geochemical Research at the Department of Earth and Ocean Sciences, University of British Columbia.

On Iron Mountain, sample 08LDi 7.4 was collected from dacitic crystal-ash tuff that is conformably overlain by a relatively thin interval of interlayered limestone and calcareous sandstone containing an assemblage of bivalves and ammonoids that were collected for identification. At Castillion Creek, sample 08LDi 32.1 was taken from the base of a stratified section with siliceous sinter, the sample originating from a rare, rhyolite ash tuff that occurs as a 20–60 cm thick layer within a black limestone-mudstone bed.

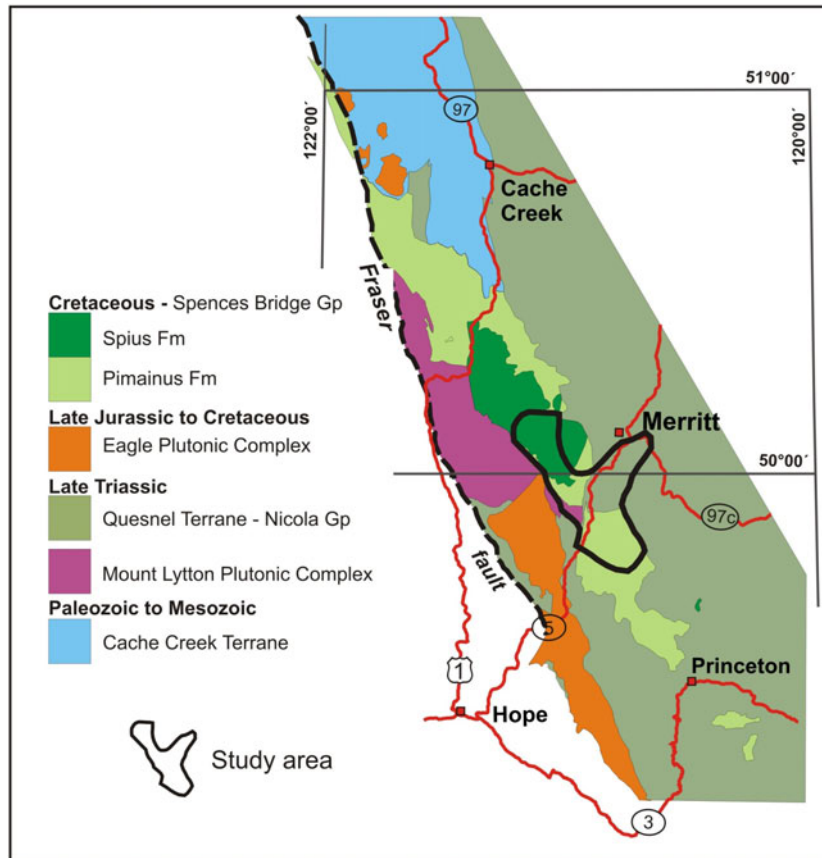


**Figure 1.** Regional geological setting of the Spences Bridge Group and location of the project area in southwestern British Columbia.

A solitary bivalve was recovered from these calcareous rocks and sent for paleontological identification.

The felsic volcanic rocks from both localities yielded identical Late Triassic (Carnian) U-Pb zircon ages of  $224.6 \pm 0.9$  Ma at Iron Mountain and  $224.5 \pm 0.3$  Ma at the Castillion Creek sinter. Fossil identifications corroborate these isotopic ages. The Iron Mountain macrofossil collections are considered to be Late Triassic, with a possible Norian to Rhaetian age suggested (Haggart, 2008). At Castillion Creek, the Triassic bivalve *Halobia*, species indeterminate, was identified from the black limestone-mudstone unit (M. Orchard, Geological Survey of Canada, pers comm, 2008). The western felsic facies (belt) of the Nicola Group has also been dated north of Merritt, where it gives a similar U-Pb zircon age of  $222.5 \pm 1.4$  Ma (Moore et al., 2000). Isotopic ages for the felsic rocks suggest that they, and accompanying sedimentary stratigraphy at Iron Mountain and Castillion Creek, are time-stratigraphic equivalents.

### **Early and Late Cretaceous Spences Bridge Group**

Thorkelson (1986) mapped the Spences Bridge Group within a 250 km<sup>2</sup> area from Shovelnose Mountain northwest to the confluence of Prospect and Spius creeks. This area straddles the Coquihalla Highway, about 25 km south of Merritt. Near Gillis Lake, stratified mid-Cretaceous rocks are particularly well exposed, and they figured prominently in formal definition and subdivision of the Spences Bridge Group in southwestern BC (Thorkelson and Rouse, 1989).

Our geological mapping overlaps Thorkelson's original work and maintains usage of his stratigraphic divisions, Pimainus and Spius formations, for the Spences Bridge Group. This study consists of 1:20 000 scale mapping and presently extends for about 50 km, from Shovelnose Mountain in the south, north-northwest through the Gillis Lake area to the Prospect Creek area in the northwest (Diakow and Barrios, 2008). Generalized stratigraphic sections, approximate thicknesses and contacts for stratigraphic units of the Spences Bridge Group between Shovelnose Mountain and Prospect Creek are shown in Figure 3, and the locations of these sections given in Figure 2.

This mapping provides stratigraphic refinements and a new U-Pb isotopic date for the Spences Bridge Group. Additional rocks were collected for U-Pb isotopic dating in 2008, but age determinations were not available for this report. These new dates will aid internal division and correlation within the Pimainus Formation and also constrain the age of the upper contact with the overlying Spius Formation.

### **PIMAINUS FORMATION**

The Pimainus Formation exhibits significant lithological diversity, in both its vertical stratigraphy and lateral facies variations, within the northwest-trending corridor mapped between Shovelnose Mountain and Prospect Creek. A somewhat continuous lateral view of the Pimainus Formation is evident in the transect from Prospect Creek southeast to the Gillis Lake area (i.e., Gillis Lake–Prospect Creek transect). At Gillis Lake, the Pimainus Formation is well stratified, inclined northeast and estimated to be about 1200 m thick. Immediately east-southeast of Gillis Lake, stratigraphic continuity of the

Pimainus Formation is severed by the north-striking Fig Lake and Coldwater faults, which demarcate the Eocene Fig Lake graben. Within the graben, crossfaults separate blocks that progressively step down northward, generally resulting in Pimainus stratigraphy being exposed mainly in the south and Eocene rocks becoming progressively more extensive farther north. The Pimainus Formation continues southeast of the graben, apparently thickening to more than 2200 m at Shovelnose Mountain (i.e., Shovelnose Mountain transect). At Shovelnose Mountain, however, orientation of stratigraphy is difficult to ascertain because of the general lack of bedding attitudes and poorer exposure; therefore, comparative thickness estimates for the Pimainus Formation are more speculative. Furthermore, internal stratigraphic correlations of Pimainus rock units between transects is difficult. However, one particularly distinctive volcanoclastic unit can be correlated with relative certainty, and correlation is corroborated by U-Pb geochronology.

### **Gillis Lake–Prospect Creek Transect**

The most lithologically diverse Pimainus stratigraphy is found in a northeast-dipping section that underlies a northwest-trending ridge near Gillis Lake (Figure 4). These rocks represent a stratigraphic reference section utilized by Thorkelson (1986) in his redefinition of the Spences Bridge Group. Remapping the geology during this study reveals mainly subaerial flows and pyroclastic volcanic units (90%), interlayered with minor sedimentary intervals containing conglomerate and sandstone. In this area, the lower contact of the Pimainus Formation is probably a nonconformity with dioritic rocks of the Late Triassic to Early Jurassic Mount Lytton Plutonic Complex, although the contact was not observed.

Pimainus stratigraphy at Gillis Lake is subdivided into ten map units. Collectively, they are at least 1200 m thick in a continuous conformable section lacking faults. Along strike, these map units are juxtaposed by high-angle faults striking northeast. Farther northwest, they diminish to only three map units adjacent to Prospect Creek, where they are poorly exposed within a section estimated to be less than 600 m thick (Diakow and Barrios, 2008). The change laterally to a simplified stratigraphy is thought to reflect primary deposition, perhaps controlled by an irregular sub-Pimainus topography. In the Gillis area, the thicker and more varied rock succession probably accumulated within a topographic low that persisted throughout active volcanism. This is indicated by tuffs and lava flows that are separated by intervals of epiclastic rocks, including four distinctive conglomerate units and other locally derived, finer sandstone units containing plant debris.

### **Lava Flows and Ash-Flow Tuffs**

Initial deposits (unit G1) of the Pimainus Formation in the Gillis Lake–Prospect Creek transect consist of grey-green andesite, of which medium-grained flows containing pyroxene (1–3%) and plagioclase (25–30%) phenocrysts are most common. Amygdaloidal flows with small chlorite- and chalcedony-filled amygdules occur but are not common. Nearly identical andesite flows recur up-section above the basal andesite in unit G7. The basal andesite is sharply overlain by a rhyolitic pyroclastic unit (unit G4), averaging 100–150 m thick. This is an important stratigraphic marker within the Pimainus Formation, as it crops out throughout the Gillis Lake–Prospect Creek transect. It correlates, on the basis of consistent lithological

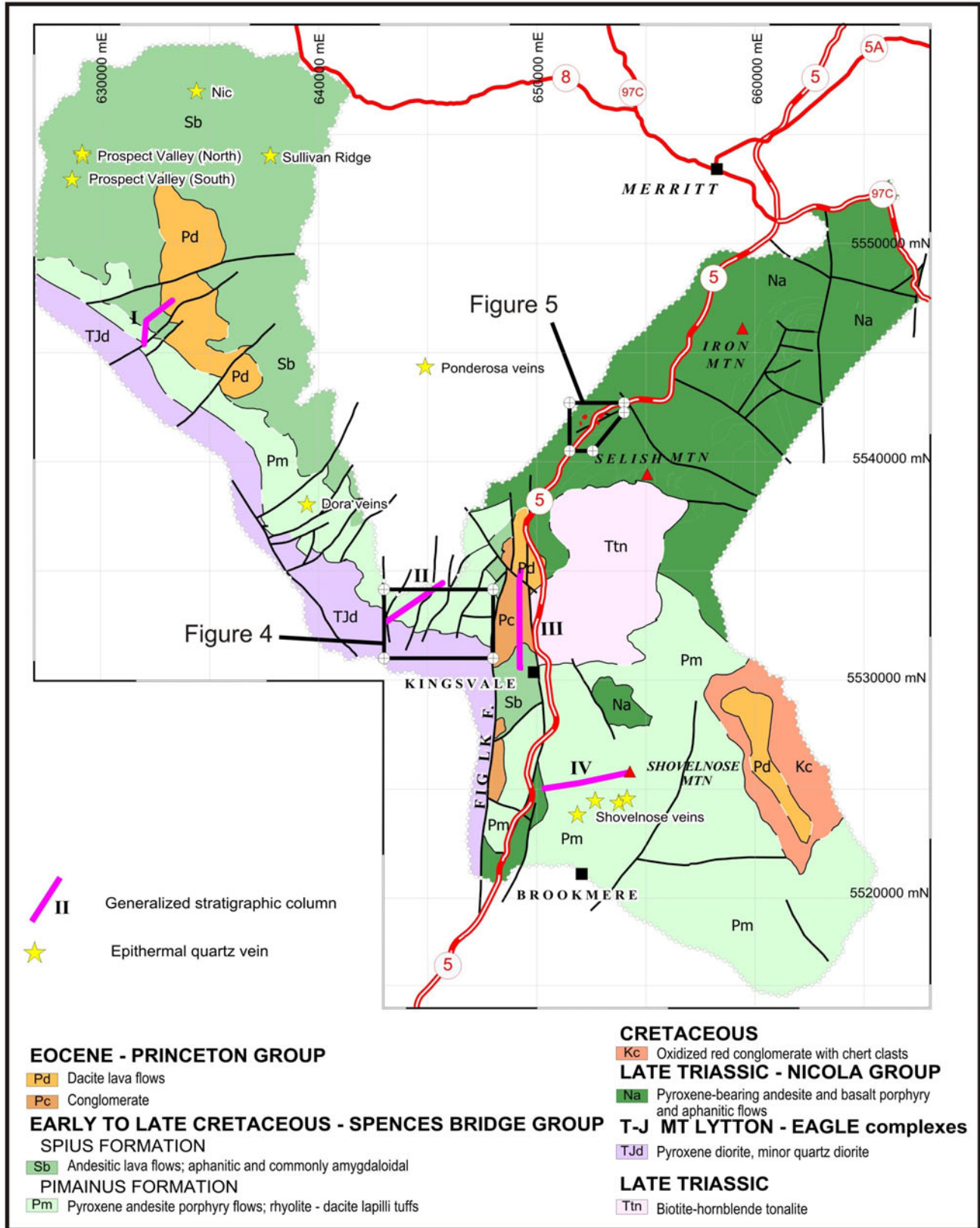


**Figure 2.** Generalized geology near Merritt, British Columbia, based on bedrock mapping in 2007 and 2008. Locations of epithermal gold-quartz vein prospects discovered since 2002 are shown.

characteristics and U-Pb isotopic age, with the large volume of rhyolitic tuffs and associated rhyolite flows underlying the lower slopes of Shovelnose Mountain (Diakow and Barrios, 2008, units PS3 and PS4). The appearance of this unit varies considerably from incompetent and rubbly weathered to indurated, massive structureless deposits that form a series of competent benches. It is distinguished by lithic pyroclasts that include light-coloured (generally whitish), clay-altered, aphanitic rhyolite; some flow-laminated rhyolite; and pink, medium-grained granitoid of

quartz monzonite to granodiorite composition. Quartz (1–2 mm in diameter) and scarcer biotite crystal fragments are widespread but can be easily overlooked owing to their small size and trace abundances. Fragments within the tuff are generally sorted and less than 2 cm in diameter, although tuff breccia sometimes alternates with lapilli tuff with or without sparse blocks. Rare charred logs, several metres long, have been observed in the unit near Prospect Creek. Tuffs from unit G4 are interpreted as a nonwelded rhyolite ash flow or ignimbrite.

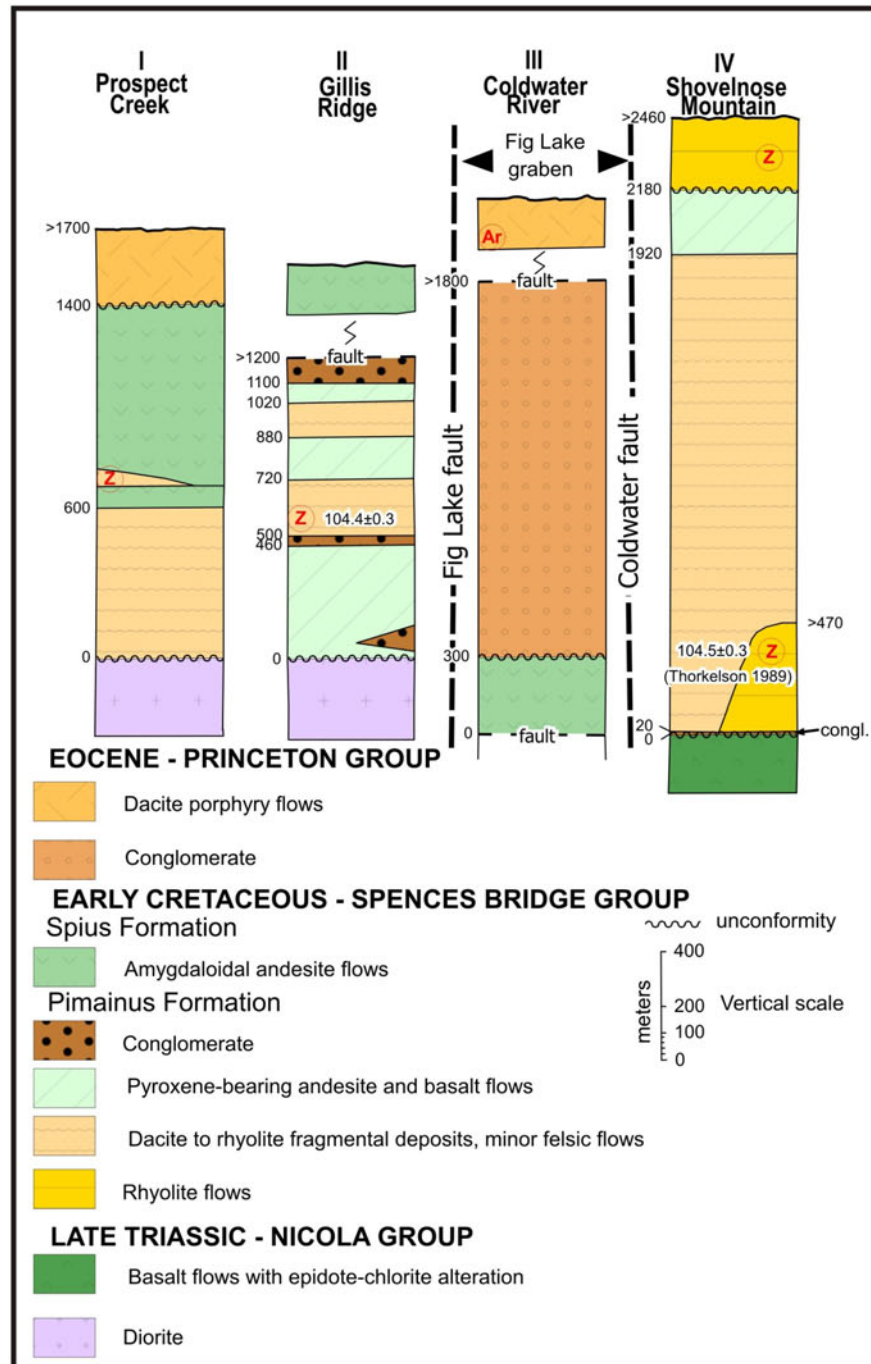
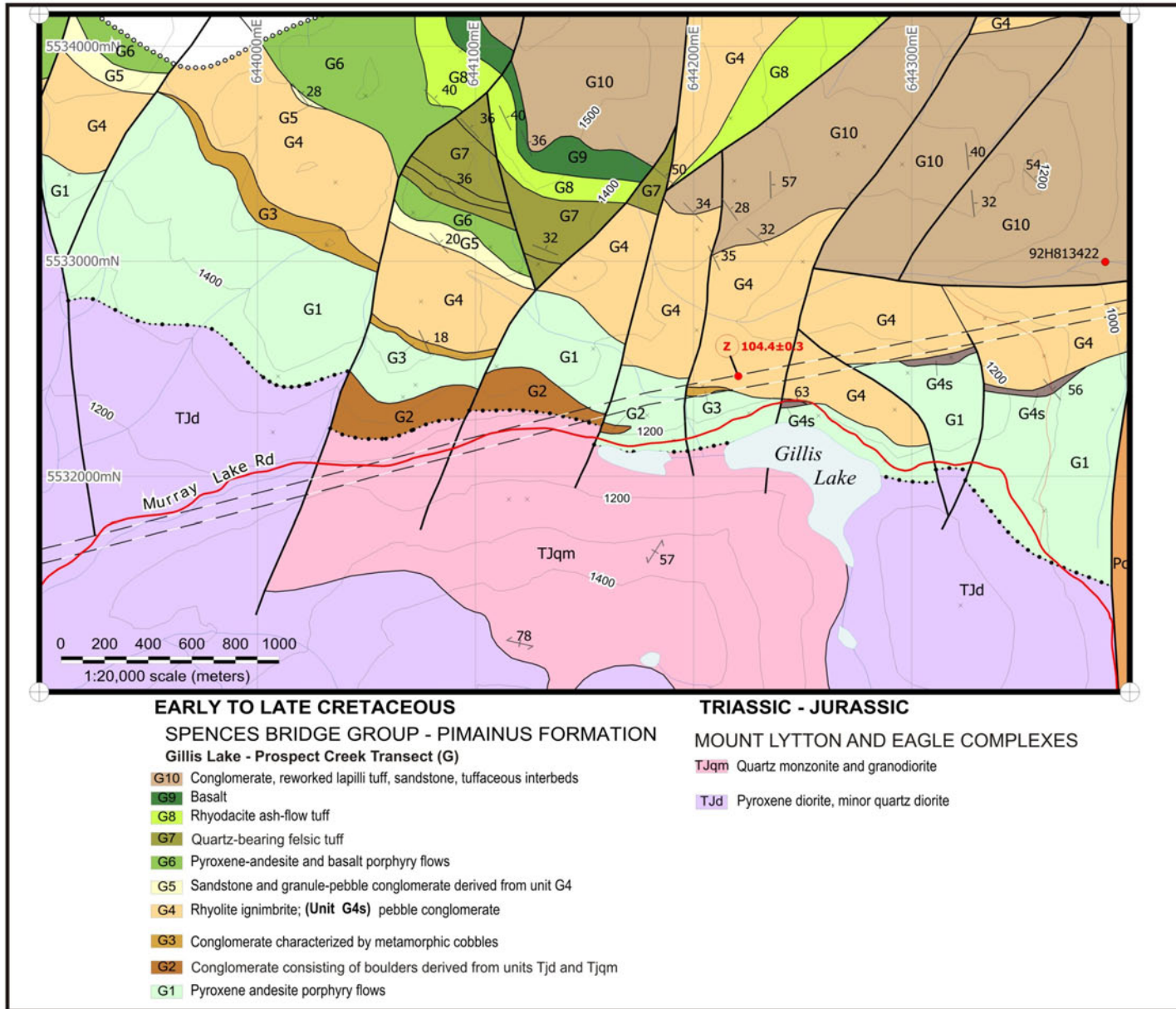


Figure 3. Generalized stratigraphic sections for rocks of the Spences Bridge Group between Shovelnose Mountain and Prospect Creek. Column locations are shown in Figure 2.



**Figure 4.** Detailed geology of the Pimainus Formation, Spences Bridge Group, at a reference area near Gillis Lake, south of Merritt. Location of Gillis Lake area is shown in Figure 2.

Minor bedded tuffs containing crystals, ash and small lithic fragments form thin-layered deposits within the otherwise massive ash flows. Cuspate vitric shards, which attest to the presence of pumice, compressed pumice and resorbed quartz phenocrysts have been observed in thin section. Other layered rocks associated with the ash-flow tuffs consist of tuffaceous sandstone made up of crystal fragments, mainly plagioclase, quartz±biotite and small volcanic lithic clasts and carbonaceous plant debris. Discrete, fine lapilli tuffs may form subordinate layers within the volcanic-derived sandstone.

A second ash-flow tuff unit (unit G8) occurs near the top of the Gillis Lake section. It occurs above pyroxene-phyric andesite (unit G7) and, in turn, is overlain by columnar-jointed basalt (unit G8) that displays a distinctive orange-brown spheroidal weathered surface. This tuff unit is distinguished from those lower in the section by monomictic juvenile lapilli and blocks composed of reddish, sparsely plagioclase-porphyrific and flow-laminated rhyodacite. Rhyolite lava flows, presumed to represent small domes or facies related to this pyroclastic flow, occur at two localities in the transect, one of which has been examined for gold mineralization (*see* 'Dora Prospect' section).

### **Conglomerate and Sandstone**

Differentiating sequentially younger and lithologically similar andesite lavas and felsic ash-flow tuff units in the Gillis Lake–Prospect Creek transect is facilitated by four distinctive conglomeratic beds dispersed at successively higher levels in the stratigraphy. The stratigraphically lowest conglomerate (unit G2) is best exposed in resistant bluffs west of Gillis Lake, where it is about 150 m thick and apparently overlies intrusive rocks concealed by colluvium in the valley. This lenticular body is partly enclosed laterally by andesite lavas from unit G1. One additional isolated exposure of the same conglomerate was found to the northwest near the upper contact of diorite with andesite, suggesting that the unit is laterally discontinuous, its distribution controlled by surface irregularities in the underlying plutonic basement. Conglomerate from unit G2 is crudely layered and composed of poorly sorted angular and subrounded boulders up to 2.2 m in diameter. The clasts have local provenance, derived from diorite and quartz monzonite phases of the Mount Lytton Plutonic Complex and underlying pyroxene-phyric andesite flows of unit G1.

The next highest conglomerate (unit G3) occurs at the contact between unit G1 andesite and overlying ash-flow tuff of unit G4. Unit G3 is a maximum of 60 m thick, pinching out over a distance of 4 km along strike. It is a polymictic cobble and boulder conglomerate composed mainly of well-rounded metamorphic clasts, dominated by foliated, intermediate composition granitoid; lesser greenschist, metasandstone and quartzite; rare schist; and locally abundant vein quartz. Evidently, the provenance of this conglomerate is an exhumed metamorphic terrain. A potential source area might be the Nicola horst, 50 km northwest, where a marginal belt, composed of metamorphic rocks broadly similar to those found in the conglomerate, has been reported (Erdmer, et al., 2002, 'Bob Lake assemblage').

Upsection, epiclastic rocks reappear as relatively thin but widespread sandstone and interbedded conglomerate (unit G5) occurring at the top of unit G4 ash-flow tuffs. A

marked change in clast types occurs in unit G5 along strike between Gillis Lake and Prospect Creek. Closer to Gillis Lake, it exhibits planar, locally crosslaminated beds of feldspar-rich sandstone and pebble-granule and local boulder conglomerate containing detrital grains of quartz, traces of biotite and rhyolitic clasts, which are indicative of erosion of the underlying ash-flow tuffs. Farther northwest, however, these rocks are supplanted by sandstone and conglomerate (Diakow and Barrios, 2008, unit G5c) dominated by granitoid clasts. In order of abundance, the clasts include diorite, quartz diorite, granodiorite and mylonitic quartz monzonite that resemble intrusive phases mapped immediately to the southwest in the Mount Lytton Plutonic Complex. Rare pebbles of vein quartz and biotite schist have also been found. Unit G5c is particularly well exposed along part of Prospect Creek, where drab olive-green sandstone forms lenses and thick beds interlayered with conglomerate in a cliff section rising about 80 m above creek level. Bedding is thick, with parallel and internal cross-bedding sometimes observed. Wood and plant debris is common everywhere within sandy layers in units G5 and G5c.

The stratigraphically highest conglomerate (unit G10) forms the top of the Gillis section. It contains numerous mauve, sparsely plagioclase-phyric rhyodacite cobbles that resemble underlying pyroclastic flow unit G8. It also contains significant interbedded sandstone, some displaying large-scale planar crossbeds. It is estimated the this unit might be several hundred metres thick, although faults are suspected. The conglomerate appears to pass imperceptibly into a thick, mixed unit composed of reworked and primary lapilli tuff beds at the top of the ridge north of Gillis Lake.

### **Shovelnose Mountain Transect**

The Shovelnose Mountain transect covers the general region extending east from the Coldwater fault to Voght valley road and south from Kane valley road to Brookmere road. In this region, stratigraphy of the Pimainus Formation is generally equivalent to that mapped in the Gillis Lake–Prospect Creek transect (for map units cited here for the Shovelnose transect, *see* Diakow and Barrios, 2008). In the Shovelnose area, however, Pimainus stratigraphy does not exhibit the diversity and sequential stratified order observed in the Gillis Lake–Prospect Creek transect. The most notable general stratigraphic difference between these transects is the considerable increase in thickness of the Pimainus Formation, due mainly to substantially greater volume of felsic fragmental rocks, particularly rhyolite lava flows, and greatly reduced epiclastic deposits in the Shovelnose section. Furthermore, stratigraphic contacts in the area are poorly defined and irregular, commonly exemplified by rhyolitic rocks that are bulbous in outline.

The base of the Pimainus Formation is believed to be an unconformity, based on contact relationships near Seymour Lake, just north of Kane valley road. Previous mapping placed a fault between the Late Triassic Coldwater pluton and the Spences Bridge succession in this locality (Thorkelson, 1986; Monger, 1989). Although a direct contact with the pluton was not observed, a small isolated exposure of conglomerate with rounded clasts of the pluton and a consistent curved contact between the pluton and overlying andesite flows (unit PS1) are adopted as indirect evidence for an unconformity. In addition, several outliers composed of similar andesite rest on the Coldwater pluton. The southern pluton margin can be placed as far south as

Voght Creek and, although it is largely concealed by overburden, the pluton crops out at creek level immediately east of the Coquihalla Highway. Between this granitic outcrop and a stratified section containing coal seams exposed along the highway, a distance of about 400 m to the south, scant evidence for a fault contact exists and the preferred interpretation is that of a nonconformity.

A stratified section along the Coquihalla Highway south of the Coldwater pluton is unique in the study area. It is distinguished by two intervals, each about 40 m thick, composed of interlayered coal beds, up to 0.5 m thick, alternating with sandstone and minor pebble conglomerate (unit PS1c). The lowest coal bed rests on pyroxene andesite flows and the uppermost coal is depositionally overlain by dacitic lapilli tuffs containing aphanitic andesite fragments and trace amounts of quartz. The area between the coal intervals is occupied by a coarse epiclastic deposit about 75 m thick. It is composed of boulder-size clasts of sandstone and lesser amygdaloidal andesite that protrude from a more recessive matrix made up of friable sandstone, coal chips and pebbles. The stratigraphic position of this unusual section within Pimainus stratigraphy is uncertain; however, because of its character and bounding volcanic rocks, it is interpreted as a lenticular deposit that has limited extent within the pyroxene andesite lava sequence of unit PS1.

Andesite flows of undetermined thickness, assigned to unit PS1, are widespread adjacent to Kane valley road and are believed to occur at the bottom of mid-Cretaceous stratigraphy at Shovelnose Mountain. Their lithological characteristics and speculated low stratigraphic position are perceived to be comparable to those of unit G1 in the Gillis Lake–Prospect Creek transect. These flows have grey-green colouration and typically exhibit porphyritic textures imparted by 25–30% medium-grained plagioclase and several percent or less pyroxene phenocrysts that often have a dull appearance due to partial replacement by chlorite. Rare amygdaloidal flow members have been observed. Celadonite is widespread along with chalcedonic silica, filling fractures in the andesite.

Up section, andesite of unit PS1 is apparently overlain by sedimentary rocks of unit PS2. Outcrops are scattered at low elevation east of the Coldwater River and generally concealed by overburden, whereas exposure improves on a hill north of Shouz Creek. An isolated occurrence of conglomerate farther south along the old CP rail bed, underlying rhyolite, may mark the southern extent of this sedimentary unit. The conglomerate contains numerous dark andesite clasts resembling the Nicola Group, and quartz-rich sandstone. An exposure along the Coquihalla Highway, about 750 m north of Coldwater Exit 256, is typical of the finer conglomerate and sandstone belonging to unit PS2. Conglomerate and sandstone of this unit are dominated by rounded cobbles and pebbles composed mainly of porphyritic andesite and sparsely plagioclase-phyric dacite. Pink granodiorite and biotite-tonalite pebbles and small cobbles are a minor component but are a characteristic and widely distributed feature of the unit. Sandstone contains abundant angular plagioclase and locally diagnostic quartz and biotite. Plant debris is widespread in most of the finer grained beds. In spite of very different lithic components, unit PS2 is believed to correlate in terms of stratigraphic position with unit G2 in the Gillis Lake–Prospect Creek transect.

Rhyolitic crystal-lithic tuff with associated sandstone and granule conglomerate containing felsic volcanic detri-

tus occupy a relatively thin outlier depositionally above unit PS2 north of Shouz Creek. This felsic tuff, designated unit PS4, and minor sedimentary rocks of unit PS4s apparently extend southward at low elevation through Shovelnose Mountain, the former unit thickening dramatically where it underlies much of the lower, southerly-facing slope. Internally, this tuff changes character over short distances, although the general dacite to rhyolite composition of the unit is maintained. Exceptions are where less voluminous volcanic rocks are interspersed and clearly contrast with the surrounding lapilli tuffs. For example, rhyolite flows (unit PS3) and pyroxene andesite (unit PS4a) sometimes display highly discordant contacts with the tuffs. Due to the relatively poor exposure and lithological variability in unit PS4, there was no representative section recognized during this study.

Unit PS4 is composed primarily of tuffs containing a variety of different fragment compositions. Felsic lapilli, typically in shades of off-white with aphanitic textures and less commonly flow laminated, are widespread and diagnostic; however, they are not necessarily the most abundant fragments. They are usually accompanied by varying proportions of green aphanitic and porphyritic andesite and mauve dacite, and sparse but widespread pink quartz monzonite fragments. Generally the tuffs are sorted and composed mainly of subangular to subrounded lapilli and few blocks. The tuff matrix is composed of crystal fragments dominated by plagioclase, quartz and commonly trace quantities of biotite. Commonly, the tuffs form resistant, massive, indurated beds where the fragments protrude from a recessive matrix. Welded fabrics were rarely observed.

Rhyolite lava flows rise from the level of the Coldwater River more than 400 m up the west-facing slope of Shovelnose Mountain (units PS3 and PS3r). They conformably overlie subhorizontal conglomerate and sandstone from unit PS2, and the apparent contact with adjacent unit PS4 tuffs is steep, giving the rhyolite the appearance of a flow dome. The rhyolite rises in a series of cliffs made up of dense, laminated flows. Vertical standing columns 60 m high occupy a zone locally at the base of the unit. Typically, the rhyolite is mauve, finely flow laminated and plagioclase porphyritic. Original glass in the rocks is replaced by small ovoid spherulites that are scattered and coalescing as they overprint flow laminations in specific layers. The mineralogy changes in rhyolite higher in the pile with the addition of minute quartz, biotite and possible slender hornblende prisms, none of which exceed 1% of the rock. Surprising is the absence of flow breccia and talus breccia. Only in a similar rhyolite unit southeast of Shovelnose Mountain is monolithic breccia associated with these lavas.

A second, homogeneous rhyolite flow unit (PS6) is found at the top of Shovelnose Mountain. It extends as a continuous sheet from the summit partway down the north slope, then turns southeast, tapering as it loses elevation to its present terminal position astride the Brookmere road. The original distribution of the unit might have been more extensive, possibly extending over much of the southern slope of the mountain where similar rocks presently crop out in a cluster of prominent knolls. These scattered exposures of rhyolite are speculated to represent remnants of a continuous rhyolite capping that existed above 1300 m elevation on the mountain. Thickness estimates for rhyolite vary from 150 to 250 m, inferred from sections at the summit.

The lower contact of the rhyolite might be an unconformity. The most compelling field evidence in support of an unconformable relationship is from a knoll approximately 4 km southeast of the Shovelnose summit. Here, rhyolite flows have a subhorizontal base, overlying a gentle northeast-inclined succession made up of older Pimainus rocks (units PS1, PS3 and PS4). Moreover, a window through the rhyolite northeast of the summit reveals boulder conglomerate directly beneath the rhyolite. This conglomerate contains well-rounded clasts up to boulder size that are composed of porphyritic andesite and dacite. Nearby, another isolated conglomerate exposure has rounded cobbles admixed with angular flow-laminated rhyolite blocks in a breccia, suggesting that flows apparently overrode loosely consolidated conglomerate.

Rhyolite from unit PS6 is best viewed along the access road to the summit of Shovelnose Mountain. Columns form a cliff a short distance southeast of the summit. Typical exposures of the rhyolite are mauve with fine, reddish flow laminations and 10–15% medium-grained plagioclase phenocrysts. The laminations vary significantly in attitude within individual outcrops and commonly outline internal flow folds. The characteristic mauve colour of the rocks is modified by incipient supergene alteration, evident as irregular patches and streaks composed of whitish clay minerals. Weathering and alteration are accompanied by the development of a narrow-spaced parting that is oriented parallel to flow laminae.

## **SPIUS FORMATION**

The Spius Formation is characterized by a thick, monotonous, andesite flow succession. In the study area, these lava flows crop out from within the Fig Lake graben, and also to the northwest where they overlie the Pimainus Formation in the Gillis Lake–Prospect Creek transect. This transect marks the southeastern limit of these flows, which extend regionally towards the northwest, blanketing an area nearly 10–15 km wide by 70 km long (Monger and McMillan, 1989). This region corresponds to the Nicoamen Plateau, a highland situated between the Nicola River to the east and, in part, the Fraser River to the west, and the hamlet of Spences Bridge to the north.

Thorkelson (1986) recognized the gradational nature of the contact between the Pimainus and Spius formations as being indicated by pyroxene andesite porphyry lavas or welded and crystal tuff, common in the Pimainus, interleaved with aphanitic and amygdaloidal andesite lavas diagnostic of the overlying Spius. Alternation of the pyroxene andesite porphyry and thinner amygdaloidal flow members can take place over hundreds of metres in elevation, as observed during this study in semicontinuous lava exposures west of Spius Creek. In this transitional contact zone, we mapped the bottom of the Spius Formation, where multiple, aphanitic or amygdaloidal flows produce brownish-weathered, rounded, low-relief exposures of fine rubble and soil. An unambiguous gradational contact is located along Prospect Creek. The lowest flows of the Spius Formation sharply bound an interbed, 30 m thick, composed of lithic-crystal tuff. Microscopically, the tuff is dominated by pumiceous lithic fragments, cusped vitric shards and 1–3% resorbed quartz-crystal fragments. It is undoubtedly related to rhyolite pyroclastic flows assigned to unit G4 of the Pimainus Formation that crop out downslope, beneath the lowest Spius flows. The tuff was sampled in 2008 for U-Pb

isotopic dating to determine timing for the onset of Spius lava eruptions.

East of the confluence of Prospect and Spius creeks, the lower contact of the Spius Formation, exposed in a roadcut, is sharp and identified by 6 m of conglomerate. Flows underlying the conglomerate, consisting of moderately to coarsely plagioclase-pyroxene-phyric andesite, have been assigned to the Pimainus Formation. Those above the conglomerate consist of aphanitic and amygdaloidal andesites and have been assigned to the Spius Formation.

From a distance, sections of the Spius Formation exhibit individual lava flows tens of metres thick stacked in parallel succession. Good exposures of this massive layered nature can be viewed from vantages along the Patchett road, looking west towards the intersection of Prospect and Spius creeks. Similar, thickly layered, gently inclined lava flows occur throughout the more remote northwestern part of the study area. The Edgar Creek and Hooshum logging roads provide access into this area. The Spius Formation is overlain above a subhorizontal unconformity by volcanic rocks of the Eocene Princeton Group.

Spius flows that usually appear well layered and gently inclined from a distance are massive with bedding difficult to discern at outcrop scale. Within any individual flow member there are, however, noticeable colour and small-scale textural variations. Brown shades are common for weathered surfaces and red-maroon shades when the surface is oxidized. Fresh rocks are typically drab grey-green. The texture of flows varies greatly, ranging from aphanitic, with and without sparse pyroxene phenocrysts, to finely to moderately pyroxene-plagioclase phyric, to amygdaloidal, in which the concentration, shape, size and composition of amygdules vary. Amygdules range from round to elongate and are filled most frequently with white quartz, chlorite and, less commonly, zeolite. The aphanitic flows display a honey yellow colour and granular texture. Interflow breccia forms irregular lenticular layers, generally oxidized and just a few metres thick. Geodes ranging up to 10 cm, and rarely to 60 cm, lined with quartz-calcite druse or completely filled with laminated greyish white agate or radiating zeolite, were found in the flows.

## **Age of the Spences Bridge Group**

Thorkelson and Rouse (1989) reported a number of K-Ar ages on whole-rock samples collected from the Spences Bridge Group near Merritt. Seven overlapping dates for the two formations range from about 94 to 79 Ma with errors of 3 Ma (1 $\sigma$ ). Based on identified palynomorph assemblages, Thorkelson and Rouse (1989) favoured a “late Albian assignment for the Pimainus Formation as well as the Spius Formation.” Thorkelson sampled rhyolite of the Pimainus Formation at Shovelnose Mountain for a U-Pb zircon date, appending the date of 104.5  $\pm$  0.3 Ma in Thorkelson and Rouse (1989). Although the geological context for the dated rhyolite was not presented in their paper, we suspect it is derived from the rhyolite dome mapped on the lower west side of the mountain, a body designated as either unit PS3 or unit PS3r in Diakow and Barrios (2008). In our mapping, this rhyolite is found stratigraphically low within the Pimainus Formation, and it represents a coherent flow facies associated with a more extensive felsic fragmental facies assigned to unit PS4.

Farther northwest near Gillis Lake, a fragmental unit (unit G4) containing felsic lithic and crystal pyroclasts similar to those in unit PS4 is correlative. In the Gillis Lake–Prospect Creek transect, these felsic deposits were interpreted as a nonwelded, low-volume, lithic-rich ash-flow tuff mapped close to the bottom of Pimainus stratigraphy. A U-Pb zircon date of  $104.4 \pm 0.3$  Ma (Albian) from this unit confirms a time-stratigraphic relationship with the topographically low felsic flows and fragmental succession at Shovelnose Mountain.

A topographically higher succession of rhyolite flows (unit PS6) drapes the summit of Shovelnose Mountain, apparently in an unconformable contact with the underlying felsic succession that includes dated Albian rhyolite. A rhyolite flow at the summit of Shovelnose Mountain was sampled (sample 08LDi 59.1) for a U-Pb isotopic age to determine if these extensive flows are part of the Pimainus Formation and, if so, to establish the duration of rhyolitic eruptions.

The gradational contact relationship observed between the Pimainus and Spius formations, manifested as coalescing felsic tuffs and amygdaloidal andesite flows, suggests that these distinctive rock units erupted in rapid succession. Onset of the massive effusive flow event that characterizes the Spius Formation will be established by U-Pb dating of sample 08LDi 14.3, which was collected from rhyolite vitric tuff of the Pimainus that occurs as an interbed, 30 m thick, between amygdaloidal flows at the base of the Spius Formation. Direct dating of the Spius Formation is difficult because of alteration and lack of suitable minerals. A black andesite glass with conchoidal fracture, the freshest lava encountered in the Spius Formation, was sampled for a whole rock  $^{40}\text{Ar}/^{39}\text{Ar}$  date (sample 08LDi 57.1). This flow is just one of many very thick planar flows comprising a homoclinal, northeast-dipping succession dissected by Teepee Creek in the northwestern part of the map area, where they host gold-bearing quartz veins at the Prospect Valley showings.

### **Early Cretaceous (?) Conglomerate (Unit Kc)**

A subhorizontal conglomerate unit is exposed intermittently in an area of at least  $21 \text{ km}^2$  east of Shovelnose Mountain, where it is estimated at between 60 and 180 m thick. This conglomerate crops out consistently adjacent to rhyolitic rocks that are tentatively assigned to the Early Cretaceous Spences Bridge Group; however, because these rock successions have not been observed in direct contact, the exact nature of the lower contact is uncertain. The top of the conglomerate unit is defined by a sharp depositional contact with the remnants of a flat-lying Eocene hornblende-dacite flow unit. The conglomerate weathers recessively and its presence in areas of poor exposure or subcrop is indicated by distinctive reddish brown soil.

The conglomerate is polymictic, generally dominated by cobble-size clasts that are supported by a matrix composed of sand and granules. The clasts are typically well rounded, oxidized red and composed of a variety of volcanic porphyries, some quartz bearing, fewer granitoid and locally abundant greyish, off-white and black chert. Sandstone containing subordinate pebbles and fewer cobbles forms interbeds within the coarser conglomerate, imparting a diffusely layered appearance in some exposures.

Preto (1979) described similar conglomeratic rocks (his unit 9) and showed their distribution northeast of the present study area, where they are either localized adjacent to major faults or occupy a medial stratigraphic position between Late Triassic Nicola Group and rocks presumed to be equivalent in age to the Early Cretaceous Spences Bridge Group.

### **Eocene Princeton Group**

Eocene volcanic rocks in the vicinity of Merritt have been mapped as part of the Princeton Group, distinguished by the presence of slender hornblende phenocrysts (Monger and MacMillan, 1989). Eocene rocks in the study area consist mainly of lava flows with a thick, subhorizontal, hornblende dacite porphyry flow sequence, more than 300 m thick, occupying a ridge north of Prospect Creek (unit Pd). The lower contact of this sequence with underlying andesitic lavas of the Spius Formation is a disconformity along which there is no evidence of erosion. A similar dacite flow unit crops out 24 km farther southeast, forming a series of isolated dome-like mounds scattered over 10 km. These isolated outcrops are interpreted to represent resistant remnants of a solitary lava flow that was deposited above oxidized red conglomerate of unit Kc.

The dacite forms thick homogeneous sections in which columns and autoclastic breccia locally contrast with typical massive, diffusely layered exposures. Platy parting in these lavas produces flaggy weathered debris. They are light grey to greyish green and exhibit porphyritic texture, dominated by 10–15% medium-grained plagioclase and up to 5% slender hornblende. In dacite flows north of Prospect Creek, pyroxene is abundant as microscopic grains in addition to hornblende.

Eocene volcanic rocks, associated with significant sedimentary rocks, occupy part of the Fig Lake graben, where they unconformably rest on rocks of the Spences Bridge Group (Thorkelson, 1989). As in adjacent regions, hornblende-phyric dacite flows dominate with subordinate, underlying, black, glassy aphanitic andesite. These dacite flows are distinguished by local flow lamination and ubiquitous, albeit sparse, quantities of biotite and quartz, in addition to prominent hornblende phenocrysts.

Sedimentary rocks of unit Pc form a significant proportion of graben fill north of Kingsvale. They are believed to underlie nearby dacitic flows; however, a stratigraphic contact has not been found and several fault strands appear to juxtapose the units. The sedimentary rocks are mainly conglomerate, with scarce finer clastic interbeds, that are estimated at more than 1800 m thick in a gently northward-dipping section exposed, in part, along the Coldwater River. Crude, thick layering within the conglomerate is sometimes accentuated by sandstone to fine conglomerate interbeds. Clasts display grading and local imbrication, suggesting fluvial transport and deposition.

The conglomerate is polyolithic and poorly sorted, containing well-rounded clasts up to 30 cm in diameter that are supported by a friable matrix composed of abundant quartz and potassium-feldspar grains. The clasts include abundant white vein quartz and granitoid, a variety of porphyritic andesite and rhyolite, and scarce jasper and schist. Some granitic clasts are distinctive, recognized as phases that form the Mount Lytton Plutonic Complex, located just a few kilometres southwest. These include chlorite-altered granodiorite–quartz monzonite with bluish translucent

quartz, foliated diorite and sparsely porphyritic rhyolite, which is a late dike phase.

## INTRUSIVE ROCKS

### **Late Triassic Diorite (Unit Td)**

Small, isolated dioritic bodies enclosed by Nicola Group strata are thought to be Late Triassic in age. The pluton near the top of Iron Mountain consists of medium- to coarse-grained gabbro and diorite, whereas a cluster of plugs southeast of Selish Mountain consists of fine-grained diorite, one of them displaying a sill-like relationship with volcanic rocks.

### **Late Triassic Coldwater Pluton (Unit Ttn)**

The Coldwater pluton crops out in an area of approximately 40 km<sup>2</sup> east of the Coldwater fault, between Selish Mountain in the north and Voght Creek in the south. The intrusion passively invades and causes minor bleaching in adjacent rocks of the Late Triassic Nicola Group, particularly along its subhorizontal northern contact. Similar thermal alteration is also evident in a screen of Nicola volcanic rocks mapped farther south. The southern and southeastern contact of the pluton is thought to be a nonconformity with overlying volcanic rocks assigned to the Early Cretaceous Spences Bridge Group. There are mainly pyroxene-phyric andesite flows, but a solitary exposure of polymictic conglomerate at the base of the succession near Seymour Lake contains tonalite clasts derived from the pluton. The pluton projects through thick gravel overburden in a few localities along Voght Creek and, at the westernmost outcrop, a strong shear fabric is developed adjacent to the Coldwater fault. Upstream, beside the Coquihalla Highway, outcrop of the intrusion at creek level marks the southernmost extent of the pluton. Immediately to the south of this locality, strata of the Spences Bridge Group are thought to drape the intrusion above a nonconformable contact. Here, exposed in steep cuts along the highway, the Spences Bridge consists of interbedded volcanic and sedimentary rocks, the latter containing intervals of coal.

The pluton is composed primarily of tonalite with a transition to quartz diorite in the north. Generally, the tonalite is light greyish white with a medium to coarse equigranular texture. The mafic minerals are dominated by fresh hornblende (20–30%) and biotite (2–5%). Biotite increases to 25% locally along the pluton margin.

Dikes crosscutting the tonalite are uncommon and typically narrow. They consist of pink, orange-weathered, fine-grained granite and rare diabase. At one locality along the pluton margin, pink aplite dikes project from the intrusion into bordering country rocks.

The pluton has produced several Late Triassic K-Ar dates (Preto et al., 1979). An unaltered tonalite collected during this study near the centre of the stock yielded an <sup>40</sup>Ar/<sup>39</sup>Ar cooling age on biotite of 212.7 ± 1.1 Ma, confirming emplacement of the Coldwater pluton in Late Triassic time.

### **Cretaceous (?) Plutons (Unit Kqm)**

Two quartz monzonite–granite bodies crop out near the top of Shovelnose Mountain. Despite being isolated

bodies 2 km apart, they have similar appearance and mineralogy, suggesting they might be apophyses of a larger pluton at depth. They are pink, coarse grained and equigranular, and contain chlorite-altered biotite as the primary mafic mineral. Pyroxene-bearing andesite of the Pimainus Formation is nearest the intrusions and lacks alteration. Because they are isolated plugs located well within Spences Bridge stratigraphy and in close proximity with rhyolite flows capping the Pimainus Formation on Shovelnose Mountain, a genetic connection is suspected.

### **Triassic–Jurassic Diorite and Quartz Monzonite (Units Tjd, Tjqm)**

Granitic rocks form a continuous border along the southwestern margin of the study area; based on regional mapping by Monger (1989), they apparently belong to two intrusive complexes that interface near the juncture of Maka and Spius creeks. These complexes are composed of broadly similar rocks but have differing emplacement ages and histories. The Mount Lytton Plutonic Complex comprises Late Triassic and Early Jurassic plutons, gneiss, amphibolite and mylonite that may represent deeper parts of the Late Triassic Nicola arc in Quesnellia (Monger, 1989). In contrast, the Eagle Plutonic Complex comprises predominantly deformed plutonic rocks that range in age from Middle Jurassic to mid-Cretaceous and maintain a record of contractional deformation at the western margin of the Intermontane Belt (Greig, 1991).

Diorite and lesser quartz diorite prevail on the ridge south of Gillis Lake and continue uninterrupted towards the northwest, underlying lower slopes adjacent to Maka and Prospect creeks. A less voluminous phase of quartz monzonite–granodiorite crosscuts the diorite and, in turn, they are both intruded by felsic dikes. Collectively, these granitoid bodies form an older base upon which rocks of the Spences Bridge Group locally lie.

Diorite to quartz diorite is the oldest intrusive phase recognized. It is grey-green and contains equigranular plagioclase, pyroxene (20–40%) and quartz in a medium-grained rock. Rare enclaves, several metres across, composed mainly of coarse pyroxene intergrown with less than 15% plagioclase, occur in the diorite. Epidote lining veinlets and chlorite replacing mafic minerals constitute weak alteration common throughout diorite. Quartz monzonite or granodiorite forms small plugs and narrow dikes intruding diorite. They are typically pinkish with a subtle green colouration due to secondary chlorite, and are coarse grained, inequigranular and weakly foliated. Bluish translucent quartz (20–25%) is diagnostic and occurs with up to 20% chlorite-altered mafic minerals. A foliation striking northwest and generally inclined southwest is prominent in both intrusive phases south of Gillis Lake; however, foliation is weak or absent elsewhere in the diorite. An intense penetrative foliation and mylonitic fabric are confined to a narrow, northwest-trending band of quartz monzonite that crops out intermittently adjacent to the fault along Maka Creek.

Nondeformed dikes, generally 1 m or less in width and rarely up to 60 m, crosscut foliated diorite and quartz monzonite phases. The dikes are pinkish to white, light orange weathered and of felsic composition. They exhibit textures varying from aphanitic aplite porphyry with up to 10% medium-grained potassium feldspar and biotite to quartz-feldspar pegmatite.

## MINERALIZATION

Two contrasting types of mineralized silica deposits are found in the study area. A new occurrence, characterized by stratiform and stratabound silica-carbonate horizons, has been discovered within shallow-marine stratified volcanic and sedimentary rocks of the Late Triassic Nicola Group. Named the 'Castillion Creek Exhalite-Sinter', they have a weakly anomalous signature for the epithermal suite of elements. No associated discordant epithermal quartz veins have been discovered. Narrow veins and veinlets with epithermal features are associated with Late Triassic subvolcanic (?) dacite, and tonalite of the Coldwater pluton (Diakow and Barrios, 2008, Table 2, samples c, d, aa, bb and cc). This suggests that high-level epithermal mineralization is possible in compositionally evolved rocks of Late Triassic age in areas where the western felsic belt of the Nicola Group crops out.

Currently, mining exploration in the Merritt region focuses on low sulphidation, epithermal gold-bearing quartz vein systems that are hosted in subaerial volcanic rocks of the Early Cretaceous Spences Bridge Group. The veins occur in differing host stratigraphies, those on Shovelnose Mountain in rhyolitic rocks of the Pimainus Formation and others, including Prospect Valley, Ponderosa, Sullivan Ridge and Nic, in the thick, andesitic flow sequence of the Spius Formation.

### **Late Triassic Castillion Creek Exhalite-Sinter Occurrence**

A Late Triassic hydrothermal system represented by stratiform silica-carbonate exhalites and sinter was discovered during the BC Geological Survey mapping survey in late 2007. This hydrothermal system and associated products are located along the Coquihalla Highway, near Castillion Creek, approximately 14 km south of Exit 286 at Merritt (Figure 2). Named the 'Castillion Creek Exhalite-Sinter', three subhorizontal siliceous zones, interlayered with Nicola Group volcanic and sedimentary rocks, are vertically stacked, with approximately 100 m elevation separating lower and upper exhalites. Sinter, superbly exposed in a roadcut, occupies a medial position relative to the exhalites. The local geology, with relative locations of siliceous horizons, is shown in Figure 5.

### **EXHALITE-SINTER CHARACTERISTICS**

Two silica exhalite horizons have sharp, conformable lower and upper contacts with both subaerial (?) mafic volcanic rocks and shallow-marine sedimentary rocks, and strike north-northeast and dip moderately southeast (~20–30°). The lower exhalite comprises two segments thought to be connected but separated by a vegetated gap. Each is composed of stratiform and stratabound silica. The southern segment is a series of resistant mounds composed of siliceous blocks, aligned along a low-lying ridge. Internally, finely laminated white and light grey silica, forming beds up to 11 cm thick, alternate with recessive carbonate layers several centimetres thick. Angular blocks of red jasperoid silica occur on the surfaces but they have not been observed *in situ*. A very old blast pit revealed chalcopyrite in fractures cutting across laminated silica, and vuggy silica in which irregular cavities are cored by sparry calcite surrounded by prismatic quartz. The northern segment is defined by semicontinuous silica subcrops traceable for

120 m and widest in a coherent layer 4 m thick. It displays lithological features resembling those in the southern segment.

The upper exhalite is a silica horizon expressed as a series of resistive mounds distributed for 500 m along a stratigraphic contact between fossiliferous black carbonate and overlying sandstone. A 200 m gap, caused by crossfaulting, breaks the continuity of the horizon. The silica layer is 1.5–3 m thick and composed of white and dark grey, internally laminated and massive silica. Finely disseminated pyrite is the only sulphide visible.

Sinter contrasts with the exhalites in dimension and appearance, attaining a strike length close to 300 m and a maximum thickness of 30 m at its northern limit, and thinning southward across a series of steep faults to around 1 m at the southern limit of cliff exposure along the Coquihalla Highway. Characteristically, the deposit is distinctly bedded, with silica beds being up to 0.5 m thick but typically thinner, and interlayered with orange-weathered, laminated siltstone and sandstone. The silica, a clear translucent variety, typically displays interlayer cavities, most of them irregular and some elongate parallel to layering. Finely disseminated pyrite is found in fine clastic interbeds. No discordant quartz veins have been found in the vicinity of the exhalites or sinter.

Chip samples collected from the exhalites and sinter were analyzed for a suite of elements by aqua regia digestion–ICP-MS at ACME Analytical Laboratories Ltd (Vancouver, BC). Table 1 is a summary of results extracted from original data given in Diakow and Barrios (2008). These data show that the epithermal suite of elements is weakly anomalous in Au, Ag, As and Hg. Sinter has significantly higher concentrations of Au, Mo, Mn, Hg and Ba than either of the exhalite zones. Silver is higher in the exhalites, the lower of which has higher average concentrations for all elements with the exception of Pb and Zn.

### **LOCAL GEOLOGICAL SETTING**

Nicola Group stratigraphy at Castillion Creek has a basal section dominated by mafic pyroxene-phyric lava flows that are abruptly overlain locally by flow-laminated rhyolite. The lowest exhalite horizon occurs within these flows. This flow unit persists upslope to the elevation of the sinter, where it forms the base for an overlying stratified volcano-sedimentary sequence, within which both sinter and the highest exhalite horizons occur.

The section of stratified rocks hosting sinter is about 30 m thick and lies directly on the underlying mafic volcanic unit. At the bottom of the section is 1.5 m of thinly bedded, grey-black limestone and mudstone that contains a 20–60 cm thick rhyolite ash-tuff interbed. A collection of bivalves was obtained from the limestone for identification, and a sample was collected from the rhyolitic tuff interbed for U-Pb zircon geochronology.

Depositionally overlying the thin carbonate is thickly bedded siltstone and coarse sandstone containing several percent disseminated pyrite grains. A massive pyroxene flow with a distinct lenticular geometry overlies these clastic rocks. Sinter immediately follows upsection, sharply overlying both the mafic flow and underlying clastic beds. The sinter is composed of silica and carbonate, forming thin beds and laminations that alternate with orange-oxidized calcareous siltstone, feldspathic sandstone and minor pebble conglomerate. Rare rhyolite ash tuff, up to 3 cm

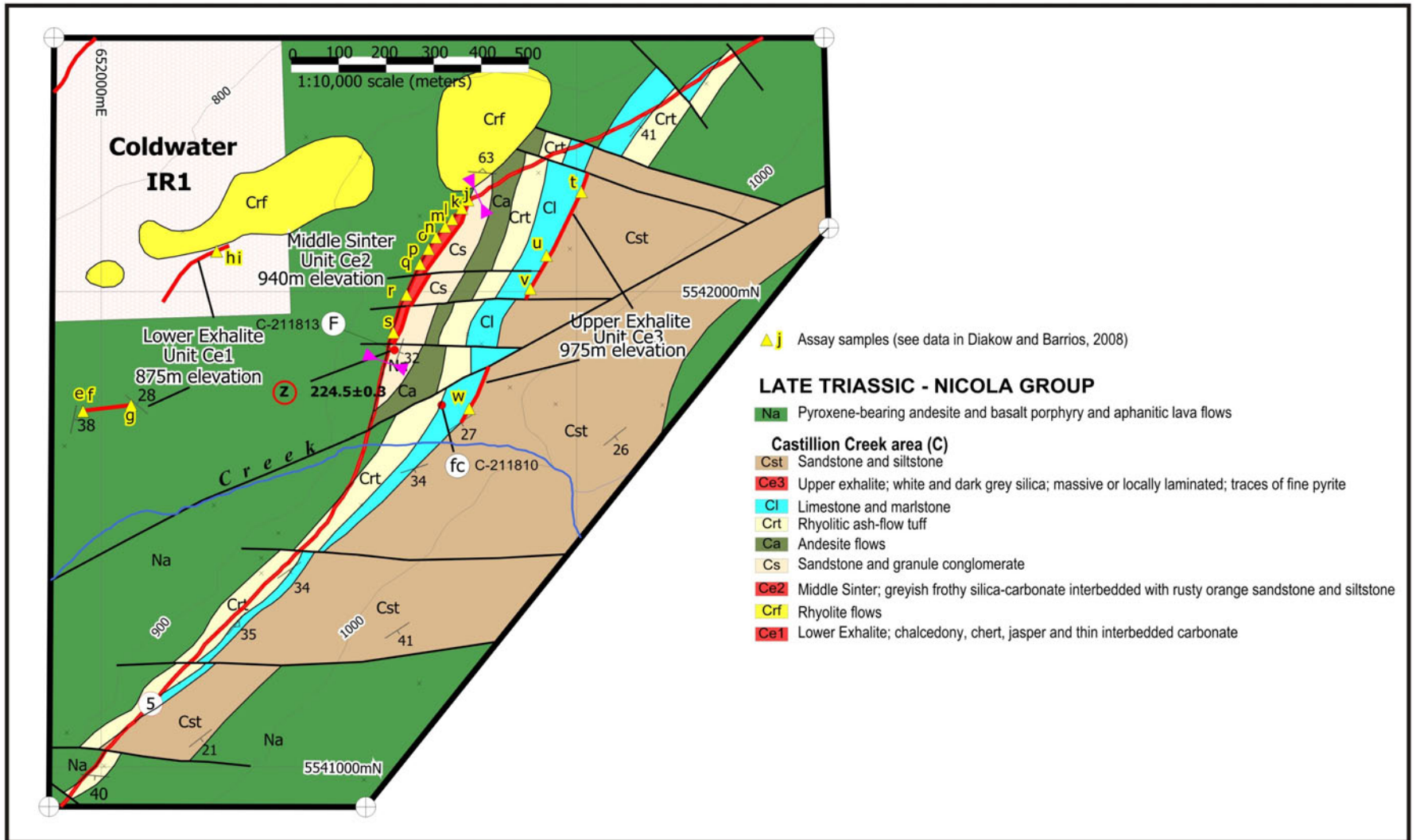


**Figure 5.** Detailed geology of the areas hosting exhalative zones near Castillion Creek. The exhalites are situated adjacent to the Coquihalla Highway within a stratified shallow-marine sequence composed of sedimentary and rhyolitic volcanic rocks of the Late Triassic Nicola Group. Location of Castillion Creek, south of Merritt, is shown in Figure 2.

thick, weathers off-white and occupies 0.5 m thick intervals within interlaminated silica and siltstone beds.

Above the sinter-sedimentary section are conformable volcanic rocks with pyroxene andesite overlain by rhyolite ash-flow tuff. The tuff contains angular white and greyish aphanitic and flow-laminated rhyolite fragments. The matrix is light green and contains an assortment of small lithic, feldspar and minor quartz fragments. Except for local thin zones that display moderate welded fabric, the deposit is generally nonwelded. Ash-flow tuff is succeeded by black limestone replete with recrystallized, thin-shelled bivalves. The highest siliceous exhalite sharply overlies limestone and is, in turn, followed upsection by a thick sedimentary unit. In the lower part of the section and sharply overlying the exhalite, parallel and crosslaminated sandstone and siltstone are interleaved with maroon lapilli tuff beds. Farther up the section, lapilli tuffs become more prevalent, and have thin accretionary lapilli interbeds. Still farther upsection, these volcanoclastic rocks pass into thick pyroxene-bearing flows occupying the mid-slope area of Selish Mountain.

The stratified section in the interval at and above the level of the sinter to the upper exhalite comprises distinctive rock types that can be traced for at least 2 km adjacent to the Coquihalla Highway. Throughout, bedding consistently strikes northeast and dips southeast at 20–30°. A series of parallel high-angle faults, oriented east-west, cut obliquely across the northeast-striking stratigraphy. In the sinter section, south-verging thrusts locally thicken the sinter horizon and underlying carbonate unit.

East-trending faults cutting post-Nicola stratigraphy have not been recognized in the study area. Curiously, there is a concentration of such structures at Castillion Creek and they delimit the lateral extent and internally shuffle the diverse stratigraphy and associated exhalative horizons. This leads us to speculate that these faults might have been active at the time of deposition and focused the hydrothermal fluids within a depositional environment that changed several times from subaerial to shallow marine.

An isolated siliceous exhalite, found 5.5 km southwest of Castillion Creek, is speculated to have developed at the same time as those at Castillion Creek. Exhalites at this locality are poorly exposed due to a thin mantle of overburden. Trenches were excavated at this locality many decades ago but are presently slumped and overgrown. Three samples collected for assays returned results comparable to those obtained from the Castillion Creek exhalites. These data are tabulated in Diakow and Barrios (2008).

## ENVIRONMENT AND AGE

Because no obvious depositional breaks were recognized in stratified rocks hosting the exhalite and sinter occurrences, it is assumed that deposition of the sequence was relatively continuous. Pre-sinter stratigraphy is dominated by massive pyroxene andesite flows, probably subaerial and periodically interrupted by submarine silica-carbonate exhalations. Unequivocal evidence for marine conditions begins at the bottom of the well-stratified sequence hosting sinter and continues upward to the upper exhalite. At the bottom of this succession, a thin black carbonate-mudstone contains the common Late Triassic marine bivalve *Halobia* (M. Orchard, Geological Survey of Canada, pers comm,

**Table 1.** Summary of assays from exhalite-sinter zones near Castillion Creek.

Element (units) <sup>1</sup>	Zone		
	Upper Exhalite (N=4)	Sinter (N=10)	Lower Exhalite (N=5)
Au (ppb)	0.7 (0.2–1.3)	15 (0.2–25)	1.8 (0.2–7)
Ag (ppb)	133 (68–187)	89 (34–120)	300 (39–879)
Cu (ppm)	10 (3–23)	13 (5–23)	296 (10–1124)
Pb (ppm)	10 (8–11)	4 (0.8–7)	4 (3–17)
Zn (ppm)	100 (26–168)	31 (10–53)	42 (3–102)
Mo (ppm)	10 (4–15)	148 (3–48)	17 (3–47)
Mn (ppm)	316 (97–458)	1567 (827–1612)	1037 (178–2294)
As (ppm)	6 (3–9)	27 (7–32)	62 (5–13)
Hg (ppm)	5 (5–6)	38 (5–58)	26 (6–48)
Sb (ppm)	0.4 (0.24–0.5)	1.3 (0.24–1.7)	1.4 (0.25–2.4)
Ba (ppm)	51 (12–160)	65 (20–151)	54 (24–71)
Tl (ppm)	1 (0.02–3.6)	0.5 (0.02–0.9)	0.07 (0.06–0.08)
Te (ppm)	0.02 (0.02–0.04)	0.03 (0.02–0.05)	0.03 (0.02–0.05)

<sup>1</sup> concentrations reported as mean (range)

2008). A thin layer of rhyolite ash tuff within this carbonate yields a U-Pb isotopic date of 224.5 ± 0.3 Ma. Rhyolite flows nearby may be temporally associated with this ash, erupted before the limy mud was consolidated. The sinter itself is interstratified, typically with finely laminated siltstone and sandstone that display parallel layering and rarely crosslaminations and small channels. Up section, evidence of deposition above sea level or alternatively in very shallow water is provided by the build-up of pyroxene flows succeeded by thin rhyolite ash-flow tuff. The tuff is locally welded and, because of its meagre thickness (typically less than 40 m), is unlikely to have developed welded structure in deep water. The abrupt upper contact of the ash flow with limestone, capped by the upper exhalite and then crosslaminated sandstone, demonstrates the change back to marine deposition.

## Epithermal Gold-Quartz Veins

### PROSPECT VALLEY (MINFILE 0921/SW 107)

The Prospect Valley showing is located 29 km west of Merritt. Access to the property is via the Petit Creek Forest Service Road to Hooshum logging road, then north along a mining road under construction by Consolidated Spire Ventures Ltd in 2008.

Prospect Valley is a low-sulphidation, epithermal stockwork-vein system carrying gold that is hosted within a homoclinal succession composed of thick andesite flows belonging to the Spius Formation. The quartz-vein system is exposed sporadically for about 1.3 km towards the northeast, maintaining random widths with interleaved country rocks of 50–150 m. Internally, this quartz-vein corridor is made up of parallel veinlets and veins, 15–75 cm wide, separated by country rocks. The veins are commonly banded, with open cavities lined by drusy quartz crystals, and some quartz breccia. Alteration observed along some veins consists of cloudy pink selvages composed of fine adularia that is accompanied by variably intense sericite-illite (?), hematite and fine-grained pyrite (Thomson, 2008). Drilling shows veining and attendant alteration localized in the hangingwall of the Early fault zone, a structure apparently striking northeast and dipping shallowly towards the northwest (Thomson, 2008). Encouraging gold values from

trench chip samples range from 0.48 to 1.58 g/t Au over 2.0 to 10.0 m.

The only historical work recorded on the property was small-scale placer mining activity along Prospect Creek, located at the south end of the property, and in the Shakan Creek drainage at the northwest corner (Thomson, 2007). Prospecting from 2001 to 2003 by Almaden Minerals Ltd, combined with follow-up on BC Regional Geochemical Stream Sediment Survey data (Jackaman and Matysek, 1994a, b), led to the discovery of chalcedonic quartz float and gold-bearing quartz-vein breccia. Early stages of exploration by the company focused on reconnaissance soil and silt sampling, and a 5 line-km IP-resistivity survey. Results from Almaden's initial exploration defined several mineralized epithermal gold zones. The main target areas were the RM-RMX zones, now called the Discovery North and South zones, respectively. In 2004, Almaden entered into a joint venture with Consolidated Spire Ventures Ltd until 2006, at which time Consolidated Spire acquired 100% ownership of the property. In 2005, Consolidated Spire collected 302 trench chip samples from 33 hand-dug trenches across the Discovery North and South zones. A 45 line-km ground magnetic and IP survey and 3734 m of diamond-drilling in 23 holes were completed in 2006. The highlight of this drill program was hole RM2006-04, which gave 2.17 g/t Au over 10.5 m, and hole RM2006-21, which showed a significant zone of stockwork veining and fault breccia between 37.2 m and 82 m. This section had a weighted average grade of 1.57 g/t Au over 45.7 m, including 14.07 g/t Ag over 11.8 m (Thomson, 2007). Work in 2007 consisted of a 1188 line-km airborne magnetic survey, followed by a 10-hole drill program totalling 1775 m. Diamond-drill hole DDH2007-02, located 85 m northwest of hole RM2006-21, returned 0.90 g/t Au and 5.86 g/t Ag over 66.82 m from similar looking stockwork quartz veinlets (Thomson, 2008).

#### **NIC (MINFILE 092I/SW 107)**

Prospecting in 2001, followed by 38 line-km of soil sampling, uncovered veins in the Discovery zone, now called the Nic zone. The Nic zone is located in the northeast corner of the Prospect Valley claim block, 24 km west-northwest of Merritt. Road access is via the Petit Creek Forest Service Road, then west on the Edgar Creek logging road.

Nic is an epithermal, low-sulphidation quartz-vein target hosted by the Spius Formation, which on the property is a thick succession of variably red oxidized, pyroxenephritic and amygdaloidal andesite lava flows. Vein segments, exposed in shallow trenches at Nic, strike northeast and dip steeply. The veins range up to 4 m long by 30 cm wide and display irregularities, such as branching veinlets and knots. They are composed of finely crystalline, white to translucent quartz accompanied by minor calcite with banding, comb, and breccia textures. Weak limonite stain occurs adjacent to the veins in the country rocks. Chip sampling across the vein returned up to 27.3 g/t Au and 209.1 g/t Ag, with an average for 40 chip samples of 1.63 g/t Au (Moore, 2005).

In 2004, Almaden optioned the Prospect Valley claims to Consolidated Spire Ventures Ltd. Between 2004 and 2005, Consolidated Spire enlarged the existing trenches, dug pits to test Au-in-soil anomalies and added a soil grid. In 2006, they drilled five holes, targeting a magnetic low that trends northeast and corresponds to the Nic zone. The

program, consisting of 1344 m of drilling to test the Nic zone, returned 3.2 g/t Au over 1.3 m from hole NIC2006-01 and 0.95 g/t Au over 6.7 m from hole NIC2006-05 (Thomson, 2007).

#### **SULLIVAN RIDGE (MINFILE 092I/SW 106)**

Reconnaissance silt, soil and rock sampling in 2004 prompted staking of the Merit claims by Almaden Minerals Ltd. Further prospecting found the Sullivan Ridge prospect, located at UTM Zone 10, 637963E, 5554070N (NAD 83; Balon, 2006). The Sullivan Ridge prospect is located 20 km west of Merritt. Access to this prospect is via the Petit Creek Forest Service Road, then onto a series of old roads heading west and then north.

A north-northeast-trending vertical structure, traceable intermittently in orange iron-carbonate-altered fault breccia for 750 m, hosts the Sullivan Ridge low-sulphidation epithermal veins. The veins occur in altered amygdaloidal, vesicular and aphanitic andesites of the Spius Formation. Branching quartz veins and veinlets locally occupy a zone 7.5 m wide and consist of white silica with comb textures. Altered country rocks nearest the veins and along the presumed fault trace are replaced by orange-brown iron carbonate and accompanied by weak pervasive silicification that obliterates primary mineralogy and textures in volcanic hostrocks. Minor disseminated pyrite, typically less than 2%, occurs in altered rocks and quartz veins. Rare malachite, azurite and grey-steel blue metallic minerals were noted in white crystalline quartz in a trench near the south end of the prospect. Almaden's chip sampling of veins in trenches returned up to 14.94 g/t Au over 0.6 m and 4.28 g/t Au over 2.5 m (Balon, 2006). A bleached and silicified zone, encountered during regional mapping, is located approximately 2 km southwest of the Sullivan Ridge prospect; a chip sample assayed 48.2 ppb Au and 444 ppb Ag (*see* data in Diakow and Barrios, 2008).

#### **PONDEROSA-AXEL RIDGE PROSPECT**

The Ponderosa property is located 16 km southwest of Merritt. Access to the property is from an old secondary forestry road that branches off Patchett road.

The epithermal, low-sulphidation vein occurrences on the Ponderosa prospect are hosted by pyroxene-andesite porphyry flows of the Spius Formation. The Axel Ridge vein forms a short but distinctive low ridge trending north and covered by thin overburden. A series of trenches across the ridge exposes a series of parallel quartz veins over a width of 12 m. The quartz is grey and white chalcedony with crustiform and colloform banded textures, as well as microcrystalline quartz, with drusy cavities and layered comb quartz (Balon, 2007). Jasper and jasper breccia were found with white microcrystalline quartz in a trench north of the Axel Ridge vein. Sparsely disseminated pyrite is present in the quartz veins, along with greyish sulphide or sulphosalt minerals.

Early work on the property by Almaden Minerals Ltd, beginning in 2002, consisted of reconnaissance geochemical silt, soil and rock sampling. Later, a grid-based soil survey, conducted in 2005 and 2006, collected 1095 soil samples. Encouraging Au-in-soil results led to the discovery of Axel Ridge, a 2000 m long soil geochemical anomaly located approximately at UTM 645000E, 5540000N. Follow-up work included hand trenching and blast-pit work that collected 29 bulk channel samples. Significant gold and silver mineralization was found at three locations in

trenches PT06-1, 2 and 3, and in numerous float samples along Axel Ridge. Channel samples from quartz-vein breccia at Axel Ridge returned values ranging from 0.11 to 6.57 g/t Au and averaging 2.22 g/t Au over 11.7 m, 1.50 g/t Au over 10 m and 2.83 g/t Au over 6.6 m (Balon, 2007).

In 2007, Almaden optioned the Ponderosa property to Strongbow Exploration Inc. Strongbow mapped the property, trenched, sampled and conducted a 6.78 line-km ground magnetic survey that culminated in a six-hole, 960 m drill program on the Axel Ridge occurrence. The magnetic survey showed a zone of subdued magnetic values trending north along Axel Ridge and an apparent dislocation of the magnetic anomaly by a fault. The geophysical survey was followed by a trenching program that included five trenches and 193 chip samples across extensions of the Almaden trenches and new prospective vein areas. Drilling tested the depth and lateral extent of the epithermal quartz veins and breccias. No significant veins were encountered at depth, although small zones of silicification and weak brecciation returned up to 68 ppb Au over a 1.15 m interval in hole PD07-03.

### DORA PROSPECT

The Dora prospect is located 24 km southwest of Merritt. Access to the property from the north is via the Patchett road, then south along the North Maka road to a branch road heading northeast and uphill to the property. Dora is owned and operated by Appleton Exploration Inc and was discovered in 2006 by silt and soil geochemistry and rock assays. The silt survey recovered three samples with values of 105, 250 and 965 ppb Au (Henneberry, 2007). An extensive soil grid, from which 3196 samples were collected, aided in delineating the Dora south and north zones, which were subsequently trenched by backhoe in 2007 and 2008.

Dora south is underlain by layered, fine nodular rhyolite flows from the Pimainus Formation. Hair-thick microveinlets of translucent quartz cut the country rocks with no obvious alteration observed. About 650 m northwest is Dora north, a zone of bleached and clay-altered porphyritic andesite of the Pimainus Formation that hosts white massive and banded quartz veins. Chip samples across nodular rhyolite and quartz in the porphyritic andesite returned values of up to 0.919 g/t Au over 6 m, 0.512 g/t Au over 5 m and 0.622 g/t Au over 3 m (Appleton Exploration Inc, 2008).

### QUARTZ VEIN PROSPECTS AT SHOVELNOSE MOUNTAIN

The Shovelnose Mountain prospect is located 30 km south-southwest of Merritt near the village of Brookmere. Access to the property is from a forestry road veering north off the Brookmere Road, west of the village. Strongbow Exploration Inc staked the Shovelnose property in 2005 and, in 2006, conducted an extensive silt sampling program followed by prospecting, mapping and soil sampling. This work led to the discovery of the Tower showing (Stewart and Gale, 2006). Further work in 2007, including a 308 line-km airborne geophysical survey and grid soil surveys, identified two new showings: the Line-6 and MIK.

The Line-6 quartz veins are located at UTM 652500E, 5524400N. These veins are up to 0.75 m wide and consist of massive chalcedony hosted in rhyolitic lapilli tuff of the Pimainus Formation. Alteration consists of weak clay replacement of fragments and matrix in the hostrock. In 2007,

Strongbow found Au values ranging from 0.49 to 4.89 g/t in 1–8 cm wide quartz veins. Trenching in 2008 uncovered wider veins and samples returned up to 1.4 g/t Au over 16.0 m in trench L6-XT-02 and 17 g/t Au over 2 m in trench L6-XT-01 (Strongbow Exploration Inc, 2008).

The MIK showing, located at UTM 653800E, 5524300N, is represented by narrow colloform-banded veins in weakly clay-altered rhyolitic lapilli tuff of the Pimainus Formation. Trenching in 2008 exposed a 30 cm wide vein, but no mineralization was observed. Quartz-vein float, sampled in 2007, returned up to 79.79 g/t Au and 94 g/t Ag; however, an *in situ* vein source was not uncovered in the 2008 trenches. Channel sampling in trench MK-XT-01 returned 1.4 g/t Au over 3 m and, in trench MK-XT-02, 1.45 g/t Au over 2 m.

The Tower showing (UTM 654150E, 5524550N) consists of rare banded chalcedony veinlets up to 1 cm wide and float pieces of chalcedony breccia up to 5 cm in size hosted in hydrothermally altered lapilli tuff of the Pimainus Formation. Fifteen pyrite-bearing quartz vein samples from the Tower showing averaged 0.22 g/t Au (Stewart and Gale, 2006).

The Brookmere quartz veinlets and stockwork at UTM 651890E, 5523745N are hosted in a sparsely plagioclase-phyric rhyolite flow. The veinlets range from several millimetres to 1.5 cm wide over a strike length of 1–2 m. They are characteristically comb textured and alteration consists only of slight bleaching of the rhyolite host. Trace amounts of crystalline disseminated pyrite was the only observed sulphide and assay samples returned no significant results (Stewart and Gale, 2006).

## ISOTOPIC AGE OF HYDROTHERMAL GOLD-QUARTZ VEIN ALTERATION

Epithermal vein prospects throughout the belt of Spences Bridge Group rocks have been visited and specimens collected of altered rocks adjacent to gold-bearing quartz veins, the principal objective being to determine the timing of hydrothermal alteration. Only at Prospect Valley is there evidence of potassium alteration, as narrow, cloudy, pink adularia selvages adjacent to quartz veins. The adularia from sample 06LDi 10.3 originates from a vein envelope at 92 m in diamond-drill hole RM2006-4 in the Prospect Valley epithermal vein system. It yielded a  $^{40}\text{Ar}/^{39}\text{Ar}$  age determination of  $104.2 \pm 0.6$  Ma. This date suggests that the hydrothermal system associated with the epithermal gold mineralization at Prospect Valley is penecontemporaneous with the Spences Bridge Group, a finding that has regional implications for the possibility for new discoveries elsewhere in the belt of Early Cretaceous rocks. On a local scale, this date also demonstrates the contemporaneity of the veins' hostrocks, the Spius Formation, and isotopically dated Pimainus Formation at Gillis Lake and Shovelnose Mountain.

## ACKNOWLEDGMENTS

We express our gratitude to Paul Schiarizza for his constructive review, which improved this paper.

## REFERENCES

- Appleton Exploration Inc (2008): Appleton Exploration Inc identifies four high priority targets at Dora 2008; *Appleton Exploration Inc*, URL <<http://appletonexploration.com/news/>> [December 2008].
- Balon, E.A. (2006): 2005 geochemical, geological, prospecting and trenching report, Merit property; *BC Ministry of Energy, Mines and Petroleum Resources*, Assessment Report 28,006, 136 pages.
- Balon, E.A. (2007): 2006 geochemical, geological, prospecting and trenching report, Ponderosa property; *BC Ministry of Energy, Mines and Petroleum Resources*, Assessment Report 28,830, 117 pages.
- Diakow, L.J. (2008): Spences Bridge bedrock mapping project: preliminary results from the Merritt region, south-central British Columbia (parts of NTS 092H/14, 15; 092I/02); in *Geological Fieldwork 2007, BC Ministry of Energy Mines and Petroleum Resources*, Paper 2008-1, pages 1–4.
- Diakow, L.J. and Barrios, A. (2008): Geology, Spences Bridge Group southwest of Merritt, British Columbia (parts of NTS 092H/14, 15 and 092I/2, 3); *BC Ministry of Energy Mines and Petroleum Resources*, Open File 2008-8, 1 map at 1:50 000 scale.
- Erdmer, P., Moore, J.M., Heaman, L., Thompson, R.I., Daughtry, K.L. and Creaser, R.A. (2002): Extending the ancient margin outboard in the Canadian Cordillera: record of Proterozoic crust and Paleocene regional metamorphism in the Nicola horst, southern British Columbia; *Canadian Journal of Earth Sciences*, Volume 39, pages 1605–1623.
- Greig, C.J. (1991): Jurassic and Cretaceous plutonic and structural styles of the Eagle Plutonic Complex, southwestern British Columbia, and their regional significance; *Canadian Journal of Earth Sciences*, Volume 29, pages 793–811.
- Haggart, J.W. (2008): Report on Triassic fossils from the Merritt region, British Columbia (NTS 92I); *Geological Survey of Canada*, unpublished Paleontological Report JWH-2008-03, 3 pages.
- Henneberry, T. (2007): Geological report Dora project; *BC Ministry of Energy, Mines and Petroleum Resources*, Assessment Report 28,946, 167 pages.
- Jackaman, W. and Matyssek, P.F. (1994a): British Columbia regional geochemical survey, NTS 92H – Hope, stream sediment and water geochemical data; *BC Ministry of Energy, Mines and Petroleum Resources*, BC RGS 39.
- Jackaman, W. and Matyssek, P.F. (1994b): British Columbia regional geochemical survey, NTS 92I – Ashcroft, stream sediment and water geochemical data; *BC Ministry of Energy, Mines and Petroleum Resources*, BC RGS 40.
- McMillan, W.J. (1981): Nicola Project—Merritt area; *BC Ministry of Energy, Mines and Petroleum Resources*, Preliminary Map 47, 2 maps at 1:25 000 scale.
- Monger, J.W.H. (1989): Geology, Hope, British Columbia; *Geological Survey of Canada*, Map 41-1989, sheet 1, scale 1:250 000.
- Monger, J.W.H. and McMillan, W.J. (1989): Geology, Ashcroft, British Columbia; *Geological Survey of Canada*, Map 42-1989, sheet 1, scale 1:250 000.
- Moore, J.M., Gabites, J.E. and Friedman, R.M. (2000): Nicola horst: toward a geochronology and cooling history; in *Slave Northern Cordillera Lithospheric Evolution (SNORCLE) Transect and Cordilleran Tectonics Workshop Meeting*, February 25–27, 2000, University of Calgary, Calgary, AB, Cook, F. and Erdmer, P., Compilers, *LITHOPROBE Secretariat, University of British Columbia*, Report 72, pages 177–185.
- Moore, M. (2005): 2005 geochemical and hand trenching report, Prospect Valley project, southern British Columbia, Canada; *BC Ministry of Energy, Mines and Petroleum Resources*, Assessment Report 28,162, 225 pages.
- Preto, V.A. (1979): Geology of the Nicola Group between Merritt and Princeton; *BC Ministry of Energy, Mines and Petroleum Resources*, Bulletin 69.
- Preto, V.A., Osatenko, M.J., McMillan, W.J. and Armstrong, R.L. (1979): Isotopic dates and strontium isotopic ratios for plutonic and volcanic rocks in the Quesnel Trough and Nicola belt, south-central British Columbia; *Canadian Journal of Earth Sciences*, Volume 16, pages 1658–1672.
- Stewart, M.L. and Gale, D.F. (2006): 2006 report on exploration activities, prospecting, mapping and geochemistry, Shovelnose property; *BC Ministry of Energy, Mines and Petroleum Resources*, Assessment Report 28 704, 53 pages.
- Strongbow Exploration Inc (2008): Strongbow assays up to 118 g/t Au at the Shovelnose property, BC trenching returns 5.1 g/t Au over 6 m; Strongbow Exploration Inc, press release, URL <<http://www.strongbowexploration.com/>> [December 2008].
- Thomson, G. (2007): 2006 geophysical, geochemical and diamond drilling report, Prospect Valley project, southern British Columbia, Canada; *BC Ministry of Energy, Mines and Petroleum Resources*, Assessment Report 29 316, 415 pages.
- Thomson, G. (2008): Prospect Valley gold property, technical report, British Columbia, Canada; unpublished NI43-101 company report, *Consolidated Spire Ventures Ltd*, Vancouver, BC, 103 pages.
- Thorkelson, D.J. (1986): Volcanic stratigraphy and petrology of the mid-Cretaceous Spences Bridge Group near Kingsvale, southwestern British Columbia; unpublished MSc thesis, *University of British Columbia*, 119 pages.
- Thorkelson, D.J. (1989): Eocene sedimentation and volcanism in the Fig Lake graben, southwestern British Columbia; *Canadian Journal of Earth Sciences*, Volume 26, pages 1368–1373.
- Thorkelson, D.J. and Rouse, G.E. (1989): Revised stratigraphic nomenclature and age determinations for mid-Cretaceous volcanic rocks in southwestern British Columbia; *Canadian Journal of Earth Sciences*, Volume 26, pages 2016–2031.



# Geology, Geochronology and Mineralization of the Chilanko Forks to Southern Clusko River Area, West-Central British Columbia (NTS 093C/01, 08, 09S)

by M.G. Mihalynuk, E.A. Orovan<sup>1</sup>, J.P. Larocque<sup>2</sup>, R.M. Friedman<sup>3</sup> and T. Bachiu<sup>4</sup>

**KEYWORDS:** regional geology, structure, litho-geochemistry, mineral potential, Clusko River, Chilanko Forks, Chilcotin River, mountain pine beetle

## INTRODUCTION

In 2008, the Beetle Impacted Zone (BIZ) project focused on bedrock mapping and resource evaluation of the Chilanko Forks (NTS 093C/01) and Clusko River (NTS 093C/09S) map areas. Located between Williams Lake and Bella Coola, in the Anahim Lake area, these map areas were targeted because of relatively good logging road access and a historical lack of mineral exploration. Building upon mapping completed in 2007 in the intervening Chezacut map area (NTS 093C/08; Mihalynuk et al., 2008a, b), results of new revision mapping in the Clusko River sheet to the north and Chilanko Forks sheet to the south are presented here, together with results from isotopic age investigation of Chezacut area map units.

Mapping and resource evaluation in 2007 demonstrated that rock exposures are more extensive and Chilcotin basalt is less extensive than previously recognized, and that further mineral exploration in the Anahim Lake region is warranted. Results of the 2008 field program echo these findings, providing further incentive for future mineral exploration in the region.

The BIZ project is one facet of a broad effort by the provincial government to stimulate economic diversification and to help reduce the long-term negative economic impact of the mountain pine beetle. As recorded by the 2004 Forest Health Survey (BC Ministry of Forests and Range, 2005a), the area of contiguous pine beetle infestation at that time was nearly coextensive with the Interior Plateau (Figure 1). Historically unprecedented in size, the beetle infestation will lead to an inevitable degradation of the trees available to the forest industry for harvest and a deceleration of the chief economic engine in central British Columbia (Ministry of Forests and Range, 2005b).

## PINE BEETLE BACKGROUND

In western North America, mountain pine beetles range from northern BC to northern Mexico. Across the interior of BC, the forest ecosystem is dominated by lodgepole pine, which at around 80 years of age, reach their maximum susceptibility to mountain pine beetle attack (Shore and Safranyik, 1992). At the outset of the current pine beetle epidemic, more than half of the pine forest stands in BC were near optimal susceptible age, largely as a consequence of fire suppression efforts. Fire suppression by government agencies was an outgrowth of the Dominion Forest Reserves Act of 1906 (Taylor, 1999) and creation of the BC Forest Service Protection Branch in 1912 (BC Ministry of Forests and Range, 2008). Particularly effective fire suppression measures have been invoked since the 1960s, such that by 2004 mature pine forest was three times as abundant as it would be in an unmanaged state (55% versus ~17%; Taylor and Carroll, 2004). Today, the BC Forest Service Protection Branch reports an initial attack fire suppression success rate of 92% (BC Ministry of Forests and Range, 2008).

The current mountain pine beetle epidemic is one of five recorded outbreaks within the past 85 years (Taylor and Carroll, 2004), although evidence for mountain pine beetle infestations extends to centuries past in the form of tree ring scars (Alfaro et al., 2004). Precise distribution and severity of infestations have been recorded only since the beginning of comprehensive aerial surveys in 1959 (e.g., Taylor and Carroll, 2004).

## LOCATION AND ACCESS

Geological bedrock mapping completed in 2008 covered an area of ~1300 km<sup>2</sup>, located approximately 200 km west of Williams Lake, midway on the Highway 20 route to Bella Coola. It includes the resort community of Puntzi Lake, a former military air base on the northern side of Highway 20 (Figure 1). Just outside the eastern map border, along Highway 20, is the community of Redstone (20 km west of the official location shown on most maps).

Six main forest service roads provide access to the map areas (Figures 1, 2). Two main roads service the Clusko River area: the Chezacut (100) Road crosses the area diagonally from the southeast (also known as the Clusko River-Thunder Mountain Road beyond the Clusko River), and a major branch known as the Scotty Meadow Road crosses the northeastern map area. Four of the main roads service the Chilanko Forks area: the Baldwin Lakes Road and the 5600 Road extend into the south-central and southeastern portion of the map area, the Clusko Main accesses the southwest, and the Puntzi Lake Road transects the south-

<sup>1</sup> Carleton University, Ottawa, ON

<sup>2</sup> University of Victoria, Victoria, BC

<sup>3</sup> Pacific Centre for Isotopic and Geochemical Research, University of British Columbia, Vancouver, BC

<sup>4</sup> Dalhousie University, Halifax, NS

This publication is also available, free of charge, as colour digital files in Adobe Acrobat® PDF format from the BC Ministry of Energy, Mines and Petroleum Resources website at <http://www.empr.gov.bc.ca/Mining/Geoscience/PublicationsCatalogue/Fieldwork/Pages/default.aspx>.

central and western parts of the map area. In the Clusko River area, low elevation roadbeds are partly constructed on glaciolacustrine deposits, which can become greasy and treacherous when rain-soaked. Hundreds of kilometres of secondary logging roads branch off the major forestry service roads, although many of these are deactivated and best accessed by mountain bike or on foot. On old logging roads or in open pine forest with sparse outcrop, foot traverses in excess of 20 km are routine.

## REGIONAL GEOLOGICAL SETTING AND PREVIOUS WORK

The Clusko River and Chilanko Forks areas are part of the Fraser Plateau (Figure 1; south-central Interior Plateau as defined by Holland, 1964). Basement rocks in this area are part of southeastern Stikine terrane, a Devonian to Jurassic arc complex, near its eastern contact with the Cache Creek terrane, a Mississippian to Early Jurassic accretionary complex. Subsequent to Middle Jurassic amalgamation of these two terranes (e.g., Ricketts et al., 1992; Mihalyuk et al., 2004), the contact was overlapped by Late Jurassic volcano-sedimentary strata, perhaps correlative with the late Jurassic Nechako/Fawnie volcanic rocks of Diakow et al. (1997) and Diakow and Levson (1997).

The southern Clusko River map area is underlain almost exclusively by supracrustal Eocene continental arc volcanic strata deposited during ~55–47 Ma extensional exhumation and cooling of kyanite-grade basement rocks characterized by ~107 Ma deformational fabrics (Friedman, 1992). Upper crustal equivalents of these Mesozoic basement rocks are well-exposed in the Chezacut and Chilanko Forks areas. Miocene, Neogene and Quaternary volcanic rocks drape the post-Eocene paleotopography and volcanic flows infill paleotopographic lows. Larocque and Mihalyuk (2009) have examined the petrogenesis of the Miocene and younger rocks in greater detail.

Previous regional bedrock geological mapping in the Anahim Lake area was conducted by Tipper (1969a; 1:250 000 scale, NTS 093C). In the Clusko River area, Tipper's mapping was revised by Metcalfe et al. (1997; 1:50 000 scale, published at approximately 1:350 000 scale, NTS 093C/09, 16, 093B/12, 13), who focused on volcanology and epithermal mineralization in the Eocene volcanic rocks. To the immediate west and south, the Tatla Lake Metamorphic Complex was mapped by Friedman (1988; 1:50 000 and 1:20 000 scales) as part of a Ph.D. study on its structural exhumation. His mapping was extended farther southwest by Mustard and van der Heyden (1997; 1:50 000 scale, NTS 092N/14E, 15). All of these sources of bedrock map data have been compiled by Massey et al. (2005) as part of the digital provincial geology map, and by Riddell (2006) to aid with petroleum resource assessment. Modern geophysical studies include the reprocessing of seismic data from hydrocarbon exploration activity undertaken in the Interior Plateau in the early 1980s (e.g., Hayward and Calvert, 2008), as well as the acquisition and interpretation of new geophysical surveys, including passive seismic tomography (e.g., Cassidy and Al-Khoubbi, 2007) and magnetotelluric imaging (e.g., Spratt and Craven, 2008).

Two main periods of hydrocarbon exploration activity, in the early 1960s and 1980s, resulted in more than 12 exploration wells drilled in the volcano-sedimentary strata,

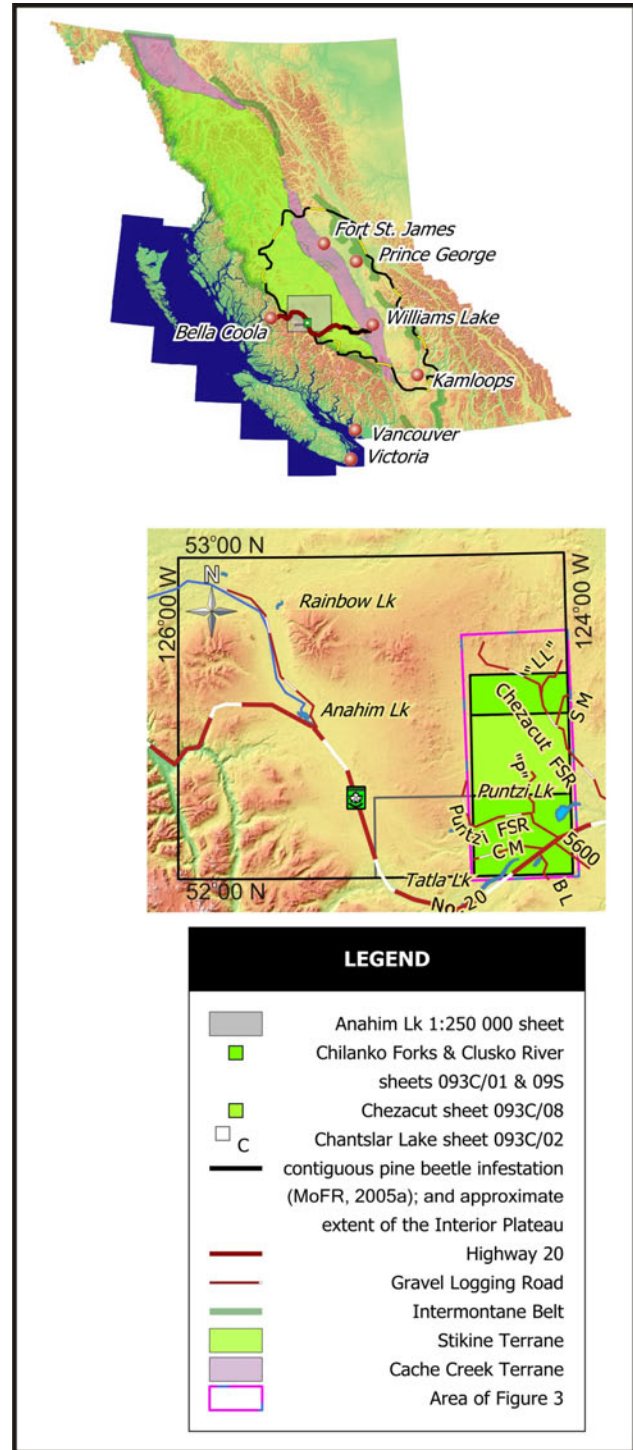


**Figure 1.** Location of the Chilanko Forks and Clusko River map area, showing features mentioned in the text. Also shown are: the area of 2005 mountain pine beetle infestation, which is nearly co-extensive with the Interior Plateau (the southern half of which is the Fraser Plateau; Holland, 1964), distribution of Stikine and Cache Creek terranes (Massey et al., 2005), and the extent of the Intermontane Belt. Road abbreviations: BL, Baldwin Lakes; CM, Clusko Main; FSR, Forest Service Road; SM, Scotty Meadow, see text.

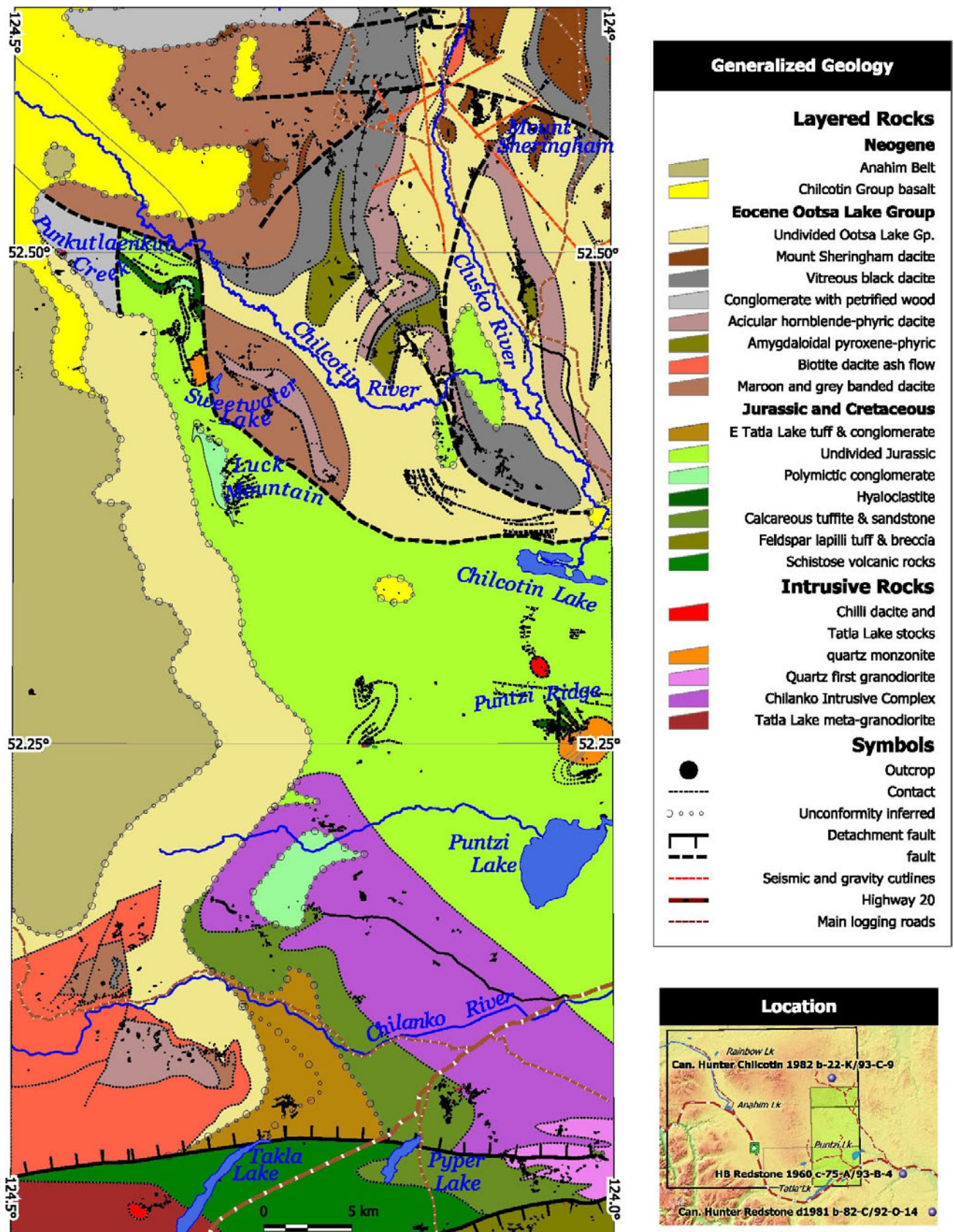


**Figure 2.** Geological sketch map showing the distribution of major units discussed in the text, new and existing showings, major access roads and sampling sites. This figure incorporates geological map data from Tipper (1969a), Massey et al. (2005), Riddell (2006) and Mihalynuk et al. (2008a).

which overlap the Stikine–Cache Creek terrane boundary (see Ferri and Riddell, 2006 for a chronology of hydrocarbon exploration). Seven of those wells have cores available for inspection at the BC Ministry of Energy, Mines and Petroleum Resources Core Facility located at Charlie Lake (Mustard and MacEachern, 2007). Three of these, from wells located 7 km north, 30 km east and 54 km southeast of the map area (see Figure 2), provide data down to 3778 m (Canadian Hunter Chilcotin 1982, b-22-K/93-C-9), 1307.5 m (Hudson Bay Redstone 1960, c-75-A/93-B-4), and 1720 m (Canadian Hunter et al. Redstone 1981, b-82-C/92-O-14). Riddell et al. (2007) reported palynological and age data from samples of the latter two wells: Late Albian palynomorphs from marine shale from 115 to 152 m underlain by marine to terrestrial strata of probable Middle to Late Albian age and, in the other well, Late Albian or Cenomanian palynomorphs from between 1210 and 1610 m. In an excellent synopsis of age and stratigraphic data, Riddell et al. (2007) report isotopic age data from the granitoid at the maximum depth penetrated (1730 m) by Canadian Hunter et al. Redstone b-82-C as  $101.4 \pm 1.9$  Ma, and a detrital age from clastic strata at 635–730 m of  $101.7 \pm 2.2$  Ma.

An Early to Middle Eocene U-Pb zircon age was obtained from volcanic rocks cored at 3121 m in Canadian Hunter Chilcotin b-22-K, essentially the same as three detrital zircon ages obtained from samples collected at depths of between 2000 and 3745 m. If the strata penetrated by Chilcotin b-22-K have not been structurally thickened, the data reported in Riddell et al. (2007) indicate an Eocene volcano-stratigraphic thickness in excess of 3745 m.

Regional glacial and fluvial physiography and surficial deposits have been mapped across the Anahim Lake area by Tipper (1971) and in more detail in the eastern Anahim Lake area by Kerr and Giles (1993; NTS 093C/01, 08, 09, 16), who also conducted till geochemical surveys (see Levson and Giles, 1997). Similarly detailed surficial surveys were conducted by Ferbey et al. (2009) in the area immediately to the east (NTS 093B/03, 04). Mihalynuk et al. (2008b) postulated that a late glacial lake occupied most valleys in the Chezacut area at elevations below 1154 m.

## FIELD TECHNIQUES

Field mapping in 2008 adapted techniques that were found to be beneficial in 2007. In particular, 1:20 000-scale digital orthophotographs (0.5 m resolution) were used extensively for the identification of areas of outcrop and definition of geological lineaments. Roadcuts added to the inventory of bedrock exposures, but only marginally. For example, rocks exposed within 15 m of roads constitute only 1.4% of those mapped within the Clusko River area, or even less than the meagre 2.4% in the Chezacut area (Mihalynuk et al., 2008b; Figure 2). Thus, mapping focused along road networks creates a falsely negative impression of the percentage of outcrop within the area. It is no accident that roads are preferentially constructed so as to avoid the high costs of blasting bedrock. Across the region, the most extensive outcrop exposures are along glacially scoured ridges and along the margins of glacial meltwater channels that are visible on 1:20 000-scale orthophotographs.

In areas with extensive till cover, clast compositions can be used as a guide to the underlying geology. Unfortunately, this technique is reliable only for basal till, whereas

the most extensive surficial cover deposits in the area mapped in 2008 are reworked glaciofluvial or potentially far-travelled hummocky glacial deposits. Contacts between units with a high magnetic contrast can be reliably mapped in the subsurface using available aeromagnetic survey data (Figure 3), as was done to create Figure 2.

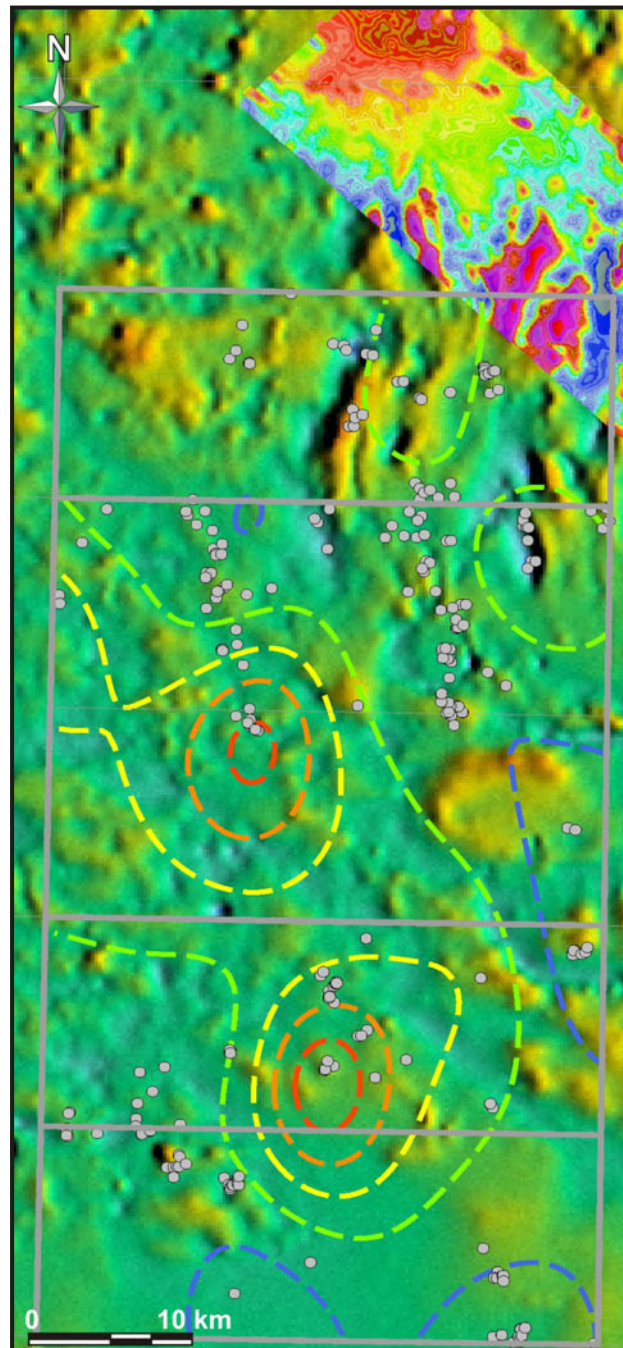


**Figure 3.** Regional aeromagnetic survey shaded total field (Geological Survey of Canada, 1994) and higher resolution total field coverage in northeastern portion of NTS 093C/09S from the Clisbako multiparameter survey; see Figure 1 for location. Overlain contoured magnetic susceptibility values range from 5 to 25, with an interval of 5 SI units. Locations of magnetic susceptibility measurements at the outcrop are shown as grey dots.

## LAYERED ROCKS

Layered rocks within the Chezacut map area were divided into four successions: Mesozoic, Eocene, Oligocene-Pleistocene or Pleistocene-Holocene by Mihalynuk et al. (2008b). Many of the units that constitute these successions extend into the current map areas (Figures 2, 3); they were described by Mihalynuk et al. (2008b) and are, therefore, not repeated here. However, units that significantly change character or may bear upon a different interpretation are described below.

### *Mesozoic*

Poorly fossiliferous Mesozoic strata were presumed by Tipper (1969a) and Mihalynuk et al. (2008b) to correlate with Late Triassic and Early Jurassic Stikine terrane volcanic arc strata. However, some strata in the Chilanko Forks area are now known to be Middle Jurassic or perhaps as young as mid-Cretaceous in age, and belong to overlap successions that are of particular interest for their hydrocarbon resource potential (e.g., Riddell and Ferri, 2008). For example, the only known fossil age determination in the Chilanko Forks area is from tuffaceous mudstone on the northern shore of Puntzi Lake (GSC locality 79765). Following publication of the Anahim Lake map in 1968, Tipper (1969b) reported that it contained poorly preserved Middle Jurassic ammonites: “According to H. Freebold a probable Bajocian age is indicated” (Tipper, 1969b, page 23). The ammonite-bearing tuffaceous mudstone unit is part of a coherent stratigraphy intruded by monzonite, for which we report a new Middle Jurassic isotopic age determination (see ‘Geochronology’ below). Coherent Mesozoic strata are common within the Chezacut area, extending from Puntzi Ridge to Puntzi Lake, in the northeastern corner of the Chilanko Forks sheet, but are not exposed farther south and east. Similar strata are expected to extend into the ~6 km<sup>2</sup> of the far southwestern corner of the southern Klusko River map area (Punkutlaenkut Creek-Chilcotin River confluence), but field conditions did not permit access to this area, which falls outside the limit of mapping shown in Figure 2. Partly correlative strata cut by, and deformed together with, a variably foliated polyphase tonalite to basaltic intrusive complex underlie much of the remaining portion of the Chilanko Forks area, except for the southeastern corner, which is underlain by Mesozoic (?) massive volcanic breccia. Another exception, the west-central part of the map area, is underlain by Eocene dacitic strata of the Ootsa Lake Group.

Map units characteristic of the coherent Mesozoic strata include: a bright green, carbonate-cemented, hyaloclastic lapilli tuff; indurated, tan and brown volcanic siltstone; orange, ‘monzonitic’ crystal lapilli tuff; and pyritic, coarse rhyolite breccia. All of these units are described in Mihalynuk et al. (2008b); units not previously described follow.

### **BAJOCIAN TUFFACEOUS SILTSTONE**

Low, recessive, friable outcrops of red-brown tuffaceous mudstone to sandstone (Figure 4a) crop out low



**Figure 4.** Mesozoic rock types, including **a)** well-bedded outcrop of Bajocian tuffaceous siltstone, **b)** massive volcanic breccia displaying typical rectilinear epidote-quartz-chlorite vein sets, and **c)** granule conglomerate portion of calcareous tuffite and sandstone.

on the southern flank of Mount Palmer and northern shore of Puntzi Lake. Mudstone appears to be interbedded with finely feldspar-phyric flows <2 m thick. Outcrops are strongly fractured and calcite veined, such that contact relationships are uncertain. Some 'flows' could in fact be dikes or unusually uniform, water-lain tuff that lacks significant winnowing or sorting.

### **VARIEGATED SILICEOUS TUFF AND RHYOLITIC FLOWS**

Rusty, white-weathering outcrops form resistant ridges, and range from coarse breccia to possible flow domes. The flows and pyroclastic rocks are typically well-indurated, with silicified clasts showing ochre, white and/or dark green ghosted margins. Thickness varies, but exposures are typically in the order of tens of metres thick. Pyritic zones are common, and pyrite can exceed 5% by volume of the rock over widths of a metre.

### **VEINED MASSIVE TUFF**

Bright green, extensively epidote-altered, blocky, orange-weathering and resistant breccia and lapilli tuff crop out across ~20 km<sup>2</sup> of southeastern NTS 093C/01. A presumably more distal lapilli- and ash tuff-dominated facies crops out sporadically north of Fit Mountain. Minor chlorite amygdaloidal flows and epiclastic strata are locally important. A feldspar crystal ash matrix is common in all tuffaceous facies. Medium-grained feldspar constitutes 10–25% of the ash and up to 35% of most fragments. Up to 5% of the rock may consist of chloritized hornblende, occurring as medium-grained subidiomorphic crystals. Sparse, altered pyroxene may also be present, but it has not been confirmed petrographically.

Green volcanic strata are locally interlayered with maroon, typically more ash-rich and breccia-poor layers <~20 m thick. In some of these layers, vague clast sorting and rounding suggest an epiclastic origin, but most contain highly angular fragments. Strain is commonly partitioned into these finer-grained units.

Extensive epidote-chlorite and quartz veining is characteristic of the massive blocky parts of the unit. Epidote-quartz veins commonly form parallel sets of veins which may range from 1 mm to ~4 cm in thickness, and are well developed across vein strike for 10 m or more (Figure 4b).

### **CALCAREOUS TUFFITE AND SANDSTONE**

Perhaps the most widespread Mesozoic sedimentary unit exposed in the Chilanko Forks-Clusko River map area is grey to blue-green volcanic tuffite and sandstone, commonly with a calcareous matrix. This unit is texturally variable, ranging from green sandstone with granule-conglomerate lags (Figure 4c) to epiclastic units with tuffaceous interbeds, to dark grey phyllitic mudstone. Limestone layers up to 10 cm thick have been observed in two localities. If better exposed, this unit could probably be subdivided into several mappable units.

The best exposures of this unit are on the hills east of Pyper Lake and in the thermal metamorphic halo of the Clusko Intrusive Complex near Puntzi Mountain. Adjacent to the complex, the carbonate matrix has been consumed through the production of secondary calcsilicate minerals: epidote or actinolite/tremolite, and rare grossular garnet.

Correlative units within the Chezacut map area (near Arc Mountain) may be the 'calcareous fossiliferous sand-

stone', 'volcanic siltstone/sandstone' and possibly, the 'calcareous chert pebble conglomerate' described in previous work (Mihalynuk et al., 2008b). Such variability in correlative units might be expected given that they are separated from those in the Chilanko Forks map area by more than 25 km.

A minimum relative age constraint on this unit is provided by the crosscutting, pre- to syndeformational Clusko Intrusive Complex. Two samples of this complex have been submitted for isotopic age determination, but neither has been completed as this paper goes to press. However, a new U-Pb age determination from the mainly undeformed 'Puntzi Ridge quartz monzonite', which cuts the presumably correlative strata within the Chezacut map area, is reported below as 160.94 ± 0.13 Ma.

## **Cretaceous Volcanic Rocks**

Volcanic rocks of Cretaceous age have not been directly dated within the Chilanko Forks to southern Clusko River area. However, Cretaceous volcanic strata are dated at 101 ± 2 Ma immediately east of the map area at Puntzi Lake, as reported by Riddell and Ferri (2008). Regionally, these rocks may correlate with the Spences Bridge Group (Thorkelson and Rouse, 1989; Diakow and Barrios, 2009). Undated volcanic rocks north of eastern Tatla Lake possibly belong to this package, as may rocks that underlie Mount Charlieboy on the southern boundary of the Chezacut map area.

### **EAST TATLA LAKE TUFF AND AUTOBRECCIA**

Olive-green or maroon, blocky to rubbly and orange- to tan-weathering tuff and breccia crop out north of the eastern end of Tatla Lake. They are vesicular and contain 20% by volume of medium- to coarse-grained, tabular plagioclase, which is commonly idiomorphic and slightly turbid, but in some outcrops can be vitreous. Vesicles are generally irregularly shaped, chlorite- or quartz-filled, with minor bright green celadonite (Figure 5a). They are less than 5 mm in diameter, and make up 5% by volume (locally up to 25%) of outcrops. Mafic minerals include chloritized biotite, less commonly hornblende, and possibly pyroxene; the latter is typically fine- to medium-grained, idiomorphic and accounts for less than 5%. Most outcrops are cut by calcite and/or zeolite (laumontite [?]) veins.

### **EAST TATLA LAKE CONGLOMERATE**

Very coarse boulder to cobble conglomerate (Figure 5b) with sparse, planar, arkosic volcanic sandstone layers appears to be entirely of local derivation, sourced from the underlying East Tatla Lake tuff and autobreccia. Unusually well-rounded boulders of chloritic, amygdaloidal, coarse-bladed feldspar porphyry flow exceeding 2 m in diameter indicate a persistent, very high-energy fluvial environment of deposition.

## **Eocene Ootsa Lake Group**

Volcanic units that compose the Eocene Ootsa Lake Group in the Chezacut map area were described by Mihalynuk et al. (2008b). These units include: basal conglomerate, acicular hornblende dacite, amygdaloidal pyroxene-phyric basalt, ochre breccia and flow lobes, dacite ash-flow tuff, maroon- and grey-banded rhyolite,

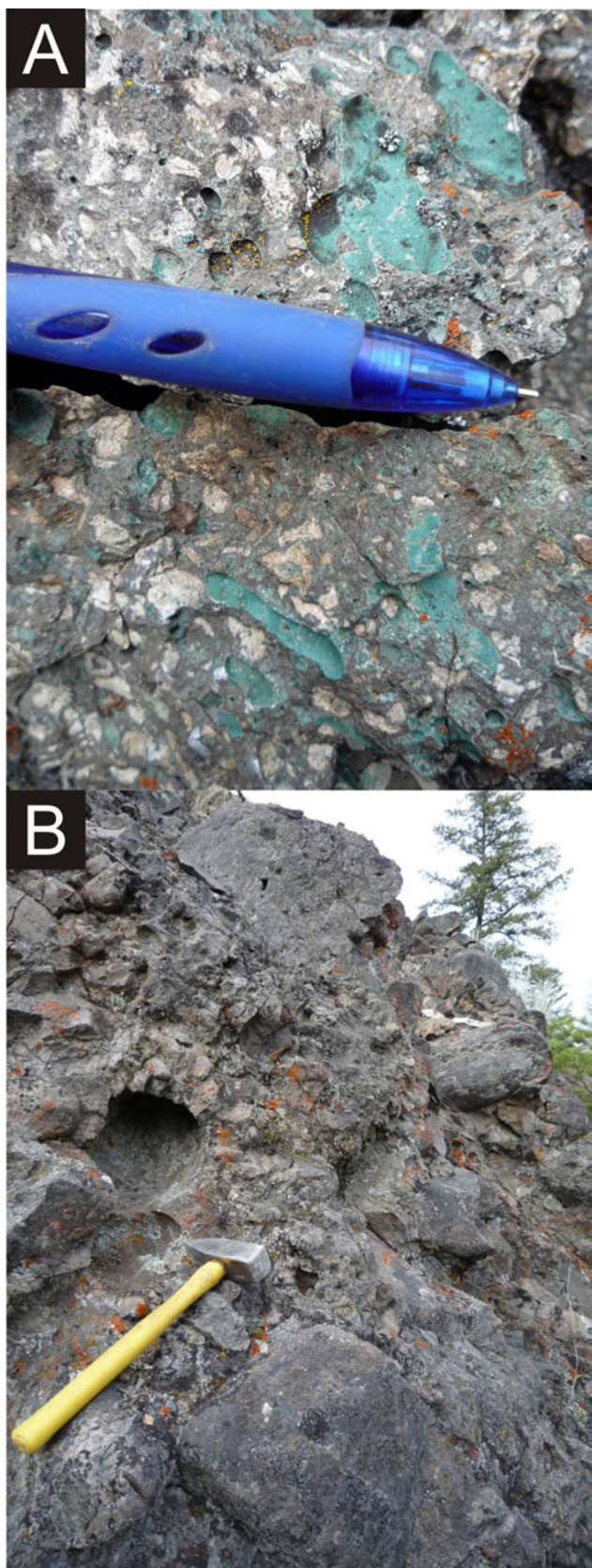


**Figure 5.** Good exposures of East Tatla Lake a) autobreccia and b) conglomerate.

and vitreous black dacite (Figure 6). Compositions are overwhelmingly dacitic as shown in Figure 7.

Fieldwork in 2008 added two additional units: a conglomerate unit with petrified wood fragments that may occur at several stratigraphic levels, and a variant of the 'vitreous black dacite' unit, that we have named the 'Mount Sheringham pyroxene dacite'.

Seven new  $^{40}\text{Ar}/^{39}\text{Ar}$  cooling age determinations for the Ootsa Lake Group within the Chezacut area show that the 'vitreous black dacite' unit is ~46–44 Ma, significantly younger than underlying units (~54–50 Ma); these data are consistent with the geochronological findings of Metcalfe et al. (1997). A full report on age determinations from Ootsa Lake Group volcanic rocks will follow when geochronological data from samples collected in 2008 become available.

### POLYMICTIC CONGLOMERATE

Although described by Mihalynuk et al. (2008b), this unit is included here as new observations bear upon the geological interpretation of the area. Bright maroon-weathering, recessive polymictic conglomerate is exposed south and west of Fit Mountain, where it displays an unconformable contact with the late Jurassic Chilanko intrusive complex diorite. Clasts appear to be derived from the underlying Jurassic terrain, including the Chilanko intrusive complex (*see below*). Characteristic maroon soil has developed above and adjacent to the unit. On the basis of local soil colour anomalies, the conglomerate is presumed to underlie an extensive area west and south of Fit Mountain, where it is sporadically exposed. This unit may represent the base of the Eocene succession in the Chilanko Forks area; however, it could also mark the basal contact of the Cretaceous section.

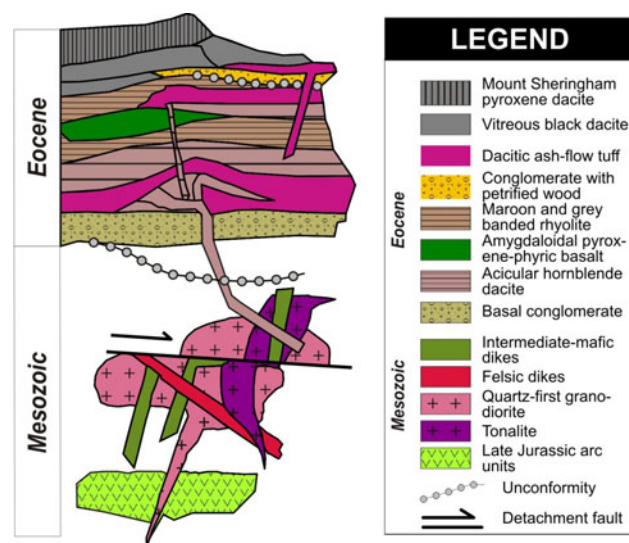


**Figure 6.** Schematic diagram of stratigraphic relationships between the major units within the Clusko River and Chilanko Forks area. See Mihalynuk et al. (2008b) for stratigraphy of the intervening Chezacut area.

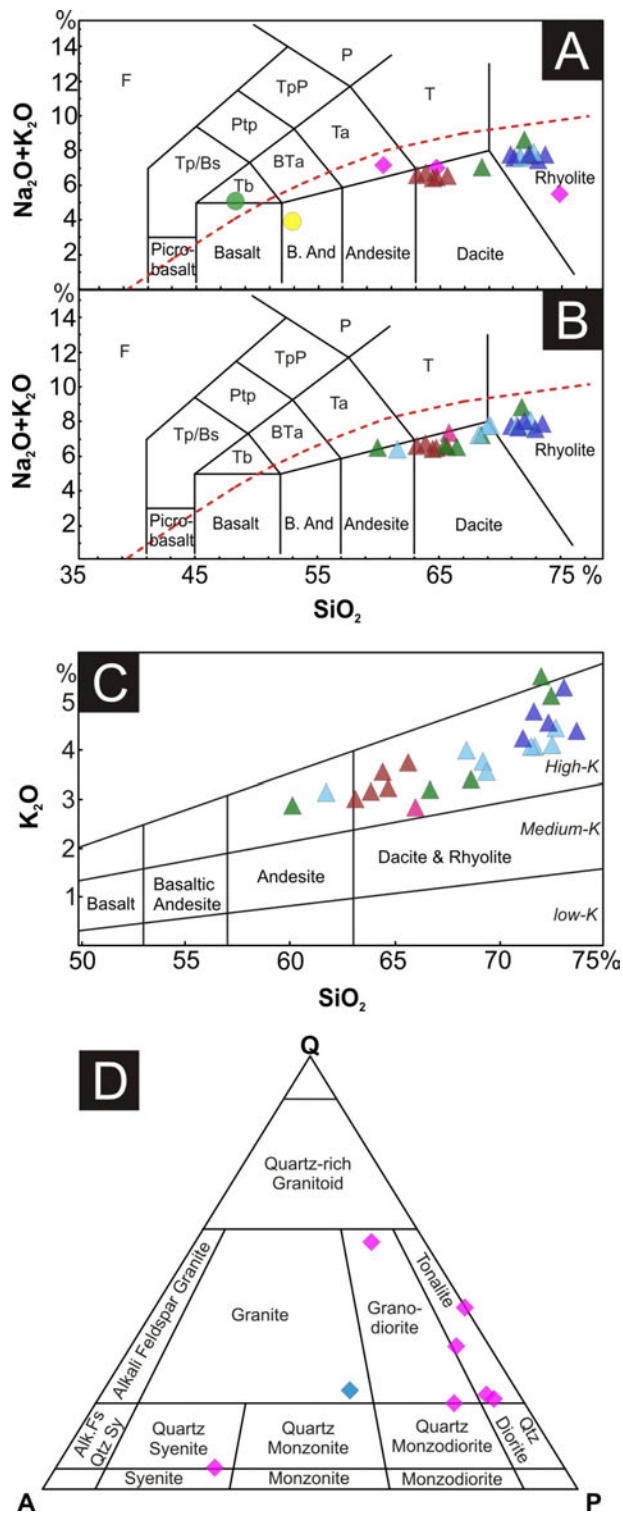


**Figure 7. a)** Total alkali-silica plot (after Le Maître, 1989) showing all 2008 whole rock samples. **b)** Total alkali-silica plot (after Le Maître, 1989) showing Eocene volcanic rocks from 2007 and 2008. **c)**  $\text{SiO}_2$ - $\text{K}_2\text{O}$  plot for Eocene volcanic rocks from 2007 and 2008. **d)** Quartz-Alkali feldspar-Plagioclase feldspar ternary diagram showing compositions of intrusions mapped in 2008. Compositions are based on visual estimates of phase proportions. F: foidite; P: phonolite; TpP: tephriphonolite; Ptp: phonotephrite; Tp/Bs: tephrite/basanite; T: trachyte; Ta: trachyandesite; Bta: basaltic trachyandesite; Tb: trachybasalt; B.And: basaltic andesite; Alk.Fs Qtz Sy: alkali feldspar quartz syenite.

### CONGLOMERATE WITH PETRIFIED WOOD CLASTS

Recessive, rusty, white- to yellow-weathering sandstone and conglomerate are common within the upper part of the Eocene succession near upper Clusko River (Figure 8a). The presence of petrified wood fragments is characteristic of this unit (Figure 8b). In some localities the unit contains bands of indurated, cherty siltstone; in other localities, the conglomerate may be strongly clay-altered and can be carved away by hand. Conglomerate clasts vary in compo-

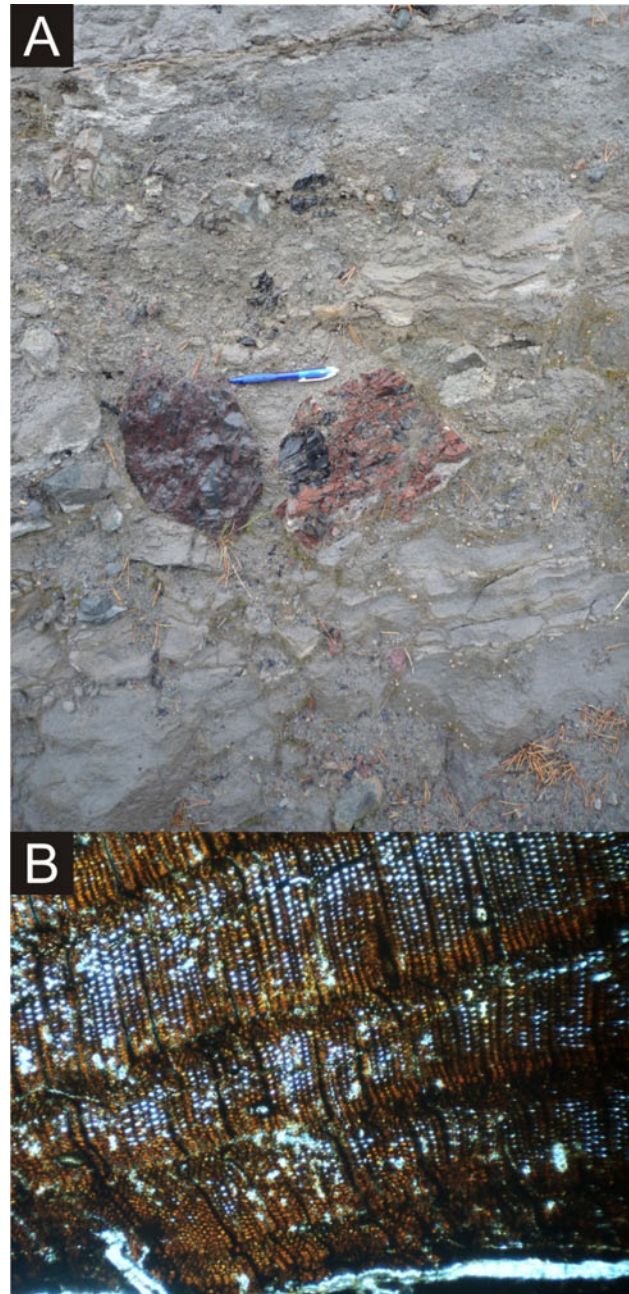


**Figure 8. a)** Very light grey- to white-weathering epiclastic conglomerate contains vitric ash flow fragments at this locality. **b)** Where the unit is more typically rusty and yellow-weathering, it invariably contains fragments of petrified wood, as seen in the thin section shown here. Long dimension of this photo represents ~2.5 mm.

sition, but quartz-phyric clasts are ubiquitous. Undulating planar bedding and low-angle cross-stratification, and channel lags are common.

### MOUNT SHERINGHAM PYROXENE DACITE

Mount Sheringham pyroxene dacite is a subunit of the ‘vitreous black dacite’ of Mihalynuk et al. (2008b) and part of the ‘Pyroxene-bearing Assemblage’ of Metcalfe et al. (1997). However, this unit contains conspicuous, amber to light lime-green quartz eyes, not described as part of the ‘vitreous black dacite’. Colour is imparted to these quartz eyes by a glass-inclusion-riddled rim (Figure 9a), interpreted as being due to a period of rapid crystal growth immediately preceding eruption. Another characteristic of this unit is the formation of spectacular columnar flows that typically range from 1 to 10 m in thickness (Figure 9b) and indicate atypically low viscosity for such a silicic composition (Figure 7).

One previously unreported feature of some amygdaloidal flows that make up the ‘vitreous black dacite’ unit, is the occurrence of a vesicle-filling, fibrous, leather-like mineral (Figure 10). It is preliminarily identified as sepiolite, but this has yet to be confirmed by x-ray diffraction analysis.

Perlitic textures are locally common within the ‘vitreous black dacite’, but none of the perlitic samples tested expanded significantly when heated.

### Neogene Volcanic Rocks

Neogene volcanic rocks in the map area encompass two broad rock packages: the Late Oligocene to Early Pleistocene Chilcotin Group, which extends over 35 000 km<sup>2</sup> of the Interior Plateau (Bevier, 1983; Andrews and Russell, 2007), and the Pleistocene to Holocene Anahim volcanic belt (Bevier, 1989; Mathews, 1989). Their characteristics have been described within the neighbouring Chezacut area (Mihalynuk et al., 2008b) and their geochemistry is the subject of a paper by Larocque and Mihalynuk (2009). Only brief descriptions of one locality within the Chilanko Forks and two within the Clusko River map area follow. Exposures are limited to the far western margin of those areas, although, significant thicknesses of Chilcotin Group basalt crop out immediately east of central Chilanko Forks map area, on the outskirts of Redstone village. Despite the relatively steep Chilanko River valley sides west of Redstone, only glaciofluvial deposits are incised and no bedrock could be found.

### DENSE FLOWS

Southwestern-most NTS 093C/09S is underlain by sporadically exposed Chilcotin Group flows. They are typical of the Chilcotin Group: grey with fine- to medium-grained, bright green olivine phenocrysts making up to 3% of the rock. Matrix consists mainly of plagioclase microlites and, locally, 1–2% idiomorphic plagioclase phenocrysts up to 1 cm long. It is characteristically spongy, with intersertal vesicles and glass in approximately equal proportions, together constituting 30% of the rock.

### SCORIA DEPOSITS

Just north of the northwestern corner of NTS 093C/09W south half is a steep-sided hill with an apron of unconsolidated black and ochre scoria and ropey bombs (Figure 11) containing fine-grained, zoned plagioclase

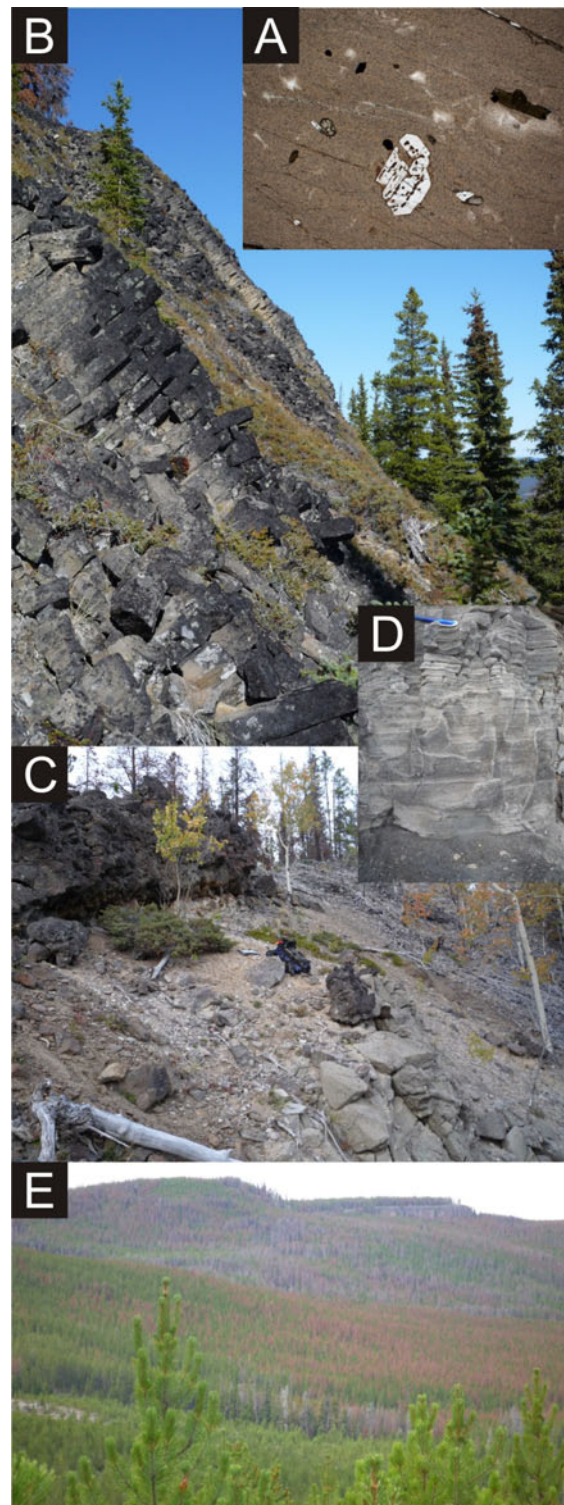


**Figure 9.** a) Embayed quartz phenocrysts within the Mount Sheringham pyroxene dacite unit display an outer growth zone with abundant glass inclusions. b) An example of well-developed columnar flows typical of this unit. c) Mount Sheringham pyroxene dacite unit sits atop light pink flow-banded dacite (view to the northeast), which pinches out to the south, above light grey epiclastic strata. d) Close-up of epiclastic strata showing trough cross-stratification and planar bedding. e) This unit is 5–10 Ma younger than most of the Ootsa Lake Group and tends to be more flat-lying than older units, as shown by the mesa in the distance.

(15%). Rare blocks contain feldspar phenocrysts up to 2 cm long. Individual blocks are hackly and vesicle-rich (~20%, up to 5 cm) and display little sign of rounding or transport (except for sparse rounded blocks of other rock types on the surface of the scoria apron).

Very low, recessive outcrops on the adjacent hill are composed of jet black scoria and crusty bombs in a poorly lithified, light brown matrix. This bedrock could be the source of scoria, although none of the unconsolidated scoria contain light brown ash matrix within vesicles or adhering to their surfaces. Thus, the scoria apron is interpreted as an essentially primary deposit, perhaps modified slightly by Late Pleistocene meltwater. These deposits are probably part of the young Anahim volcanic belt.

### BLOCKY FLOW TOP

Only the low, drift-covered northwestern corner of the Chilanko Forks map area is interpreted as underlain by Neogene volcanic rocks consisting of extensive monolithic block fields interpreted as nearcrop. The blocks are tabular, up to 3 m in diameter and 2 m thick; many of these blocks appear to fit together in jigsaw fashion and are there-



**Figure 10.** Photomicrograph of fibrous sepiolite (?). Grey, leathery tongues of this mineral developed as it infilled flattened vesicles within flow tops of the 'vitreous black dacite' unit. Long dimension of the photo represents ~2.5 mm.



**Figure 11.** Scoria deposit in the western half of the Clusko River area (south half).

fore interpreted as part of the same, originally intact, auto-brecciated flow unit. No sign of overlying glacial debris is apparent. Thus, the blocks are interpreted as part of a late to post-Pleistocene unit, perhaps part of the Anahim volcanic belt.

## GLACIOGENIC DEPOSITS

Glaciogenic deposits are widespread within the Chilanko Forks area, and are volumetrically dominated by thick glaciofluvial blankets within the main Tatla Lake, Puntzi Creek and Puntzi Lake valleys. Glacial deposits have been discussed as part of a study by Levson and Giles (1997), were mapped by Kerr and Giles (1993), and extend to the east where they were the subject of surficial mapping and till surveys conducted by Ferbey et al. (2009). Readers are referred to these publications for more details.

Glaciolacustrine deposits are preserved sporadically throughout the southeastern Anahim map area. Well-bedded lacustrine strata are exposed along the Clusko River and Puntzi Lake valleys, where they locally exceed 10 m in thickness. In the Chezacut area, they are interpreted as having been deposited by a late glacial lake that inundated approximately 65% of the map area up to an elevation of ~1150 m.

## INTRUSIVE ROCKS

Proportional distribution of plutonic intrusive rocks increases southward in the map area, from near zero in the southern half of the Clusko River area to at least 30% in the Chilanko Forks map area. Dikes related to Eocene volcanism are widely dispersed throughout the region, but to the south are greatly outnumbered by those of suspected Jurassic age. In the southeastern map area, swarms of dikes cut a >30 km northwest-elongate polyphase plutonic body that is bisected by the Chilanko River. Collectively, the dikes and pluton are informally referred to as the 'Chilanko intrusive complex'. In the areas mapped, the northwestern limit of the complex is the 'Sweetwater Lake' monzonite, a separate body located in the Chezacut map area.

### *Chilanko intrusive complex*

Tonalite is the most common rock type within the Chilanko intrusive complex (Figure 7), but constituent phases include diorite to granodiorite, monzodiorite and, rarely, granite. Dikes are common, in some places constituting >50% of broad exposures. Dikes range in composition from basalt to felsite and pegmatite of probable granitic composition. Dikes of intermediate composition tend to be the most strongly foliated. Constituent plutonic phases are also commonly foliated. Mafic phases within both plutons and dikes consist of amphibole and biotite, which typically account for less than 10% by volume of the rock, although they may account for as much as 25% (Figure 12a). Subhedral hornblende is often altered to actinolite±chlorite and biotite is commonly pervasively altered to chlorite. Plagioclase varies in habit from tabular euhedral to subhedral and is partly to mostly replaced by white mica, epidote and calcite. It has a composition of  $An_{30\pm5}$ , although plagioclase as calcic as  $An_{50}$  was observed within samples of quartz syenite. Interstitial potassium feldspar is commonly turbid due to very fine-grained clay alteration (probably kaolinite). Quartz typically displays

sutured margins; very quartz-rich samples contain cataclastically reduced quartz grains. Vein assemblages of quartz, calcite, actinolite, epidote and/or prehnite are widespread. Apatite, titanite and zircon are common accessory minerals.

Two plutonic phases within the Chilanko intrusive complex are noteworthy: a uniform body of tonalite at Fit Mountain, and variably foliated quartz-porphyritic granodiorite, herein referred to as the 'quartz-first granodiorite'. Samples of both units were collected for geochronological age determination, but analyses were not yet complete as this paper went to press.

#### **FIT MOUNTAIN TONALITE**

Blocky, salmon-orange and grey-weathering, medium-grained tonalite underlies Fit Mountain, and typically contains hornblende and lesser biotite as mafic phases (~35% combined). Medium- to fine-grained quartz and milky white plagioclase account for ~25% and 40% of the rock volume. Fit Mountain tonalite is commonly altered and green-tinged with minor epidote and chlorite veins ranging from millimetres to centimetres in thickness. Magnetite (0.25%) occurs as granular patches, giving the unit a moderately high magnetic susceptibility (~15 SI). Traces of fine-grained lemon-yellow titanite are common. Unlike most parts of the Chilanko intrusive complex, this body is only locally foliated, particularly at the highest elevations on the western side of Fit Mountain. On the eastern side, an area of chlorite-magnetite alteration contains veins of chalcocopyrite and bornite (*see* 'Mineralization' below).

#### **QUARTZ-FIRST GRANODIORITE**

Blocky or tabular, white-pink and tan-weathering granodiorite is light yellow-green on fresh surfaces due to pervasive chloritization of mafic minerals and sericitization of feldspars. It is characteristically quartz porphyritic and holocrystalline, with medium-grained quartz, feldspar and biotite intergrown between coarse knots of grey quartz (Figure 13). Both strongly foliated and nonfoliated variants are common within the southeastern Chilanko Forks map area.

#### ***Eocene Tatla Lake Stock***

North of Tatla Lake, a widely jointed biotite granodiorite stock weathers into rounded, light grey to tan blocks and appears light grey to nearly white on fresh surfaces. Originally mapped by Friedman (1988), who obtained from it an isotopic age of 47.5 Ma, the stock cuts, and is chilled against, strongly foliated granodiorite of the Tatla Lake Metamorphic Complex. It is not foliated.

Tatla Lake stock is medium-grained and subhedral holocrystalline, and contains minor biotite (3–7%) and smoky quartz (35%). Myrmekitic intergrowths of interstitial quartz and potassium feldspar are common. Very minor alteration is limited to rare replacement of biotite by chlorite, and slight turbidity in plagioclase due to secondary white mica. Accessory phases include euhedral titanite and sparse rutile.

### **GEOCHRONOLOGY**

In the Chezacut area, three ~1 km<sup>2</sup> intrusive bodies were mapped and sampled for geochronological age determination by Mihalyuk et al. (2008a, b). One of these, the

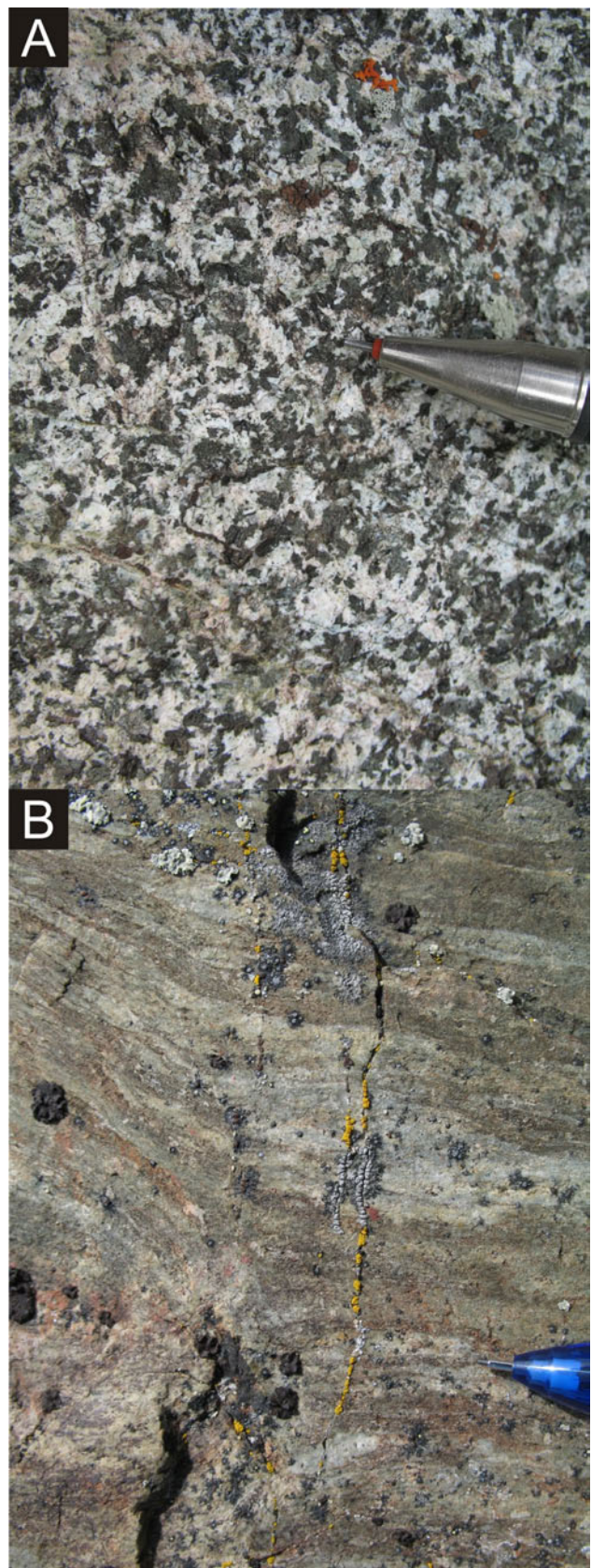


**Figure 12.** a) Nonfoliated quartz diorite phase within the Chilanko intrusive complex. b) Foliated calcareous country rocks adjacent to the contact of the complex.

Chili dacite stock, is of Eocene age; the other two, the Puntzi Ridge quartz monzonite and the 'Sweetwater Lake' monzonite (Figure 2) are of Late Jurassic age. We report on the geochronological age data from these two older intrusions.

All sample preparation and analytical work for the U-Pb and  $^{40}\text{Ar}/^{39}\text{Ar}$  isotopic ages presented here was conducted at the Pacific Centre for Isotopic and Geochemical Research (PCIGR) at the Department of Earth and Ocean Sciences, University of British Columbia.

U-Pb isotopic age determinations reported here (Table 1) are from data acquired by Thermal Ionization Mass Spectrometry (U-Pb TIMS). Argon-40/argon-39 isotopic age determinations are from data acquired by the laser-induced step-heating technique (Table 2). Details of both analytical techniques are presented in Logan et al. (2007).

### Sample Descriptions

Samples collected for isotopic age determination are from southeastern and northwestern Chezacut map area. A grapefruit-sized sample was collected from the southeastern pluton, the Puntzi Ridge quartz monzonite (sample site MMI07-45-1, Table 2, Figure 2). The medium-grained, orange, porphyritic monzonite body was sampled at this site (Figure 14a) because it contains vitreous black biotite (5%) and hornblende (15%) an unusual occurrence as both minerals are normally dull green and turbid due to alteration. Accessory minerals include magnetite (~5%), pyrite (~0.25%) and traces of chalcopyrite. Outcrops near the sample site are cut by millimetre-thick sheeted K-feldspar and epidote veins.

Pink, medium-grained, holocrystalline monzonite is the main rock type within the northwestern intrusive body, the 'Sweetwater Lake' monzonite. It contains 3–4% interstitial quartz (locally up to 10%), ~45% K-feldspar, 40% plagioclase, 10% hornblende and 5% biotite. However, pervasive epidote and chlorite alteration attacks calcic cores of plagioclase and renders identification of the mafic minerals difficult. It was necessary to collect a ~20 kg sample from which a sufficient volume of zircons could be extracted (sample site MMI07-48-6, Figure 2).



Figure 13. Quartz-first granodiorite shows typical early porphyritic knots of quartz within a holocrystalline matrix.

### U-Pb Protolith Age

Zircon was separated from an approximately 20 kg sample of monzonite using a standard mineral separation technique, which includes crushing, grinding, Wilfley (wet shaker) table, heavy liquids and magnetic separation, followed by hand picking. Eight air abraded single grains selected for analysis were processed using techniques reported in Logan et al. (2007). One of these grains was lost during processing prior to mass spectrometry and two gave weak or unstable signals that did not yield usable data. Analytical results from the remaining five grains are listed in Table 1 and plotted in Figure 15. All data overlap concordia at the 2 $\sigma$  confidence level (Figure 15a), with the five-point weighted average of overlapping  $^{206}\text{Pb}$ - $^{238}\text{U}$  dates at 160.94  $\pm$  0.13 Ma (Figure 15b) taken as the best estimate for the age of the rock.

### $^{40}\text{Ar}/^{39}\text{Ar}$ Cooling Age

Both biotite and hornblende were separated from sample MMI07-45-1. The biotite separate yielded a humped-

Table 1. U-Pb TIMS analytical data for zircon from 'Sweetwater Lake' monzonite.

Grain <sup>1</sup>	Wt <sup>2</sup> (mg)	U <sup>3</sup> (ppm)	Pb <sup>4</sup> (ppm)	$^{206}\text{Pb}^5$ $^{204}\text{Pb}$	$^{207}\text{Pb}^6$ $^{206}\text{Pb}$	Pb <sup>7</sup> (pg)	Th/U <sup>8</sup>	Isotopic ratios $\pm 1\sigma, \%$ <sup>9</sup>			corr. coef.	% <sup>10</sup> discordant	Apparent ages $\pm 2\sigma, \text{Ma}$ <sup>11</sup>		
								$^{206}\text{Pb}/^{238}\text{U}$	$^{207}\text{Pb}/^{235}\text{U}$	$^{207}\text{Pb}/^{206}\text{Pb}$			$^{206}\text{Pb}/^{238}\text{U}$	$^{207}\text{Pb}/^{235}\text{U}$	$^{207}\text{Pb}/^{206}\text{Pb}$
Sample MMI07-48-6															
B	5.2	436.0	11.6	3992	69.4	0.9	0.599	0.02530 $\pm$ 0.10	0.1719 $\pm$ 0.2	0.04928 $\pm$ 0.15	0.599	0.0	161.1 $\pm$ 0	161.1 $\pm$ 1	161.1 $\pm$ 7.2/7.2
D	7.0	798.0	23.2	12620	233.2	0.7	0.886	0.02532 $\pm$ 0.15	0.1724 $\pm$ 0.2	0.04939 $\pm$ 0.10	0.801	3.3	161.2 $\pm$ 0	161.5 $\pm$ 1	166.6 $\pm$ 4.8/4.8
F	7.3	547.0	14.6	6564	111.1	1.0	0.563	0.02526 $\pm$ 0.19	0.1716 $\pm$ 0.2	0.04927 $\pm$ 0.15	0.765	-0.2	160.8 $\pm$ 1	160.8 $\pm$ 1	160.5 $\pm$ 7.0/7.1
G	5.5	1484.0	43.0	14590	267.1	0.9	0.888	0.02525 $\pm$ 0.08	0.1717 $\pm$ 0.1	0.04932 $\pm$ 0.06	0.859	1.3	160.8 $\pm$ 0	160.9 $\pm$ 0	162.8 $\pm$ 3.0/3.0
H	4.4	843.0	24.4	10800	200.2	0.5	0.725	0.02529 $\pm$ 0.07	0.1720 $\pm$ 0.1	0.04932 $\pm$ 0.11	0.725	1.2	161.0 $\pm$ 0	161.1 $\pm$ 0	163.0 $\pm$ 5.1/5.2

<sup>1</sup>All single grains, air abraded.

<sup>2</sup>Grain mass determined on Sartorius SE2 ultra-microbalance to  $\pm 0.1$  microgram.

<sup>3</sup>Corrected for spike, blank (0.2 pg  $\pm 50\%$ , 2 $\sigma$ ), and mass fractionation, which is directly determined with  $^{233}\text{U}$ - $^{235}\text{U}$  spike.

<sup>4</sup>Radiogenic Pb; data corrected for spike, fractionation, blank and initial common Pb; mass fractionation correction of 0.23% /amu  $\pm 40\%$  (2 $\sigma$ ) is based on analysis of NBS-982 throughout course of study; blank Pb correction of 0.5-0.9 pg  $\pm 40\%$  (2 sigma) with composition of  $^{206}\text{Pb}/^{204}\text{Pb} = 18.5 \pm 2\%$ ,  $^{207}\text{Pb}/^{204}\text{Pb} = 15.5 \pm 2\%$ ,  $^{208}\text{Pb}/^{204}\text{Pb} = 36.4 \pm 2\%$ , all at 2 $\sigma$ ; initial common Pb compositions based on Stacey and Kramers (1975) model Pb at the interpreted age of the rock.

<sup>5</sup>Measured ratio corrected for spike and fractionation.

<sup>6</sup>Ratio of radiogenic to common Pb.

<sup>7</sup>Total weight of common Pb calculated with blank isotopic composition.

<sup>8</sup>Model Th/U ratio calculated from radiogenic  $^{207}\text{Pb}/^{206}\text{Pb}$  ratio and  $^{207}\text{Pb}/^{206}\text{Pb}$  age.

<sup>9</sup>Corrected for spike, fractionation, blank and initial common Pb.

<sup>10</sup>Discordance in % to origin.

<sup>11</sup>Age calculations are based on decay constants of Jaffey et al. (1971).

Table 2. Ar isotopic data from Puntzi Ridge quartz monzonite.

Laser Power(%)	Isotope Ratios $^{40}\text{Ar}/^{39}\text{Ar}$	$^{38}\text{Ar}/^{39}\text{Ar}$	$^{37}\text{Ar}/^{39}\text{Ar}$	$^{36}\text{Ar}/^{39}\text{Ar}$	Ca/K	Cl/K	% $^{40}\text{Ar}$ atm f $^{39}\text{Ar}$	$^{40}\text{Ar}/^{39}\text{ArK}$	Age	
Sample MMI07-45-1										
2	115.2233 ±0.0055	1.4680 ±0.0111	4.4609 ±0.0167	0.3364 ±0.0175	15.3	0.322	85.82	17.1	16.330 ±1.724	145.43 ±14.75
2.2	283.1358 ±0.0941	0.3750 ±0.4352	1.8510 ±1.5255	0.8857 ±0.1339	6.043	0.04	88.65	0.12	25.512 ±26.303	222.34 ±215.67
2.4	111.6997 ±0.0503	0.4008 ±0.1464	0.5939 ±1.0879	0.3098 ±0.0712	1.934	0.074	76.98	0.36	21.394 ±5.056	188.26 ±42.25
2.7	75.2856 ±0.0215	0.2663 ±0.0507	1.0841 ±0.8500	0.1936 ±0.0556	3.678	0.049	73.67	1.33	18.459 ±2.989	163.56 ±25.32
3	41.1631 ±0.0127	0.1311 ±0.0354	0.6036 ±0.3130	0.0810 ±0.0396	2.09	0.023	55.16	2.97	17.398 ±0.938	154.55 ±7.99
3.3	29.4392 ±0.0075	0.2237 ±0.0480	1.2511 ±0.2216	0.0418 ±0.0504	4.354	0.046	38.53	5.5	17.319 ±0.636	153.88 ±5.41
3.6	26.7454 ±0.0064	0.4487 ±0.0188	2.2229 ±0.0844	0.0337 ±0.0370	7.752	0.099	33.89	8.74	17.172 ±0.386	152.62 ±3.29
4	22.4389 ±0.0047	1.9552 ±0.0095	5.4533 ±0.0142	0.0198 ±0.0222	19.11	0.45	21.26	29.2	17.568 ±0.158	155.99 ±1.34
4.3	20.9618 ±0.0063	1.6863 ±0.0139	4.5753 ±0.0276	0.0146 ±0.0587	16.01	0.387	14.83	13.2	17.475 ±0.280	155.21 ±2.39
4.6	19.9892 ±0.0074	1.3166 ±0.0177	3.5043 ±0.0155	0.0111 ±0.0582	12.25	0.301	10.86	12.1	17.352 ±0.236	154.16 ±2.01
4.9	20.0264 ±0.0128	0.3988 ±0.0290	1.4738 ±0.0565	0.0112 ±0.0929	5.176	0.088	11.84	9.35	17.002 ±0.383	151.17 ±3.26
Total/Average	39.4907 ±0.0013	1.3023 ±0.0028	7.2375 ±0.0031	0.0775 ±0.0067	13.31	0.171			100	17.246 ±0.160

J = 0.005141 ±0.000012

Volume  $^{39}\text{ArK}$  = 96.16

Integrated Date = 153.25 ±2.75

Volumes are  $1\text{E}^{13}$  cm<sup>3</sup> NPT

Neutron flux monitors: 28.02 Ma FCs (Renne et al., 1998)

Isotope production ratios: ( $^{38}\text{Ar}/^{39}\text{Ar}$ )K=0.0302 ±0.00006, ( $^{37}\text{Ar}/^{39}\text{Ar}$ )Ca=1416.4 ±0.5, ( $^{36}\text{Ar}/^{39}\text{Ar}$ )Ca=0.3952 ±0.0004,

Ca/K=1.83 ±0.01( $^{37}\text{ArCa}/^{39}\text{ArK}$ ).

shaped release spectrum with no reliable plateau age, suggesting the presence of excess argon. In addition, the computed inverse isochron ages are not reasonable. The best age estimate that can be obtained from the biotite data is the integrated plateau age of  $155.9 \pm 0.5$ , but this is suspect and made redundant with a well-behaved hornblende separate. The hornblende plateau age of  $155.1 \pm 1.2$  Ma represents

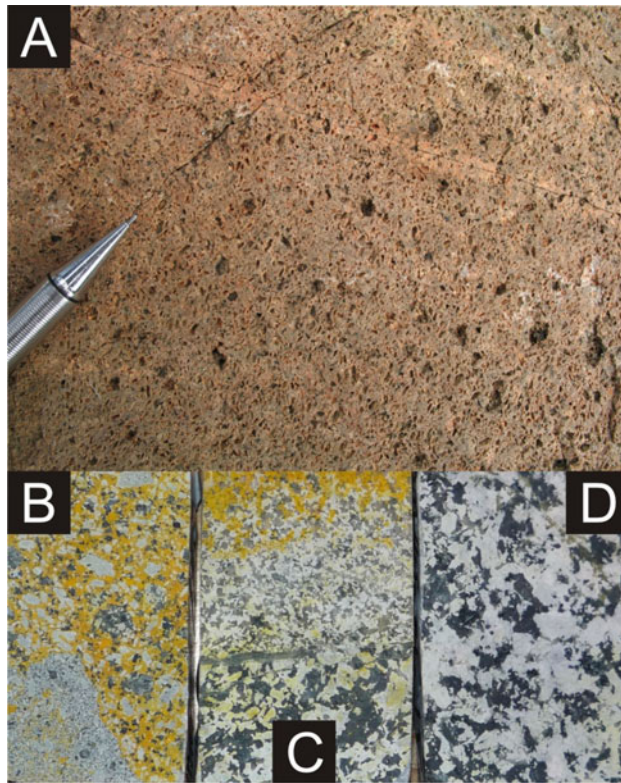


Figure 14. a) Typical exposure of Puntzi Ridge quartz monzonite and b) thin section cut-off with yellow-stained K-feldspar from a high-level tuffaceous equivalent of the monzonite. c) Chilanko Igneous Complex quartz diorite with finer-grained, crosscutting monzogranite dike and d) unaltered quartz diorite of the complex.

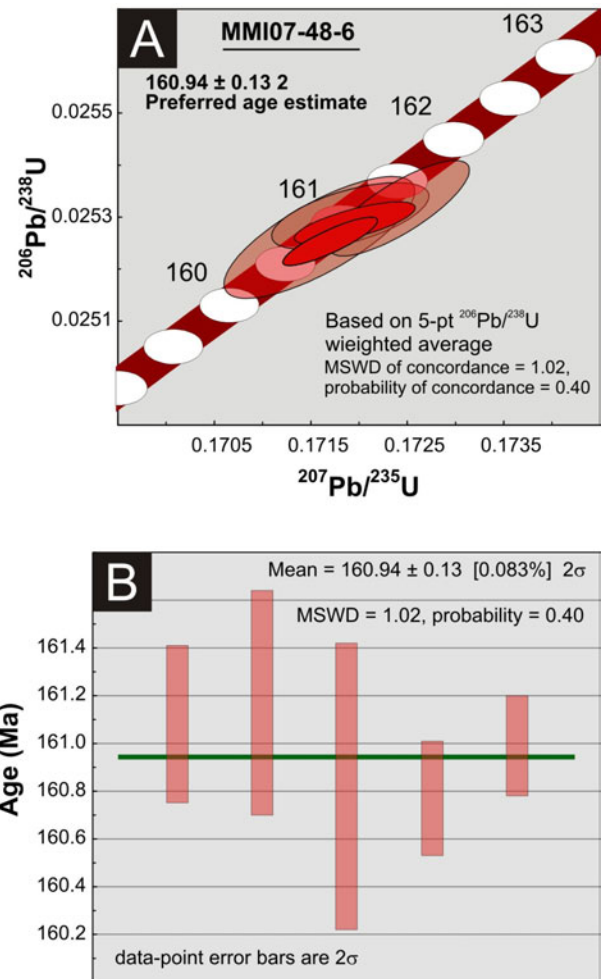


Figure 15. a) Concordia plots for U-Pb TIMS data for sample MMI07-48-6. The  $2\sigma$  error ellipses for individual analytical fractions are in red. Concordia bands include  $2\sigma$  errors on U decay constants. b) Mean square weighted deviates (MSWD) plot for the five fractions. Box heights are  $2\sigma$ .

90.7% of the  $^{39}\text{Ar}$  released (Figure 16a, only the highest temperature step is omitted). The age is confirmed by an inverse isochron model age for the six high temperature steps which yields  $154.4 \pm 2.9$  Ma (Figure 16b).

### Implications of Geochronology

Polyphase, variably foliated dioritic parts of the northern ‘Sweetwater Lake’ monzonite intrusion are very similar to parts of the Chilanko intrusive complex, which underlies much of the southeastern Chilanko Forks area (Figure 2). Penetrative fabrics are lacking within the main ‘Sweetwater Lake’ monzonitic body. Similarly, undeformed monzonitic phases are seen to cut the more foliated parts of the Chilanko intrusive complex (Figure 14c). If this correlation is correct, a relative age relationship is demonstrated, consistent with the isotopic ages reported here.

Mihalynuk et al. (2008b) suggested that although the Puntzi Ridge quartz monzonite cuts structurally lower Mesozoic arc strata, it may be comagmatic with some of the younger Mesozoic tuffaceous rocks (Figure 14b).

An implication of the foregoing inferences is that both the growth of the middle arc succession and deformation affecting the Chilanko intrusive complex are bracketed at between ~161 and ~152 Ma. This deformation age is consistent with syndeformational fabrics within the complex (see next section), and appears coeval with deformation in southwest Anahim Lake map area (van der Heyden, 2004).

## STRUCTURE AND DEFORMATION

Youngest rocks within the region, those of the Oligocene-Pleistocene Chilcotin Group and/or Pleistocene-Holocene Anahim volcanic belt, are not folded. However, Mihalynuk et al. (2008b) showed that even the youngest rocks appear to be cut by high angle reverse faults. No evidence of such deformation was observed in the sparse exposures of these rocks within the Chilanko Forks or Klusko River areas.

Pervasive deformational fabrics were probably formed in Late Jurassic, mid-Cretaceous and Early Eocene times. At least two stages of deformation have affected Mesozoic rocks, including Late Jurassic rocks within the Tatla Lake Metamorphic Complex (Friedman, 1988) and probable correlative rocks deformed at a higher crustal level (Mihalynuk and Friedman, 2009) and now included within the informally named Chilanko intrusive complex. In contrast, the Eocene Ootsa Lake Group displays only locally developed cleavage.

### Jurassic Deformation

Jurassic deformation is indicated by the syndeformational intrusive fabrics preserved within the Chilanko intrusive complex. Such fabrics include crosscutting of foliated intrusive phases by phases that appear compositionally identical, but which are weakly to nonfoliated. If the Klusko Intrusive Complex is dated at ~161–152 Ma, as argued above, then synemplacement metamorphism is broadly correlative with that within the Atnarko Crystalline Complex (western part of NTS 093C). The U-Pb metamorphic ages of those rocks are interpreted as  $158.8 \pm 0.3$  Ma and  $157 \pm 11$  Ma, based on metamorphic zircon from ductilely sheared metarhyolite, and syn- to late-kinematic quartz diorite (van der Heyden, 2004), respectively. These

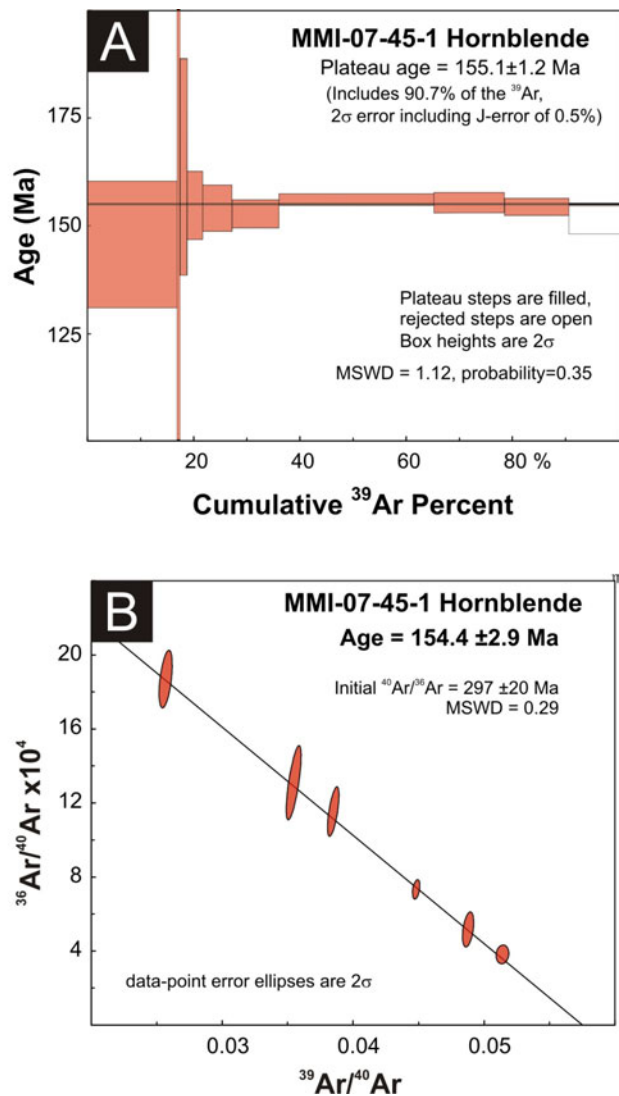


**Figure 16. a)** Step heating Ar gas release spectra for hornblende sample MMI07-45-1. Filled plateau steps produce an age of  $155.1 \pm 1.2$  Ma (90.7% of  $^{39}\text{Ar}$ , rejected step is open). Box heights at each step are  $2\sigma$ . **b)** The Ar isotope ratio correlation plots for plateau steps in a) provide a reliable age determination of  $154.4 \pm 2.9$  Ma, identical within error to the plateau age.

ages span the Middle–Upper Jurassic boundary of  $156.6 \pm 2.0$ – $2.7$  Ma (Pálffy et al., 2000).

### Late Eocene-Oligocene Deformation

Broad folds are interpreted to deform the Ootsa Lake Group with production of local, open parasitic folds and axial cleavage. This cleavage is well developed only locally, but in such localities it is obvious, causing platy segmentation of outcrops with folia passing through clasts. Such fabric should not be confused with much more common flow foliation that also results in platy parting, but does not pass through fragments or clasts contained within the flows. Axial cleavage is best developed 4 km southeast of Thunder Mountain, along strike of the Mesozoic uplift and fold hinge mapped in the Chezacut area (Mihalynuk et al., 2008a). Another fold mapped by Mihalynuk et al. (2008a), about 8 km farther west, could not be verified by mapping

along strike to the north. It may not exist, as in the reinterpretation offered in Figure 2, or it may die out as it passes from the southern to the northern part of the Chezacut map area. In most other parts of the Clusko River area, tilting of Eocene strata is probably due to block faulting.

The age of deformation of the Ootsa Group has not been conclusively constrained. However, the tendency of the upper, younger units (~46–44 Ma, see ‘Ootsa Lake Group’ above) to lie flat (Figure 9e) while the underlying rocks (~54–50 Ma) are moderately tilted, suggests an intervening period of deformation. This age of deformation is consistent with a rapid regional cooling at ~50 Ma, as determined from fission tracks (Riddell and Ferri, 2008) and extensional faulting in the nearby Tatla Lake Metamorphic Complex between  $55 \pm 3$  and  $47 \pm 1.5$  Ma (Friedman, 1988), which is herein postulated to extend to southeastern Chilanko Forks area; see also Mihalynuk et al., 2009) where deformed Jurassic rocks are widely affected by block faulting.

Beautifully corrugated and polished fault planes (Figure 17) have a spacing of ~5–10 m within intermittently exposed, ductilely deformed Chilanko intrusive complex rocks in the southeastern corner of NTS 093C/01. Fault planes are lined with comminuted quartz and epidote, dip moderately east and generally display normal to slightly oblique offsets (although overprinted fault plane fabrics with reverse offset are not uncommon). These faults cut an earlier shallow, intense mylonite fabric (Figure 18a) and subhorizontal west-trending folds. Mylonite is overprinted by sets of centimetre-scale, domino-style normal faults (Figure 18b); with increasing downdip offset on these normal faults, the mylonite becomes brecciated (Figure 18c). The breccia consists of cemented quartz and chlorite. We tentatively interpret the brecciation as recording a ductile to brittle transition at a detachment fault. The corrugated, moderately east-dipping normal faults are antithetic with respect to top-to-the-west motion documented on extensional shear zones of the Tatla Lake Metamorphic Complex (Friedman, 1988) and are typical of early brittle shears within the brittle-ductile transition zone footwall of detachment faults (e.g., Sacramento Mountains core complex; Stewart and Argent, 2000). Locally derived clastic rocks atop the sheared intrusive rocks are likely deposited in small synextensional basins within a few hundred verti-



**Figure 17.** Moderately east-dipping, beautifully corrugated and polished brittle fault plane.

cal metres of the detachment surface. Unlike the main detachment fault, which exhumes high grade rocks in the core of the Tatla Lake Metamorphic Complex, the detachment fault mapped within the southeast portion of the Chilanko Forks map area is a relatively minor structure and shows little evidence of major crustal omission across it.

Middle to upper amphibolite-grade lower plate rocks of the Tatla Lake Metamorphic Complex are separated from greenschist-grade upper plate rocks by a 1–2.5 km thick ‘ductilely sheared assemblage’ (DSA; Friedman,

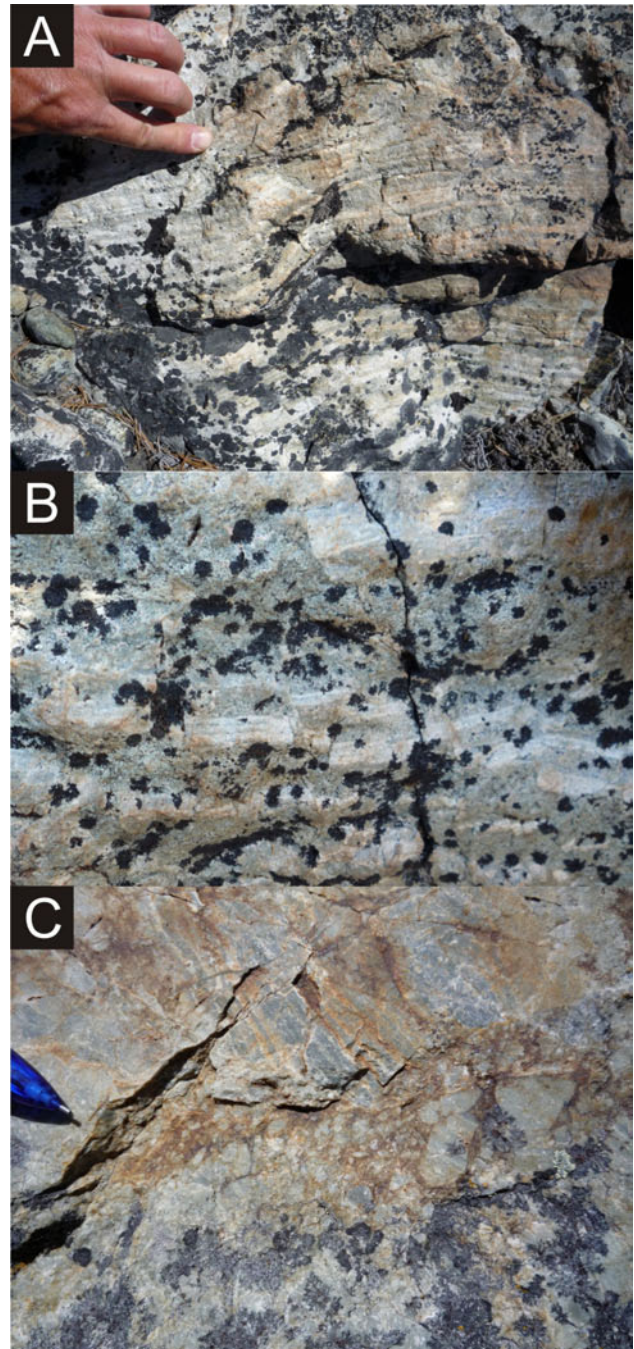


**Figure 18.** a) Well-developed mylonitic fabric locally includes ptynitic veins. b) Domino-style brittle faults cutting the mylonitic fabric. c) Increased offset on brittle faults produces disaggregated and recemented breccia.

1988). Within the Chilanko Forks area, rocks belonging to the DSA crop out north and south of Takla Lake. To the north, they consist of strongly foliated biotite granodiorite and, to the south, they are strongly foliated and lineated green schistose rocks, probably former volcanoclastic strata.

## MINERALIZATION

Within the Chilanko Forks area and southern half of the Clusko River area, only two mineral occurrences are recorded in MINFILE: ‘Chilcotin River East’ (MINFILE 093C 014) and ‘Chilcotin River West’ (MINFILE 093C 013). Both of these “consist...of copper mineralization within...Ootsa Lake Group intermediate to felsic volcanic and related rocks” (MINFILE, 2007) north of the Chilcotin River in NTS 093C/09S. Neither showing was encountered during the course of our mapping. Within the intervening Chezacut map area, several new mineral occurrences were discovered by Mihalynuk et al. (2008b).

Newmac Resources Inc. is owner and operator of the CA prospect (Chilanko River property), located just 6 km west of the southern Chilanko Forks map area. Here mineralization consists of disseminated chalcocopyrite within a locally foliated quartz diorite-andesite dike complex (Fleming, 1996) that is almost certainly correlative with the Chilanko intrusive complex. Within, or adjacent to the Chilanko complex, three copper showings were found during the course of mapping in the 2008 field season: the Fit, ET and Ejewra showings (see Table 3 and Figure 2 for locations). Scattered angular sericite-altered float displaying an epithermal geochemical signature was also found adjacent to the complex. North of Tatla Lake, intrafolial chalcocopyrite and malachite were found within a ~3.5 m<sup>3</sup> erratic of gneissic granodiorite. North of Chilanko River, a sample of altered Eocene tuff returned elevated As and Au (INAA: 18 ppm, 83 ppb). Analyses of grab samples obtained from these showings are listed in Table 3.

### Fit Showing

Minor copper-silver mineralization is found in scattered tonalite outcrops and angular boulders over a ~50 m<sup>2</sup> area about 0.75 km northeast of Fit Mountain summit. Mineralization within the intrusion accompanies chlorite-magnetite alteration. It consists of veinlets and disseminations

of chalcocopyrite and subordinate bornite together with epidote-magnetite-chlorite-quartz-calcite veining (Figure 19a, b) and matrix replacement. Analyses of samples collected returned up to 0.18% Cu, 2.2 g/t Ag, and 20 ppb Au (MMI08-6-3, Table 3). Attempts to track the mineralized zone beyond the local outcrops were not successful, although mineralization crops out ~1.2 km to the northwest in the thermal-metamorphic halo of the Fit Mountain tonalite. Within the contact zone, strongly altered (chlorite-calcite±epidote±albite+scapolite (?)) and brecciated outcrop is exposed over a ~10 m<sup>2</sup> area. A grab sample of the altered and mineralized breccia returned 0.37% Cu, 2.87 g/t Ag and 63 ppb Au.

### Ejewra Showing

A grab sample collected approximately 4 km southeast of Fit Mountain (EOR08-13-3, Table 3) returned 0.58% Cu, 4.2 g/t Ag and 40 ppb Au. A large angular block (probable erratic) 1.1 km to the northwest contained more than 10% pyrite and a grab sample collected from it contained 7.47 g/t Te (and lesser concentrations of the above noted elements). It is worthwhile noting that the probable erratic is up-ice of the outcrop sample and must be derived from a separate mineralized zone (or one that is continuous for over 1 km).

### ET Showing

About 2.5 km northeast of Pyper Lake and 0.8 km west of the Chilanko igneous complex contact, variably foliated tuffaceous rocks (Figure 19c) contain veins of quartz-calcite (±rhodochrosite)-epidote-chlorite±chalcocite and malachite, which make up the ET showing (Figure 2). Veins up to 15 cm thick contain irregular knots of chalcocite up to 2 cm across. Grab samples collected from various veins contain up to 0.12% Cu, 2.8 g/t Ag and 0.2 g/t Au (Table 3).

Abundant, fist-sized, angular, rusty float is scattered over several square metres of hillside ~1.8 km south of the ET showing. Portions of five angular quartz- and sericite-altered clasts were combined and analyzed. Results show elevated base metal values, including 0.4 g/t Ag, 11.9 ppm As, 22 ppm Hg, as well as 84 and 55 ppb Au (via ICP and INAA methods, respectively; MMI08-31-3, Table 3). These results correspond to an epithermal geochemical signature and may warrant further evaluation given the abun-

Table 3. Analytical subset for selected grab samples.

Sample ID	Name	Location	Latitude	Method Longitude	Cu	Pb	Zn	Ag	Au	Te	Hg	As	Zn	Ag	Au	As
					ICP-MS (ppm)	ICP-MS (ppm)	ICP-MS (ppm)	ICP-MS (ppb)	ICP-MS (ppb)	ICP-MS (ppm)	ICP-MS (ppm)	INAA (ppm)	INAA (ppb)	INAA (ppb)	INAA (ppm)	
EOR08-13-3	Ejewra	Fit Mtn. S	52.18	-124.22	5826.64	5.84	170.6	4199	40	0.88	85	2.8	<50	<5	44	9.2
EOR08-13-5	Ejewra float	Fit Mtn. S	52.19	-124.23	99.02	3.91	61.7	101	7	7.47	<5	4.3	<50	<5	<2	6.0
MMI08-2-2	no name: float	Fit Mtn. S	52.16	-124.25	8.69	0.94	20.5	45	<0.2	0.80	309	1.0	<50	<5	<2	4.8
MMI08-5-1	Chili	Chezacut SE	52.31	-124.03	1473.66	23.84	195.5	13186	93	4.42	<5	17.0	230	23	120	34.2
MMI08-5-1rep	Chili	Chezacut SE	52.31	-124.03	1565.99	24.51	188.3	14477	101	4.80	<5	15.8	240	24	120	35.4
MMI08-6-3	Fit	Fit Mtn	52.21	-124.24	1861.30	7.02	95.1	2226	20	0.17	<5	1.9	<50	<5	27	5.9
MMI08-6-8B	Fit	Fit Mtn	52.22	-124.25	3707.11	10.25	57.5	2872	63	0.19	7	0.7	<50	<5	<2	9.5
MMI08-13-7	no name	Chilanko R. N	52.12	-124.40	28.99	2.73	44.4	10	<0.2	<0.02	<5	0.5	<50	<5	83	18.0
MMI08-31-3	no name	Pyper Lk. E	52.05	-124.13	131.77	42.12	52.8	443	84	4.37	22	11.9	<50	<5	55	2.7
MMI08-31-12	ET	Pyper Lk. NE	52.07	-124.14	1152.92	1.42	14.2	853	15	<0.02	<5	<0.1	<50	<5	29	1.0
MMI08-31-12rep	ET	Pyper Lk. NE	52.07	-124.14	1214.07	1.39	13.3	987	202	0.03	5	<0.1	<50	<5	29	1.0
MMI08-41-6	Erratic	Tatla Lk N of E	52.02	-124.37	4040.24	1.61	10.5	2465	11	0.12	<5	1.1	<50	<5	8	3.0
TBA08-38-4	ET	Pyper Lk.	52.03	-124.04	1276.51	51.22	246.4	2857	2	0.26	5	0.9	260	<5	<2	4.0
<b>Detection limit</b>					<b>0.01</b>	<b>0.01</b>	<b>0.1</b>	<b>2</b>	<b>1</b>	<b>0.02</b>	<b>5</b>	<b>0.1</b>	<b>50</b>	<b>5</b>	<b>2</b>	<b>0.5</b>

Notes: INAA, instrumental neutron activation analysis; ICP-MS, inductively coupled plasma mass spectrometry  
A full list of samples and elements analyzed can be obtained for both INAA and ICP-MS suites from  
[http://www.em.gov.bc.ca/Mining/GeolSurv/Publications/catalogue/cat\\_geof.htm](http://www.em.gov.bc.ca/Mining/GeolSurv/Publications/catalogue/cat_geof.htm)

dance and angularity of the clasts, which suggest a nearby source.

### Erratic

North of eastern Tatla Lake an erratic of foliated granodiorite contains intrafolial chalcopyrite-malachite and tetrahedrite(?). One grab sample yielded 0.4% Cu and 2.4 g/t Ag. Mineralization is confined to one ~20 cm thick

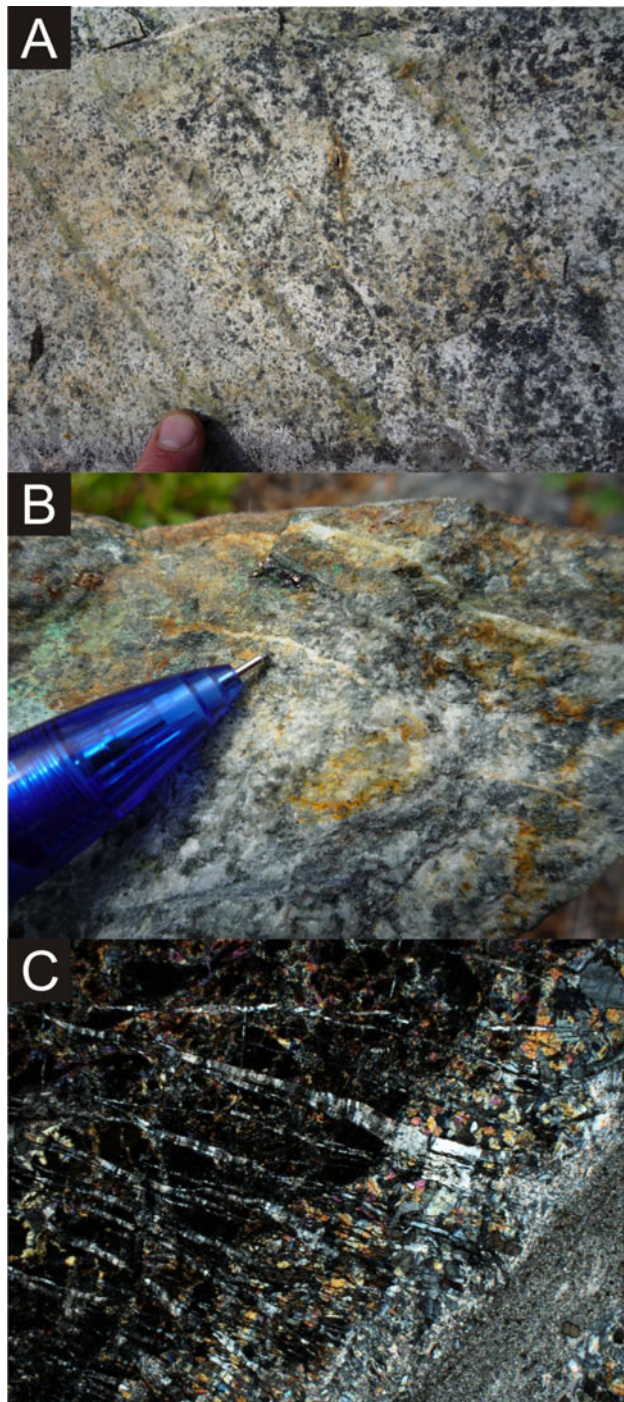


**Figure 19.** a) Sheeted veins within Fit Mountain tonalite. b) Veinlets contain chalcopyrite and bornite. c) Abundant calcite veinlets within foliation in epidotized tuff near the ET showing.

foliaform zone (Figure 20). Even though this large (~3.5 m<sup>3</sup>) erratic lies within 100 m of outcrop, a thorough search of the surrounding ~1 km<sup>2</sup> did not reveal any mineralized bedrock or other mineralized erratics.

### Regional Mineral Potential

Some hints of epithermal mineralization within the Eocene Ootsa Lake Group were revealed by analysis of altered tuffs from north of the Chilanko River and from quartz- and sericite-altered float south of the ET showing. However, if the frequency of discovery during our 2008 field mapping in the Chilanko Forks area (NTS 093C/01) can be used as an indicator, the greatest potential for future discoveries lies within the Chilanko intrusive complex. Our findings are confirmed by the work of Newmac Resources Inc. and predecessors at the Chilanko property in adjacent parts of NTS 093C/02. Thus, this >330 km<sup>2</sup> complex, together with rocks in the adjacent thermal metamorphic halo, warrants further systematic exploration.

### ACKNOWLEDGMENTS

T. Ullrich processed the <sup>40</sup>Ar/<sup>39</sup>Ar samples and generated the step release data, spectra and inverse isochron plots. J. Riddell offered peer review of this paper. P. Metcalfe is thanked for his candid discussions with regards to former data density in the southern Clusko map area. R. Lett provided rock solid reliability in the delivery of geochemical data with fine quality control for this and past unacknowledged years. Assistance with mineral separation and mass spectrometry was provided by H. Lin and Y. Feng helped with grain selection, pre-treatment and sample dissolution/processing. J. Wardle was always close at hand to lend assistance in the field. M. and A. McMath were tremendously accommodating hosts at our Puntzi Lake base camp.



**Figure 20.** Erratic of strongly foliated granodiorite contains a 20 cm thick foliaform zone of malachite+tetrahedrite (?).

### REFERENCES

Alfaro, R., Campbell, R., Vera, P., Hawkes, B. and Shore, T. (2004): Dendroecological reconstruction of mountain pine beetle outbreaks in the Chilcotin Plateau of British Columbia; in Mountain Pine Beetle Symposium: Challenges and

- Solutions, T.L. Shore, J.E. Brooks and J.E. Stone, Editors, *Natural Resources Canada*, Canadian Forest Service, Pacific Forestry Centre, Information Report BC-X-399, pages 245–256.
- Andrews, G.D.M. and Russell, J.K. (2007): Mineral exploration potential beneath the Chilcotin Group (NTS 0920, P, 093A, B, C, F, G, I, J, K), south-central British Columbia: preliminary insights from volcanic facies analysis; in *Geological Fieldwork 2006, BC Ministry of Energy, Mines and Petroleum Resources*, Paper 2007-1 and Geoscience BC, Report 2007-1, pages 229–238.
- BC Ministry of Forests and Range (2005a): The state of British Columbia's forests 2004; *BC Ministry of Forests and Range*, URL <<http://www.for.gov.bc.ca/hfp/sof/2004/>> [November 2007].
- BC Ministry of Forests and Range (2005b): British Columbia's Mountain Pine Beetle Action Plan 2005-2010; *Government of British Columbia*, 20 pages, URL <[http://www.for.gov.bc.ca/hfp/mountain\\_pine\\_beetle/actionplan/2005/actionplan.pdf](http://www.for.gov.bc.ca/hfp/mountain_pine_beetle/actionplan/2005/actionplan.pdf)> [October 2, 2006].
- BC Ministry of Forests and Range (2008): About Us; *BC Ministry of Forests and Range*, URL <<http://bcwildfire.ca/AboutUs/>> [October 2008].
- Bevier, M.L. (1983): Regional stratigraphy and age of Chilcotin Group basalts, south-central British Columbia; *Canadian Journal of Earth Sciences*, Volume 20, pages 515–524.
- Bevier, M.L. (1989): A lead and strontium isotopic study of the Anahim volcanic belt, British Columbia: additional evidence for widespread suboceanic mantle beneath western North America; *Geological Society of America Bulletin*, Volume 101, pages 973–981.
- Cassidy, J. and Al-Khoubbi, I. (2007): A passive seismic investigation of the geological structure within the Nechako Basin; in *The Nechako Initiative-Geoscience Update, BC Ministry of Energy, Mines and Petroleum Resources*, Petroleum Geology Open File 2007-1, pages 7–57, URL <[http://www.empr.gov.bc.ca/OG/oilandgas/petroleumgeology/ConventionalOilAndGas/InteriorBasins/Documents/The\\_Nechako\\_Initiative-Geoscience\\_Update\\_2007.pdf](http://www.empr.gov.bc.ca/OG/oilandgas/petroleumgeology/ConventionalOilAndGas/InteriorBasins/Documents/The_Nechako_Initiative-Geoscience_Update_2007.pdf)> [November 2008].
- Diakow, L.J. and Barrios, A. (2009): Geology and mineral occurrences of the mid-Cretaceous Spences Bridge Group near Merritt, southern British Columbia (parts of NTS 092H/14, 15, 092I/02, 03); in *Geological Fieldwork 2008, BC Ministry of Energy, Mines and Petroleum Resources*, Paper 2009-1, pages 63–80.
- Diakow, L.J. and Levson, V.M. (1997): Bedrock and surficial geology of the southern Nechako Plateau, central British Columbia; *BC Ministry of Energy, Mines and Petroleum Resources*, Geoscience Map 1997-2, scale 1:100 000.
- Diakow, L.J., Webster, I.C.L., Richards, T.A. and Tipper, H.W. (1997): Geology of the Fawnie and Nechako Ranges, southern Nechako Plateau, central British Columbia (93F/2, 3, 6, 7); in *Interior Plateau Geoscience Project: Summary of Geological, Geochemical and Geophysical Studies*; *BC Ministry of Energy, Mines and Petroleum Resources*, Paper 1997-2, pages 7–30.
- Ferbey, T., Vickers, K.J., Hietava, T.J.O. and Nicholson, S.C. (2009): Quaternary geology and till geochemistry of the Redstone and Loomis Lake map areas, central British Columbia (NTS 93B/04, 05); in *Geological Fieldwork 2008, BC Ministry of Energy, Mines and Petroleum Resources*, Paper 2009-1, pages 117–126.
- Ferri, F. and Riddell, J. (2006): The Nechako Basin project: new insights from the southern Nechako Basin; in *Summary of Activities 2006, BC Ministry of Energy, Mines and Petroleum Resources*, Paper 2007-2, pages 89–124.
- Fleming, D.B. (1996): Chilanko River property; *BC Ministry of Energy, Mines and Petroleum Resources*, Assessment Report 24324, 10 pages (plus appendices and maps), URL <<http://www.em.gov.bc.ca/DL/ArisReports/24324.PDF>> [November 2008].
- Friedman, R.M. (1988): Geology and geochronology of the Eocene Tatla Lake metamorphic core complex, western edge of the Intermontane Belt, British Columbia: Ph.D. thesis, *The University of British Columbia*, 348 pages.
- Friedman, R.M. (1992): P-T-t path for the lower plate of the Eocene Tatla Lake metamorphic core complex, southwestern Intermontane Belt, British Columbia; *Canadian Journal of Earth Sciences*, Volume 29, pages 972–983.
- Friedman, R.M. and Armstrong, R.L. (1988): Tatla Lake Metamorphic Complex: an Eocene metamorphic core complex on the southwestern edge of the Intermontane Belt of British Columbia; *Tectonics*, Volume 7, pages 1141–1166.
- Geological Survey of Canada (1994): Magnetic residual total field, Interior Plateau of British Columbia; *Geological Survey of Canada*, Open File 2785, 19 maps at 1:100 000 and 1:250 000 scale.
- Hayward, N. and Calvert, A. (2008): Structure of the south-eastern Nechako Basin, British Columbia: results of seismic interpretation and first-arrival tomographic inversion; in *Back to Exploration (extended abstract)*, CSPG CSEG CWLS Convention, Calgary, pages 612–616, URL <<http://www.cspg.org/conventions/abstracts/2008abstracts/027.pdf>> [November 2008].
- Holland, S.S. (1964): Landforms of British Columbia; *BC Ministry of Energy, Mines and Petroleum Resources*, Bulletin 48 (revised 1976), 138 pages.
- Jaffey, A.H., Flynn, K.F., Glendenin, L.E., Bentley, W.C. and Essling, A.M. (1971): Precision measurement of half-lives and specific activities of  $^{235}\text{U}$  and  $^{238}\text{U}$ ; *Physical Review C*, Volume 4, pages 1889–1906.
- Kerr, D.E. and Giles, T.R. (1993): Surficial geology of the Chezacut map area (NTS 93C/8); *BC Ministry of Energy, Mines and Petroleum Resources*, Open File 1993-17, scale 1:50 000.
- Larocque, J.P. and Mihalynuk, M.G. (2009): Geochemical character of Neogene volcanic rocks of the central beetle-infested zone, south-central British Columbia (NTS 093B, C); in *Geological Fieldwork 2008, BC Ministry of Energy, Mines and Petroleum Resources*, Paper 2009-1, pages 109–116.
- LeMaître, R.W., Bateman, P., Dudek, A., Keller, J., Le Bas, M.J., Sabine, P.A., Schmid, R., Sorensen, H., Streckeisen, A., Wooley, A.R. and Zanettin, B. (1989): A Classification of Igneous Rocks and Glossary of Terms; *Blackwell Scientific Publications*, Oxford, United Kingdom, 193 pages.
- Levson, V.M. and Giles, T.R. (1997): Quaternary geology and till geochemistry studies in the Nechako and Fraser plateaus, central British Columbia (NTS 93C/1, 8, 9, 10; F/2, 3, 7; 93L/16; 93M/1); in *Interior Plateau Geoscience Project: Summary of Geological, Geochemical and Geophysical Studies*, L.J. Diakow, P. Metcalfe and J. Newell, Editors, *BC Ministry of Energy, Mines and Petroleum Resources*, Paper 1997-2, pages 121–145.
- Logan, J.M., Mihalynuk, M.G., Ullrich, T. and Friedman, R.M. (2007): U-Pb ages of intrusive rocks and  $^{40}\text{Ar}/^{39}\text{Ar}$  plateau ages of copper-gold-silver mineralization associated with alkaline intrusive centres at Mount Polley and the Iron Mask Batholith, southern and central British Columbia; in *Geological Fieldwork 2006, BC Ministry of Energy, Mines and Petroleum Resources*, Paper 2007-1, pages 93–116, URL <<http://www.em.gov.bc.ca/DL/GSBPubs/GeoFldWk/2006/11-Logan.pdf>> [November 2008].
- Massey, N.W.D., MacIntyre, D.G., Desjardins, P.J. and Cooney, R.T. (2005): Digital geology map of British Columbia: whole province; *BC Ministry of Energy, Mines and Petroleum Resources*, GeoFile 2005-1, scale 1:250 000, URL

- <<http://www.empr.gov.bc.ca/Mining/Geoscience/PublicationsCatalogue/GeoFiles/Pages/2005-1.aspx>>.
- Mathews, W.H. (1989): Neogene Chilcotin basalts in south-central British Columbia: geology, ages, and geomorphic history; *Canadian Journal of Earth Sciences*, Volume 26, pages 969–982.
- Metcalfe, P., Richards, T.A., Villeneuve, M.E., White, J.M. and Hickson, C.J. (1997): Physical and chemical volcanology of the Eocene Mount Clisbako volcano, central British Columbia (93B/12, 13; 93C/9, 16); in Interior Plateau Geoscience Project: Summary of Geological, Geochemical and Geophysical Studies, L.J. Diakow, P. Metcalfe and J. Newell, Editors, *BC Ministry of Energy, Mines and Petroleum Resources*, Paper 1997-2, pages 31–61.
- Mihalynuk, M.G., Erdmer, P., Ghent, E.D., Cordey, F., Archibald, D.A., Friedman, R.M. and Johannson, G.G. (2004): Coherent French Range blueschist: subduction to exhumation in <2.5 m.y.?; *Geological Society of America*, Bulletin, Volume 116, pages 910–922.
- Mihalynuk, M.G., Peat, C.R., Terhune, K. and Orovan, E.A. (2008a): Regional geology and resource potential of the Chezacut map area, central British Columbia (NTS 093C/08); in Geological Fieldwork 2007, *BC Ministry of Energy, Mines and Petroleum Resources*, Paper 2008-1, pages 117-134, URL <<http://www.em.gov.bc.ca/DL/GSBPubs/GeoFldWk/2007/13-Mihalynuk-Chezacut34526.pdf>> [November 2008].
- Mihalynuk, M.G., Peat, C.R., Orovan, E.A., Terhune, K., Ferbey, T. and McKeown, M.A. (2008b): Chezacut area geology (NTS 93C/8); *BC Ministry of Energy, Mines and Petroleum Resources*, Open File 2008-2, scale 1:50 000, URL <<http://www.empr.gov.bc.ca/Mining/Geoscience/PublicationsCatalogue/OpenFiles/2008/Pages/2008-2.aspx>> [November 2008].
- Mihalynuk, M.G. and Friedman, R.M. (2009): First isotopic age constraints for the Dean River Metamorphic belt, Anahim Lake area: implications for crustal extension and resource evaluation in west-central British Columbia; in Geological Fieldwork 2008, *BC Ministry of Energy, Mines and Petroleum Resources*, Paper 2009-1, pages 101–108.
- MINFILE (2007): MINFILE BC mineral deposits database; *BC Ministry of Energy, Mines and Petroleum Resources*, URL <<http://www.minfile.ca>> [November 2007].
- Mustard, P.S. and MacEachern J.A. (2007): A detailed facies (sedimentological and ichnological) evaluation of archived hydrocarbon exploration drill core from the Nechako Basin, BC; in The Nechako Initiative-Geoscience Update, *BC Ministry of Energy, Mines and Petroleum Resources*, Petroleum Geology Open File 2007-1, pages 7-57, URL <[http://www.empr.gov.bc.ca/OG/oilandgas/petroleumgeology/ConventionalOilAndGas/InteriorBasins/Documents/The\\_Nechako\\_Initiative-Geoscience\\_Update\\_2007.pdf](http://www.empr.gov.bc.ca/OG/oilandgas/petroleumgeology/ConventionalOilAndGas/InteriorBasins/Documents/The_Nechako_Initiative-Geoscience_Update_2007.pdf)> [November 2008].
- Mustard, P.S. and Van der Heyden, P. (1997): Geology of the Tatla Lake and east half of Bussel Lake; in Interior Plateau Geoscience Project: Summary of Geological, Geochemical and Geophysical Studies, L.J. Diakow, P. Metcalfe and J. Newell, Editors, *BC Ministry of Energy, Mines and Petroleum Resources*, Paper 1997-2, pages 103–122.
- Pálffy, J., Smith, P.L. and Mortensen, J.K. (2000): A U-Pb and <sup>40</sup>Ar-<sup>39</sup>Ar time scale for the Jurassic; *Canadian Journal of Earth Sciences*, Volume 37, pages 923–944.
- Ricketts, B.D., Evenchick, C.A., Anderson, R.G. and Murphy, D.C. (1992): Bowser Basin, northern British Columbia; constraints on the timing of initial subsidence and Stikinia-North America terrane interactions; *Geological Society of America*, Geology, Volume 20, pages 1119–1122.
- Riddell, J.M. (2006): Geology of the southern Nechako Basin (NTS 92N, 92O, 93C, 93F, 93G), sheet 3 of 3-geology with contoured gravity underlay; *BC Ministry of Energy, Mines and Petroleum Resources*, Petroleum Geology Map 2006-1, scale 1:400 000.
- Riddell, R. and Ferri, F. (2008): Nechako Project Update; in Geoscience Reports 2008, *BC Ministry of Energy, Mines and Petroleum Resources*, pages 67–77.
- Riddell, J.M., Ferri, F., Sweet, A.R. and O’Sullivan, P.B. (2007): New geoscience data from the Nechako Basin project; in The Nechako Initiative-Geoscience Update 2007, *BC Ministry of Energy, Mines and Petroleum Resources*, Petroleum Geology Open File 2007-1, pages 59-98, URL <[http://www.empr.gov.bc.ca/OG/oilandgas/petroleumgeology/ConventionalOilAndGas/InteriorBasins/Documents/The\\_Nechako\\_Initiative-Geoscience\\_Update\\_2007.pdf](http://www.empr.gov.bc.ca/OG/oilandgas/petroleumgeology/ConventionalOilAndGas/InteriorBasins/Documents/The_Nechako_Initiative-Geoscience_Update_2007.pdf)> [November 2008].
- Shives, R.B.K. and Carson, J.M. (1994): Multiparameter airborne geophysical survey of the Clisbako River area, Interior Plateau, British Columbia (parts of 093 B/12, 93 C/9, 93 C/16); *Geological Survey of Canada*, Open File 2815, 56 pages, URL <[http://edg.rncan.gc.ca/geochem/metadata\\_rel\\_e.php?rel=of02815](http://edg.rncan.gc.ca/geochem/metadata_rel_e.php?rel=of02815)> [November 2008].
- Shore, T.L. and Safranyik, L. (1992): Susceptibility and risk rating systems for the mountain pine beetle in lodgepole pine stands; *Forestry Canada*, Pacific Forestry Centre, Information Report BC-X-336, 17 pages, URL <[http://bookstore.cfs.nrcan.gc.ca/detail\\_e.php?catalog=3155](http://bookstore.cfs.nrcan.gc.ca/detail_e.php?catalog=3155)>.
- Spratt J. and Craven J. (2008): A first look at the electrical resistivity structure in the Nechako Basin from magnetotelluric studies west of Nazko, B.C. (NTS 092 N, O; 093 B, C, F, G); in Geoscience Reports 2008, *BC Ministry of Energy, Mines and Petroleum Resources*, pages 119–127.
- Stacey, J.S. and Kramer, J.D. (1975): Approximation of terrestrial lead isotope evolution by a two-stage model; *Earth and Planetary Science Letters*, Volume 26, pages 207–221.
- Stewart S.A. and Argent J.D. (2000): Relationship between polarity of extensional fault arrays and presence of detachments; *Journal of Structural Geology*, Volume 22, Number 6, pages 693–711.
- Taylor, S.W. (1999): 100 years of federal forestry in British Columbia; *Forest History Association of British Columbia*, BC Forest History Newsletter, Number 57, pages 1–7.
- Taylor, S.W. and Carroll, A.L. (2004): Disturbance, forest age, and mountain pine beetle outbreak dynamics in BC: a historical perspective; in Mountain Pine Beetle Symposium: Challenges and Solutions, T.L. Shore, J.E. Brooks and J.E. Stone, Editors, Natural Resources Canada, Canadian Forest Service, *Pacific Forestry Centre*, Information Report BC-X-399, pages 41–51.
- Tipper, H.W. (1969a): Geology, Anahim Lake; *Geological Survey of Canada*, Map 1202A, scale 1:253 440.
- Tipper, H.W. (1969b): Mesozoic and Cenozoic geology of the northeast part of Mount Waddington map-area (92N), Coast District, British Columbia; *Geological Survey of Canada*, Paper 68-33, 103 pages.
- Tipper, H.W. (1971): Surficial geology, Anahim Lake; *Geological Survey of Canada*, Map 1289A, scale 1:250 000.
- Thorkelson, D.J. and Rouse, G.E. (1989): Revised stratigraphic nomenclature and age determinations for mid-Cretaceous volcanic rocks in southwestern British Columbia; *Canadian Journal of Earth Sciences*, Volume 26, pages 2016–2031.
- van der Heyden, P. (2004): Uranium-lead and potassium-argon ages from eastern Bella Coola and adjacent parts of Anahim Lake and Mount Waddington map areas, west-central British Columbia; in Current Research 2004, *Geological Survey of Canada*, Paper 2004-A2, 14 pages.

## ERRATUM

LEGEND	
<i>Neogene</i>	
●	Anahim belt volcanic rocks
●	Chilcotin Group
<i>Eocene Ootsa Lake Group</i>	
▲	Mount Sheringham pyroxene dacite
▲	Vitreous black dacite
▲	Dacite ash-flow
▲	Acicular hornblende dacite
▲	Dacite ash-flow (with biotite)
<i>Intrusive rocks</i>	
◆	Tatla Lake Stock
◆	Chilanko Intrusive Complex

Legend for figure 7 omitted from the original published volume.

# First Isotopic Age Constraints for the Dean River Metamorphic Belt, Anahim Lake area: Implications for Crustal Extension and Resource Evaluation in West-Central British Columbia

by M.G. Mihalynuk and R.M. Friedman<sup>1</sup>

**KEYWORDS:** isotopic dating, Dean River metamorphic belt, Anahim Lake geology, Tatla Lake Metamorphic Complex, detachment mineralization, polymetallic fault-related, deposit model

## INTRODUCTION

Reconnaissance field studies conducted as part of the Beetle Impacted Zone project included investigation of the Dean River metamorphic belt in northwestern Anahim Lake map area (Figure 1; for an introduction to the Beetle Impacted Zone project (BIZ), its mandate and deliverables to date, see Mihalynuk, 2007a, b and Mihalynuk et al., 2007, 2008, 2009). Aims of the reconnaissance investigation were: to ascertain the type of protoliths and their geological setting, evaluate their mineral resource potential and establish the nature of the basal contact and pre-Miocene topography. We collected samples for isotopic age determination as an aid to correlation with rock packages for which the mineral potential is more clearly understood. Based on MINFILE records, (MINFILE, 2008), no mineral occurrences or mineral tenures are currently known to exist within the Dean River metamorphic belt (DRMB). We present the age data here together with field and microscopic observations, which support a correlation with rocks in the Tatla Lake Metamorphic Complex.

## LOCATION

Rocks of the Dean River metamorphic belt are shown by Schiarizza et al. (1994) to extend from Lily Lake near Ulkatcho to the headwaters of Puntzi Creek near Chantslar Lake (northwestern to south-central Anahim Lake map area, NTS 093C; Figure 1). This area corresponds largely with the eastern headwaters of the Dean River. Fieldwork was focused on a broad area of discontinuous exposure near Rainbow Lake, 45 km north of Anahim Lake. The main Dean River forest service road, which originates at the northern outskirts of Anahim Lake village, provides access to the area. A subsidiary logging road departs from the main road between Far and Tanswanket creeks and DRMB rocks are exposed in the roadbed within a kilometre of the Tanswanket Creek crossing. Fieldwork in this area was

aided by lack of undergrowth due to a forest fire in the summer of 2006 (Figure 2).

## GEOLOGICAL SETTING AND PREVIOUS WORK

Little is known about the DRMB other than its regional distribution as compiled by Schiarizza et al. (1994), which is mainly based upon regional mapping by Tipper (1969). Tipper included rocks of the DRMB in his "Unit 4...mainly gneisses that occur in a belt northeast of the Coast Mountains and can be traced 40 miles to the northwest and more than 60 miles southeast". At its southern limit, Unit 4 included parts of the Tatla Lake Metamorphic Complex (TLMC; Friedman, 1988). In observance of the limits of the TLMC mapped by Friedman (1988), Schiarizza et al. (1994) sought to distinguish the northern continuation of Tipper's northwest-trending belt of metamorphic rocks, and named them the 'Dean River metamorphic belt' (Figure 2). In a study aimed at the Miocene and younger volcanic rocks of the Ilgachuz Range, Souther and Souther (1994) extended the TLMC to include DRMB rocks near Rainbow Lake. Souther and Souther showed that, like the TLMC along strike to the southeast, these rocks display a dominantly east-striking foliation and a contact with presumably less deformed Early Jurassic Hazelton Group volcanic rocks, which are obscured by glacial cover.

## SAMPLE DESCRIPTIONS

Dean River metamorphic belt rocks in the Rainbow Lake area include dacite, tonalite, mafic tuff and volcanic metasediment. All display evidence of at least two phases of deformation, typically a mylonitic foliation which is crumpled and locally overprinted by a late mylonitic fabric.

Dacite occurs as low, glaciated, slabby or blocky, light grey to white outcrops. Protolith textures are common in all but the most intensely mylonitized rocks. Relict flattened crystal-rich clasts are interpreted as lapilli, but they could be a product of attenuated and dismembered dikelets. A lapilli clast origin is preferred as crystal fragments (relict, not cataclastic) and embayed quartz eyes are common (Figure 3). Typical porphyroclasts include medium-grained plagioclase (~15%, and probably minor sanidine), quartz eyes (~5%), and sparse remnants of biotite (<1%), which can be difficult to distinguish from secondary biotite. The predominant secondary minerals are fine- to medium-grained muscovite, which may account for 25% of the rock, and fine-grained secondary calcite (up to 10%). Much of the rock consists of comminuted quartz and feldspar. Shear

<sup>1</sup> Pacific Centre for Isotopic and Geochemical Research, University of British Columbia, Vancouver, BC

This publication is also available, free of charge, as colour digital files in Adobe Acrobat® PDF format from the BC Ministry of Energy, Mines and Petroleum Resources website at <http://www.empr.gov.bc.ca/Mining/Geoscience/PublicationsCatalogue/Fieldwork/Pages/default.aspx>.

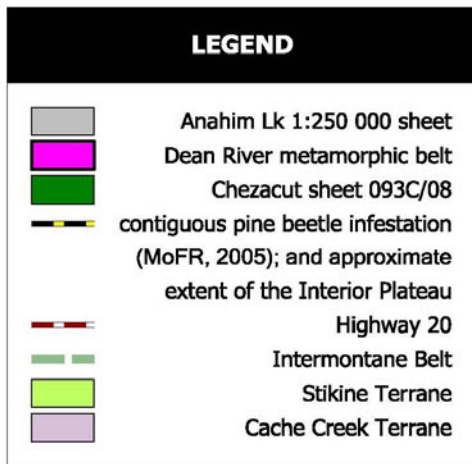
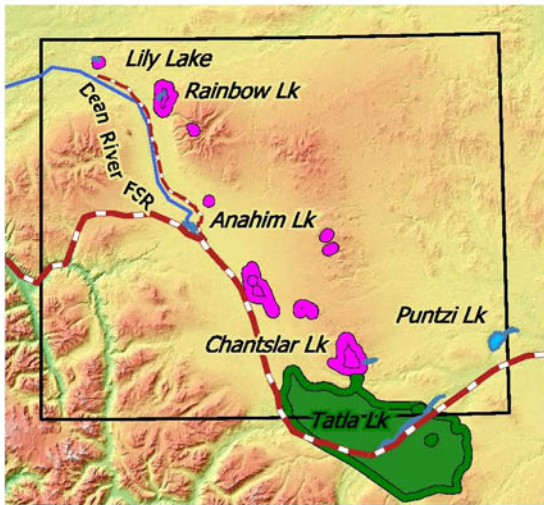


**Figure 1.** Location map showing the Interior Plateau, Beetle Impacted Zone, Intermontane Belt and constituent terranes. Magnified Anahim Lake inset shows the Tatla Lake Metamorphic Complex, Dean River metamorphic belt and geographic features mentioned in the text.

sense indicators include rotated feldspar porphyroclasts and incipiently developed S-C fabrics (Figure 4), but variations in the sense of offset are suggestive of folded shear zone boundaries.

## ISOTOPIC AGE DETERMINATION

Three samples of the dacite unit were selected for isotopic age determination. One of the least deformed and least metamorphosed outcrops was sampled for U-Pb age determination. A strongly schistose and white mica-rich sample and a late (Figure 5), relatively undeformed quartz-

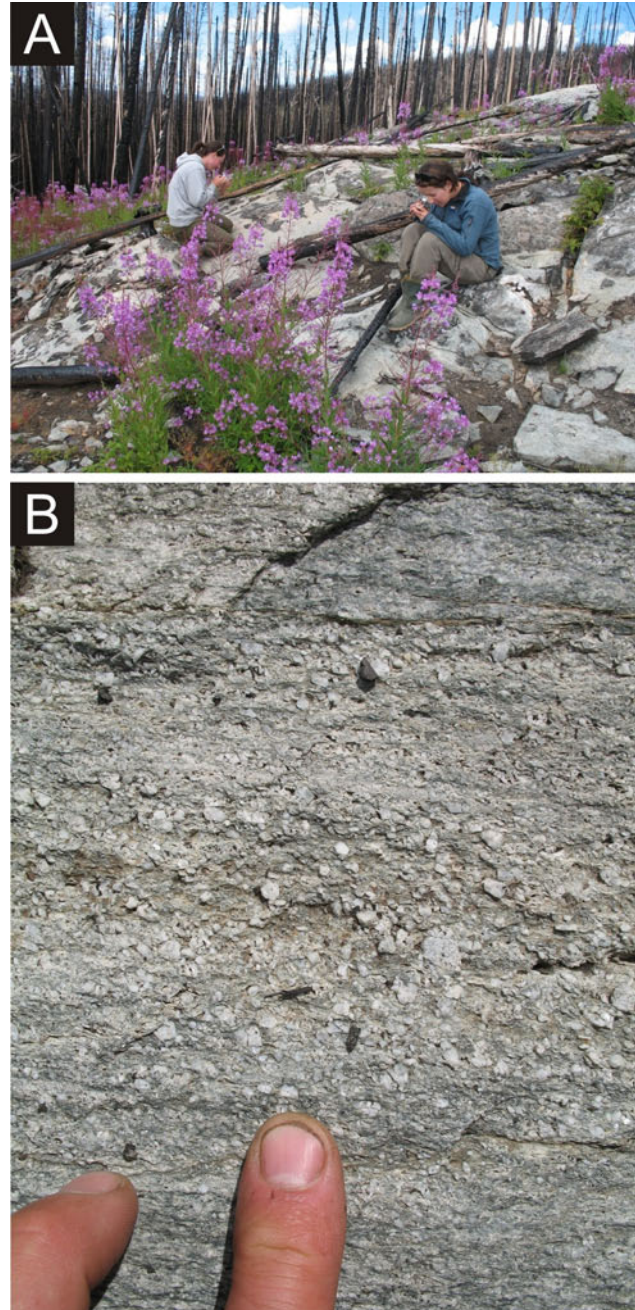


**Figure 2.** a) General nature of the outcrop shown in this 2006 photo (view ~north). b) Close-up view of typical fragmented crystal-rich dacite, like that sampled for U-Pb isotopic age determination.

feldspar segregation (Figure 4c) were sampled for  $^{40}\text{Ar}/^{39}\text{Ar}$  age determination.

All sample preparation and analytical work for the U-Pb and  $^{40}\text{Ar}/^{39}\text{Ar}$  isotopic ages presented here was conducted at the Pacific Centre for Isotopic and Geochemical Research (PCIGR) at the Department of Earth and Ocean Sciences, University of British Columbia.

The U-Pb isotopic age determinations reported here were acquired by thermal ionization mass spectroscopy (U-Pb TIMS). The  $^{40}\text{Ar}/^{39}\text{Ar}$  isotopic age determinations were

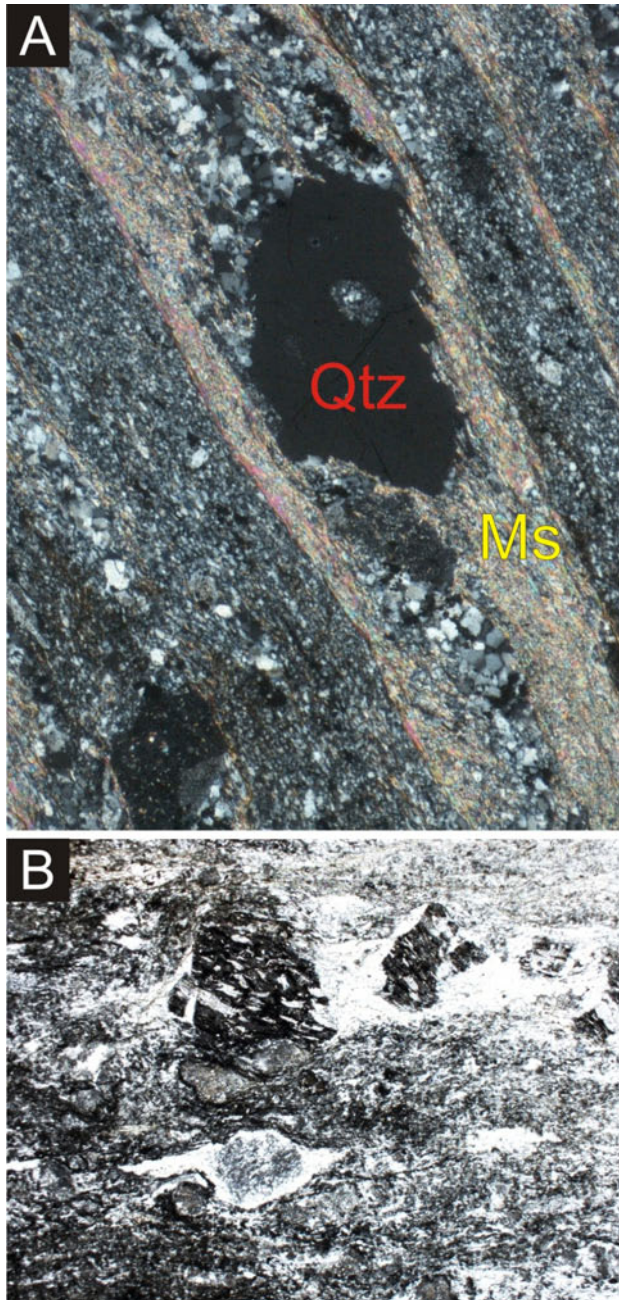


**Figure 3.** Photomicrographs of **a)** embayed quartz (Qtz) and muscovite (Ms) concentrated along folia in strongly foliated dacite such as that sampled for  $^{40}\text{Ar}/^{39}\text{Ar}$  age determination; **b)** fragmented and rotated trachytic volcanic granules in sedimentary unit display pressure shadows. Long dimensions of photos represent 2.5 and 5 mm, respectively.

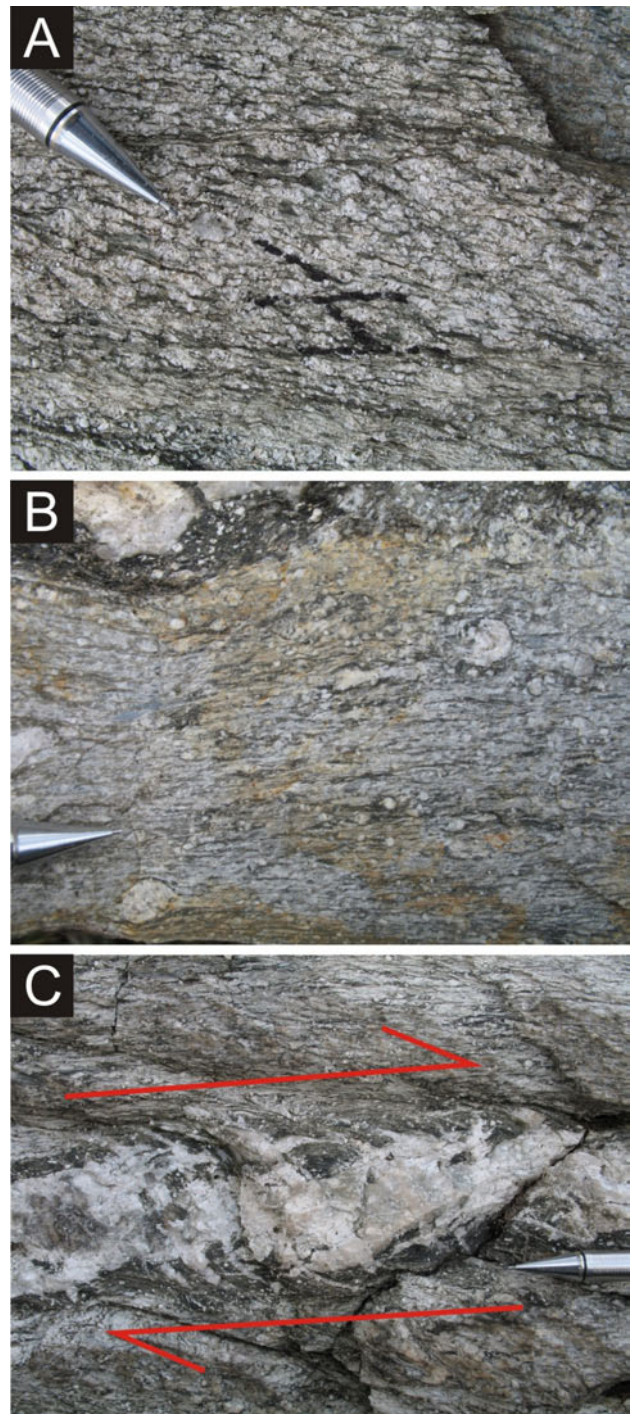


**Figure 4.** Outcrops displaying shear sense indicators: **a)** foliated, white mica-rich part of the unit and S-C developed within moderately foliated dacite, **b)** strong S2 (crenulation cleavage) developed with preserved porphyroclasts displaying mainly dextral shear sense, although one -type porphyroclast (below pencil tip) appears to display sinistral shear sense (mineral elongation is within the fabric plane and ~ parallel to outcrop surface in both a) and b); **c)** relatively undeformed quartz-feldspar segregation (sampled for  $^{40}\text{Ar}/^{39}\text{Ar}$  age determination without success) within a brittle sigmoid shear zone (dextral shear sense indicated).

acquired by the laser-induced step-heating technique. Details of the both analytical techniques are presented in Logan et al. (2007).

### U-Pb protolith age

Zircon was separated from dacite sample MMI07-33-3 using standard mineral separation techniques (crushing, grinding, Wilfley [wet shaker] table, heavy liquids and magnetic separation), followed by hand picking. Five air-abraded single zircon grains were analyzed with results plotted in Figure 6 and listed in Table 1. All data overlap concordia at the 2 $\sigma$  confidence level. Dispersion of Pb-U dates are attributed to minor Pb loss; the weighted average of overlapping  $^{206}\text{Pb}$ - $^{238}\text{U}$  dates for older grains A and B at  $150.2 \pm 0.3$  Ma is taken as the best estimate for the age of the rock (Figure 7). However, because zircons were only air abraded (not chemically abraded), Pb loss for grains A and B cannot be ruled out and this estimate should be considered as a minimum age. The weighted average of  $^{207}\text{Pb}$ - $^{235}\text{U}$  dates for all analyzed grains at ca. 153 Ma gives a rough measure of the maximum age allowed with the current data set. We will refine the age of this rock by analyzing several zircon grains that have undergone chemical abrasion pre-treatment (Mundil et al., 2004; Mattinson, 2005).

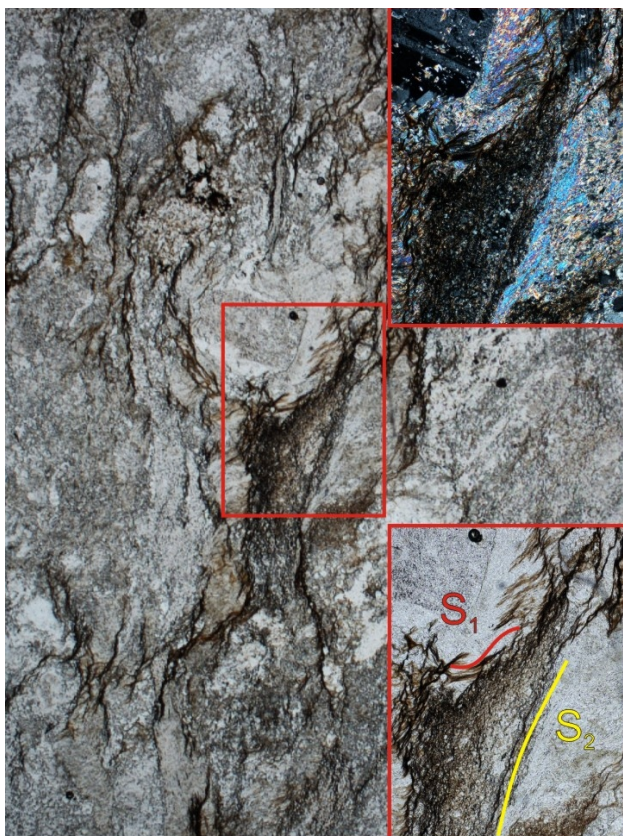


**Figure 5.** Photomicrograph of Dean River metamorphic belt dacite showing plagioclase porphyroclast and higher magnification inset in both plane polarized (bottom right) and cross polarized light (top right). Note abundant muscovite with high birefringence. Long dimension of photo represents ~5 mm.

### $^{40}\text{Ar}/^{39}\text{Ar}$ cooling age

No useful data was acquired from the sample of syn- to post-kinematic quartz-feldspar segregation, probably because the feldspar was albite and not sufficiently K-rich. The white mica sample did yield useful results, although the release spectrum was plagued by excess argon (Figure 8) as indicated by the rising steps within the spectrum. Excess argon is present when the initial  $^{40}\text{Ar}/^{36}\text{Ar}$  value is  $>295.5$  Ma (Table 2). This condition is mitigated by the isochron plots shown in Figure 9a, b, which produce reliable cooling ages of  $49.9 \pm 0.5$  Ma.

## REGIONAL CORRELATION AND IMPLICATIONS

Protoliths and structural fabrics within the DRMB are similar to those within the ductilely sheared assemblage of the TLMC. We suggest that the instincts of Tipper (1969) and Souther and Souther (1994) led them to correctly correlate metamorphic rocks in northwestern through south-central Anahim Lake area. That the TLMC is more extensive than originally mapped by Friedman (1988) is not surprising given that his limits of the TLMC were governed in large part by the extent of his map coverage. Furthermore, Friedman and Armstrong (1988) hypothesized a crustal-scale shear zone linking core complexes on both sides of the Intermontane Belt (Figure 1); such a shear zone may also provide a linkage between intracontinental transform faults (Struik, 1993). If correct, a more widespread manifestation of the crustal-scale shear zone is to be expected. For example, it should be imaged in Lithoprobe deep-seismic experiment data (as predicted by Friedman and Armstrong, 1988). However, the current interpretation of most shallowly-dipping reflectors observed on the Southern Cordilleran Lithoprobe transect (about 250 km southeast) is as trans-Cordilleran thrust faults (Cook et al., 1992). Regional-scale detachment faults might also be imaged by confidential industry seismic data that has been recently re-processed (e.g., Hayward and Calvert, 2008) or by magnetotelluric data (e.g., Spratt and Craven, 2008), but in-

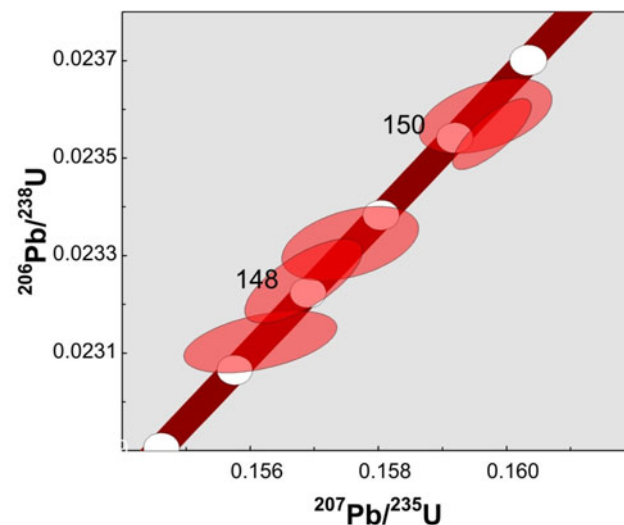


**Figure 6.** Concordia plots for U-Pb TIMS data for sample MMI07-33-3. The 2 $\sigma$  error ellipses for individual analytical fractions are in red. Concordia bands include 2 $\sigma$  errors on U decay constants.

**Table 1.** U-Pb thermal ionization mass spectrometry (TIMS) analytical data for zircon from sample MMI07-33-3, metadacite of the Dean River metamorphic belt.

Fraction <sup>1</sup>	Weight <sup>2</sup> (mg)	U <sup>3</sup> (ppm)	Pb <sup>4</sup> (ppm)	<sup>206</sup> Pb <sup>5</sup> <sup>204</sup> Pb	Pb <sup>6</sup> Pbc	Pb <sup>7</sup> (pg)	Th-U <sup>8</sup>	Isotopic ratios ±1σ (%) <sup>9</sup>			corr. coeff.	% <sup>10</sup> discordant	Apparent ages ±2σ (Ma) <sup>11</sup>		
								<sup>206</sup> Pb/ <sup>238</sup> U	<sup>207</sup> Pb/ <sup>235</sup> U	<sup>207</sup> Pb/ <sup>206</sup> Pb			<sup>206</sup> Pb- <sup>238</sup> U	<sup>207</sup> Pb- <sup>235</sup> U	<sup>207</sup> Pb- <sup>206</sup> Pb
<b>Sample MMI07-33-3</b>															
A	8.1	712.0	17.6	6459	109.5	1.3	0.544	0.02355 ± 0.13	0.1598 ± 0	0.18787 ± 0.05	0.779	5.0	150.0 ± 0.4	150.5 ± 0.4	157.8 ± 4.6/4.6
B	7.7	308.0	7.5	3194	53.3	1.1	0.490	0.02359 ± 0.13	0.1597 ± 0	0.18783 ± 0.09	0.440	1.5	150.3 ± 0.4	150.4 ± 0.7	152.6 ± 11.1/11.2
C	5.5	389.0	9.5	3505	58.9	0.9	0.530	0.02325 ± 0.15	0.1568 ± 0	0.18767 ± 0.05	0.707	-2.5	148.2 ± 0.5	147.9 ± 0.7	144.6 ± 7.9/8.0
D	5.4	323.0	8.0	2787	48.0	0.9	0.583	0.02333 ± 0.13	0.1576 ± 0	0.18771 ± 0.05	0.402	-0.8	148.6 ± 0.4	148.6 ± 0.8	147.5 ± 11.8/11.9
E	5.0	307.0	7.4	1686	28.0	1.3	0.490	0.02312 ± 0.11	0.1562 ± 0	0.18493 ± 0.13	0.466	-0.2	147.4 ± 0.3	147.4 ± 0.9	147.1 ± 12.9/13.0

<sup>1</sup>All single grains, air-abraded.

<sup>2</sup>Grain mass determined on Sartorius SE2 ultra-microbalance to ±0.1 microgram.

<sup>3</sup>Corrected for spike, blank (0.2 pg ±50%, 2σ), and mass fractionation, which is directly determined with <sup>423</sup>U/<sup>429</sup>U spike.

<sup>4</sup>Radiogenic Pb; data corrected for spike, fractionation, blank and initial common Pb; mass fractionation correction of 0.23% /amu ±40% (2σ) is based on analysis of NBS-982 throughout

course of study; blank Pb correction of 0.5-1.0 pg ±40% (2σ) with composition of <sup>206</sup>Pb/<sup>204</sup>Pb = 18.5 ±2%; <sup>207</sup>Pb/<sup>204</sup>Pb = 15.5 ±2%; <sup>208</sup>Pb/<sup>204</sup>Pb = 36.4 ±2%, all at 2σ; initial common Pb compositions based on the Stacey and Kramer (1975) model Pb at the interpreted age of the rock at 150 Ma.

<sup>5</sup>Measured ratio corrected for spike and fractionation.

<sup>6</sup>Ratio of radiogenic to common Pb.

<sup>7</sup>Total weight of common Pb calculated with blank isotopic composition.

<sup>8</sup>Model Th-U ratio calculated from radiogenic <sup>206</sup>Pb/<sup>206</sup>Pb ratio and <sup>206</sup>Pb/<sup>206</sup>Pb age.

<sup>9</sup>Corrected for spike, fractionation, blank and initial common Pb.

<sup>10</sup>Discordance in % to origin.

<sup>11</sup>Age calculations are based on decay constants of Jaffey et al., 1971.

terpretation and regional integration of these datasets are not yet complete. That a regionally-developed zone of Eocene detachment existed in the mid-crust seems necessary to explain normal faulting in central BC, which moderately tilts strata across tens of thousands of square kilometres (Lowe et al., 2001). Eocene crustal extension is also consistent with apatite and zircon fission track data from widespread localities that indicate rapid cooling between 55 and 50 Ma (Riddell et al., 2007). Breakaway zones, where ductile offset in the ductile mid-crust is transferred to the upper brittle crust through arrays of normal faults, are interpreted in the Puntzi Lake area (Mihalynuk et al., 2009) and may explain rapid lateral variations in Cretaceous and Tertiary Nechako Basin strata which appear as elongate sub-basins (e.g., as interpreted by Riddell et al., 2007).

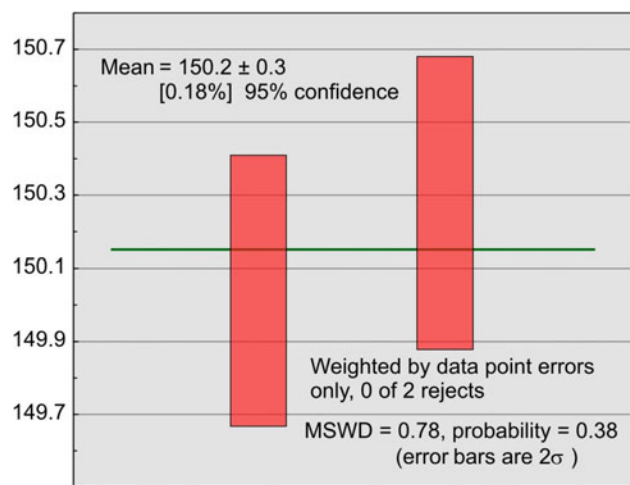


Figure 7. Mean square weighted deviates (MSWD) plot for the two most concordant fractions. Box heights are 2 .

Estimates of the structural omission across the main detachment zone can be deduced from the paleobarometric data in Friedman (1988). He shows an omission of roughly 13.5 km (~4.5 kbar); although at the limits of error for the geobarometers used, the thickness of missing crust ranges from ~3 to 24 km (~1–8 kbar). Closer to the central axis of the Intermontane Belt, minimum depth of any regional detachment fault is only constrained as >3778 m at the Chilcotin B-22-K hydrocarbon exploration well, about 80 km east-southeast of Rainbow Lake, which ends in undeformed volcanic rocks. Fifty kilometres south of the well, Tipper's Unit 4 metamorphic rocks are exposed at surface, requiring a regional dip on an interpreted single intervening detachment fault surface of more than 4.5 degrees.

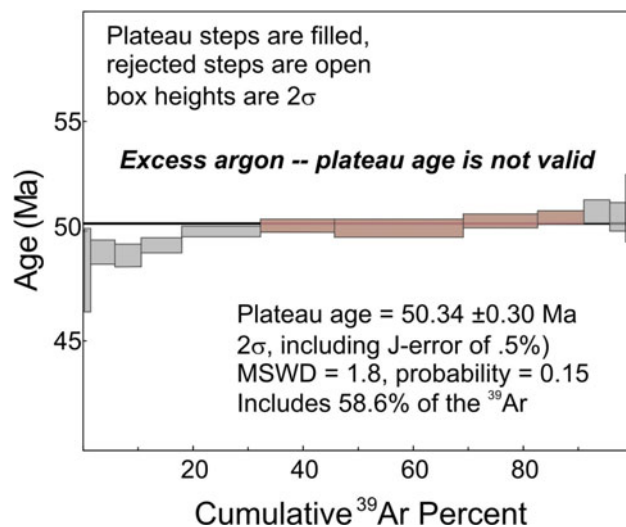


Figure 8. Step-heating Ar gas release spectra for sample MMI07-33-3. Rising steps indicate a problem with excess argon.

Table 2.  $^{40}\text{Ar}/^{39}\text{Ar}$  step-heating gas release data from sample MMI07-33-3, metadacite of the Dean River metamorphic belt.

Laser Power (%)	Isotope Ratios $^{40}\text{Ar}/^{39}\text{Ar}$	$^{38}\text{Ar}/^{39}\text{Ar}$	$^{37}\text{Ar}/^{39}\text{Ar}$	$^{36}\text{Ar}/^{39}\text{Ar}$	Ca/K	Cl/K	% $^{40}\text{Ar}$ atm f $^{39}\text{Ar}$	$^{40}\text{Ar}^*/^{39}\text{ArK}$	Age
<b>Sample MMI07-33-3</b>									
2	30.9386 ± 0.0148	0.0498 ± 0.0628	0.0391 ± 0.1694	0.0683 ± 0.0434	0.122	0.005	60.63	0.3 10.905 ± 0.854	98.82 ± 7.53
2.2	10.6132 ± 0.0063	0.0226 ± 0.0744	0.0272 ± 0.1116	0.0183 ± 0.0380	0.092	0.001	45.87	1.08 5.240 ± 0.210	48.16 ± 1.91
2.4	6.4570 ± 0.0061	0.0148 ± 0.0574	0.0518 ± 0.0324	0.0038 ± 0.0445	0.183	0	14.1	4.43 5.330 ± 0.060	48.98 ± 0.55
2.6	5.8561 ± 0.0074	0.0132 ± 0.0790	0.1303 ± 0.0238	0.0018 ± 0.0739	0.462	0	5.5	4.8 5.316 ± 0.057	48.84 ± 0.52
2.8	5.6854 ± 0.0051	0.0132 ± 0.0436	0.0205 ± 0.0381	0.0010 ± 0.0781	0.072	0	2.83	7.32 5.365 ± 0.037	49.30 ± 0.34
3	5.6263 ± 0.0047	0.0124 ± 0.0474	0.0104 ± 0.0657	0.0005 ± 0.0355	0.037	0	1.61	14.3 5.436 ± 0.027	49.94 ± 0.24
3.2	5.6253 ± 0.0053	0.0122 ± 0.0280	0.0084 ± 0.0481	0.0004 ± 0.1134	0.029	0	1.02	13.5 5.464 ± 0.033	50.19 ± 0.30
3.4	5.6025 ± 0.0078	0.0122 ± 0.0550	0.0062 ± 0.0314	0.0004 ± 0.1050	0.022	0	1.36	23.3 5.452 ± 0.045	50.08 ± 0.41
3.6	5.6857 ± 0.0052	0.0122 ± 0.0379	0.0070 ± 0.0391	0.0006 ± 0.1129	0.025	0	1.65	13.5 5.489 ± 0.035	50.42 ± 0.32
3.8	5.8171 ± 0.0053	0.0123 ± 0.0410	0.0110 ± 0.0278	0.0010 ± 0.0533	0.038	0	2.85	8.31 5.507 ± 0.034	50.58 ± 0.31
4	5.9400 ± 0.0086	0.0127 ± 0.0953	0.0153 ± 0.0888	0.0013 ± 0.0790	0.053	0	2.95	4.72 5.537 ± 0.059	50.85 ± 0.53
4.2	6.1000 ± 0.0080	0.0132 ± 0.1530	0.0200 ± 0.0706	0.0020 ± 0.0931	0.07	0	4.13	2.96 5.510 ± 0.072	50.61 ± 0.65
4.4	6.4442 ± 0.0103	0.0128 ± 0.1512	0.0254 ± 0.1070	0.0031 ± 0.1744	0.088	0	4.35	1.56 5.554 ± 0.170	51.00 ± 1.54
<b>Total/Average</b>	<b>5.7405 ± 0.0012</b>	<b>0.0126 ± 0.0091</b>	<b>0.0347 ± 0.0035</b>	<b>0.0008 ± 0.0147</b>	<b>0.064</b>	<b>0</b>	<b>100</b>	<b>5.464 ± 0.008</b>	

Notes

J = 0.005163 ± 0.000012

Volume  $^{39}\text{ArK}$  = 701.22

Integrated age = 50.19 ± 0.18

Gas volume measurements to 10-13 cm<sup>3</sup> NPT

Neutron flux monitors: 28.02 Ma FCs (Renne et al., 1998)

Isotope production ratios: ( $^{40}\text{Ar}/^{39}\text{Ar}$ )K = 0.0302 ± 0.00006, ( $^{37}\text{Ar}/^{39}\text{Ar}$ )Ca = 1416.4 ± 0.5, ( $^{36}\text{Ar}/^{39}\text{Ar}$ )Ca = 0.3952 ± 0.0004, Ca/K = 1.83 ± 0.01 ( $^{37}\text{ArCa}/^{39}\text{ArK}$ ).

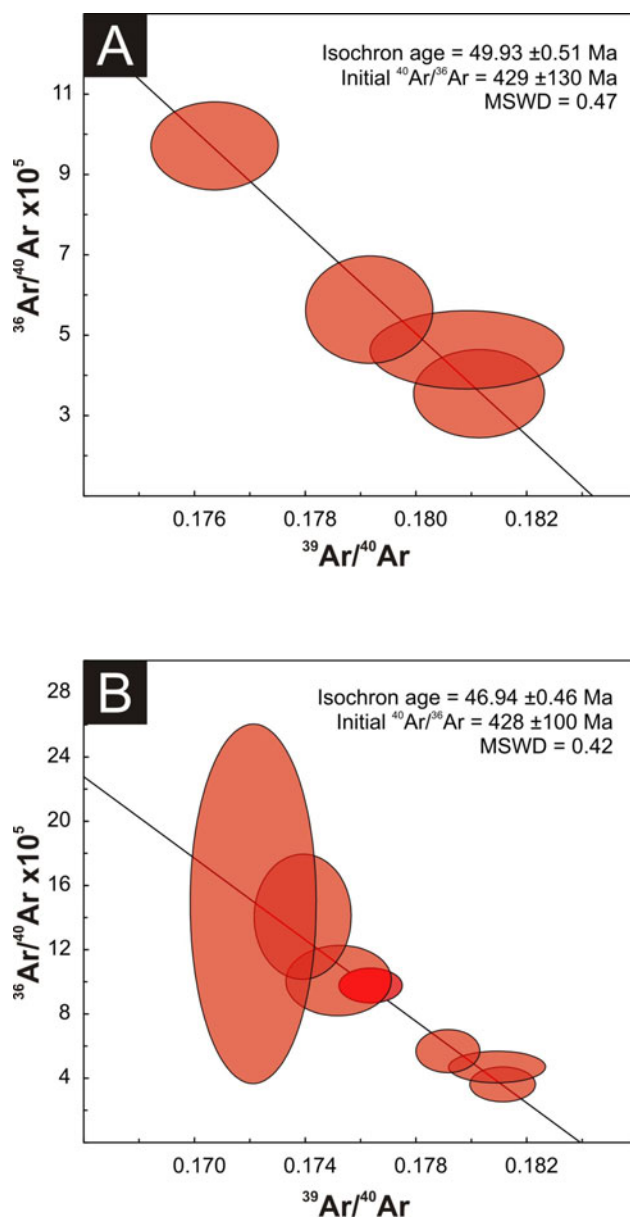


**Figure 9.** Ar isotope ratio correlation plots for **a)** plateau steps (N=4, see Figure 8), and **b)** plateau plus higher temperature steps (N=7). Both isochrons provide reliable age determinations which we report as  $49.9 \pm 0.5$  Ma.

Currently the crust within the Anahim Lake area is between 30 and 35 km thick as defined by the Mohorovicic discontinuity (Moho) extrapolated from the Lithoprobe transect (Cook et al., 1992) and as imaged in teleseismic data from the western Anahim Lake area. Preliminary interpretation of newly acquired teleseismic data from the Nechako Basin indicate a depth to the Moho of 35–40 km (J. Cassidy, personal communication, 2008), similar to the Moho depth near the eastern edge of the Coast Belt as imaged by Joshua Calkins et al. at the University of Arizona (in Cassidy and Al-Khoubbi, 2007; see their Figure 7). Including the omitted crustal section based upon the forgoing arguments, the pre-Eocene crust was probably in the order of 45–50 km thick (although post-Eocene cooling has probably depressed the Moho slightly).

Accuracy of models of the Eocene detachment surface, as well as thickness and composition of the crust affected by extension, are important considerations for resource assessment. Such considerations are especially germane for petroleum source-rock potential as the shallow crust may have been translated tens of kilometres by detachment, and rocks below any detachment fault are likely to have been subjected to significantly higher temperatures and pressures than those in the immediate hangingwall. Additionally, in the southwest United States, detachment faults are recognized as principal control on one group of polymetallic (Cu-Au-Ag-Pb-Zn) deposits. The detachment fault-related polymetallic deposit model (Wilkins et al., 1986) is a largely unexplored deposit type in BC. Small, scattered copper showings in the metamorphic rocks in southeastern Anahim Lake map area (Mihalynuk et al., 2009) may be an early indication of the exploration opportunities that exist for this type of mineralization, especially if the Tatla Lake metamorphic complex is part of a much more regional detachment system.

## ACKNOWLEDGMENTS

T. Ullrich processed the  $^{40}\text{Ar}/^{39}\text{Ar}$  samples and generated the step release data, spectra and inverse isochron plots. L. Diakow conscientiously reviewed an earlier draft of this paper. J. Cassidy kindly offered advice based upon the most recently available teleseismic data. Assistance with mineral separation and mass spectrometry was provided by H. Lin; Y. Feng helped with grain selection, pretreatment and sample dissolution/processing.

## REFERENCES

- BC Ministry of Forests and Range (2005): The state of British Columbia's forests 2004; *BC Ministry of Forests and Range*, URL <<http://www.for.gov.bc.ca/hfp/sof/2004/>> [November 2007].
- Cassidy, J. and Al-Khoubbi, I. (2007): A passive seismic investigation of the geological structure within the Nechako Basin; in *The Nechako Initiative—Geoscience Update*, *BC Ministry of Energy, Mines and Petroleum Resources*, Petroleum Geology Open File 2007-1 pages 7–57, URL <[http://www.empr.gov.bc.ca/OG/oilandgas/petroleumgeology/ConventionalOilAndGas/InteriorBasins/Documents/The\\_Nechako\\_Initiative-Geoscience\\_Update\\_2007.pdf](http://www.empr.gov.bc.ca/OG/oilandgas/petroleumgeology/ConventionalOilAndGas/InteriorBasins/Documents/The_Nechako_Initiative-Geoscience_Update_2007.pdf)> [November 2008].
- Cassidy, J.F., Al-Khoubbi, I. and Kim, H.S. (2008): Mapping the structure of the Nechako Basin using passive source seismology; in *Geoscience BC Summary of Activities 2007*, *Geoscience BC*, Report 2008-1, pages 115–120.
- Cook, F.A., Varsek, J.L., Clowes, R.M., Kanasevich, E.R., Spencer, C.S., Parrish, R.R. Brown, R.L., Carr, S.D., Johnson, B.J. and Price, R.A. (1992): LITHOPROBE crustal reflection structure of the southern Canadian Cordillera 1, foreland thrust and fold belt to Fraser River fault; *Tectonics*, Volume 11, pages 12–35.
- Friedman, R.M. (1988): Geology and geochronology of the Eocene Tatla Lake Metamorphic Core Complex, western edge of the Intermontane Belt, British Columbia; Ph.D. thesis, *University of British Columbia*, 348 pages.
- Friedman, R.M. and Armstrong, R.L. (1988): Tatla Lake metamorphic complex: an Eocene metamorphic core complex on the southwestern edge of the Intermontane Belt of British Columbia; *Tectonics*, Volume 7, pages 1141–1166.
- Friedman, R.M. (1992): P-T-t path for the lower plate of the Eocene Tatla Lake metamorphic core complex, southwest-

- ern Intermontane Belt, British Columbia; *Canadian Journal of Earth Sciences*, Volume 29, pages 972–983.
- Hayward, N. and Calvert, A.J. (2008): Structure of the south eastern Nechako Basin, south-central British Columbia (NTS 092N, O; 093B, C): preliminary results of seismic interpretation and first-arrival tomographic modelling; in *Geoscience BC Summary of Activities 2007*, *Geoscience BC*, Report 2008-1, pages 129–134.
- Jaffey, A.H., Flynn, K.F., Glendenin, L.E., Bentley, W.C., Essling, A.M. (1971): Precision measurement of half-lives and specific activities of  $^{235}\text{U}$  and  $^{238}\text{U}$ ; *Physical Review C*, Volume 4, pages 1889–1906.
- Logan, J.M., Mihalynuk, M.G., Ullrich, T. and Friedman, R.M. (2007): U-Pb ages of intrusive rocks and  $^{40}\text{Ar}/^{39}\text{Ar}$  plateau ages of copper-gold-silver mineralization associated with alkaline intrusive centres at Mount Polley and the Iron Mask batholith, southern and central British Columbia; in *Geological Fieldwork 2006*, *BC Ministry of Energy, Mines and Petroleum Resources*, Paper 2007-1, pages 93–116, URL <<http://www.em.gov.bc.ca/DL/GSBPubs/GeoFldWk/2006/11-Logan.pdf>> [November 2008].
- Lowe, C., Enkin, R.J. and Struik, L.C. (2001): Tertiary extension in the central British Columbia Intermontane Belt: magnetic and paleomagnetic evidence from the Endako region; *Canadian Journal of Earth Sciences*, Volume 38, pages 657–678.
- Mattinson, J.M. (2005): Zircon U-Pb chemical abrasion (“CA-TIMS”) method: combined annealing and multi-step partial dissolution analysis for improved precision and accuracy of zircon ages; *Chemical Geology*, Volume 220, pages 47–66.
- Mihalynuk, M.G. (2007a): Evaluation of mineral inventories and mineral exploration deficit of the Interior Plateau Beetle Infested Zone (BIZ); in *Geological Fieldwork 2006*, *BC Ministry of Energy, Mines and Petroleum Resources*, Paper 2007-1, pages 137–142, URL <<http://www.em.gov.bc.ca/DL/GSBPubs/GeoFldWk/2006/14-Mihalynuk.pdf>> [November 2007].
- Mihalynuk, M.G. (2007b): Neogene and Quaternary Chilcotin Group cover rocks in the Interior Plateau, south-central British Columbia: a preliminary 3-D thickness model; in *Geological Fieldwork*, *BC Ministry of Energy, Mines and Petroleum Resources*, Paper 2007-1, pages 143–147, URL <<http://www.em.gov.bc.ca/DL/GSBPubs/GeoFldWk/2006/15-Mihalynuk.pdf>> [November 2007].
- Mihalynuk, M.G., Erdmer, P., Ghent, E.D., Cordey, F., Archibald, D.A., Friedman, R.M. and Johannson, G.G. (2004): Coherent French Range blueschist: subduction to exhumation in <2.5 m.y.?; *Bulletin of the Geological Society of America*, Volume 116, pages 910–922.
- Mihalynuk, M.G., Harker, L.L., Lett, R. and Grant, B. (2007): Results of reconnaissance surveys in the Interior Plateau Beetle Infested Zone (BIZ); *BC Ministry of Energy, Mines and Petroleum Resources*, GeoFile 2007-5, URL <<http://www.empr.gov.bc.ca/Mining/Geoscience/PublicationsCatalogue/GeoFiles/Pages/2007-5.aspx>> [November 2007].
- Mihalynuk, M.G., Peat, C.R., Terhune, K. and Orovan, E.A. (2008): Regional geology and resource potential of the Chezacut map area, central British Columbia (NTS 093C/08); in *Geological Fieldwork 2007*, *BC Ministry of Energy, Mines and Petroleum Resources*, Paper 2008-1, pages 117–134, URL <<http://www.em.gov.bc.ca/DL/GSBPubs/GeoFldWk/2007/13-Mihalynuk-Chezacut34526.pdf>> [November 2008].
- Mihalynuk, M.G., Orovan, E.A., Larocque, J.P., Friedman, R.M. and Bachiu, T. (2009): Geology, geochronology and mineralization of the Chilanko Forks to southern Clusko River area, British Columbia (NTS 93C/01, 08, 09S); in *Geological Fieldwork 2008*, *BC Ministry of Energy, Mines and Petroleum Resources*, Paper 2009-1, pages 81–100.
- MINFILE (2008): MINFILE BC mineral deposits database; *BC Ministry of Energy, Mines and Petroleum Resources*, URL <<http://www.minfile.ca>> [November 2008].
- Mundil, R., Ludwig, K.R., Metcalfe, I. and Renne, P.R. (2004): Age and timing of the Permian mass extinctions: U/Pb dating of closed-system zircons; *Science*, Volume 305, pages 1760–1763.
- Renne, P.R., Swisher, C.C., III, Deino, A.L., Karner, D.B., Owens, T. and DePaolo, D.J. (1998): Intercalibration of standards, absolute ages and uncertainties in  $^{40}\text{Ar}/^{39}\text{Ar}$  dating; *Chemical Geology*, Volume 145, Numbers 1–2, pages 117–152.
- Riddell, J.M., Ferri, F., Sweet, A.R. and O’Sullivan, P.B. (2007): New geoscience data from the Nechako Basin project; in *The Nechako Initiative—Geoscience Update 2007*, *BC Ministry of Energy, Mines and Petroleum Resources*, Petroleum Geology Open File 2007-1, pages 59–98, URL <[http://www.empr.gov.bc.ca/OG/oilandgas/petroleumgeology/ConventionalOilAndGas/InteriorBasins/Documents/The\\_Nechako\\_Initiative-Geoscience\\_Update\\_2007.pdf](http://www.empr.gov.bc.ca/OG/oilandgas/petroleumgeology/ConventionalOilAndGas/InteriorBasins/Documents/The_Nechako_Initiative-Geoscience_Update_2007.pdf)> [November 2008].
- Schiarezza, P., Panteleyev, A., Gaba, R.G., Glover, J.K. (1994): Geological compilation of the Cariboo-Chilcotin area, south-central British Columbia (NTS 92J, K, N, O, P; 93A, B, C, F, G, H); *BC Ministry of Energy, Mines and Petroleum Resources*, Open File 1994-7, scale 1:250 000, URL <<http://www.empr.gov.bc.ca/Mining/Geoscience/PublicationsCatalogue/OpenFiles/1994/Pages/1994-7.aspx>> [November 2008].
- Souther, J.G. and Souther, M.E.K. (1994): Geology, Ilgachuz Range and adjacent parts of the Interior Plateau, British Columbia; *Geological Survey of Canada*, Map 1845A, scale 1:50 000.
- Spratt, J. and Craven, J. (2008): A first look at the electrical resistivity structure in the Nechako Basin from magnetotelluric studies west of Nazko, British Columbia (NTS 092 N, O; 093 B, C, F, G); *Geoscience Reports 2008*, *BC Ministry of Energy, Mines and Petroleum Resources*, pages 119–127.
- Stacey, J.S., Kramer, J.D. (1975): Approximation of terrestrial lead isotope evolution by a two-stage model; *Earth and Planetary Science Letters*, Volume 26, pages 207–221.
- Struik, L.C. (1993): Intersecting intracontinental Tertiary transform fault systems in the North American Cordillera; *Canadian Journal of Earth Sciences*, Volume 30, pages 1262–1274.
- Tipper, H.W. (1969): Geology, Anahim Lake; *Geological Survey of Canada*, Map 1202A, scale 1:253 440.
- Wilkins, Joe, Jr., Beane, R.E., and Heidrick, T.L., 1986, Mineralization related to detachment faults: a model; in *Frontiers in Geology and Ore Deposits of Arizona and the Southwest*, Beatty, B. and Wilkinson, P.A.K., Editors, *Arizona Geological Society Digest*, Volume 16, pages 108–117.

# Geochemical Character of Neogene Volcanic Rocks of the Central Beetle-Infested Zone, South-Central British Columbia (NTS 093B, C)

by J.P. Larocque and M.G. Mihalynuk

**KEYWORDS:** alkaline magmatism, geochemistry, Neogene volcanic rocks, Chilcotin group, Anahim volcanic belt

## INTRODUCTION

Volcanic rocks have formed along the length of the North American Cordillera during the Neogene and Quaternary periods. Volcanism of this age is dominantly alkaline and extends throughout central British Columbia and the southern Yukon Territory. Distinct provinces of alkaline magmatism have been identified in BC, including the northern Cordillera volcanic province, the Chilcotin Group and the Anahim volcanic belt (e.g., Edwards and Russell, 2000). Of these, the latter two occur within the Beetle-Infested Zone and represent the youngest units mapped by Mihalynuk et al. (2008). A major-element geochemical investigation of the contemporaneous Anahim volcanic belt and Chilcotin Group basalts suggests that their compositions are controlled by a common process.

## PREVIOUS WORK

### *Anahim Volcanic Belt*

The Anahim volcanic belt is a well-studied east-trending chain of Neogene shield volcanoes and intrusions extending from coastal BC west of Bella Coola, into the interior of the province (Figure 1). There is a well-defined age progression from west to east along the belt (Souther, 1986). The oldest expressions of magmatism in the Anahim volcanic belt are the coastal Bella Bella dikes and the King Island pluton, dated at 14.5–12.5 Ma and 13–10.3 Ma, respectively. Discrete volcanic centres occur east of Bella Coola, including the Rainbow Range, the Ilgachuz Range, the Itcha Range and the Nazko cones, which range systematically in age from 8.7 to 0.34 Ma (Bevier, 1978; Souther, 1986; Souther et al., 1987). With the exception of the Nazko lavas, all volcanic activity along the Anahim volcanic belt began with early shield-building felsic eruptions, which were later capped by mafic flows (Bevier, 1978; Souther, 1984; Charland and Francis, 1993). These late-stage mafic lavas range in composition from hawaiite through alkali olivine basalt to basanite, with a trend of progressive Si-undersaturation in later eruptions (e.g., Charland and Francis, 1993). Work on the Itcha Range has

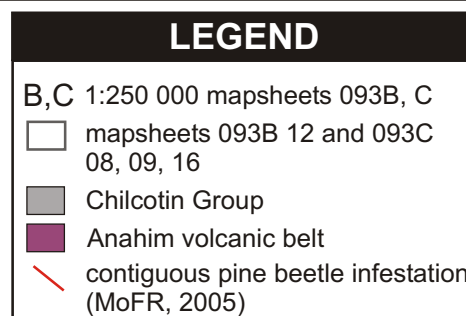
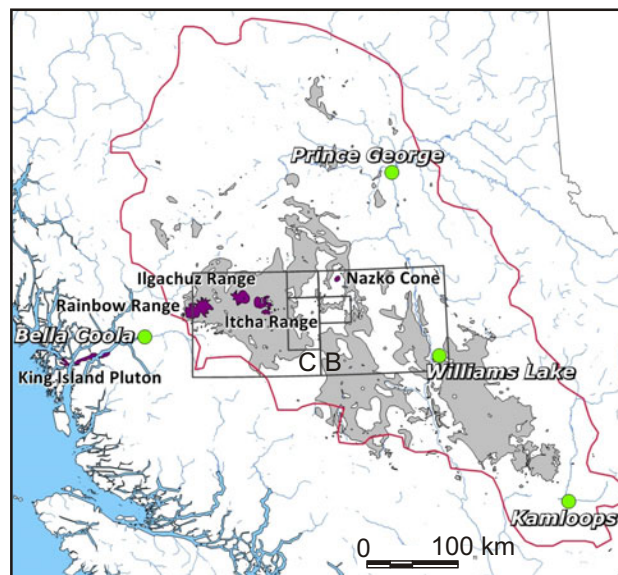


**Figure 1.** Location of fieldwork area with respect to the Chilcotin Group and Anahim volcanic belt volcanic centres.

shown that the hawaiite can be produced through the fractionation of olivine+clinopyroxene from primitive alkali olivine basalt at the base of the crust (Charland et al., 1995), while the basanite requires a distinct parental magma based on trace-element ratios (Charland and Francis, 1993).

### *Chilcotin Group*

The Chilcotin Group ranges in age from 34 to 1 Ma, with periods of high eruption rates at 16–14 Ma, 9–6 Ma and 3–1 Ma (Mathews, 1989). Extrusive rocks include subaerial and subaqueous basaltic lava and pyroclastic rocks, while minor gabbroic to basaltic plugs are interpreted to represent lava vents (Bevier, 1983). The basalts are transitional from alkali olivine basalt to quartz-normative basalt. The Chilcotin Group is broadly contemporaneous

*This publication is also available, free of charge, as colour digital files in Adobe Acrobat® PDF format from the BC Ministry of Energy, Mines and Petroleum Resources website at <http://www.empr.gov.bc.ca/Mining/Geoscience/PublicationsCatalogue/Fieldwork/Pages/default.aspx>.*

ous with both the Anahim volcanic belt and the calcalkaline Pemberton and Garibaldi volcanic belts to the southwest, and has been interpreted as having formed in a backarc basin behind the Cascadia-Garibaldi arc (Souther, 1977; Bevier, 1983). Once believed to cover up to 50 000 km<sup>2</sup> of the south-central interior of BC with an average thickness of 70 m (Bevier, 1983), recent mapping suggests a significantly smaller aerial extent (~36 500 km<sup>2</sup>), and topographic modelling shows that the basaltic cover is relatively thin (<50 m), except where the flows have filled paleochannels (Andrews and Russell, 2007; Mihalynuk, 2007).

A number of important petrological observations were made by Bevier (1983) pertaining to the Chilcotin Group basalts, including that

- they are commonly aphyric, with olivine as the dominant phenocryst phase;
- the most magnesian olivine composition is Fo<sub>83</sub>, too low for the basalts to be primary melts of peridotite containing Fo<sub>89-92</sub>; and
- the major-element compositional array cannot be modelled by fractional crystallization.

## GEOCHEMISTRY OF NEOGENE MAFIC LAVAS

### Anahim Volcanic Belt

Major-element geochemistry of the mafic lava flows of the Anahim volcanic belt reveals systematic changes in the degree of Si-undersaturation along the belt (Figure 2), paralleling changes in the geochemistry of late mafic flows at individual centres. The trends defined by individual volcanic centres are readily explained by fractionation of olivine+clinopyroxene±plagioclase, phases that are present as phenocrysts in mafic lava from the Anahim volcanic belt. If the data is filtered to minimize the effects of crystal sorting, however, a different story emerges. Lava flows having

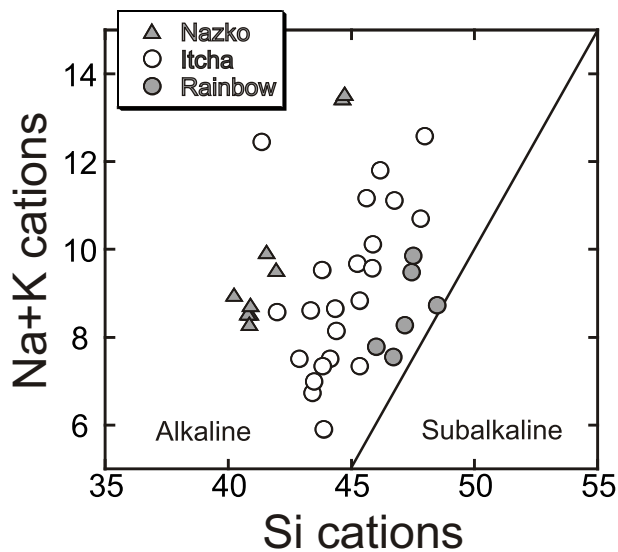


**Figure 2.** Plot of Na+K versus Si (in cation units) showing trends among the Rainbow Range, Itcha Range, and Nazko cone volcanic centres of the Anahim volcanic belt. Data from Bevier (1978), Charland and Francis (1993), Charland et al. (1995) and Souther et al. (1987). The alkaline-subalkaline line is from Charland and Francis (1993).

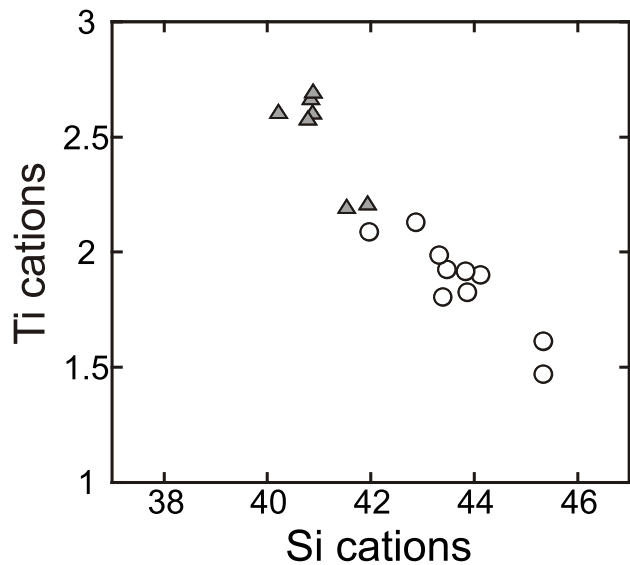


**Figure 3.** Plot of Ti versus Si, showing Itcha Range and Nazko cone lavas having >8 wt. % MgO (anhydrous).

>8 wt. % MgO form an array that cannot be explained by olivine+clinopyroxene fractionation (Figure 3).

### Chilcotin Group

The Chilcotin Group basalts (also filtered for lava flows with >8 wt. % MgO) form poorly defined trends in most major-element space. Like the primitive lava of the Anahim volcanic belt, they display behaviour that is incompatible with olivine fractionation, or indeed any combination of olivine, clinopyroxene, plagioclase, spinel and/or Fe-Ti oxide fractionation (Figure 4). Likewise, the trend cannot be explained by varying degrees of partial melting of an anhydrous peridotite source, as the incompatible elements do not correlate with indices of partial fusion. Bevier (1983) took such behaviour to indicate chemical heterogeneity in the source region, requiring the Chilcotin Group basalts to have been generated by different degrees of partial melting of a source with a heterogeneous distribution of incompatible elements. The negative correlation of Mg (a proxy for the extent of partial melting) with K and Ti requires that regions that melted to the greatest extent (producing the highest Mg basalts) also had the highest incompatible-element concentrations (Figure 4). This trend could be explained by the melting of a hydrous K- and Ti-bearing phase, such as amphibole or phlogopite. Hydrous fluids have the effect of depressing the peridotite solidus, and the more water present, the greater the degree of partial melting at a given temperature (e.g., Hirose and Kawamoto, 1995). Regions of high amphibole or phlogopite concentration would have released more water upon melting, depressing the peridotite solidus to a greater extent, and yielding comparatively large melt fractions (those with the highest Mg contents). While there is little correlation between Pb isotopic ratios and K in the Chilcotin Group basalts, K and Sr isotopic ratios do correlate as expected. One possible explanation for the Pb isotopic ratios is that the process that created heterogeneous mantle metasomatism immediately predated the generation of Chilcotin Group melts without sufficient time for Pb isotopic differentiation.

A decreasing alkali concentration with an increasing degree of silica saturation is a geochemical characteristic that persists from the basalt array to the most primitive lavas of the Anahim volcanic belt, and suggests that a similar process governs their geochemistry (Figure 5). As with the Chilcotin subset, this greater trend cannot be explained by any reasonable fractionation assemblage, or by partial melting of an anhydrous peridotite source. Incompatible minor and trace elements also display colinearity, the further suggestion of a common process (Figure 6). With this in mind, the origins of the most Si-undersaturated members of the spectrum may shed light on the nature of the process responsible for this geochemical trend.

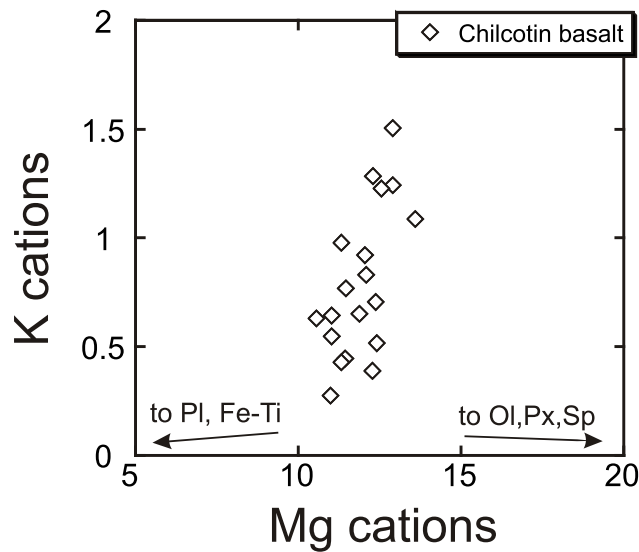


**Figure 4.** Plot of K versus Mg, showing Chilcotin Group basalts having >8 wt. % MgO (anhydrous). The locations of common anhydrous minerals are also shown. Abbreviations: Fe-Ti, magnetite-ilmenite; Ol, olivine; Pl, plagioclase; Px, pyroxene; Sp, spinel. Data from Bevier (1983).

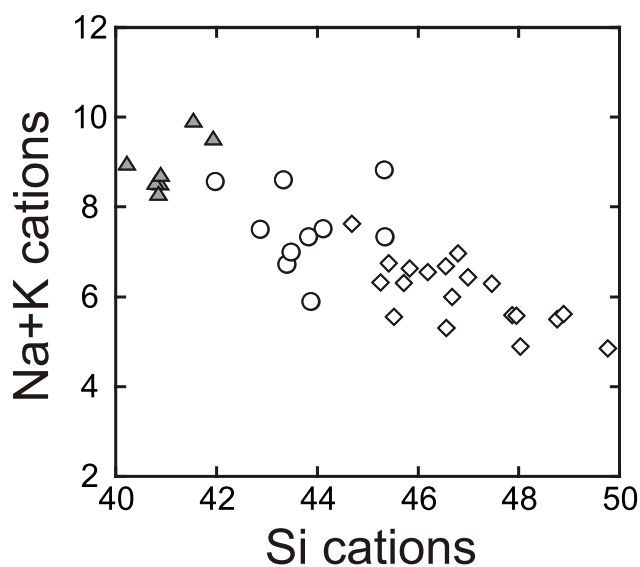


**Figure 5.** Plot of Na+K versus Si showing Itcha Range, Nazko cone and Chilcotin Group lavas with >8 wt. % MgO.

## GENERATION OF HIGHLY UNDERSATURATED MAFIC ALKALINE MAGMA

Strongly Si-undersaturated magmas such as olivine nephelinite and basanite have been attributed to a variety of processes, including low-degree melts of peridotite, melting of Si-poor garnet pyroxenite and melting of amphibole in metasomatized mantle (e.g., Francis and Ludden, 1995; Kogiso et al., 2003; Pilet et al., 2008).

Experimental work has demonstrated that low-degree partial melts of anhydrous peridotite can produce strongly Si-undersaturated liquids at elevated pressures (Hirose and Kushiro, 1993). Partial melting trends for anhydrous peridotite compositions, however, can neither replicate the Ca/Al ratios of highly undersaturated magma, nor the positive slope of Ca/Al in the olivine nephelinite-alkali olivine basalt array (Francis and Ludden, 1995). In addition, such

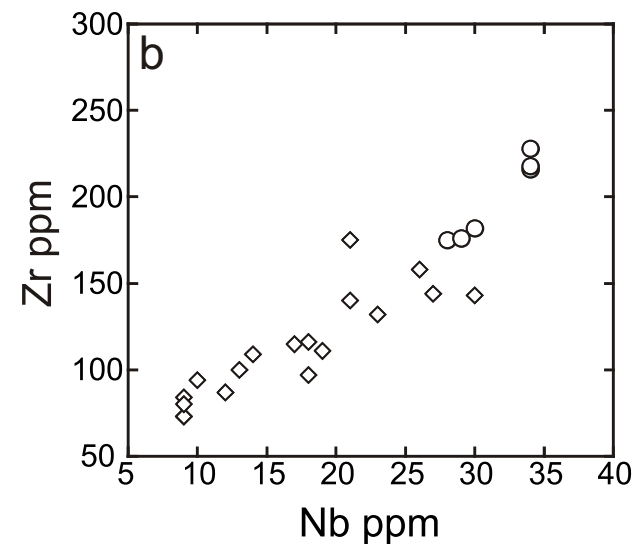
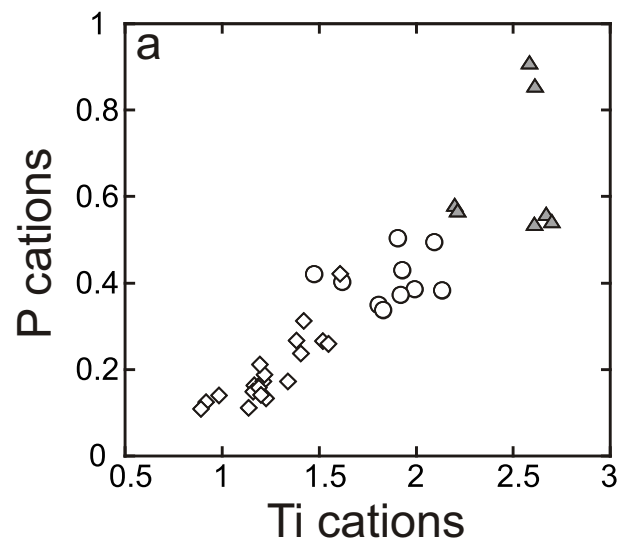


**Figure 6.** a) Plot of P versus Ti, showing Anahim volcanic belt lavas and Chilcotin Group basalts. Dataset as in Figure 5. b) Plot of Nb versus Zr. Dataset shows only Chilcotin and Itcha data because published Nazko data lacks trace elements.

source compositions cannot reproduce the elevated Ti content of alkaline magma in general (Pilet et al., 2008). Silica-deficient garnet pyroxenite has been suggested as the source of undersaturated magma, in part because of their elevated Ti contents. Below pressures of at least 50 kbar (~150 km depth), however, partial melts of such compositions do not reproduce the elevated K concentrations of alkaline magma (Pilet et al., 2008). Experimental investigations of the melting behaviour of amphibole at upper mantle conditions reveal that it melts incongruently to form clinopyroxene+spinel±olivine+liquid at pressures below 15 kbar, and to form clinopyroxene+garnet+liquid at pressures above 15–20 kbar (Ólafsson and Eggler, 1983). Experimental liquids are highly undersaturated, with nephelinitic compositions (Pilet et al., 2008). Francis and Ludden (1995) offer compelling evidence that the olivine nephelinite–basanite transition in the northern Cordillera corresponds to the exhaustion of amphibole in the source region. Experimental work by Pilet et al. (2008) shows that this model also explains the trace-element patterns of basanitic lava. As such, the melting of amphibole appears to best explain the major- and trace-element systematics of highly undersaturated mafic alkaline lava.

## PETROGENESIS

While there is compelling evidence for the role of amphibole in the generation of nephelinitic to basanitic magma, it remains to be seen how such highly undersaturated compositions are related to the alkali olivine basalts of the Anahim volcanic belt and the Chilcotin Group. It has been suggested that the basanite-alkali olivine basalt spectrum represents the two-step melting of a heterogeneous amphibole-bearing mantle assemblage, whereby initial amphibole-derived melts are progressively diluted with peridotite-derived basalt (Wilkinson, 1991; Francis and Ludden, 1995). More recently, it has been proposed that the spectrum largely reflects equilibration between amphibole-derived melts and subsolidus peridotite (Pilet et al., 2008). The silica content of primary melts is largely insensitive to the degree of partial melting and source composition, and instead is controlled by the pressure at which melting occurs (Hirose and Kushiro, 1993). Nephelinitic liquids produced by the melting of amphibole are out of equilibrium with surrounding peridotite at pressures below those at which nephelinitic melts would be generated from anhydrous peridotite (>50 kbar; extrapolated from data of Hirose and Kushiro, 1993). At pressures within the spinel stability field, nephelinitic liquids will essentially leach silica from orthopyroxene by transforming it into olivine and thereby increasing the Si content of the liquid to bring it into equilibrium with the surrounding mantle (Lundstrom et al., 2000). Experiments show that this reaction occurs on experimental timescales (Ólafsson and Eggler, 1983; Pilet et al., 2008). An important aspect of this reaction is that, given that the maximum pressure at which amphibole is stable in the mantle is ~30 kbar (Wallace and Green, 1991), strongly Si-undersaturated melts derived from amphibole must avoid equilibration with the surrounding mantle peridotite if they are to reach the surface unmodified.

If the compositional spectrum reflects the simple addition of silica to an originally nephelinitic melt, as required by the reaction with orthopyroxene to produce olivine, then it is to be expected that element ratios, such as K/Na and Mg#, should remain unchanged as the Si content increases.

For K/Na at least, this is not the case (Figure 7). The K/Na behaviour of the basanite–alkali olivine basalt (AOB) array indicates a progressive dilution of K by Na, most likely caused by the melting of clinopyroxene, suggesting that some degree of peridotite (or pyroxenite) partial melting has taken place. Likewise, the Na+K–Si and Ti–Si systematics of the basanite–AOB array cannot be explained by the addition of silica to nephelinite or basanite, but rather appear to reflect the dilution of nephelinite or basanite with relatively low-pressure (10–15 kbar) peridotite melts (Figure 8). The most suitable basaltic end members are near-solidus melts produced under hydrous conditions.

The basalt dilution model, however, has a major flaw: no ‘standard’ peridotite composition is capable of producing an end-member melt with the observed Fe contents (Figure 8c). The Mg# does not change significantly from nephelinite to Si-saturated basalt; in the dilution model, there ought to be a gradual increase in Mg# with increasing Si (Figure 8d). Perhaps coincidentally, the alkaline array clusters along a tie joining nephelinite with pure silica. Francis (1995) has shown that primitive intraplate lavas worldwide appear to require a source that is richer in Fe than the mantle source of mid-ocean ridge and subduction-related basalt. Therefore, either the mantle that is furnishing the Si-saturated end member is significantly richer in Fe than is indicated by Cordilleran peridotite xenoliths (e.g., Nicholls et al., 1982), or there is a decoupling of compatible and incompatible elements such that incompatible elements reflect dilution of the amphibole-derived melt with hydrous peridotite melts, while compatible elements reflect the reaction of nephelinitic melts with orthopyroxene.

This view provides an alternative explanation for why the Chilcotin Group basalts cannot be related by fractionation processes: their compositions may be unmodified by any crystal fractionation processes, and may instead be controlled either by dilution, by the addition of silica or both. The question naturally arises as to why there are no highly undersaturated compositions reported from the Chilcotin Group. This suggests that either the Chilcotin Group basalt source region had a low amphibole:peridotite melt ratio, or that amphibole-derived melts equilibrated with the surrounding peridotite at shallow depths. Conversely, the highly undersaturated AVB lavas must come from a source rich in amphibole, and must have travelled to the surface rapidly enough to avoid equilibration to higher silica concentrations.

## TECTONIC IMPLICATIONS

Neogene to Quaternary volcanism along the length of the Cordillera appears to be controlled by plate boundary interactions between the North American Plate and its outboard oceanic counterparts (Thorkelson and Taylor, 1989; Edwards and Russell, 2000). Paleosubduction models suggest that a spreading ridge flanked by the Kula and Farallon plates began to subduct beneath the North American Plate during the Late Cretaceous, since which time a slab window has developed beneath virtually the entire northern Canadian Cordillera (Figure 9; Thorkelson and Taylor, 1989). The Kula Plate has been completely subducted, while the Juan de Fuca and Explorer plates are all that is left of the Farallon Plate. A southern slab window formed during the Miocene, when the Farallon-Pacific Ridge subducted, and underlies much of the Basin-and-Range Province of the southwestern United States (Thorkelson

and Taylor, 1989). For the past 5 Ma, volcanism in the Basin-and-Range Province has been dominantly Si-undersaturated (Fitton et al., 1991). The spatial and temporal coincidence of alkaline magmatism and slab windows is therefore highly suggestive.

Because of its linear expression, the Anahim volcanic belt has been variably interpreted as the product of a mantle plume, a propagating rift and a slab window-related edge-effect (e.g., Bevier et al., 1979). Its spatial coincidence with the southern edge of the Cordilleran slab window makes the latter interpretation attractive (Figure 9). The trend of the Anahim volcanic belt does, however, parallel the projected trend of the Yellowstone plume track (Johnston and Thorkelson, 2000), implying that the Anahim trend is consistent with the North American Plate's motion over a steady-state hotspot. The Chilcotin Group has been interpreted as an ensialic backarc basin, forming behind the Pemberton and Garibaldi volcanic belts as a result of subduction of the Juan de Fuca Plate beneath North Amer-

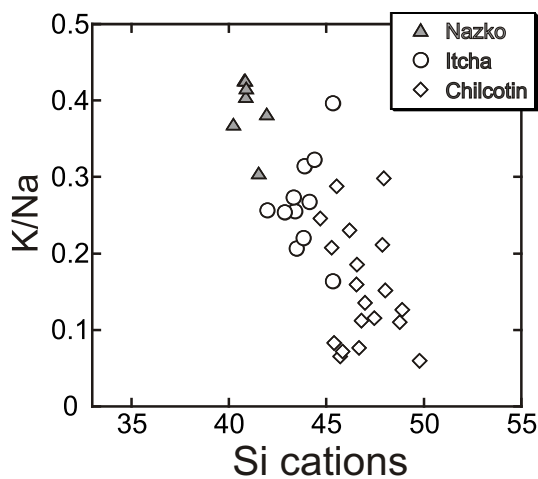


Figure 7. Plot of K/Na versus Si. Dataset as in Figure 5.

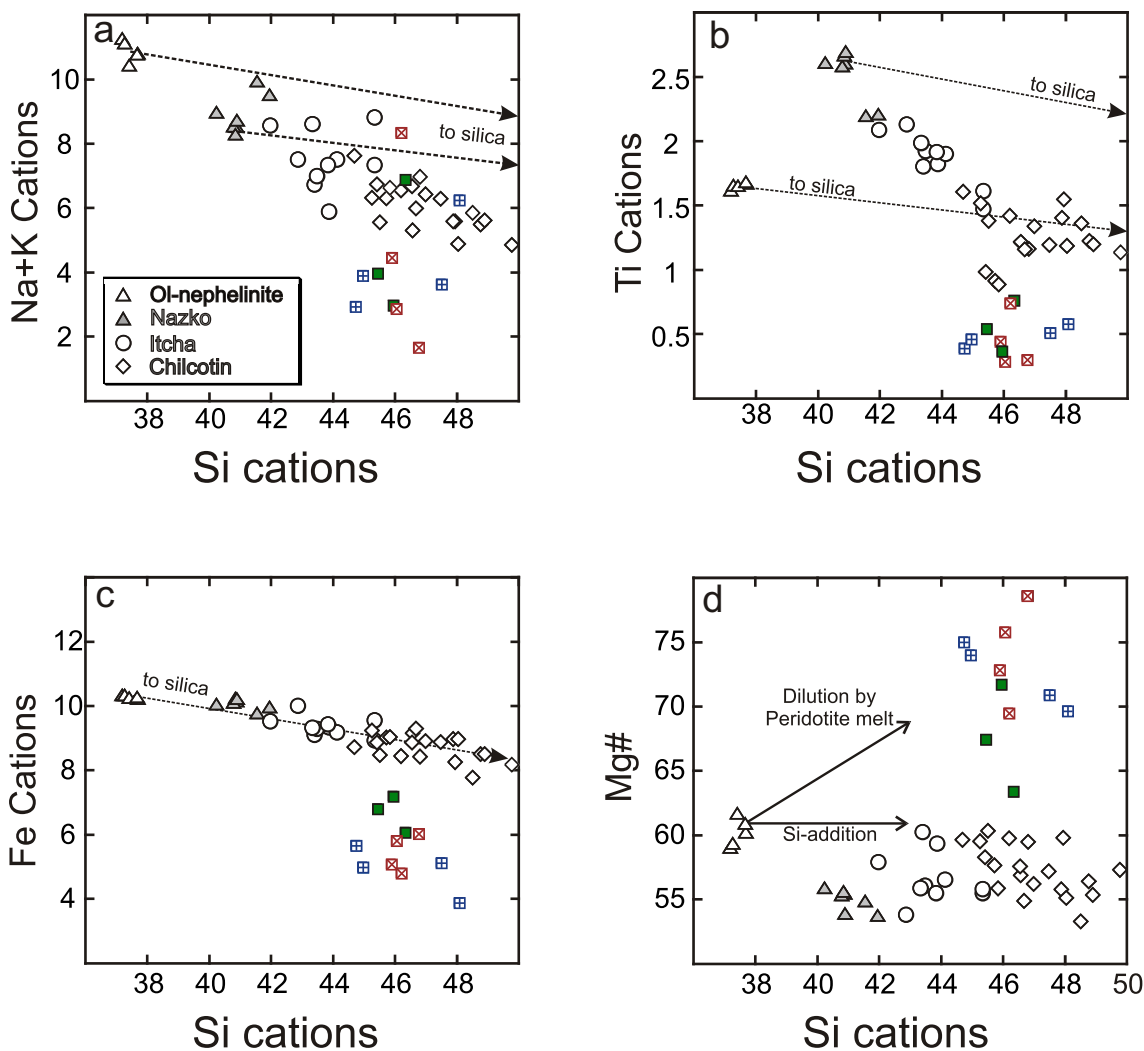


Figure 8. a) Plot of Na+K versus Si. b) Plot of Ti versus Si. c) Plot of Fe versus Si. d) Plot of Mg# versus Si (Mg# =  $100 \cdot \text{Mg}/(\text{Mg} + \text{Fe}_{\text{T}})$ ), with solid arrows showing trends expected from the dilution of nephelinite with peridotite melts, and by the addition of silica to nephelinite. Dataset as in Figure 5, with olivine nephelinite from Francis and Ludden (1995). Partial melts of spinel lherzolite at 10 kb also shown: solid green square, HK-66 (Hirose and Kushiro, 1993); open blue square with cross, KLB-1 (Hirose and Kushiro, 1993); open red square with x, KLB-1 hydrous (Hirose and Kawamoto, 1995). Dashed tie lines link olivine nephelinite and basanite with pure silica (100Si), indicating a Si-addition trend.

ica (Souther, 1977; Bevier, 1983). Thorkelson and Taylor (1989) suggest that, like the Anahim volcanic belt, the Chilcotin Group is also related to slab window edge-effects, although it is difficult to explain why the basalts should extend so far south of the projected slab window.

Because of the slope of the amphibole-out curve in P-T space, amphibole melting cannot be induced directly by decompression, and requires a thermal perturbation to drive the ambient mantle temperature out of the amphibole stability field (Figure 10). This can be accomplished by the upwelling of 'normal' asthenospheric mantle, without needing to infer the existence of an anomalously hot plume. In the Anahim volcanic belt, this upwelling is most likely generated by perturbation in the asthenosphere due to the foundering of the Farallon plate edge. The systematic age progression along the belt would then reflect the migration of this perturbation with continued subduction. If the interpretation of the Chilcotin Group as having formed in a backarc setting is correct, then frictional drag of the mantle wedge by the subducting Juan de Fuca Plate may create a minor convection cell in which the Chilcotin Group melt was produced above the upwelling arm. In either case, hot upwelling asthenospheric mantle comes into contact with amphibole-bearing lithospheric mantle, and in the course of thermal re-equilibration, the amphibole melts, generating nephelinitic to basanitic liquids and hydrous fluids (Figure 10).

## CONCLUSIONS

Neogene alkaline volcanism in the central interior of BC requires a heterogeneous mantle source. The behaviour of incompatible elements such as K and Ti are best explained by varying concentrations of amphibole in the source regions of alkaline lava. Highly undersaturated alkaline compositions, such as nephelinite and basanite, appear to represent the spectrum of incongruent melts of amphibole (Francis and Ludden, 1995; Pilet et al., 2008). The coherent geochemical behaviour of primitive lavas ranging in composition from basanite to quartz-normative basalt in the Anahim volcanic belt and the Chilcotin Group suggests that a common process controls this compositional array. Incompatible element behaviour seems to require the dilution of amphibole-derived nephelinite and basanite with hydrous peridotite melts. Compatible elements, by contrast, suggest the reaction of nephelinite and basanite with orthopyroxene in order to attain equilibrium with mantle peridotite. The reason for the disconnection between compatible and incompatible element behaviour is unclear; an avenue for future work.

The breakdown of amphibole in the lithospheric mantle requires a thermal push. In the case of the Chilcotin Group basalts, this is most likely accomplished by extension and asthenospheric upwelling due to subduction-induced convection in the mantle wedge. In the case of the Anahim volcanic belt, this may be a result of asthenospheric upwelling caused by the sinking of the Farallon Plate edge, as suggested by Thorkelson and Taylor (1989).

## ACKNOWLEDGMENTS

Discussions with Graham Nixon, Dante Canil and Don Francis have helped to organize the ideas presented in this contribution. Graham Nixon also kindly reviewed the

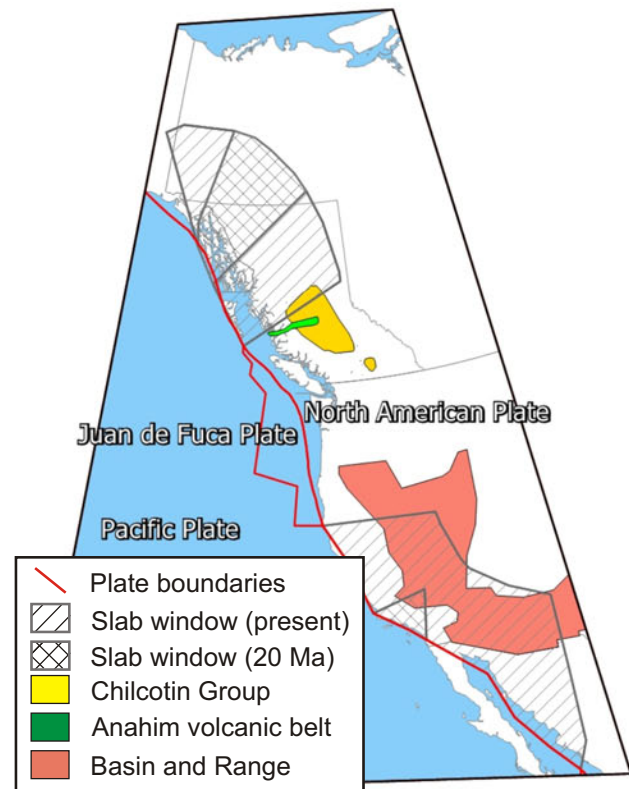


**Figure 9.** Western North America, showing the approximate locations of slab windows at 20 Ma and at present, with respect to Neogene alkaline provinces mentioned in the text. Projected slab windows are from Edwards and Russell (2000) and Thorkelson and Taylor (1989).

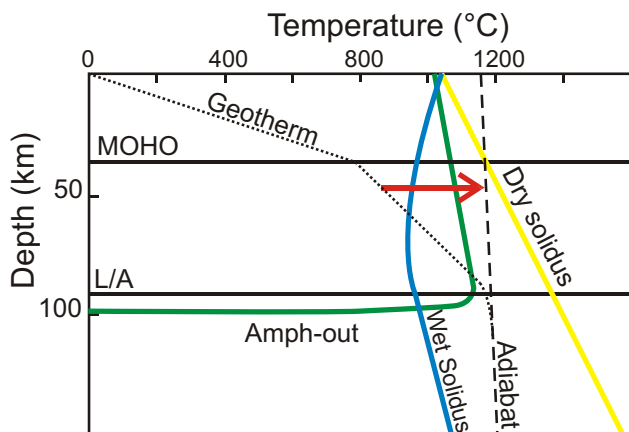


**Figure 10.** Pressure-temperature phase diagram for the crust and upper mantle beneath central BC. Crustal geotherm, crust-mantle boundary and lithosphere-asthenosphere boundary from Harder and Russell (2006). Dry and water-saturated peridotite solidi and amphibole stability field adapted from Francis and Ludden (1995). Adiabāt gradient assumed to be 1.2°C/kbar. The red arrow shows the thermal effect of upwelling asthenospheric mantle impinging on cooler amphibole-bearing lithospheric mantle. Abbreviations: Moho, Mohorovicic discontinuity; L/A, lithosphere-asthenosphere boundary.

manuscript, although we absolve him of any association with the views of alkaline magmatism expressed herein.

## REFERENCES

- Andrews, G.D.M. and Russell, J.K. (2007): Mineral exploration potential beneath the Chilcotin Group, south-central BC: preliminary insights from volcanic facies analysis; in *Geological Fieldwork 2006, BC Ministry of Energy, Mines and Petroleum Resources*, Paper 2007-1 and *Geoscience BC*, Report 2007-1, pages 229–238.
- Bevier, M. (1978): Field relations and petrology of the Rainbow Range shield volcano, west-central British Columbia; M.Sc. thesis, The University of British Columbia, 100 pages.
- Bevier, M., Armstrong, R.L. and Souther, J.G. (1979): Miocene peralkaline volcanism in west-central British Columbia—its temporal and plate-tectonic setting; *Geology*, Volume 7, pages 389–392.
- Bevier, M. (1983): Implications of chemical and isotopic compositions for petrogenesis of Chilcotin Group basalts, British Columbia; *Journal of Petrology*, Volume 24, pages 207–226.
- Charland, A. and Francis, D. (1993): Stratigraphy and geochemistry of the Itcha volcanic complex, central British Columbia; *Canadian Journal of Earth Science*, Volume 30, pages 132–144.
- Charland, A., Francis, D. and Ludden, J. (1995): The relationship between the hawaiites and basalts of the Itcha volcanic complex, central British Columbia; *Contributions to Mineralogy and Petrology*, Volume 121, pages 289–302.
- Edwards, B.R. and Russell, J.K. (2000): Distribution, nature, and origin of Neogene–Quaternary magmatism in the northern Cordilleran volcanic province, Canada; *GSA Bulletin*, Volume 112, pages 1280–1295.
- Fitton, J.G., James, D. and Leeman, W.P. (1991): Basic magmatism associated with late Cenozoic extension in the western United States: compositional variations in space and time; *Journal of Geophysical Research*, Volume 96, pages 13693–13711.
- Francis, D. (1995): The implications of picritic lavas for the mantle sources of terrestrial volcanism; *Lithos*, Volume 34, pages 89–105.
- Francis, D. and Ludden, J. (1995): The signature of amphibole in mafic alkaline lavas, a study in the northern Canadian Cordillera; *Journal of Petrology*, Volume 36, pages 1171–1191.
- Harder, M. and Russell, J.K. (2006): Thermal state of the upper mantle beneath the northern Cordilleran volcanic province (NCVP), British Columbia, Canada; *Lithos*, Volume 87, pages 1–22.
- Hirose, K. and Kushiro, I. (1993): Partial melting of dry peridotites at high pressures: determination of compositions of melts segregated from peridotite using aggregates of diamond; *Earth and Planetary Science Letters*, Volume 114, pages 477–489.
- Hirose, K. and Kawamoto, T. (1995): Hydrous partial melting of lherzolite at 1 GPa: the effects of H<sub>2</sub>O on the genesis of basaltic magmas; *Earth and Planetary Science Letters*, Volume 133, pages 463–473.
- Johnston, S.T. and Thorkelson, D.J. (2000): Continental flood basalts: episodic magmatism above long-lived hotspots; *Earth and Planetary Science Letters*, Volume 175, pages 247–256.
- Kogiso, R., Hirschmann, M.M. and Frost, D.J. (2003): High-pressure partial melting of garnet pyroxenite: possible mafic lithologies in the source of ocean island basalts; *Earth and Planetary Science Letters*, Volume 216, pages 603–617.
- Lundstrom, C.C., Gill, J. and Williams, Q. (2000): A geochemically consistent hypothesis for MORB generation; *Chemical Geology*, Volume 162, pages 105–126.
- Mathews, W.H. (1989): Neogene Chilcotin basalts in south-central British Columbia; *Canadian Journal of Earth Sciences*, Volume 26, pages 969–982.
- Mihalynuk, M.G. (2007): Neogene and Quaternary Chilcotin Group cover rocks in the Interior Plateau, south-central British Columbia: a preliminary 3-D thickness model; in *Geological Fieldwork 2006, BC Ministry of Energy, Mines and Petroleum Resources*, Paper 2007-1, pages 143–148.
- Mihalynuk, M.G., Peat, C.R., Terhune, K. and Orovan, E.A. (2008): Regional geology and resource potential of the Chezacut map area, central British Columbia (NTS 093C/08); in *Geological Fieldwork 2007, BC Ministry of Energy, Mines and Petroleum Resources*, Paper 2008-1, pages 117–134.
- Nicholls, J., Stout, M.Z. and Fiesinger, D.W. (1982): Petrologic variations in Quaternary volcanic rocks, British Columbia, and the nature of the underlying upper mantle; *Contributions to Mineralogy and Petrology*, Volume 79, pages 201–218.
- Olafsson, M. and Eggler, D.H. (1983): Phase relations of amphibole, amphibole-carbonate, and phlogopite-carbonate peridotite: petrologic constraints on the asthenosphere; *Earth and Planetary Science Letters*, Volume 64, pages 305–315.
- Pilet, S., Baker, M.B. and Stolper, E.M. (2008): Metasomatized lithosphere and the origin of alkaline lavas; *Science*, Volume 320, pages 916–919.
- Souther, J.G. (1977): Volcanic and tectonic environments in the Canadian Cordillera—a second look; in *Volcanic Regimes in Canada, Geological Association of Canada, Special Paper 16*, pages 3–24.
- Souther, J.G. (1984): The Ilgachuz Range, a peralkaline shield volcano in central British Columbia; in *Current Research, Part A, Geological Survey of Canada, Paper 84-1A*, pages 1–9.
- Souther, J.G. (1986): The western Anahim belt: root zone of a peralkaline magma system; *Canadian Journal of Earth Science*, Volume 23, pages 895–908.
- Souther, J.G., Clague, J.J. and Mathewes, R.W. (1987): Nazco cone: a Quaternary volcano in the eastern Anahim belt; *Canadian Journal of Earth Science*, Volume 24, pages 2477–2485.
- Thorkelson, D.J. and Taylor, R.P. (1989): Cordilleran slab windows; *Geology*, Volume 17, pages 833–836.
- Wallace, M.E. and Green, D.H. (1991): The effect of bulk composition on the stability of amphibole in the upper mantle: implications for solidus positions and mantle metasomatism; *Mineralogy and Petrology*, Volume 44, pages 1–9.
- Wilkinson, J.F.G. (1991): Mauna Loa and Kilauea tholeiites with low ‘ferromagnesian-fractionated’ 100Mg/(Mg<sup>+</sup>Fe<sup>2+</sup>) ratios: primary liquids from the upper mantle?; *Journal of Petrology*, Volume 32, pages 863–907.



# Quaternary Geology and Till Geochemistry of the Redstone and Loomis Lake Map Areas, Central British Columbia (NTS 093B/04, 05)

by T. Ferbey, K.J. Vickers, T.J.O. Hietava<sup>1</sup> and S.C. Nicholson<sup>2</sup>

**KEYWORDS:** geochemistry, surficial geology, Quaternary geology, drift exploration, till geochemical survey

## INTRODUCTION

This paper summarizes Quaternary geology mapping and till geochemistry studies conducted as part of the regional mineral potential assessment of the Redstone and Loomis Lake map areas (NTS 093B/04, 05; Figure 1). This study was initiated to complement an ongoing regional bedrock mapping program and mineral potential assessment being conducted in NTS 093C/01, 08 and 09 (Mihalynuk et al., 2008a, b), and a previous surficial mapping and till geochemical survey in NTS 093C/01, 08, 09 and 16 (Giles and Kerr, 1993; Proudfoot, 1993; Lett et al., 2006). Historic gold and silver prospects (e.g., Chili prospect, MINFILE 093C 015; MINFILE, 2008; Clisbako prospect, MINFILE 093C 015), as well as newly discovered copper (e.g., Punky, Orovain, Vampire and Gumbo) and gold and silver showings (e.g., Pyro, Mihalynuk et al., 2008a, b), occur within Mesozoic to Eocene volcanic rocks adjoining the study area. These strata are thought to extend into the study area but an extensive cover of glacial drift makes this speculative. As a result, and despite its mineral potential, the study area has been overlooked and considered a frontier area by the mineral exploration community. There are no known metallic mineral occurrences within the study area and there is no staked ground.

The objectives of this study are to characterize and delineate the Quaternary materials that occur in NTS 093B/04 and 05 and establish the regional ice-flow history; and assess the mineral potential of covered bedrock (subcrop) using a till geochemistry survey.

The goal of this study is to provide the mineral exploration community with new, high-quality, regional-scale, geochemical data, which will help guide exploration efforts in this drift-covered area. Integrating interpretations of these data with other historic geological and geochemical data collected by the British Columbia Geological Survey (BCGS), Geological Survey of Canada (GSC) and Geoscience BC provides a new exploration tool. The study area falls within the mountain pine beetle infestation zone,

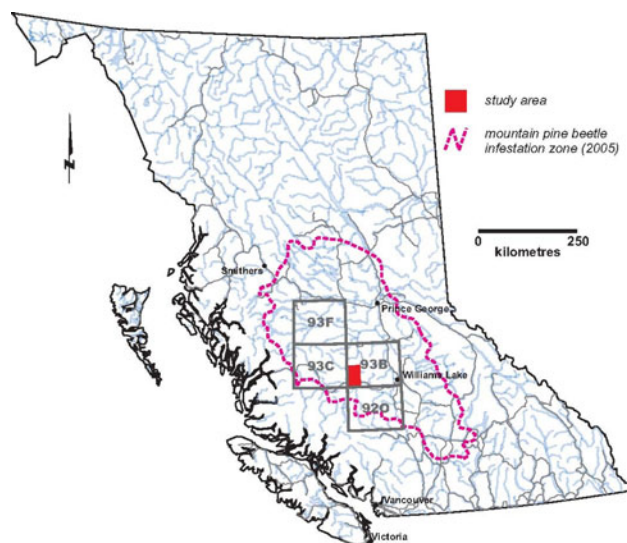


Figure 1. Location of study area, central British Columbia.

which has been a focus of provincial and federal economic diversification initiatives. It is hoped that data from this study will contribute to long-term economic diversification from increased mineral exploration.

## LOCATION AND PHYSIOGRAPHY

During the 2008 field season, detailed sedimentological, glacial history and till geochemical studies were conducted in Redstone and Loomis Lake (NTS 093B/04, 05; Figure 1). The area is located approximately 150 km west of Williams Lake, British Columbia, within the Fraser Plateau, a subdivision of the Interior Plateau physiographic region (Holland, 1976). The area can be described as flat to gently rolling with a relatively undissected upland (Figure 2). An exception to this are the broad valleys of the Chilcotin River and its larger tributaries (e.g., Chilanko and Chilko rivers), which are incised below the plateau surface (Tipper, 1971). The subdued plateau topography is largely attributed to the subhorizontal, Late Oligocene to Pleistocene Chilcotin Group basalt flows thought to underlie it. Mantling these basalt flows is a sequence of glacial drift.

Valley settings have thick sequences of Quaternary, and locally pre-Late Wisconsinan, sediments while the upland or plateau surface is dominated by till. At 1377 m asl, Mount Alexis is the highest, named elevation in the area. North of Temapho Lake, the plateau surface rises to over 1500 m asl in a series of unnamed peaks and ridges (Figure 2). For the most part, bedrock outcrop is limited to higher elevations, meltwater channel flanks, and recent

<sup>1</sup>University of Oulu, Oulu, Finland

<sup>2</sup>University of Guelph, Guelph, ON

This publication is also available, free of charge, as colour digital files in Adobe Acrobat® PDF format from the BC Ministry of Energy, Mines and Petroleum Resources website at <http://www.empr.gov.bc.ca/Mining/Geoscience/PublicationsCatalogue/Fieldwork/Pages/default.aspx>.



**Figure 2.** View of study area looking south towards Mount Alexis (centre of the background), central British Columbia. Note the flat to gently rolling topography in foreground and higher peaks and ridges in background.

scarps that define the larger Chilanko, Chilcotin and Chilko river valleys.

Homesteads and cattle ranches characterize the study area. Redstone (population 500), located south of Punt Lake on the north bank of Chilanko River, is the largest established community. The southern portion of the study area is traversed by Highway 20 and the remainder is accessible using an extensive network of Forest Service roads.

## BEDROCK GEOLOGY

The bedrock geology was first described by Tipper (1959). This work was compiled by Massey et al. (2005) and recently studied in greater detail locally by Ferri and Riddell (2006) and Riddell and Ferri (2008) as part of an assessment of oil and gas potential of the Nechako Basin. Adjacent to the study area, an ongoing regional bedrock mapping and mineral potential assessment in NTS 093C/01, 08 and 09 has yielded new occurrences of metallic mineralization (Mihalynuk et al., 2008a, 2009).

The main geological subdivisions found in the study area, as summarized from Tipper (1959), Diakow et al. (1997) and Massey et al. (2005), are as follows. The study is situated within the Stikine terrane, close to its eastern contact with the Cache Creek terrane (Monger et al., 1991). The oldest rocks are found in the westernmost portion of NTS 093B/04 and belong to the Early to Middle Jurassic Hazelton Group. Locally, they are composed of andesite and basalt with related tuff, breccia and volcanoclastic deposits, which resulted from subaerial and submarine volcanism. Submarine sedimentary rocks, associated with activity in an island arc, are also locally present. These are all overlain by a sedimentary succession of fluvial conglomerate, sandstone and siltstone from the Early and Late Cretaceous Skeena Group. These rocks are locally exposed in the Chilko River valley, south and southwest of Sisters Hills, and northwest of Temapho Lake.

Subduction-related arc volcanism resumed within the Stikine terrane in the Late Cretaceous, changing to a continent margin setting with subaerial volcanism in the Paleogene. Paleogene assemblages include the Ootsa Lake and Endako groups. Eocene volcanic deposits of the Ootsa Lake Group are widespread at Sisters Hills, and underlie

topographically higher terrain in much of the northern portion of NTS 093B/05. They consist of a diverse succession, ranging from rhyolite to basalt, and were mapped in detail to the west by Mihalynuk et al. (2008a, b). They include maroon-brown basalt flows and breccia, acicular hornblende dacite flows, maroon and grey flow-banded rhyolite, and vitreous black dacite. In NTS 093C, conglomerate is locally found lying at the base of the Ootsa Lake Group, unconformably overlying the older Jurassic Hazelton Group.

Within the study area, Eocene to Oligocene volcanic rocks of the Endako Group unconformably overlie the Ootsa Lake Group. They occupy higher ground in the northern portion of NTS 093B/05 and to the northeast of Sisters Hills. They consist mainly of inclined, massive to crudely stratified andesite to basaltic andesite flows. Although the flows can include vesicular and amygdaloidal varieties, characteristically they are dense, black and aphanitic.

The youngest rock unit consists of basalt flows and associated volcanoclastic rocks that unconformably overlie older rock units and are correlated with the Late Oligocene to Pleistocene Chilcotin Group. These rocks consist of distinctly layered, subhorizontal, relatively thin flows, commonly with columnar structures associated with shield-like volcanic centres, interpreted to occur north of the study area (Mihalynuk et al., 2008a). When compared to other basalt within the study area, they differ and are dark brown to grey, highly vesiculated, and contain unaltered phenocrysts of olivine and feldspar. Fine-grained, less vesiculated varieties have a felted grey-brown texture.

Geological maps by Tipper (1959) and Massey et al. (2005) show that upwards of 70% of the study area is underlain by basalt of the Chilcotin Group. Although the areal extent of these rocks within the Nechako Plateau is certainly significant, recent work by Mihalynuk et al. (2008a, b, 2009) and Andrews and Russell (2007) demonstrated that this cover may not be as widespread or thick as originally thought. This is positive for mineral exploration and drift prospecting, as these recent studies report significant thickness variations and even windows through Chilcotin Group flow sequences exposing older more prospective basement units.

Massive granite occupies the southwest corner of NTS 093B/04. It is interpreted to be part of an intrusive body mapped by Tipper (1969) and Mihalynuk et al. (2009) to the west. Mihalynuk et al. (2008a, b, 2009) reported positive correlation between intrusive bodies and intrusion-hosted veins with copper mineralization. As this is the only intrusive body within the study area, a higher density of till samples was collected down-ice, to the northeast, in order to investigate a potential association with mineralization.

## Mineral Occurrences

There are no known metallic mineral occurrences within the study area. To the west, however, historic gold and silver prospects are known within the eastern portion of NTS 093C (e.g., Chili, MINFILE 093C 011; Chilcotin River East and West, MINFILE 093C 013 and 093C 014; Baez, MINFILE 093C 015; Clisbako, MINFILE 093C 016), as well as newly discovered copper (e.g., Punky, Orovain, Vampire and Gumbo) and gold and silver showings (e.g., Pyro). Lett et al. (2006) and Mihalynuk et al. (2008a) provided summaries of these occurrences.

## QUATERNARY GEOLOGY

The Quaternary geology of the study area was first described by Tipper (1971) in a glacial features map at a 1:250 000 scale. The BC Ministry of Environment, Lands and Parks (1976a, b) produced 1:50 000 scale soils and landforms maps for NTS 093B/04 and 05. Other Quaternary geological studies have been conducted in the region in areas adjacent to NTS 093B (Figure 1; e.g., Giles and Kerr, 1993; Proudfoot, 1993; Levson and Giles, 1997; Mate and Levson, 1999; Mate and Levson, 2000; Plouffe and Levson, 2001). The following is a summary of data collected during the 2008 field season.

## Surficial Geology

Detailed sedimentological and stratigraphic descriptions were conducted at 266 stations within the study area (Figure 3). These stations were selected with the objective of gaining a better understanding of Quaternary processes during the Late Wisconsinan and of the area's glacial history. Most Quaternary exposures were the result of logging-related activity (e.g., roadcuts and borrow and gravel pits) but also included natural exposures (e.g., sides of valleys and meltwater channels, tree throws) and hand-dug soil pits. Exposures ranged from a few to several tens of

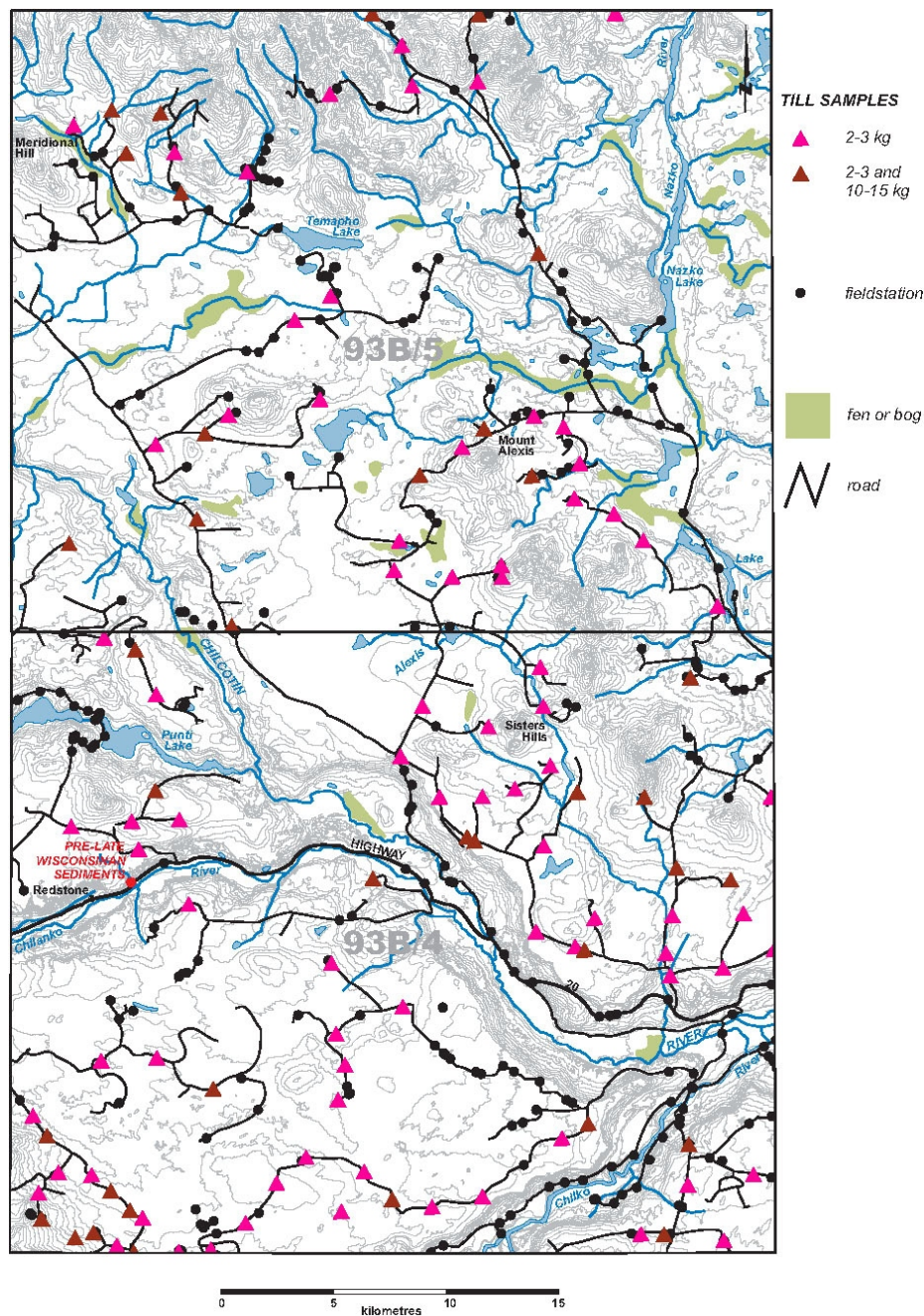


Figure 3. Location of field stations and till samples within the study area, central British Columbia.



**Figure 4.** Pre-Late Wisconsinan sequence of sand, gravel and tephra, near Redstone, British Columbia. The overlying Late Wisconsinan Fraser glaciation basal till is shown with an asterisk (\*).

metres in height. In the case of hand-dug soil pits, depth only occasionally exceeded 1 m below surface.

### PRE-LATE WISCONSINAN

Exposed in a 12 m vertical section are the oldest sediments to occur in the study area (Figure 3). Preliminary data indicate that this is a 6.8 m thick sequence of pre-Late Wisconsinan stratified sand, gravel and tephra (Figure 4). These pre-Late Wisconsinan sediments are unconformably overlain by 2.2 m of basal till and 3.0 m of glaciofluvial gravel deposited during full glacial and retreat-phase conditions, respectively, of the Late Wisconsinan Fraser glaciation. The thick crossbedded sand and gravel succession that occurs in the lower portion of the section is lithologically distinct from the gravel that overlies the Late Wisconsinan basal till as the succession appears to be devoid of intrusive clasts. A 30 to 50 cm thick, grey horizon of silt-sized material of possible volcanic origin separates the lower sand and gravel from a 2.5 m thick unit of interbedded buff to white tuff and oxidized and indurated silt. The tuff is rhyolitic, with biotite and feldspar crystals up to 1.0 mm across. The 40 to 60 cm thick indurated and oxidized silt horizons that separate tuff layers could be weakly developed paleosols. This exposure, and another exposure located 5 km to the east on Highway 20, is believed to be the first observation of pre-Late Wisconsinan sediments in the area. More detailed work is required to confirm these interpretations.

### LATE WISCONSINAN GLACIAL SEDIMENTS

The dominant surficial material found in the study area is diamict. Based on physical characteristics such as matrix texture and proportion, modal clast size and clast shape, and surface expression, the sediments are divided into two genetically separate units. The first, and likely dominant in terms of areal extent, is a grey, sand-rich, gravelly diamict. In this diamict, characteristics such as vertical jointing, subhorizontal fissility and compaction or over-consolidation are lacking. Clast shape is commonly subangular to subrounded and modal clast size is small pebble but ranges from granule to large pebble. The unit is clast rich compared to the second diamict described below and the proportion of matrix is typically 55 to 75%. Near surface (in the upper 1 to 2 m), this matrix can be oxidized and clasts, in particular intrusive rock types, can be weathered. The



**Figure 5.** Hummocky, englacial or supraglacial till, central British Columbia.

lower contact of this diamict, observed in only a few localities, is gradational downward into a grey, silt-rich, overconsolidated diamict (described below). Minimum thickness is ~1 m and ranges up to several metres in some areas.

The surface expression of this sand-rich, gravelly diamict, as observed in aerial photographs and in the field, is distinctive. The upper surface is typically undulating to hummocky and commonly has pebble to boulder-sized clasts sitting at surface (Figure 5). The physical and geomorphological characteristics are consistent with till of englacial or supraglacial origin. The transport history of this till facies can be complex and this uncertainty precluded sampling for till geochemistry. Windows through this facies to an underlying silt-rich, overconsolidated diamict are occasionally found. This underlying material is an ideal sample medium for a till geochemical survey and is described below.

The underlying silt-rich, overconsolidated diamict is grey and is the other commonly occurring diamict within the study area. This diamict is massive; vertical jointing and subhorizontal fissility are locally well developed (Figure 6). Matrix proportion ranges from 65 to 85%. Modal clast size is small pebble and ranges from granule to large pebble. Clast shape is typically subangular to subrounded but locally, down-ice from larger river valleys, there can be a concentration of rounded, subdiscoidal to spherical clasts and a more sandy textured matrix. These clasts are interpreted to have been incorporated by the Cordilleran Ice Sheet as it moved across existing valley fills.

This diamict can occur at surface or underlie the englacial or supraglacial till unit described above. Its surface expression is also distinctive. The morphology of the upper surface is variable and can be rolling or ridged (e.g., in the case of fluted, drumlinized or crag-and-tail terrain) or a more subtle variation of the bedrock surface it blankets. At some sites, this basal till directly overlies grooved and striated Chilcotin Group basalt flows. The texture, primary structures and degree of consolidation of this unit are consistent with those of subglacially derived diamict (Dreimanis, 1989) and this unit is interpreted as basal till.

## LATE WISCONSINAN RETREAT-PHASE SEDIMENTS

Late-glacial ice-marginal and retreat-phase glaciofluvial sand and gravel commonly occur, within and adjacent to meltwater channels, as terrace and outwash deposits in the larger Chilanko, Chilcotin and Chilko river valleys. Meltwater channels can be isolated features a few metres across and tens of metres long, or can be complex kilometre-scale meltwater channel systems composed of multiple tributary channels. The most prominent is located in the eastern portion of NTS 093B/05 and hosts the Alexis and Nazko lakes system. Surficial materials in these systems range from moderately well-sorted, silty sand to cobble gravel. Tipper (1971) proposed that this meltwater channel system was the outlet for a Late Wisconsinan glacial lake that occupied the Chilcotin River valley, a product of damming of the Chilcotin River at its confluence with the Fraser River by a late-glacial readvance of ice from the Cariboo Mountains to the west across the Fraser Plateau. Based on the elevation of the drainage divide that separates the modern-day Nazko River watershed from that of Chilcotin River, a minimum upper elevation for this glacial lake is 1047 m asl.

Glaciolacustrine sediment associated with this ice-dammed lake dominates the larger river valleys such as Chilanko, Chilcotin and Chilko, and many of their tributaries (Figure 7). The sediment is typically parallel-laminated and bedded silt and fine sand. Near lake margins, the silt and fine sand are interbedded with coarse sand, and ripples and cross-stratification are common. They are commonly deeply gullied and can be associated with valley-side, mass-wasting deposits. The juxtaposition of large-scale esker systems in the bottom of Chilcotin River valley, upstream of the confluence of Chilcotin and Chilanko rivers, and in the bottom of Chilko River valley, upstream of the confluence with Chilcotin River, against these glaciolacustrine sediments is both impressive and a curiosity as they demonstrate a contrast in depositional environments. These esker systems are composed of sand and pebble- to cobble-sized gravel ridges up to 50 m high and 2 km long. They are free of any fine-grained glaciolacustrine sediments. Their occurrence suggests that large stagnant ice



**Figure 6.** Silt-rich, overconsolidated diamict (interpreted to be basal till), central British Columbia. Note well-developed jointing and subhorizontal fissility. The maroon hue is attributed to the colour of its source rock, Ootsa Lake Group volcanic rocks that occur up-ice of this exposure.

masses were sitting at least locally in the Chilcotin River and upper Chilko valleys while they were flooded.

## HOLOCENE DEPOSITS

Glacial units are typically capped on steeper valley slopes by colluvial deposits. The parent material of these deposits can be pre-existing glacial sediment or Chilcotin Group basalt flows that have moved downslope from bedrock scarps that rim larger valleys (e.g., Chilanko, Chilcotin, Chilko valleys). Historic mass-wasting deposits can be clearly seen in aerial photographs while ongoing translational displacement of Chilcotin Group basalt blocks can be observed on the ground. Holocene organic deposits in the study area are typically found bordering small lakes or flooring some of the larger glaciofluvial meltwater channels and channel systems.

## Ice-Flow History

The study area was covered by the Cordilleran Ice Sheet during the Late Wisconsinan Fraser glaciation (Tipper, 1971). The occurrence of crag-and-tail features on higher ground within the north and southeast parts of NTS 093B/04 (>1330 m asl) and 093B/05 (>1400 m asl), and the northeast-tapering drift tail of an unnamed peak in the southwest part of 093B/04 (Figure 8), provide a minimum elevation for this ice of approximately 1500 m asl. The consistent orientation of these landform-scale features with striations, grooves and other drumlins and flutings at lower elevation shows that ice movement through the study area was relatively unaffected by topography during the glacial maximum (Figure 9). A minor deflection can be observed when comparing ice-flow indicators occurring in the southwest to those in the northwest and north, a result of the interaction of northeast-flowing ice from the Coast Mountains with westward-flowing ice from the Cariboo Mountains. The confluence and turning of these two ice flows occurred during the Late Wisconsinan glacial maximum to the east of this map area, near the Fraser River valley (Tipper, 1971).

Both bidirectional (e.g., flute) and unidirectional (e.g., drumlin, crag-and-tail) landform-scale, ice-flow indicators, in various topographic settings, can be observed in aerial photographs and on the ground. In both cases, the features (Figure 9) trend  $035^{\circ}$  (in the northwest and north) to



**Figure 7.** View of glaciolacustrine sequence in Chilcotin River valley, central British Columbia.

055° (in the southwest). The preservation and definition of these features can vary; excellent examples can be observed where topographic features are oriented perpendicular to regional ice flow. For example, on the east side of the upper Chilcotin River valley (upstream of its confluence with Chilanko River), clear, well-defined drumlins and crag-and-tail features up to 60 m across can be observed in the valley bottom for 850 m up the valley side onto the plateau surface. Excellent examples of crag-and-tail features occur on much of the higher ground in the vicinity of Sisters Hills. Smaller, outcrop-scale features such as striations and grooves are rare. These, and outcrop-scale roches moutonnées, consistently trend 048 to 052° (Figure 9). The orientations of ice-flow indicators observed as part of this study are in general agreement with areas to the west in NTS 093C (Giles and Kerr, 1993; Proudfoot, 1993; Lett et al., 2006; Mihalynuk et al., 2008a, b) and with data and interpretations presented by Tipper (1971).

The proximity of the study area to accumulation centres such as the Coast and Cariboo mountains resulted in a complex late-glacial and deglacial history. To the west, a late-glacial readvance was identified by Tipper (1971), Giles and Kerr (1993) and Proudfoot (1993) and named the Ahahim Lake advance. Piedmont lobes, fed by valley glaciers originating in the Coast Mountains to the west, flowed onto the Fraser Plateau and fanned out to the north, east and southeast. Based on differential ice-flow directions and the occurrence of pitted and kettled terrain, a limit of this advance has been placed within the eastern portions of NTS 093C (Tipper, 1971; Giles and Kerr, 1993; Proudfoot, 1993). A similar readvance is thought to have occurred east of the study area. There, ice advanced west out of the Cariboo Mountains and fanned out onto the Fraser Plateau. Lateral overflow channels and intersections of drumlinoid forms associated with this readvance, and those associated with the northeasterly flow of the Cordilleran Ice Sheet during the Late Wisconsinan glacial maximum, indicate that this readvance crossed and extended up to 30 km west of the Fraser River valley (Tipper, 1971). It has also been proposed that a late-glacial advance, named the Kleena Kleene, occurred down Kleena Kleene, Tatlayoko, Tatla and Chilko valleys. Along the Tatla Lake valley, an elevation limit of approximately 1200 m asl has been suggested for this advance (Tipper, 1971).

Deglaciation was dominated by thinning and downwasting of ice masses (cf. Fulton, 1991). This resulted in higher ground being exposed first, leaving valleys choked with stagnant ice. Hummocky till, glaciofluvial deposits and eskers (in valley settings and on the plateau surface) are evidence in support of this interpretation. In the northern part of the study area, these deglacial features are likely related to the Cordilleran Ice Sheet during the waning stages of the Fraser glaciation. In the southern portions of the study area, however, it is unclear whether they are related to retreat of the Cordilleran Ice Sheet or to the later Kleena Kleene readvance. The occurrence of lateral melt-water channels and a rare recessional moraine (Figure 10) suggest that there was some minor component of marginal retreat during deglaciation.

## TILL GEOCHEMICAL SURVEYS

Till geochemical surveys have not been conducted within the study area. Till samples were collected, however, within NTS 093C/01, 08, 09 and 16 to assess the mineral



**Figure 8.** View of an unnamed peak in the southwest of NTS 093B/04 (looking north-northwest), central British Columbia. Note the drift tail of this crag-and-tail that tapers towards the northeast.

potential of these areas (Giles and Kerr, 1993; Proudfoot, 1993; Lett et al., 2006). Plouffe and Ballantyne (1994), Plouffe (1997) and Plouffe et al. (2001) conducted till geochemistry surveys to the north and south of the study area. To the north of the study area, in the Fawnie Creek map area (093F/03), Cook et al. (1995) conducted a comparative study on the ability of regional lake sediment and till geochemistry surveys to identify known mineral occurrences. In this study, till identified all seven known prospects in the study area with >95th percentile element concentrations. Nine of eleven potential new geochemical prospects presented in the study were also identified with till samples, which had >95th percentile concentrations of multiple elements.

## Sample Media

Basal till, a first derivative of bedrock (Shilts, 1993), is transported in a relatively linear fashion parallel to ice-flow direction, down-ice from its bedrock source. The contrast between elevated and background geochemical values is clear and the area represented by till samples with elevated values can be areally more extensive than that of their bedrock source. The geochemical patterns found in basal till produce a regional signature that is in contrast to residual soils and bedrock-derived colluvium, which typically reflect more local geochemical variations in bedrock (Levson, 2001). The relatively simple transport history of basal till makes it an effective tool for tracing elevated geochemical values back to their bedrock source. In the Canadian Cordillera, the efficiency of conducting a till geochemistry survey, and the quality of geochemical interpretations, are largely dependent on appropriate sample material, access and the detail to which the region's Quaternary and ice-flow history can be determined.

While conducting a till geochemistry program, it is imperative that the sample medium is correctly identified. This ensures consistency between sample sites and understanding of the origin and mode of sediment transport and deposition (Levson, 2001). To this end, sedimentological data, such as texture, colour, thickness, primary and secondary structures, density, matrix percentage, clast mode, shape and presence of striae, were collected at each site in order to ensure the proper discrimination of basal till from other sediment types such as colluvium, debris flows and

glaciolacustrine diamict. As well, at each sample site, notes were made of type of exposure sampled, terrain map unit, sample site geomorphology (e.g., topographic position, aspect, slope, drainage), stratigraphy, and type and thickness of soil horizons present. This information can be critical when interpreting resultant geochemical data. Clasts in till were examined in detail at most sites; data such as lithology, angularity, size, presence of striae, and occurrence of mineralization were recorded. From these data, inferences on clast provenance were made and allow insight into local, covered bedrock units.

For this study, major, minor and trace-element geochemical analyses of till will be conducted on the silt- plus clay-sized (<0.063 mm) and the clay-sized (<0.002 mm) fractions. Traditionally, the silt- plus clay-sized (<0.063 mm) fraction is most commonly used as it can be separated quickly and cost effectively (Levson, 2001). For this study, the clay-sized (<0.002 mm) fraction in basal till will also be analyzed as the contrast between elevated and background element concentrations can be higher. This contrast is due to the tendency of some base metals (more specifically, chalcophile elements such as copper, zinc and lead) to con-

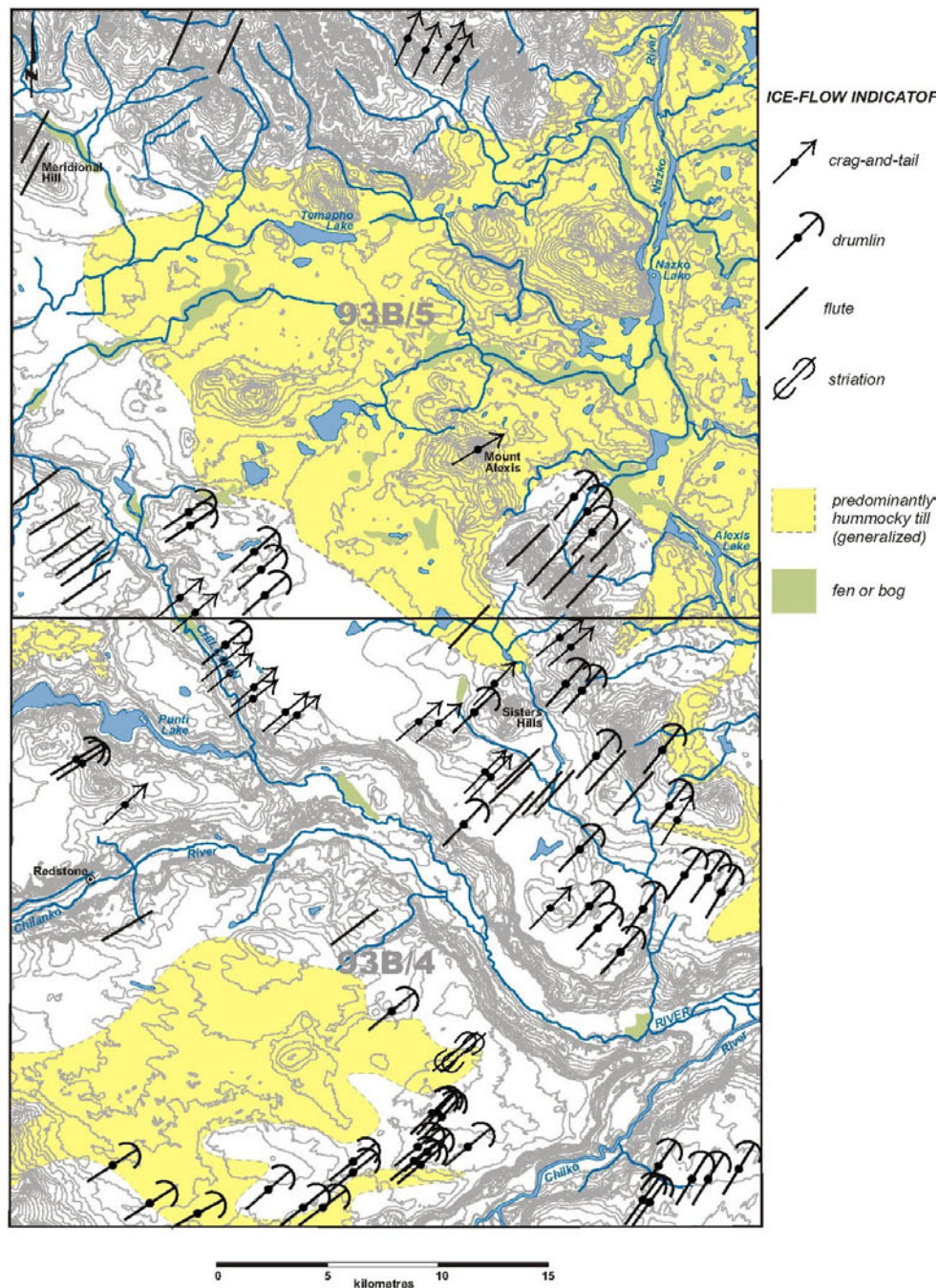


**Figure 9.** Summary of ice-flow indicators observed as part of this study, central British Columbia. Areas of hummocky till (englacial or supraglacial origin) are shown in yellow (*adapted from Tipper, 1971*).

concentrate in this fraction due to the high cation exchange capacity of clay-sized particles (Nikkarinen et al., 1984; Shilts, 1984, 1995; DiLabio, 1995).

Heavy mineral separations are planned for the medium- to very coarse-grained sand (0.25–2.0 mm) fraction, while gold grain counts will be conducted on the very coarse-grained sand fraction and smaller (<2.0 mm). Gold grains in till, based on their morphology and abundance, can provide insight into transport history and genesis. These data can also provide insight into the genesis of source rocks through identification and analysis of heavy mineral assemblages (Averill, 2001).

### Sample Types

As part of this study, 117 basal till samples (2–3 kg) were collected for major, minor and trace-element geochemical analyses, while 38 basal till samples (10–15 kg) were collected for analysis of heavy mineral concentrates and for gold grain counts. Sample sites were selected to optimize spatial coverage, taking into account ice-flow direction and availability of appropriate sample material. The average till sample density for the survey is one sample per 15 km<sup>2</sup>. This is lower than other regional-scale till geochemistry surveys conducted in central British Columbia, which had sample densities of approximately one sample per 5 to 10 km<sup>2</sup>. The lower density is mainly due to the absence of appropriate sample media in the study area and to limited access (e.g., deactivated Forest Service roads, private land or lack of roads). Till samples were collected mainly from roadcuts but also from soil pits and gullies. Average sampling depth was 100 cm below surface but ranged from 45 to 510 cm.

### Laboratory Methods

Till samples collected for major, minor and trace-element analyses are being sieved, decanted and centrifuged to produce a silt- plus clay-sized (<0.063 mm) and clay-sized (<0.002 mm) fraction. This sample preparation is being conducted at the Geological Survey of Canada's Sedimentology Laboratory (Ottawa, ON), following procedures outlined by Girard et al. (2004). Heavy mineral samples have been sent to Overburden Drilling Management (ODM; Nepean, ON) where heavy mineral (0.25–2.0 mm) and gold grain (<2.0 mm) concentrates are being produced using a combination of gravity tabling and heavy liquid separation techniques.

For the 2–3 kg samples, minor and trace-element analyses (37 elements) will be conducted on splits of the silt-plus clay-sized (<0.063 mm) and clay-sized (<0.002 mm) fractions, respectively, by inductively coupled plasma mass spectrometry (ICP-MS), following an aqua regia digestion. Major element analyses will be conducted on a split of the silt- plus clay-sized (<0.063 mm) fraction only, using inductively coupled plasma emission spectrometry (ICP-ES), following a lithium metaborate/tetraborate fusion and dilute nitric acid digestion. This analytical work will be conducted by Acme Analytical Laboratories Limited (Vancouver).

Also as part of this project, a split of the silt- plus clay-sized (<0.063 mm) fraction will be analyzed for 35 elements by instrumental neutron activation analysis (INAA) at Activation Laboratories Limited (Ancaster, ON). Additionally, INAA determinations will be conducted on bulk



**Figure 10.** Northwest-trending recessional moraine, a glacial feature not commonly observed on the Nechako Plateau, central British Columbia. View is towards the southeast.

heavy mineral concentrates produced from the 10–15 kg samples. Heavy mineral picking, scanning electron microscopy (SEM) analyses on difficult-to-identify heavy mineral grains, and pebble counts may be conducted at a later date on these concentrates. Minor and trace-element concentrations, as well as the abundance of heavy minerals and gold grains, will be used to assess whether the additional analyses are warranted.

In each block of 20 samples submitted for major, minor and trace-element analyses, 16 are routine field samples. The remaining four samples are quality control measures, utilized in both the sample collection and sample analysis components of the study, to differentiate true geochemical trends from those that reflect random and systematic sampling or analytical errors. Quality control measures include the use of field duplicates, analytical duplicates and control standards.

## IMPLICATIONS FOR MINERAL EXPLORATION

The single biggest challenge in assessing the area's mineral potential is the cover of englacially or supraglacially derived till, which is not a favourable sample medium for a till geochemical survey. The quality of geochemical determinations, and the interpretations that follow, are entirely dependent on the quality of field sample selection. Although challenging, till geochemical surveys can be successfully completed in areas with the physiographic and geological characteristics encountered in NTS 093B/04 and 05. An initial review of existing surficial geology map data and aerial photographs can help identify most likely till occurrences, such as where rolling or ridged till occurs (e.g., fluted, drumlinized or crag-and-tail terrain), or where thin till conforms to an underlying bedrock surface. Melt-water channels, even those surrounded by glaciofluvial sediments or hummocky till, should be investigated as they can expose underlying basal till units on their flanks. Areas with hummocky till can offer windows through this material into an underlying basal till. Investigating these areas, however, remains a secondary priority.

Interpretation of glacial history can be a challenge in areas with similar physiographic and geological character-

istics. For this study, the streamlined landform record is relatively well preserved and provides a reliable indication of ice-flow direction during the Fraser glaciation maximum. Smaller-scale features, such as grooves, striations or rat tails which provide insight into local variation of ice flow, however, are rare. Although not part of this study, till fabric analyses can provide insight into ice-flow history when other data are lacking. Because till fabric analysis is time consuming and may not be conclusive, however, these analyses should be conducted as a lower priority.

It is worth considering a multimedia approach to geochemical sampling in areas where basal till is not extensive. Raw geochemical data from different sample media (e.g., till, colluvium or bedrock) cannot be combined for interpretation. Integration of interpretations of different sample media, however, is recommended. Local, bedrock-derived colluvium could be sampled, as could locally derived colluvium whose parent material can be confidently identified as basal till. Stream sediment sampling could also be considered.

## SUMMARY AND FUTURE WORK

During the Late Wisconsinan glacial maximum, the Cordilleran Ice Sheet moved northeast across the study area, depositing a silt-rich, overconsolidated, basal till. Fluted, drumlinized and crag-and-tail terrain is common where topographic features such as valley sides and peaks or ridges are oriented perpendicular to the regional ice-flow direction. There is good agreement between ice-flow indicators in valley settings, on the plateau surface, and in the higher ground in the south and eastern portions of the study area, indicating that ice flowed generally unaffected by topography.

The late-glacial history appears to be complex and readvances from the Coast Mountains, and further to the east out of the Cariboo Mountains, have left their mark. The dominant material type is an englacial or supraglacial till. It is unclear whether this gravelly and hummocky till is derived from the stagnation and downwasting of Late Wisconsinan Cordilleran Ice Sheet or at least in part related to the east and northeastward late-glacial readvance of glaciers from the Coast Mountains. Hummocky glaciofluvial deposits and eskers (located in valleys and on the plateau) provide evidence for ice-stagnation. In contrast to this, a rare recessional moraine in the northwest portion of the study area suggests that ice-marginal retreat occurred at least locally. A thick sequence of silt commonly occurs in the Chilanko, Chilcotin and Chilko river valleys. These were deposited in an ice-dammed lake following a late-glacial readvance of ice from the Cariboo Mountains west across the Fraser Plateau, which dammed Chilcotin River at its confluence with Fraser River.

The dominance of a gravelly, englacial or supraglacial till presents a challenge to till geochemistry assessment and the evaluation of bedrock mineral potential. This till facies is not appropriate for a till geochemical survey, and as a result the total number of till samples collected and resultant sample density are less than ideal. A silt-rich, overconsolidated, jointed and fissile basal till (the sample medium of choice) occurs at surface within the study area and in windows through the gravelly till unit. Samples of this facies were collected for major, minor and trace-element analyses and for heavy mineral separations and gold grain counts. At the time of writing, geochemical determinations

and heavy mineral separations were in progress. These data, and accompanying glacial features and surficial geology maps, are planned for release as soon as available in 2009.

## ACKNOWLEDGMENTS

The Geological Survey of Canada (Natural Resources Canada) is gratefully acknowledged for sample processing and analyses support through the Mountain Pine Beetle Program. Camp and field logistics were shared with M.G. Mihalyuk, E.A. Orovan, T. Bachiu, J. Larocque and J. Wardel. Those colleagues are thanked for excellent breakfasts and even finer company. This work benefited from discussions with R.E. Lett and A. Plouffe on analytical methods and techniques. M.G. Mihalyuk, L.J. Diakow and G.T. Nixon are thanked for their comments and insight into the local bedrock geology. A. and M. MacMath (Kokanee Bay Fishing Resort) are thanked for their hospitality. This manuscript benefited from a thorough review by P. Erdmer.

## REFERENCES

- Andrews, G.D.M. and Russell, J.K. (2007): Mineral exploration potential beneath the Chilcotin Group (NTS 092O, P; 093A, B, C, F, G, J, K), south-central British Columbia: preliminary insights from volcanic facies analysis; in *Geological Fieldwork 2006, BC Ministry of Energy, Mines and Petroleum Resources*, Paper 2007-1 and *Geoscience BC*, Report 2007-1, pages 229–238.
- Averill, S.A. (2001): The application of heavy indicator mineralogy in mineral exploration with an emphasis on base metal indicators in glaciated metamorphic and plutonic terrains; in *Drift Exploration in Glaciated Terrain*, McClenaghan, M.B., Bobrowsky, P.T., Hall, G.E.M. and Cook, S.J., Editors, *Geological Society*, Special Publication Number 185, pages 69–81.
- British Columbia Ministry of Environment, Lands and Parks (1976a): Soils and landforms 93B/4; *BC Ministry of Environment, Lands and Parks*, Resource Analysis Branch, 1:50 000 scale map.
- British Columbia Ministry of Environment, Lands and Parks (1976b): Soils and landforms 93B/5; *BC Ministry of Environment, Lands and Parks*, Resource Analysis Branch, 1:50 000 scale map.
- Cook, S.J., Levson, V.M., Giles, T.R. and Jackaman, W. (1995): A comparison of regional lake sediment and till geochemistry surveys: a case study from the Fawnie Creek area, central British Columbia; *Exploration Mining Geology*, Volume 4, pages 93–101.
- Diakow, L.J., Webster, I.C.L., Richards, T.A. and Tipper, H.W. (1997): Geology of the Fawnie and Nechako ranges, southern Nechako Plateau, central British Columbia; in *Interior Plateau Geoscience Project: Summary of Geological, Geochemical and Geophysical Studies*, Diakow, L.J. and Newell, J.M., Editors, *Geological Society of Canada*, Open File 3448 and *BC Ministry of Employment and Investment*, Paper 1997-2, pages 7–30.
- DiLabio, R.N.W. (1995): Residence sites of trace elements in oxidized till; in *Drift Exploration in the Canadian Cordillera*, Bobrowsky, P.T., Sibbick, S.J., Newell, J.M. and Matysek, P., Editors, *BC Ministry of Energy, Mines and Petroleum Resources*, Paper 1995-2, pages 139–148.
- Dreimanis, A. (1989): Tills: their genetic terminology and classification; in *Genetic Classification of Glacigenic Deposits*,

- Goldthwait, R.P. and Matsch, C.L., Editors, *A.A. Balkema*, Rotterdam, pages 17–83.
- Ferri, F. and Riddell, J. (2006): The Nechako basin project: new insights from the southern Nechako basin; in *Summary of Activities 2006, BC Ministry of Energy, Mines and Petroleum Resources*, pages 89–124.
- Fulton, R.J. (1991): A conceptual model for growth and decay of the Cordilleran Ice Sheet; *Géographie physique et Quaternaire*, Volume 45, pages 333–339.
- Giles, T.R. and Kerr, D.E. (1993): Surficial geology in the Chilanko Forks and Chezacut areas (93C/1, 8); in *Geological Fieldwork 1992, BC Ministry of Energy, Mines and Petroleum Resources*, Paper 1993-1, pages 483–490.
- Girard, I., Klassen, R.A. and Laframboise, R.R. (2004): Sedimentology laboratory manual, Terrain Sciences Division; *Geological Survey of Canada*, Open File 4823, 137 pages.
- Holland, S.S. (1976): Landforms of British Columbia: a physiographic outline; *BC Ministry of Energy, Mines and Petroleum Resources*, Bulletin 48, 138 pages.
- Lett, R.E., Cook, S.J. and Levson, V.M. (2006): Till geochemistry of the Chilanko Forks, Chezacut, Clusko River and Toil Mountain area, British Columbia; *BC Ministry of Energy, Mines and Petroleum Resources*, GeoFile 2006-1, 272 pages.
- Levson, V.M. (2001): Regional till geochemical surveys in the Canadian Cordillera: sample media, methods, and anomaly evaluation; in *Drift Exploration in Glaciated Terrain*, McClenaghan, M.B., Bobrowsky, P.T., Hall, G.E.M. and Cook, S.J., Editors, *Geological Society*, Special Publication, Number 185, pages 45–68.
- Levson, V.M. and Giles, T.R. (1997): Quaternary geology and till geochemistry studies in the Nechako and Fraser Plateaus, central British Columbia (NTS 93C/1, 8, 9, 10; F/2, 3, 7; L/16; M/1); in *Interior Plateau Geoscience Project: Summary of Geological, Geochemical and Geophysical Studies*, Diakow, L.J. and Newell, J.M., Editors, *Geological Society of Canada*, Open File 3448 and *BC Ministry of Employment and Investment*, Paper 1997-2, pages 121–145.
- Massey, N.W.D., MacIntyre, D.G., Desjardins, P.J. and Cooney, R.T. (2005): Digital geology map of British Columbia - whole province; *BC Ministry of Energy, Mines and Petroleum Resources*, GeoFile 2005-1, 1:250 000 scale map.
- Mate, D.J. and Levson, V.M. (1999): Quaternary geology of the Marilla map sheet (NTS 93F/12); in *Geological Fieldwork 1998, BC Ministry of Energy, Mines and Petroleum Resources*, Paper 1999-1, pages 25–32.
- Mate, D.J. and Levson, V.M. (2000): Quaternary geology of the Marilla map area (NTS 93F/12); *BC Ministry of Energy, Mines and Petroleum Resources*, Open File 2000-9, 1:50 000 scale map.
- Mihalynuk, M.G., Orovan, E.A., Larocque, J.P., Friedman, R.M. and Bachiu, T. (2009): Geology, geochronology and mineralization of the Chilanko Forks to southern Clusko River area, British Columbia (NTS 93C/01, 08, 09S); in *Geological Fieldwork 2008, BC Ministry of Energy, Mines and Petroleum Resources*, Paper 2009-1, pages 81–100.
- Mihalynuk, M.G., Peat, C.R., Terhune, K. and Orovan, E.A. (2008a): Regional geology and resource potential of the Chezacut map area, central British Columbia (NTS 093/08); in *Geological Fieldwork 2007, BC Ministry of Energy, Mines and Petroleum Resources*, Paper 2008-1, pages 117–134.
- Mihalynuk, M.G., Peat, C.R., Orovan, E.A., Terhune, K., Ferbey, T. and McKeown, M.A. (2008b): Chezacut area geology (NTS 93C/08); *BC Ministry of Energy, Mines and Petroleum Resources*, Open File 2008-2, 1:50 000 scale map.
- MINFILE (2008): MINFILE BC mineral deposits database; *BC Ministry of Energy, Mines and Petroleum Resources*, URL <<http://www.empr.gov.bc.ca/Mining/Geoscience/MINFILE/Pages/default.aspx>> [December 16, 2008].
- Monger, J.W.H., Wheeler, J.O., Tipper, H.W., Gabrielse, H., Harms, T., Struik, L.C., Campbell, R.B., Dodds, C.J., Gehrels, G.E. and O'Brien, J. (1991): Cordilleran terranes (Chapter 8: Upper Devonian to Middle Jurassic assemblages); in *Geology of the Cordilleran Orogen in Canada*, Gabrielse, H. and Yorath, C.J., Editors, *Geological Survey of Canada*, Geology of Canada Series Number 4, pages 281–327.
- Nikkarinen, M., Kallio, E., Lestinen, P. and Äyräs, M. (1984): Mode of occurrence of copper and zinc in till over three mineralized areas in Finland; *Journal of Geochemical Exploration*, Volume 21, pages 239–247.
- Plouffe, A. (1997): Reconnaissance till geochemistry on the Chilcotin Plateau (92O/5 and 12); in *Interior Plateau Geoscience Project: Summary of Geological, Geochemical and Geophysical Studies*, Diakow, L.J., Metcalfe, P. and Newell, J., Editors, *BC Ministry of Energy, Mines and Petroleum Resources*, Paper 1997-2, pages 145–157.
- Plouffe, A. and Ballantyne, S.B. (1994): Regional till geochemistry, Mount Tatlow and Elkin Creek area, British Columbia (92O/5 and O/12); *Geological Survey of Canada*, Open File 2909, 62 pages.
- Plouffe, A. and Levson, V.M. (2001): Late Quaternary glacial and interglacial environments of the Nechako River - Cheslatta Lake area, central British Columbia; *Canadian Journal of Earth Sciences*, Volume 38, pages 719–731.
- Plouffe, A., Levson, V.M. and Mate, D.J. (2001): Till geochemistry of the Nechako River map area (NTS 93F), central British Columbia; *Geological Survey of Canada*, Open File 4166, 66 pages.
- Proudfoot, D.N. (1993): Drift exploration and surficial geology of the Clusko River and Toil Mountain map sheets (93C/9, 16); in *Geological Fieldwork 1992, BC Ministry of Energy, Mines and Petroleum Resources*, Paper 1993-1, pages 491–498.
- Riddell, R. and Ferri, F. (2008): Nechako Project update; in *Geoscience Report 2008, BC Ministry of Energy, Mines and Petroleum Resources*, pages 67–77.
- Shilts, W.W. (1984): Till geochemistry in Finland and Canada; *Journal of Geochemical Exploration*, Volume 21, pages 95–117.
- Shilts, W.W. (1993): Geological Survey of Canada's contributions to understanding the composition of glacial sediments; *Canadian Journal of Earth Sciences*, Volume 30, pages 333–353.
- Shilts, W.W. (1995): Geochemical partitioning in till; in *Drift Exploration in the Canadian Cordillera*, Bobrowsky, P.T., Sibbick, S.J., Newell, J.M. and Matysek, P., Editors, *BC Ministry of Energy, Mines and Petroleum Resources*, Paper 1995-2, pages 149–163.
- Tipper, H.W. (1959): Geology, Quesnel; *Geological Survey of Canada*, Map 12-1959, 1:253 440 scale.
- Tipper, H.W. (1969): Geology, Anahim Lake; *Geological Survey of Canada*, Map 1202A, 1:250 000 scale.
- Tipper, H.W. (1971): Glacial geomorphology and Pleistocene history of central British Columbia; *Geological Survey of Canada*, Bulletin 196, 89 pages.

# Geology and Mineral Occurrences of the Quesnel River Map Area, central British Columbia (NTS 093B/16)

by J.M. Logan and D.P. Moynihan<sup>1</sup>

**KEYWORDS:** Quesnel River, Quesnel terrane, Cache Creek terrane, Mesozoic copper-gold metallogeny, Nicola Group stratigraphy, Dragon Lake limestone, alkalic Cu-Au porphyry mineralization, copper, gold

## INTRODUCTION

Regional mapping in the Quesnel area was initiated by the British Columbia Geological Survey in 2006 and continued in 2008 as part of a multiyear program designed to study and promote exploration of BC porphyry deposits in Quesnellia. The 2007–2008 fieldwork was a continuation of regional mapping and mineral deposits studies initiated in the area around Mount Polley (Logan and Mihalynuk, 2005; Logan et al., 2007a, b), and extended coverage north-westward to the area north and east of Quesnel. The 2008 project area covers the 1:50 000 scale Quesnel River map area (NTS 093B/16; Figure 1) and ties in with 1:50 000 scale mapping carried out last year in the Cottonwood River map area (Logan, 2008) to the north.

The project objectives are to

determine the arc history and tectonics of the Quesnel terrane to understand the evolution of magmatism and porphyry mineralization over the life of the arc (ca. 230–185 Ma); and

update the mineral potential knowledge base of the area.

The Quesnel River map area is bounded on the west by the Fraser fault system and bisected diagonally from north-west to southeast by the Pinchi fault system, which marks the boundary between the Cache Creek and Quesnel terranes. West of the Quesnel River, Jurassic sedimentary rocks, derived in part from the Quesnel terrane and correlative with the Ashcroft Formation (Travers, 1978) in southern BC, overlie Cache Creek rocks and mask the terrane boundary with Quesnellia. Triassic to Jurassic volcanic and plutonic arc rocks and associated sedimentary rocks that form the Quesnel terrane crop out east of the Quesnel River. Basement to the Quesnel terrane in southern BC is the Harper Ranch Group (Devonian–Permian arc). Basement to the Quesnel terrane in central BC is unknown, but late Early Cambrian limestone is reported from a single location along its western margin (Struik, 1984). This small isolated exposure of recrystallized limestone, reported to con-

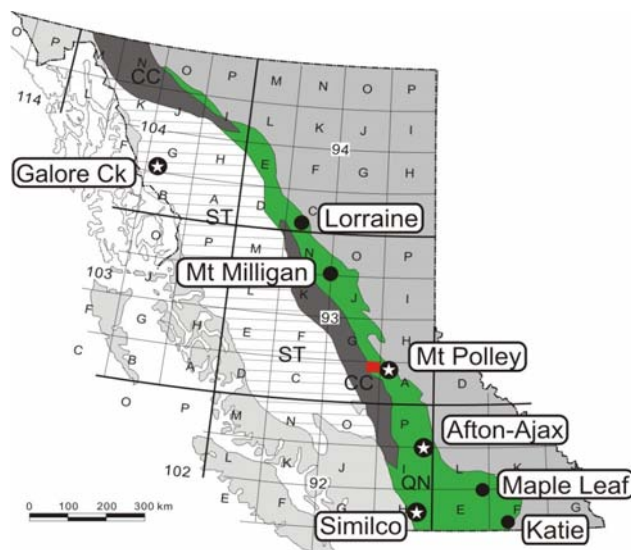


**Figure 1.** Location of the Quesnel River (NTS 093B/16) map area, marked with a red box. The Quesnel terrane is shown in green, and the Cache Creek terrane in grey. The locations of Cu-Au-Ag±PGE alkaline porphyry deposits are also shown.

tain archaeocyathids (52.936 N, 122.355 W), was visited and sampled, along with Mesozoic limestone occurrences, during current fieldwork.

## REGIONAL GEOLOGY

The study area lies along the eastern margin of the Intermontane Belt close to its boundary with the Omineca Belt, in south-central British Columbia (Figure 1).

The Quesnel terrane represents an extensive (>2000 km), west-facing, calcalkaline to alkaline, Late Triassic to Middle Jurassic arc that developed marginal to the western margin of North America (Mortimer, 1987; Mihalynuk et al., 1994). It is characterized by Mesozoic arc volcanic and sedimentary rocks of the Nicola, Takla and Stuhini groups, and coeval plutonic rocks that intrude and inflate the sequence.

At the latitude of the study area, the Intermontane Belt is underlain mainly by Late Paleozoic to Early Mesozoic arc volcanic, plutonic and sedimentary rocks of the Quesnel terrane and coeval rocks of the oceanic Cache Creek terrane. The southern Quesnel terrane consists of a geochemically and isotopically primitive, Late Triassic to Early Jurassic magmatic-arc complex that formed above an east-dipping subduction zone (Mortimer, 1987). The Cache Creek terrane, with its Late Triassic (Patterson and Harakal, 1974; Ghent et al., 1996) blueschist-facies rocks,

<sup>1</sup> Department of Geoscience, University of Calgary, Calgary, AB

This publication is also available, free of charge, as colour digital files in Adobe Acrobat® PDF format from the BC Ministry of Energy, Mines and Petroleum Resources website at <http://www.empr.gov.bc.ca/Mining/Geoscience/PublicationsCatalogue/Fieldwork/Pages/default.aspx>.

represents the remnants of this subduction-accretionary complex (Travers, 1978; Mihalynuk et al., 2004).

The chemical and facies architecture of the Nicola Group rocks records an eastward shift in magmatism from calcalkaline in the fore-arc volcanoclastic-dominated successions to alkalic across the arc into back-arc Middle to Late Triassic, fine-grained clastic rocks (the black phyllite unit of Rees, 1987). The eastern boundary of the Quesnel terrane is marked by the Eureka thrust (Struik, 1988), an easterly-verging fault zone interpreted to have formed during accretion of Quesnellia to North America. The variably sheared mafic and ultramafic rocks of the Crooked amphibolite that occupy this boundary are assigned to the Slide Mountain terrane, a Late Paleozoic marginal-basin assemblage (Schiarrizza, 1989; Roback et al., 1994) of oceanic basalt and chert that separated Quesnellia from North America until its closure, beginning in the Late Paleozoic (Klepacki and Wheeler, 1985), and final collapse in the Early Jurassic (Nixon et al., 1993). The footwall to the Eureka thrust comprises the Proterozoic to Paleozoic Snowshoe Group rocks of the Barkerville subterrane (Struik, 1986), a northern extension of the Kootenay terrane (Monger and Berg, 1984), which are pericratonic and likely represent distal sedimentation of ancestral North America (Colpron and Price, 1995). By Middle Jurassic time, Stikinia had collided with Quesnellia, resulting in demise of the Cache Creek subduction zone (173 Ma) and stitching of the boundary in the northern Cordillera by ca. 172 Ma plutons (Mihalynuk et al., 2004). At the same time, the Quesnel terrane, Slide Mountain terrane, and Barkerville and Cariboo subterrane were imbricated and thrust eastward onto the North American craton (Nixon et al., 1993).

The tectonic boundary between the Kootenay and Quesnel terranes is intruded by the Cretaceous Naver pluton north of the study area (Struik et al., 1992; Moynihan and Logan, 2009). Tertiary volcanic rocks and feeder dikes of the Eocene Endako Group, Oligocene to Miocene sedimentary rocks and Miocene flood basalt of the Chilcotin Group are the youngest rocks in the region (Rouse and Mathews, 1979; Mathews, 1989).

Quesnel arc magmatism and associated porphyry mineralization migrated eastward with time, beginning in the west ca. 215–210 Ma with emplacement of plutons and development of calcalkaline Cu-Mo±Au deposits at Highland Valley and Gibraltar. New data suggest that mineralization at Highland Valley postdates intrusion of the Guichon batholith by up to 4 Ma (Ash et al., 2007). To the east, at Mount Polley in the central axis of the arc, alkaline magmatism and Cu-Au mineralization took place ca. 205 Ma. A chain of similar deposits extends the length of the Intermontane Belt (Barr et al., 1976; Figure 1). In the south, they are associated with the Iron Mask batholith (Afton, Ajax and Crescent) and Copper Mountain intrusions (Copper Mountain, Ingerbelle) and, to the north, with the Hogem batholith (Kwanika). Uplift and erosion of the fore arc produced sub-Jurassic unconformities as magmatism shifted east and culminated with intrusion of calcalkaline composite plutons, consisting of quartz monzodiorite (ca. 202 Ma) and granodiorite (195–193 Ma) phases (Schiarrizza and Macauley, 2007) in the south (Takomkane, Thuya, Wild Horse and Pennask), and deposition of volcanoclastic and sedimentary rocks across the terrane. Copper-molybdenum mineralization is associated with the Takomkane (Woodjam) and Pennask batholiths

(Brenda). A temporally unrelated, ca. 183 Ma, synaccretionary pulse of alkaline magmatism and Cu-Au mineralization is recognized at Mount Milligan, 275 km northwest of Mount Polley. Postaccretion plutons in the central Quesnel belt include the Middle Jurassic (ca. 163 Ma) Quesnel River leucogranite, with its associated Cu-Au-Mo mineralization, and the mid-Cretaceous (ca. 104 Ma) Bayonne suite of plutons, with associated Mo mineralization at the Boss Mountain deposit and the Anticlimax showing.

## STRATIGRAPHY

The Quesnel River map area is underlain by the Quesnel and Cache Creek terranes, two major elements of the Intermontane Belt of the Canadian Cordillera. The contact is covered but inferred to transect the map area from northwest to southeast, following the approximate trend of the Quesnel River. This is based upon projecting Cache Creek rocks exposed north of the map area along the Fraser River at the confluence with the Cottonwood River (Struik et al., 1990) to outcrops on Beedy Creek, a tributary of Beaver Creek (Tipper, 1959, 1978) located south of the area. Cache Creek basement has been intersected in drilling east of Kersley in the southwest corner of the map area (Sproule and Associates, 1953). The terrane boundary is assumed to be a steeply dipping linear feature.

The Quesnel terrane comprises two main rock packages: a Middle to Late Triassic Eastern Sedimentary succession, consisting of the Black pelite and Cottonwood River successions; and the Late Triassic Western Volcanoclastic succession, itself consisting of the Maroon Volcanoclastic and Green Volcanoclastic successions (Figures 2, 3).

The Cache Creek terrane is overlain by three main rock packages: an Early to Middle (?) Jurassic Dragon Mountain succession, an Eocene volcanic succession, and Oligocene to Miocene sedimentary rocks (Figure 3).

Unconsolidated Recent and glacial deposits are thick and cover the majority of the map area (Figure 2).

### Nicola Group

#### EASTERN SEDIMENTARY SUCCESSION

##### BLACK PELITE SUCCESSION

Outcrops are scarce and varied north of the Swift River in the northeast corner of the map area. They include massive to well-bedded pyroxene-phyric volcanoclastic units; rusty weathering, very fine grained, cherty, green and black argillaceous rocks; thin, interlayered, siliceous, muscovite-bearing siltstone and phyllite; and thinly banded calcareous volcanoclastic rocks. Detrital quartz and muscovite in quartzite beds imply a continental margin rather than a fore-arc volcanic setting. The northwestern continuation of the black, fine-grained, siliceous and calcareous clastic rocks structurally overlies sheared serpentinite of the Crooked amphibolite in the Cottonwood map area (Logan, 2008). These fine-grained black clastic rocks are correlated with the Middle and Late Triassic Black phyllite unit of Rees (1987). The Black pelite succession is considered to be broadly coeval with the eastern volcanoclastic Nicola Group and may be an eastern back-arc facies onto which arc volcanic and volcanoclastic rocks were deposited (Bloodgood, 1987; Rees, 1987; Panteleyev et al., 1996).

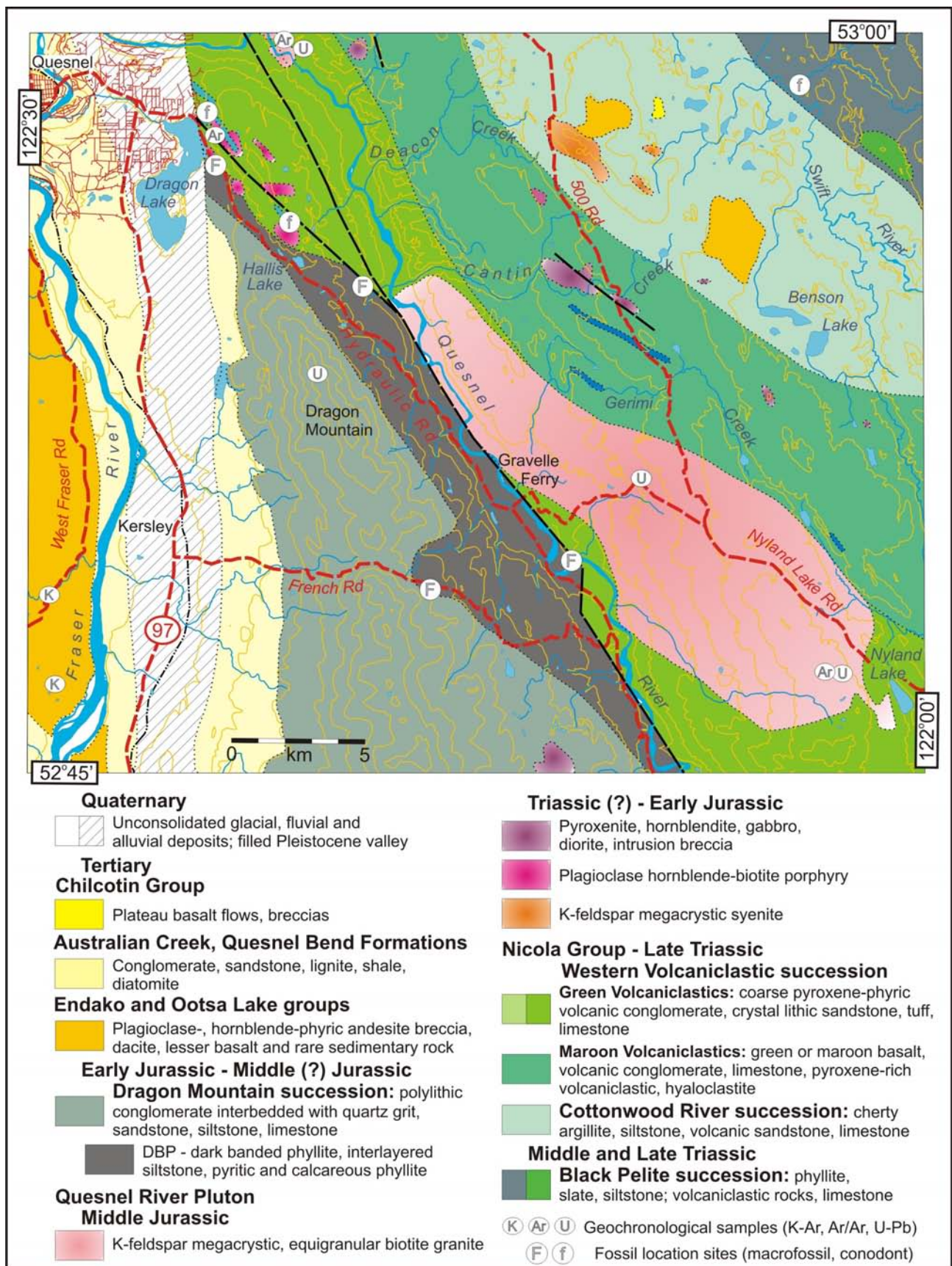


**Figure 2.** Generalized geology of the Quesnel River map area, based on 2008 fieldwork and interpretation of airborne geophysical data (Carson et al., 2006). The map shows the location of geochronological, microfossil and macrofossil samples.

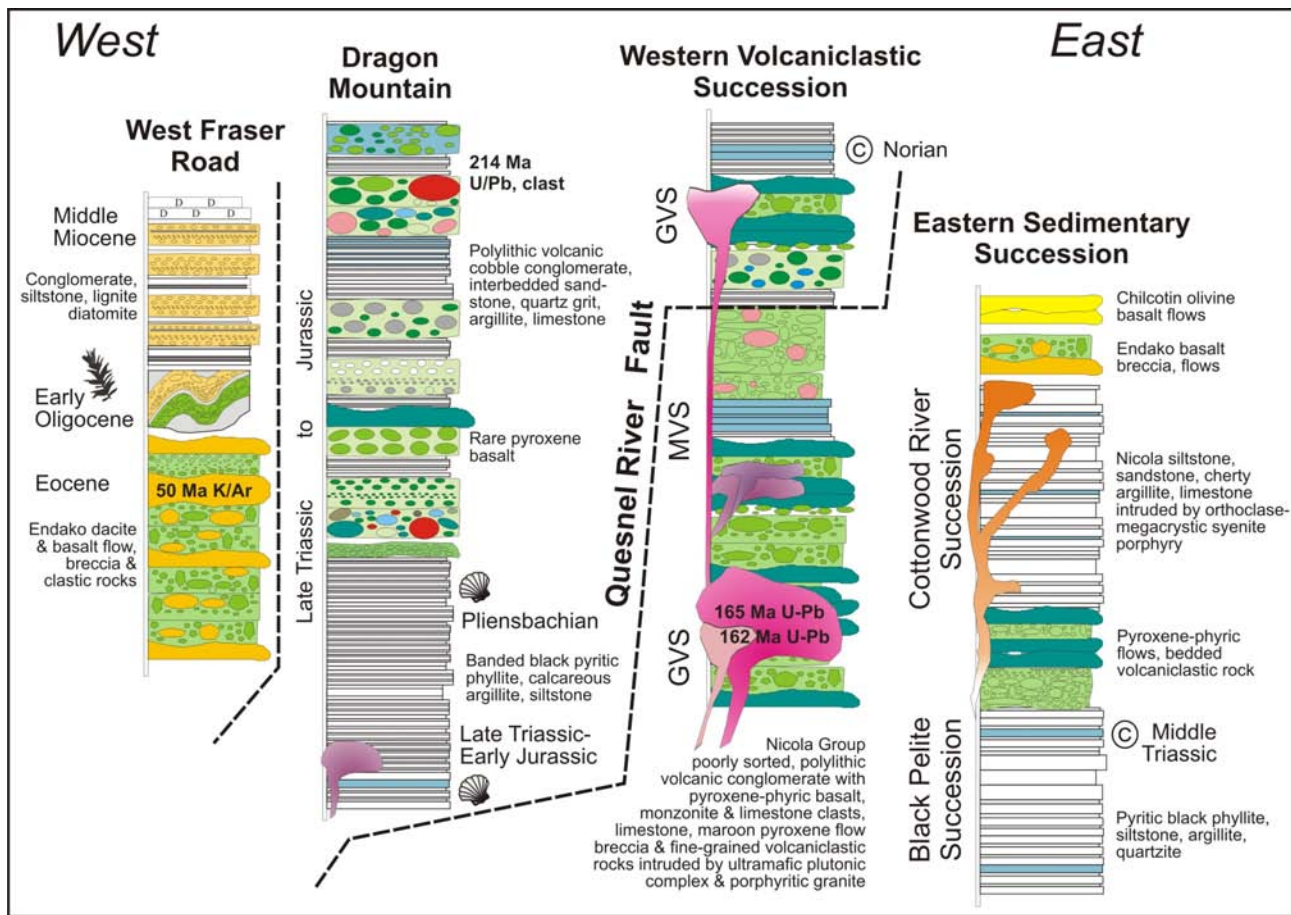


**Figure 3.** Schematic stratigraphic sections for Nicola Group volcanic and sedimentary successions, the Dragon Mountain sedimentary succession, and Tertiary Endako volcanic and younger sedimentary rocks in the Swift River, Cantin Creek-Quesnel River, Dragon Mountain and Fraser River portions of the Quesnel River map area. Abbreviations: GVS, Green Volcaniclastic succession; MVS, Maroon Volcaniclastic succession.

Middle Triassic conodonts have been identified by M. Orchard (pers comm, 2008) from limestone interbedded with fine-grained volcaniclastic rocks and siltstone of the Eastern Sedimentary succession exposed in the Swift River (Figure 3).

### COTTONWOOD RIVER SUCCESSION

The Cottonwood River succession is dominated by fine-grained, volcanic-derived clastic sedimentary rocks that are best exposed along the length of the Cottonwood River in NTS 093G/01 (Logan, 2008). It forms a continuous belt extending south from the Naver pluton, through and beyond the current map area, and has similarities with the Gavin Lake succession in the Mount Polley area (Logan and Bath, 2006).

In the Quesnel River map area, the Cottonwood River succession is dominated by thin, wavy-laminated, cryptic-bedded, grey, green, buff and black cherty argillite, volcanic siltstone, slate and grey or buff limestone that form a belt of rocks approximately 9 km wide between the 500 Road and the Swift River (Figures 2, 3). The succession consists mainly of dark, rusty-weathering cherty argillite and fine-grained, parallel-laminated volcanic siltstone. Bedding is difficult to recognize in outcrop, specifically in the massive, conchoidally fractured siliceous argillite. Well-bedded intervals of green- or orange-weathering, nor-

mally graded crystal and lithic sandstone and rare conglomeratic beds are found throughout the belt. Another distinctive unit recognized along the length of the belt is thickly bedded to massive, green volcanic sandstone characterized by centimetre-scale, angular rip-up clasts of grey cherty argillite. In addition, centimetre-thick grey limestone beds occur interlayered with the cherty argillite sequence or rarely as thicker, buff-coloured silty limestone interbedded with the phyllite. Relatively minor amounts of dark green, coarse, pyroxene-phyric volcaniclastic units occur interbedded with other sedimentary rocks along the eastern margin of the belt.

In a series of outcrops close to the eastern boundary of the Cotton River succession, an intraclastic *mélange*-type fabric is visible on highly weathered surfaces. Clasts of relatively intact rock are wrapped by a matrix fabric that is defined by compositional layering and contains numerous tight-isoclinal folds. As these fabrics have highly variable orientations and cleavage is not visible in the outcrops, this deformation probably occurred before full lithification of the rock. These textures are only visible on highly weathered surfaces; elsewhere, the rock appears massive. Bedding was not identified in this area, and the full extent and significance of this disrupted zone is not known.

The upper contact with the Western Volcaniclastic succession is not well established but inferred from the verti-

cal-gradient aeromagnetic map. Samples of limestone and calcareous black siltstone from the Cottonwood River succession have been submitted to the Geological Survey of Canada micropaleontology laboratory in Vancouver.

## WESTERN VOLCANICLASTIC SUCCESSION

The Western Volcaniclastic succession of the Nicola Group forms a northwest-trending, 10–12 km wide belt of subaqueous and subordinate subaerial volcanic rocks that defines the western part of the Quesnel terrane in the Cottonwood River and Quesnel River map areas. It extends southeastward into the Mount Polley area, where it occupies a medial position between the Black phyllite and Gavin Lake sedimentary successions (Logan and Bath, 2006). The pyroxene crystal-rich sandstone, volcaniclastic breccia and conglomerate horizons contain abundant detrital magnetite and a relatively high magnetic susceptibility, which is evident on the airborne magnetic maps. The stratigraphy of the Western Volcaniclastic succession (Bailey, 1989; Lu, 1989) is similar to that described in the Hydraulic map area (Bailey, 1988, Panteleyev et al., 1996; Logan and Mihalynuk, 2005). It comprises pyroxene-phyric basalt breccia, limestone, heterolithic volcanic conglomerate, crystal-lithic sandstone and fine-grained heterolithic volcaniclastic rocks of Late Triassic age (Orchard, 2007b), and rare quartz-bearing tuff and tuffaceous sedimentary rocks of Early Jurassic age (Figures 2, 3).

In the Quesnel River map area, the Western Volcaniclastic succession is divisible into two age-equivalent units: the Maroon Volcaniclastic succession (MVS) in the east and the Green Volcaniclastic succession (GVS) in the west. Contact relationships between these two and with the fine clastic rocks of the Cottonwood River succession are not well constrained. Along most of its length, the western boundary of the Western Volcaniclastic succession is marked by the Quesnel River fault (Figures 2, 3).

The majority of outcrops in the Maroon Volcaniclastic unit consist of massive, green and/or maroon, pyroxene-phyric and aphyric basalt; monomictic basalt breccia flows; hyaloclastite; and associated volcaniclastic rocks. Basalt flows are approximately 5 m thick and characterized by brecciated margins. Flows vary from coarse, crowded pyroxene porphyry to sparse and aphyric, commonly highly vesicular varieties. Overlying and interbedded with fine maroon volcaniclastic material are fine-grained grey, green and maroon argillite and siltstone with discontinuous decimetre-thick beds of dolomitic limestone. Late Triassic (Norian) conodonts have been identified by M. Orchard (pers comm, 2008) from equivalent limestone exposed in the Cottonwood River, north of Ten Mile Lake (093G/01). Green and maroon polymictic volcanic and plutonic-dominated volcaniclastic and conglomeratic units form the uppermost strata in the belt. They are chaotic to well-sorted, boulder- to granule-size clastic units dominated by coarse pyroxene-phyric basalt and plagioclase-phyric basaltic andesite. Minor amounts of pink-weathering porphyritic monzonite are also present. Clasts are supported by a matrix of coarse lithic and crystal sand; bedding is rarely observed (Figure 4). Rocks are variably green and/or maroon and hematitic, suggesting marine and subaerial deposition, and diagenetic and/or metamorphic alteration.

The Green Volcaniclastic succession is best exposed in the area between Dragon Lake and the Quesnel River, where it extends south to the Quesnel River pluton as a 5 km wide belt of pyroxene-phyric breccia; maroon and green,

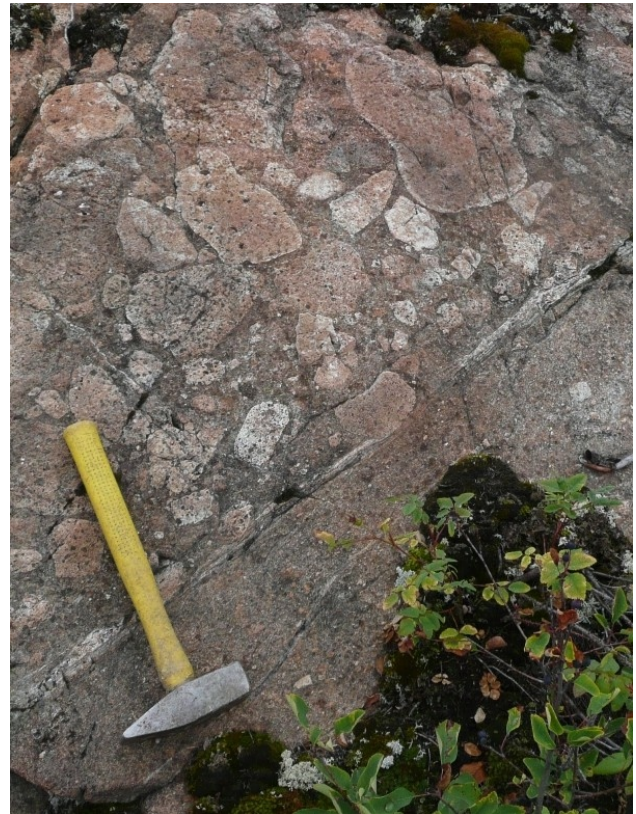


**Figure 4.** Coarse, pyroxene-phyric, basalt-dominated, chaotic, matrix-supported boulder and granule conglomerate beds of the Late Triassic Western Volcaniclastic succession. Outcrop located midway between Nyland and Benson lakes.

pyroxene- and plagioclase-phyric volcaniclastic and massive polyolithic conglomerate; green tuffaceous rocks; and limestone (Figures 2, 3). The relationship between rock types is complicated by faults and the intrusion of numerous small, Early Jurassic, high-level stocks and dikes, including acicular hornblende diorite, plagioclase porphyry and Middle Jurassic equigranular granite. Narrow discrete mylonite zones cut the intrusive rocks. Struik (1984) established a stratigraphy for the Triassic Dragon Lake rocks that included, from oldest to youngest, conglomerate, volcaniclastic greywacke, shale, tuff, limestone, calcareous shale and pyroxene-phyric flows. He also distinguished a Jurassic sequence consisting of aphyric basalt, sandstone, micritic nonfossiliferous limestone, andesite and shale. Our regional-scale mapping did not distinguish a separate Jurassic volcanic and sedimentary sequence. It is from this area that an isolated outcrop of Early Cambrian limestone (archaeocyathid-bearing) was reported (Tipper, 1978; Struik, 1984).

Re-examination of this limestone was undertaken after samples collected in 2005 returned a single Late Triassic (Early Norian) conodont identification (Orchard, 2007a). Contact relationships with the country rock are not exposed (Struik, 1984; this study). The limestone is flanked on the west and east by purple- and pale green-mottled, phyllitic volcaniclastic rocks consisting of plagioclase and pyroxene breccia, crystal-rich lapillistone, sandstone and thin-laminated siltstone beds locally characterized by 0.5–1 mm black calcite crystals. The southern boundary is masked by medium-grained, weakly trachytic, acicular hornblende

porphyry diorite. The limestone unit consists of white-, grey- and buff-weathering, fine phyllitic micrite and yellow-weathering, medium- to coarse-grained, crinoid ossicle-rich grainstone (B. Pratt, pers comm, 2007). The latter contains numerous spherical and elliptical crinoid stems, a few of which possess a central void core or circular outer wall with radial partitions. No archaeocyathids are present.

The uppermost stratigraphy of the Green Volcaniclastic succession is exposed around the Hydraulic Road, east of Dragon Lake, where it generally fines upward from coarse, polymictic volcanic conglomerate and clastic rocks through limestone with or without pyroxene-phyric flows to dark banded phyllite. The same tripartite stratigraphic relationship—pyroxene-phyric volcaniclastic rocks, limestone and dark banded phyllite—that occurs east of Dragon Lake is also present at the southern boundary of the map area south of the Quesnel River pluton. Here however, the pyroxene-phyric volcaniclastic rocks are more extensively recrystallized (Figures 5, 6) and the limestone has been converted to a marble.

Interbedded with the volcaniclastic rocks along the Quesnel River are well-sorted, planar-laminated argillite and siltstone units and metre-thick chaotic slump deposits of sedimentary- and volcanic-derived material. These



**Figure 5.** Foliated and metamorphosed pyroxene-phyric basalt and limestone-dominated volcaniclastic rocks of the Green Volcaniclastic succession, exposed in the Quesnel River at the southern boundary of the map area.

coarse-grained intervals consist of angular boulder- to granule-size volcanic clasts and centimetre-size rip-up clasts of cherty argillite supported within a matrix of pyroxene- and plagioclase-rich sand. The grain-flow deposits are dominated by clasts of pyroxene-phyric basalt.

At Hallis Lake, the Nicola Group is fossiliferous (Struik, 1984) and Norian in age; however, along strike and upsection (Hydraulic and French roads) are similar, fine-grained black siltstone and phyllite that contain Sinemurian fossils (Tipper, 1978; Petersen et al., 2004). The upward fining of volcaniclastic rocks and the presence of black, fine-grained calcareous rocks at the top of the Triassic GVS are similar to lower parts of the Sinemurian phyllite and siltstone interbedded with volcanic conglomerate of the Dragon Mountain succession.

### **Dragon Mountain Succession**

A thick (>500 m) package of alternating coarse- and fine-grained, arc-derived sedimentary rocks defines a north-tapering wedge-shaped area extending 45 km north from the Gibraltar mine to Dragon Lake. The resistant, massive, coarse conglomerate that dominates this sequence underlies Dragon Mountain and the south-trending highlands that separate the southward-flowing Fraser River and

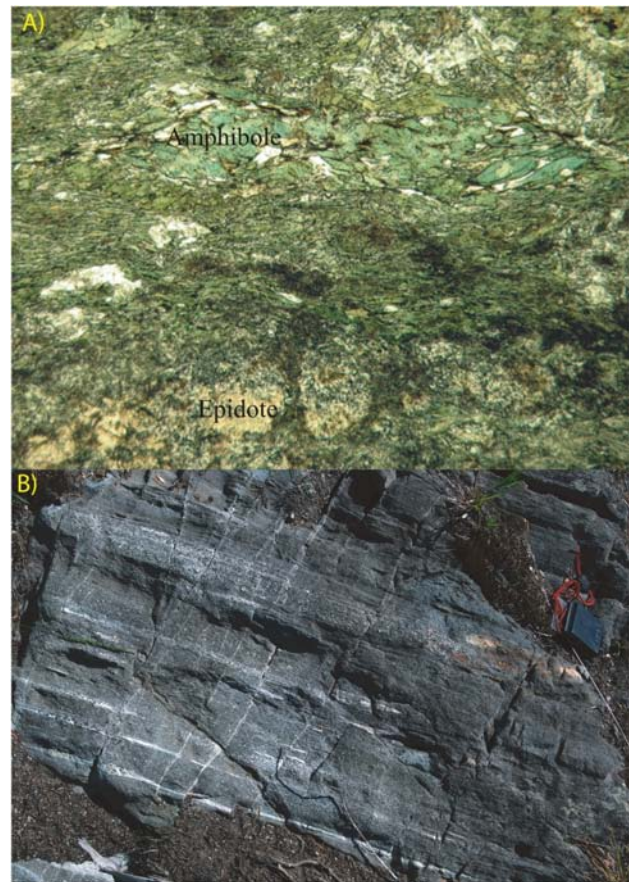


**Figure 6.** **A)** Photomicrograph of metamorphosed mafic volcaniclastic rocks containing amphibole, epidote and plagioclase; the amphibole needles define a mineral lineation (3 mm field of view). **B)** This rock forms part of a distinctive, banded volcaniclastic unit in the Green Volcaniclastic succession of the Nicola Group. Outcrop located 7.5 km southwest of Nyland Lake.

the northward-flowing Quesnel River. Interlayered with the massive to thickly bedded conglomerate and forming approximately 40% of the sequence are finer grained silicic and calcareous sedimentary rocks. Early workers included these sedimentary rocks in the upper part of the Quesnel River Group and, from fossil collections identified by H. Frebold, ascribed them an Early Jurassic (Pliensbachian) age (Tipper, 1978). The British Columbia digital geology map (Massey et al. 2005) correlates the Dragon Mountain sedimentary succession with the Ashcroft Formation of southern BC. In the type area, the Ashcroft Formation is mainly dark carbonaceous shale with minor lenses of fine sandstone and thin siltstone, and contains fossils that range in age from Early to Middle Jurassic (Frebold and Tipper, 1969; Travers, 1978). A basal conglomerate, several metres thick and containing granitic rocks in a calcareous sandy matrix, marks the base of the unit that nonconformably overlies the Guichon Creek batholith.

The Dragon Mountain succession within the Quesnel River map area consists of a two-fold subdivision: a lower package of interlayered black and dark grey phyllite and light grey siltstone; and an upper package of interbedded polyolithic cobble conglomerate, sandstone, quartz grit, siltstone and limestone. The lower unit is characterized by alternating dark and light, mainly 0.2–1 cm thick layers of phyllite and siltstone that give it a dark banded appearance in outcrop and the field name of ‘Dark banded phyllite’. Siliceous, pyritic and carbonaceous, and calcareous varieties of siltstone and phyllite layers are 0.5–2.0 cm thick and make up 30% of the outcrop. phyllite often shows good crenulations, whereas the siltstone does not.

The upper unit consists of massive conglomerate, rich in green and grey polyolithic volcanic and plutonic clasts, interbedded with a diverse package of finer grained sedimentary rocks that include pale grey-cream, parallel-bedded siltstone and shale; pale green, fine-grained sandstone and siltstone-shale; white to grey quartz grit; and grey, green and white limestone to limy granule conglomerate. The unit also contains rare pyroxene-phyric basalt flows. The conglomerate is massive to thickly bedded with mainly boulder- to cobble-size clasts of Nicola Group volcanic and sedimentary rocks and associated intrusions. Clast types include coarse pyroxene-phyric basalt; plagioclase-phyric and aphyric, epidote-altered intermediate volcanic rocks; limestone; hornblende±biotite granite; quartz-phyric intrusive rocks; and rare conglomerate (Figure 7).

The contact relationship between the upper and lower packages is believed to be depositional because similar stratigraphic relationships occur in exploration diamond-drilling north of the Gibraltar mine (Bysouth et al., 1995). There, a flat-lying, pyritic black argillite and greywacke sequence, at least 130 m thick, forms the basal member of Jurassic sedimentary and volcanic rocks that unconformably (?) overlie penetratively deformed chert and metavolcanic rocks of the Cache Creek Group and Late Triassic tonalite-trondhjemite of the Granite Mountain pluton (Bysouth, 1987). This same relationship is postulated for the Quesnel

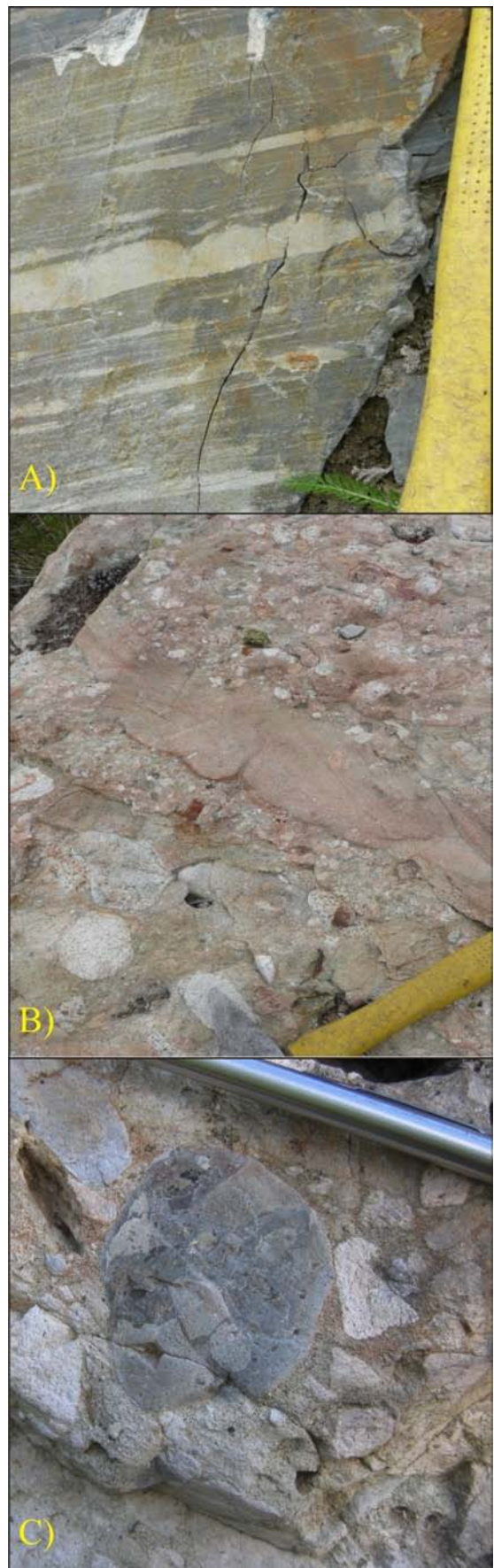


**Figure 7.** Rocks of the upper Dragon Mountain succession include **A)** parallel-layered and flaser-bedded, grey siltstone and buff sandstone; **B)** normal-graded, matrix-supported polymictic conglomerate with granite, epidote alteration, limestone and volcanic clasts in a coarse granule to sand matrix; **C)** detail of recycled volcanic conglomerate clast.

River map area, but here the lower contact is depositional with Nicola Group volcanoclastic and sedimentary rocks.

Dark banded phyllite (DBP) of the Dragon Mountain succession is faulted against the Middle Jurassic Quesnel River pluton and metavolcaniclastic rocks of the Nicola Group around Gravelle Ferry. The western contact with the Oligocene to Miocene sedimentary rocks is assumed to be faulted along a north-trending structure (Rouse and Mathews, 1979) that parallels the Fraser River.

In proximity to the Quesnel River fault, the DBP is cut by pale green to orange, Fe-carbonate-altered, fine- to medium-grained, pyroxene-porphyritic monzodiorite dikes. Dikes vary from centimetres to metres thick. They are altered and deformed together with the banded phyllite. Alteration varies from weak chlorite-biotite to pervasive and texturally destructive Fe-carbonate-sericite-quartz. Mineral assemblages include chlorite, biotite, muscovite, carbonate, Cr-mica, serpentine and pyrite. Pyroxene phenocrysts (5 mm) are variably altered to hornblende-biotite or entirely replaced by muscovite, producing a distinctive coarse, muscovite-rich, Fe-carbonate rock.

Petersen et al. (2004) assigned an upper Pliensbachian (Kunae Zone) age to the dark-banded phyllite unit cropping out along the French Creek Road. Fossils from the top of Dragon Mountain, collected and reported on by Struik (1984), are Late Triassic, and a U-Pb zircon age from a clast of plagioclase-porphyritic dacite, collected from the same location, yielded a Late Triassic (214 ± 4 Ma) age (Petersen, 2001; Breitsprecher and Mortensen, 2004). Thin-banded black graphitic and calcareous phyllite and siltstone are exposed in the Quesnel River on the Gillis Ranch, south of Gravelle Ferry. A collection of aulacocerids (belemnites) from an outcrop underlying the dogleg meander in the river have been tentatively identified by T. Poulton (pers comm, 2008) as late Triassic to Early Jurassic in age. Limestone samples collected from this same section have been submitted to the Geological Survey of Canada micropaleontology laboratory in Vancouver. In addition, poorly preserved ammonites collected from the north end of the DBP unit exposed in Schiste Creek have been tentatively identified as Middle Jurassic (T. Poulton, pers comm, 2008). Interbedded with black and grey siltstone, argillite and limestone are white-weathering quartz grit and quartz wacke. A 20 kg sample of the quartz-bearing grit was collected and submitted to the Pacific Centre for Isotopic and Geochemical Research (PCIGR) laboratory at the University of British Columbia (UBC) for detrital zircon analysis to determine a maximum age.

## EOCENE ENDAKO GROUP

An Eocene assemblage of pyroclastic rocks, lava flows and limited sedimentary rocks forms the steep bluffs west of the Fraser River at Kersley, in the southwestern corner of the map area. At this spot, 300–400 m of volcanic stratigraphy is incised and well exposed by Narcosli Creek. Most of the Eocene lavas in the map area are andesite with lesser basalt (Rouse and Mathews, 1979) and include autobreccias, monomictic and diamictic debris deposits that predominate over coherent flows, tuffs and sedimentary rocks (Figure 8). The majority of the exposures in the Narcosli Creek area consist of grey-, green- and red-weathering, plagioclase-phyric andesite breccias; cream-coloured coherent dacite flows; and crystal tuffs interbedded with decimetre-thick coarse block to lapilli breccias of black and grey scoriaceous andesitic basalt. The units trend north-

westerly or southerly with moderate east dips. Polygonal and closely spaced (millimetre-scale) orthogonal cooling fractures characterize fine-grained hornblende-biotite dacite units, and hematitic flow breccias are developed at the base of metre-thick coherent grey andesite flows. Pink-to mauve-weathering, grey, plagioclase-phyric andesite consists of plagioclase, hornblende and rare biotite phenocrysts in an aphyric glassy matrix. Phenocrysts locally define a trachytic flow fabric. Phenocrysts include euhedral bimodal plagioclase (2 and 10 mm, 15%) and hornblende (5–7 mm, 10%) in a fine matrix of feldspar and quartz microlites.

Two exposures of well-bedded, pale-green- to yellow-weathering sandstone, siltstone and conglomerate dominated by felsic volcanic clasts underlie the western side of the map area, 8 km south of Quesnel. The sedimentary rocks are poorly consolidated and include thick-bedded, normal-graded, medium-grained sandstone containing kaolinite-altered feldspar, quartz, plagioclase and biotite crystals; fine siltstone and shale; organic-rich lignite horizons; and channel-cut coarse boulder conglomerate containing shale rip-up clasts and coarse plant material. It is uncertain whether these two exposures represent intraflow Eocene sedimentary rocks or are part of the Oligocene Australian Creek Formation or Miocene Fraser Bend Formation.

East of the Fraser River, scattered outcrops of flat-lying basalt or basaltic-andesite flows cap the highlands east of the 500 Road. The lavas comprise massive grey, brown or black coherent flows interlayered with clastic units of variegated orange, pink-maroon, brown and ochre, block to lapilli breccia. They are locally columnar jointed. The ba-



**Figure 8.** Coarse, monomictic, hornblende-plagioclase-porphyritic andesite block breccia forms cliffs west of the Fraser River, south of Narcosli Creek. Photo is 1 m across.

salt is aphyric to porphyritic with plagioclase and pyroxene phenocrysts; aligned plagioclase phenocrysts locally define a trachytic texture. The basalt is almost always vesicular and commonly filled with white, grey or chalcedonic silica or calcite.

These volcanic rocks have been dated by K-Ar techniques at 50–44 Ma (49–42 Ma ages of Rouse and Mathews [1979] recalibrated using new decay constants of Dalrymple [1979]). The rocks are age correlative with the Kamloops Group of south-central BC and the Endako Group to the northwest.

### **TERTIARY SEDIMENTARY ROCKS**

Early investigations of the Tertiary rocks in Quesnel include work by Selwyn (1872) and Dawson (1877). Lay (1939, 1940, 1941) described the stratigraphy; Rouse and Mathews (1979) refined its nomenclature and provided palynology and K-Ar age constraints.

In the map area, the Tertiary sedimentary rocks occupy a 15 km wide by 50 km long belt along the Fraser River and tributaries in the area north and south of Quesnel (Figure 2). Here, three mid-Tertiary formations, the Australian Creek, Fraser Bend and Crownite, appear to be confined to a broad valley cut in the pre-Tertiary rocks (Lay, 1940; Rouse and Mathews, 1979), which parallels the present Fraser River. The Early Oligocene Australian Creek Formation includes lignite, clay, silt, sand and gravel. The succession is deformed and separated from the Lower to Middle Miocene Fraser Bend Formation and younger units by an angular unconformity (Figure 3). The Fraser Bend consists of flat-lying, well-sorted gravel and alternating finer and less well sorted gravel and silt, clay and seams of lignite. The overlying Crownite Formation is almost pure diatomite with some clay (Figure 3; Hora, 2008).

### **CHILCOTIN GROUP**

Early Miocene to Pleistocene basalt flows and associated pyroclastic and sedimentary rocks of the Chilcotin Group cover an area of approximately 25 000 km<sup>2</sup>, extending from the Okanagan Highland to the Nechako Plateau (Mathews, 1989). In the field area, basalt mapped as Chilcotin occurs as a single, small, isolated, flat-lying exposure capping a hill in the northeastern corner of the map. The lava comprises single or multiple columnar-jointed flow units separated by a thin breccia. Lavas are primarily olivine phyric in a fine-grained grey groundmass.

Diatomite underlies the basalt in a continuous belt west of the Fraser River (Rouse and Mathews, 1979; Hora, 2008).

### **Quaternary Cover**

Unconsolidated Pleistocene and Recent sediments, comprising deglaciation outwash, lake and drift deposits, cover much of the area. These deposits are locally very thick and bedrock is limited to deeply incised creeks and rivers, and hilltops. A major north-trending Pleistocene valley, now infilled with younger sediments, has been documented to the east of the present Fraser River (Figure 2; Rouse and Mathews, 1979).

Gravel and sand eskers and/or drumlins trend north-westerly, and the direction of glacial-ice movement is generally interpreted to have been from southeast to northwest. Overburden thickness varies from 20 to 75 m in the centre of the map to substantially thicker accumulations of glacial

lacustrine deposits. West of the Fraser River, the plateau is covered by a basal till with irregular patches of gravel. Drumlins, eskers and striae indicate glacial ice movement was from south to north.

### **Intrusive Rocks**

Intrusive rocks within the Quesnel River map area include a Late Triassic suite (R. Friedman, pers comm, 2006) of alkalic quartz-undersaturated rocks; an Early Jurassic suite of calcalkalic quartz-saturated rocks that forms the constructive period of Quesnel arc magmatism; a Middle Jurassic synkinematic suite of calcalkalic magmatism (T. Ullrich, pers comm, 2006; Logan et al., 2007) that coincides with amalgamation of Quesnellia to North America; and an Eocene suite of alkalic magmatic rocks represented by mafic dikes. A postaccretion suite of Cretaceous plutons intrudes the Quesnel arc north of the current study area (Struik et al., 1992; T. Ullrich, pers comm, 2006; Logan et al., 2007a) but has not been recognized in the Quesnel River area.

### **LATE TRIASSIC TO EARLY JURASSIC**

The Late Triassic to Early Jurassic intrusions are predominantly small, complex plutonic bodies distributed in linear trends that closely follow the regional structural grain and gross lithological packages. Bailey (1989, 1990) subdivided the Late Triassic and Early Jurassic suites on the basis of composition and texture into two groups (7A and B). Our work and studies in the Cottonwood River map area has recognized a third suite, described below (Logan, 2008).

Subunit 7A consists of pyroxene diorite, monzonite and syenite with lesser clinopyroxenite, peridotite and gabbro, and corresponds to Alaskan-type mafic to ultramafic plutonic complexes. Throughout BC, these are spatially and genetically associated with Late Triassic to Early Jurassic volcanic arc rocks of the Nicola-Takla-Stuhini groups in the Quesnel and Stikine terranes (Irvine, 1974; Mortimer, 1987; Nixon et al., 1997). Locally, these plutonic complexes intrude the Western Volcaniclastic succession of the Nicola Group, have elevated concentrations of magnetite and correspond to magnetic highs on residual total magnetic field plots. Similar mafic complexes are present in the Cottonwood River map area to the north (Logan, 2008) and farther south in the Canim Lake area (Schiarizza and Macauley, 2007). These mafic-ultramafic complexes have radiometric crystallization and cooling ages that span the Early Jurassic (Sinemurian to Pliensbachian) from 192 to 183 Ma (Schiarizza and Macauley, 2007; T. Ullrich, pers comm, 2008).

### **Cantin Creek Mafic-Ultramafic Complex**

The Cantin Creek mafic intrusive complex is a north-west-trending composite body that straddles the upper reaches of Cantin Creek, northeast of the centre of the map. It does not crop out but is defined by exploration percussion- and diamond-drilling (Fox, 1985, 1990; MacDonald, 1991). The complex is concentrically zoned, with a melanocratic margin of commingling pyroxenite, gabbro and diorite, and a more felsic interior of monzonite to syenite. Whether faulting has dismembered a single pluton or been localized along the margins of two separate bodies is uncertain, but sheared gabbro/pyroxenite and wide fault zones intersected in drilling indicate that the complex has

undergone substantial deformation. The following lithological descriptions are summarized from diamond-drill logs summarized in assessment reports (Fox, 1985, 1990; MacDonald, 1991).

Pyroxene gabbro is a medium- to coarse-grained, equigranular, melanocratic rock consisting of 80% chloritic mafic minerals dominated by either clinopyroxene or hornblende, with biotite, 20% stubby grey plagioclase and 2–3% magnetite. The pyroxene-biotite diorite is a medium-grained, equigranular rock consisting of 50% blocky to lath-shaped white plagioclase, 30% greenish pyroxene and 10% books and irregular flakes of biotite and magnetite. Leucocratic, felsic intrusive rocks spatially associated with the mafic phases include white, stubby, plagioclase±biotite porphyry and K-feldspar±hornblende porphyry syenite.

### **Potassium-Feldspar Megacrystic Intrusions**

Subunit 7B of Bailey (1989, 1990) is primarily syenite in composition and is characterized by megacrysts of orthoclase. In the Cottonwood (NTS 093G/01) and Quesnel River map areas, megacrystic orthoclase syenite intrudes the sedimentary Cottonwood River succession of the Nicola Group, has low concentrations of magnetite and is indistinct on residual total magnetic field plots. A close spatial and temporal association between orthoclase-megacrystic syenite and Cu-Au mineralization has been suggested for the Northeast zone at Mount Polley (Logan et al., 2007a), but there the syenite dikes are intruding the main magmatic axis of the arc, which is composed primarily of volcanic and volcanoclastic rocks.

In this map area, brilliant white-weathering, orange, pink and grey syenite intrudes and alters fine clastic sedimentary rocks of the Cottonwood River succession east of the 500 Road. The intrusions consist of northwest-elongated bodies, ranging from <1 km to 3.2 km in size, of distinctive, crowded, megacrystic, orthoclase porphyritic syenite that crop out in an area extending for approximately 5 km southeast of the 500 Road. The intrusions are complex, comprising equigranular, hornblende quartz syenite containing sparse (2–3%) megacrysts of orthoclase; crowded, coarse-grained, orthoclase-megacrystic syenite containing aligned orthoclase crystals up to 5 cm in length that form 80% of the rock; and fine-grained pink syenite. Apophyses and margins to the plugs have chilled textures characterized by fine-grained green syenite containing rare broken orthoclase megacrysts and partially digested xenoliths of argillite. Cutting all phases of the syenite and the hornfelsed country rock are sheeted and stockwork quartz veins (Figure 9). The syenite has low magnetic susceptibility and therefore no distinctive geophysical signature to distinguish it from the sedimentary rocks on the regional aeromagnetic maps.

The syenite comprises euhedral, lath-shaped orthoclase megacrysts (1.5–3 cm, 50–80%) in a fine to medium equigranular groundmass of orthoclase (0.1–1 mm, 10–25%), plagioclase (1–7 mm, 10%), hornblende (0.2–1 mm, 1–10%), and trace amounts of biotite, sphene, apatite and pyrite.

Early exploration drilling of the Northeast zone at Mount Polley revealed a close association between ore-grade mineralization and the appearance of K-feldspar-megacrystic syenite clasts in the breccias (P. McAndless, pers comm, 2005). Isotopic dating has substantiated a close temporal relationship between the crystallization age of the



**Figure 9.** Crowded, orthoclase-megacrystic hornblende syenite cut by sheeted quartz vein sets; locally contains sparse galena and potassium-alteration envelopes.

K-feldspar porphyritic syenite dikes (U-Pb zircon, 205.1 ±0.3 Ma) and the mineralization and alteration system (Ar/Ar biotite, 205.2 ±1.2 Ma) at Mount Polley. Samples of the crowded orthoclase-megacrystic porphyritic syenite have been collected and submitted to the PCIGR-UBC laboratory for crushing and heavy mineral separation to establish if there are sufficient zircon or titanite grains to proceed with U-Pb dating.

### **Subvolcanic Plagioclase Porphyry**

Grey to white, biotite-hornblende-plagioclase porphyritic andesite (?) or subvolcanic quartz monzodiorite porphyry crop out in the area east of Dragon Lake (Figure 2). The rocks are coarsely porphyritic with tabular, white plagioclase phenocrysts <1 cm in diameter and noticeably finer, acicular hornblende and biotite crystals in a green aphanitic matrix. Quartz commonly forms phenocrysts 1–4 mm in size that constitute up to 5% of the rock.

Brecciated lithic fragments, crystal shards and eutaxitic textures in correlative rocks of the Cottonwood map area (Jonnes and Logan, 2007) indicate extrusive as well as intrusive characteristics for this unit. Hornblende from the plagioclase crystal tuff at Mouse Mountain returned an Early Jurassic cooling age of 192 ±1.3 Ma (Logan, 2008).

## MIDDLE JURASSIC

### *Quesnel River Pluton*

The Quesnel River pluton is exposed on the northeast side of the Quesnel River and dominates the central and southwestern parts of the map area. It is a 23 km long by 7 km wide, northwest-trending complex granitoid. The northern margin of the pluton is not exposed; the northwestern contact, which follows the Quesnel River, is faulted against Late Triassic to Early Jurassic DBP; and its southern contact intrudes metavolcaniclastic rocks of the GVS.

The pluton consists dominantly of medium- to coarse-grained, equigranular or K-feldspar–megacrystic hornblende-biotite monzogranite. This monzogranite forms the main core of the pluton. It has generally low magnetic susceptibility and is manifested as a large magnetic low on regional airborne magnetic maps. Marginal phases to the main monzogranite body are exposed around the southern margin of the pluton and include gabbro, pyroxenite, biotite diorite, quartz-eye porphyritic granite and late-stage pegmatite and aplite dikes. These units are mineralogically and texturally distinctive but not regionally extensive, and are therefore not shown on the map.

The monzogranite is mainly a leucocratic, pink, equigranular or sparsely K-feldspar–megacrystic rock. Grain size ranges from 3 to 7 mm, with 1–5 cm, euhedral, tabular microcline phenocrysts present locally. Thin sections show 30–40% plagioclase, 30–35% microcline (<10% perthitic microcline megacrysts), 25–30% rounded quartz, 5–7% biotite and 3–5% hornblende. Accessory minerals include sphene, zircon and magnetite.

A 15 kg sample of pink hornblende-biotite granite was collected from the southern end of the Quesnel River pluton and dated using thermal ionization mass spectrometry (TIMS) and inductively coupled plasma–mass spectrometry (ICP-MS) U-Pb techniques at the PCIGR-UBC laboratory. Zircons extracted from the sample yielded a Middle Jurassic crystallization age of  $165.6 \pm 0.3$  Ma for the orthoclase megacrystic phase of the granite. A second sample was collected from close to the centre of the pluton, where a southeast-trending mylonite zone cuts the monzogranite. Zircons from this location yielded an age of  $158.2 \pm 0.3$  Ma (R. Friedman, pers comm., 2007), thus providing a maximum age for deformation of the pluton.

To further constrain the cooling history of the unit, hornblende and biotite were separated from the granite and analyzed using Ar/Ar incremental-step heating techniques at the PCIGR-UBC laboratory. The hornblende data are complex and inconclusive. The hornblende spectrum indicated excess argon and did not yield an interpretable plateau age. An inverse isochron analysis on five points gave an isochron age of  $118.6 \pm 8.8$  Ma, with an initial  $^{40}\text{Ar}/^{36}\text{Ar}$  intercept of  $802 \pm 17$  Ma. Reanalyses of the hornblende sample produced a different isochron age ( $77.62 \pm 0.5$  Ma) and an initial  $^{40}\text{Ar}/^{36}\text{Ar}$  intercept ( $1599 \pm 430$  Ma) that was much higher than the first run (T. Ullrich, pers comm, 2007). However, the second age does match the biotite isochron age (below). Biotite separated from this same sample gave a well-defined Ar/Ar plateau age of  $77.62 \pm 0.5$  Ma, utilizing 74.5% of the  $^{39}\text{Ar}$ , and an inverse isochron age of  $77.4 \pm 0.79$  Ma with an initial Ar intercept of  $299 \pm 10$  Ma (T. Ullrich, pers comm, 2007).

The marginal phases of the pluton are typically more mafic; they also have higher magnetite contents than the

monzogranite and, as a result, contribute to the annular magnetic anomaly that surrounds the pluton. In addition, banded magnetite-rich rocks form parts of the metavolcaniclastic sequence adjacent to the southern margin of the Quesnel River pluton. These likely represent metamorphosed, thinly bedded, fine-grained calcareous volcaniclastic horizons and must also contribute to the magnetic anomaly surrounding the main body of the pluton. Rounded mafic inclusions of foliated pyroxenite, amphibolite, hornblende-biotite diorite and partially digested metavolcanic rocks are also concentrated in marginal zones of the pluton. In these rocks, clinopyroxene is typically partially or fully replaced by hornblende.

The biotite quartz monzodiorite is a medium- to coarse-grained mesocratic rock that, in places, contains coarse (up to 20 mm) tabular phenocrysts of biotite. Some of the large phenocrysts consist of aggregates of biotite, suggesting late-stage replacement of hornblende. The coarse phenocrysts of biotite are randomly oriented but portray a graphic textural intergrowth with feldspars and quartz. Minor amounts of 1–2 mm, tabular pyroxene crystals occur interstitial to the biotite phenocrysts (Figure 10).

One of the youngest phases of the Middle Jurassic magmatic suite is a fine-grained, leucocratic, quartz-eye



**Figure 10.** Contact zone between coarse, platy biotite quartz monzodiorite (marginal phase) and medium-grained, equigranular biotite monzogranite (main phase) of the Quesnel River pluton.

porphyritic granite. It occurs as metre- to decimetre-wide dikes and stocks cutting the Quesnel River pluton and pyroxene volcanoclastic and sedimentary rocks exposed along the Quesnel River at the Kate showing. The granite is characteristically rusty weathering due to finely disseminated pyrite and variable quartz–Fe-carbonate alteration; as a result, it has low magnetic susceptibility. A diagnostic feature is the presence of up to 10%, 1–3 mm euhedral quartz phenocrysts scattered individually or as crystal aggregates throughout a fine-grained feldspar-plagioclase-quartz matrix. Mafic minerals, including biotite (up to several percent) and rare hornblende, are commonly replaced by sericite, carbonate and pyrite.

A 15 kg sample of quartz-porphyritic granite was collected from an outcrop exposed in the Quesnel River at the Kate showing, located approximately 9 km east of Quesnel. Zircons were extracted and four single zircon grains analyzed using thermal ionization mass spectrometry (TIMS) U–Pb geochronological techniques. The resulting  $^{206}\text{Pb}/^{238}\text{U}$  ages were Late Triassic (233.0 and 201.4 Ma), Early Jurassic (182.1 Ma) and Middle Jurassic (162.4 Ma). The zircon with the Middle Jurassic age (162 Ma) was interpreted to be xenocryst free and reflect the crystallization age of the granite (R. Friedman, pers comm, 2007). Xenocryst-rich zircons with 162 Ma rims and primarily Late Triassic cores have been extracted from Middle Jurassic quartz-eye porphyry at Gavin Lake (Logan et al., 2007a).

Fine- to medium-grained leucocratic biotite granite apophyses emanate from the southern margin of the Quesnel River pluton and crosscut the epidote-amphibolite–facies metavolcanic country rocks at a high angle to schistosity. A sample of one of these dikes was collected for U–Pb zircon dating to constrain the age of penetrative foliation. Results are pending.

## EOCENE

East-trending biotite lamprophyre dikes crosscut the metavolcanoclastic rocks and quartz-feldspar-biotite porphyry intrusions in the canyon section of the Quesnel River, 9.5 km east of Quesnel. They are also found in the dark banded phyllite of the Dragon Mountain succession. The mafic dikes consist of two varieties, distinguished on the basis of biotite phenocryst size: a fine-grained variety with biotite crystals ranging from <1 to 1 mm and a variety with coarse euhedral biotite books up to 6 mm in length in an aphanitic dark groundmass. The dikes are moderately to strongly magnetic and display fine-grained chilled margins.

Argon/argon step-heating of biotite separates from one of these dikes returned a good plateau age of  $51.89 \pm 0.32$  Ma, utilizing 83.3% of the  $^{39}\text{Ar}$  released in steps 7 through 11. The inverse isochron solution gave an age of  $51.82 \pm 0.38$  Ma, with an initial Ar intercept of  $309 \pm 48$  Ma (T. Ullrich, pers comm, 2007).

## STRUCTURE

Most rocks in the area are penetratively deformed. Fine-grained clastic rocks have a slaty or phyllitic cleavage defined by aligned phyllosilicate minerals and elongated quartz grains. Volcanoclastic rocks are also penetratively deformed, but a coarser grained matrix leads to a more spaced, scaly cleavage resulting from pressure solution and alignment of metamorphic minerals. Fabrics in the

volcanoclastic rocks are also defined by stretched clasts, lapilli and mineral aggregates. However, ductile deformation fabrics are not evident in part of the northeastern half of the map area. For descriptive purposes, the area has been divided into five southeast-trending structural domains (Figure 11).

### Domain I

This domain includes the polyolithic conglomerate, fine-grained volcanoclastic rocks, banded limestone and grit beds of the Dragon Mountain succession. The foliation (S1) dips quite uniformly to the northeast, with a mean orientation of  $281/66$ . Measured bedding (S0) orientations have mostly shallow dips and are spread along a girdle whose axis trends almost horizontally southeast, approximately parallel to the long axes of stretched clasts. The main cleavage (S1) is locally overprinted by spaced cleavages with widely varying orientations.

### Domain II

This domain consists exclusively of the dark banded phyllite and siltstone belonging to the lower part of the Dragon Mountain succession. The main cleavage (S1) is parallel to bedding except in the hinge zones of tight to isoclinal F1 folds, which are rarely exposed (Figure 12). The parallel S0/S1 fabric is folded around gently plunging strike-parallel axes. This is manifested in crenulations of micaceous layers, centimetre-scale buckles of quartz veins/layers and larger scale folds between outcrops. These folds are gentle-close and typically have a spaced S2 fabric parallel to their axial planes. Axial planes are variable and dip from northeast to southwest. Fault discontinuities are common in the dark banded phyllite unit at a variety of scales (Figure 13).

### Domain III

The Quesnel River pluton and the surrounding mafic volcanoclastic rocks are included in domain III. A penetrative fabric is developed in volcanoclastic conglomerate and associated finer grained sedimentary rocks. A fabric is also well developed in mafic phases around the margins of the Quesnel River pluton. Large parts of the central, felsic part of the Quesnel Lake pluton are unfoliated to weakly foliated. However, this area also includes numerous discrete mylonitic shear zones (Figure 14). These shear zones dip approximately  $60^\circ$  to the southwest, with stretching lineations typically plunging around  $40^\circ$  to the southeast. Curvature of the foliation into these zones and asymmetric delta porphyroclasts suggest oblique-dextral movement. A second, spaced tectonic fabric is evident in some of the volcanoclastic units of domain III. These spaced cleavages have highly variable orientations. Bedding features are scarce in much of this area, but most recorded values dip southwest.

### Domain IV

Rocks of the Maroon Volcanoclastic succession and the Cottonwood River succession are not penetratively deformed. They are affected by brittle deformation and locally spaced fabrics are developed; however, unlike other Mesozoic rocks in the area, they do not record any significant ductile strain.

## Domain V

This domain approximately coincides with the Black pelite succession. There is generally a cleavage parallel to compositional layering in phyllite that is locally folded around shallow-plunging axes. There is no penetrative fabric in coarse volcanoclastic rocks. Measured cleavage and bedding dip mostly to the northeast in this domain but, as elsewhere, data are limited.

## Major Faults

The dominant map-scale structural features of the area are northwest-trending faults. The Quesnel River fault is a steep, northwest-trending structure that follows the Quesnel River. It has been interpreted to represent one of the strands of the Pinchi fault zone that separates Cache Creek from Quesnel (Bailey, 1990). It juxtaposes foliated Middle Jurassic granite and Late Triassic metavolcanic rocks with Late Triassic (?) to Early Jurassic black banded phyllite along most of its length.

Bailey (1990) showed the map area to be regularly dissected by northeasterly-trending, high-angle extensional faults. Although they are rarely observed in outcrop, he interpreted them from aeromagnetic patterns. No substantive evidence for significant faults with this orientation was found during the current study.

The Chiaz fault (Bailey, 1988) is a north-trending arcuate fault that follows the eastern boundary of the map area for approximately 40 km northwards from the Quesnel River fault. The fault has a well-defined aeromagnetic signature that crosscuts the northwest-trending regional aeromagnetic grain. Bailey (1990) estimated a minimum of 4 km of dextral displacement along this structure and at least 5 km of vertical displacement (west side up) from offset of granite exposed at its southern end in the Quesnel River and the distribution of basalt across the fault. Additional evidence to support right lateral displacement along this structure is the northwest-trending contact of the Cottonwood River succession of sedimentary rocks and the Western Volcanoclastic succession (located 5 km southeast of Robertson Lake), which displays at least 10 km of

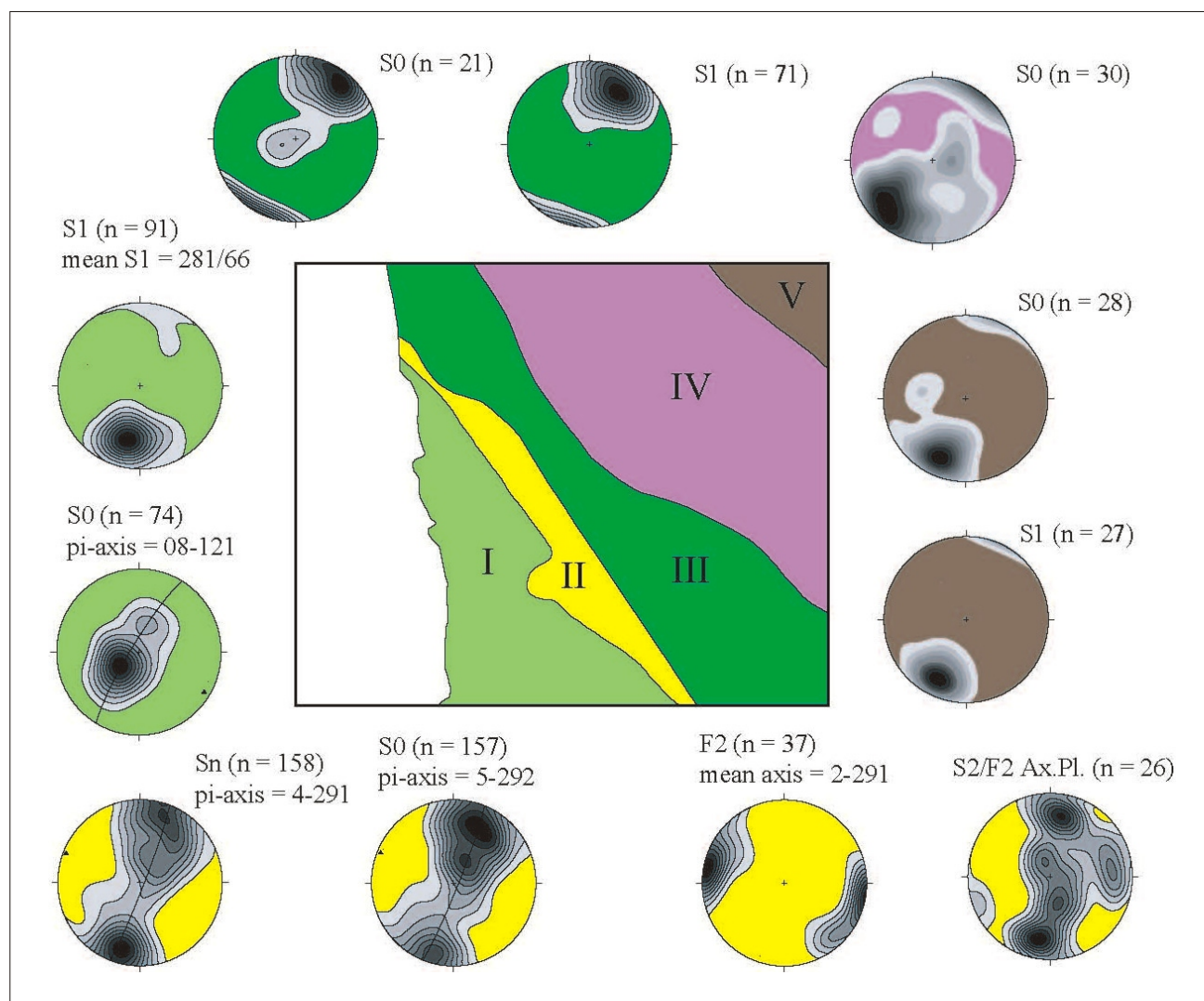


**Figure 11.** Equal-area lower-hemisphere stereonet projections of structural data from the Quesnel River map area. The map area has been divided into five structural domains (I to V) east of the Fraser River, and the data are colour coded to these areas.

dextral displacement before it reappears east of Nyland Lake.

The Oligocene rocks of the Australian Creek Formation trend northerly and dip generally shallowly, with the exception of a well-developed anticline exposed along the east bank of the Fraser River, 6 km south of Quesnel (Figure 15; Rouse and Mathews, 1979).

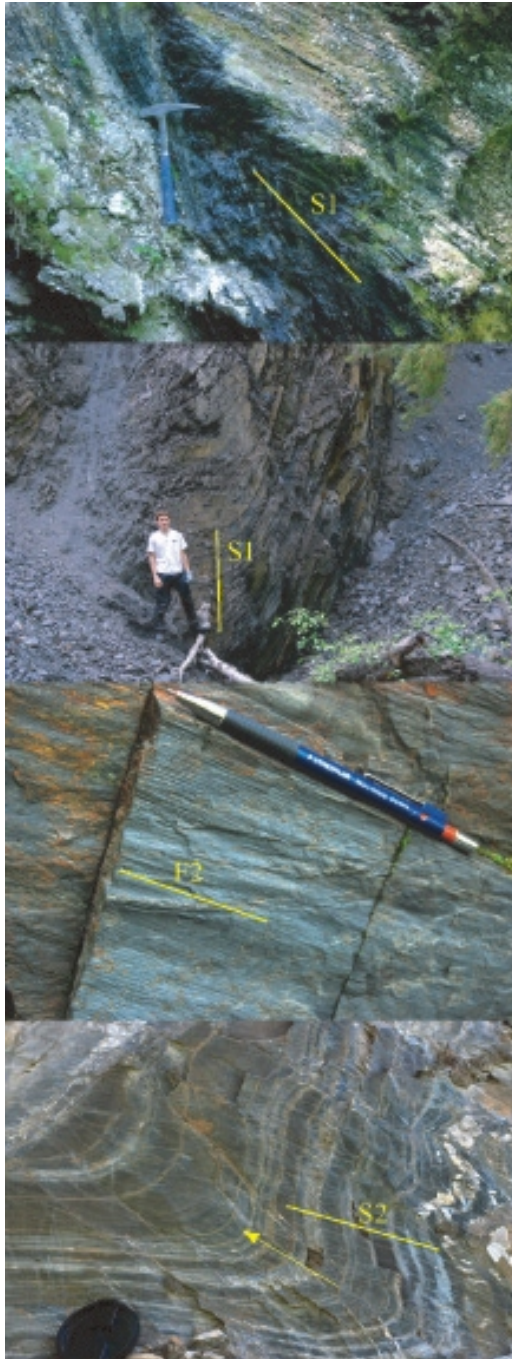


**Figure 12.** Folds in the dark banded phyllite (structural domain II): **A)** tight F1 fold with gently plunging axis; S1 is axial planar; **B)** larger scale F1 fold exposed in stream canyon; the left limb of the fold has been faulted off; **C)** F2 crenulations of S0/S1 surface in dark phyllite; **D)** F2 fold of banded phyllite with spaced S2; the fold facing direction is given by graded bedding.



**Figure 13.** Small-scale faults in the dark banded phyllite (Dragon Mountain succession). Note the truncation of the layers on which the hammer rests.

## METAMORPHISM

Phyllite in the northeastern part of the area (Black pelite succession) and close to the Quesnel River (dark banded phyllite) has chlorite+muscovite+quartz+plagioclase assemblages, with biotite locally present. Mafic volcanic and volcanoclastic rocks in the northern part of the Green Volcanoclastic succession (GVS) and the Dragon Mountain succession contain amphibole, plagioclase, epidote, carbonate and chlorite. Pyroxene crystals are fully or partly converted to amphibole or chlorite, quartz-epidote veins and replacement pods are widespread, and the rocks have an overall green appearance. In the southern part of the Green Volcanoclastic succession, chlorite is absent and mafic metavolcanic rocks have the assemblage amphibole+epidote+plagioclase. Metamorphic amphibole is aligned parallel to foliation and locally displays a lineation. Although transformed mineralogically, many rocks retain their volcanoclastic or volcanic texture—phenocrysts and detrital crystals are discernible in almost all rocks that are sufficiently coarse grained. Metamorphic mineral assemblages in the area indicate greenschist-facies metamorphism, possibly reaching epidote-amphibolite facies in the southern GVS.

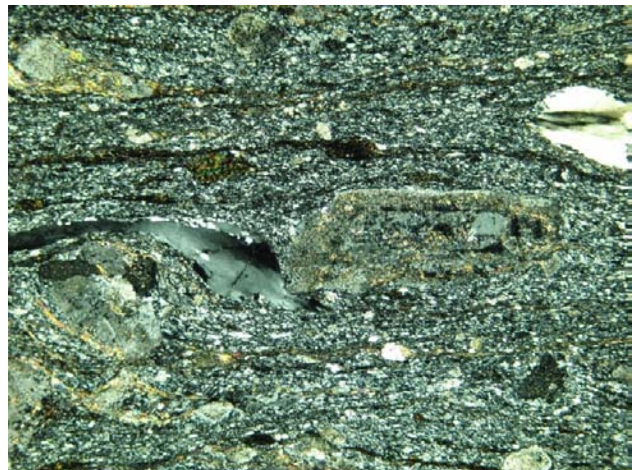


**Figure 14.** Photomicrograph of mylonite zone in Middle Jurassic K-feldspar-megacrystic monzogranite of the Quesnel River pluton (3 mm field of view; crossed polars).

In contrast, mafic volcanoclastic rocks belonging to structural domain IV have not been substantially affected by metamorphic recrystallization. Many volcanoclastic and volcanic rocks in the Maroon Volcanoclastic succession retain their maroon-coloured matrix and clasts rather than being green. They lack epidote veins and pods and, although plagioclase crystals are altered, detrital pyroxene crystals are commonly fresh. Rocks in this domain therefore differ from those elsewhere in two respects: they were not ductilely deformed and they are much less extensively hydrated and recrystallized.

Volcanic rocks of the Endako and Ootsa Lake groups experienced zeolite facies metamorphism, and the Tertiary sedimentary rocks are unmetamorphosed.

Alteration zones have developed in the volcanoclastic and sedimentary country rocks peripheral to igneous bodies in the map area. With the exception of the Quesnel River pluton, the alteration zones are generally limited to narrow zones of less than 100 m. At the southern end of the Quesnel River pluton, garnet+actinolite+epidote±biotite overprint the metavolcanic rocks immediately adjacent to the contact with the granite. Assuming a vertical contact, the alteration extends 2–400 m outwards from the granite.

Fine-grained black sedimentary units of the Cottonwood River succession are intruded by a cluster of small, north-trending, crowded megacrystic, orthoclase syenite porphyry stocks. Adjacent to the syenite, the sedimentary rocks are variably altered to a fine-grained, brown to dark purple biotite-chlorite-pyrite±pyrrhotite hornfels. Overprinting the hornfels are fracture-controlled, pale, anastomosing bleached zones of Na- and/or K-enriched hydrothermal alteration. Late-stage (?) sheeted quartz veins and stockworks extend beyond the pluton margins into the hornfelsed country rocks. Minor sulphides of Fe, Cu and Pb occur locally. Small, composite, mafic to ultramafic stocks and plugs of hornblende, diorite, monzonite and syenite intrude green volcanoclastic rocks of the Western Volcanoclastic succession along a medial northwest-trending axis. Dark hornfels and potassic alteration overprints green volcanic rock, with skarn and calcsilicate alteration occurring in calcareous volcanoclastic horizons (MINFILE 093B 027; MINFILE, 2008). No sulphide introduction was recognized.



**Figure 15.** Upright anticlinal fold in Oligocene Australian Creek Formation conglomerate, sandstone and siltstone units, exposed between the railroad line and the Fraser River, 6 km south of Quesnel.

## MINERALIZATION

With the exception of Tertiary and younger placer, coal and diatomite occurrences, mineralization in the Quesnel River area is related to Mesozoic subduction-generated arc magmatism and high-level emplacement of stocks and plutons that occupy the northeastern half of the map area (Figure 16, Table 1).

Two past-producing surficial placer Au deposits are located along the Quesnel River, and sub-bituminous coal and lignite beds are known to occur within sections of the late Early Oligocene Australian Creek Formation exposed in the Fraser River valley. East of the study area, diatomite overlies the coal-bearing stratigraphy (Rouse and Mathews, 1979; Hora, 2008).

North of the map area, limited production is recorded for the alkalic Cu-Au porphyry mineralization at Mouse Mountain (Sutherland Brown, 1957), and showings of Mo and W mineralization occur near the western margin of the Naver pluton. South of the map area, Cu±Mo porphyry mineralization associated with calcalkaline intrusive complexes at the Gibraltar mine, and Cu±Au porphyry and propylitic Au replacement associated with alkaline intrusive centres at the Mount Polley mine and the QR mine, respectively, represent important exploration models for this part of the Nicola Arc.

Proven and probable reserves at Gibraltar (0.2% Cu cut-off) total 472.4 Mt of 0.315% Cu and 0.008% Mo, with an additional 958 Mt of measured and indicated resources at 0.298% Cu and 0.008% Mo (Taseko Mines Limited, 2008). Proven and probable reserves at Mount Polley incorporate the open pit mining of the Southeast zone, C2 zone and the Springer zone, in addition to the Wight and Bell pits, and total 55.6 Mt at 0.36% Cu, 0.30 g/t Au and 0.66 g/t Ag (Imperial Metals Corporation, 2008), with an additional measured and indicated resource of 104.8 Mt at 0.295% Cu, 0.304 g/t Au and 0.19 g/t Ag. Reserves for the QR mine, estimated by Kinross Gold Corporation on January 1, 1997, were 1.57 Mt grading 3.99 g/t Au, with the main zone hosting an estimated 0.6 Mt at 4.4 g/t Au (MINFILE 093A 121). Development and milling operations at the mine have recommenced, with the first gold pour reported in November 2007 (Cross Lake Minerals Ltd., 2007).

Mineralization in the map area includes

Au±Cu developed in potassic, skarn and propylitic alteration assemblages in calcareous volcanoclastic rocks adjacent to the Cantin Creek mafic-ultramafic plutonic complex;

Cu-Au-Mo associated with elevated As-Sb-Bi±Pb-Zn geochemical signatures adjacent to the Middle Jurassic calcalkaline Quesnel River pluton, apophyses and related stocks located northeast of Dragon Lake; and weak silicification and pyritic alteration zones with elevated base metals developed peripheral to K-feldspar–megacrystic quartz syenite bodies that intrude the Cottonwood succession (Table 1).

Thirty-two rock geochemical samples were collected from alteration and mineralization over the course of three summers (2006, 2007 and 2008) mapping in the Quesnel River map area (Table 2). The majority of these samples (30) were collected northeast of the Quesnel River fault and attest to the higher mineral potential of the volcanic and plutonic Nicola Group rocks that underlie this area.

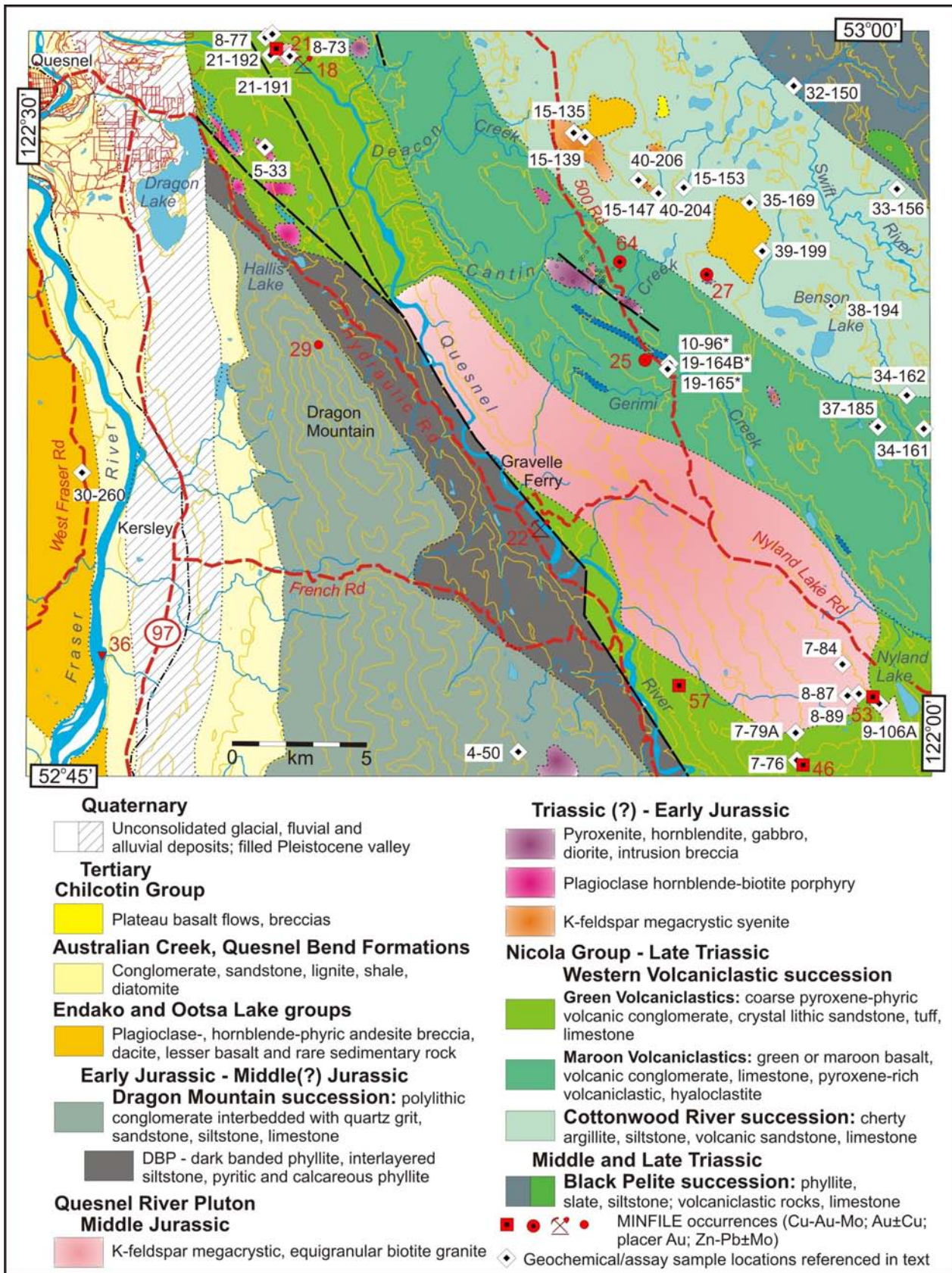


**Figure 16.** Geology the Quesnel River map area, showing the distribution of MINFILE occurrences described in Table 1 and geochemical/assay sample locations listed in Table 2. The numbers accompanying the MINFILE occurrences and geochemical/assay sample locations correspond to the last part of the 'MINFILE No.' in Table 1 and 'Station No.' in Table 2, respectively.

Table 1. MINFILE occurrences within the Quesnel River map area (NTS 093B/16).

MINFILE No.	Name (Status)	UTM (Zone 10)		Commodity	Description
		East	North		
<b>Surficial Placers:</b>					
093B 018	<b>Quesnel Canyon</b> (developed prospect)	543330	5871755	Au	•Raised bench of Tertiary glacial fluvial deposits consisting of coarse cobble gravels unconformably overlying Nicola Group basement. Test pits and bulk samples have established indicated reserves of 61 785 m <sup>3</sup> grading 0.48 g/m <sup>3</sup> Au (Dolphin, 1988).
093B 022	<b>Ainsworth, Sardine Flats,</b> (past producer)	552675	5854326	Au	•Most of the gold production from the Quesnel River has come from dredging operations, but a significant amount of gold has been won from Tertiary benches located adjacent to the present river level.
<b>Sedimentary/Volcanic-Hosted Cu:</b>					
093B 025	<b>Lynda, BI, Phantom</b> (showing)	556604	5860736	Cu, Ag	•Late Triassic Nicola stratigraphic package comprising maroon volcanoclastic rocks and basalt, dolomitic limestone and green polyolithic volcanoclastic unit intruded by alkalic trachytic dikes. The limestone is brecciated and mineralized with disseminated pyrite and tetrahedrite; malachite and azurite coat weathered surfaces. Stratigraphically lower maroon basalt and volcanoclastic rocks contain native Cu replacing vesicles and fractures suggestive of red bed Cu–style mineralization.
<b>Au-Quartz Veins:</b>					
093B 064	<b>Cantin Creek, Deacon</b> (showing)	555633	5863970	Au	•Propylitic, Fe-carbonate and silica alteration of intermediate to mafic, pyroxene-phyric volcanic flow and clastic volcanic rocks intruded by mafic-ultramafic intrusive complex. Best intersection of 2.64 g/t Au over 1.6 m (Miller-Tait, 2004).
093B 053	<b>Nyland Lake</b> (showing)	566632	5847792	Au	•Nicola Group metavolcanoclastic rocks are hornfelsed and skarned adjacent to the contact with granite and diorite of the Quesnel River pluton. Garnet, diopside, epidote, pyrite and biotite alteration assemblages and dike swarms of pegmatite, aplite and quartz characterize the contact zone which contains, anomalous Au values. In addition, anomalous Au values in heavy-mineral pan separates are reported from creeks draining the area (Troup and Freeze, 1985).
<b>Porphyry Cu, Mo, Au:</b>					
093B 021	<b>Kate</b> (showing)	542770	5871781	Cu, Mo, Au	•Pyroxene phyric flows, volcanoclastic and tuffaceous argillite-sandstone are intruded by stocks and dikes of Middle Jurassic biotite-feldspar porphyry and quartz porphyry. Pyrite-silica and antkenitic alteration is closely associated with fracture-controlled chalcocopyrite mineralization. Best surface assay returned 1.32% Cu over 4 m in quartz porphyry (Fraser, 1974).
093B 057	<b>TARN, AND, ALSO</b> (showing)	558007	5848206	Cu, Ag, Au, Mo	•Mineralization consists of Cu, Mo, Ag and Au in silicified, skarned and hornfelsed country rock within the contact aureole of Quesnel River diorite. Pyrite > pyrrhotite with minor chalcocopyrite, chalcocite and rosettes of molybdenite are disseminated or occupy fractures in both the country rocks and the dioritic intrusion.
<b>Polymetallic Veins:</b>					
093B 027	<b>AB, XL, ANO</b> (showing)	558875	5863537	Pb, Ag	•The showing is underlain by cherty argillite, siltstone and fine-grained tuffaceous rocks of the Cottonwood River succession adjacent to its contact with volcanic and volcanoclastic rocks of the Western Volcanoclastic succession. The area is intruded by a small composite diorite to monzonite intrusive complex. Ubiquitous pyrite and minor galena and tetrahedrite reported (Holland, 1968).
093B 029	<b>COUSIN JACK</b> (showing)	544456	5860764	Pb, Ag, Au	•Mineralization consists of galena and pyrite in quartz stringers within an oxidized sheared zone cutting sedimentary and volcanic rocks located on the east side of Dragon mountain. The zone, about 6 m wide and 150 m long, strikes at 068°. A grab sample of vein material assayed 1.24 g/t Au, 130.6 g/t Ag and 9% Pb (Lay, 1935). Actual location uncertain.
093B 046	<b>MANDY, BLACK BEAR</b> (showing)	562654	5845297	Ag, Cu, Au, Sb, Zn	• East-trending quartz-ankerite veins up to 1.4 m wide occupy shears cutting Nicola metavolcanic rocks. The main vein, explored by a 6 m decline, follows a 90 cm wide east-trending shear zone and contains 5–10% patchy tetrahedrite with chalcocopyrite. A 1.5 m chip sample of the quartz-ankerite vein yielded 3.3 % Cu, 0.02 % Pb, 0.45 % Zn, 435 g/t Ag and 0.65 g/t Au (Durfell, 1986).
<b>Coal:</b>					
093B 036	<b>Quesnel Coal</b> (developed prospect)	536527	5849079	Cl	•A number of coal zones containing sub-bituminous "B" and "C" rank coal are present in the lower portion of the Fraser River Member of Lower Oligocene Age.

Table 2. Assays of rock samples collected during 2006, 2007 and 2008 fieldwork, Quesnel River map area (NTS 093B/16); anomalous values are highlighted in yellow.

Station Number	Easting	Northing	Element	Ag	As	Au	Ba	Bi	Ca	Cd	Ce	Co	Cr	Cu	Fe	Hf	K	La	Li	Mg	Mn	Mo	
			Units	ppm	ppm	ppb	ppm	ppm	%	ppm	ppm	ppm	ppm	ppm	ppm	%	ppm	%	ppm	ppm	%	ppm	ppm
			Method	TICP	TICP	FAIC	TICP	TICP	TICP	TICP	TICP	TICP	TICP	TICP	TICP	TICP	TICP	TICP	TICP	TICP	TICP	TICP	TICP
			Det'n Limit	2	0.5	2	50	0.02	0.01	0.01	3	0.1	5	0.01	0.01	0.1	0.01	0.5	0.1	0.01	1	0.01	
06JLO5-33	542390	5868110		<.1	1	3	1523	0.1	2.19	0.2	22	6.5	67.1	2.6	2.09	1.2	2.17	9.8	5.7	0.41	432	0.1	
06JLO8-73	542745	5871773		6.5	76	610	56	4.8	6.82	0.2	29	12.6	67.5	433	4.53	1.6	2.32	13.9	15.1	3.01	775	160.1	
06JLO8-77	541996	5872630		<.1	1	9	1827	<.1	1.74	<.1	28	4.9	73	12.8	1.88	1.1	1.96	14	6.6	0.67	277	0.4	
06JLO10-96*	557499	5860024		0.3	11	6	640	<.1	9.16	0.1	32	49.9	138.8	468.6	9.27	1.8	0.9	16.8	28.4	5.00	2013	0.6	
06JLO13-123	572109	5843437		<.1	6	16	3232	<.1	4.55	0.2	22	20.8	48.3	32.4	5.54	2	2.94	10	9.2	2.41	1205	0.4	
06JLO15-135	554295	5868601		0.4	1	7	634	0.5	2.5	11	21	6.5	181.8	92.1	2.63	2.6	2.21	13	8.3	0.61	288	73.8	
Acme Q/C				0.4	<1	2	603	0.6	2.49	10.7	21	6.2	181.3	91.4	2.62	2.7	2.28	13	7.7	0.61	290	73.1	
06JLO15-139	553872	5868759		<.1	1	2	1019	0.9	0.65	0.1	8	2.5	122.6	3.2	1.11	1	2.45	4.4	7.1	0.22	326	0.5	
06JLO19-164B*	557449	5860053		1.1	16	6	1000	0.1	5.41	0.2	21	20.6	21.1	5504.5	5.66	2.5	3.96	10.1	25.4	2.24	1824	2.6	
06JLO19-165*	557554	5860041		0.1	8	<.1	828	0.1	8.66	0.2	38	43.4	220.2	29.2	7.89	1.6	1.45	21.6	24.1	5.38	1329	0.3	
07GLE32-152	565793	5868491		<.1	<.1	27	1798	<.1	3.95	0.1	30	15.9	75.7	51.8	4.36	2.5	3.55	17.7	15	1.87	1029	0.2	
07GLE32-150	562370	5870651		0.1	5	<2	3794	<.1	3.76	0.1	15	21.8	25.5	69.6	6.65	0.8	1.45	6.7	45.1	2.17	1876	0.5	
07GLE33-156	565923	5866792		0.3	5	5	945	0.2	1.22	1.9	24	16.4	68.6	120.1	5.05	2.1	2.61	13	25.3	1.97	497	9.2	
07GLE34-161	567016	5857871		0.2	5	16	1581	0.1	5.05	0.2	20	21.1	74.5	102.7	5.26	1.6	3.57	10.6	25.9	2.27	1136	1.7	
07GLE34-162	566371	5859110		<.1	86	12	172	0.2	0.07	0.1	143	0.9	40.9	14.1	3.64	2.4	8.4	76.6	15.4	0.08	1130	14.3	
07GLE35-169	560442	5866226		0.1	2	14	1165	<.1	6.17	0.1	65	43.3	271.7	46.9	7.21	3.8	1.46	33.1	10.8	4.73	1165	0.9	
07GLE37-185	565309	5857927		0.1	5	-	1866	<.1	4.11	0.1	19	11.6	30.7	25.7	4.85	1.7	1.78	8.8	4.3	1.48	1165	0.1	
07GLE38-194	563515	5862414		0.1	<.1	53	42	0.4	2.18	14.6	28	19.1	98.4	140.4	5.04	2.3	3.22	15.3	51.6	1.27	647	140.5	
07GLE39-199	560935	5864426		0.1	3	8	1445	<.1	5.9	0.2	90	36	168.4	70.6	7.95	5.2	1.61	45.7	10	2.22	992	1.6	
07GLE40-204	557049	5866543		0.2	5	28	1643	0.3	0.46	0.2	14	3.6	55.2	54.3	2.61	1.9	3.7	7.3	15.5	0.22	197	6.5	
07GLE40-206	556298	5867023		0.1	6	-	1360	0.1	0.06	<.1	3	<.2	13.3	3.2	0.27	0.5	4.68	2	74.7	0.04	11	1.2	
08JLO4-50	552051	5845674		-0.1	-1	-2	25	-0.1	1.47	0.1	-1	1.7	266	4.8	1.38	-0.1	0.04	0.3	2.4	0.12	1756	0.5	
08JLO7-76	562473	5845444		-0.1	-1	-2	253	-0.1	0.05	-0.1	10	1.7	128	2.4	0.93	0.2	1.74	5.4	8	0.13	119	0.2	
08JLO7-79A	562367	5846491		-0.1	-1	-2	572	-0.1	1.11	-0.1	33	0.6	85	2.1	1.01	0.1	1.46	14.6	4.7	0.23	883	0.2	
08JLO7-84	564080	5849065		-0.1	-1	-2	237	-0.1	0.07	-0.1	9	1.6	106	2.1	0.96	0.3	1.71	4.7	7.5	0.13	125	0.2	
08JLO7-84rep				-0.1	-1	6	232	0.3	0.08	0.1	9	1.8	112	2.8	0.96	0.3	1.69	4.9	7.2	0.13	129	0.5	
08JLO8-87	564279	5847897		-0.1	-1	-2	3361	0.1	3	-0.1	57	19.1	45	31.1	4.76	2.1	2.86	25.3	26.2	1.2	917	0.3	
08JLO8-89	564704	5847971		-0.1	-1	-2	47	0.6	15.59	0.3	10	30.9	114	15.9	7.47	1.1	0.03	4.5	1.8	2.67	1985	0.3	
08JLO9-106A	565467	5847615		-0.1	4	40	449	-0.1	7.72	0.2	16	23.1	70	31.2	5.43	0.9	0.66	7.2	17	2.48	1193	0.8	
08JLO15-147	557050	5866539		0.2	3	11	1756	0.3	0.7	0.4	14	5.3	47	37.5	2.2	2.2	3.73	7.1	13.5	0.19	425	4.2	
08JLO15-153	557990	5866763		0.7	1	5	288	0.2	2.29	0.9	16	15	81	73.2	4.01	3	2.17	7.2	16.7	1.64	725	4.8	
08JLO21-191	543155	5871686		3.9	165	684	12	91.1	6.9	0.6	7	14.2	113	151.4	15.27	0.2	0.46	3.8	8	2.96	838	130	
08JLO21-192	542447	5872422		-0.1	1	13	155	0.9	2.7	0.1	3	8	37	4.4	1.23	0.9	0.36	1	1.3	0.08	311	0.8	
08JLO30-260	535708	5855910		0.1	-1	-2	1094	-0.1	3.23	0.2	55	17.4	67	32.3	4.68	5.9	2.58	23.7	6.4	0.98	649	2.1	
Std CANMET WPR1				0.6	<.1	<.1	19	0.1	1.61	0.2	5	174	2370.6	1692	10.96	0.5	0.09	1.9	4.6	18.57	1352	0.3	
Std WPR-1/SY4				0.6	-1	-0.1	19	0.1	1.61	0.2	5	174	2370.6	1692	10.96	0.5	0.09	1.9	4.6	18.57	1352	0.3	
Recommended				0.7	1.4	0.042	22	0.19	1.43	0.43	6	180	3300	1640	9.93	0.61	0.165	2.2	4.2	18.69	1549	0.9	
% Difference				3.8	300.0	122.4	3.7	15.5	3.0	18.3	4.5	0.8	8.2	0.8	2.5	5.0	14.7	3.7	2.3	0.2	3.4	25.0	

Table 2 (continued)

Station Number	Easting	Northing	Element	Na	Nb	Ni	P	Pb	Rb	S	Sb	Sc	Sn	Sr	Th	Ti	U	V	W	Y	Zn	Zr
			Units	%	ppm	ppm	%	ppm	ppm	%	ppm	ppm	ppm	ppm	ppm	ppm	%	ppm	ppm	ppm	ppm	ppm
			Method	TICP	TICP	TICP	TICP	TICP	TICP	TICP	TICP	TICP	TICP	TICP	TICP	TICP	TICP	TICP	TICP	TICP	TICP	TICP
			0.001		0.1	0.001	0.01		0.02	0.02	0.1		0.5	0.2	0.001	0.5	2	1		0.1		
06JLO5-33	542390	5868110		3.11	1.5	12.4	0.07	17.2	49.6	0.4	3	5	0.8	224	2.7	0.11	1.30	50	0.5	4.9	71	20.8
06JLO8-73	542745	5871773		0.04	3.7	25.7	0.08	101.1	58.8	2.7	138.3	5	0.8	214	3.4	0.21	6.20	89	18.4	11.9	90	48.2
06JLO8-77	541996	5872630		3.93	7.5	17.3	0.06	9.8	51.4	<1	0.4	4	1.3	582	3.8	0.22	1.30	35	1.2	5.8	43	21.6
06JLO10-96*	557499	5860024		3.08	2.7	36.5	0.35	7.6	21.8	-0.1	0.1	46	0.9	1023	2.3	0.54	-	335	0.4	16	116	44.2
06JLO13-123	572109	5843437		2.69	3.2	14.7	0.17	2.4	48.8	0.3	1	17	0.6	841	3.2	0.52	1.40	252	0.6	15.8	57	61.2
06JLO15-135	554295	5868601		2.10	5.6	52.9	0.06	73.8	50.9	1	0.4	13	1.1	368	2.3	0.38	4.80	888	0.9	34.4	543	90.4
Acme Q/C				2.08	5.3	52.6	0.06	72.1	48.3	1	0.4	13	1.1	360	2.3	0.40	4.80	891	0.9	34.6	543	87.9
06JLO15-139	553872	5868759		1.70	5.5	8.3	0.03	31.7	48.9	<1	0.1	2	2.7	289	1.3	0.10	0.60	110	0.2	4.6	36	28.9
06JLO19-164B*	557449	5860053		2.75	5.4	3.1	0.20	-	41.1	0.1	0.3	8	1	958	2.6	0.39	-	187	1.1	15.3	113	89.6
06JLO19-165*	557554	5860041		2.40	3	52.8	0.28	-	23.7	<1	0.1	35	1	1053	3.2	0.46	-	275	0.6	13	80	44.5
07GLE32-152	565793	5868491		3.90	6.3	21.2	0.13	5.7	93.2	<1	0.3	15	0.7	1030	4.90	0.33	2.7	195	0.5	12.3	48	81.3
07GLE32-150	562370	5870651		3.72	2	11.5	0.12	3.6	33.8	0.5	0.5	16	0.8	637	0.60	0.53	0.5	254	0.3	10.2	125	18.1
07GLE33-156	565923	5866792		2.24	4.4	32.1	0.13	10.5	64.4	0.4	1.7	20	1.1	363	3.30	0.47	3.1	407	0.5	16.8	190	65.6
07GLE34-161	567016	5857871		3.73	3.1	30.5	0.16	13.3	66.3	0.5	0.3	15	0.6	1535	1.40	0.34	1	246	0.3	14.5	94	48.6
07GLE34-162	566371	5859110		1.06	68.1	11.4	0.03	8.9	113.1	1.9	6.5	1	6.3	126	5.00	0.06	0.8	20	6.6	11.5	58	83
07GLE35-169	560442	5866226		2.03	8.8	195.3	0.26	7.6	36.9	0.1	0.1	26	1	916	2.30	0.82	0.8	243	0.3	20.1	92	146.2
07GLE37-185	565309	5857927		2.93	1.8	3.3	0.11	3.4	39.1	0.2	0.6	14	0.4	532	2.40	0.36	1	175	1	14.4	58	53.2
07GLE38-194	563515	5862414		4.18	9.9	72.8	0.11	16.6	57	4	0.4	14	1.3	339	3.10	0.34	6.1	666	0.6	22.8	665	73.3
07GLE39-199	560935	5864426		3.53	16.8	115	0.48	8.7	29.9	0.1	0.1	20	1.6	1259	2.80	1.09	1.2	237	0.5	21.4	115	189.2
07GLE40-204	557049	5866543		2.70	7.3	8.5	0.07	28.2	101.6	0.3	0.9	6	0.8	521	2.30	0.23	2.3	87	1	7.9	53	59.9
07GLE40-206	556298	5867023		0.77	9.4	0.4	0.01	17.7	45.1	0.1	0.8	1	1.2	1038	1.20	0.05	0.8	108	0.8	1.1	8	23.4
08JLO4-50	552051	5845674		0.06	-0.1	4.7	0.00	0.8	1.7	-0.1	0.2	1	0.3	48	0.10	0.01	-0.1	2	0.2	0.8	46	1.7
08JLO7-76	562473	5845444		3.94	1.2	9.1	0.02	10.3	56.2	-0.1	0.9	1	0.4	93	2.60	0.03	2.4	24	0.6	0.7	27	4.9
08JLO7-79A	562367	5846491		3.32	5.9	2	0.02	7.7	33.6	-0.1	0.2	1	0.9	237	2.80	0.08	0.8	-1	0.2	7.5	47	3.9
08JLO7-84	564080	5849065		4.22	1.1	8.7	0.03	10.9	52.9	-0.1	1	1	0.4	89	1.90	0.03	1.8	25	0.5	0.8	24	5.9
08JLO7-84rep				4.09	1.2	9.2	0.02	12	52.3	-0.1	1.1	1	0.5	85	2.30	0.04	2.2	25	0.6	0.9	22	4.7
08JLO8-87	564279	5847897		3.45	3.6	8.9	0.25	30.7	70.5	-0.1	0.1	10	1	820	5.60	0.31	1.8	155	0.2	11.5	93	91.1
08JLO8-89	564704	5847971		0.10	0.8	23.6	0.05	9	1.7	-0.1	0.9	38	0.5	560	0.80	0.42	1.5	389	0.9	18.7	98	31.5
08JLO9-106A	565467	5847615		3.18	1	24.7	0.08	4.2	22.3	-0.1	0.3	28	0.3	294	1.60	0.39	1.6	236	0.6	15.2	76	19
08JLO15-147	557050	5866539		2.76	9.7	7.1	0.06	38.6	107.8	0.1	1	4	0.9	714	2.90	0.22	2.7	79	0.7	9.4	64	82.3
08JLO15-153	557990	5866763		3.69	3	18.9	0.11	13.1	39.1	2.4	0.6	23	1.2	294	1.10	0.54	1.3	181	1.6	30.4	127	90.6
08JLO21-191	543155	5871686		0.03	0.3	29.4	0.02	154	15.8	>10.0	66.7	3	0.3	168	0.30	0.05	9.9	62	3.9	6.3	154	5.6
08JLO21-192	542447	5872422		7.14	2.3	1.9	0.03	3.6	10.1	1.2	1.5	2	0.3	209	0.70	0.09	0.6	30	6.8	2.2	9	19
08JLO30-260	535708	5855910		3.13	14.8	31.8	0.23	10.4	73	-0.1	0.1	12	1.3	671	5.70	0.61	2	138	0.6	15.1	88	248.1
Std CANMET WPR1				0.017	1.8	3150.9	0.018	5.7	3.8	0.8	0.7	11	0.7	6	0.3	0.204	0.1	72	0.1	4.3	94	14.2
Std CANMET WPR1				0.017	1.8	3150.9	0.018	5.7	3.8	0.8	0.7	11	0.7	6	0.3	0.204	0.1	72	0.1	4.3	94	14.2
Recommended					2.4	2900	0.013	6	5	0.9	0.9	12	1.1	7	0.4	0.179	0.2	65			95	18
% Difference				50.0	7.1	2.1	8.1	1.3	6.8	2.9	6.3	2.2	11.1	3.8	7.1	3.3	16.7	2.6	50.0	50.0	0.3	5.9

## Late Triassic (?) to Jurassic Zn-Pb±Mo-Au Mineralization

Quartz-sulphide vein mineralization at the AB-XL showing (MINFILE 093B 027; Table 1) is associated with small stocks of orthoclase-megacrystic syenite and a monzonite, which intrude sedimentary rocks of the Cottonwood River succession.

Miarolitic, orthoclase-megacrystic syenite intrusions underlie the 10 km<sup>2</sup> area that extends from the headwaters of Deacon Creek southeast across the 500 Road. They are composite bodies consisting of 1) coarse-grained, equigranular, orthoclase- and hornblende-phenocrystic syenite, intruded by 2) crowded, orthoclase-megacrystic porphyry syenite and 3) fine-grained dikes of orthoclase. Sheeted and stockwork quartz veins crosscut all three phases of the intrusion and the fine-grained black and green argillite and phyllite country rocks. The veins are late-stage, brittle quartz±orthoclase veins that occasionally display orthoclase alteration envelopes. The vein quartz is massive and white, with crystals oriented perpendicular to vein walls or zones of bullish white quartz filling brittle fractures and healing breccia zones. In addition, the quartz occupies miarolitic cavities and comb quartz layers, and rarely is mineralized with pyrite and sparse galena. The mean principal orientation for quartz veins cutting the syenite is 347 /72 , but these sheeted vein sets are commonly cut by a younger orthogonal set of veins trending 250 /80 .

Samples of the orthoclase-megacrystic syenite (07GLE40-204, -206, 08JLO14-140A, 08JLO15-147), the sheeted quartz veins and stockwork that cut the intrusion (06JLO15-139), and hornfelsed, quartz-veined argillaceous country rock (06JLO15-135) that host the intrusions were collected and analyzed to assess the potential of this suite of alkalic intrusions to host Cu-Au mineralization. The results in Table 2 indicate that the highest anomalies occur in the altered and quartz-veined country rocks adjacent to the syenite. Argillite sample 06JLO15-135 is hornfelsed and silicified by discrete vitreous quartz veinlets with wide alteration envelopes, typically 2–3 times the width of the veinlet, and returned elevated Zn, Pb, Cd, ±Cu±Mo values (Figure 17). The quartz veins sampled that cut the intrusions contained only background values. However, crosscutting vein samples yet to be analyzed contain disseminated galena. Two of the four syenite samples contained slightly elevated Au values but no coincident anomalous values for other elements.

A northwest-trending ridge of rusty-weathering black argillite and lesser green siltstone is located north of Benson and Robertson lakes. The rocks are massive, with faint, cryptic, fine laminations suggestive of bedding. They possess a splintery or conchoidal fracture pattern resulting from silica or hornfels alteration. Bailey (1989) showed an intrusive body of grey porphyritic syenite (his unit 7B) northeast of this location that could account for the observed hornfels alteration. Pale greenish alteration envelopes and bleaches the argillite adjacent to centimetre-scale, sulphide-rich quartz veins. Where vein density is high, disseminated pyrite occurs throughout the argillite. Grab samples from this location (07GLE38-194) returned anomalous values for Zn, Cd and Mo, with slightly elevated Cu and Au (Table 2). This element association is similar to that of mineralization associated with sediment-hosted, K-feld-

spar–megacrystic syenite that intrudes sedimentary rocks of the Cottonwood succession.

## Early Jurassic Au±Cu Mineralization

### CANTIN CREEK

The Cantin Creek showing (MINFILE 093B 064) is located west and east of the 500 Road, approximately 10 km north of its junction with the Nyland Lake Road in the upper reaches of Cantin Creek. It was explored first in 1964 (Bacon, 1964) and again in the late 1980s and early 1990s, with substantial geophysical, geochemical and diamond-drilling (~4000 m) programs looking for another QR-type deposit (Fox, 1975, 1985, 1990; Goodall and Fox, 1989). Outcrop is scarce and historical drilling intersected between 40 and 90 m of overburden consisting of gravel and water-soaked clay (Fox, 1985). Recent exploration has included additional diamond-drilling designed to test induced-polarization (IP) and geochemical targets peripheral to, and distal from, the Cantin Creek stock (Miller-Tait, 2004). The stock is a mafic-ultramafic complex composed of pyroxenite, diorite and gabbro. Early exploration drilling focused on defining the extent and metal content of this



**Figure 17.** Hornfelsed and veined argillite of the Cottonwood River succession, located peripheral to crowded orthoclase-megacrystic syenite. Pyrite±pyrrhotite vein stockworks are characterized by pale anastomosing bleached alteration envelopes of Na and/or K- alteration.

body. Assay results from more than 150 one-metre sample intervals of the pyroxenite, gabbro and diorite returned low Au values of <50 ppb (Fox, 1985) to 5 ppb (Goodall and Fox, 1989), while felsic intrusions averaged 15 ppb and locally up to 130 ppb (Goodall and Fox, 1989). However, the best assay results were intersected in marble=calcsilicate skarn and propylitic alteration zones peripheral to the main Cantin Creek stock.

Interbedded hornfels, diopside and garnet calcsilicate and marble intruded by narrow felsic dikes in drillhole G-10 returned a high value of 3690 ppb Au and seven one-metre samples with values greater than 1000 ppb Au (Goodall and Fox, 1989). Propylitically altered basalt cut by 2–5 m wide felsic dikes intersected in drillhole 20 returned 16 one-metre samples with greater than 100 ppb Au and one of 1779 ppb Au (Fox, 1990). Auriferous calcite-fluorite veining in pyroxene-plagioclase-phyric breccia, intersected between 131 and 139 m in drillhole 21, returned 1.8 g/t Au over 8 m. Drillhole 25 was drilled to test the IP anomaly located northeast of the stock and returned some of the more continuous mineralization (Fox, 1990). Anomalous Zn and Cu values (1 m samples as high as 1.9% Zn and 0.2% Cu) with low Au values were intersected in pyritic epidote hornfels between 63 and 73 m; propylitized calcareous volcanoclastic rocks between 112 and 120 m returned 212 ppb Au over 8 m; a 6 m interval of propylitic basalt between 136 and 142 m returned 1.7 g/t Au and low Zn and Cu values; and a felsic dike intersected at 151 m returned 391 ppb Au over 3 m. Fox (1990) concluded that the mineralized material and local stratigraphic section at Cantin Creek were typical of the QR Au deposit.

#### LYNDA

The Lynda showing (MINFILE 093B 025) is located 3 km south of the Cantin Creek showings in outcrops exposed along the 500 Road. It is characterized by sedimentary/volcanic-hosted Cu mineralization consisting of finely disseminated tetrahedrite and chalcocite replacements of limestone, and stratabound native Cu replacements of amygdules, vesicles and fractures in basalt flows and volcanoclastic rocks. Malachite and azurite are common on weathered surfaces. A 1 m chip sample of mineralized dolomitic limestone returned 2445 ppm Cu, 69 ppm Pb, 321 ppm Zn, 3600 ppb Hg, 3.4 ppm Ag and 15 ppb Au (Turner, 1983). Geochemical analyses of altered and mineralized maroon volcanic rocks (06JLO10-96 and 19-165) that underlie the limestone and an alkalic dike (JLO19-164b) are listed in Table 2. The volcanic rocks show anomalous Cu values but low Au, Ag and base-metal contents.

### **Middle Jurassic Cu-Au-Mo Mineralization**

#### KATE

The Kate showing (MINFILE 093B 053) is located in the Quesnel River canyon, approximately 9 km upstream from Quesnel. Pyroxene-phyric flows and volcanoclastic and fine-grained sedimentary rocks of the Late Triassic Nicola Group are intruded by a suite of quartz-saturated Jurassic stocks and Eocene mafic dikes. Contacts are sharp, crosscutting and chilled for subsequent phases. Textures suggest an early fine-grained equigranular monzodiorite, followed by a feldspar-quartz-biotite-porphyrific monzonite, and a late phase of quartz-porphyrific granite.

All units except the cemented Tertiary gravel are cut by metre-wide, east-trending, biotite lamprophyre dikes.

Sulphide mineralization comprises pyrite, chalcopyrite and minor tetrahedrite in fractures, and quartz-carbonate veins and disseminations in the metavolcanic country rock peripheral to the quartz porphyry granite. Carbonate and sericite alteration accompanies mineralization. In zones of high-density fracturing, Fe-carbonate replacement is pervasive, texturally destructive and produces pink- to buff-coloured rock. An assemblage of dolomite, pyrite, calcite, quartz and sericite dominates this alteration. Secondary minerals include malachite, azurite and hematite. Two geochemical samples of sulphide mineralization (05JLO8-73 and 08JLO21-191) were collected from the Quesnel River canyon at the Kate showing (Figure 18). Results show a multi-element suite of elevated to anomalous values for Au, Ag, As, Bi, Cu, Mo, Sb, Pb and Zn (Table 2).

At Mouse Mountain, these Middle Jurassic Fe-carbonate alteration zones (trending north and east) overprint the Late Triassic alkalic alteration assemblage and can dilute Cu-Ag grades of the monzonite-related mineralization. Zones of Fe-carbonate alteration are characterized by elevated As, Sb and Mo values (Jonnes and Logan, 2007).

#### MANDY

The Mandy showing (MINFILE 093B 046) is located 1.3 km south of the southern margin of the Quesnel River pluton in hornfelsed metavolcanoclastic rocks of the Nicola Group. Mineralization is hosted in Fe-carbonate (ankeritic)-quartz veins developed in sheared metavolcanic rocks and includes sporadic Cu, Zn, Ag and Au values



**Figure 18.** Massive, fine-grained pyrite vein with Fe-carbonate and silica alteration envelope, hosted in metavolcanic rocks adjacent to a quartz porphyry intrusion at the Kate occurrence (MINFILE 093B 053).

over widths of 1.5 m. The veins strike easterly, dip steeply north and occupy an en échelon northeasterly-stepping distribution. They are sheeted, milky white massive quartz banded with discontinuous blebs and layers of sulphides that include pyrite, chalcopyrite and tetrahedrite.

A grab sample of tetrahedrite-mineralized vein material from pit 1, which is explored by a 6 m decline, returned 13.54% Cu, 1530 g/t Ag, 2.36 g/t Au and 7.49% Sb (Larabie, 1985). A random chip sample across 1.5 m of the same quartz-ankerite vein, hosted in sheared metabasalt, yielded 3.3% Cu, 0.02% Pb, 0.45% Zn, 435 g/t Ag, 0.65 g/t Au and 0.29% As (Durfeld, 1986). Elevated As and Sb values suggest the presence of tennantite ( $\text{Cu}_{12}\text{As}_4\text{S}_{13}$ ) in addition to tetrahedrite ( $\text{Cu}_{12}\text{Sb}_4\text{S}_{13}$ ) within the veins. A weakly pyritized north-trending Fe-carbonate alteration zone crosscuts quartz-epidote±pyrite-replaced volcanoclastic rocks in an exploration pit adjacent to the logging road access. A grab sample from this alteration zone is barren (Table 2, station 08JLO7-76.).

## TARN

The Tarn showing (MINFILE 093B 057) is located 1.5 km northeast of the Quesnel River in epidote-amphibolite-facies metavolcanic rocks of the Green Volcanoclastic succession. The showing is spatially associated with an aeromagnetic high coincident with the southwestern contact aureole of the Quesnel River pluton. Sparse Cu, Mo, Au and Ag mineralization has developed along fractures and as local disseminations in the metavolcanic rocks adjacent to hornblende-biotite monzogranite, coarse biotite quartz monzodiorite and felsite units that characterize the southern margin of the pluton. Trenching and sampling around the original discovery site returned values that averaged 0.67% Cu, 0.029% Mo, 7.3 g/t Ag and 0.4 g/t Au (Campbell et al., 1981). Follow-up rock sampling of skarn-, chlorite- and silica-altered metavolcanic, felsite, diorite and feldspar porphyry units could duplicate but not expand these anomalies beyond the original showings. Soil geochemistry recognized anomalous Cu, Mo, Ag and Au values, but their erratic distribution led Campbell et al. (1981) to conclude there was not an economic target present on the property.

The mineralized showings were not sampled during the current mapping project.

## NYLAND LAKE

The Nyland Lake showing (MINFILE 093B 053) is classified incorrectly as a Mo showing located in the centre of Nyland Lake. Assessment reports covering the area indicate anomalous Au values in heavy-mineral pan concentrates and concluded a lode Au potential for the area (Troup and Freeze, 1985). The area, approximately 1.5 km west of Nyland Lake, contains the east-trending altered contact between Nicola Group metavolcanic rocks and granite of the Quesnel River pluton. Calcsilicate and sulphide assemblages overprint the metavolcanic rocks adjacent to the southern contact zone of the pluton, which is characterized by abundant narrow granite apophyses and aplite and pegmatite dikes. A single grab sample of epidote-garnet-chlorite-quartz-altered metavolcanic rock, taken adjacent to the contact with granite, returned a Au-only anomaly of 40 ppb (Table 2).

## MISCELLANEOUS MINERALIZATION

Geochemical grab sample 07GLE34-162 consists of strongly altered (bleached, silicified and pyritized), grey to green, fine-grained volcanoclastic rock cut by sulphide-bearing centimetre-thick quartz veins. Bleaching and surface oxidation have produced an outcrop of brown-, orange- and green-weathered rock that returned anomalous values in As, Nb and W (Table 2). The sample site is located close to the contact between the Cottonwood River succession and the Western Volcanoclastic succession.

Molybdenum mineralization is associated with aplite dikes cutting diorite at the Daphne showing (MINFILE 093A 123), located immediately adjacent to the southeast corner of NTS area 093B/16. Molybdenite occurs with quartz in stringers, as specks in the aplite and as fracture coatings in the diorite (Petersen, 1976).

## CONCLUSIONS

The Quesnel River map area includes Middle Triassic to Early Jurassic sedimentary, volcanic and plutonic rocks of the Quesnel terrane and younger units that overlie the Cache Creek terrane in the southwestern part of the map area.

These younger rocks include Jurassic Dragon Mountain sedimentary rocks; Eocene dacite and basalt; Oligocene to Miocene sedimentary rocks; and thick accumulations of unconsolidated Quaternary deposits. The thickest accumulation of Quaternary deposits is preserved in a 4 km wide, north-trending Pleistocene valley that follows the east side of the Fraser River.

The Nicola Group has been divided into two main units in the Quesnel River map area: an Eastern Sedimentary succession (ESS) and Western Volcanoclastic succession (WVS). These can be traced northwestward along strike into correlative Nicola units of the Cottonwood map area (Logan et al., 2008) and southeast into the Mount Polley area (Logan et al., 2007b). The ESS comprises a package of disrupted, green and grey cherty argillite, siltstone, limestone and tuffaceous sandstone that correlates with the Cottonwood River succession (Logan, 2008), and a mixed package of pyroxene volcanoclastic rocks and Middle Triassic dark phyllite, siltite and slate that correlate with the Eastern Volcanoclastic and Black pelite successions to the north in the Cottonwood map area (Logan et al., 2008). The WVS is a pyroxene-rich volcanoclastic succession, characterized by green and maroon, polyolithic volcanic conglomerate interbedded with limestone, maroon and/or green pyroxene basalt, and fine-grained, bedded volcanoclastic rocks, that correlates with rocks of the same name in the Cottonwood map area (Logan, et al., 2008). The Cottonwood River succession and conformably overlying Western Volcanoclastic succession are Late Triassic or older because the upper part of the succession is cut by monzonite of the Late Triassic (207 Ma) Mouse Mountain stock.

The isolated limestone located north of Hallis Lake has been reinterpreted as a crinoid ossicle-rich, Late Triassic grainstone rather than a Cambrian archaeocyathid-bearing rock (Tipper, 1978).

The area southeast of the Quesnel River is underlain by a coarsening-upward sequence of sedimentary rocks of Triassic (?)/Early Jurassic to Middle (?) Jurassic age that comprises a lower package of black, thin-banded phyllite and pyritic and calcareous argillite and siltstone, and an upper

sequence of thick-bedded or massive, volcanic- and plutonic-clast conglomerate, quartz grit, limestone and greywacke. The Ashcroft Formation of southern BC formed in a fore-arc basin from material shed from the uplifted Nicola volcanic-plutonic arc and Cache Creek accretionary wedge (Travers, 1978). A similar interpretation is postulated for the Dragon Mountain succession in the Quesnel River map area. Cache Creek rocks form the basement to the southwestern part of the map area, where they are overlain mainly by the Dragon Mountain succession. A gradational stratigraphic contact between the Late Triassic Green Volcaniclastic succession (Nicola Group) and Early Jurassic Dragon Mountain succession is apparent east of Dragon Lake, suggesting that deposition was continuous from Late Triassic through early Jurassic. This implies that the Dragon Mountain succession is an overlap assemblage linking the Cache Creek basement rocks in the map area to the Nicola Group fore-arc (Quesnel terrane) prior to the end of the Late Triassic. This interpretation is further supported by relationships at the Gibraltar mine, 30 km to the south. Here 212 Ma subduction-generated arc plutons intrude Cache Creek rocks that probably occupied a fore-arc setting to the nascent Nicola arc prior to the culmination, in the Late Triassic, of Nicola Group arc magmatism.

Intrusive rocks in the map area include the Early Jurassic (ca. 193 Ma) Polaris suite of mafic-ultramafic complexes, synkinematic Middle Jurassic (165, 160, 158 Ma) suite of granite, and Tertiary (ca. 50 Ma) suite of alkalic mafic dikes. Discrete brittle shear zones with oblique-dextral sense of shear cut across the Middle Jurassic Quesnel River pluton.

Mineralization in the Quesnel River map area is associated with emplacement of high-level intrusions and comprises a Late Triassic (?) to Early Jurassic episode characterized by Zn-Pb±Mo-Au, an Early Jurassic episode of Au±Cu and a Middle Jurassic episode of Cu-Au-Mo deposition.

An early Miocene tectonic event produced anticlines in Oligocene sedimentary rocks.

## ACKNOWLEDGMENTS

Fieldwork in the Quesnel River map area, undertaken between 2006 and 2008, benefited from the capable and enthusiastic field assistance of a number of people: Leslie Able, Graham Leroux and Brian Hawes from the University of Victoria; Matt McManus from Camosun College; and Stewart Butler from Malspina College. Many thanks are extended to Mike J. Orchard and Terry Poulton of the Geological Survey of Canada for providing micro- and macrofossil identifications, and to Richard Friedman and Thomas Ullrich of the Pacific Centre for Isotopic and Geochemical Research at the University of British Columbia for providing the geochronological analyses that are so critical to these mapping projects. This program was partially funded through the Geological Survey of Canada's Geoscience for Pine Beetle program.

## REFERENCES

- Ash, C.H., Reynolds, P.H., Creaser, R.A. and Mihalynuk, M.G. (2007):  $^{40}\text{Ar}/^{39}\text{Ar}$  and Re-O isotopic ages for hydrothermal alteration and related mineralization at the Highland Valley Cu-Mo deposit (NTS 0921), southwestern British Columbia; in *Geological Fieldwork 2006, BC Ministry of Energy, Mines and Petroleum Resources*, Paper 2007-1, pages 19–24.
- Bacon, W.R. (1964): Geological, geochemical and geophysical report on the Gerimi and Sam claim group, Quesnel River area; submitted by Mastodon-Highland Bell Mines Ltd, *BC Ministry of Energy, Mines and Petroleum Resources*, Assessment Report 639.
- Bailey, D.G. (1988): Geology of the central Quesnel belt, Hydraulic, south-central British Columbia (93A/12); in *Geological Fieldwork 1987, BC Ministry of Energy, Mines and Petroleum Resources*, Paper 1988-1, pages 147–153.
- Bailey, D.G. (1989): Geology of the central Quesnel belt, Swift River, south-central British Columbia (93B/16, 93A/12, 93G/1); in *Geological Fieldwork 1988, BC Ministry of Energy, Mines and Petroleum Resources*, Paper 1989-1, pages 167–172.
- Bailey, D.G. (1990): Geology of the central Quesnel Belt, British Columbia; *BC Ministry of Energy, Mines and Petroleum Resources*, Open File 1990-31, 1:100 000 scale map with accompanying notes
- Barr, D.A., Fox, P.E., Northcote, K.E. and Preto, V.A. (1976): The alkaline suite porphyry deposits: a summary; in *Porphyry Deposits of the Canadian Cordillera*, Sutherland Brown, A., Editor, *Canadian Institute of Mining and Metallurgy*, Special Volume 15, pages 359–367.
- Bloodgood, M.A. (1987): Deformational history, stratigraphic correlations and geochemistry of eastern Quesnel Terrane rocks in the Crooked Lake area, central British Columbia, Canada; unpublished MSc thesis, *University of British Columbia*, Vancouver, BC, 165 pages.
- Breitsprecher, K. and Mortensen, J.K. (2004): BC Age 2004A-1: a database of isotopic age determinations for rock units from British Columbia; *BC Ministry of Energy, Mines and Petroleum Resource*, Open File 2004-03.
- Bysouth, G.D. (1987): Diamond drill report on the ZE group, Cariboo Mining Division; submitted by Gibraltar Mines Ltd., *BC Ministry of Energy, Mines and Petroleum Resources*, Assessment Report 15764.
- Bysouth, G.D., Campbell, K.V., Barker, G.E. and Gagnier, G.K. (1995): Tonalite-trondhjemite fractionation of peraluminous magma and the formation of syntectonic porphyry copper mineralization, Gibraltar mine, central British Columbia; in *Porphyry Deposits of the Northwestern Cordillera of North America*, Schroeter, T.G., Editor, *Canadian Institute of Mining, Metallurgy and Petroleum*, Special Volume 46, pages 201–213.
- Campbell, C.J., Hardy, J.L. and Hodgson, G.D. (1981): Geology, geochemistry and geophysics of the B.C. Miller claims; submitted by Riocanex Inc, *BC Ministry of Energy, Mines and Petroleum Resources*, Assessment Report 9891.
- Carson, J.M., Dumont, R., Potvin, J., Shives, R.B.K., Harvey, B.J.A. and Buckle, J.L. (2006): Geophysical series – NTS 93G/1, 93G/8 and 93B/16 – Cottonwood, British Columbia; *Geological Survey of Canada*, Open File 5288, 10 maps at 1:50 000 scale.
- Colpron, M. and Price, R.A. (1995): Tectonic significance of the Kootenay Terrane, southeastern Canadian Cordillera: an alternative model; *Geology*, Volume 23, pages 25–28.
- Cross Lake Minerals Ltd. (2007): QR gold mine commences operations; Cross Lake Minerals Ltd., press release, September 11, 2007, URL <[http://www.crosslakeminerals.com/s/NewsReleases.asp?ReportID=207636&\\_Type=NewsReleases&\\_Title=QR-Gold-Mine-Commences-Operations](http://www.crosslakeminerals.com/s/NewsReleases.asp?ReportID=207636&_Type=NewsReleases&_Title=QR-Gold-Mine-Commences-Operations)> [November 2008].
- Dalrymple, G.B. (1979): Critical tables for conversion of K-Ar ages from old to new constants; *Geology*, Volume 7, pages 558–560.

- Dawson, G.M. (1877): Report on explorations in British Columbia; *Geological Survey of Canada*, Reports on Explorations and Surveys of 1875–76, pages 233–280.
- Dolphin, K. (1988): Quesnel canyon placer project; submitted by Freegold Recovery Inc, *BC Ministry of Energy, Mines and Petroleum Resources*, Assessment Report 16736.
- Durfeld, R.M. (1986): Geochemical and geological report on the Mandy property; submitted by Mandalla Resources Ltd, *BC Ministry of Energy, Mines and Petroleum Resources*, Assessment Report 15130.
- Fox, P.E. (1975): Alkaline rocks and related mineral deposits of the Quesnel Trough, British Columbia (abstract); *Geological Association of Canada–Mineralogical Association of Canada*, Joint Annual Meeting, Program with Abstracts, page 12.
- Fox, P.E. (1985): Drilling report on the Gerimi claims, Cantin Creek area, BC; submitted by Dome Exploration (Canada) Limited, *BC Ministry of Energy, Mines and Petroleum Resources*, Assessment Report 13765.
- Fox, P.E. (1990): Drilling report on the Gerimi 1 to 7 claims, Cantin Creek area, BC; submitted by Placer Dome Inc, *BC Ministry of Energy, Mines and Petroleum Resources*, Assessment Report 20125.
- Fraser (1974): Geology of the Kate group, Cariboo Mining Division; submitted by Noranda Exploration Company Ltd, *BC Ministry of Energy, Mines and Petroleum Resources*, Assessment Report 4914.
- Frebald, H. and Tipper, H.W. (1969): Lower Jurassic rocks and fauna near Ashcroft, British Columbia and their relation to some granitic plutons (92-1); *Geological Survey of Canada*, Paper 69-23, 20 pages.
- Ghent, E.D., Erdmer, P., Archibald, D.A. and Stout, M.Z. (1996): Pressure-temperature and tectonic evolution of Triassic lawsonite-aragonite blueschists from Pinchi Lake, British Columbia; *Canadian Journal of Earth Sciences*, Volume 33, pages 800–810.
- Goodall, G.N. and Fox, P.E. (1989): Drilling report on the Gerimi claims, Cantin Creek area, BC; submitted by Placer Dome Inc, *BC Ministry of Energy, Mines and Petroleum Resources*, Assessment Report 18783.
- Holland, S.S. (1968): Ab, Ano, XI; in Annual Report of the BC Minister of Mines and Petroleum Resources for 1967, *BC Ministry of Energy, Mines and Petroleum Resources*, page 124.
- Hora, Z.D. (2008): Diatomite resource assessment in the Quesnel area, central British Columbia; in Geological Fieldwork 2007, *BC Ministry of Energy, Mines and Petroleum Resources*, Paper 2008-1, pages 31–38.
- Imperial Metals Corporation (2008): Imperial updates mineral reserve and mineral resource estimates for Mount Polley and Huckleberry resource; Imperial Metals Corporation, press release, March 31, 2008, URL <[http://www.imperialmetals.com/s/News-2008.asp?ReportID=294096&\\_Type=News-Release-2008&\\_Title=Imperial-Updates-Mineral-Reserve-and-Mineral-Resource-Estimates-for-Mount-P](http://www.imperialmetals.com/s/News-2008.asp?ReportID=294096&_Type=News-Release-2008&_Title=Imperial-Updates-Mineral-Reserve-and-Mineral-Resource-Estimates-for-Mount-P)> [November 2008].
- Irvine, T.N. (1974): Alaskan-type ultramafic-gabbroic rocks in the Aiken Lake, McConnell Creek and Toodoggone map-areas; *Geological Survey of Canada*, Paper 76-1A, pages 76–91.
- Jonnes, S. and Logan, J.M. (2007): Bedrock geology and mineral potential of Mouse Mountain (NTS 093G/01), central British Columbia; in Geological Fieldwork 2006, *BC Ministry of Energy, Mines and Petroleum Resources*, Paper 2007-1 and *Geoscience BC*, Report 2007-1, pages 55–66.
- Klepacki, D. W., and Wheeler, J.O. (1985): Stratigraphic and structural relations of the Milford, Kaslo and Slocan groups, Goat Range, Lardeau and Nelson map areas, British Columbia; in Current Research, Part A, *Geological Survey of Canada*, Paper 85-1A, pages 277–286.
- Larabee, E.N. (1985): Geological, geochemical and geophysical report on the Mandy property; submitted by Mandalla Resources Ltd, *BC Ministry of Energy, Mines and Petroleum Resources*, Assessment Report 14816.
- Lay, D. (1935): Cousin Jack, Quesnel Mining Division, northeastern mineral survey district (No. 2); in Annual Report of the BC Minister of Mines for 1934, *BC Ministry of Energy, Mines and Petroleum Resources*, page C29.
- Lay, D. (1939): Baker Creek; in BC Minister of Mines Report for 1938, *BC Ministry of Energy, Mines and Petroleum Resources*, pages C36–C39.
- Lay, D. (1940): Fraser River Tertiary drainage history in relation to placer gold deposits; *BC Ministry of Energy, Mines and Petroleum Resources*, Bulletin 3, pages 1–30.
- Lay, D. (1941): Fraser River Tertiary drainage history in relation to placer gold deposits, part II; *BC Ministry of Energy, Mines and Petroleum Resources*, Bulletin 11, pages 1–75.
- Logan, J.M. (2008): Geology and mineral occurrences of the Quesnel Terrane, Cottonwood map sheet, central British Columbia (NTS 093G/01); in Geological Fieldwork 2007, *BC Ministry of Energy, Mines and Petroleum Resources*, Paper 2008-1, pages 69–86.
- Logan, J.M. and Bath, A.B. (2006): Geochemistry of Nicola Group basalt from the central Quesnel Trough at the latitude of Mount Polley (NTS 093A/5, 6, 11, 12), central BC; in Geological Fieldwork 2005, *BC Ministry of Energy, Mines and Petroleum Resources*, Paper 2006-1, pages 83–98.
- Logan, J.M. and Mihalynuk, M.G. (2005): Regional geology and setting of the Cariboo, Bell, Springer and Northeast Porphyry Cu-Au zones at Mount Polley, south-central British Columbia; in Geological Fieldwork 2004, *BC Ministry of Energy, Mines and Petroleum Resources*, Paper 2005-1, pages 249–270.
- Logan, J.M., Bath, A.B., Mihalynuk, M.G., Ullrich, T.D., Friedman, R. and Rees, C.J. (2007b): Regional geology of the Mount Polley area, central British Columbia; *BC Ministry of Energy, Mines and Petroleum Resources*, Geoscience Map 2007-1.
- Logan, J.M., Leroux, G. and Able, L. (2008): Regional geology of the Cottonwood area, central British Columbia (NTS 093G/01); *BC Ministry of Energy, Mines and Petroleum Resources*, Open File 2008-06.
- Logan, J.M., Mihalynuk, M.G., Ullrich, T. and Friedman, R.M. (2007a): U-Pb ages of intrusive rocks and  $^{40}\text{Ar}/^{39}\text{Ar}$  plateau ages of copper-gold-silver mineralization associated with alkaline intrusive centres at Mount Polley and the Iron Mask batholith, south and central British Columbia; in Geological Fieldwork 2006, *BC Ministry of Energy, Mines and Petroleum Resources*, Paper 2007-1 and *Geoscience BC*, Report 2007-1, pages 93–116.
- Lu, J. (1989): Geology of the Cantin Creek area Quesnel River, (93B/16); in Geological Fieldwork 1988, *BC Ministry of Energy, Mines and Petroleum Resources*, Paper 1989-1, pages 173–181.
- MacDonald, R.C. (1991): 1991 diamond drilling program Gerimi 1 to 7 claims, Cantin Creek area, BC; submitted by Phelps Dodge Corporation of Canada, Limited, *BC Ministry of Energy, Mines and Petroleum Resources*, Assessment Report 21461.
- Massey, N.W.D., MacIntyre, D.G., Desjardins, P.J. and Cooney, R.T. (2005): Digital geology map of British Columbia: whole province; *BC Ministry of Energy, Mines and Petroleum Resources*, GeoFile 2005-1.
- Mathews, W.H. (1989): Neogene Chilcotin basalts in south-central British Columbia; *Canadian Journal of Earth Sciences*, Volume 26, pages 969–982.

- MINFILE (2008): MINFILE BC mineral deposits database; *BC Ministry of Energy, Mines and Petroleum Resources*, URL <<http://www.empr.gov.bc.ca/Mining/Geoscience/MINFILE/Pages/default.aspx>> [November 2008].
- Mihalynuk, M.G., Erdmer, P., Ghent, E.D., Cordey, F., Archibald, D.A., Friedman, R.M. and Johannson, G.G. (2004): Coherent French Range blueschist: subduction to exhumation in <2.5 m.y.?; *Geological Society of America Bulletin*, Volume 116, numbers 7–8, pages 910–922.
- Mihalynuk, M.G., Nelson, J. and Diakow, L. (1994): Cache Creek terrane entrapment: oroclinal paradox within the Canadian Cordillera; *Tectonics*, Volume 13, pages 575–595.
- Miller-Tait, J. (2004): Diamond drilling report on the Cantin Creek property; submitted by Cross Lake Minerals Ltd, *BC Ministry of Energy, Mines and Petroleum Resources*, Assessment Report 27548.
- Monger, J.W.H. and Berg, H.C. (1984): Lithotectonic terrane map of western Canada and southeastern Alaska: in *Lithotectonic Terrane Maps of the North American Cordillera*, Siberling, N.J. and Jones, D.L., Editors, *United States Geological Survey*, Open File Report 84-523.
- Mortimer, N. (1987): The Nicola Group: Late Triassic and Early Jurassic subduction-related volcanism in British Columbia; *Canadian Journal of Earth Sciences*, Volume 24, pages 2521–2536.
- Moynihan, D.P. and Logan, J.M. (2009): Geological relationships on the western margin of the Naver pluton, central British Columbia (NTS 093G/08); in *Geological Fieldwork 2008*, *BC Ministry of Energy, Mines and Petroleum Resources*, Paper 2009-1, pages 153–162.
- Nixon, G.T., Archibald, D.A., and Heaman, L.M. (1993): <sup>40</sup>Ar-<sup>39</sup>Ar and U-Pb geochronometry of the Polaris Alaskan-type complex, British Columbia; precise timing of Quesnellia-North America interaction, *Geological Association of Canada-Mineralogical Association of Canada*, Joint Annual Meeting, Program with Abstracts, Volume 17, p. 76.
- Nixon, G. T., Hammack, J.L., Ash, C.H., Cabri, L.J., Case, G., Connelly, J.N., Heaman, L.M., Laflamme, J.H.G., Nuttall, C., Paterson, W.P.E. and Wong, R.H. (1997): Geology and platinum-group-element mineralization of Alaskan-type ultramafic-mafic complexes in British Columbia; *BC Ministry of Energy, Mines and Petroleum Resources*, Bulletin 93, 141 pages.
- Orchard, M.J. (2007a): Report on conodonts and other microfossils, Quesnel (93B); *Geological Survey of Canada*, Conodont Data File, Report No. MJO-2007-29.
- Orchard, M.J. (2007b): Report on conodonts and other microfossils, Quesnel (93A) Telegraph Creek (104G); *Geological Survey of Canada*, Conodont Data File, Report No. MJO-2007-18.
- Panteleyev, A., Bailey, D.G., Bloodgood, M.A. and Hancock, K.D. (1996): Geology and mineral deposits of the Quesnel River-Horsefly map area, central Quesnel Trough, British Columbia; *BC Ministry of Energy, Mines and Petroleum Resources*, Bulletin 97, 156 pages.
- Patterson, I. and Harakal, J. (1974): Potassium-argon dating of blueschists from Pinchi Lake, central British Columbia; *Canadian Journal of Earth Sciences*, Volume 11, pages 1007–1011.
- Petersen, D.B. (1976): Geological, geochemical and geophysical report on the Nyland Lake/Quesnel Area; submitted by Rio Tinto Canadian Exploration, *BC Ministry of Energy, Mines and Petroleum Resources*, Assessment Report 6076.
- Petersen, N.T. (2001): Provenance of Jurassic sedimentary rocks of Quesnellia: implications for paleogeography; unpublished MSc thesis, *University of British Columbia*, 153 pages.
- Petersen, N.T., Smith, P.L., Mortensen, J.K., Creaser, R.A. and Tipper, H.W. (2004): Provenance of Jurassic sedimentary rocks of south-central Quesnellia, British Columbia: implications for paleogeography; *Canadian Journal of Earth Sciences*, Volume 41, pages 103–125.
- Rees, C.J. (1987): The Intermontane-Omineca Belt boundary in the Quesnel Lake area, east-central British Columbia: tectonic implications based on geology, structure and paleomagnetism; unpublished PhD thesis, *Carleton University*, Ottawa, ON, 421 pages.
- Roback, R.C., Sevigny, J.H. and Walker, N.W. (1994): Tectonic setting of the Slide Mountain terrane, southern British Columbia; *Tectonics*, Volume 13, pages 1242–1258.
- Rouse, G.E. and Mathews, W.H. (1979): Tertiary geology and palynology of the Quesnel area, British Columbia; *Bulletin of Canadian Petroleum Geology*, Volume 27, pages 418–445.
- Schiarizza, P. (1989): Structural and stratigraphic relationships between the Fennell Formation and Eagle Bay Assemblage, western Omineca Belt, south-central British Columbia: implications for Paleozoic tectonics along the paleocontinental margin of western North America; unpublished MSc thesis, *University of Calgary*, Calgary, AB, 343 pages.
- Schiarizza, P. and Macauley, J. (2007): Geology and mineral occurrences of the Hendrix Lake area, south-central British Columbia (93A/02); in *Geological Fieldwork 2006*, *BC Ministry of Energy, Mines and Petroleum Resources*, Paper 2007-1 and *Geoscience BC*, Report 2007-1, pages 179–202.
- Selwyn, A.R.C. (1872): Journal and report on British Columbia by Mr. Selwyn: *Geological Survey of Canada*, Report on Progress for 1871–72, pages 16–72.
- Sproule, J.C. and Associates (1953): Report on geological survey of British Columbia petroleum and natural gas permit No. 549; *British Columbia Department of Mines and Petroleum Resources*, unpublished report, pages 1–16.
- Struik, L.C. (1984): Stratigraphy of Quesnel terrane near Dragon Lake, Quesnel map area, central British Columbia; *Geological Survey of Canada*, Paper 84-1A, pages 113–116.
- Struik, L.C. (1986): Imbricated terranes of the Cariboo gold belt with correlations and implications for tectonics in southeastern British Columbia; *Canadian Journal of Earth Sciences*, Volume 23, pages 1047–1061.
- Struik, L.C. (1988): Regional imbrication within Quesnel Terrane, central British Columbia, as suggested by conodont ages; *Canadian Journal of Earth Sciences*, Volume 25, pages 1608–1617.
- Struik, L.C., Fuller, E.A. and Lynch, T.E. (1990): Geology of Prince George (east half) map area (93G/E); *Geological Survey of Canada*, Open File 2172.
- Struik, L.C., Parrish, R.R. and Gerasimoff, M.D. (1992): Geology and age of the Naver and Ste Marie plutons, central British Columbia; in *Radiogenic Age and Isotopic Studies: Report 5*; *Geological Survey of Canada*, Paper 91-2, pages 155–162.
- Sutherland Brown, A. (1957): Mouse Mountain (53° 122° S.E.); in *Minister of Mines Annual Report 1956*, *BC Ministry of Energy, Mines and Petroleum Resources*, page 33.
- Taseko Mines Limited (2008): Taseko Mines Limited Gibraltar reserve update; Taseko Mines Limited, press release, December 11, 2008, URL <[http://www.tasekomines.com/tko/NewsReleases.asp?ReportID=331641&\\_Type=NewsReleases&\\_Title=Taseko-Mines-Ltd.-Gibraltar-Reserve-Update](http://www.tasekomines.com/tko/NewsReleases.asp?ReportID=331641&_Type=NewsReleases&_Title=Taseko-Mines-Ltd.-Gibraltar-Reserve-Update)> [December 22, 2008].
- Tipper, H.W. (1959): Quesnel map area, British Columbia; *Geological Survey of Canada*, Map 12-1959.
- Tipper, H.W. (1978): Northeast part of Quesnel (93B) map area, British Columbia; in *Current Research, Part A*, *Geological Survey of Canada*, Paper 78-1A, pages 67–68.
- Travers, W.B. (1978): Overturned Nicola and Ashcroft strata and their relations to the Cache Creek Group, southwestern

Intermontane Belt, British Columbia; *Canadian Journal of Earth Sciences*, Volume 15, pages 99–116.

Troup, A.G. and Freeze, J.C. (1985): Geochemical report on the Nyland Lake gold property, Cariboo Mining Division, BC; submitted by A.T. Syndicate, *BC Ministry of Energy, Mines and Petroleum Resources*, Assessment Report 13640.

Turner, J. A. (1983): Geological and geochemical report on the Phantom 1 claim, Cariboo Mining Division; submitted by Newmont Exploration of Canada Ltd, *BC Ministry of Energy, Mines and Petroleum Resources*, Assessment Report 11458.

# Geological Relationships on the Western Margin of the Naver Pluton, Central British Columbia (NTS 093G/08)

by D.P. Moynihan<sup>1</sup> and J.M. Logan

**KEYWORDS:** Quesnel, Slide Mountain, Kootenay, Barkerville, Crooked amphibolite, Snowshoe Group, Nicola Group, Naver pluton, deformation, metamorphism, contact aureole

## INTRODUCTION

The Naver pluton occupies approximately 700 km<sup>2</sup> southeast of Prince George in east-central British Columbia (Figures 1, 2). It comprises mostly granite and granodiorite. The pluton intrudes rocks of the Nicola Group, the Crooked amphibolite and the Snowshoe Group, and crosscuts tectonically significant boundaries between these units. The pluton was studied by Struik et al. (1992), who obtained U-Pb zircon and monazite crystallization ages of ca. 113 Ma and described the pluton as being nonfoliated except directly adjacent to faults.

Here we report on observations made during preliminary mapping of the southwestern part of NTS map area 093G/08 (1:50 000), incorporating the western part of the Naver pluton and adjacent metasedimentary and metavolcanic rocks. A primary finding is that rather than being a homogeneous post-tectonic intrusion, the Naver pluton is a composite body including a deformed western part. The post-tectonic 113 Ma part of the composite body was intruded at shallow levels into low-grade metamorphic rocks, resulting in a Buchan-type contact aureole. This contrasts with the older part, which was penetratively deformed with midcrustal amphibolite-facies rocks and lacks a contact aureole.

## REGIONAL GEOLOGY

The Naver pluton intrudes across the boundaries separating the Quesnel, Slide Mountain and Kootenay terranes, three major tectonic components of the Canadian Cordillera (Figure 1).

The Quesnel terrane represents an extensive (>2000 km) west-facing calcalkaline-alkaline Late Triassic–Early Jurassic arc that developed outboard or proximal to the western margin of North America. It is characterized by Mesozoic arc volcanic and sedimentary rocks of the



**Figure 1.** Location of the NTS 093G/08 map sheet, marked with a red box. The Quesnel terrane is shown in green and the Cache Creek terrane in dark grey. The locations of Cu-Au-Ag±PGE alkaline porphyry deposits are also shown.

Nicola, Takla and Stuhini groups and coeval plutonic rocks. At this latitude, the western part of the Nicola Group is dominated by forearc volcanoclastic-dominated successions that grade eastward across the arc into backarc Middle–Late Triassic fine-grained clastic rocks (the black phyllite unit of Rees, 1987). Rocks of the Nicola Group record an eastward shift in the locus of magmatism through time and a change from early calcalkaline to alkaline magmatism.

The eastern margin of the Quesnel terrane is marked by a discontinuous belt of variably sheared mafic and ultramafic rocks of the Crooked amphibolite. These rocks are assigned to the Slide Mountain terrane, a Late Paleozoic marginal basin assemblage (Schiarizza, 1989; Roback et al., 1994) of oceanic basalt and chert that separated Quesnellia from North America. The Eureka thrust, an east-verging thrust fault, marks the eastern boundary of the Slide Mountain terrane (Struik, 1986). The footwall to the Eureka thrust comprises Proterozoic–Paleozoic Snowshoe Group rocks of the Barkerville subterrane, a northern extension of the Kootenay terrane (Monger and Berg, 1984), which are pericratonic and likely represent distal sedimentation of ancestral North America (Colpron and Price, 1995). In this region, a conglomerate close to the base of the Nicola Group contains foliated clasts derived

<sup>1</sup>Department of Geoscience, University of Calgary, Calgary, AB

This publication is also available, free of charge, as colour digital files in Adobe Acrobat® PDF format from the BC Ministry of Energy, Mines and Petroleum Resources website at <http://www.empr.gov.bc.ca/Mining/Geoscience/PublicationsCatalogue/Fieldwork/Pages/default.aspx>.



## VOLCANICLASTIC UNIT (T<sub>NV</sub>)

The volcanoclastic unit is dominated by green- or orange-weathering conglomerate with boulder- to granule-size volcanic and subvolcanic clasts. Conglomerate is interbedded with finer-grained reworked deposits of lithic and crystal sandstone and siltstone, and lesser fine cherty sedimentary rocks. The sandstone and siltstone are well sorted and commonly display normal grading. These epiclastic units are interlayered with coarse pyroxene-phyric±pyroxene-plagioclase-phyric basaltic breccia flows and hyaloclastite deposits.

This unit is correlative with similar rocks to the southeast that have yielded Middle–Late Triassic conodonts (M. Orchard, pers comm, 2007). The magnetic susceptibility values in this area are low, while correlative pyroxene-phyric volcanoclastic rocks located southeast of the study area (NTS 093G/01 and 093B/16) have moderate–high magnetic susceptibility and a distinctive geophysical signature on regional aeromagnetic maps.

## Jurassic Mafic Intrusion

An elongate, northwest-trending mafic-ultramafic composite intrusion crops out within the Nicola Group in the southwest corner of the study area (Figure 2). The intrusion consists mainly of commingling melanocratic and leucocratic phases of gabbro, pyroxenite and hornblende; with lesser porphyritic biotite quartz diorite and felsic segregations. The intrusion is sheared, cut by numerous brittle northwest-trending faults and has been extensively altered to chlorite, epidote and serpentine. Metasomatic alteration has produced decimetre-wide sections of rock containing 75–85% coarse biotite and chlorite. The base- and precious-metal content of the intrusion is low (Kowalchuk, 1988).

Similar mafic complexes are present in the Cottonwood map area (Logan, 2008) and farther south in the Canim Lake area (Schiarrizza and Macauley, 2007). Radiometric crystallization and cooling ages from these complexes span the Early Jurassic (Sinemurian–Pliensbachian) from 192 to 183 Ma (Schiarrizza and Macauley, 2007; T. Ullrich, pers comm, 2008).

## Naver Pluton

The Naver pluton is a composite body including an undeformed eastern and southern part and a deformed western part. Radiometric dating of the undeformed parts of the pluton has yielded U–Pb crystallization ages of 113 Ma and K–Ar biotite cooling ages of 107–98 Ma (Struik et al., 1992). A sample of the deformed western margin was collected and submitted to the Pacific Centre for Isotopic and Geochemical Research at The University of British Columbia for U–Pb and <sup>40</sup>Ar/<sup>39</sup>Ar dating. Results are pending.

## NAVER II PLUTON

Most of the Naver pluton is, as described by Struik et al. (1992), undeformed orthoclase-megacrystic biotite granite–granodiorite with a variable texture from equigranular to megacrystic. Biotite is contained throughout, locally accompanied by muscovite or hornblende adjacent to contacts, with local alteration of hornblende, biotite and plagioclase. This part of the body includes the eastern two-thirds of the main subspherical northern part, and the elongate

tail that cuts across terrane boundaries (Figure 2). We refer to this as the Naver II pluton.

## NAVER I PLUTON

The Naver I pluton is an elongate, foliated body occupying the northwest part of the composite Naver pluton. It trends parallel to strike and is truncated by the Naver II pluton at its southern end. Its western margin is a gradational zone tens of metres wide comprising country rock mixed with sheets of granite and pegmatite, which are commonly approximately parallel to foliation (Figure 3a). The percentage of country rock decreases eastward across the transition zone, but elongate strike-parallel inclusions are common at a variety of scales throughout the body. The foliation in screens of country rock is consistently oriented parallel to that outside the pluton. These features suggest the Naver I pluton grew by the progressive intrusion of dikes whose orientation was influenced by foliation planes.

Rocks of the Naver I pluton are deformed biotite granodiorite that have undergone recrystallization and grain-size reduction. Large K-feldspar crystals up to 1.5 cm are locally preserved, but porphyroclasts of K-feldspar and plagioclase are typically <5 mm in length. These porphyroclasts sit in a fine-grained, strained matrix of quartz, plagioclase, myrmekite, biotite and accessory phases, with secondary chlorite and muscovite. Locally, where the pluton is well foliated and highly porphyroclastic, the rock takes on the appearance of augen gneiss. Biotite is the only mafic silicate phase present, and primary muscovite is restricted to rocks adjacent to inclusions of the Snowshoe Group. Here it is often concentrated in thin granitic veins, which sometimes also contain garnet. Muscovite and garnet are common in pegmatite on the gradational western margin of the pluton, where granitic sheets are intermixed with country rock.

The boundary between the Naver I and Naver II plutons is constrained by field observations, but the precise location shown in Figure 2 is inferred from aeromagnetic data. The extent to which aeromagnetic patterns accurately define the boundary will be tested during the 2009 field season. The two-fold subdivision adopted here is preliminary; future work may show that it is an oversimplification.

## STRUCTURAL GEOLOGY

### Deformation of the Naver I Pluton

Granitic rocks belonging to the Naver I phase are foliated and lineated (Figure 3b, c). The S–L fabric is defined by aligned biotite crystals, flattened and elongated quartz-feldspar aggregates and quartz lenses. In most places the foliation (S<sub>NG</sub>) has a moderate dip to the southwest and the stretching lineation (L<sub>NG</sub>) pitches steeply, approximately down the dip of the foliation (Figure 4a). In a few locations around the margins, steep foliations with anomalous strikes were measured. Due to the lack of exposure, the relationship between these fabrics and the dominant southeast-trending fabric is unknown, but in some of these locations there are superimposed localized foliated zones oriented close to average S<sub>NG</sub>.

There is a general westward increase in the intensity of deformation within the Naver I body—deformed granite on the western margin forms slabby outcrops parallel to the topographic slope (Figure 3b), whereas outcrops farther

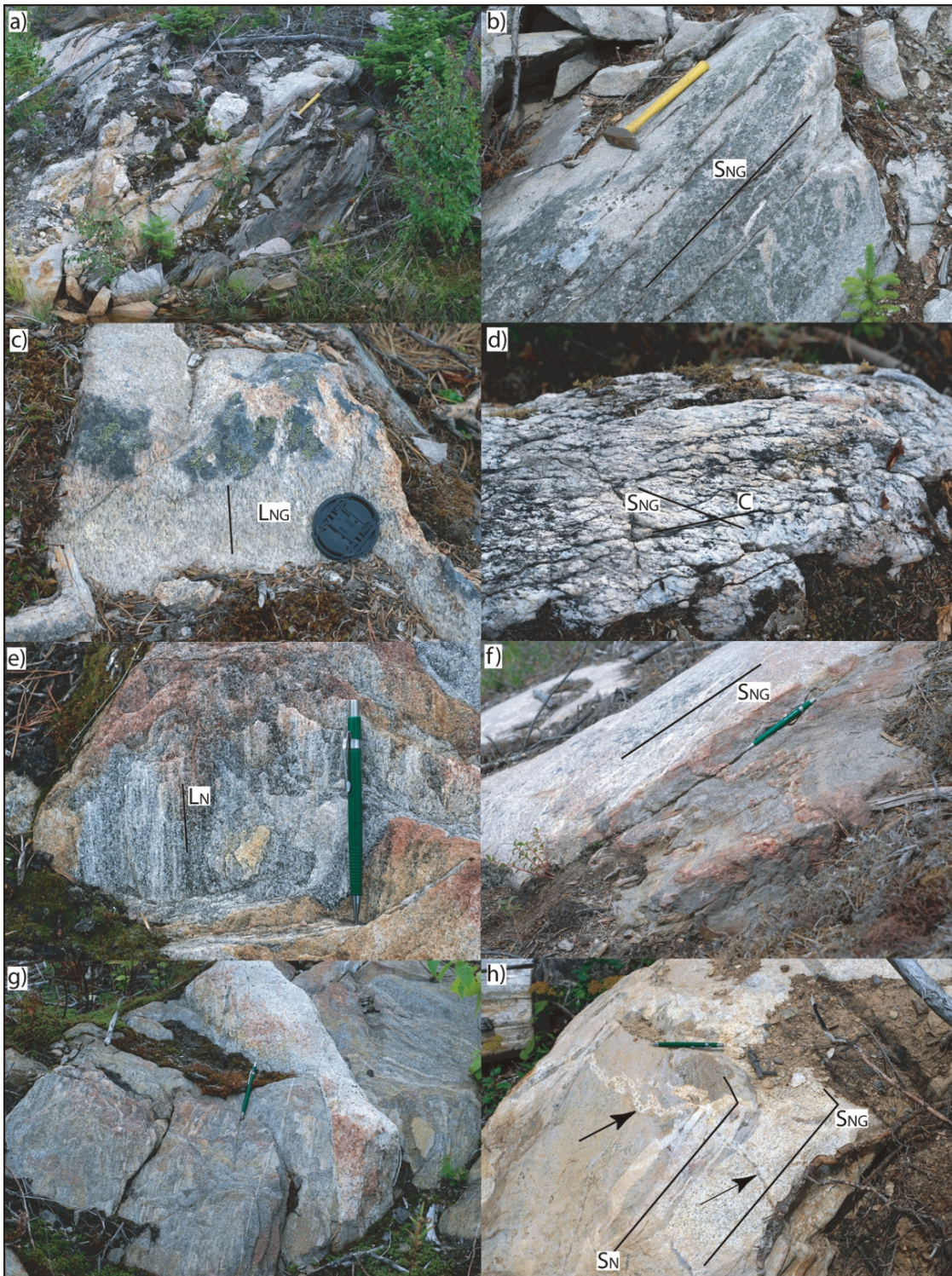


**Figure 3.** **a)** Outcrop on the western margin of the Naver I pluton showing rocks of the Snowshoe Group intruded by a granitic sheet, rock hammer for scale. **b)** Foliated granite of the Naver I pluton forms slabby outcrops, rock hammer for scale. **c)** Mineral lineation ( $L_{NG}$ ) defined by aligned biotite and elongate quartz-feldspar aggregates, viewed on the  $S_{NG}$  surface, lens cap for scale. **d)** Two foliations displaying S-C relationship on the western margin of the Naver I pluton. The shape fabric ( $S_N$ ) is cut by discrete shear bands (SB); width of field of view is 20 cm **e)** Downdip mineral and intersection lineations in the Snowshoe Group on the margin of the Naver I pluton, pencil for scale. **f)** Fold of the dominant fabric ( $S_N$ ) in the Snowshoe Group on the margin of the Naver I pluton; its axial plane is parallel to average  $S_N$ . The granitic sheet cuts  $S_N$ , but is foliated parallel to average  $S_N$ , pencil for scale. **g)** Granitic dike intruded into the Snowshoe Group on the margin of the Naver I pluton. The dike cuts  $S_N$ , but is itself foliated parallel to  $S_N$ , pencil for scale. **h)** Granitic dike foliated parallel to  $S_N$  in the Snowshoe Group host. This is cut by a thin granitic vein, which is folded. The axial planes of these folds are parallel to  $S_N$  in the Snowshoe Group schist, pencil for scale.

east are more massive and the fabric is less well developed. On the western margin of the Naver I intrusion, two fabrics are locally developed (Figure 3d). The S-L fabric is cut by discrete shear bands, forming S-C or S-C' geometry. These fabrics indicate west-side-down (normal-sense) shearing, approximately parallel to  $L_{NG}$ . Normal-sense shearing is also indicated by sigmoidal recrystallized tails on K-feldspar porphyroclasts. These features suggest the Naver I body was deformed by a west-side-down (normal-sense) simple or general shear, which was concentrated on its western margin.

### Deformation of the Snowshoe and Nicola Groups

#### $D_N$

The dominant planar tectonic fabric ( $S_N$ ) in the Snowshoe and Nicola groups on the western margin of the Naver I pluton dips moderately to steeply to the southwest (Figure 4b). It is variably expressed as a continuous, disjunctive or crenulation cleavage and is typically parallel to compositional layering. A planar fabric with the same orientation is developed in the Slide Mountain rocks. A mineral lineation ( $L_N$ ) is visible in rocks that are sufficiently coarse-grained, namely schist of the Snowshoe Group and some parts of the volcanic Nicola Group. Wherever observed together, mineral lineations ( $L_N$ ) and intersection lineations ( $L_{NI}$ , intersection of  $S_N$  with  $S_0$ ) are parallel. These lineations pitch at highly variable (shallow–very steep) angles on  $S_N$  from the south-southeast (Figure 3e).

Shear band cleavage (S-C' fabric), indicating west-side-down shearing and extension along  $S_N$ , is developed in the Snowshoe Group close to its contact with the Nicola Group (around UTM Zone 10, 5917368N, 0537392E, NAD 83). This is the only well-exposed section across the contact that was mapped and metamorphic contrasts suggest the two units are in normal fault contact (*see below*). It is not known whether this postulated fault passes northeast or southwest of ultramafic rocks where they are present along this boundary.

#### $D_{N+1}$

Around the western margin of the Naver I pluton, close folds of  $S_N$ , whose axial planes are approximately parallel to average  $S_N$ , are developed. Axes of these folds pitch gently to steeply on  $S_N$  from the south-southeast. Some of these folds are truncated by granitic dikes of the Naver I pluton (Figure 3f). Folds of  $S_N$  are also locally developed in enclaves of the Snowshoe Group within the Naver I pluton where  $S_N$  lies at a high angle to  $S_{NG}$ . Although these folds are classified as  $F_{N+1}$  (Figure 4), they can plausibly be interpreted as resulting from progressive  $D_N$  rather than a distinct episode of deformation.

#### $D_{N+2}$

The youngest ductile structures recognized are crenulations ( $F_{N+2}$ ), which plunge approximately downdip. These crenulations are gentle–open, with axial planes at a high angle to strike. Crenulations with these orientations and characteristics postdate the formation of porphyroblasts of andalusite and cordierite in the contact aureole; this folding therefore postdates the intrusion of the Naver I pluton at 113 Ma. Larger-scale  $F_{N+2}$  folding is interpreted to be responsible for the significant variation in the orientation of  $S_N$  across the area, as measured values of  $S_N$  are

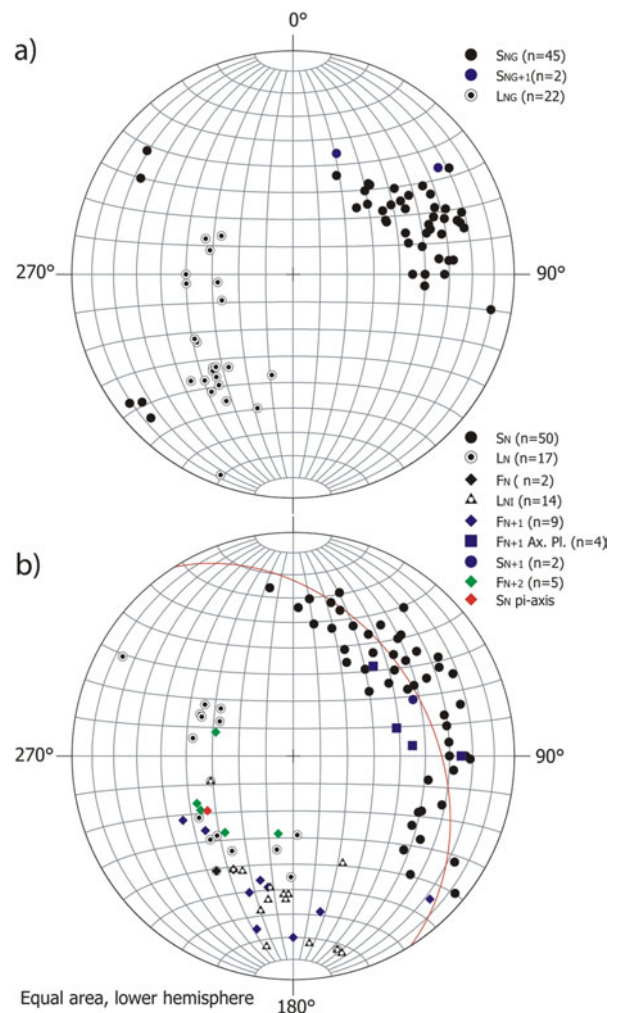


**Figure 4.** Equal-area lower-hemisphere stereonet projections of structural data from the western margin of the Naver I pluton and adjacent rocks: **a)** data from the Naver I pluton; **b)** data from rocks of the Snowshoe Group, Crooked amphibolite and Nicola Group (black phyllite unit) adjacent to the western margin of the intrusion.

spread along a girdle whose  $\sigma_1$ -axis approximately coincides with the orientation of  $F_{N+2}$  crenulation axes.

### Relationship of Structures in the Naver I Pluton to those in the Snowshoe and Nicola Groups

The planar fabric ( $S_N$ ) in the Snowshoe Group and  $S_{NG}$  in the Naver I pluton have the same overall orientation. Granitic dikes on the western margin of the Naver I pluton typically cut  $S_N$ , but exhibit a foliation ( $S_{NG}$ ) that is parallel to  $S_N$  (Figure 3g). This implies that the strain that produced  $S/L_{NG}$  in the Naver I pluton is a subset of the strain that produced  $S/L_N$  in the Snowshoe Group. The Naver I and its host were deformed together and display congruent kinematic indicators. The simplest interpretation, adopted here, is that each of these units records the same period of west-side-down simple or general shear. It is possible that this deformation was synchronous with the intrusion of the Naver I pluton; the presence of variably deformed, cross-cutting dikes (Figure 3h) is compatible with, but not diagnostic of, syntectonic intrusion.

The planar fabric ( $S_N$ ) in the Nicola Group is parallel to that in the Snowshoe Group, and crenulations of  $S_{N-1}$  are locally preserved in each. There is evidence in the region for deformation of the Snowshoe Group prior to the deposition of the Nicola Group (McMullin et al., 1990), but earlier structures restricted to the Snowshoe Group were not identified in the course of this study.

## METAMORPHIC PETROLOGY

### Regional Metamorphism

Rocks of the Nicola Group have undergone regional greenschist-facies metamorphism. This is manifested in chlorite-muscovite-quartz-plagioclase assemblages in phyllitic metapelite of the black phyllite unit, and chlorite-plagioclase ( $\pm$ epidote) assemblages in metabasite of the volcanoclastic unit. Biotite is absent from phyllite but is present, along with amphibole, in calcisilicate belonging to  $T_{NV}$ .

In contrast, garnet and biotite are widely distributed in metapelitic schist and micaceous quartzite of the Snowshoe Group (this study; Struik et al., 1992), and the metapelite is coarser-grained than its Triassic equivalents. Amphibolite is also present in the Snowshoe Group. All nonequant metamorphic minerals are aligned in the plane of  $S_N$  in both the Snowshoe and the Nicola groups.

The difference in metamorphic grade between the Nicola and Snowshoe groups is exemplified by a series of outcrops west of the Naver I pluton (northeast from UTM Zone 10, 5917157N, 0537203E). Here, there is intermittent exposure in a small stream gully for a cross-strike distance of approximately 260 m. Chlorite-zone phyllite of the Nicola Group is exposed in the southwest, whereas outcrops of Snowshoe Group schist at the northeast end of the section include the assemblage kyanite-staurolite-garnet-biotite-muscovite-chlorite(retrograde)-plagioclase-ilmenite (Figure 5). No direct P-T estimates have been obtained from these rocks, but schist with this assemblage forms under conditions of approximately 650–700°C and 6.5–8 kb in metapelites of widely varying bulk composition.

The kyanite zone metapelite exhibits shear band cleavage ( $S-C'$  fabric) indicating west-side-down (normal-sense) shearing. Overgrowth by kyanite of sigmoidal foliation traces between these shear bands attests to a temporal overlap between normal-sense shearing and peak Barrovian metamorphism.

Given the large difference in metamorphic grade over a cross-strike distance of approximately 260 m, and the evidence for normal-sense shearing in the amphibolite-facies rocks, the Snowshoe Group–Nicola Group contact is interpreted as a normal fault/shear zone.

### Contact Metamorphism

A contact metamorphic aureole extends approximately 1 km from the western boundary of the Naver II pluton. Here, the assemblage cordierite-andalusite-biotite-quartz-plagioclase-ilmenite is widely developed in metapelitic rocks of the black phyllite unit of the Nicola Group (Figure 6). Porphyroblasts of cordierite and andalusite overgrow the  $S_N$  foliation (locally a crenulation cleavage) with no preferred orientation, giving rise to a hornfelsic texture.

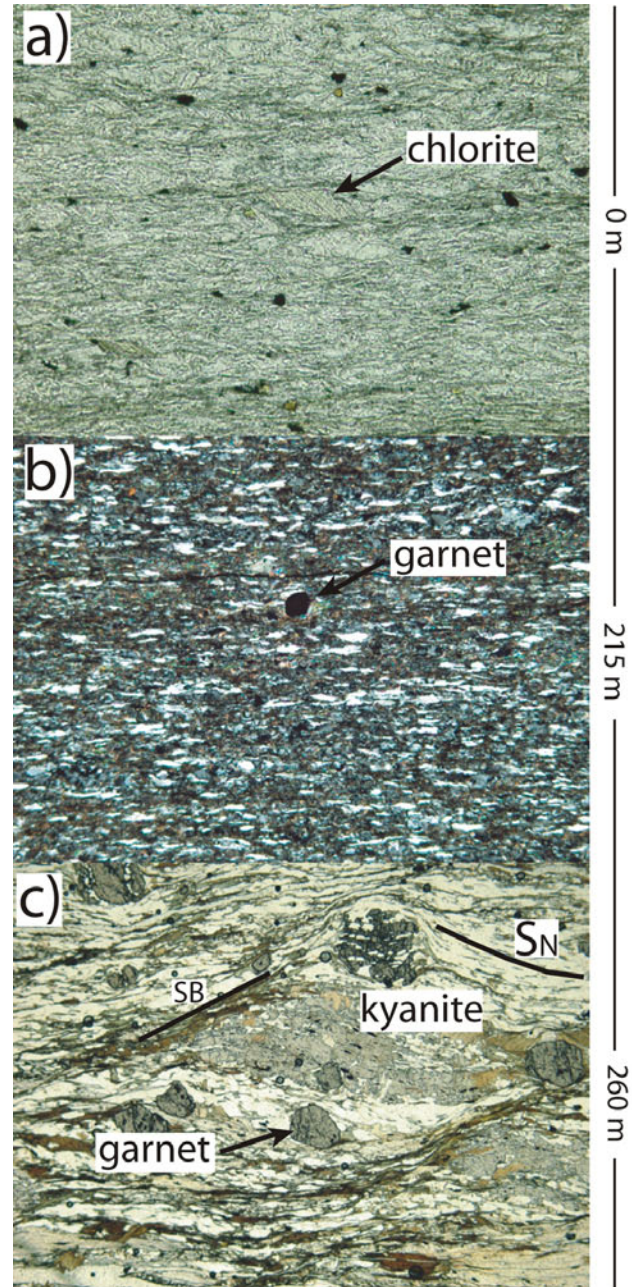


**Figure 5.** Photomicrographs of three rocks sampled perpendicular to the metamorphic discontinuity at the Nicola Group–Snowshoe Group boundary; the rock shown in a) is separated from the rock shown in c) by a cross-strike distance of 260 m: a) greenschist-facies Nicola Group phyllite with chlorite- and muscovite-rich matrix and small chlorite porphyroblasts; field of view = 1.5 mm; b) phyllite/fine-grained schist with biotite- and muscovite-rich matrix and small garnet crystals; field of view = 3 mm; c) Snowshoe Group kyanite-garnet schist with well-developed shear bands; kyanite crystals overgrow sigmoidal deflections into west-side-down shear bands; field of view = 6 mm; the large change in metamorphic grade across this transect and the evidence for normal-sense shearing in the Snowshoe Group suggests the Nicola Group–Snowshoe Group contact is a fault or shear zone.



**Table 1.** Whole-rock x-ray fluorescence (XRF) major-element analysis of 08DMO36-393: a metapelitic hornfels sample from the contact aureole of the Naver pluton.

<b>SiO<sub>2</sub></b>	56.79%
<b>TiO<sub>2</sub></b>	1.10%
<b>Al<sub>2</sub>O<sub>3</sub></b>	22.98%
<b>Fe<sub>2</sub>O<sub>3</sub></b>	7.06%
<b>MnO</b>	0.07%
<b>MgO</b>	1.80%
<b>CaO</b>	1.01%
<b>Na<sub>2</sub>O</b>	1.53%
<b>K<sub>2</sub>O</b>	2.04%
<b>P<sub>2</sub>O<sub>5</sub></b>	0.16%
<b>Ba</b>	0.08%
<b>LOI</b>	4.66%
<b>Total</b>	99.28%

ical crustal density, this means that the 113 Ma Naver II pluton was intruded at a depth of approximately 10 km or less.

This diagram also places a constraint on the regional metamorphism undergone by Nicola Group phyllite prior to the intrusion of the Naver II pluton. As these rocks did not develop biotite, garnet or staurolite during regional metamorphism, the temperature cannot have exceeded approximately 510–540°C (depending on pressure).

## DISCUSSION

The interpretations presented here are based on a small dataset and are preliminary. Nevertheless, the new observations contradict previous work and require a revised interpretation of the Naver pluton and its contact relations.

The main, younger part of the Naver pluton has a simple history. It was intruded into the upper crust at 113 Ma, after deformation and metamorphism of surrounding rocks, and cooled below approximately 280°C (the closure temperature of biotite) by 107–98 Ma (Struik et al., 1992). It crosscuts structures and places a minimum age on major boundaries between units.

The older part of the Naver pluton lacks a contact aureole and does not cut across strike. Instead it was deformed with middle-amphibolite-facies rocks that recrystallized in the middle crust. Normal-sense shearing in the Snowshoe Group overlapped with peak metamorphism, and if the same period of normal-sense shearing affected the Naver I pluton, it must also have been deformed and metamorphosed under the same conditions.

All the rocks in the area were exhumed to shallow levels by 113 Ma. The difference in pressure between the Barrovian regional metamorphism in the Snowshoe Group and the Buchan contact metamorphism provides an estimate of net exhumation of the Snowshoe Group between the time of peak deformation and the intrusion of the Naver II body. The difference is approximately 5 kb, implying approximately 18 km of exhumation during this interval.

The Naver II pluton provides a lower age limit to the deformation in all units. It crosscuts the deformation fabrics and the postulated normal fault between the Snowshoe and Nicola groups. Work is underway to ascertain the crystallization age of the Naver I pluton, but at this time the only absolute constraints are provided by the depositional ages of the units themselves. The Ste Marie pluton, which was intruded at 167 Ma, is post-tectonic with respect to the regional foliation in the surrounding Nicola Group. It is therefore likely that deformation and metamorphism in the Nicola Group around the Naver pluton predated the intrusion of the Ste Marie pluton. However, the possibility that, as in the Cariboo Mountains, metamorphism and deformation in the higher-grade rocks are younger than at shallower structural levels (Reid, 2003) cannot be ruled out.

The Snowshoe Group–Nicola Group contact is interpreted as a normal fault or shear zone due to the large, discrete contrast in metamorphic grade and the presence of normal-sense kinematic indicators close to the contact. No evidence for thrust-sense shearing was observed. Snowshoe Group rocks record a higher metamorphic grade than the Nicola Group black phyllite along strike to the southeast (Logan, 2008; Struik, 1988), and the possibility that the contact is a normal fault elsewhere along this boundary is worthy of investigation. This postulated normal fault is much older than similar Tertiary structures in southeast BC (Parrish et al., 1988) as it is truncated by the Naver II pluton. The only ductile structures that are demonstrably younger than 113 Ma are  $F_{N+2}$  folds, which postdate the Naver II contact aureole.

## ACKNOWLEDGMENTS

Thanks to Matthew McManus and Stewart Butler for assistance in the field and to Christopher Coueslan for reviewing the manuscript.

## REFERENCES

- Colpron, M. and Price, R.A. (1995): Tectonic significance of the Kootenay Terrane, southeastern Canadian Cordillera: an alternative model; *Geology*, Volume 23, pages 25–28.
- de Capitani, C. and Brown, T.H. (1987): The computation of chemical equilibrium in complex systems containing non-ideal solutions; *Geochimica et Cosmochimica Acta*, Volume 51, pages 2639–2652.
- Ghent, E.D., Erdmer, P., Archibald, D.A. and Stout, M.Z. (1996): Pressure-temperature and tectonic evolution of Triassic lawsonite-aragonite blueschists from Pinchi Lake, British Columbia; *Canadian Journal of Earth Sciences*, Volume 33, pages 800–810.
- Holland, T.J.B. and Powell, R. (1990): An enlarged and updated internally consistent thermodynamic dataset with uncertainties and correlations: the system  $K_2O-Na_2O-CaO-MnO-MgO-FeO-Fe_2O_3-Al_2O_3-TiO_2-SiO_2-C-H_2O_2$ ; *Journal of Metamorphic Geology*, Volume 8, pages 89–124.
- Holland, T.B.J. and Powell, R. (2003): Activity-composition relations for phases in petrological calculations: an asymmetric multicomponent formulation; *Contributions to Mineralogy and Petrology*, Volume 145, pages 492–501.
- Kowalchuck, J.M. (1988): Diamond drilling report on the Yardley Lake property, Cariboo Mining Division, BC; submitted by Gabriel Resources, *BC Ministry of Energy, Mines and Petroleum Resources*, Assessment Report 15926, 247 pages.
- Logan, J.M. (2008): Geology and mineral occurrences of the Quesnel Terrane, Cottonwood map sheet, central British Co-

- lumbia (NTS 093G/01); in *Geological Fieldwork 2007, BC Ministry of Energy, Mines and Petroleum Resources*, Paper 2008-1, pages 69–85.
- Logan, J.M. and Moynihan, D.P. (2009): Geology and mineral occurrences of the Quesnel River map area, central British Columbia (NTS 093B/16); in *Geological Fieldwork 2008, central British Columbia, BC Ministry of Energy, Mines and Petroleum Resources*, Paper 2009-1, pages 127–152.
- Logan, J.M., Bath, A.B., Mihalynuk, M.G., Ullrich, T.D., Friedman, R. and Rees, C.J. (2007): Regional geology of the Mount Polley area, central British Columbia; *BC Ministry of Energy, Mines and Petroleum Resources*, Geoscience Map 2007-1, scale 1:50 000.
- McMullin, D.W.A., Greenwood, H.J. and Ross, J.V. (1990): Pebbles from Barkerville and Slide Mountain terranes in a Quesnel Terrane conglomerate: evidence for pre-Jurassic deformation of the Barkerville and Slide Mountain terranes; *Geology*, Volume 18, pages 962–965.
- Massey, N.W.D., MacIntyre, D.G., Desjardins, P.J. and Cooney, R.T. (2005): Digital geology map of British Columbia: whole province; *BC Ministry of Energy, Mines and Petroleum Resources*, Geofile 2005-1.
- Mihalynuk, M.G., Erdmer, P., Ghent, E.D., Cordey, F., Archibald, D.A., Friedman, R.M. and Johannson, G.G. (2004): Coherent French Range blueschist: subduction to exhumation in <2.5 m.y.?; *Geological Society of America Bulletin*, Volume 116, Number 7/8, pages 910–922.
- Monger, J.W.H. and Berg, H.C. (1984): Lithotectonic terrane map of western Canada and southeastern Alaska: in *Lithotectonic Terrane Maps of the North American Cordillera*, Siberling, N.J. and Jones, D.L., Editors, *United States Geological Survey*, Open File Report 84-523.
- Parrish, R., Carr, S. and Parkinson, D. (1988): Eocene extensional tectonic and geochronology of the southern Omineca Belt, British Columbia and Washington; *Tectonics*, Volume 7, pages 181–212.
- Patterson, I. and Harakal, J. (1974): Potassium-argon dating of blueschists from Pinchi Lake, central British Columbia; *Canadian Journal of Earth Sciences*, Volume 11, pages 1007–1011.
- Rees, C.J. (1987): The Intermontane-Omineca belt boundary in the Quesnel Lake area, east central British Columbia: tectonic implications based on geology, structure and paleomagnetism; Ph.D. thesis, Carleton University, 421 pages.
- Reid, L.F. (2003): Stratigraphy, structure, petrology, geochronology and geochemistry of the Hobson Lake area (Cariboo Mountains, British Columbia) in relation to the tectonic evolution of the southern Canadian Cordillera; Ph.D. thesis, University of Calgary, 221 pages.
- Roback, R.C., Sevigny, J.H. and Walker, N.W. (1994): Tectonic setting of the Slide Mountain Terrane, southern British Columbia; *Tectonics*, Volume 13, pages 1242–1258.
- Schiarizza, P. (1989): Structural and stratigraphic relationships between the Fennell Formation and Eagle Bay assemblage, western Omineca Belt, south-central British Columbia: implications for Paleozoic tectonics along the paleocontinental margin of western North America; M.Sc. thesis, University of Calgary, 343 pages.
- Schiarizza, P. and Macauley, J. (2007): Geology and mineral occurrences of the Hendrix Lake area, south-central British Columbia (093A/02); in *Geological Fieldwork 2006, BC Ministry of Energy, Mines and Petroleum Resources*, Paper 2007-1 and *Geoscience BC*, Report 2007-1, pages 179–202.
- Struik, L.C. (1986): Imbricated terranes of the Cariboo gold belt with correlations and implications for tectonics in southeastern British Columbia; *Canadian Journal of Earth Sciences*, Volume 23, pages 1047–1061.
- Struik, L.C. (1988): Structural geology of the Cariboo gold mining district, east-central British Columbia; *Geological Survey of Canada*, Memoir 421, 100 pages.
- Struik, L.C., Parrish, R.R. and Gerasimoff, M. D. (1992): Geology and age of the Naver and Ste Marie plutons, central British Columbia; in *Radiogenic Age and Isotopic Studies: Report 5*, *Geological Survey of Canada*, Paper 91-2, pages 155–162.
- Tinkham, D.K. and Ghent, E.D. (2005): Estimating P-T conditions of garnet growth with isochemical phase diagram sections and the problem of effective bulk composition; *The Canadian Mineralogist*, Volume 43, pages 35–50.
- Travers, W.B. (1977): Overturned Nicola and Ashcroft strata and their relations to the Cache Creek Group, southwestern Intermontane Belt, British Columbia; *Canadian Journal of Earth Sciences*, Volume 15, pages 99–116.



# Lithogeochemistry of the Spanish Mountain Gold Deposit, British Columbia (NTS 093A/11W)

by K. Paterson<sup>1</sup>, R.E. Lett and K.Telmer<sup>1</sup>

**KEYWORDS:** lithogeochemistry, alteration, Spanish Mountain, mineral deposits, Au, Carlin-type deposits, sediment-hosted disseminated Au deposits.

## INTRODUCTION

The Spanish Mountain mineral property, located in the Cariboo region of central British Columbia is approximately 6 km east of the community of Likely in NTS map area 093A/11W (Figure 1). The deposit is hosted within a metasedimentary package of the Quesnel Terrane that occupies the hangingwall to the Eureka thrust, a structure that separates the Quesnel Terrane of the Intermontane Belt from the Kootenay Terrane of the Omineca Belt. The main geotectonic framework of the area includes the Cache Creek, Quesnel, Slide Mountain and Kootenay terranes (Figure 2). Skygold Ventures Ltd. currently owns 100% interest in the Spanish Mountain property and has been participating in the exploration of the property since 2003.

Sediment-hosted vein-type deposits along the Carlin trend in Nevada contain >200 million oz of Au (production+reserves+resources) and these deposits account for a large portion of production in the United States (Sillitoe, 2008). A similar style of Au deposits have also been discovered in China, Russia, Mexico, Southeast Asia and South America (Lefebure et al., 1999) and it has been suggested that accreted terranes such as Quesnel and Stikine, with basement carbonate rock types and associated intrusive events could host this type of sediment-related Au mineralization (Poulson, 1996). The Spanish Mountain property is described as an orogenic- or sediment-hosted Au deposit (Singh, 2008) based on the calcareous argillite hostrocks with microscopic Au, alteration style and tectonic setting. Spanish Mountain does not possess the same geochemical signature as sediment-hosted Au deposits described by Schroeter and Poulson (1996). To date, the only pathfinder element identified is Au.

## FIELDWORK

Fieldwork was undertaken in June 2008, and consisted of a broad sampling of bedrock lithological units identified on the property by Skygold Ventures Ltd. (Singh, 2008). Skygold detected a negative correlation between Mg and

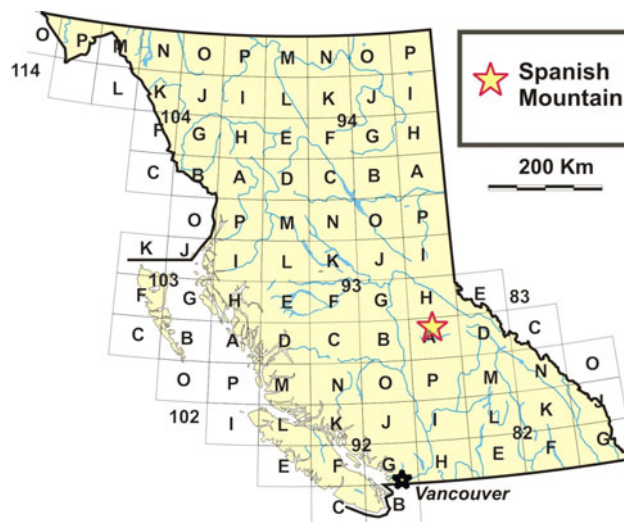


Figure 1. Location of the Spanish Mountain study area, central BC.

Mn within Au-bearing rock types from an examination of their lithogeochemical data (Singh, 2008). Interest lies in inferring how the geochemistry of Au-bearing zones and barren rock differ from each other and from those of previous sediment-hosted Au deposits. With this in mind, 35 surface outcrop samples were obtained, targeting Mg-Fe carbonate-enriched samples often containing substantial

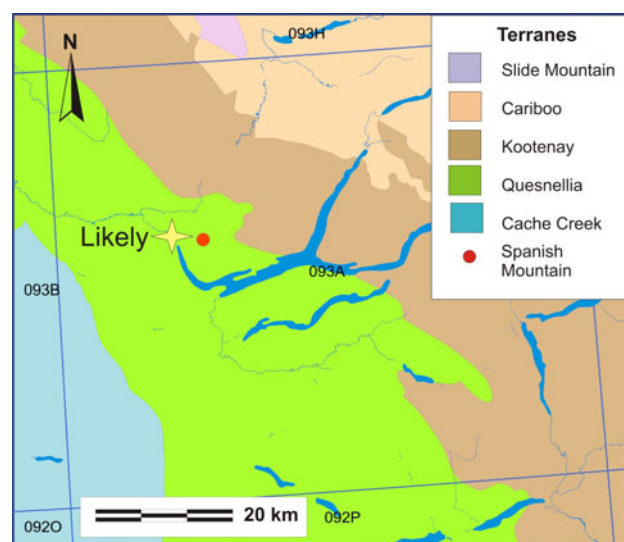


Figure 2. Geology of NTS map area 093A showing the relationship of host Quesnel Terrane to that of the Kootenay Terrane.

<sup>1</sup>School of Earth and Ocean Sciences, University of Victoria, Victoria, BC

This publication is also available, free of charge, as colour digital files in Adobe Acrobat® PDF format from the BC Ministry of Energy, Mines and Petroleum Resources website at <http://www.empr.gov.bc.ca/Mining/Geoscience/PublicationsCatalogue/Fieldwork/Pages/default.aspx>.

sericite. The majority of samples collected were of the more competent wacke and siltstone units due to the emphasis on collecting unweathered samples to obtain suitable material for laser ablation inductively coupled-plasma mass spectrometry (ICP-MS) analysis. However, hostrocks for the majority of Au mineralization are phyllite and argillite, which are typically deeply weathered and oxidized. Skygold Ventures Ltd. generously donated 18 additional samples of diamond-drill core to supplement the surface outcrop samples. These samples provided examples of relatively unoxidized barren and ore-grade specimens. Figure 3 shows the location of samples taken for geochemical analysis and for preparation of thick and thin sections.

## SAMPLE ANALYSIS

All rock samples were prepared for geochemical analysis at the BC Geological Survey (BCGS) Laboratory in Victoria, BC. Rock samples were first crushed to <2 mm using a jaw crusher fitted with hardened chromium-steel plates, then split into 100–200 g subsamples using a Jones splitter. Subsamples were taken from the <2 mm material for milling. A tungsten-carbide (W-C) ring and puck mill

was used to mill one subsample of the jaw-crushed material for major oxide analysis, while a second subsample for minor- and trace-element analysis was prepared using a chrome-steel (Cr-Fe) ring and puck mill. A quartz sand was milled between each sample to minimize intersample contamination. Time and care were taken to choose fresh rock surfaces, but due to the extreme surface oxidation and extensive heterogeneity of veining within samples, milled portions may contain minor built-in bias of certain elements (e.g., SiO<sub>2</sub>). Duplicate samples were inserted to monitor analytical precision, and known rock standards were added to measure accuracy.

A portion of each milled sample was analyzed for major oxides at Global Discovery Laboratories Ltd. (Vancouver, BC) on a fused disk with a Siemens Model SRS 3000 x-ray fluorescence spectrometer. Hafnium, niobium and zirconium (high field-strength elements) were also analyzed by x-ray fluorescence using a lithium metaborate-tetraborate pressed pellet and a Siemens SRS 3000 x-ray fluorescence spectrometer. Loss on ignition (LOI) was also determined at 1100°C by Global Discovery Laboratories. Other subsamples of the Cr-Fe milled material were analyzed for 42 trace elements at Acme Analytical Laboratories (Vancouver, BC) by hydrofluoric-perchloric-nitric-hydrochloric acid digestion followed by a combination of inductively coupled plasma-emission and mass spectrometry (ICP-ES and ICP-MS) as well as for 37 major and trace elements by a less rigorous aqua regia (HCl, HNO<sub>3</sub>, H<sub>2</sub>O) digestion followed by ICP-MS. The samples were also analyzed by Acme Analytical Laboratories for carbonate C by hydrochloric acid digestion and Leco combustion. A further set of subsamples was analyzed for 33 elements including Au and a selection of rare-earth elements by instrumental neutron activation analysis (INAA). Selected samples were analyzed for rare-earth elements at Memorial University (St. John's, NL) by sodium peroxide sinter and ICP-MS. The advantage of using different nondestructive and extraction (total and partial) methods for analyzing elemental concentrations is that the data produced should aid in determining the most reliable analytical method for a given element or Group of elements in further research. Table 1 summarizes detection limits for elements analyzed by the different methods. Twenty-six selected rock specimens were sectioned at the BC Geological Survey and cut samples sent to Vancouver Petrographics (Langley, BC) for thin and thick section preparation.

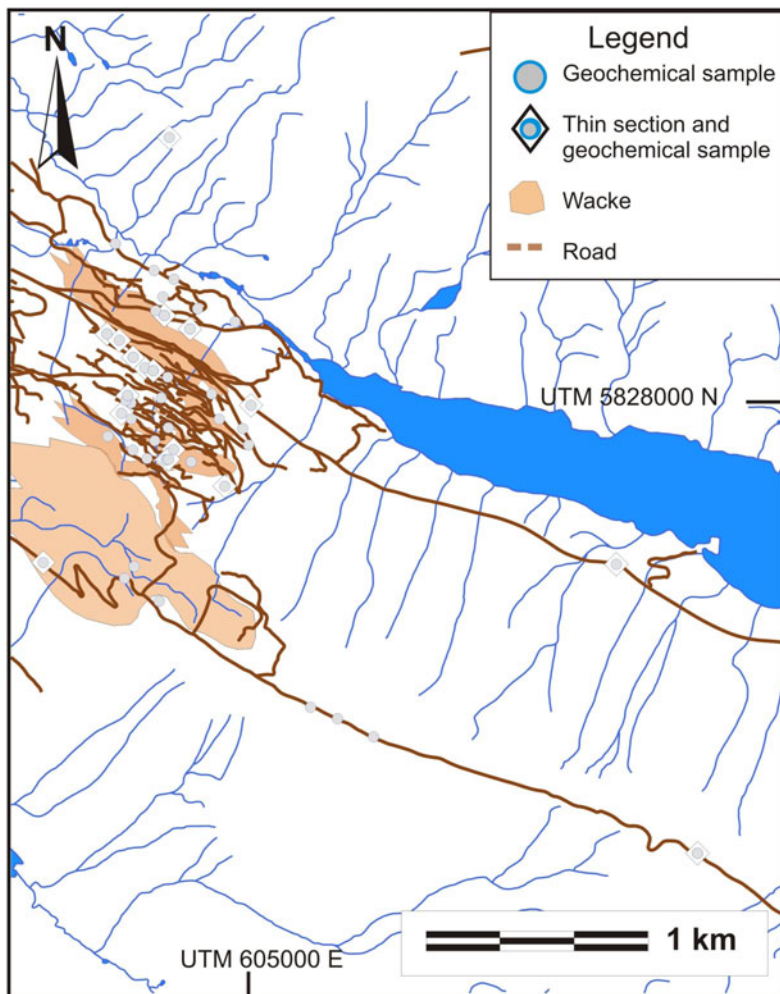


**Figure 3.** The Spanish Mountain property, with sample locations for petrographic and geochemical analysis highlighted. Wacke surface trace provided by Skygold Ventures Ltd.

## GEOLOGY

### Regional Geology

Gold mineralization at Spanish Mountain is hosted in metasedimentary rocks of the Late Triassic to Early Jurassic Nicola Group (Bloodgood, 1988) or its northern equivalent the Takla Group (Rees, 1987). In the eastern part of the property, these sedi-

Element	XRF	AR	ICP-MS	HF ICP-MS	INAA	REE	Other
Units	ppm	ppm	ppm	ppm	ppm	ppm	%
Ag		0.002	0.1		5		
Al		200	100				
As		0.1	1		0.5		
Au		0.0002	0.1		0.002		
B		20					
Ba		0.5	1		50		
Bi		0.02	0.1				
Be			1				
Br					0.5		
Ca		200	100		10000		
Cd		0.01	0.1				
Ce			1		3	0.14	
Co		0.1	0.2		1		
Cr		0.5	1		5		
Cs					1		
Cu		0.01	0.1				
Dy						0.3	
Ho						0.06	
Er						0.24	
Eu					0.2	0.18	
Fe		200	100		100		
Ga		0.1				0.35	
Hf			0.1		1	0.39	
Hg		0.005			1		
Ho						0.06	
Ir					0.005		
K		200	100				
La		0.5	0.1		0.5	0.18	
Li			0.1				
Lu					0.05	0.09	
LOI							0.01
Mg		200	100				
Mn		1	1				
Mo			0.1		1		
Na		20	10		100		
Nb	3		0.1				
Nd					5	1.1	
Ni		0.1	0.1		20		
P		10	10				
Pb		0.01	0.1				
Pr						0.11	
Rb			0.1		15		
S		400	1000				
Sb		0.02	0.1		0.1		
Sc		0.1	1		0.1		
Se		0.1			3		
Sm					0.1	0.8	
Sn			0.1		200		
Sr		0.5	1		500		
Ta			0.1		0.5	0.42	
Tb					0.2	0.08	
Te		0.02					
Th		0.1	0.1		0.2	0.08	
Ti		10	1000				
Tl		0.02					
Tm						0.05	
U		0.1	0.1		0.5		
V		2	1				
W		0.1	0.1		1		
Y	3		0.1				
Yb					0.2	0.41	
Zn		0.1	1		50		
Zr	3		0.1				
CO <sub>2</sub>							0.02

**Table 1.** Instrumental detection limits for elements determined by pressed pellet x-ray fluorescence (XRF), aqua regia digestion-ICP-MS (AR-ICP-MS), hydrofluoric-perchloric-hydrochloric-nitric acid digestion and combination of ICP-MS and ICP-ES (HF ICP-MS) and instrumental neutron activation analysis (INAA). Rare-earth element (REE) and carbonate carbon by LECO combustion. Detection limit for a major oxide (e.g., SiO<sub>2</sub>, Al<sub>2</sub>O<sub>3</sub>) by fused-disc XRF is 0.01%.



**Figure 4.** Altered wacke displaying oxidized Mg-Fe-rich carbonate (right of image) and pervasive sericite alteration that resembles silica flooding (08KAP-02-04, UTM Zone 11, 604143 N, 5827859E, NAD 83).



**Figure 5.** Typical argillite with graphitic fracture surface showing rusty weathered pyrite, Fe-Mg carbonate and a displaced and distorted quartz vein (08KAP 04-07, UTM Zone 11, 604310N, 5828487E, NAD 83).

mentary rocks overlie the Middle Triassic black phyllite, which forms the basement Member of the Quesnel Terrane. The Middle-Late Triassic age constraint for the hostrocks in the study area comes from conodonts found in the vicinity of Quesnel Lake (Struik, 1983; Struik and Orchard, 1985). The Crooked amphibolite of the Late Paleozoic Slide Mountain Terrane (Schiarizza, 1989) separates the Quesnel Terrane to the west from the Kootenay Terrane in the east. Adjacent to the Spanish Mountain property, the Kootenay Terrane is composed of Paleozoic meta-

sedimentary rocks of the Snowshoe Group and the Quesnel Lake orthogneiss. Southwest of Spanish Mountain, the sequence grades stratigraphically upwards into a sequence of volcanic wacke and associated volcanic rocks of the Nicola Group (Bloodgood, 1988).

### Property Geology, Alteration and Mineralization

The host sedimentary rocks for Au mineralization and alteration are calcareous argillite, siltstone and wacke. Northern parts of the property are dominated by fissile black, thin-bedded argillite and siltstone with graphitic fracture surfaces. Quartz veins are present throughout argillite sequences with variable characteristics: containing pyrite, carbonate and rare galena; barren, highly deformed, or relatively undeformed and follow wavy bedding surfaces. The variation in quartz vein geometry and style demonstrate that fluid flow has been important throughout the deformational history. Surface outcrops of the main zone (Singh, 2008) are chiefly composed of wacke, siltstone and argillite sequences. The wacke is grey to buff white in colour with variable amounts of disseminated and well-formed cubic pyrite that is generally less than 5% of the rock. The siltstone is grey to black colour, occurring as thin beds and rounded boudins within phyllitic members. In the main zone, there is also wide variation in the character of the quartz veins hosted in the more competent wacke. It is of note that quartz veins within this unit have historically produced the highest Au assay values on the property (Singh, 2008). The siltstone and wacke have been intruded

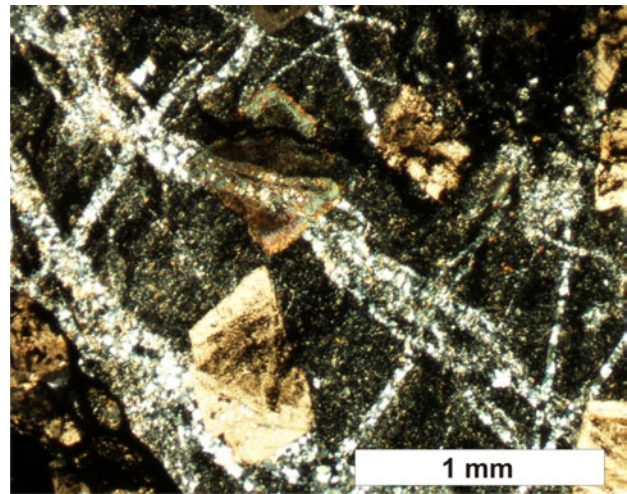


**Figure 6.** Thin section of siltstone displaying quartz veinlet interaction with rhombic carbonate. Interactions include termination, deflection and inclusion of quartz with or without carbonate remobilization (drillcore sample, UTM Zone 11, 604544 N, 5828363E, NAD 83).

by minor mafic dikes, which are altered to a dark green colour and contain Cr-rich mica. Similar Cr-mica alteration occurs as subangular to angular fragments within the wacke sequence. Figures 4 and 5 show examples of the wacke and graphitic argillite.

Alteration on the property consists of extensive iron carbonate, dolomite and sericite replacement and obliteration

**Table 2.** Summary of selected statistics for major and trace elements in Spanish Mountain rock samples. Abbreviations: ARMS, aqua regia digestion and ICP-MS; HFMS, hydrofluoric-perchloric-hydrochloric-nitric acid digestion and ICP-MS/ICP-ES; INAA, instrumental neutron activation analysis; CO<sub>2</sub> by HCl, digestion and LECO combustion; LOI, loss on ignition; XRF, x-ray fluorescence.

Analytical Method	Units	Rock Type									
		Wacke	Siltstone	Argillite	Wacke	Siltstone	Argillite	Wacke	Siltstone	Argillite	
		Mean	Mean	Mean	95th %ile	95th %ile	95th %ile	Max	Max	Max	
SiO <sub>2</sub>	XRF	%	58.12	53.93	64.10	83.47	74.85	78.18	86.70	80.72	78.95
Al <sub>2</sub> O <sub>3</sub>	XRF	%	12.45	14.36	10.59	17.24	17.83	16.59	17.72	20.39	17.93
Fe <sub>2</sub> O <sub>3</sub>	XRF	%	5.03	6.21	4.79	8.07	9.30	8.52	8.19	11.43	8.84
MnO	XRF	%	0.13	0.14	0.19	0.22	0.21	0.58	0.25	0.24	0.77
MgO	XRF	%	3.56	3.33	2.54	11.79	6.09	5.78	12.17	6.11	7.14
CaO	XRF	%	4.66	4.83	3.52	6.85	8.06	7.54	6.88	8.76	7.82
Na <sub>2</sub> O	XRF	%	2.18	2.62	1.07	4.08	5.18	2.08	4.73	6.61	2.11
LOI		%	10.34	10.48	9.12	21.55	16.05	16.97	22.43	17.46	17.34
Cu	HFMS	ppm	44.0	95.4	49.2	90.8	207.8	91.3	157.4	285.0	107.9
Pb	HFMS	ppm	6.7	9.5	25.1	12.5	28.1	91.9	21.5	35.8	153.7
Ni	HFMS	ppm	64.00	36.80	37.40	391.20	91.40	63.10	425.40	175.60	65.70
CO <sub>2</sub>	LECO	%	7.67	7.88	5.47	16.55	12.89	11.77	16.70	14.28	13.22
Y	XRF	ppm	20	18	19	39	31	33	120	34	33
Zr	XRF	ppm	139	96	122	437	200	208	512	203	265
Nb	XRF	ppm	8	7	14	15	10	38	19	18	55
Au	INAA	ppb	118.6	329.4	33.9	420.9	1230.0	177.5	1820.0	5030.0	339.0
As	INAA	ppm	55.7	62.9	40.6	193.5	155.0	80.8	315.0	274.0	83.4
Ba	INAA	ppm	695	970	1029	1368	2000	2145	1470	2630	2410
La	INAA	ppm	12.3	16.2	17.9	24.8	26.0	32.9	25.4	48.4	41.1
Lu	INAA	ppm	0.33	0.41	0.42	0.56	0.64	0.70	0.59	0.71	0.73
Ag	ARMS	ppb	282.4	393.2	731.6	1333.8	782.0	3450.0	1678.0	1673.0	6623.0
S	ARMS	%	0.34	0.65	0.74	1.36	1.85	3.75	2.87	4.42	6.09
Hg	ARMS	ppb	4	3	18	12	8	77	26	8	137

tion of the majority of primary textures of all sedimentary units. Metamorphism has resulted in multiple stages of Fe-carbonate and/or high-Mg dolomite recrystallization that give the rocks a knotted appearance. Oxidation of Fe-bearing carbonate and pyrite has given the rocks a characteristic brown spotted appearance in many surface exposures. Muscovite alteration is also extensive throughout the property, occurring as fine-grained sericite, usually comprising between 20 and 40% of the matrix, but as high as 60% in some samples. Pyrite is observed as fine-grained disseminations throughout the wallrock, concentrated in veins and as euhedral cubes up to 2 cm. As many as three stages of pyrite growth have been identified by the University of Tasmania (Singh, 2008), but are nearly impossible to differentiate in hand sample.

## PETROLOGY

Our petrographic analysis was designed to recognize possible mineralization vectors associated with carbonate mineralogy and to select samples for laser ablation ICP-MS at the University of Victoria. Mineral identification by microscopic examination of thin sections has been complemented by x-ray diffraction of 12 samples at Global Discovery Laboratories, Vancouver. The initial examination of the thin sections indicates that carbonate species occur in multiple generations; as irregular porphyroblasts with locally remobilized grain edges, well-formed zoned and unzoned prismatic rhombs, and patchy interlocking sections in intensely altered rock types. Figure 6 shows a thin section of an altered siltstone. Studying the different styles of carbonate replacement and observations of carbonate microchemistry will provide us with insight into the evolution of hydrothermal fluids responsible for wallrock alteration.

## LITHOGEOCHEMISTRY—PRELIMINARY RESULTS

Results from whole-rock and trace-element geochemistry have been obtained and an analysis of the data is in progress. Preliminary results are listed in Table 2, together with rock types assigned in the field. Initial examination confirms previous studies of the mineralization: that Au-bearing samples have low values of As, Hg, Sb, Ba, Ag, Ba and Tl, elements identified by Schroeter and Poulson (1996) to be characteristic geochemical signatures of sediment-hosted Au deposits. This leads to the hypothesis that the chemistry of mineralization at Spanish Mountain differs from that of the better-studied Carlin-trend deposits. By obtaining and analyzing detailed geochemistry of the hostrocks, the intriguing potential exists in developing a new model explaining some of the unique characteristics of this sediment-hosted Au system. Refinement of hostrock types based on geographic and stratigraphic distribution will be part of ongoing undergraduate thesis work to better characterize alteration patterns of this deposit. Table 2 lists mean, 95<sup>th</sup> percentile and maximum values for selected major oxides, minor and trace elements, LOI and carbonate C for samples classified as wacke, siltstone and argillite. This tripartite classification scheme may be revised after more detailed petrographic analysis. The statistics in Table 2 reveal that wacke samples have higher SiO<sub>2</sub>, MgO, Ni, carbonate C, Zn and As, whereas siltstone samples have higher

Fe<sub>2</sub>O<sub>3</sub>, CaO, Cu and Au. Argillite samples have higher Pb, Nb, Ba, La, Ag, S and Hg.

## CONCLUSIONS

Preliminary petrographic and geochemical analysis of surface outcrop and diamond-drill core samples from the Spanish Mountain property has revealed

multiple generations of carbonate alteration minerals, including irregular porphyroblasts with locally remobilized grain edges, well-formed zoned and unzoned prismatic calcite rhombs, and patchy interlocking carbonate minerals in intensely altered rocks;

principal rock types hosting Au mineralization at the Spanish Mountain deposit that display distinctive major oxide, minor- and trace-element chemistries; and a geochemical signature displayed by Spanish Mountain rock types that differs from previously discovered sediment-hosted Au deposits.

Further research into why elements such as As, Hg and Sb are in such low concentrations in the Spanish Mountain deposit leads to the exciting potential of a new deposit model for Au deposits in BC.

Among techniques that will be used to complete a study of alteration and lithogeochemistry are x-ray diffraction, rare-earth element analysis by sodium peroxide sinter-ICP-MS and laser ablation-ICP-MS analysis. Results and an analysis of the data will be reported in the senior author's University of Victoria Honours BSc thesis. It is anticipated that a detailed analysis of hostrock geochemistry and mineralogy will provide a better understanding of Au mineralization processes in the Spanish Mountain deposit.

## ACKNOWLEDGMENTS

We would like to thank Jessica Doyle for her enthusiasm and assistance during fieldwork and throughout the summer. Permission from Scott Weeks, Skygold Ventures Ltd, to visit the Spanish Mountain property and collect samples is very much appreciated. Bob Singh is thanked for very generously spending time to advise on the geology and chemistry of the deposit and to suggest a practical focus for the study. We would also like to thank Roger MacDonald, Andrea Stevens and Bronwyn Azar of Skygold Ventures Ltd. for their expertise and hospitality during fieldwork. Gratitude is extended to Jim Logan for carefully editing a preliminary draft of this paper.

## REFERENCES

- Bloodgood, M.A. (1988): Geology of the Quesnel Terrane in the Spanish Lake area, central British Columbia; in *Geological Fieldwork 1987, BC Ministry of Energy, Mines and Petroleum Resources*, Paper 1988-1, pages 139–146.
- Lefebure, D.V., Brown, D.A. and Ray, G.E. (1999): The British Columbia sediment-hosted gold project; in *Geological Fieldwork 1998, BC Ministry of Energy, Mines and Petroleum Resources*, Paper 1999-1, pages 165–178.
- Poulson, K.H. (1996): Carlin-type Au deposits and their potential occurrence in the Canadian Cordillera; *Geological Survey of Canada*, Current Research Paper 1996-A, pages 1–9.
- Rees, C.J. (1987): The Intermontane-Omineca Belt boundary in the Quesnel Lake area, east central British Columbia: tec-

- tonic implications based on geology, structure and paleomagnetism; PhD thesis, Carleton University, 421 pages
- Schiarizza, P. (1989): Structural and stratigraphic relationships between the Fennell Formation and Eagle Bay Assemblage, western Omineca Belt, south-central British Columbia: implications for Paleozoic tectonics along the paleocontinental margin of western North America; M.Sc. thesis, University of Calgary, 343 pages.
- Schroeter, T.G. and Poulson, K.H. (1996): Carbonate hosted disseminated Au-Ag; in *Selected British Columbia Mineral Deposit Profiles, Volume 2*, D.V. Lefebure, and T. Hoy, Editors, *BC Ministry of Energy, Mines and Petroleum Resources*, Open File 1996-13, pages 9–12.
- Sillitoe, R.H. (2008): Major Au deposits and belts of the North and South American Cordillera: distribution, tectonomagmatic settings, and metallogenic considerations; *Economic Geology*, Volume 103, pages 663–687.
- Singh, R.B. (2008): Technical report on the Spanish Mountain property for Skygold Ventures Ltd.; NI43-101 Report 92 pages.
- Struik, L.C. (1983): Bedrock geology of Spanish Lake (93A/11) and parts of adjoining map areas, central British Columbia; *Geological Survey of Canada*, Open File Map 920, scale 1:50 000.
- Struik, L.C. and Orchard, M.J. (1985): Late Paleozoic conodonts from ribbon chert delineate imbricate thrusts within the Antler Formation of the Slide Mountain Terrane, central British Columbia; *Geology*, Volume 13, pages 794–798.

# Geology and Mineral Occurrences of the Murphy Lake Area, South-Central British Columbia (NTS 093A/03)

by P. Schiarizza, K. Bell and S. Bayliss

**KEYWORDS:** Quesnel terrane, Nicola Group, Takomkane batholith, Spout Lake pluton, Kamloops Group, Chilcotin Group, copper, molybdenum, gold

## INTRODUCTION

The Takomkane Project is a multiyear bedrock mapping program initiated by the British Columbia Geological Survey in 2005. This program is focused on Mesozoic arc volcanic and plutonic rocks of the Quesnel terrane in the vicinity of the Takomkane batholith, which crops out in the northern Bonaparte Lake (NTS 092P) and southern Quesnel Lake (NTS 093A) map areas. Mapping during the 2005 through 2007 field seasons covered the Canim Lake, Hendrix Lake and Timothy Lake map areas, and is summarized by Schiarizza and Boulton (2006a, b), Schiarizza and Macauley (2007a, b), Schiarizza and Bligh (2008) and Schiarizza et al. (2008). Here, we present preliminary results from the fourth and final year of mapping for the Takomkane Project, which was carried out by a four-person crew from mid-June to the end of August 2008. This work covers 950 km<sup>2</sup> of generally subdued topography encompassing parts of the Fraser Plateau and Quesnel Highland physiographic provinces, including NTS map area 093A/03 and a small part of adjoining area 093A/06 (Figure 1). This area is within the traditional territories of the Northern Secwepemc te Qelmuw and Esketemc First Nations. Access to most parts of the map area is easily achieved via extensive networks of logging and forest service roads that connect to Highway 97 at 100 Mile House, Lac La Hache and 150 Mile House.

The Takomkane Project builds on the geological framework established by the reconnaissance-scale mapping of Campbell and Tipper (1971) and Campbell (1978), the metallogenic studies of Fox (1975) and Barr et al. (1976), and, more recently, relatively detailed mapping programs by Panteleyev et al. (1996), Schiarizza and Israel (2001) and Schiarizza et al. (2002a–c). Our geological interpretation of the Murphy Lake area also incorporates data found in assessment reports available through the BC Geological Survey's Assessment Report Indexing System (ARIS), and airborne magnetic and radiometric data from a number of recent surveys funded by the Geological Survey of Canada, Geoscience BC and various industry partners (Carson et al., 2006a, b; Dumont et al., 2007).

---

*This publication is also available, free of charge, as colour digital files in Adobe Acrobat® PDF format from the BC Ministry of Energy, Mines and Petroleum Resources website at <http://www.empr.gov.bc.ca/Mining/Geoscience/PublicationsCatalogue/Fieldwork/Pages/default.aspx>.*

## REGIONAL GEOLOGICAL SETTING

The Takomkane Project area is underlain mainly by rocks of the Quesnel terrane, which is characterized by a Late Triassic to Early Jurassic magmatic arc complex but also includes late Paleozoic arc sequences and, in southernmost BC, late Paleozoic rocks of more oceanic aspect (Monger et al., 1991). The Quesnel terrane occurs along most of the length of the Canadian Cordillera. It is flanked to the east by assemblages of Proterozoic to Paleozoic siliciclastic, carbonate and local volcanic rocks of ancestral North American affinity, but is commonly separated from these rocks by an intervening assemblage of late Paleozoic oceanic basalt and chert assigned to the Slide Mountain terrane. The Cache Creek terrane, dominated by late Paleozoic and early Mesozoic oceanic basalt, chert and limestone, occurs to the west of the Quesnel terrane and is generally interpreted as part of the accretion-subduction complex that was responsible for generating the Quesnel magmatic arc (Travers, 1978; Struik et al., 2001). Although some tectonic models depict the Quesnel terrane as part of an allochthonous crustal fragment that was accreted to the North American continental margin in Early Jurassic time (e.g., Monger et al., 1982), numerous studies have demonstrated older stratigraphic, provenance and geochemical linkages between North American rocks and those of the Slide Mountain and Quesnel terranes (Campbell, 1971; Klepacki and Wheeler, 1985; Schiarizza, 1989; McMullin et al., 1990; Roback and Walker, 1995; Ferri, 1997; Erdmer et al., 2001; Unterschutz et al., 2002; Thompson et al., 2006). One set of tectonic models formulated to explain these linkages, as well as evidence for regional Permo–Triassic deformation, has the Late Paleozoic arc of the Quesnel terrane forming on a crustal fragment that separated from ancestral North America during back-arc extension that produced the Slide Mountain marginal ocean basin. This fragment then returned to proximity with the continental margin during Permo–Triassic collapse of the Slide Mountain basin, prior to formation of the Mesozoic arc that characterizes the Quesnel terrane (Smith, 1979; Schiarizza, 1989; Roback and Walker, 1995; Ferri, 1997; Dostal et al., 2001). Thompson et al. (2006) suggested that, in parts of southern BC, there was little or no separation of this western crustal fragment from the continental margin, and that both the late Paleozoic and Mesozoic arc sequences of the Quesnel terrane are therefore autochthonous and were deposited above North American continental crust.

In southern and central BC, the early Mesozoic arc of the Quesnel terrane is represented mainly by Middle to Upper Triassic volcanic and sedimentary rocks of the Nicola Group, together with abundant Late Triassic to Early Jurassic calcalkaline and alkaline intrusions (Schau, 1970; Preto, 1977, 1979; Mortimer, 1987; Panteleyev et al.,

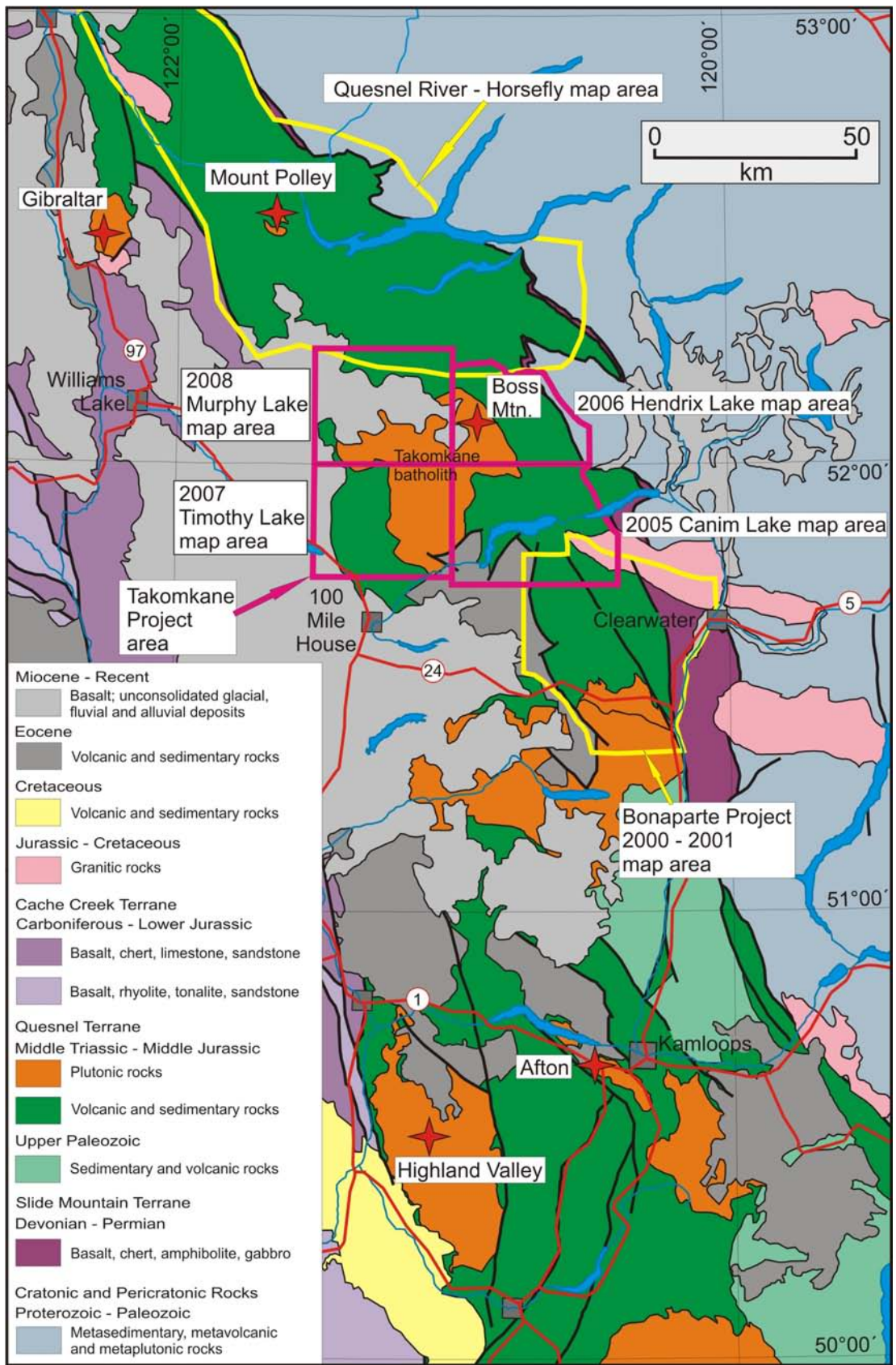


**Figure 1.** Regional geological setting of the Takomkane Project area, showing the areas mapped in 2005, 2006, 2007 and 2008, as well as the area mapped during the 2000–2001 Bonaparte Project, and the Quesnel River–Horsefly map area of Panteleyev et al. (1996). Stars denote locations of selected major mineral deposits.

1996). The Nicola Group is characterized by volcanic and volcanic-derived sedimentary rocks but also includes an eastern sedimentary facies of dark grey siltstone and slate intercalated with quartzite and quartz sandstone (Bloodgood, 1990; Schiarizza et al., 2002a). The volcanic rocks consist mainly of augite-phyric basalt and andesite that belong to a high-potassium to shoshonitic rock series, but low-potassium calcalkaline volcanic rocks form a distinctive western belt in southern BC (Preto, 1977; Mortimer, 1987). Lower to Middle Jurassic sandstone and conglomerate rest unconformably above the Triassic successions at scattered localities within the belt (Travers, 1978; Monger and McMillan, 1989; Schiarizza et al., 2002a; Logan and Mihalyuk, 2005a), and an assemblage of Lower Jurassic shoshonitic to calcalkaline arc volcanic rocks, assigned to the Rosslund Group, is a prominent component of the southeastern part of the terrane (Höy and Dunne, 1997). These Lower Jurassic volcanic rocks occur well east of the axis of Triassic arc magmatism, but rest above Triassic sedimentary rocks that are correlated with the eastern sedimentary facies of the Nicola Group.

The structural geology of the Quesnel terrane includes generally poorly understood faults that exerted controls on Late Triassic volcanic-sedimentary facies distributions and the localization of plutons and associated mineralization and alteration systems (Preto, 1977, 1979; Nelson and Bellefontaine, 1996; Logan and Mihalyuk, 2005b; Schiarizza and Tan, 2005). In central and southern BC, east-directed thrust faults and associated folds, of Permian-Triassic and/or Early Jurassic age, are documented within the eastern part of the Quesnel terrane and the structurally underlying rocks of the Slide Mountain terrane (Rees, 1987; Struik, 1988a-c; Schiarizza, 1989; Ferri, 1997). Younger structures include west- to southwest-verging folds, in part of early Middle Jurassic age, that deform the east-directed thrust faults (Ross et al., 1985; Brown et al., 1986; Rees, 1987; Schiarizza and Preto, 1987), and prominent systems of Eocene dextral strike-slip and extensional faults (Ewing, 1980; Panteleyev et al., 1996; Schiarizza and Israel, 2001).

The Quesnel terrane is an important metallogenic province, particularly for porphyry deposits containing copper, gold and molybdenum. The world-class Highland Valley copper-molybdenum porphyry deposits occur in calcalkaline plutonic rocks of the Late Triassic Guichon Creek batholith (Casselman et al., 1995), which is hosted in the western calcalkaline belt of the Nicola Group (Figure 1). Copper-gold porphyry deposits, such as the Mount Polley and Afton mines, are associated with slightly younger, latest Triassic alkaline plutons that are hosted by the main belt of shoshonitic volcanic and volcanoclastic rocks of the Nicola Group (Mortensen et al., 1995; Logan and Mihalyuk, 2005a, b). Cospatial with these latest Triassic alkaline plutons is a belt of large, Early Jurassic calcalkaline plutons that includes the Takomkane, Thuya, Wild Horse, Pennask and Bromley batholiths. These plutons locally host copper-molybdenum-gold porphyry deposits, such as the past-producing Brenda mine (Weeks et al., 1995) and the Southeast zone of the Woodjam property (this report). Much younger calcalkaline plutons of mid-Cretaceous age intrude the Quesnel and adjacent terranes, and host porphyry molybdenum deposits, including the past-producing Boss Mountain mine (Soregaroli and Nelson, 1976; Macdonald et al., 1995).

## GEOLOGICAL UNITS

The distribution of the main geological units within the Murphy Lake map area is shown on Figure 2, and schematic vertical cross-sections are presented on Figure 3. The bedrock geology is dominated by Late Triassic to Early Jurassic volcanic, volcanoclastic and plutonic rocks of the Quesnel terrane, but also includes two substantial accumulations of Eocene volcanic and sedimentary rocks assigned to the Kamloops Group. Basalt of the Miocene to Pliocene Chilcotin Group is represented by a few exposures in the northwestern part of the map area, and two outliers of Quaternary basalt are mapped in the southeastern part of the area.

The oldest rocks of the Quesnel terrane comprise volcanic and sedimentary rocks of the Late Triassic Nicola Group, which crop out mainly in the western part of the map area but also occur in two small areas near Tisdall Lake in the northeast. The most areally extensive units of the Quesnel terrane are plutonic rocks, represented mainly by the alkaline Spout Lake pluton and the calcalkaline Takomkane batholith. Smaller intrusive units include an ultramafic-mafic complex located north of Tisdall Lake, two stocks of coarse plagioclase porphyry west of Woodjam Creek and a small monzonite plug south of the McIntosh Lakes.

### *Nicola Group*

The Nicola Group, originally named for exposures on the south side of Nicola Lake (Dawson, 1879), comprises a diverse assemblage of Middle and Upper Triassic volcanic, volcanoclastic and sedimentary rocks that crop out over a broad area in south-central BC. The name is applied to Triassic rocks in the Takomkane Project area following Campbell and Tipper (1971) and Panteleyev et al. (1996), although the Triassic rocks in the Quesnel Lake map area have also been referred to as Quesnel River Group (Campbell, 1978) or Takla Group (Rees, 1987). The former term has generally been superseded by Nicola Group, and the latter continues to be applied to Triassic rocks in central and northern BC that correlate with the Nicola Group (e.g., Nelson and Bellefontaine, 1996; Schiarizza and Tan, 2005).

On Figure 4, the Nicola Group in the Takomkane Project area is subdivided into four general map units. The easternmost rocks of the group, assigned to the Lemieux Creek succession, comprise dark grey slate and siltstone with local intercalations of limestone and quartz sandstone. These rocks pass westward and structurally upward into a broad belt of pyroxene- and feldspar-rich sedimentary and volcanic rocks referred to as the volcanoclastic succession. The volcanoclastic succession includes several internal units of coarse volcanic breccia and pyroxene-phyric basalt. One of these, at the top of the succession, is separated out on Figure 4 and referred to as the basalt-breccia unit. This unit crops out mainly as a continuous belt along the eastern margin of the Takomkane batholith, but also occurs west of the batholith, where it forms the uppermost part of the volcanoclastic succession between Spout Lake and the McIntosh Lakes. There, it is overlain by the fourth map unit, which is referred to as the polyolithic breccia succession. This succession consists mainly of polyolithic breccia and conglomerate with intercalated feldspathic sandstone, and is the uppermost unit of the Nicola Group exposed in the Takomkane Project area.

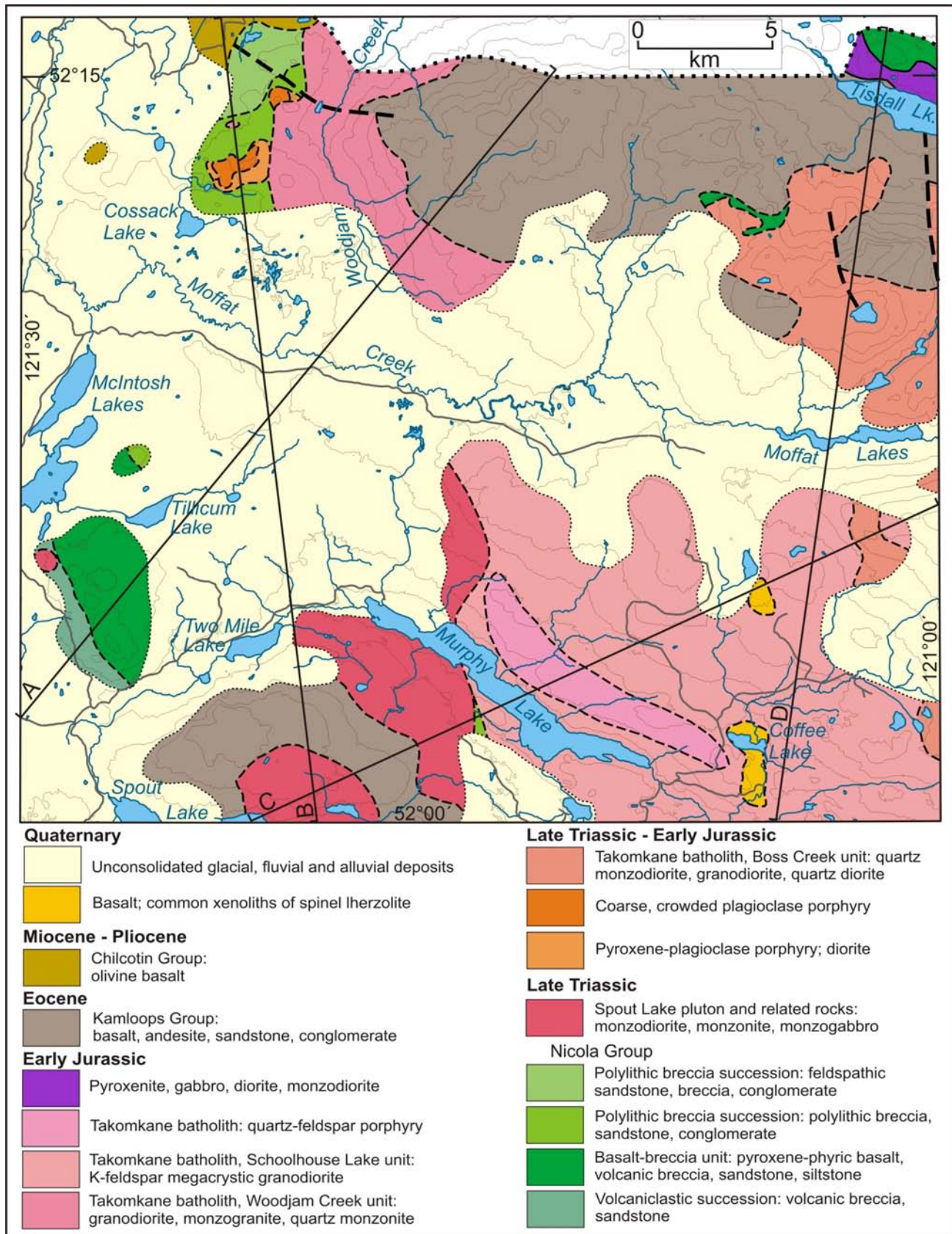


Figure 2. Generalized geology of the Murphy Lake map area, based mainly on 2008 fieldwork.

The Nicola Group is not a major component of the Murphy Lake map area, but substantial exposures occur in two localities in the western part of the area, south of the McIntosh Lakes and west of Woodjam Creek (Figure 2). The exposures south of the McIntosh Lakes comprise rocks of the volcanoclastic succession overlain to the east-northeast by the basalt-breccia unit. The basalt-breccia unit is in turn overlain by the polyolithic breccia succession in an isolated set of exposures on a low hill east of the southern lake. The northwest-dipping interval west of Woodjam Creek comprises rocks of the polyolithic breccia succession, which is subdivided into a lower unit of mainly coarse breccia and conglomerate, and an upper unit dominated by feldspathic sandstone. Nicola Group rocks elsewhere in the Murphy Lake map area include exposures near Tisdall Lake that are assigned to the basalt-breccia unit, and an exposure south of Murphy Lake, between the Spout Lake pluton and the Takomkane batholith, that is included in the polyolithic breccia succession.

### VOLCANICLASTIC SUCCESSION

The volcanoclastic succession is represented by a narrow belt of exposures south of the McIntosh Lakes. Here, the succession consists mainly of volcanic breccia (Fig-

ure 5), with local intercalations of massive to thin-bedded sandstone. The breccia is mainly medium to dark green or greyish green, and weathers rusty brown to greenish brown; locally, however, the fragments weather to a variety of colours, mainly in shades of green, grey and maroon, imparting a mottled colour to the rock. Fragments are mainly feldspar- and feldspar-pyroxene-phyric basalt, but the clast population also includes aphyric volcanic rock, feldspar-hornblende-pyroxene-phyric basalt or andesite, and limestone. The fragments commonly range from a few millimetres to a few centimetres in size, but locally are more than 10 cm across. They are typically angular to sub-rounded, poorly sorted and matrix supported. The matrix consists of sand-size grains of feldspar, accompanied by a smaller proportion of mafic minerals and dark volcanoclastic grains.

The breccia of the volcanoclastic succession is massive to vaguely stratified, and was probably derived from mass-flow deposits. Locally, thick breccia units are separated by narrow intervals, only a few tens of centimetres wide, of thin-bedded feldspathic sandstone and siltstone. The succession also includes thicker units of massive sandstone, as represented by a single isolated exposure of dark green,

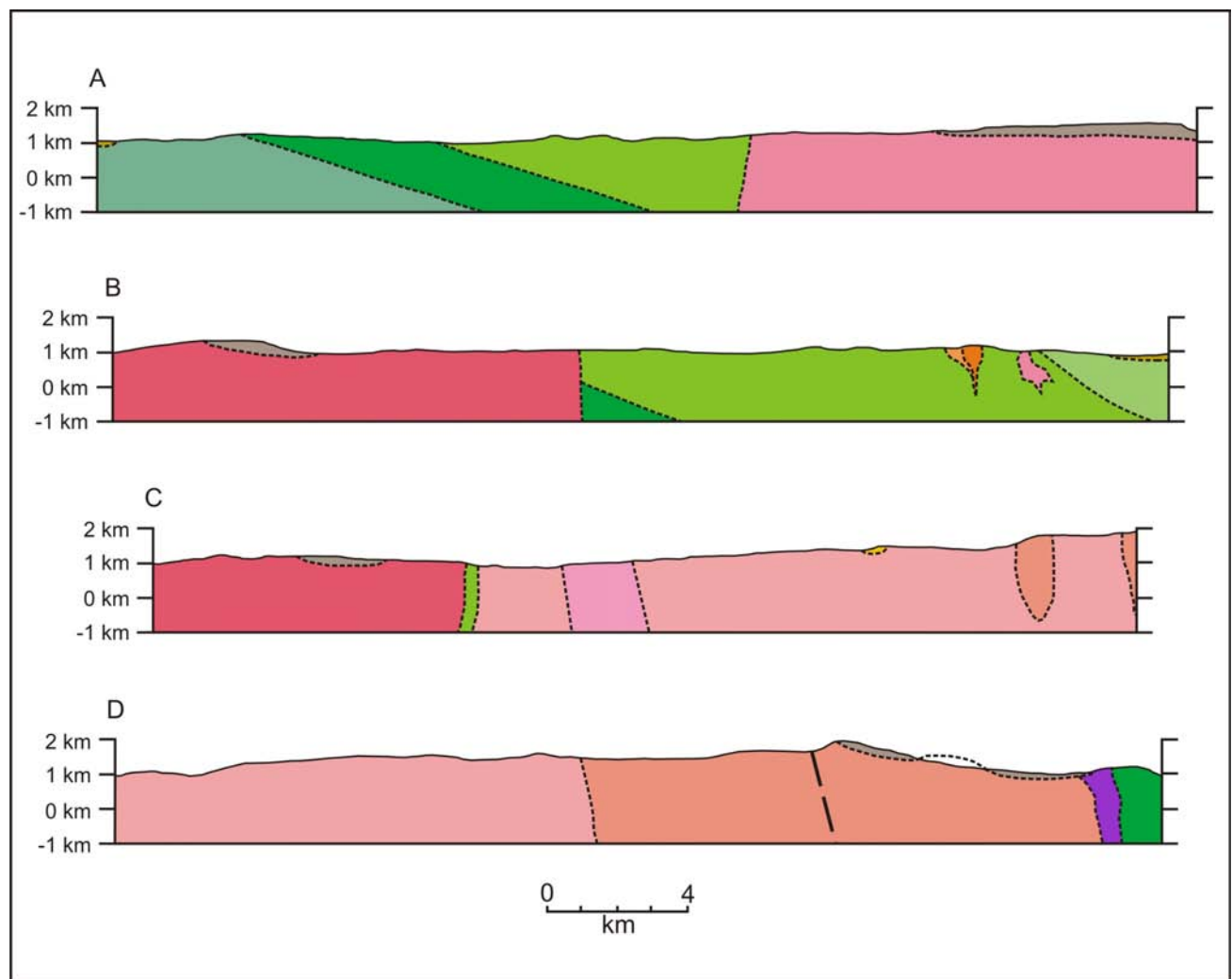
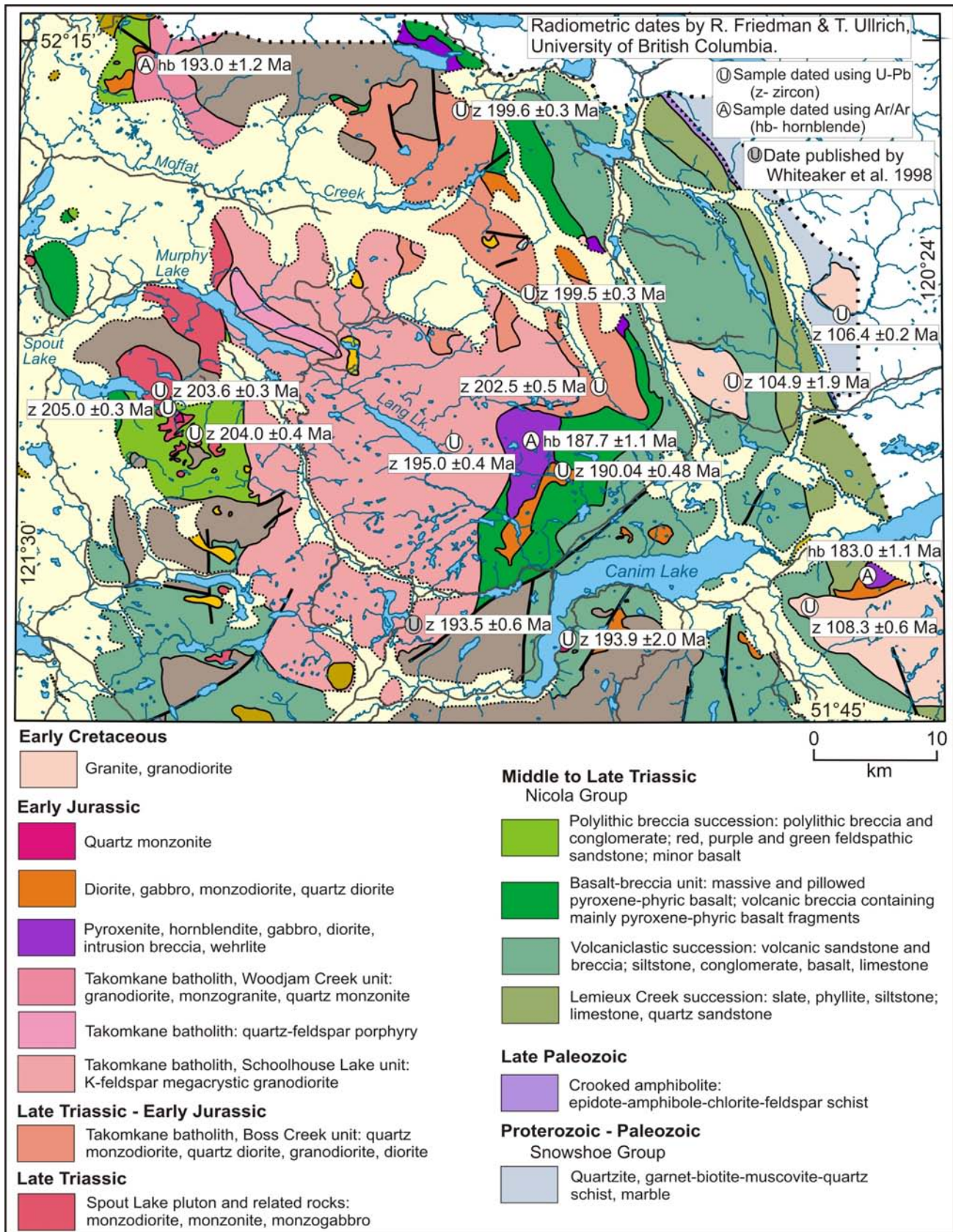


Figure 3. Schematic vertical cross-sections along the lines shown in Figure 2. See Figure 2 for legend.



**Figure 4.** Simplified geology of the entire 2005–2008 Takomkane Project area, showing major subdivisions of the Nicola Group and locations of isotopically dated samples of plutonic rocks. Legend for Tertiary and Quaternary units shown in Figure 2.

rusty-brown-weathered, coarse-grained feldspathic sandstone in its upper part, west of Tillicum Lake.

The volcanoclastic succession is not dated within the Murphy Lake map area. Correlative rocks to the south include a prominent lens of limestone, 10 km southeast of Lac La Hache, that has yielded fossils of Late Triassic, probably Norian age (Campbell and Tipper, 1971).

### BASALT-BRECCIA UNIT

The basalt-breccia unit consists of pillowed to massive basalt and basalt breccia, characterized by abundant, coarse pyroxene phenocrysts. It is well exposed on the hills and ridges south of the McIntosh Lakes, where it is underlain by the volcanoclastic succession and overlain by the polyolithic breccia succession (Figure 3, section A). It also occurs northeast of Tisdall Lake and as a thin screen beneath Eocene cover on the margin of the Takomkane batholith, southwest of the lake.

The basalt-breccia unit south of the McIntosh Lakes is dominated by dark green, brownish-weathered, massive to pillowed basalt. The basalt typically comprises 10–30% pyroxene phenocrysts, 2–8 mm in size, and smaller but equally or more abundant feldspar phenocrysts, in a fine-grained, variably epidote-calcite-chlorite-altered groundmass. Amygdules of epidote and/or calcite are common locally, and varioles were noted rarely in some exposures of pillowed basalt. Irregular veins and patches of calcite-epidote are a common feature, particularly in pillowed units.

Medium to dark green, greenish-brown to rusty-brown weathered volcanic breccia is a subordinate but significant component of the basalt-breccia unit south of the McIntosh Lakes, and makes up most of the unit in the two exposure belts near Tisdall Lake. Fragments are angular to subrounded, and commonly range from less than 1 cm to 8 cm in size, although some exposures include fragments that are more than 20 cm across. The fragments consist mainly of pyroxene- and pyroxene-feldspar-phyric basalt, although clasts of limestone, pyroxenite and volcanic sandstone occur locally. There may be considerable textural variation among basalt fragments, mainly with respect to size, abundance and proportion of phenocrysts, but most are characterized by coarse pyroxene phenocrysts that commonly range up to 8 mm in size (Figure 6). The frag-

ments are typically supported in a matrix made up of sand- to granule-size grains of mainly pyroxene and feldspar.

Pyroxene-feldspar sandstone and gritty sandstone is a relatively minor component of the basalt-breccia unit in the Tisdall Lake area. It either forms massive units that have indistinct contacts with enclosing breccia, or narrow thin-bedded intervals up to a few metres thick. Dark grey, rusty-weathered, laminated to thin-bedded siltstone forms an interval at least 10 m thick that was traced for 1.3 km within the basalt-breccia unit south of the McIntosh Lakes.

### POLYLITHIC BRECCIA SUCCESSION

The polyolithic breccia succession crops out mainly in the northwest corner of the map area, where it forms a north-northwest-dipping panel that is subdivided into a lower unit of mainly coarse breccia and an upper unit of mainly feldspathic sandstone with local intercalations of breccia and conglomerate (Figure 2). A few exposures of polyolithic breccia also occur east of the McIntosh Lakes, and demonstrate the stratigraphic position of the polyolithic breccia succession, above the basalt-breccia unit. A single exposure of hornfelsed, thin-bedded sandstone, siltstone and skarn, located between the Spout Lake pluton and Takomkane batholith south of Murphy Lake, is also included in the polyolithic breccia succession. These rocks resemble thin-bedded intervals within the polyolithic breccia succession near the Nemrud skarn occurrence, along the margin of the Takomkane batholith just south of the Murphy Lake map area (Scharizza and Bligh, 2008).

The breccias of the polyolithic breccia unit have an overall light to dark green or greenish grey colour, and commonly weather to light shades of brown, greenish brown or beige. They are typically matrix supported and poorly sorted, with angular to subrounded clasts that commonly range from a few millimetres to 6 cm in size, and are locally as large as 12 cm. The clast population is dominated by fine-grained, equigranular to weakly porphyritic feldspathic rocks but also includes porphyritic volcanic clasts containing variable proportions of feldspar, pyroxene and hornblende phenocrysts, and clasts of medium-grained gabbro/diorite and monzodiorite (Figure 7). The matrix consists mainly of feldspar with scattered mafic mineral grains. The feldspar is mainly plagioclase, but commonly includes a substantial proportion of pinkish



**Figure 5.** Volcanic breccia of the Nicola Group volcanoclastic succession, south of the McIntosh Lakes.



**Figure 6.** Volcanic breccia with coarse pyroxene porphyry basalt fragments, Nicola Group basalt-breccia unit, north of Tisdall Lake.

grains that may be K-feldspar and/or hematite-altered plagioclase. The polyolithic breccias are typically massive, but some exposures display weak stratification. Locally, this stratification is accented by the intercalation of narrow intervals of thin-bedded feldspathic sandstone, gritty sandstone and siltstone.

The upper unit of the polyolithic breccia succession consists mainly of medium- to coarse-grained, locally gritty, feldspathic sandstone. It is mostly medium green to grey-green and weathers rusty brown to light greenish brown, but in some exposures is red to purple on weathered and fresh surfaces. The clastic feldspar grains are mainly plagioclase, but commonly include pinkish K-feldspar and/or hematitic plagioclase, which are at least in part the products of alteration. Bedding is evident mainly as a planar platy to flaggy parting, but thin to medium beds are locally well defined by distinct units of contrasting grain size, ranging from siltstone to gritty sandstone. Matrix-supported pebble to cobble conglomerate and conglomeratic sandstone occur locally as thicker beds, and contain clasts that are similar in composition and texture to those in the underlying breccia unit.

Volcanic rocks were not positively identified within either the upper or lower unit of the polyolithic breccia succession, but both units include exposures of fine-grained feldspathic rock, locally with scattered coarser grains of feldspar and/or mafic minerals, of uncertain origin. It is suspected that most of these are feldspathic sandstone and gritty sandstone with textures obscured by hornfels development and/or alteration. However, some might be volcanic rocks and/or high-level dioritic to monzodioritic intrusions.

Rocks assigned to the polyolithic breccia succession in the Murphy Lake map area are readily correlated with similar rocks mapped to the south between Spout Lake and Mount Timothy ('polyolithic breccia' and 'red sandstone-conglomerate' units of Schiarizza and Bligh, 2008). The succession is inferred to be Late Triassic because it sits stratigraphically higher than the volcanoclastic succession, which is dated regionally as Late Triassic, and is cut by the Late Triassic Peach Lake stocks southeast of Spout Lake (Figure 4).



**Figure 7.** Breccia of the Nicola Group polyolithic breccia unit, east of the McIntosh Lakes.

## Plutonic Rocks of the Quesnel Terrane

### SPOUT LAKE PLUTON

The Spout Lake pluton, of mainly monzodiorite to monzonite composition, crops out in the southwestern part of the Murphy Lake map area. It measures at least 16 km north-south by 9 km east-west, but the western and northern limits are obscured by Quaternary drift. The pluton apparently intrudes the basalt-breccia unit and polyolithic breccia succession of the Nicola Group along its south and southeast margins, and is cut by the Schoolhouse Lake unit of the Takomkane batholith to the northeast, but none of these contacts are exposed. The southern part of the pluton is locally overlapped by Eocene volcanic rocks of the Kamloops Group.

Most exposures of the Spout Lake pluton consist of light-grey-weathered, medium- to coarse-grained, equigranular monzodiorite to monzonite. Mafic minerals commonly constitute 15–20% of the rock. The mafic component is typically clinopyroxene with lesser biotite, but some rocks contain hornblende and biotite. Quartz is locally present as a minor constituent, and apatite is conspicuous in thin sections. Planar dikes of fine- to medium-grained, equigranular to porphyritic monzonite, monzodiorite, syenite and diorite are common, as are veins and irregular patches of pegmatite, ranging from monzonite to granite in composition (Figure 8).

Darker grey, coarse-grained, equigranular monzogabbro forms a distinctive unit within the eastern part of the Spout Lake pluton south of Murphy Lake. Mafic minerals typically form about 30% of the rock and consist mainly of clinopyroxene, with minor amounts of altered olivine evident in thin section. Clinopyroxenite locally forms irregular patches and lenses, up to 20 cm across, within the monzogabbro, and dikes of monzodiorite, monzonite, syenite and pegmatite, similar to those found elsewhere in the pluton, are common (Figure 9). Where observed, contacts between monzogabbro and the more typical monzodiorite are highly irregular, with no clear indication of the relative ages of the two units, although xenoliths of melanocratic gabbro that might be related to the monzo-



**Figure 8.** Monzodiorite of the Spout Lake pluton containing a xenolith of melanocratic gabbro and cut by a pegmatite dike and a younger fine-grained monzonite dike, 3 km south of the west end of Murphy Lake.

gabbro unit occur locally within the monzodiorite, as shown in Figure 8.

A sample of fairly typical monzodiorite collected from the southern part of the Spout Lake pluton in 2007 yielded a Late Triassic U-Pb zircon date of  $203.6 \pm 0.3$  Ma (Figure 4). A sample of monzogabbro collected from the eastern part of the pluton in 2008 has also been submitted for U-Pb dating, but the results are not yet available.

### MONZONITE PLUG SOUTH OF THE MCINTOSH LAKES

A small intrusive plug, less than 1 km in diameter, cuts the volcanoclastic succession of the Nicola Group south of the McIntosh Lakes. It consists of pinkish-brown-weathered, medium-grained, equigranular monzonite, containing about 25% clinopyroxene and traces of hornblende and biotite. Fine-grained monzodiorite forms part of the south-eastern margin of the plug, and narrow dikes of fine-grained syenite locally cut the main monzonite and monzodiorite phases. The plug is undated but may be related to the Spout Lake pluton and the monzodiorite to monzonite stocks south of Peach Lake, two of which have yielded Late Triassic U-Pb zircon dates of  $204.0 \pm 0.4$  Ma and  $205.0 \pm 0.3$  Ma (Figure 4; Schiarizza and Bligh, 2008).

### TAKOMKANE BATHOLITH

The Takomkane batholith is a large, composite pluton that measures 56 km north-south by 20–33 km east-west (Figure 4). It cuts the Spout Lake pluton and several different units of the Nicola Group, and is itself cut by several Early Jurassic ultramafic-mafic plutons and the Early Cretaceous Boss Mountain Mine stock. Locally it is nonconformably overlain by volcanic successions of Eocene, Miocene and Quaternary age. The Takomkane batholith consists of two major subdivisions: the Late Triassic to Early Jurassic Boss Creek unit and the Early Jurassic Schoolhouse Lake unit (Figure 4; Schiarizza and Boulton, 2006a). Both of these units are present in the Murphy Lake map area, as are two additional mappable units: a quartz-feldspar porphyry that is within the Schoolhouse Lake unit; and the Woodjam Creek unit, which is texturally distinct but compositionally similar to the Schoolhouse Lake unit, and forms the northwestern part of the batholith.

#### *Boss Creek Unit*

The Boss Creek unit forms the northeastern part of the Takomkane batholith, and underlies a belt about 35 km long that extends southeastward from the eastern part of the Murphy Lake area into the Canim Lake map area. Within the Murphy Lake map area, it is well exposed along several sets of ridges north of the Moffat Lakes. It consists mainly of light grey, medium- to coarse-grained, equigranular quartz monzodiorite to granodiorite, locally grading to quartz diorite and diorite. Mafic minerals typically form 15–25% of the rock. These commonly consist of hornblende with lesser amounts of biotite, but locally include clinopyroxene, biotite and hornblende. Rounded xenoliths of fine-grained dioritic rock are scattered sparsely through some exposures and, in one isolated exposure south of the east end of the Moffat Lakes, medium-grained diorite hosts numerous xenoliths of coarse-grained gabbro, diorite and hornblende.

Samples of biotite-pyroxene-hornblende quartz monzodiorite from near the southern and northern limits of the Boss Creek unit have yielded U-Pb zircon dates of 202.5



**Figure 9.** Monzogabbro containing irregular patches of pyroxenite, Spout Lake pluton, southwest of Murphy Lake.

$\pm 0.5$  Ma and  $199.6 \pm 0.3$  Ma, respectively (Figure 4). A sample of hornblende-biotite granodiorite collected between these two sites has yielded a U-Pb zircon date of  $199.5 \pm 0.3$  Ma. These dates indicate crystallization of the Boss Creek unit at about the Triassic–Jurassic boundary, which has been placed at  $199.6 \pm 0.7$  Ma by Pálffy et al. (2000).

#### *Schoolhouse Lake and Quartz-Feldspar Porphyry Units*

The Schoolhouse Lake unit is the main component of the Takomkane batholith, with exposures extending from Moffat Creek southward 40 km to the southern margin of the batholith at Bridge Creek (Figure 4). It is remarkably homogeneous throughout this area, comprising light grey to pinkish grey, coarse- to medium-grained, hornblende-biotite granodiorite to monzogranite characterized by K-feldspar megacrysts up to 5 cm in size and, commonly, quartz grains and aggregates up to 1 cm in size. Mafic minerals typically make up 10–20% of the rock, with hornblende predominating over biotite. Variations in composition and texture occur mainly along the margins of the unit, where equigranular granodiorite and tonalite have been noted locally.

Pegmatite and aplite dikes, generally less than 1 m wide, are a widespread but relatively minor component of the Schoolhouse Lake unit. Thicker dikes of grey to pink quartz porphyry and quartz-feldspar porphyry also occur; in the Timothy Lake map area, these dikes were noted in both the Schoolhouse Lake unit and the adjacent Nicola Group (Schiarizza and Bligh, 2008). In the Murphy Lake map area, a northwest-trending unit of quartz-feldspar porphyry, up to 1800 m wide, has been traced for 11 km within the Schoolhouse Lake unit on the northeast side of Murphy Lake. It consists of quartz and K-feldspar phenocrysts in a fine-grained sugary groundmass of feldspar and quartz, accompanied by relatively minor amounts of biotite and hornblende. The phenocrysts are typically 4–10 mm in size, but K-feldspar megacrysts are locally as large as 3 cm. We suspect that this unit is broadly related to the enclosing Schoolhouse Lake unit, and of similar Early Jurassic age. This interpretation will be tested with U-Pb dating of zircons from a sample collected during the 2008 field season.

Outcrop distribution within the Murphy Lake and Hendrix Lake map areas suggests that the contact between the Schoolhouse Lake and Boss Creek units is irregular and complex (Figure 4). The contact is not well exposed, however, and the relative ages of the two units have been established through isotopic dating. The Schoolhouse Lake unit has yielded U-Pb zircon crystallization ages of  $193.5 \pm 0.6$  Ma from a sample near Ruth Lake (Whiteaker et al., 1998), and  $195.0 \pm 0.4$  Ma from a sample near Lang Lake (Figure 4). These dates indicate that the Schoolhouse Lake unit is younger than the Boss Creek unit by about 5 Ma.

### Woodjam Creek Unit

The Woodjam Creek unit makes up the northwestern part of the Takomkane batholith, where it is represented by good exposures on both sides of Woodjam Creek. It cuts the polyolithic breccia succession of the Nicola Group to the west, and is overlain by Eocene volcanic and sedimentary rocks to the east. It is also in contact with undated plugs of feldspar porphyry and feldspar-pyroxene porphyry along its western margin, but relative ages have not been established. The contacts between the Woodjam Creek unit and the Boss Creek and Schoolhouse Lake units are obscured by large areas of Eocene and Quaternary cover.

The Woodjam Creek unit consists mainly of light grey, light pinkish-grey to white weathered, hornblende-biotite granodiorite, monzogranite, quartz monzonite and quartz monzodiorite. This range in rock names does not reflect a wide compositional range for the unit, but rather a fairly restricted range of compositions that plot near the mutual contact point of these four fields on a QAP diagram. Texturally, the rocks are isotropic, medium to coarse grained and generally equigranular, although some exposures feature K-feldspar and hornblende grains, up to 1 cm long, that are coarser than other mineral grains. Mafic minerals, mainly hornblende with relatively minor amounts of biotite, commonly form 10–15% of the rock. Dikes of aplite, pegmatite and quartz-feldspar porphyry are a widespread but volumetrically minor component of the unit.

The Woodjam Creek unit resembles the Schoolhouse Lake unit, but generally has less quartz and does not contain the large K-feldspar megacrysts that characterize the latter unit. Logan et al. (2007) reported that hornblende from a sample collected on the west side of Woodjam Creek yielded a well-defined Ar/Ar cooling age of  $193.0 \pm 1.2$  Ma, which they interpreted as an approximate crystallization age. This date suggests a temporal relationship between the Woodjam Creek and Schoolhouse Lake units. A sample collected from the east side of Woodjam Creek during the 2008 field season has been submitted for U-Pb dating of zircons to further evaluate the crystallization age of the unit.

### TISDALL LAKE ULTRAMAFIC-MAFIC COMPLEX

The Tisdall Lake complex comprises ultramafic and mafic plutonic rocks that crop out on the northeast side of Tisdall Lake. These rocks intrude the Nicola Group basalt-breccia unit to the northeast, and are overlain by Eocene volcanic rocks to the south. They are inferred to intrude the Boss Creek unit of the Takomkane batholith beneath the Eocene cover (Figure 3, section D).

Eastern exposures of the Tisdall Lake complex comprise complex mixtures of dark green, coarse-grained hornblende clinopyroxenite; medium- to coarse-grained

melanocratic gabbro; grey, medium-grained diorite; and light grey, fine- to medium-grained leucodiorite. The hornblende clinopyroxenite, which contains accessory biotite and magnetite, is the oldest phase present and forms irregular patches ranging from less than 1 m to more than 10 m across. Melanocratic gabbro forms smaller patches that have sharp to gradational contacts with the clinopyroxenite. Mafic minerals make up 40–80% of the gabbro and include clinopyroxene, hornblende and minor biotite. Variations in modal composition are typically complex and irregular, but rare patches display modal layering. Grey diorite dominates large areas of outcrop, and also occurs as dikes cutting clinopyroxenite and gabbro. Leucodiorite occurs as narrow dikes and irregular veins cutting all other rock types, and locally forms the matrix of intrusion breccia that contains xenoliths of clinopyroxenite, gabbro and diorite (Figure 10).

Western exposures of the Tisdall Lake complex consist mainly of grey, medium- to coarse-grained, equigranular diorite. The diorite locally encompasses patches of less homogeneous, varitextured diorite to gabbro, and locally contains xenoliths of clinopyroxenite and melanocratic gabbro. Pegmatitic quartz monzodiorite forms dikes and irregular patches within the dioritic rocks, and dominates some areas along the north contact of the complex.

The Tisdall Lake complex correlates with two similar ultramafic-mafic plutonic complexes that crop out along the eastern margin of the Takomkane batholith farther south (Figure 4). These are referred to as the Hendrix Lake complex (Scharizza and Macauley, 2007a) and the Iron Lake complex (Scharizza and Boulton, 2006a). These ultramafic-mafic plutons are assigned Early Jurassic ages based on isotopic dating of the Iron Lake complex (Figure 4).

### STOCKS EAST OF WOODJAM CREEK

Two separate stocks that cut the Nicola Group polyolithic breccia succession along the western margin of the Takomkane batholith, in the northwest corner of the map area, consist of coarse plagioclase porphyry, partially enveloped by finer grained feldspar-pyroxene porphyry and, locally, fine-grained hornblende-phyric diorite. The coarse porphyry units are characterized by 30–40% plagioclase



**Figure 10.** Hornblende clinopyroxenite, grey diorite and leucodiorite of the Tisdall Lake ultramafic-mafic complex, north of Tisdall Lake.

phenocrysts, commonly 6–10 mm long and locally up to 2 cm long, within an aphanitic groundmass of randomly oriented plagioclase microlites and fine opaque material (Figure 11). Ovoid to irregularly shaped green alteration patches, from a few millimetres to 3 cm in size, are also a common feature. They consist mainly of actinolite and epidote, locally accompanied by feldspar and specularite. Some of these look like amygdules, whereas others appear to represent alteration of feldspar and mafic phenocrysts. The finer grained porphyry along the margins of the stocks comprises 50% feldspar and mafic phenocrysts, 1–6 mm in size, within an aphanitic groundmass. The mafic phenocrysts have a pyroxene habit, but are seen in thin section to be pale green amphibole, possibly an alteration product. Irregular patches and lenses of green, grey and red sandstone occur locally within the finer grained porphyry near the margin of the southern stock, and are inferred to be screens of hematite-altered country rock.

The plagioclase porphyry stocks cut the polyolithic breccia succession of the Nicola Group, so are Late Triassic or younger. They may also be in contact with the Woodjam Creek unit of the Takomkane batholith, but contact relationships were not observed. The stocks resemble some coarse plagioclase-phyric flows within the Eocene Kamloops Group (Schiarizza and Bligh, 2008), but are suspected to be Mesozoic, in part because they display significant epidote-chlorite-hematite alteration, typical of Mesozoic rocks in the area.

### **Kamloops Group**

Eocene volcanic and sedimentary rocks in the Quesnel Lake map area were assigned to the Kamloops Group by Campbell (1978). The group underlies substantial areas in the northern and southwestern parts of the Murphy Lake map area (Figure 2), where it consists of mafic volcanic flows and subordinate amounts of volcanic breccia, conglomerate and sandstone. These gently dipping rocks rest unconformably above a number of different Mesozoic units, including the Nicola Group, the Spout Lake pluton, the Takomkane batholith, and the Tisdall Lake ultramafic-mafic complex (Figure 3).

The Kamloops Group in the Murphy Lake map area is represented in large part by dark grey, grey-brown to rusty-brown weathered, pyroxene-plagioclase-phyric basalt or



**Figure 11.** Coarse plagioclase porphyry from stock west of Woodjam Creek.

andesite flows and related flow breccia. Flows are typically massive to weakly columnar-jointed, but are friable in places due to pervasive platy fractures. Olivine-pyroxene-phyric basalt flows are also present, and fine-grained, aphyric andesite forms a significant part of the succession near Tisdall Lake. Vesicles within the volcanic rocks are commonly filled with chalcedonic quartz, calcite or zeolite minerals (Figure 12).

Sedimentary intervals scattered throughout the volcanic succession consist mainly of friable, yellow-brown to red weathered pebble conglomerate, with local intercalations of lithic wacke (Figure 13). The conglomerate contains mafic to intermediate volcanic-lithic clasts, probably derived from the Eocene succession, and local chips of woody material. Conglomerate near the base of the Eocene section in the northern outcrop belt also includes granitic clasts derived from the underlying Takomkane batholith, and is intercalated with quartz-feldspar sandstone and gritty sandstone.

### **Chilcotin Group**

The Chilcotin Group comprises flat-lying basalt flows and related rocks, of Early Miocene to Early Pleistocene age, that are distributed over much of the Interior Plateau of south-central BC (Bevier, 1983; Mathews, 1989; Andrews and Russell, 2007). The group is represented by a few scattered exposures in the northwest corner of the Murphy Lake map area, where it is inferred to rest unconformably above the Nicola Group and the Woodjam Creek unit of the Takomkane batholith. These exposures comprise medium to dark grey, grey-brown to rusty-brown weathered, variably vesicular, fine-grained basalt. A thin section from one of the exposures consists mainly of plagioclase, clinopyroxene, olivine and opaque minerals, arranged in a subophitic texture. A Chilcotin basalt sample collected from an exposure just west of the Murphy Lake map area, near the south end of the McIntosh Lakes, yielded a Late Miocene K-Ar whole-rock date of  $8.7 \pm 0.4$  Ma (Mathews, 1989).

### **Quaternary Basalt**

Flat-lying basalt flows of probable Quaternary age overlie the Schoolhouse Lake unit of the Takomkane



**Figure 12.** Andesite with amygdules of chalcedonic quartz, Eocene Kamloops Group, west of Tisdall Lake.

batolith in two separate areas in the southeastern part of the map area (Figure 2). The southern outlier is locally well exposed along the creek that drains the southeast end of Coffee Lake, where it is represented by columnar-jointed flows with a combined thickness of several tens of metres. Exposure is poor elsewhere, although sufficient to confirm that it is these flows that generate pronounced positive anomalies on aeromagnetic maps of the area. The basalt is dark grey, aphanitic and, in part, weakly vesicular. It contains xenocrysts ( $\pm$ phenocrysts) of olivine and numerous mantle and crustal xenoliths, generally less than 5 cm across but locally ranging up to 12 cm in size. The mantle xenoliths are mainly lherzolite. The crustal xenoliths show a wide range of textures and compositions, and include quartzfeldspathic gneiss, quartz diorite, diorite and layered gabbro.

Exposures of similar xenolith-bearing basalt occur just to the east of the Murphy Lake map area, on Takomkane Mountain (Schiarizza and Macauley, 2007a), as well as to the south, on and around Mount Timothy (Schiarizza and Bligh, 2008). They are assigned a Quaternary age because, on Takomkane Mountain, the basalt rests on a glaciated surface, but the associated cinder cone has been sculpted by subsequent glacial action (Sutherland Brown, 1958). These basalt outliers are probably related to the Quaternary Wells Gray volcanic field to the east (Hickson and Souther, 1984).

## STRUCTURE

Outcrop-scale structures within the Murphy Lake map area consist mainly of brittle faults and fractures that are more common in Mesozoic rocks than in Eocene rocks of the Kamloops Group. Rocks of the Nicola Group basalt-breccia unit north of Tisdall Lake commonly display a steeply dipping, northwest-striking schistosity, but penetrative foliations elsewhere are restricted to rare, narrow, local shear zones.

Nicola Group rocks south of the McIntosh Lakes apparently form a homoclinal succession that dips at moderate angles to the northeast (Figure 3, section A), whereas the panel of Nicola rocks exposed west of Woodjam Creek dips at moderate angles to the north-northwest (Figure 3, section B). The regional significance of these orientations is difficult to evaluate because the exposures are isolated from other Nicola rocks by tens of kilometres of plutonic rock to the east, and extensive Quaternary and Miocene cover to the west. Rocks of the basalt-breccia unit north of Tisdall Lake dip steeply to the southwest, which is consistent with their position along the west edge of a thick panel of Nicola rocks that generally dips and faces to the southwest above a basal contact with the Crooked amphibolite (Figure 4; Schiarizza and Macauley, 2007a, b).

Eocene rocks are flat lying to gently dipping wherever bedding orientations were observed. Two northerly-trending faults are inferred to the south of Tisdall Lake from abrupt juxtapositions of flat-lying Eocene rocks against rocks of the Takomkane batholith. The Eocene rocks are apparently down-dropped between the faults in a small graben structure. A northwest-trending fault in the north-western corner of the map area is likewise inferred from an apparent offset, down-dropped to the north, of the basal Eocene contact above the Takomkane batholith. This fault may also be partly responsible for a pronounced jog in the contact between the batholith and the Nicola Group (Fig-



**Figure 13.** Conglomerate and conglomeratic sandstone, Eocene Kamloops Group, east of Woodjam Creek.

ure 2). Relief on the basal Eocene contact elsewhere is inferred to be due mainly to Eocene paleotopography.

Although Eocene or younger faults are clearly present, many of the outcrop-scale faults observed within Mesozoic units are inferred to be pre-Eocene because these structures are much more prevalent in the older rocks. Steeply dipping faults with northwest, north and northeast strikes are most common. Topographic lineaments with these orientations are also common but, with the exception of the mapped Eocene or younger faults, none have been proven to be controlled by major faults.

## MINERAL OCCURRENCES

Metallic mineral occurrences are found mainly in the southwest and northwest parts of the Murphy Lake map area (Figure 14). Those in the southwest are copper showings within the Spout Lake pluton. Those in the northwest include porphyry-style copper-molybdenum-gold mineralization within the Woodjam Creek unit of the Takomkane batholith, as well as copper-gold mineralization within the adjacent Nicola Group. Occurrences elsewhere in the map area include two showings southwest of Tisdall Lake that are associated with the Boss Creek unit of the Takomkane batholith, and a copper occurrence within the Schoolhouse Lake unit of the batholith southwest of the Moffat Lakes.

### *Occurrences in the Spout Lake Pluton*

#### **CLEO (MINFILE 093A 044) AND BORY (MINFILE 093A 063)**

The Cleo and Bory showings comprise minor amounts of chalcopyrite disseminated in monzonite of the Spout Lake pluton. The Cleo showing is located about 1.5 km south of the west end of Murphy Lake and was discovered in 1971 during exploration on the Cleo claim group by Nitro Development Inc. (Kirwin, 1971). The Bory showings are located north and northeast of the east end of Two Mile Lake (Aulis, 1993). They are named after the Bory claim group, which covered this area in the early 1970s (Sutherland and Brown, 1971).

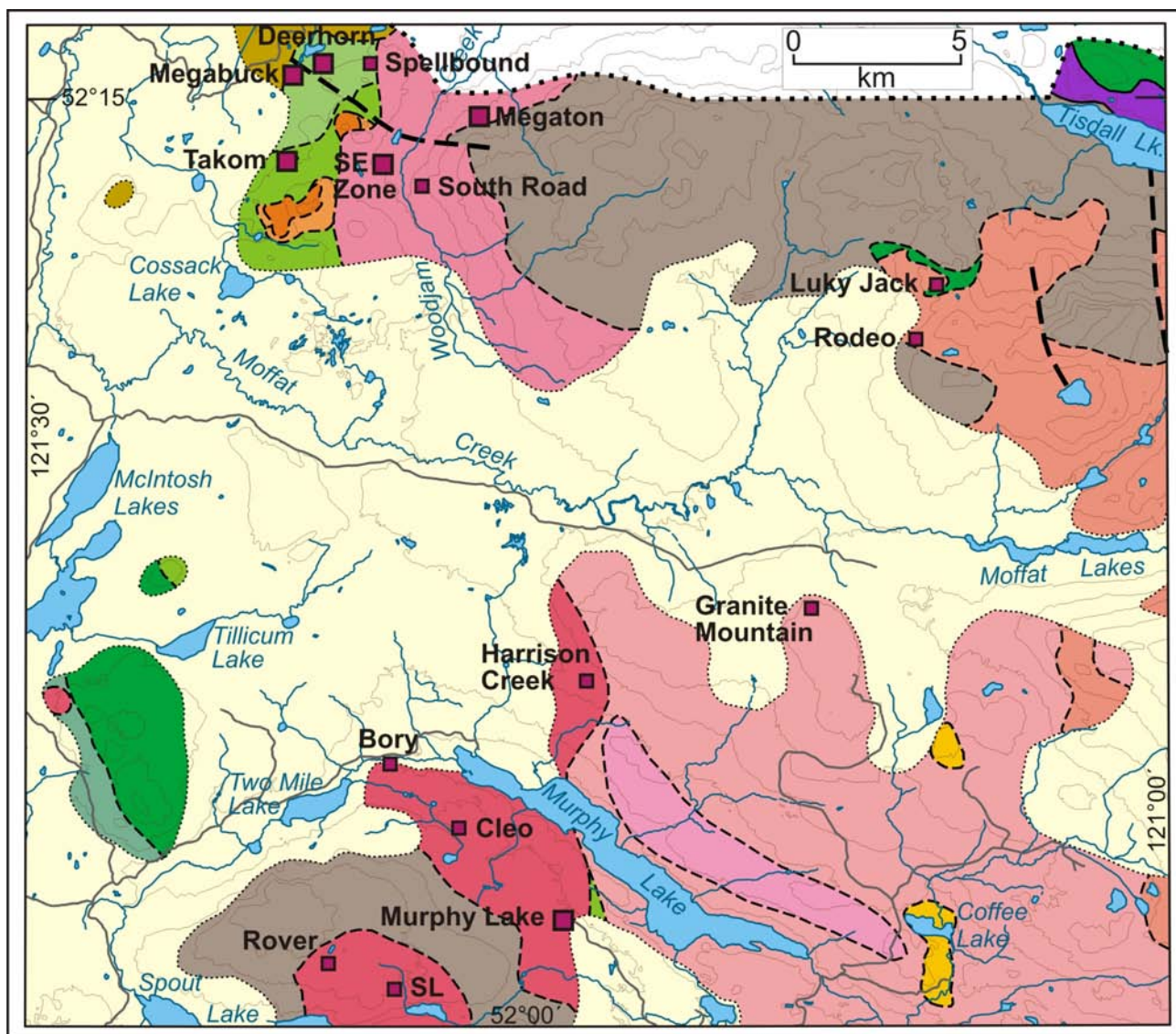


Figure 14. Mineral occurrences in the Murphy Lake map area. See Figure 2 for legend.

### MURPHY LAKE (MINFILE 093A 073)

The Murphy Lake occurrence is located 2 km south-west of Murphy Lake, within an area of commingled monzodiorite, monzonite and monzogabbro of the Spout Lake pluton. Outcrops in this area contain scattered, minor occurrences of chalcopyrite and bornite (Aulis, 1993), but the most significant mineralization was discovered during a seven-hole diamond-drill program by Regional Resources Ltd. and GWR Resources Inc. in 1995 (von Guttenberg, 1996). Hole ML95-01 intersected 45 m of 0.20% Cu, and hole ML95-06, drilled 115 m to the north, intersected 53 m of 0.34% Cu and 0.04 g/t Au. These intersections were interpreted as part of a steeply dipping, north-striking mineralized zone, 30–35 m in true width and open to depth and along strike (von Guttenberg, 1996). Candorado Operating Company Ltd. drilled five additional holes in 2004 (Ostler, 2005) and two holes in 2007 (Koffyberg, 2008). These programs confirmed widespread, low-grade copper values, but did not define any continuous zones of major mineralization. One hole, ML04-1, was drilled between holes ML95-

01 and ML95-06, but did not intersect the mineralized zone interpreted by von Guttenberg (Ostler, 2005).

Sulphide minerals at the Murphy Lake occurrence are mainly pyrite and chalcopyrite, but locally include minor amounts of bornite or molybdenite. The sulphides occur along fractures, in K-feldspar veins and as disseminations. Locally, in diamond-drill hole ML95-06, chalcopyrite occurs in veins, 10–15 cm thick, with chlorite and quartz (von Guttenberg, 1996).

### SL (MINFILE 093A 113) AND ROVER

The SL and Rover occurrences comprise minor amounts of disseminated chalcopyrite and bornite within the southern part of the Spout Lake pluton. The SL showing (occurrence 2 of Janes, 1967) was discovered in 1966 during a prospecting program by Coranex Ltd. that followed the discovery of anomalous copper in silt samples during a reconnaissance geochemical survey. This initiated staking of the Rover claim group and follow-up exploration that led to the discovery of several additional minor occurrences.

The most significant of these, occurrences 4 and 9 of Janes (1967), are shown as the Rover showing on Figure 14. There has been little subsequent work on these showings, although the SL occurrence was briefly mentioned by Vollo (1973) in a report on geophysical and geochemical surveys over the SL claim group by Craigmont Mines Ltd., and Aulis (1993) noted disseminated chalcopyrite at the Rover showing in a report describing an exploration program on the Two Mile Lake claim group by Regional Resources Ltd.

### **HARRISON CREEK**

The Harrison Creek occurrence, discovered during our 2008 mapping program, is located in the eastern part of the Spout Lake pluton, north of Murphy Lake. It comprises pyrite, chalcopyrite, magnetite and malachite within and along quartz–epidote–K-feldspar veins that cut monzodiorite. A grab sample of this mineralized vein material returned 1671 ppm Cu, 1432 ppb Ag and 105 ppb Au (Schiarizza et al., 2009, sample 08SBA-18).

### **Occurrences near Woodjam Creek**

The area around Woodjam Creek has a protracted history of mineral exploration, dating from at least the mid-1960s, largely focused on the Megabuck and Takom (formerly WL) occurrences. Exposures of the polyolithic breccia succession and the western part of the Takomkane batholith throughout this area display moderate to intense epidote alteration, locally accompanied by K-feldspar, tourmaline, magnetite and calcite. The known mineral occurrences are currently covered by two claim groups. The Woodjam property in the west was assembled by Wildrose Resources Ltd. in 1998 and currently is jointly owned by Cariboo Rose Resources Ltd. (40%) and Fjordland Exploration Inc. (60%). It encompasses the Megabuck, Takom and Spellbound occurrences, as well as the newly discovered Southeast and Deerhorn zones. The area east of the Woodjam property is covered by the Megaton claim group, which was staked by H. Wahl and J. Brown-John in 1996 and encompasses the Megaton and South Road occurrences (Figure 14).

### **MEGABUCK (MINFILE 093A 078)**

The Megabuck zone is located near the northern boundary of the Murphy Lake map area, 2.5 km west of the Takomkane batholith. The few small outcrops observed during our 2008 fieldwork comprise grey-green gritty feldspathic sandstone cut by quartz veinlets that carry pyrite and chalcopyrite. A grab sample of mineralized rock returned 1431.92 ppm Cu, 29.27 ppm Mo and 1226 ppb Au (Schiarizza et al., 2009, sample 08PSC-260). The host-rocks are assigned to the upper unit of the Nicola Group polyolithic breccia succession, as are good exposures of sandstone, conglomerate and breccia located about 1 km to the east and southeast. Small exposures of basalt, belonging to the Miocene–Pliocene Chilcotin Group, occur 500 m west of the mineralized outcrops.

The first drilling on the Megabuck occurrence comprised two diamond-drill holes by Exploram Minerals Ltd. in 1974 (Cruz, 1974a). Subsequent exploration has included diamond-drill programs by Placer Development Ltd. in 1983 and 1984, by Phelps Dodge Corp. in 1999, and by Fjordland Exploration Inc. from 2002 to 2007 (in part summarized by Peters, 2007). These programs have outlined a complex but approximately tabular mineralized

zone about 175 m thick that trends northeast and dips about 45° to the southeast (Peters, 2005, 2007). Drill-tested mineralization has a 300 m strike length and extends 400 m down dip; it is truncated by mineralized faults to the northeast and east, but remains open to depth and to the southwest. Notable intersections from Fjordland's 2004 drilling program, designed mainly to test the mineralization at depth, include 0.81 g/t Au and 0.12% Cu over 378 m in hole 04-32, and 0.77 g/t Au and 0.13% Cu over 397.5 m in hole 04-37 (Peters, 2005).

Mineralization in the Megabuck zone consists of chalcopyrite, pyrite and minor amounts of bornite, which occur in several generations of quartz and quartz-calcite veins and stockworks, and also as disseminations and along fractures. Complex alteration assemblages include quartz, carbonate, epidote, K-feldspar, magnetite, hematite, chlorite and sericite (Campbell and Pentland, 1983; Peters, 2005). The hostrocks have been interpreted by some workers as a layered sequence of tuff, volcanic breccia and volcanic-derived sedimentary rocks (e.g., Campbell and Pentland, 1983), whereas others have indicated that the zone includes a significant proportion of premineralization dioritic to monzonitic intrusive rocks (e.g., Peters, 2005, 2007). The age of mineralization is partially constrained by an Ar/Ar cooling age of  $163.67 \pm 0.84$  Ma on biotite from a post-mineralization quartz-feldspar porphyry dike (Logan et al., 2007).

### **DEERHORN (MINFILE 093A 204)**

The Deerhorn zone, located about 1 km northeast of the Megabuck zone, comprises mineralization that was encountered during a 2003 diamond-drilling program by Fjordland Exploration Inc., designed to test an area of anomalous copper in soils coincident with an IP anomaly that extends east-northeast from the Megabuck zone. The best mineralization came from hole DH-03-30, which intersected a breccia zone with quartz-carbonate veining and semimassive chalcopyrite, grading 0.90% Cu and 42.3 ppb Au over 15.4 m (Peters, 2004). Evaluation of this area is in its early stages, but diamond-drill hole WJ-06-70, 600 m northeast of hole DH-03-30, also encountered copper mineralization (Peters, 2007), as did two holes drilled on a separate IP anomaly in 2008, about 1 km north of DH-03-30 (Cariboo Rose Resources Ltd., 2008).

### **SPELLBOUND (MINFILE 093A 205)**

The Spellbound showing is within hornfelsed sandstone of the polyolithic breccia succession near the contact of the Takomkane batholith, about 2.3 km east of the Megabuck zone. It comprises minor amounts of chalcopyrite and pyrite in quartz stockworks within a broader area of tourmaline-epidote alteration. The mineralization was discovered by Noranda Exploration Company Ltd. in 1992, but has received little subsequent attention. A grab sample collected during an exploration program by Fjordland Minerals Ltd. in 2001 returned 1992 ppm Cu and 13 ppb Au (Peters, 2002, sample V-9).

### **TAKOM (MINFILE 093A 206)**

The Takom zone is 2.5 km south of the Megabuck zone. Bedrock exposure is limited to a couple of old trenches and road scrapes, and consists of variably silicified and pyritic granodiorite to quartz monzodiorite that resembles the Woodjam Creek unit of the Takomkane batholith. Small exposures of pyrite-altered breccia occur a

few hundred metres east of the granitic outcrops, and there are good exposures of epidote±tourmaline-altered breccia in a cut block about 700 m to the south. These breccia exposures are assigned to the polyolithic breccia succession of the Nicola Group.

Exploram Minerals Ltd. tested the area with three diamond-drill holes in 1974 and another hole in 1977 (Cruz, 1974b, 1977). One of the holes, 74-3, intersected 1.3 g/t Au and 0.13% Cu over a 10.7 m interval that also included 1.5 m of 0.028% MoS<sub>2</sub> (Carne, 1984). Fjordland Exploration Inc. drilled eight reverse-circulation holes and one diamond-drill hole in 2005, to test coincident IP and copper-in-soils anomalies. The results were encouraging, and included an intersection grading 0.10 g/t Au and 0.12% Cu over the bottom 82.6 m of the diamond-drill hole (Peters, 2006, hole 05-48). A 526.4 m diamond-drill hole in 2006 intersected 0.033 g/t Au and 0.058% Cu over 464.0 m, and included several higher grade intersections (Peters, 2007, hole 06-71). The hostrocks intersected in Fjordland's drillholes are described mainly as feldspathic volcanics, volcanoclastics and breccias, cut by granitic intrusive rocks and hornblende porphyry. Mineralization consists of chalcopyrite, pyrite, magnetite and minor molybdenite, which occur in quartz stringers, as disseminations and along fractures.

## SOUTHEAST ZONE

The Southeast zone is a porphyry-style copper-molybdenum-gold occurrence hosted by the Woodjam Creek unit of the Takomkane batholith. It is located on low, drift-covered ground a short distance west of Woodjam Creek, about 2.5 km east of the Takom occurrence. The mineralization was discovered in the late summer and fall of 2007, when Fjordland Exploration Inc. initiated a drilling program to test an IP chargeability anomaly identified by a geophysical survey conducted earlier that year. Three widely spaced vertical diamond-drill holes that were completed during the program were mineralized from top to bottom. The best grades came from hole WJ-07-79, which intersected 203.55 m grading 0.34% Cu and 0.014% Mo (Fjordland Exploration Inc., 2008a). Drilling began again in the spring of 2008 and, by the end of summer, a total of 15 vertical holes, totalling 6059 m, had been drilled in the Southeast zone; all were mineralized from the bedrock surface to the bottom of the hole (Fjordland Exploration Inc., 2008b). The deepest hole (WJ-08-82) extended to 700.4 m and intersected 570.9 m grading 0.24% Cu, 0.013% Mo and 0.028 g/t Au. The highest copper and gold grades so far recorded are from hole WJ-08-84, which intersected 226.77 m grading 0.93% Cu, 0.003% Mo and 0.40 g/t Au, including 51.00 m grading 1.61% Cu, 0.004% Mo and 0.84 g/t Au. Drilling has so far covered less than a third of the 1.5 km by 1.0 km IP anomaly, and mineralization remains open in all directions (Fjordland Exploration Inc., 2008b).

Mineralization in the Southeast zone consists of pyrite, chalcopyrite and molybdenite, which occur along fractures, in quartz veinlets and as disseminations. A core sample from diamond-drill hole WJ-07-79 was submitted to R. Creaser at the University of Alberta for Re-Os dating of molybdenum, and returned a model age of 196.9 ± 0.9 Ma (J. Logan, pers comm, 2008). This Early Jurassic age demonstrates that mineralization was broadly synchronous with crystallization of the host Woodjam Creek unit of the Takomkane batholith.

## MEGATON

The Megaton copper occurrence is hosted by the Woodjam Creek unit of the Takomkane batholith on the east side of Woodjam Creek, about 3 km northeast of Fjordland's Southeast zone. The initial discovery, made in the late summer of 1995 and followed up in the spring of 1996, comprised blocks of limonite- and malachite-stained granodiorite in a road bank within a new cut block. This led to staking of the Megaton claim group and several trenching programs, carried out from 1996 to 2006, that uncovered a significant area of copper mineralization (Wahl, 1996, 2002, 2006). The Megaton claims were subsequently optioned by Northern Rand Resource Corp., who carried out a major drilling program over the Megaton showing during the summer of 2008.

Trenches and drill roads on the Megaton showing expose highly fractured granodiorite, with fracture-controlled clay and limonite alteration, and abundant malachite and azurite, mainly along fractures and shears. Native copper is also reported, as are local occurrences of bornite, chalcopyrite and traces of molybdenite (Wahl, 2002, 2006). The sulphide minerals and their alteration products occur along fractures, in quartz veins and as disseminations.

The initial phase of diamond-drilling carried out by Northern Rand Resource Corp. consisted of 3186 m in 15 holes. Only a few preliminary results have been released, including intersections of 0.256% Cu over 13.9 m, 0.237% Cu over 7.1 m, and 0.340% Cu over 26 m, in hole MT 07a (Northern Rand Resource Corp., 2008).

## SOUTH ROAD

The South Road showing is within the southern part of the Megaton claim group, on the slopes east of Woodjam Creek, about 1200 m southeast of Fjordland's Southeast zone. The mineralized outcrops were discovered in 1996, in the drainage ditch along a newly constructed logging road (Wahl, 1996). The mineralization consists of pyrite, chalcopyrite, malachite and local traces of molybdenite, which occur along fractures and shears cutting granodiorite of the Takomkane batholith (Woodjam Creek unit). Part of the original showing was re-exposed with a hand trench in 2002 (Wahl, 2002), but it has not received any subsequent attention.

## **Occurrences Associated with the Boss Creek and Schoolhouse Lake Units of the Takomkane Batholith**

### RODEO AND LUKY JACK OCCURRENCES

The Rodeo and Luky Jack occurrences are located 6–8 km southeast of Tisdall Lake. The TL claims, held by the Bethlehem Copper Corporation, were staked over this area in 1980 and were explored by Cominco Ltd. in 1981 with a program that included geological mapping, a soil geochemical survey and an induced-polarization geophysical survey (Rebic, 1981; Jackisch, 1981). Minor amounts of chalcopyrite and malachite, as disseminations and fracture-coatings, were identified at this time within quartz monzodiorite of the Takomkane batholith. Part of the area was re-staked as the Rodeo claims in 1998, to cover mineralization exposed in a pit excavated for road-fill during logging operations by Weldwood of Canada Ltd (Wahl, 1998). The adjoining Luky Jack claims were staked at the same time, to cover a

zinc-in-soils geochemical anomaly and an adjacent IP geophysical anomaly, both identified by Cominco in 1981.

The Rodeo showing consists of chalcopyrite, locally with malachite and azurite, that occurs as disseminations, blebs and fracture-fillings associated with alteration and vein assemblages that include quartz, magnetite, epidote, K-feldspar and sericite. The hostrock is mainly quartz monzodiorite of the Takomkane batholith. A grab sample collected during the present study contained 6335.27 ppm Cu, 3824 ppb Ag and 212 ppb Au (Schiarizza et al., 2009, sample 08KBE-140). A short diamond-drill hole directed under the mineralized exposures in 2001 did not intersect any significant mineralization (Wahl, 2004).

The Luky Jack showing is located about 1800 m north-northeast of the Rodeo occurrence, and has been explored with trenches and two short diamond-drill holes (Wahl, 1998, 2004). It comprises quartz veins and stockworks that locally contain minor amounts of sphalerite and chalcopyrite, and are associated with alteration assemblages that include epidote, magnetite, K-feldspar and sericite. Hostrocks include the Boss Creek unit of the Takomkane batholith and adjacent breccias and flows of the Nicola Group.

### GRANITE MOUNTAIN OCCURRENCE

The Granite Mountain copper occurrence is hosted by the Schoolhouse Lake unit of the Takomkane batholith, 5 km west-southwest of the Moffat Lakes. A group of claims covering this area was referred to as the Granite Mountain property by Bailey (2007), who described a small program of geological mapping and soil sampling. Mineralization consists of minor chalcopyrite and malachite marginal to shear-zone-hosted quartz veins, and minor malachite staining along joints within granodiorite to the south of the veins (Bailey, 2007).

### ACKNOWLEDGMENTS

We thank Patrick Young for his capable and enthusiastic assistance during fieldwork, and Jean and Mike Peake for their excellent hospitality at Eagle Creek. We also thank Jim Logan for discussions concerning the geology and metallogeny of the region, and Nick Massey for editing an earlier version of the manuscript. This program was partially funded through the Geological Survey of Canada's Geoscience for Pine Beetle program.

### REFERENCES

- Andrews, G.D.M. and Russell, J.K. (2007): Mineral exploration potential beneath the Chilcotin Group (NTS 0920, P; 093A, B, C, F, G, J, K), south-central British Columbia: preliminary insights from volcanic facies analysis; in *Geological Fieldwork 2006, BC Ministry of Energy, Mines and Petroleum Resources*, Paper 2007-1 and *Geoscience BC*, Report 2007-1, pages 229–238.
- Aulis, R.J. (1993): Geological and geochemical surveys on the Lac La Hache property (Two Mile Lake group); *BC Ministry of Energy, Mines and Petroleum Resources*, Report 23089, 45 pages.
- Bailey, D.G. (2007): 2007 exploration, Granite Mountain project, Moffat Lakes, Cariboo Mining Division, British Columbia; *BC Ministry of Energy, Mines and Petroleum Resources*, Assessment Report 29405, 18 pages.
- Barr, D.A., Fox, P.E., Northcote, K.E. and Preto, V.A. (1976): The alkaline suite porphyry deposits—a summary; in *Porphyry Deposits of the Canadian Cordillera*, Sutherland Brown, A., Editor, *Canadian Institute of Mining and Metallurgy*, Special Volume 15, pages 359–367.
- Bevier, M.L. (1983): Regional stratigraphy and age of Chilcotin Group basalts, south-central British Columbia; *Canadian Journal of Earth Sciences*, Volume 20, pages 515–524.
- Bloodgood, M.A. (1990): Geology of the Eureka Peak and Spanish Lake map areas, British Columbia; *BC Ministry of Energy, Mines and Petroleum Resources*, Paper 1990-3, 36 pages.
- Brown, R.L., Journeay, J.M., Lane, L.S., Murphy, D.C. and Rees, C.J. (1986): Obduction, backfolding and piggyback thrusting in the metamorphic hinterland of the southeastern Canadian Cordillera; *Journal of Structural Geology*, Volume 8, pages 255–268.
- Campbell, K.V. (1971): Metamorphic petrology and structural geology of the Crooked Lake area, Cariboo Mountains, British Columbia; unpublished PhD thesis, *University of Washington*, 192 pages.
- Campbell, R.B. (1978): Geological map of the Quesnel Lake map-area, British Columbia; *Geological Survey of Canada*, Open File 574, scale 1:125 000.
- Campbell, R.B. and Tipper, H.W. (1971): Bonaparte Lake map area, British Columbia; *Geological Survey of Canada*, Memoir 363, 100 pages.
- Campbell, S. and Pentland, W. (1983): A diamond drilling report on the Horsefly property, LS #1, AB #3 and #4 mineral claims, Horsefly, British Columbia, Cariboo Mining Division; *BC Ministry of Energy, Mines and Petroleum Resources*, Assessment Report 12522, 85 pages.
- Cariboo Rose Resources Ltd. (2008): New mineralized zone discovered by drilling at the Woodjam, BC Project; Cariboo Rose Resources Ltd., news release, October 1, 2008.
- Carne, J.F. (1984): Geological and geochemical report on the Ravioli 85-1 group, Ravioli 85-2 group, Ravioli 85-3 group, Cariboo Mining Division; *BC Ministry of Energy, Mines and Petroleum Resources*, Assessment Report 13741, 16 pages.
- Carson, J.M., Dumont, R., Potvin, J., Shives, R.B.K., Harvey, B.J.A., Buckle, J.L. and Cathro, M. (2006a): Geophysical Series, NTS 93A/3, 93A/2, 93A/6, 93A/7, 92P/14, Eagle (Murphy) Lake, British Columbia; *Geological Survey of Canada*, Open File 5292, 10 maps at 1:50 000 scale.
- Carson, J.M., Dumont, R., Potvin, J., Shives, R.B.K., Harvey, B.J.A. and Buckle, J.L. (2006b): Geophysical Series, NTS 93A/2, 93A/3, 92P/14, 92P/15, McKinley Creek, British Columbia; *Geological Survey of Canada*, Open File 5293, 10 maps at 1:50 000 scale.
- Casselmann, M.J., McMillan, W.J. and Newman, K.M. (1995): Highland Valley porphyry copper deposits near Kamloops, British Columbia: a review and update with emphasis on the Valley deposit; in *Porphyry Deposits of the Northwestern Cordillera of North America*, Schroeter, T.G., Editor, *Canadian Institute of Mining, Metallurgy and Petroleum*, Special Volume 46, pages 161–191.
- Cruz, E.D. (1974a): Assessment work submission on the HS claims, Cariboo Mining Division, British Columbia; *BC Ministry of Energy, Mines and Petroleum Resources*, Assessment Report 5237, 102 pages.
- Cruz, E.D. (1974b): Assessment work submission on the WL claims, Cariboo Mining Division, British Columbia; *BC Ministry of Energy, Mines and Petroleum Resources*, Assessment Report 5411, 78 pages.
- Cruz, E.D. (1977): Assessment work submission on the WL claims, Cariboo Mining Division, British Columbia; *BC Ministry of Energy, Mines and Petroleum Resources*, Assessment Report 6315, 49 pages.

- Dawson, G.M. (1879): Preliminary report on the physical and geological features of the southern portion of the interior of British Columbia; in Report of Progress, 1877–1878, Part B, *Geological Survey of Canada*, pages 1B–187B.
- Dostal, J., Church, B.N. and Höy, T. (2001): Geological and geochemical evidence for variable magmatism and tectonics in the southern Canadian Cordillera: Paleozoic to Jurassic suites, Greenwood, southern British Columbia; *Canadian Journal of Earth Sciences*, Volume 38, pages 75–90.
- Dumont, R., Potvin, J., Carson, J.M., Harvey, B.J.A., Coyle, M., Shives, R.B.K. and Ford, K.L. (2007): Geophysical Series, Eagle (Murphy) Lake 93A/3, British Columbia – Bonaparte Lake East geophysical survey; *Geological Survey of Canada*, Open File 5496 and *Geoscience BC*, Map 2007-3-9, 10 maps at 1:50 000 scale.
- Erdmer, P., Heaman, L., Creaser, R.A., Thompson, R.I. and Daughtry, K.L. (2001): Eocambrian granite clasts in southern British Columbia shed light on Cordilleran hinterland crust; *Canadian Journal of Earth Sciences*, Volume 38, pages 1007–1016.
- Ewing, T.E. (1980): Paleogene tectonic evolution of the Pacific Northwest; *Journal of Geology*, Volume 88, pages 619–638.
- Ferri, F. (1997): Nina Creek Group and Lay Range assemblage, north-central British Columbia: remnants of late Paleozoic oceanic and arc terranes; *Canadian Journal of Earth Sciences*, Volume 34, pages 854–874.
- Fjordland Exploration Inc. (2008a): Woodjam's Southeast zone returns 0.40% copper and 0.014% molybdenum over 113.8 metres; Fjordland Exploration Inc., news release, January 18, 2008.
- Fjordland Exploration Inc. (2008b): Woodjam Project: Southeast zone drilling intersects 200.76 metres of 1.01% copper and 0.44 g/t gold open to depth; Fjordland Exploration Inc., news release, October 14, 2008.
- Fox, P.E. (1975): Alkaline rocks and related mineral deposits of the Quesnel Trough, British Columbia (abstract); *Geological Association of Canada*, Symposium on Intrusive Rocks and Related Mineralization of the Canadian Cordillera, Program and Abstracts, page 12.
- Hickson, C.J. and Souther, J.G. (1984): Late Cenozoic volcanic rocks of the Clearwater–Wells Gray area, British Columbia; *Canadian Journal of Earth Sciences*, Volume 21, pages 267–277.
- Höy, T. and Dunne, K.P.E. (1997): Early Jurassic Rosland Group, southern British Columbia: part I—stratigraphy and tectonics; *BC Ministry of Energy, Mines and Petroleum Resources*, Bulletin 102, 123 pages.
- Jackisch, I. (1981): Geophysical survey on the Tisdall group, Horsefly area, Cariboo Mining Division, British Columbia; *BC Ministry of Energy, Mines and Petroleum Resources*, Assessment Report 9370, Part 2, 19 pages.
- Janes, R.H. (1967): Geochemical report, Rover, fourteen miles north-northeast of Lac La Hache; *BC Ministry of Energy, Mines and Petroleum Resources*, Assessment Report 949, 25 pages.
- Kirwin, G.L. (1971): Geomagnetic-geochemical survey, Cleo claim group, Cariboo Mining District, British Columbia; *BC Ministry of Energy, Mines and Petroleum Resources*, Assessment Report 3387, 11 pages.
- Klepacki, D.W. and Wheeler, J.O. (1985): Stratigraphic and structural relations of the Milford, Kaslo and Slocan groups, Goat Range, Lardeau and Nelson map areas, British Columbia; in Current Research, Part A, *Geological Survey of Canada*, Paper 85-1A, pages 277–286.
- Koffyberg, A. (2008): Assessment report on airborne geophysical interpretation, prospecting, soil geochemistry and drill program, Murphy Lake property, Cariboo Mining Division, British Columbia; *BC Ministry of Energy, Mines and Petroleum Resources*, Assessment Report 29754, 262 pages.
- Logan, J.M. and Mihalynuk, M.G. (2005a): Regional geology and setting of the Cariboo, Bell, Springer and Northeast porphyry Cu-Au zones at Mount Polley, south-central British Columbia; in Geological Fieldwork 2004, *BC Ministry of Energy, Mines and Petroleum Resources*, Paper 2005-1, pages 249–270.
- Logan, J.M. and Mihalynuk, M.G. (2005b): Porphyry Cu-Au deposits of the Iron Mask batholith, southeastern British Columbia; in Geological Fieldwork 2004, *BC Ministry of Energy, Mines and Petroleum Resources*, Paper 2005-1, pages 271–290.
- Logan, J.M., Mihalynuk, M.G., Ullrich, T. and Friedman, R.M. (2007): U-Pb ages of intrusive rocks and  $^{40}\text{Ar}/^{39}\text{Ar}$  plateau ages of copper-gold-silver mineralization associated with alkaline intrusive centres at Mount Polley and the Iron Mask batholith, southern and central British Columbia; in Geological Fieldwork 2006, *BC Ministry of Energy, Mines and Petroleum Resources*, Paper 2007-1 and *Geoscience BC*, Report 2007-1, pages 93–116.
- Macdonald, A.J., Spooner, E.T.C. and Lee, G. (1995): The Boss Mountain molybdenum deposit, central British Columbia; in Porphyry Deposits of the Northwestern Cordillera of North America, Schroeter, T.G., Editor, *Canadian Institute of Mining, Metallurgy and Petroleum*, Special Volume 46, pages 691–696.
- Mathews, W.H. (1989): Neogene Chilcotin basalts in south-central British Columbia: geology, ages, and geomorphic history; *Canadian Journal of Earth Sciences*, Volume 26, pages 969–982.
- McMullin, D.W.A., Greenwood, H.J. and Ross, J.V. (1990): Pebbles from Barkerville and Slide Mountain terranes in a Quesnel terrane conglomerate: evidence for pre-Jurassic deformation of the Barkerville and Slide Mountain terranes; *Geology*, Volume 18, pages 962–965.
- Monger, J.W.H. and McMillan, W.J. (1989): Geology, Ashcroft, British Columbia (92I); *Geological Survey of Canada*, Map 42-1989, sheet 1, 1:250 000 scale.
- Monger, J.W.H., Price, R.A. and Tempelman-Kluit, D.J. (1982): Tectonic accretion and the origin of the two major metamorphic and plutonic belts in the Canadian Cordillera; *Geology*, Volume 10, pages 70–75.
- Monger, J.W.H., Wheeler, J.O., Tipper, H.W., Gabrielse, H., Harms, T., Struik, L.C., Campbell, R.B., Dodds, C.J., Gehrels, G.E. and O'Brien, J. (1991): Part B—Cordilleran terranes; in Upper Devonian to Middle Jurassic Assemblages, Chapter 8 of Geology of the Cordilleran Orogen in Canada, Gabrielse, H. and Yorath, C.J., Editors, *Geological Survey of Canada*, Geology of Canada, Number 4, pages 281–327 (also *Geological Society of America*, The Geology of North America, Volume G-2).
- Mortensen, J.K., Ghosh, D.K. and Ferri, F. (1995): U-Pb geochronology of intrusive rocks associated with copper-gold porphyry deposits in the Canadian Cordillera; in Porphyry Deposits of the Northwestern Cordillera of North America, Schroeter, T.G., Editor, *Canadian Institute of Mining, Metallurgy and Petroleum*, Special Volume 46, pages 142–158.
- Mortimer, N. (1987): The Nicola Group: Late Triassic and Early Jurassic subduction-related volcanism in British Columbia; *Canadian Journal of Earth Sciences*, Volume 24, pages 2521–2536.
- Nelson, J.L. and Bellefontaine, K.A. (1996): The geology and mineral deposits of north-central Quesnellia; Tezzeron Lake to Discovery Creek, central British Columbia; *BC Ministry of Energy, Mines and Petroleum Resources*, Bulletin 99, 112 pages.
- Northern Rand Resource Corp. (2008): Northern Rand drills 26 metres of 0.34% Cu at Megaton; Northern Rand Resource Corp., news release, September 9, 2008.

- Ostler, J. (2005): Geological mapping, drilling, and geophysical surveys on the Mur and Copper property areas; *BC Ministry of Energy, Mines and Petroleum Resources*, Assessment Report 27712, Part A, 222 pages.
- Pálffy, J., Smith, P.L. and Mortensen, J.K. (2000): A U-Pb and  $^{40}\text{Ar}/^{39}\text{Ar}$  time scale for the Jurassic; *Canadian Journal of Earth Sciences*, Volume 37, pages 923–944.
- Panteleyev, A., Bailey, D.G., Bloodgood, M.A. and Hancock, K.D. (1996): Geology and mineral deposits of the Quesnel River–Horsefly map area, central Quesnel Trough, British Columbia; *BC Ministry of Energy, Mines and Petroleum Resources*, Bulletin 97, 155 pages.
- Peters, L.J. (2002): Assessment report, including induced polarization and magnetometer surveys, on the Woodjam property, Woodjam 5 (367190) claim and Woodjam 6–12 (367883–89) claims, Cariboo Mining Division, British Columbia; *BC Ministry of Energy, Mines and Petroleum Resources*, Assessment Report 26838, 35 pages.
- Peters, L.J. (2004): Assessment report, including diamond drilling, on the Woodjam property, Woodjam 5 (367190) claim and Woodjam 6–12 (367883–89) claims, Cariboo Mining Division, British Columbia; *BC Ministry of Energy, Mines and Petroleum Resources*, Assessment Report 27330, 60 pages.
- Peters, L.J. (2005): Assessment report, including diamond drilling, on the Woodjam property, Woodjam 5 (367190) claim, Woodjam 6–12 (367883–89) claims, Woodjam 14 (412157) claim, Cariboo Mining Division, British Columbia; *BC Ministry of Energy, Mines and Petroleum Resources*, Assessment Report 27735, 220 pages.
- Peters, L.J. (2006): Assessment report, including diamond and reverse circulation drilling, on the Woodjam property, Woodjam 5 (367190) claim, Woodjam 6–12 (367883–89) claims, Woodjam 14 (412157) claim, Cariboo Mining Division, British Columbia; *BC Ministry of Energy, Mines and Petroleum Resources*, Assessment Report 28419, 234 pages.
- Peters, L.J. (2007): Assessment report, including diamond drilling, on the Woodjam property, Cariboo Mining Division, British Columbia; *BC Ministry of Energy, Mines and Petroleum Resources*, Assessment Report 28823, 447 pages.
- Preto, V.A. (1977): The Nicola Group: Mesozoic volcanism related to rifting in southern British Columbia; in *Volcanic Regimes in Canada*, W.R.A. Baragar, L.C. Coleman and J.M. Hall, Editors, *Geological Association of Canada*, Special Paper 16, pages 39–57.
- Preto, V.A. (1979): Geology of the Nicola Group between Merritt and Princeton; *BC Ministry of Energy, Mines and Petroleum Resources*, Bulletin 69, 90 pages.
- Rebic, Z. (1981): Geochemical and geological report on the Tisdall Lake group (claims 1 and 2), Horsefly area, Cariboo Mining Division, British Columbia; *BC Ministry of Energy, Mines and Petroleum Resources*, Assessment Report 9370, Part 1, 32 pages.
- Rees, C.J. (1987): The Intermontane-Omineca belt boundary in the Quesnel Lake area, east-central British Columbia: tectonic implications based on geology, structure and paleomagnetism; unpublished PhD thesis, *Carleton University*, 421 pages.
- Roback, R.C. and Walker, N.W. (1995): Provenance, detrital zircon U-Pb geochronometry, and tectonic significance of Permian to Lower Triassic sandstone in southeastern Quesnelia, British Columbia and Washington; *Geological Society of America Bulletin*, Volume 107, pages 665–675.
- Ross, J.V., Fillipone, J., Montgomery, J.R., Elsby, D.C. and Bloodgood, M. (1985): Geometry of a convergent zone, central British Columbia, Canada; *Tectonophysics*, Volume 119, page 285–297.
- Schau, M.P. (1970): Stratigraphy and structure of the type area of the Upper Triassic Nicola Group in south-central British Columbia; in *Structure of the Southern Canadian Cordillera*, Wheeler, J.O., Editor, *Geological Association of Canada*, Special Paper 6, pages 123–135.
- Schiarizza, P. (1989): Structural and stratigraphic relationships between the Fennell Formation and Eagle Bay Assemblage, western Omineca Belt, south-central British Columbia: implications for Paleozoic tectonics along the paleocontinental margin of western North America; unpublished MSc thesis, *University of Calgary*, Calgary, Alberta, 343 pages.
- Schiarizza, P. and Bligh, J.S. (2008): Geology and mineral occurrences of the Timothy Lake area, south-central British Columbia (NTS 092P/14); in *Geological Fieldwork 2007*, *BC Ministry of Energy, Mines and Petroleum Resources*, Paper 2008-1, pages 191–211.
- Schiarizza, P. and Boulton, A. (2006a): Geology and mineral occurrences of the Quesnel Terrane, Canim Lake area (NTS 092P/15), south-central British Columbia; in *Geological Fieldwork 2005*, *BC Ministry of Energy, Mines and Petroleum Resources*, Paper 2006-1 and *Geoscience BC*, Report 2006-1, pages 163–184.
- Schiarizza, P. and Boulton, A. (2006b): Geology of the Canim Lake area, NTS 92P/15; *British Columbia Ministry of Energy, Mines and Petroleum Resources*, Open File 2006-8, 1:50 000 scale.
- Schiarizza, P. and Israel, S. (2001): Geology and mineral occurrences of the Nehalliston Plateau, south-central British Columbia (92P/7, 8, 9, 10); in *Geological Fieldwork 2000*, *BC Ministry of Energy, Mines and Petroleum Resources*, Paper 2001-1, pages 1–30.
- Schiarizza, P. and Macauley, J. (2007a): Geology and mineral occurrences of the Hendrix Lake area (NTS 093A/02), south-central British Columbia; in *Geological Fieldwork 2006*, *BC Ministry of Energy, Mines and Petroleum Resources*, Paper 2007-1 and *Geoscience BC*, Report 2007-1, pages 179–202.
- Schiarizza, P. and Macauley, J. (2007b): Geology of the Hendrix Lake area, NTS 93A/02; *BC Ministry of Energy, Mines and Petroleum Resources*, Open File 2007-3, 1:50 000 scale.
- Schiarizza, P. and Preto, V.A. (1987): Geology of the Adams Plateau–Clearwater–Vavenby area; *BC Ministry of Energy, Mines and Petroleum Resources*, Paper 1987-2, 88 pages.
- Schiarizza, P. and Tan, S.H. (2005): Geology and mineral occurrences of the Quesnel Terrane between the Mesilinka River and Wrede Creek (NTS 94D/8, 9), north-central British Columbia; in *Geological Fieldwork 2004*, *BC Ministry of Energy, Mines and Petroleum Resources*, Paper 2005-1, pages 109–130.
- Schiarizza, P., Bell, K. and Bayliss, S. (2009): Geology of the Murphy Lake area, NTS 093A/03; *BC Ministry of Energy, Mines and Petroleum Resources*, Open File 2009-3, 1:50 000 scale.
- Schiarizza, P., Bligh, J.S., Bluemel, B. and Tait, D. (2008): Geology of the Timothy Lake area, NTS 92P/14; *BC Ministry of Energy, Mines and Petroleum Resources*, Open File 2008-5, 1:50 000 scale.
- Schiarizza, P., Heffernan, S. and Zuber, J. (2002a): Geology of Quesnel and Slide Mountain terranes west of Clearwater, south-central British Columbia (92P/9, 10, 15, 16); in *Geological Fieldwork 2001*, *BC Ministry of Energy, Mines and Petroleum Resources*, Paper 2002-1, pages 83–108.
- Schiarizza, P., Heffernan, S., Israel, S. and Zuber, J. (2002b): Geology of the Clearwater–Bowers Lake area, British Columbia (NTS 92P/9, 10, 15, 16); *BC Ministry of Energy, Mines and Petroleum Resources*, Open File 2002-15, 1:50 000 scale.
- Schiarizza, P., Israel, S., Heffernan, S. and Zuber, J. (2002c): Geology of the Nehalliston Plateau (92P/7, 8, 9, 10); *BC Ministry of Energy, Mines and Petroleum Resources*, Open File 2002-4, 1:50 000 scale.
- Smith, R.B. (1979): Geology of the Harper Ranch Group (Carboniferous-Permian) and Nicola Group (Upper Triassic) north-

- east of Kamloops, British Columbia; unpublished MSc thesis, *University of British Columbia*, Vancouver, BC, 202 pages.
- Soregaroli, A.E. and Nelson, W.I. (1976): Boss Mountain; in Porphyry Deposits of the Canadian Cordillera, Sutherland Brown, A., Editor, *Canadian Institute of Mining and Metallurgy*, Special Volume 15, pages 432–443.
- Struik, L.C. (1988a): Crustal evolution of the eastern Canadian Cordillera; *Tectonics*, Volume 7, pages 727–747.
- Struik, L.C. (1988b): Regional imbrication within Quesnel Terrane, central British Columbia, as suggested by conodont ages; *Canadian Journal of Earth Sciences*, Volume 25, pages 1608–1617.
- Struik, L.C. (1988c): Structural geology of the Cariboo gold mining district, east-central British Columbia; *Geological Survey of Canada*, Memoir 421, 100 pages.
- Struik, L.C., Schiarizza, P., Orchard, M.J., Cordey, F., Sano, H., MacIntyre, D.G., Lapierre, H. and Tardy, M. (2001): Imbricate architecture of the upper Paleozoic to Jurassic oceanic Cache Creek Terrane, central British Columbia; *Canadian Journal of Earth Sciences*, Volume 38, pages 495–514.
- Sutherland Brown, A. (1958): Boss Mountain; in Annual Report of the Minister of Mines for 1957, *BC Ministry of Energy, Mines and Petroleum Resources*, pages 18–22.
- Sutherland, D.B. and Brown, D.H. (1971): Interim report on the induced polarization and resistivity survey on the Bory Mineral claims, Murphy Lake, British Columbia, Cariboo Mining District; *BC Ministry of Energy, Mines and Petroleum Resources*, Assessment Report 3232, 58 pages.
- Thompson, R.I., Glombick, P., Erdmer, P., Heaman, L.M., Lemieux, Y. and Daughtry, K.L. (2006): Evolution of the ancestral Pacific margin, southern Canadian Cordillera: insights from new geologic maps; in Paleozoic Evolution and Metallogeny of Pericratonic Terranes at the Ancient Pacific Margin of North America, Canadian and Alaskan Cordillera, Colpron, M. and Nelson, J., Editors, *Geological Association of Canada*, Special Paper 45, pages 433–482.
- Travers, W.B. (1978): Overturned Nicola and Ashcroft strata and their relations to the Cache Creek Group, southwestern Intermontane Belt, British Columbia; *Canadian Journal of Earth Sciences*, Volume 15, pages 99–116.
- Unterschutz, J.L.E., Creaser, R.A., Erdmer, P., Thompson, R.I. and Daughtry, K.L. (2002): North American margin origin of Quesnel terrane strata in the southern Canadian Cordillera: inferences from geochemical and Nd isotopic characteristics of Triassic metasedimentary rocks; *Geological Society of America Bulletin*, Volume 114, pages 462–475.
- Vollo, N.B. (1973): Geophysical and geochemical report on the 93A/3 SL group of Craigmont Mines Limited at Lac La Hache, British Columbia; *BC Ministry of Energy, Mines and Petroleum Resources*, Assessment Report 4697, 12 pages.
- von Guttenberg, R. (1996): Regional Resources Ltd., GWR Resources Inc., Lac La Hache Project, 1995 drill program, Cariboo and Clinton Mining divisions, British Columbia, NTS 92P/14, 93A/3; *BC Ministry of Energy, Mines and Petroleum Resources*, Assessment Report 25368, 256 pages.
- Wahl, H. (1996): Preliminary exploration, including trenching, on the Megaton claim group, Cariboo Mining Division; *BC Ministry of Energy, Mines and Petroleum Resources*, Assessment Report 25084, 58 pages.
- Wahl, H. (1998): Preliminary report of exploration and trenching on the Rodeo/Luky Jack mineral claims, Cariboo Mining Division; *BC Ministry of Energy, Mines and Petroleum Resources*, Assessment Report 25733, 40 pages.
- Wahl, H. (2002): Report of 2002 exploration on the Megaton–TNT mineral claims, Cariboo Mining Division, central British Columbia; *BC Ministry of Energy, Mines and Petroleum Resources*, Assessment Report 27157, 52 pages.
- Wahl, H. (2004): Preliminary core drilling, Rodeo/Luky Jack porphyry Zn-Pb-Cu project, Cariboo Mining Division; *BC Ministry of Energy, Mines and Petroleum Resources*, Assessment Report 27384, 35 pages.
- Wahl, H. (2006): Megaton project, results of April 2006 trenching, Cariboo Mining Division; *BC Ministry of Energy, Mines and Petroleum Resources*, Assessment Report 28743, 52 pages.
- Weeks, R.M., Bradburn, R.G., Flintoff, B.C., Harris, G.R. and Malcolm, G. (1995): The Brenda mine: the life of a low-cost porphyry copper-molybdenum producer (1970–1990), southern British Columbia; in Porphyry Deposits of the Northwestern Cordillera of North America, Schroeter, T.G., Editor, *Canadian Institute of Mining, Metallurgy and Petroleum*, Special Volume 46, pages 192–200.
- Whiteaker, R.J., Mortensen, J.K. and Friedman, R.M. (1998): U-Pb geochronology, Pb isotopic signatures and geochemistry of an Early Jurassic alkalic porphyry system near Lac La Hache, British Columbia; in *Geological Fieldwork 1997*, *BC Ministry of Energy, Mines and Petroleum Resources*, Paper 1998-1, pages 33-1–33-13.



# Southern Nicola Project: Whipsaw Creek–Eastgate–Wolfe Creek Area, Southern British Columbia (NTS 092H/01W, 02E, 07E, 08W)

by N.W.D. Massey, J.M.S. Vineham and S.L. Oliver

**KEYWORDS:** Nicola Group, Eagle pluton, Eastgate–Whipsaw metamorphic belt, Princeton, Quesnellia, mineral deposits

## INTRODUCTION

The Southern Nicola Project area is located on the eastern boundary of Manning Park, about 15 km southwest of the town of Princeton (Figure 1). Tectonically, the project area lies at the western edge of Quesnellia, just inboard of the bounding Pasayten fault, and includes the southernmost exposures of the Late Triassic Nicola Group.

Mapping by Rice (1947), Preto (1972) and Monger (1989) has outlined the essential distribution of Nicola Group strata in the Princeton area (NTS 092H/SE) and their relationships to younger intrusive and volcano-sedimentary sequences. To the east of the Boundary fault, rocks of the Nicola Group are assigned to the ‘eastern belt’ (Preto, 1979; Mortimer, 1987) and display an alkalic affinity. They host the important porphyry and skarn deposits of the Copper Mountain area (Preto, 1972). To the west, the rocks of the Nicola Group were not assigned to any of the three major belts by Monger (1989), although Mortimer (1987) included them in the calcalkaline ‘western belt’.

Adjacent to the Eagle Plutonic Complex in the west, rocks correlated with the Nicola by Rice (1947) and Monger (1989) are remarkable for being more highly deformed and metamorphosed. This belt also shows significant lithological differences to the immediately adjacent Nicola volcanic rocks, and is the host to volcanogenic massive sulphide (VMS) deposits (e.g., Red Star and S and M properties). These dissimilarities in rock type and the presence of VMS deposits cast some doubt on the correlation with the Nicola Group. The belt may be equivalent to the Late Permian to Early Triassic Sitlika-Kutcho sequences, including volcanic rocks and intrusions from the Ashcroft area (Childe et al., 1997), about 150 km north-northwest of Princeton.

Mapping in 2008 focused in the area to the southwest of Princeton (Figure 1). The map area stretches from the Wolfe Creek area and Copper Mountain southwest to Eastgate and the boundary of Manning Park and west to the Whipsaw Creek and Hudson Bay Meadows areas. In 2009, mapping will continue northwards from Whipsaw Creek to the Tulameen and Otter Lake areas.

---

*This publication is also available, free of charge, as colour digital files in Adobe Acrobat® PDF format from the BC Ministry of Energy, Mines and Petroleum Resources website at <http://www.empr.gov.bc.ca/Mining/Geoscience/PublicationsCatalogue/Fieldwork/Pages/default.aspx>.*

## PREVIOUS WORK

The Princeton area has a mining history dating from the discovery of placer gold in the 1860s. The first geological report for the area was that of Bauerman (1885), based on work done during the Boundary Commission Expedition of 1859–1861. Regional geological studies were undertaken by Dawson (1877), who defined and described the rocks of the Nicola Group. Subsequent mapping in the Princeton and adjacent areas was undertaken by Camsell (1913), Bostock (1940a, b), Rice (1947), Preto (1972, 1979), Coates (1974), Ray and Dawson (1987) and Monger (1989). Coal-bearing units of the Princeton Group have been described by Camsell (1913), Shaw (1952a, b), Hills (1962) and McMechan (1983), while industrial minerals have been described by Read (1987, 2000). Detailed investigations of the intrusions and associated copper mineralization at Copper Mountain were reported by Dolmage (1934), Fahrni (1951), Montgomery (1967), Preto (1979) and Stanley et al. (1995). No systematic mapping of Quaternary deposits, soils or terrain features has been undertaken in the area.

## GEOLOGY

The results of this summer’s mapping are summarized in Figures 2 and 3.

### *Stratified Units*

#### LATE TRIASSIC NICOLA GROUP

The Nicola Group contains the oldest exposed rocks in the area and is the main focus of this project. Rocks previously assigned to the group can be subdivided into three packages. To the east, from Wolfe Creek to the Pasayten River, the Nicola Group sedimentary and volcanic rocks have been assigned to the eastern belt (Preto, 1979; Mortimer, 1987). Rocks to the west, in the Whipsaw–Hudson Bay Meadows area, are presently unassigned to any of the Nicola Group belts. The higher grade metamorphic rocks at the western edge of the map area are herein renamed the ‘Eastgate–Whipsaw metamorphic belt’. As outlined above, their correlation with the Nicola Group is equivocal. The metamorphic belt is in fault contact with the Nicola Group proper (Figure 2).

#### *Eastern Part of Map Area*

Within the map area, the eastern Nicola Group comprises an unnamed lower sequence of clastic sedimentary rocks, overlain by a mixed volcanic and volcanic sediment package, called the Wolfe Creek Formation by Preto (1972).

### Lower Unnamed Sedimentary Rocks

The lower sedimentary sequence is dominated by interbedded black argillite, grey siltstone and sandstone. Finer grained beds are laminated and may have a limy or siliceous matrix. Coarser beds can be graded, laminated or crossbedded, and show bottom structures such as load structures. Beds vary from millimetres to several centimetres thick. Matrix-supported, polymictic pebble to cobble conglomerate layers are intercalated with the finer sedimentary rocks. The clasts are dominantly clastic sedimentary, although sometimes include rare limestone and volcanic material. Limestone beds were not observed but have been reported by Preto (1972).

Grey, orange-weathering crystal and lapilli tuffs are seen bedded in the argillite and siltstone along Placer Mountain Forest Service road. Lapilli are pyroxene-feldspar porphyry, occasionally vesicular and angular in shape.

The matrix is chloritic with a fine- to medium-grained calcareous cement that appears to be altered in places to skarn, with minor disseminated pyrite, chalcocopyrite and arsenopyrite.

In the southern reaches of Placer Creek, east of the Boundary fault, the sedimentary rocks take on a pronounced phyllitic character. This phyllite is fine grained and dark grey to black with a silvery sheen to the foliation. Beds vary in thickness, reaching up to 10 cm, and have undergone polyphase folding in many areas. Sandy beds tend to lighter grey feldspar-sericite schist. Conglomerate is weakly foliated.

### Wolfe Creek Formation

Rocks of the Wolfe Creek Formation are primarily volcanic in origin. Within the map area, they consist of units of volcanic breccia and lapilli tuff, as well as tuffaceous sand-

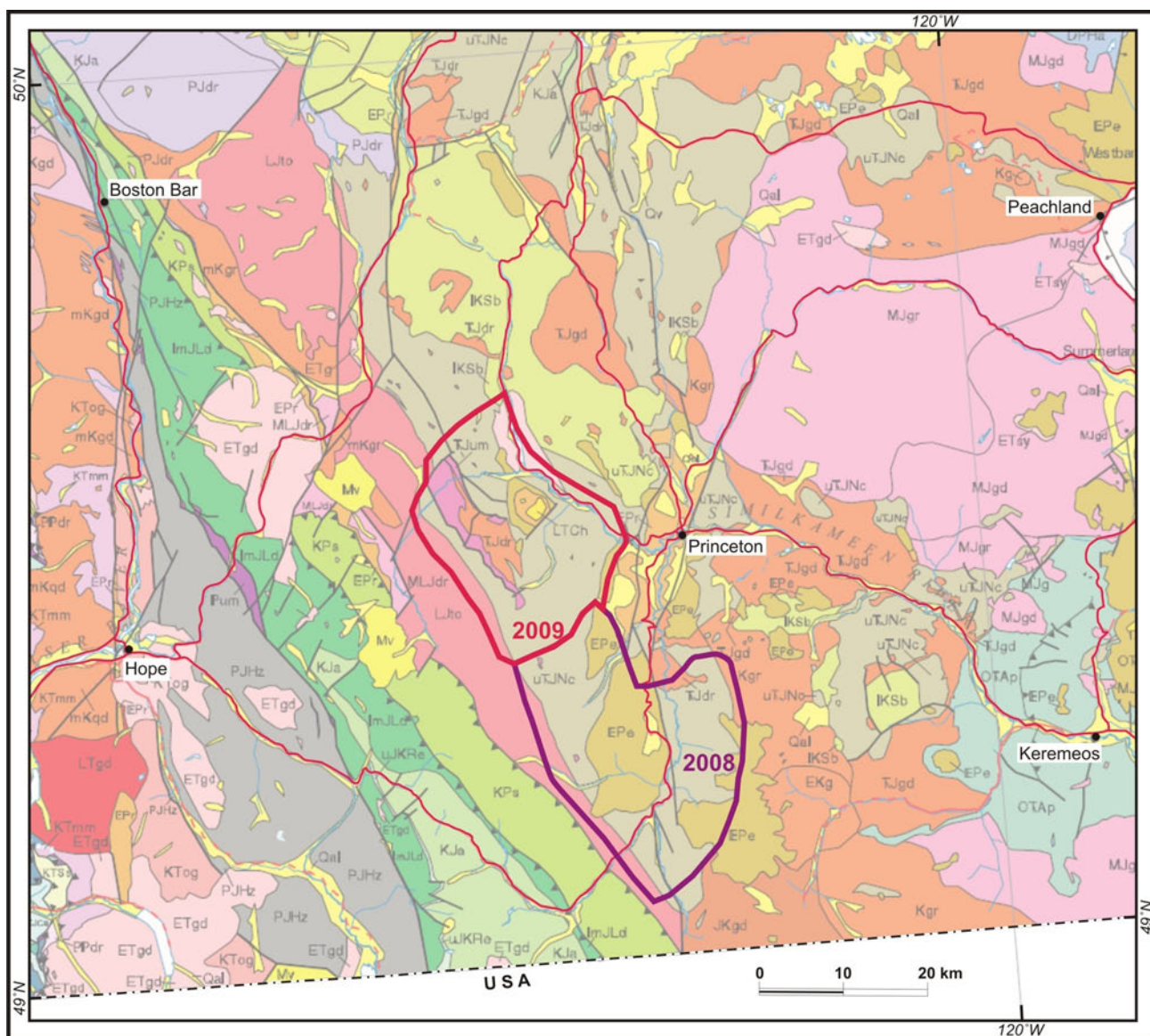


**Figure 1.** Location of the Southern Nicola Project. Geology base map derived from Massey et al. (2005). Boxes outline the area mapped in 2008 and proposed for 2009. Rocks of the Nicola Group are labelled uTJNc. For other units see Massey et al. (2005).

stone and siltstone. These units are intermixed, but no consistent stratigraphic sequence was determinable.

The fragmental volcanic beds include the interbedded pyroxene-feldspar tuff, lapilli tuff, breccia and agglomerate that are characteristic of the Nicola Group in other areas. They are light grey in colour, weathering to green-grey with orange-stained fracture surfaces. Lithic clasts vary from angular to subrounded and are typically 3–5 cm across, ranging up to 20–25 cm in breccia and agglomerate. They are dominantly pyroxene-feldspar–porphyritic basalt and basaltic andesite, showing a wide variation in proportions and sizes of phenocrysts. Aphyric basalt can also be seen. The clasts are usually matrix supported. The matrix is medium to coarse sand sized, containing feldspar and pyroxene crystals as well as small lithic clasts and chlorite. Epidote, chlorite and calcite occur as alteration minerals in clasts and matrix, and also in veins. Quartz veins are also common. Development of hornfels is common adjacent to the Copper Mountain intrusions, rendering original fabrics cryptic.

Tuffaceous sedimentary rocks comprise well-bedded siltstone, sandstone and conglomerate, and minor cherty argillite. Sandstone units are medium to coarse grained and grey on fresh surfaces, weathering to grey or orange-brown. They are generally massive but may show some grading. They contain abundant subhedral to broken feldspar, pyroxene and lithic fragments in a chlorite matrix. Conglomerate units are polyolithic with a variety of rounded to angular clasts. Volcanic clasts are usually pyroxene or pyroxene-feldspar porphyry, but one cobble to boulder conglomerate on the Wolfe-Belgie Branch 1 road contained large boulders of spherulitic obsidian, quartz-eye rhyolite and chert. These are the only felsic rocks observed in the Wolfe Creek Formation within the map area. The sedimentary rocks show pervasive chlorite alteration, veinlets and patches of epidote, and minor amounts of disseminated pyrite.

### **Western Part of Map Area**

The Nicola Group in the western half of the map area is lithologically similar to that in the east, although differing in details of stratigraphic succession. Here, clastic sedimentary rocks—black argillite interbedded with grey to green-grey siltstone and sandstone similar to those in the east—are intercalated with feldspathic tuff, tuff breccia, tuffaceous sandstone, pebbly sandstone and fine-grained cherty siltstone. Pyroxene is rare to absent in these beds. Thin grey limestone beds occur interbedded with argillite along the Lamont Main road.

The clastic sediment and feldspathic volcanoclastic unit passes westwards, and probably upwards, into typical Nicola pyroxene-feldspar tuff, lapilli tuff and breccia. However, in contrast to the eastern part of the map area, most of the exposed volcanic rocks are deformed and schistose. The change from massive to schistose rocks is transitional and gradual from east to west. Initially, the tuff and lapilli tuff look massive in outcrop but display a weak foliation on broken surfaces. This foliation becomes progressively more penetrative to the west. Finer grained tuff produces bluish green-grey chlorite schist. Relict pyroxene is chloritized and varies from euhedral shapes (Figure 4a) to being smeared along the schistosity. Clasts in lapilli tuff and breccia are undeformed to slightly flattened (Figure 4b). Chloritic rims may develop around the clasts, with

feathering of their terminations occurring along the foliation.

### **Eastgate-Whipsaw Metamorphic Belt**

Rocks of the Eastgate-Whipsaw metamorphic belt are quite distinct from those of the Nicola Group in either the eastern or western parts of the map area. They are quite heterogeneous but can be divided into three northwest-trending lithological assemblages that show increasing metamorphic grade from greenschist in the east to amphibolite in the west. Foliation and bedding dip to the west, but the stratigraphic significance, or even the stratigraphic integrity, of the three divisions remains unclear. Mineral exploration activity in the S and M camp suggests significant faulting within the package (*see below*), although none was directly observed during the course of mapping.

#### **Amphibolite**

Amphibolite forms the western unit of the metamorphic belt and is intruded by the Eagle pluton along its western margin. The amphibolite is overall dark grey to black in colour and typically medium to coarse grained and well foliated, and consists of alternating mafic- and felsic-rich layers (Figure 5a). It comprises black to greenish black amphibole, white feldspar, quartz and minor biotite and magnetite. The elongate amphiboles are usually larger than the subhedral feldspar and quartz, and show marked alignment parallel to the compositional layering, although without distinct lineation. The amphibolite is presumably of volcanic protolith, but generally no relict textures remain. However, some relict pyroxene crystals and cryptic clast outlines are observed in outcrops to the east of Huckleberry Creek (unofficial name) and in the Hudson Bay Meadows area (Figure 5b).

#### **Quartzite–Biotite–Quartz Schist**

This subunit occurs in the centre of the metamorphic belt, predominantly to the south in the Eastgate–Pasayten Creek area. It is a package of interbedded quartzite, biotite quartzite, actinolite-biotite quartzite, biotite-quartz schist and minor chlorite schist (Figure 6a) that probably derives mainly from siliceous sediments. Quartzite units are white with orange-brown oxide staining on surfaces. They are recrystallized with a medium to coarse saccharoidal texture. They can be massive but often contain disseminated biotite flakes or thin sericite or biotite layers that impart a foliation to the rock. Distinctive actinolite±biotite quartzite contains black to green actinolite needles that vary from 0.1 to 3 cm in size (Figure 6b). The needles form randomly oriented single crystals, clots and sheaves that lie along the foliation surfaces. Subrounded, blue-black magnetite is also found in some quartzite beds.

Biotite-quartz schist is made up of 50–60% black biotite plates that range up to 3–5 mm in size and define good foliations. Sugary quartz is finer grained and interstitial to the biotite. Contacts between quartzite and biotite schist vary from sharp to gradational. Grey marble occurs as rare thin interbeds within biotite schist in the Pasayten River area. Marble is also reported in trenches and drillcore on the S and M property (*see below*).

#### **Mixed Metavolcanic–Metasedimentary Schist**

This is a very heterogeneous package of schist that lies along the eastern margin of the metamorphic belt. It includes fine- to medium-grained, dark to light grey or grey-

green chlorite, chlorite-quartz and chlorite-sericite schists (Figure 7), and pale buff-orange to silvery grey sericite, sericite-quartz±feldspar and sericite-chlorite schists and paper schists (Figure 8a). Red and blue rounded quartz eyes are common in some sericite schist. Biotite and magnetite may be minor phases in some chlorite schist. Quartz veins are common, often boudinaged or tightly folded.

The schists appear to be derived from fine-grained laminated sediments or volcanic tuffs and tuffaceous sediments. Original volcanic fabrics are not preserved, although relict chloritized pyroxene is seen in chlorite schist in the Whipsaw Creek area.

Pale grey to red and blue banded, fine-grained saccharoidal quartzite occurs near the Redstar showing and is prob-

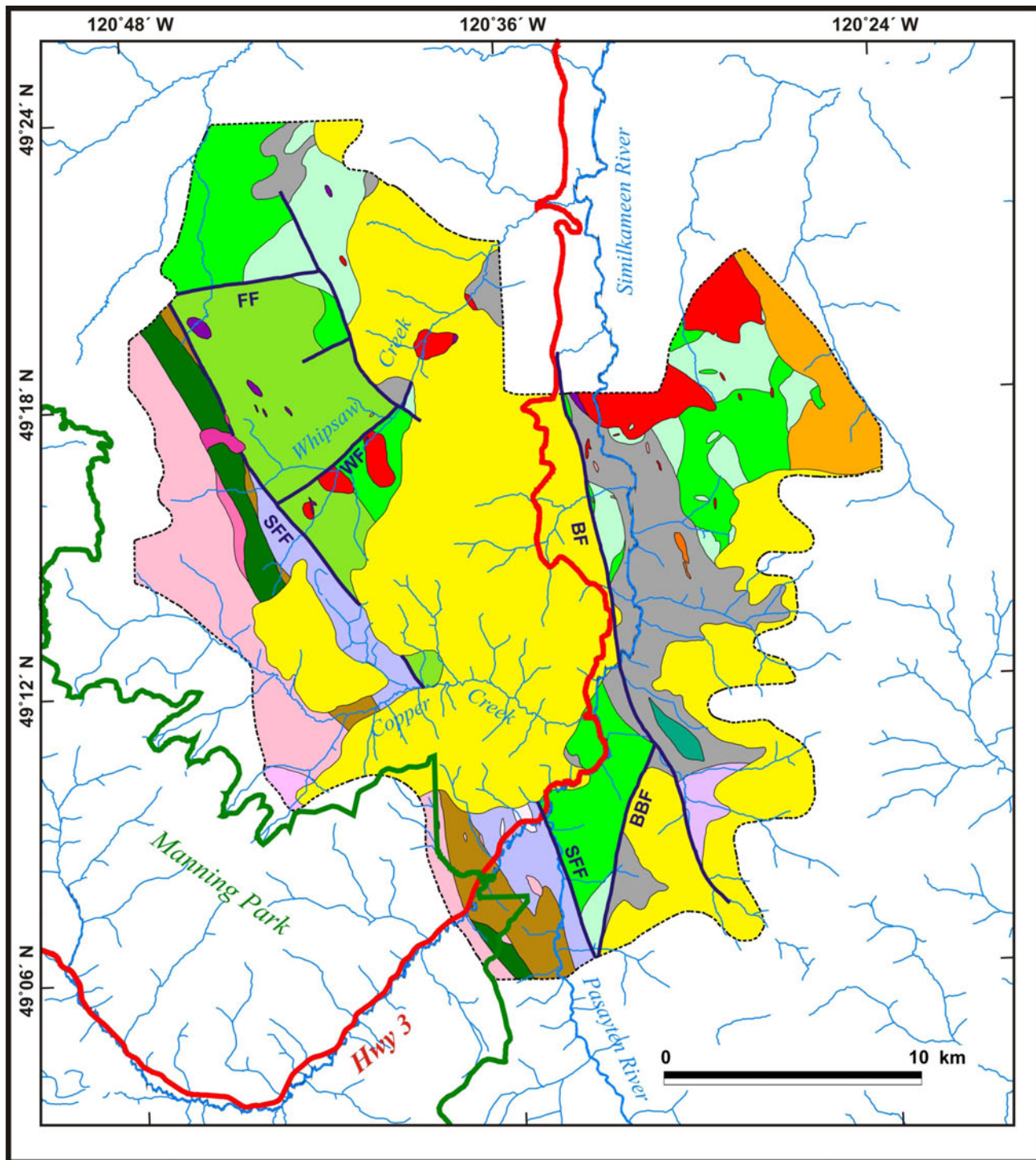


**Figure 2.** Geology of the 2008 map area. See Figure 3 for key to geological units. Abbreviations: BF, Boundary fault; BBF, Baby Buggy fault; SFF, Similkameen Falls fault; WF, Whipsaw Creek fault; FF, Frenchy Creek fault.

ably a meta-chert (Figure 8b). This is massive to weakly foliated with fine-grained sericite along cleavage planes. Other minor rock types include massive grey to grey-green metabasalt and massive to weakly cleaved, white to bluish pink, quartz-eye biotite rhyolite. Weakly foliated, white to pale buff, leucocratic quartz-feldspar porphyry forms several dikes and a small stock in the Similkameen Falls area. It is unclear if this porphyry is correlative with the schist or related to the younger Eagle pluton.

### PRINCETON GROUP

Eocene rocks of the Princeton Group occur at higher elevations in the central and eastern parts of the map area (Figure 2). They lie unconformably on the Nicola Group and all older intrusive rocks. Significant paleorelief is evident on the unconformity and was estimated at more than 300 m by McMechan (1983).

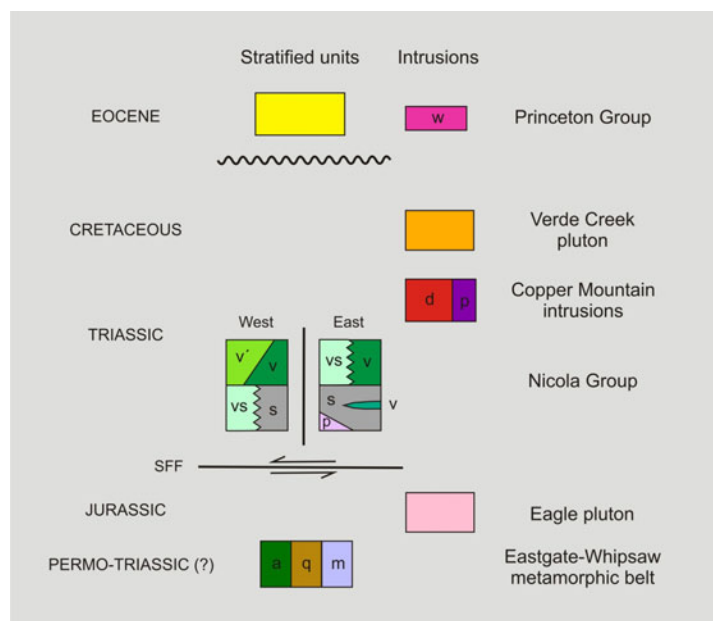
Within the map area, the Princeton Group is a heterogeneous sequence of mafic to felsic, mostly subaerial, alkalic volcanic and minor clastic sedimentary rocks. Exposure is often limited and discontinuous, and stratigraphic relationships are difficult to infer. Read (2000) correlated the volcanic rocks (not designated on Figure 2) with the Cedar Formation, formerly called the 'Lower Volcanic Formation' (Shaw, 1952a; McMechan, 1983), and suggested a Middle Eocene age based on whole-rock K-Ar dating. He also correlated conglomerate and sandstone of the Sunday Creek area with the overlying Allenby Formation, also of Middle Eocene age.

The volcanic rocks vary widely in lithology and composition, from mafic to felsic, aphyric to porphyritic, and massive to volcanoclastic, often changing character within tens of metres. Although generally quite fresh in appearance, the volcanic rocks can show a variety of weathering colours, with pink and purple hues common but including some very distinctive blue-green shades. Zeolite was observed in some vesicles and vugs, and is reported in tuffaceous sedimentary rocks (Read, 1987).

Volcanic units of intermediate composition are most common and generally display porphyritic textures. These include varieties of feldspar-pyroxene, feldspar-



**Figure 4.** Schistose volcanic rocks of the Nicola Group: **a)** relict pyroxene crystals in chlorite schist (field station 08JVI22-07-02; UTM Zone 10, 5459675N, 667153E, NAD83); **b)** schistose pyroxene lapilli tuff; clasts are flattened within the foliation (08NMA31-09; UTM 5465573N, 667794E).



hornblende and feldspar-pyroxene±hornblende andesite; megacrystic feldspar andesite; hornblende-biotite-feldspar and feldspar-hornblende±quartz dacites; and monolithic and heterolithic andesitic lapilli tuffs, pyroxene and feldspar crystal tuffs, and fine-grained dacitic tuff. Felsic units include massive, light grey to white or pink, rhyolite, quartz and feldspar crystal tuffs, and lithic rhyolite tuff. Mafic units are dark grey or brown in colour and massive, although occasionally columnar jointed or vesicular. Minor phenocrysts of olivine, pyroxene, feldspar or analcite were observed.

Interbedded with the volcanic units are volcanic breccia, conglomerate and finer clastic sedi-

**Figure 3.** Geological units in the map area. Nicola Group abbreviations: s, clastic sedimentary rocks; p, phyllite; v, volcanic rocks; vs, volcanoclastic sedimentary rocks; v', schistose volcanic rocks. Eastgate-Whipsaw metamorphic belt abbreviations: a, amphibolite; q, quartzite-biotite-quartz schist; m, mixed metavolcanic-metasedimentary unit. Intrusive units abbreviations: w, Whipsaw porphyry; d, diorite; p, pyroxenite; SFF, Similkameen Falls fault.

mentary rocks. Clasts in the breccia and conglomerate beds vary from pebble to boulder size and are polymictic, with clasts of rhyolite to basalt, beige claystone, grey siltstone and rarely granite. Other beds include black or purple argillite, light grey tuffaceous sandstone, fine- to medium-grained light grey sandstone, and light grey felsic gritstone.

### **Intrusive Rocks**

Several phases of intrusions have been observed, mostly peripheral to the map area. These include the Late Triassic–Early Jurassic Copper Mountain intrusions, the Middle–Late Jurassic Eagle pluton and the Cretaceous Verde Creek pluton.

#### **LATE TRIASSIC–EARLY JURASSIC INTRUSIONS**

##### **Copper Mountain Intrusions**

The Copper Mountain intrusions include four main bodies (Preto, 1972), of which only two, the Copper Mountain and Voigt stocks, fall within the map area. These bodies intrude and cause hornfels alteration of the Nicola Group

rocks. Uranium-lead dating of zircon and titanite from various phases of the body suggests an age of 206–200 Ma (Mortensen et al., 1995).

The Copper Mountain stock was mapped by Dolmage (1934) and Montgomery (1967) as a concentrically zoned, differentiated intrusion grading from an outer mafic diorite through monzonite into a syenite core. Only the outer mafic zone occurs within the map area. The diorite is white to grey with a pinkish colour on weathered surfaces. It is equigranular and medium to coarse grained (averaging 1–2 mm in size), and displays a typical salt-and-pepper texture. Mineralogically, the diorite has approximately equal proportions of subhedral to euhedral, creamy white K-feldspar and grey subvitreous plagioclase. Colour indices range from 30 to 35, with principal mafic minerals being pyroxene and lesser hornblende and/or biotite. The Copper Mountain diorite has a high magnetic susceptibility, with an average range of 10–50 and highs of 90–140, and easily deflects a pen magnet. Epidote and chlorite veinlets, some with potassic alteration halos, are fairly pervasive throughout the diorite. Sparse xenoliths are seen in a few outcrops, including fine-grained hornfelsed metasedimentary rocks and mafic pyroxene porphyry.

Coarse biotite-olivine pyroxenite is associated with the diorite in the lower reaches of Friday Creek. The pyroxenite is dominantly black pyroxene with green trans-

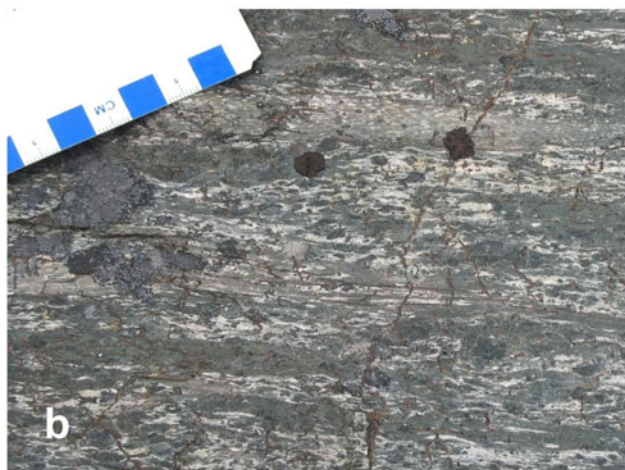
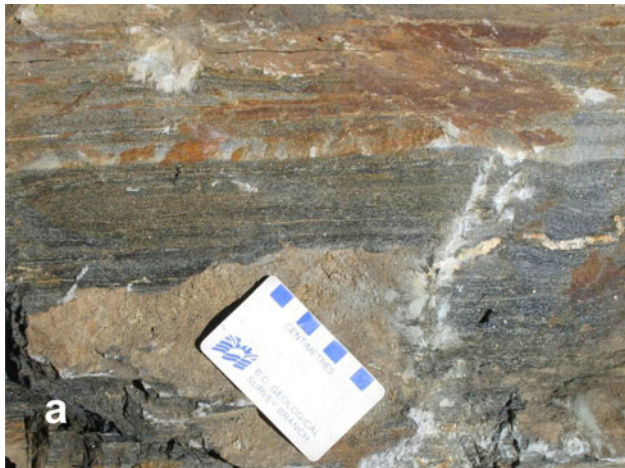


**Figure 5.** Amphibolites of the Eastgate-Whipsaw metamorphic belt: **a)** well-foliated medium-grained amphibolite (field station 08NMA16-04; UTM Zone 10, 5442156N, 674387E, NAD83); **b)** amphibolite with relict pyroxene crystals and cryptic clast outlines (08NMA30-09; UTM 5460351N, 664310E).



**Figure 6.** Quartzite–biotite–quartz schist of the Eastgate-Whipsaw metamorphic belt: **a)** interbedded quartzite, biotite quartzite and biotite-quartz schist; note schistosity is subparallel to bedding (field station 08NMA20-11; UTM Zone 10, 54448316N, 673430E, NAD83); **b)** coarse actinolite needles and sheaves in biotite quartzite (08NMA17-06; UTM 5442201N, 675785E).

lucent olivine, black magnetite and sparse white feldspar. Biotite forms very coarse grained pegmatite-like patches, as well as smaller grains scattered within the pyroxenite. It can be associated with pink K-feldspar veins and alteration patches, some of which show malachite staining, suggesting that it may result, at least in part, from potassic alteration of the original olivine pyroxenite.

Microdiorite and mafic pyroxene porphyry occur as minor intrusions associated with the Copper Mountain stock.

The Voigt stock consists of green-grey, equigranular, fine- to medium-grained diorite that weathers to a light grey colour. Feldspar is mostly white plagioclase, while mafic minerals are dominantly pyroxene with lesser biotite. A hornblende-rich phase, with minor pyroxene and biotite, was also observed. As with the Copper Mountain diorite, the Voigt stock is quite magnetic. Two types of crosscutting veinlets are found throughout the intrusion. The first, and most common, is epidote-chlorite veinlets, and the second is K-feldspar-filled veinlets. Epidote alteration patches are also commonly seen within the diorite.

#### **Other Diorite and Pyroxenite Stocks**

Several small stocks of mafic diorite and pyroxenite are found intruding Nicola Group rocks in the Whipsaw Creek area. Their correlation is uncertain, however, as they may be related to the Copper Mountain intrusions or to the Late Triassic Tulameen Complex (Nixon et al., 1997).



**Figure 7.** Interlaminated chlorite and sericite schists (meta-argillite-metasiltstone interbeds) in the Eastgate-Whipsaw metamorphic belt (field station 08NMA23-12-02; UTM Zone 10, 5457516N, 6660687E, NAD83).

The diorite is fine to medium grained and has typical grey salt-and-pepper fresh surfaces with brown or brick red to grey weathered surfaces. It is composed primarily of white feldspar and greenish black hornblende, with colour indices varying from 30 to 50 in most outcrops, but up to 70 in melanocratic phases. Minor minerals include rare euhedral biotite flakes, pyroxene or quartz.

Pyroxenite is dark green to black on fresh surfaces and weathers dark grey. It is coarse grained with crystals ranging from 1 to 3 cm. Pyroxene constitutes 80–90% of the rock, the rest being chlorite, magnetite and minor feldspar. Epidote-chlorite veinlets are common; serpentinite and calcite alteration is rare. The pyroxenite outcrops separately from but close to the diorite. Contacts are rarely seen but suggest that the diorite is intrusive into the pyroxenite.

#### **JURASSIC-CRETACEOUS EAGLE PLUTONIC COMPLEX**

The Eagle Plutonic Complex lies along the western margin of the map area (Figure 2), intruding and being deformed with the Eastgate-Whipsaw metamorphic belt. Greig (1992) described the complex immediately to the



**Figure 8.** Metavolcanic-metasedimentary rocks of the Eastgate-Whipsaw metamorphic belt: **a)** sericite-chlorite paper schist with two obliquely crosscutting schistosity (field station 08NMA19-01; UTM Zone 10, 54469396N, 674182E, NAD83); **b)** s-fold in laminated quartzite (meta-chert; 08NMA18-06-01; UTM 5447070N, 674145E).

north. Within the map area, most outcrops belong to Grieg's 'Eagle tonalite', although, in the absence of petrographic data, these were called biotite granodiorite in the field, which terminology is retained here. Greig et al. (1992) reported Middle–Late Jurassic U–Pb zircon ages for the Eagle tonalite.

The biotite granodiorite is a syntectonic intrusion with varying texture and fabrics. A range of foliate fabrics from massive to gneissic is seen in the granodiorite, particularly in the marginal portions.

Massive phases are equigranular to seriate, varying in grain size from 3–5 mm to 5–6 mm. White feldspar forms subhedral laths. Translucent grey quartz is irregular, often interstitial to feldspar and biotite, and may be smaller in grain size. Biotite is typically black and micaceous and makes up 10–25% of the rock. Minor epidote and red garnet are common. Finer grained microgranodiorite (1–2 mm grain size) is of similar mineral composition, although more melanocratic with up to 50% biotite.

Weakly foliated granodiorite is similar to the massive phase, except that biotite shows a marked alignment (Figure 9a), may cluster and may also be coarser grained. In fo-

liated phases, biotite forms penetrative sheets, or folia, that break the granodiorite into layers 1–10 cm thick (Figure 9b). Within the layers between folia, biotite is aligned parallel to the folia. White feldspar megacrysts up to 1–2 cm can be associated with the biotite folia, giving a very distinctive spotted look to surfaces. Biotite folia may be folded into tight isoclinal folds (Figure 9c)

Biotite gneiss occurs in the Whipsaw Creek area, marginal to the intrusion (Figure 9d). Layers of biotite or biotite-feldspar alternate with leucocratic feldspar-quartz layers. The gneiss is intruded and included by massive granodiorite. The mineralogy of the gneiss contrasts with that of the amphibolite of the adjacent Eastgate-Whipsaw metamorphic belt and suggests that it may be related to the 'Eagle gneiss' unit of Greig (1992).

Coarse quartz-feldspar-biotite pegmatite and leucocratic feldspar-quartz aplite intrude all phases of the granodiorite, massive or foliated. Rare muscovite granite, probably related to muscovite granite in the mid-Cretaceous Fallslake Plutonic Suite (Greig, 1992; Greig et al., 1992), occurs as a minor phase in the southern Copper Creek area, as well as occasional thin dikes. The granite contains both pink and white feldspars, quartz, muscovite,



**Figure 9.** Foliated rocks of the Eagle Plutonic Complex: **a)** weakly foliated biotite granodiorite (field station 08NMA24-05; UTM Zone 10, 5457745N, 663754E, NAD83); **b)** biotite folia between layers of weakly foliated biotite granodiorite (08NMA24-06; UTM 5457773N, 663966E); **c)** folded foliation in gneissic granodiorite (08NMA25-07; UTM 5456645N, 661853E); **d)** biotite gneiss intruded by massive biotite granodiorite (08NMA27-02; UTM 5459801N, 663688E).

biotite and minor red garnet. Pink K-feldspar may form megacrysts up to 2 cm in size.

### CRETACEOUS VERDE CREEK QUARTZ MONZONITE

Quartz monzonite of the Verde Creek stock is variable in texture from medium to coarse grained, and from equigranular to porphyritic. It is generally pinkish grey to grey in colour, weathering buff to orange with dark iron and manganese staining on fracture surfaces. The quartz monzonite is leucocratic, with white plagioclase, pinkish K-feldspar and clear quartz. Myrmekitic intergrowths of quartz and feldspar are common. Quartz contents are commonly about 10–15% but range up to 25% in more granitic phases. Mafic minerals range from 2 to 7%, with hornblende usually more common than biotite. Mirolitic vugs, lined with brown-red-stained quartz crystals, are common. The vugs are usually elongate and can be as long as 7 cm. Minor intrusive phases include a distinctive needle hornblende porphyry, characterized by long, thin laths of hornblende up to 2.5 cm long. Contacts with the quartz monzonite are equivocal and perhaps transitional. Pink feldspar porphyry, possibly a chill phase of the quartz monzonite, is occasionally seen as xenoliths within the margin of the quartz monzonite stock.

Rice (1947) correlated the Verde Creek stock with the Otter granite and assigned it an “Upper Cretaceous or later” age. Preto reported two K-Ar ages of  $101 \pm 4$  Ma and  $98 \pm 4$  Ma (recalculated to  $102 \pm 8$  Ma and  $100 \pm 8$  Ma, respectively, by Breitspacher and Mortensen [2004]) from biotite of the Verde Creek stock, which suggest a late Early Cretaceous age.

### TERTIARY (?) INTRUSIONS

Many minor intrusions occur through out the map area. A bimodal suite of dikes in the area around and to the east of Copper Mountain has been called the ‘Mine Dykes’ in the older literature (Preto, 1972). These are dominated by buff to cream, quartz and pink feldspar porphyries and aphyric fine-grained felsite. They demonstrate characteristic Liesegang rings or ‘picture rock’ alteration. Minor brown-weathering, black, aphyric mafic dikes are also found. The age of the ‘Mine Dykes’ is uncertain. They may be comagmatic with the Eocene Princeton Group volcanic rocks, although Preto (1972) suggested a Late Cretaceous to Early Tertiary age.

Intermediate to felsic dikes of more certain correlation with the Princeton Group are ubiquitous in the map area. They include feldspar basalt; pyroxene, pyroxene-feldspar and hornblende±feldspar andesite porphyries; hornblende-feldspar, feldspar and aphyric dacites; and rare rhyolite.

The Whipsaw porphyry forms a small stock and associated dikes in the Fortyfive Mile Creek area, north of Whipsaw Creek. This grey to pink porphyry is marked by abundant (20–30%) white to pink feldspar laths, up to 5–8 mm in size. Quartz is less abundant (1–5%) and forms smaller (1–3 mm) rounded crystals. Hornblende and biotite phenocrysts are tabular, greenish black and often altered to epidote, making identification difficult. Disseminated sulphides and malachite staining are observed in some outcrops. The age of the Whipsaw porphyry is unknown. It intrudes the Eagle pluton and may be correlated with porphyries of the Late Cretaceous Otter Lake suite in the Tulameen area to the north. Alternatively, it may be comagmatic with the Princeton Group.

## STRUCTURE

### Folds

Coarse clastic sedimentary rocks of the Princeton Group in the Sunday Creek area have been correlated by Read (1987) with the Allenby Formation, which overlies the older volcanic rocks of the Cedar Formation in the core of the Kennedy Lake syncline. This runs north-south, subparallel and adjacent to the Boundary fault. Limited outcrop and scarcity of structural information preclude identification of other major folds within the Princeton Group in the map area.

In the eastern half of the map area, lack of regional markers and suspected facies changes within the volcanic and volcanoclastic rocks of the Nicola Group render the identification of major folds difficult. Observed bedding attitudes generally strike north-northwesterly in the north and become more northwesterly to the south. Dips are steep, 60–80° to both the northeast and the southwest, perhaps suggesting some upright isoclinal folding. Shallower east-northeasterly dips, about 45°, occur in the Wolfe Creek area, south of Copper Mountain.

Schistosity in the western part of the Nicola Group are subparallel to bedding where both are observed, and to bedding in nonfoliated units. They strike north-northwesterly with shallow to moderate (20–45°) westerly dips. Dips steepen in the west to 60–70°, closer to the Similkameen Falls fault. East-northeasterly-striking schistosity is found to the south of the Frenchy Creek fault and also adjacent to the Whipsaw Creek fault. The age of deformation within the Nicola Group rocks is unknown.

The metamorphic rocks of the Eastgate-Whipsaw metamorphic belt and Middle–Late Jurassic, syntectonic granodiorite of the Eagle pluton show variable, moderate to steep (60–90°) westerly dipping schistosity that parallels the belt orientation. Two schistosity are discernible in some outcrops crosscutting at an acute angle (Figure 8a). It is often difficult to determine the relative order of formation of these schistosity, which may have resulted from progressive deformation rather than two separate events. Minor S- and Z-folds of the foliations, intrafolial quartz pods or granodiorite bands (Figure 9c) show variable plunges from steep to shallow and trending to either the northwest or the southeast. Anomalous northeast- and north-northeast-striking schistosity and bedding attitudes are found just west of the Pasayten River. The westerly-dipping structures within the Eastgate-Whipsaw metamorphic belt match those reported by Greig (1992) farther to the north.

### Major Faults

The majority of Princeton Group volcanic and sedimentary units in the central part of the map area accumulated within a half-graben bounded on its eastern side by the Boundary fault (Figure 2). This subvertical normal fault was first identified by Preto (1972), and confirmed by Read (1987) in an area to the north. Present mapping continues the trace of the fault to the south, where it curves into the valley of Placer Creek. A smaller Tertiary graben is indicated to the west of Placer Creek, bounded by the Boundary and Baby Buggy faults. Despite considerable movement during the Eocene, the Boundary fault is part of a larger sys-

tem extending to the north and suspected by Preto (1979) to have been established early in the geological history of the region, controlling the facies distributions and pluton emplacement within the Nicola Arc.

Three northeast- to east-northeast-trending faults are interpreted within the western Nicola Group volcanic rocks (Figure 2). Massive, nonschistose, feldspathic volcanoclastic rocks and pyroxene lapilli tuffs and breccias occur on the south side of Whipsaw Creek valley, intruded by massive diorite and pyroxenite. In marked contrast, north-northwesterly-trending schistose pyroxene-phyric volcanic rocks occur on the north side of the valley. Similarly, the Frenchy Creek fault separates nonfoliated rocks to the north from schistose volcanic rocks to the south. The age of this faulting is unknown, but postdates schistosity generation in the volcanic rocks.

The Eastgate-Whipsaw metamorphic belt is separated from Nicola Group volcanic rocks by the northwest-trending Similkameen Falls fault. This is best seen along Highway 3 about 1 km south of Similkameen Falls (Figure 10). Here the fault places northeast-trending interbedded sericite and chlorite schists against massive pyroxene lapilli tuff of the Nicola Group. The fault trace appears to be linear, continuing to the southeast along the Pasayten River and to the northwest into the Hudson Bay Meadows area, and is therefore interpreted to be steep. The age of the fault is unknown. It terminates the easterly-trending faults in the western belt of the Nicola Group. It also appears to acutely crosscut the three lithological assemblages of the Eastgate-Whipsaw metamorphic belt, suggesting that it postdates the Middle-Late Jurassic deformation. The fault trace is sealed by the Whipsaw porphyry and overlain by Princeton Group strata. Motion must have therefore concluded before the Eocene.

## MINERALIZATION

Some 38 mineral occurrences are reported for the map area in the MINFILE database (Table 1; MINFILE, 2008). Sixteen of these occurrences lie in the northeast corner of the map area (Figure 11) and are related to the Copper Mountain alkalic porphyry Cu-Au system, which has been

described in detail by several authors, including Dolmage (1934), Fahrni (1951), Montgomery (1967) and Preto (1979). Within the map area, showings display a variety of styles, including veins, stockworks, shear zones or disseminated chalcopryrite-bornite-pyrite mineralization hosted in Copper Mountain diorite, Voigt diorite or Nicola Group volcanic and sedimentary rocks. Platinum and palladium minerals are found in faults and shears in Copper Mountain pyroxenite and diorite.

Both the Red Star and S and M massive sulphide camps occur in rocks of the Eastgate-Whipsaw metamorphic belt. At the Red Star, mineralization is hosted by a wide zone of strongly sheared, strongly schistose quartz-sericite-pyrite schist, sericite schist and chlorite schist of the metavolcanic-metasedimentary subunit. Intense sericitization is characteristic over the entire Red Star horizon; silicification and pyritization are also common. Several styles of mineralization have been identified, including pyritized silicified schist; white sugary quartz-carrying pyrite, sphalerite, chalcopryrite and galena; and glassy quartz with patches or blebs of pyrite, chalcopryrite and rarely bornite with chalcocite. Pyrrhotite, tetrahedrite, Au and tellurides have also been reported. The best mineralization is associated with the Main zone, which extends north-south for 480 m and generally consists of disseminated sphalerite and chalcopryrite in quartz veins and sweats within highly sheared, sericitic schist. Significant sphalerite, chalcopryrite with galena, Ag and Au mineralization was reported from the underground workings, which have since caved in. A lens of massive, coarse-grained sphalerite, pyrite and chalcopryrite occurs within the Main zone. Minor bornite, galena, molybdenite and pyrrhotite are also present. Gangue minerals include quartz, barite, kaolinite and sericite.

In the S and M camp, mineralization is hosted in a north-trending fault zone that cuts schist of the metavolcanic-metasedimentary subunit and amphibolite. The brecciated fault zone varies from 5 m to greater than 10 m in width and extends for about 1.5 km. The breccia contains 2.5–25 cm fragments in a matrix of sheared clayey rock and fault gouge that may be cemented by ankerite, dolomite or calcite. Many of the breccia fragments consist of massive to semimassive sulphides, comprising sphalerite, galena, pyrite, chalcopryrite and argentite with carbonate. Pyrite,



**Figure 10.** Similkameen Falls fault, separating chlorite and sericite schists of the Eastgate-Whipsaw metamorphic belt (EWsc) from massive pyroxene lapilli tuff of the Nicola Wolfe Creek Formation (TrNwc; station 08NMA21-02; UTM Zone 10, 5447430N, 675927E, NAD83).

**Table 1:** Mineral occurrences in the map area (from MINFILE, 2008). Note that only the principal name is shown for each occurrence for brevity. Deposit type codes: C01, surficial placer; D01, open-system zeolite; D03, volcanic redbed Cu; G04, Besshi massive sulphide; G06, Noranda/Kuroko massive sulphide; I01, A-quartz vein; I05, Ag-Pb-Zn±Au polymetallic veins; I06, Cu±Au veins; K01, Cu skarn; K02, Pb-Zn skarn; L01, subvolcanic Cu-Ag-Au (As-Sb); L03, alkalic porphyry Cu-Au; L04, porphyry Cu±Mo±Au.

MINFILE number	Name	Status	Commodities	Latitude	Longitude	Deposit type	Zone	Easting	Northing
<b>Copper Mountain camp</b>									
092HSE021	Falum	Showing	Cu, Au	49.338050	-120.471100	L03	10	683705	5468113
092HSE022	Azurite	Showing	Cu	49.330280	-120.480000	L03	10	683089	5467227
092HSE027	Jennie Silkman	Prospect	Cu, Au	49.312780	-120.508100	L03	10	681115	5465214
092HSE029	Marquis of Lome	Prospect	Cu, Ag	49.291940	-120.513900	L03, K01	10	680767	5462884
092HSE031	Johnston	Showing	Cu	49.291390	-120.533100	L03	10	679375	5462777
092HSE033	Friday Creek	Prospect	Cu, Au, Ag, Pd, Pt	49.300000	-120.560600	L03	10	677345	5463669
092HSE044	St. Louis Fraction	Showing	Cu, Ag	49.284720	-120.536400	L03	10	679157	5462028
092HSE092	Skagit 1 Fraction	Prospect	Cu, Ag	49.291940	-120.506400		10	681312	5462902
092HSE109	OX	Showing	Cu	49.268610	-120.521100	L03	10	680327	5460274
092HSE114	Reco	Prospect	Cu, Au, Ag	49.285280	-120.545300	L03, L01	10	678509	5462069
092HSE121	Enterprise	Showing	Cu	49.290550	-120.540800	L03	10	678813	5462666
092HSE132	TAS	Showing	Cu	49.279450	-120.449700	D03, L03, L01	10	685479	5461651
092HSE192	Y	Showing	Cu	49.284440	-120.487500	L01, G04	10	682713	5462114
092HSE193	Y 46	Showing	Cu	49.295280	-120.467800	L01, G04	10	684107	5463366
092HSE194	Elk No. 1 Fraction	Showing	Cu	49.290000	-120.546700	L03	10	678391	5462590
092HSE195	Ilk	Prospect	Cu, Au, Ag, Pd	49.293890	-120.555600	L03	10	677731	5463002
<b>Red Star camp</b>									
092HSE067	Red Star	Past Producer	Zn, Cu, Ag, Au, Pb, Mo	49.149720	-120.610000	G06, I05	10	674279	5446850
092HSE068	Pasayten	Prospect	Cu, Au, Ag, Pb	49.156390	-120.591100	G06, I05	10	675632	5447635
092HSE069	Knob Hill	Prospect	Cu, Ag, Zn, Au	49.146670	-120.626700	G06, I05	10	673074	5446472
092HSE093	Paw	Showing	Cu, Au, Ag	49.154450	-120.621100	I06	10	673452	5447350
092HSE191	Golden Crown	Showing	Cu, Au, Ag	49.153340	-120.586100	L01, G06	10	676008	5447307
<b>S and M camp</b>									
092HSE072	Knight and Day	Prospect	Zn, Pb, Au, Ag, Cu	49.262780	-120.732800	I05, G04	10	664950	5459142
092HSE073	S and M	Past Producer	Pb, Zn, Cu, Ag, Au	49.275550	-120.736100	I05, G04	10	664665	5460555
092HSE097	Metestoffer	Prospect	Zn, Au, Ag, Cu, Pb	49.261390	-120.746100	I05, G04, I06	10	663984	5458958
092HSE098	Five Fissures	Prospect	Pb, Zn, Ag, Cu, Au	49.267780	-120.733600	I05, G04, I06	10	664873	5459696
092HSE206	T.G.S.	Showing	Zn, Cu	49.282500	-120.746100	G04	10	663915	5461305
092HSE207	BZ	Prospect	Zn, Cu, Ag, Au, Mo, Pb	49.277500	-120.745600	G04	10	663971	5460750
<b>Whipsaw camp</b>									
092HSE102	Whipsaw	Prospect	Cu, Mo, Ag	49.293330	-120.759400	L04	10	662909	5462480
092HSE074	Marian	Prospect	Zn, Cu, Au, Ag, Pb, Mo	49.277500	-120.757500	I05, G04, K01, K02	10	663103	5460724
<b>Others</b>									
092HSE042	Wilmac	Showing	Cu	49.375550	-120.679700		10	668424	5471795
092HSE071	Silver Moon	Prospect	Au, Ag, Zn, Cu, Pb	49.196950	-120.553900	I01	10	678200	5452230
092HSE077	Riv	Showing	Au, Ag	49.355000	-120.601400	I01, L01	10	674183	5469688
092HSE081	Mazie	Prospect	Pb, Ag	49.274720	-120.700000	G06, I05	10	667294	5460541
092HSE105	Ski	Showing	Cu	49.348610	-120.604700		10	673963	5468970
092HSE112	Nev	Showing	Cu	49.292500	-120.658100	L04, K01	10	670283	5462611
092HSE124	Goldroop	Past Producer	Zn, Cu, Pb, Au, Ag	49.335560	-120.626900	G06, I05	10	672395	5467468
092HSE168	Sunday Creek	Prospect	Zeolite	49.248610	-120.584200	D01	10	675811	5457902
092HSE236	Whipsaw Creek Placer	Past Producer	Au, Pt	49.306390	-120.649700	C01	10	670841	5464174

sphalerite, galena and chalcopyrite also occur as disseminations and blebs in quartz-carbonate veinlets ranging from a few millimetres to 40 cm wide, and in quartz veins that are generally up to 15 cm in width.

Porphyry Cu-Mo mineralization is associated with the Whipsaw porphyry and its hostrocks of the Eagle Plutonic Complex and the Eastgate-Whipsaw metamorphic belt. It may also partially overprint the massive sulphide mineralization in the adjacent S and M camp. Sulphide mineralization is developed over a widespread area, as disseminations and fracture fillings, and in quartz and calcite veins. Pyrite is most abundant, ranging from 2 to 10%, particularly within altered porphyry. Trace amounts of chalcopyrite, molybdenite, bornite, chalcocite and covellite occur with up to 10% magnetite, primarily in the Eastgate-Whipsaw metamorphic belt and Eagle Plutonic Complex hostrocks flanking the stock, and in feldspar porphyry dikes and sills.

The chalcopyrite is closely associated with pyrite and occurs as disseminations in the porphyry and schist, as fracture fillings and in quartz-carbonate veins in schist. Molybdenite forms fine-grained coatings along fractures and along margins of quartz and quartz-carbonate veins in the porphyry and surrounding hostrocks. Bornite is closely associated with pyrite and occurs as fine disseminations in the porphyry. Thin blebs and rounded coatings of chalcocite and covellite are present in porphyry dikes to the south. Epidote and chlorite are the most common alteration minerals. Argillic alteration is best developed in the margins of the stock. The porphyry also exhibits quartz-sericite alteration, which appears to be associated with the argillic alteration. Feldspars are replaced by kaolinite and minor epidote and sericite in the more altered sections of the stock. The main mineralization occurs along the stock's northern contact and near the southern contact, where a

southeastward-trending apophysis extends from the main body. Sphalerite, pyrite, pyrrhotite and chalcocopyrite with minor galena and molybdenite in garnet-epidote-diopside or quartz-epidote skarn on the Marian showing is peripheral to, and possibly related to, the Whipsaw porphyry Cu-Mo mineralization.

Other mineral showings in the map area include a variety of quartz veins with either gold or sulphides; zeolite in Eocene volcanoclastic sedimentary rocks; and placer Au and Pt.

Table 2 reports the results of analyses of various mineralized grab samples from the map area. These form three

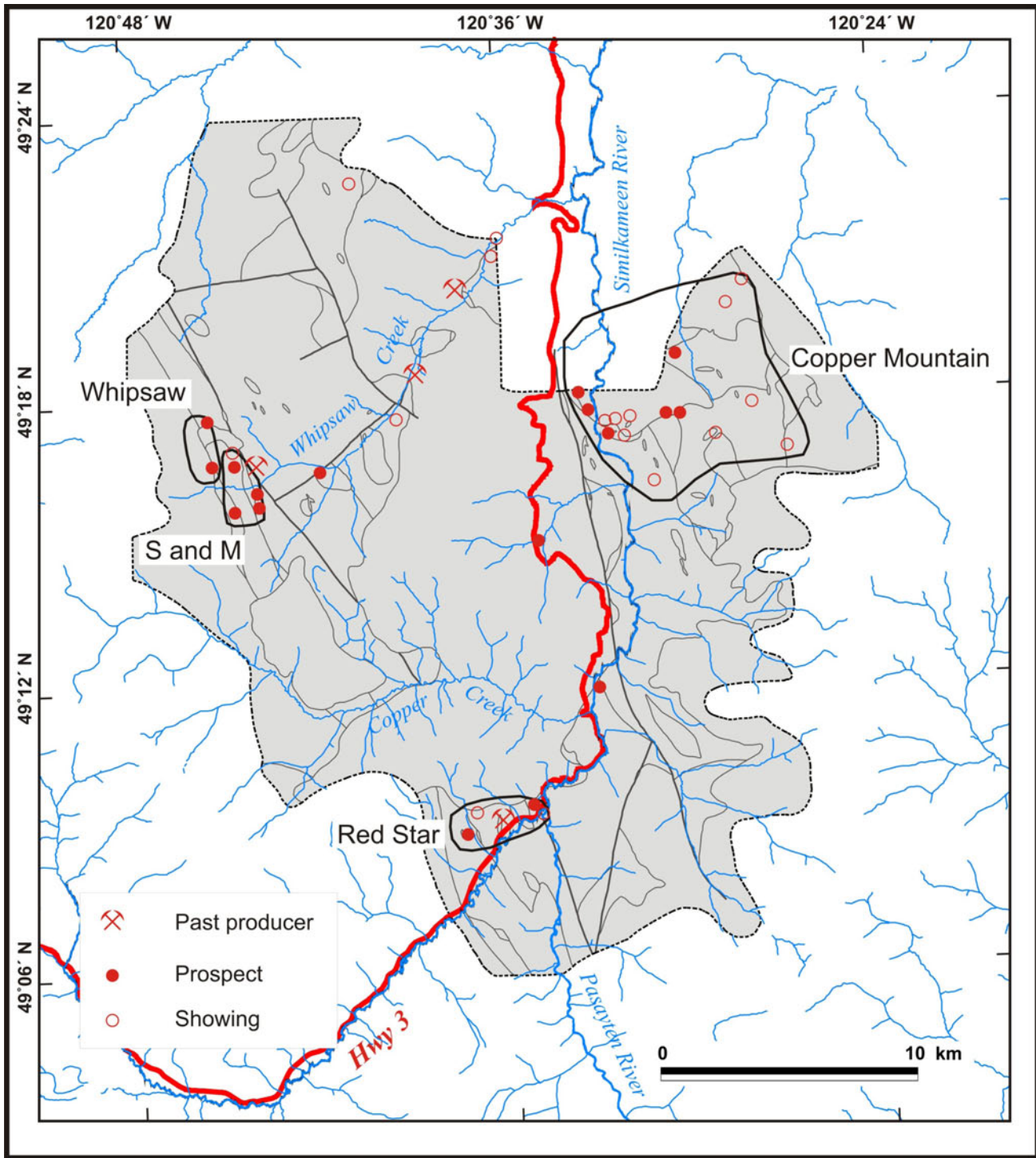


**Figure 11:** Locations of mineral occurrences in the map area. Important camps are outlined and labelled. Geological contacts and faults in the grey map area are as in Figure 2.

**Table 2.** Analyses for selected elements on mineralized grab samples collected in the map area in 2008. Samples crushed and milled in a Cr steel mill. Analyses by ACME Analytical Laboratories Ltd. (Vancouver) using inductively coupled plasma–mass spectrometry after HCl-HNO<sub>3</sub> digestion.

Sample No	Latitude	Longitude	Zone	Northing	Easting	Lab No.	Mo (ppm)	Cu (ppm)	Pb (ppm)	Zn (ppm)	Ag (ppb)	Au (ppb)	As (ppm)	Sb (ppm)	S (%)
a) Sulphide mineralization associated with the Whipsaw porphyry															
08NMA28-01	49.289038	-120.765018	10	5461990	662519	61556	50.31	456.75	1.24	34.9	541	2.9	1.1	0.03	0.89
08SOL18-13A	49.298642	-120.759313	10	5463070	662902	61548	0.49	722.35	0.78	139.7	651	1.6	0.5	0.07	1.49
08SOL18-13B	49.298642	-120.759313	10	5463070	662902	61550	4.61	595.70	0.74	106.8	710	1.7	0.7	0.07	0.70
08SOL18-14A	49.297318	-120.762781	10	5462915	662655	61546	1.12	238.52	1.09	69.2	177	1.7	0.8	0.02	0.92
08SOL18-14B	49.297318	-120.762781	10	5462915	662655	61547	0.93	665.15	1.33	55.0	582	3.9	1.6	0.03	1.90
b) Calcareous tuffs, partially skarned															
08NMA12-03-01	49.182849	-120.510861	10	5450765	681387	61564	0.87	46.86	3.55	29.9	60	1.5	-0.1	0.22	1.45
08NMA12-03-02	49.183064	-120.511271	10	5450788	681357	61719	0.76	22.76	4.70	45.7	133	3.2	1.8	0.24	1.53
08NMA12-03-03	49.183655	-120.512382	10	5450851	681274	61562	0.73	76.91	1.78	35.4	31	4.7	3.9	0.20	1.03
08NMA12-05-01	49.184253	-120.515249	10	5450910	681063	61563	1.39	101.73	1.91	56.7	47	1.3	1.3	0.15	1.64
c) Iron carbonate–silica alteration zones															
08NMA29-07A	49.311243	-120.687187	10	5464629	668103	61554	0.24	23.70	2.07	22.5	59	1.5	0.5	0.03	-0.02
08NMA29-07B	49.311243	-120.687187	10	5464629	668103	61555	0.13	196.37	1.86	57.8	91	23.2	0.4	-0.02	-0.02
08NMA32-07A	49.347796	-120.686680	10	5468693	668015	61551	0.44	79.31	1.14	64.4	143	0.9	105.9	0.15	0.20
08NMA32-07B	49.347796	-120.686680	10	5468693	668015	61552	0.47	75.46	1.68	52.3	85	1.8	78.5	0.10	0.11
08NMA32-07C	49.347796	-120.686680	10	5468693	668015	61553	0.28	122.23	0.78	60.6	238	2.6	152.2	0.13	0.23
08NMA32-07C-Rep	49.347796	-120.686680	10	5468693	668015	61565	0.31	133.05	0.98	64.3	267	3.5	155.6	0.14	0.23
08NMA32-08	49.347328	-120.687886	10	5468638	667929	61560	1.83	66.79	3.94	49.4	172	2.6	136.0	0.28	-0.02
08NMA32-10	49.348220	-120.680290	10	5468754	668478	61561	0.19	7.60	0.58	35.6	16	12.1	63.4	0.07	-0.02
08NMA32-13	49.339153	-120.681716	10	5467743	668405	61557	0.76	94.71	1.16	51.4	242	4.9	122.5	0.09	0.05
08NMA32-14	49.335878	-120.682731	10	5467377	668343	61558	17.79	87.18	3.10	222.3	236	4.5	76.1	0.22	0.02
08NMA33-06	49.311319	-120.653013	10	5464714	670586	61559	0.18	65.40	0.45	55.9	88	13.7	28.7	0.07	0.45
08SOL21-04	49.365024	-120.669913	10	5470646	669174	61549	0.99	56.02	2.88	64.2	293	2.9	3.8	0.43	0.04

groupings (Figure 12). Assays of grab samples northwest of the Whipsaw property show reasonably anomalous Cu, Mo and Ag values, suggesting that the Whipsaw porphyry Cu system could be extended.

The calcareous matrix of volcanic rocks within the lower Nicola sedimentary sequence is variably altered to

skarn with some visible sulphides. Analyses of grab samples, however, proved to be unremarkable.

Several grab samples were collected in the northwestern part of the map area, where several areas of orange-brown iron carbonate-silica alteration occur in Nicola volcanic rocks and possibly the Princeton Group. The samples

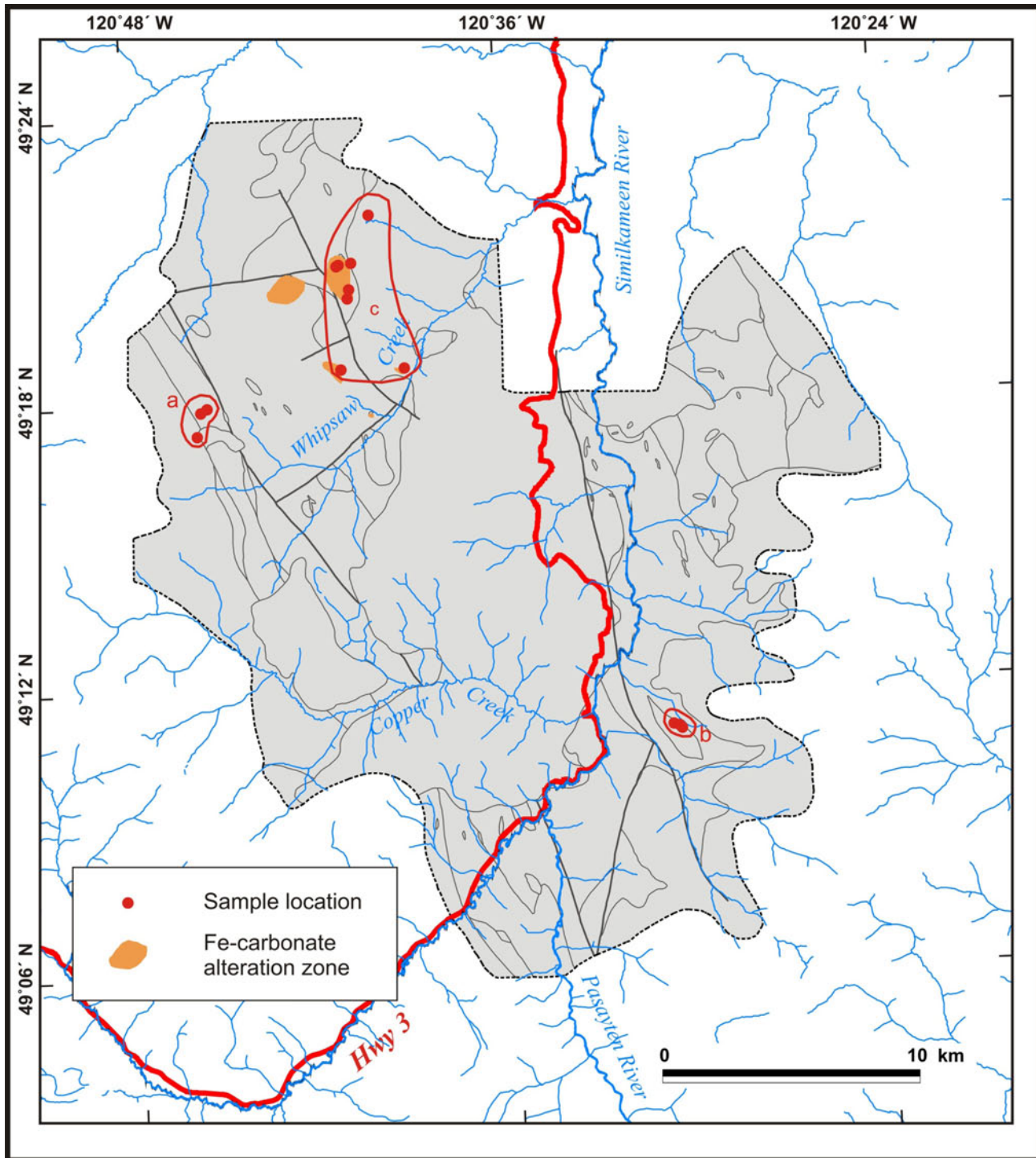


**Figure 12.** Locations of assay samples (see Table 2 for analyses and identification of groupings). Geological contacts and faults in the grey map area are as in Figure 2.

are somewhat variable but do show some elevated As and Ag values and moderate Au and Cu. The full extent and continuity of this alteration is unknown. No MINFILE occurrences are reported in this area and there is little recorded work in assessment reports.

## ACKNOWLEDGMENTS

The authors are much indebted to Rob Marshall of Weyerhaeuser (Princeton), Frank Joe of Stuwix Resources Ltd. (Merritt) and Peter Holbeck and Richard Joyes of Copper Mountain Mining Corporation for all their invaluable help and advice during the planning stages of this project. The authors also acknowledge the indispensable and tireless assistance of Scott Jasechko during fieldwork and in the office. Paul Schiarizza offered invaluable comments on an earlier draft of this manuscript.

## REFERENCES

- Bauerman, H. (1885): Report on the geology of the country near the forty-ninth parallel of north latitude west of the Rocky Mountains; *Geological Survey of Canada*, Report of Progress 1882–83–84, part B, pages 5–42.
- Bostock, H.S. (1940a): Map of Hedley area; *Geological Survey of Canada*, Map 568A, scale 1:63 360.
- Bostock, H.S. (1940b): Map of Wolfe Creek area; *Geological Survey of Canada*, Map 569A, scale 1:63 360.
- Breitspacher, K. and Mortensen, J.K. (2004): BC Age 2004A-1: a database of isotopic age determinations for rock units from British Columbia; *BC Ministry of Energy, Mines and Petroleum Resources*, Open File 2004-3, URL <<http://www.empr.gov.bc.ca/Mining/Geoscience/PublicationsCatalogue/OpenFiles/2004/Pages/2004-3.aspx>> [December 16, 2008].
- Camsell, C. (1913): Geology and mineral deposits, Tulameen District, British Columbia; *Geological Survey of Canada*, Memoir 26, 188 pages.
- Childe, F.C., Friedman, R.M., Mortensen, J.K. and Thompson, J.F.H. (1997): Evidence for Early Triassic felsic magmatism in the Ashcroft (92I) map area, British Columbia; in *Geological Fieldwork 1996*, *BC Ministry of Energy, Mines and Petroleum Resources*, Paper 1997-1, pages 117–123, URL <<http://www.empr.gov.bc.ca/Mining/Geoscience/PublicationsCatalogue/Fieldwork/Pages/GeologicalFieldwork1996.aspx>> [December 16, 2008].
- Coates, J.A. (1974): Geology of Manning Park area, British Columbia; *Geological Survey of Canada*, Bulletin 238, 177 pages.
- Dawson, G.M. (1877): Report on explorations in British Columbia, *Geological Survey of Canada*, Report of Progress, 1875–76, pages 233–265.
- Dolmage, V. (1934): Geology and ore deposits of Copper Mountain, British Columbia; *Geological Survey of Canada*, Memoir 171, 69 pages.
- Fahrni, K.C. (1951): Geology of Copper Mountain; *Bulletin of the Canadian Institute of Mining and Metallurgy*, volume 44, pages 317–324.
- Greig, C.J. (1992): Jurassic and Cretaceous plutonic and structural styles of the Eagle Plutonic Complex, southwestern British Columbia, and their regional significance; *Canadian Journal of Earth Sciences*, volume 29, pages 793–811.
- Greig, C.J., Armstrong, R.L., Harakal, J.E., Rinkle, D and van der Hayden, P. (1992): Geochronometry of the Eagle Plutonic Complex and the Coquihalla area, southwestern British Columbia; *Canadian Journal of Earth Sciences*, volume 29, pages 812–829.
- Hills, L.V. (1962): Glaciation, structures and micropalaeontology of Princeton coalfield, British Columbia; unpublished MSc thesis, *University of British Columbia*.
- Massey, N.W.D., MacIntyre, D.G., Desjardins, P.J. and Cooney, R.T. (2005): Geology of British Columbia; *BC Ministry of Energy, Mines and Petroleum Resources*, Geoscience Map 2005-3, scale 1:1 000 000, URL <<http://www.empr.gov.bc.ca/Mining/Geoscience/PublicationsCatalogue/Maps/GeoscienceMaps/Pages/2005-3.aspx>> [December 16, 2008].
- McMechan, R.D. (1983): Geology of the Princeton Basin; *BC Ministry of Energy, Mines and Petroleum Resources*, Paper 1983-3, 52 pages, URL <<http://www.empr.gov.bc.ca/Mining/Geoscience/PublicationsCatalogue/Papers/Pages/1983-3.aspx>> [December 16, 2008].
- MINFILE (2008): MINFILE BC mineral deposits database; BC Ministry of Energy, Mines and Petroleum Resources, URL <<http://www.empr.gov.bc.ca/Mining/Geoscience/MINFILE/Pages/default.aspx>> [December 16, 2008].
- Monger, J.W.H. (1989): Geology, Hope, British Columbia; *Geological Survey of Canada*, Map 41-1989, scale 1:250 000.
- Mortensen, J.K., Ghosh, D.K. and Ferri, F. (1995): U-Pb geochronology of intrusive rocks associated with copper-gold porphyry deposits in the Canadian Cordillera; in *Porphyry Deposits of the Northwestern Cordillera of North America*, Schroeter, T.G., Editor, *Canadian Institute of Mining, Metallurgy and Petroleum*, Special Volume 46, pages 142–158.
- Montgomery, J.H. (1967): Petrology, structure and origin of the Copper Mountain intrusions near Princeton, British Columbia; unpublished PhD thesis, *University of British Columbia*.
- Mortimer, N. (1987): The Nicola Group: Late Triassic and Early Jurassic subduction-related volcanism in British Columbia; *Canadian Journal of Earth Sciences*, volume 24, pages 2521–2536.
- Nixon, G.T., Hammack, J.L., Ash, C.A., Cabri, L.J., Case, G., Connelly, J.N., Heaman, L.M., Laflamme, J.H.G., Nuttall, C.N., Paterson, W.P.E. and Wong, R.H. (1997): Geology and platinum-group-element mineralization of Alaskan-type ultramafic-mafic complexes in British Columbia; *BC Ministry of Energy, Mines and Petroleum Resources*, Bulletin 93, 142 pages, URL <<http://www.empr.gov.bc.ca/Mining/Geoscience/PublicationsCatalogue/BulletinInformation/BulletinsAfter1940/Pages/Bulletin93.aspx>> [December 16, 2008].
- Preto, V.A. (1972): Geology of Copper Mountain; *BC Ministry of Energy, Mines and Petroleum Resources*, Bulletin 59, 87 pages, URL <<http://www.empr.gov.bc.ca/Mining/Geoscience/PublicationsCatalogue/BulletinInformation/BulletinsAfter1940/Pages/Bulletin59.aspx>> [December 16, 2008].
- Preto, V.A. (1979): Geology of the Nicola Group between Merritt and Princeton; *BC Ministry of Energy, Mines and Petroleum Resources*, Bulletin 69, 90 pages, URL <<http://www.empr.gov.bc.ca/Mining/Geoscience/PublicationsCatalogue/BulletinInformation/BulletinsAfter1940/Pages/Bulletin69.aspx>> [December 16, 2008].
- Ray, G.E. and Dawson, G.L. (1987): Geology and mineral occurrences in the Hedley gold camp, southern British Columbia; *BC Ministry of Energy, Mines and Petroleum Resources*, Open File 1987-10, scale 1:20 000, URL <<http://www.empr.gov.bc.ca/Mining/Geoscience/Publications/OpenFiles/OF1987-10/toc.htm>> [November 2008].
- Read, P.B. (1987): Tertiary stratigraphy and industrial minerals, Princeton and Tulameen basins, British Columbia; *BC Ministry of Energy, Mines and Petroleum Resources*, Open File 1987-19, scale 1:25 000, URL <<http://www.empr.gov.bc.ca/>>

[Mining/Geoscience/PublicationsCatalogue/OpenFiles/1987/Pages/1987-19.aspx](http://www.empr.gov.bc.ca/Mining/Geoscience/PublicationsCatalogue/OpenFiles/1987/Pages/1987-19.aspx) [December 16, 2008].

Read, P.B. (2000): Geology and industrial minerals of the Tertiary basins, south-central British Columbia; *BC Ministry of Energy, Mines and Petroleum Resources*, GeoFile 2000-03, 110 pages, URL <<http://www.empr.gov.bc.ca/Mining/Geoscience/PublicationsCatalogue/GeoFiles/Pages/2000-3.aspx>> [December 16, 2008].

Rice, H.M.A. (1947): Geology and mineral deposits of the Princeton map-area, British Columbia; *Geological Survey of Canada*, Memoir 243, 136 pages.

Shaw, W.S. (1952a): The Princeton coalfield, British Columbia; *Geological Survey of Canada*, Paper 52-12, 28 pages.

Shaw, W.S. (1952b): The Tulameen coalfield, British Columbia; *Geological Survey of Canada*, Paper 52-19, 13 pages.

Stanley, C.R., Holbeck, P.M., Huyck, H.L.O., Lang, J.R., Preto, V.A.G., Blower, S.J. and Bottaro, J.C. (1995): Geology of the Copper Mountain alkalic porphyry copper-gold deposits, Princeton, British Columbia; *in* Porphyry Deposits of the Northwestern Cordillera of North America, Schroeter, T.G., Editor, *Canadian Institute of Mining, Metallurgy and Petroleum*, Special Volume 46, pages 537–564.

# Carbonate-Hosted, Nonsulphide, Zinc-Lead Deposits in the Southern Kootenay Arc, British Columbia (NTS 082F/03)

by G.J. Simandl<sup>1,3</sup> and S. Paradis<sup>2,3</sup>

**KEYWORDS:** zinc deposit, nonsulfide, carbonate-hosted, hemimorphite, cerussite, oxide, Salmo district

## INTRODUCTION

Carbonate-hosted, nonsulphide, base-metal (CHNSBM) deposits are commonly overlooked during the selection of exploration targets. Under favourable geological, climatic, topographic and hydrological conditions, the weathering of a variety of carbonate-hosted, sulphide deposits may result in the formation of economically significant CHNSBM deposits. The primary objective of this paper is to provide conceptual background on CHNSBM deposits, supply concrete examples of direct-replacement, nonsulphide deposits from the Salmo district, British Columbia (NTS 082F/03) and demonstrate that the area has significant potential to host undiscovered wallrock-replacement-type CHNSBM deposits. The secondary objective is to explain the importance of deposit morphology and its spatial orientation in the preservation of such deposits within glaciated areas of southeastern BC.

## CARBONATE-HOSTED, NONSULPHIDE, BASE-METAL DEPOSITS

Nonsulphide deposits were the main source of zinc prior to the 1930s but following the development of differential flotation and breakthroughs in smelting technology, the mining industry turned its attention to sulphide ore. Today, most zinc is derived from sulphide ore (Hitzman et al., 2003). The situation, however, is changing as evidenced by the successful operation of a dedicated processing plant to extract zinc metal, through direct acid leaching, solid-liquid separation, solvent extraction and electrowinning, from nonsulphide and mixed ores mined at the Skorpion mine, Namibia. Geological information on CHNSBM deposits was reviewed by Hitzman et al. (2003). The CHNSBM deposits are interpreted to be of either supergene or hypogene origin (Hitzman et al., 2003; Sangster, 2003). The formation of supergene deposits is well established but

uncertainty remains regarding hypogene CHNSBM deposits.

In this paper, we concentrate on nonsulphide deposits formed in supergene environments from carbonate-hosted, sulphide, base-metal deposits (such as Mississippi Valley-type [MVT], sedimentary-exhalative [SEDEX], Irish-type or vein-type deposits and, to lesser extent, skarns). When carbonate-hosted, base-metal sulphide mineralization is subject to intense weathering, metals are liberated by the oxidation of sulphide minerals. The metals can be trapped locally, forming direct-replacement, nonsulphide, ore deposits (Heyl and Bozion, 1962; Hitzman et al., 2003) also referred to as “residual” ore by Reichert and Borg (2008).

A schematic section of an idealized direct-replacement deposit is shown in Figure 1a. During the formation of a direct-replacement CHNSBM deposit, primary ore (protore) is oxidized, and base metals pass into solution and are redistributed and trapped within space originally occupied by the protore. Depending on the extent of replacement of the sulphides by base-metal and iron-bearing nonsulphide minerals (oxides, silicates, carbonates and phosphates), the resulting ore is called mixed (combination of sulphide and nonsulphide ore) or nonsulphide ore (also referred to as oxide ore). If the base metals liberated by the oxidation of sulphide ore are not trapped locally, they are transported by percolating waters down and away from the sulphide protore and may form wallrock-replacement CHNSBM deposits (Figure 1b). Wallrock-replacement deposits can be located in proximity to protore or several hundreds of metres away (Heyl and Bozion, 1962; Hitzman et al., 2003; Reichert and Borg, 2008). Alternatively, if the metal-bearing solutions do not encounter conditions favourable for trapping within nonsulphide minerals (by direct- or wallrock-replacement processes), metals are dispersed in low concentration over large areas (i.e., without forming economic ore deposits).

Heyl and Bozion (1962) and Hitzman et al. (2003) also described residual and karst-fill, supergene, nonsulphide, base-metal deposits formed by mechanical or chemical transport followed by accumulation of previously formed nonsulphide mineralization in karst depressions and underground systems. These deposits are typically high grade and small tonnage. We do not discuss these deposit types here. The main nonsulphide Zn-, Pb- and Fe-bearing minerals and their characteristics are listed in Table 1. The reader is referred to Hitzman et al. (2003) for a more complete list.

Historically, most CHNSBM deposits were thought to be small; some deposits and districts, however, have tonnage comparable to world-class sulphide deposits, especially if mixed ores are also considered (Figure 2). The Balmat deposit (New York), which is a large stratiform, carbonate-hosted, Zn sulphide deposit, is shown for comparison. The Balmat deposit has a near-surface

<sup>1</sup> British Columbia Ministry of Energy, Mines and Petroleum Resources, Victoria, BC

<sup>2</sup> Geological Survey of Canada, Pacific Division, Sidney, BC

<sup>3</sup> School of Earth and Ocean Sciences, University of Victoria, Victoria, BC

This publication is also available, free of charge, as colour digital files in Adobe Acrobat® PDF format from the BC Ministry of Energy, Mines and Petroleum Resources website at <http://www.empr.gov.bc.ca/Mining/Geoscience/PublicationsCatalogue/Fieldwork/Pages/default.aspx>.

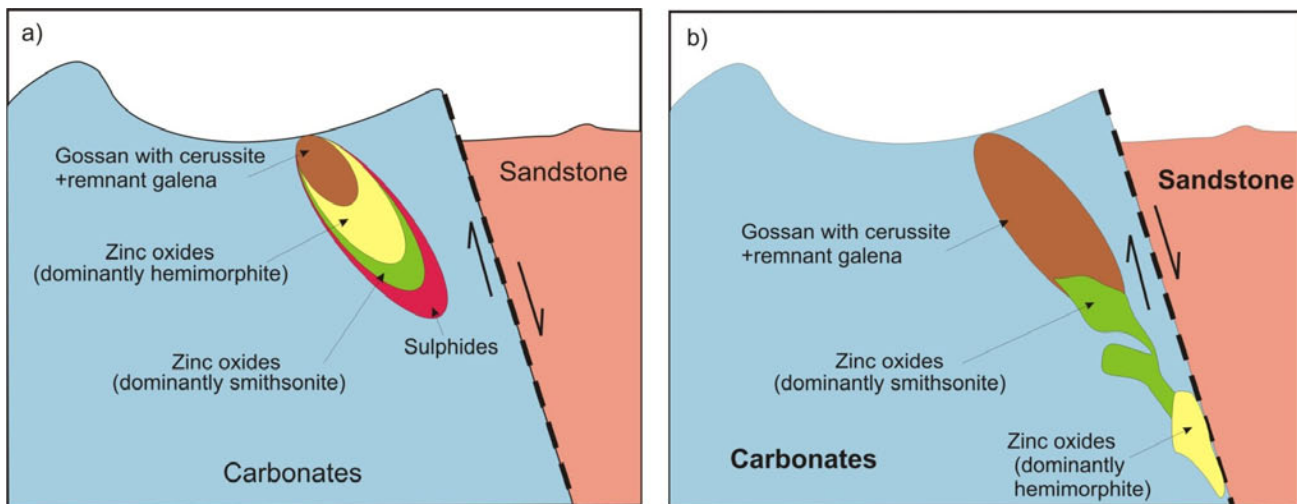


**Figure 1.** Idealized sections of carbonate-hosted, nonsulphide, base-metal deposits: a) direct-replacement deposit; b) wallrock-replacement deposit (modified from Heyl and Bozion, 1962; Hitzman et al., 2003).

nonsulphide component of <100 000 tonnes at 10–29% Zn (too small to show on Figure 2). Skorpion (Namibia), which has 60 million tonnes of mixed resource grading 6–8% Zn and 1–2% Pb and 24.6 million tonnes of oxide resource grading 10.6% Zn, and Mapimi (Mexico), which has 6 million tonnes at 15% Zn, 10% Pb and 500 g/t Ag, are examples of large, high-grade, nonsulphide deposits (Corrans et al., 1993; Titley, 1993).

A summary of Zn and Pb grades of major CHNSBM deposits is presented in Figure 3. Where the data are available, the Pb and Zn content of sulphide protore and mixed (nonsulphide and sulphide) ores that are genetically related to CHNSBM mineralization are also shown. CHNSBM mineralization has higher Zn and lower Pb content than mixed ore and/or the sulphide protore (Figure 3) from which it was derived. Wallrock-replacement deposits are commonly rich in Zn and poor in Pb relative to the direct-replacement CHNSBM deposits.

The above summary is an oversimplification. The oxidation of base-metal ore is commonly a multicyclic process (Hitzman et al., 2003). Diversity in the type of protore, and the multicyclic nature and variations in near-surface geological processes result in a wide spectrum of CHNSBM ores. Reichert and Borg (2008) proposed two extremes of CHNSBM ores, “red ores” and “white ores”. Red ores consist commonly of Fe-oxyhydroxides, goethite, hematite, hemimorphite, smithsonite, hydrozincite and cerussite. They typically contain >20% Zn, >7% Fe and Pb±As. White ores, consisting commonly of smithsonite, hydrozincite and minor Fe-hydroxides, contain <40% Zn, <7% Fe and very low concentrations of Pb. The stability of hemimorphite is largely dictated by the activity of silica within the system. Hemimorphite may be present within red or white ores. Red ores are found largely in the settings where the direct-replacement process (Figure 1a), as defined by Hitzman et al. (2003), predominates. White ore, at the opposite end of the spectrum, may be found as replacement of breccia clasts and wallrock or as breccia cement or open-space filling. It may be located tens to several hundreds of metres from the nearest sulphide ore, mixed ore, red ore or gossan. From metallurgical and environmental considerations, white ores are simpler and preferable.

## REGIONAL GEOLOGY

The area of interest is located in the Kootenay Arc of southeastern BC (Figure 4). The Kootenay Arc is an arcuate belt of complexly deformed rocks extending at least 400 km from near Revelstoke to the southwest across the Canada–United States border (Fyles, 1964). The Kootenay Arc lies between the Purcell Anticlinorium in the Purcell Mountains to the east and the Monashee metamorphic complex to the west (Figure 4). The Arc consists of a thick succession of thrust-imbricated Proterozoic to Lower Mesozoic miogeoclinal to basinal strata of sedimentary and volcanic protoliths (Brown et al., 1981).

Colpron and Price (1995) outlined a regionally coherent stratigraphic succession in the Kootenay Arc. The lower part is composed of siliciclastic and carbonate rocks of the Eocambrian Hamill Group and Mohican Formation. These are overlain by the archaeocyathid-bearing carbonate rocks of the Lower Cambrian Badshot Formation and its equivalent, the Reeves Member of the Laib Formation (Fyles and Eastwood, 1962; Fyles, 1964; Read and Wheeler, 1976), which host a number of Zn–Pb sulphide deposits. The Badshot Formation is characterized by calcitic dolomitic marble. Schist is locally interlayered with the marble. In the southern part of the Kootenay Arc, the carbonate rocks are overlain by siliciclastic, basinal shale and mafic volcanic rocks of the Lower Paleozoic Lardeau Group (Colpron and Price, 1995). Polyphase deformation has transposed bedding and locally obscured primary stratigraphic relationships (Colpron and Price, 1995).

## GEOLOGICAL SETTING OF THE CARBONATE-HOSTED SULPHIDE DEPOSITS

The Kootenay Arc hosts numerous carbonate-hosted Zn–Pb deposits (Höy, 1982; Nelson, 1991). The carbonate-hosted Zn–Pb deposits are distributed along the Kootenay Arc. The main concentrations define the Salmo and Duncan camps in southern BC. Smaller deposits characterize the northern part of the Kootenay Arc (Figure 4). The deposits, commonly referred to as “Kootenay Arc-type de-

**Table 1.** Selected nonsulphide Zn-, Pb- and Fe-bearing minerals and their characteristics.

	<b>Formula</b>	<b>Colour</b>	<b>Lustre</b>	<b>Density</b>	<b>Hardness</b>	<b>Comments</b>
<b>Main Zn-bearing minerals</b>						
Smithsonite	ZnCO <sub>3</sub>	white	earthy, dull	4.5	4.4	soluble in HCl, botroidal, reniform, earthy or granular; may be fluorescent, greenish or bluish or whitish in ultraviolet light
Hemimorphite	Zn <sub>4</sub> Si <sub>2</sub> O <sub>7</sub> (OH) <sub>2</sub> ·H <sub>2</sub> O	white, brown, greenish grey	vitreous	3.6	5	weakly soluble in HCl, massive, botroidal, stalactitic
Hydrozincite	Zn(CO <sub>3</sub> ) <sub>2</sub> (OH) <sub>6</sub>	white, pale yellow, pale grey	pearly	3.6–3.8	2–2.5	massive, fibrous, bladed aggregates; fluorescent pale blue or lilac in ultraviolet light; soluble in acids and amonia
Sauconite	Na <sub>0.2</sub> Zn <sub>3</sub> Si <sub>3</sub> AlO <sub>10</sub> (OH) <sub>2</sub> ·4(H <sub>2</sub> O)	white, pale brown, reddish brown	dull, earthy	2.45 (variable)	1.0–2.0	earthy, clay-like texture
Willemite	ZnSiO <sub>4</sub>	white, green, red, brown, black, pinkish, bluish	vitreous/resinous	3.9–4.2	5.5	massive, granular, prismatic; fluorescent green in short ultraviolet light
Zn-bearing aragonite	(Zn,Ca)CO <sub>3</sub>	white, grey, yellowish	vitreous	3	3.5–4.0	fluorescent green in short ultraviolet light; effervesces in HCl; fibrous, prismatic, columnar
Minrecordite	CaZn(CO <sub>3</sub> ) <sub>2</sub>	white to colourless, brown, blue-green	vitreous to pearly	3.5	3.5–4	rhombohedral, sometimes saddle-shaped
<b>Main Pb-bearing minerals</b>						
Cerussite	PbCO <sub>3</sub>	colourless, white, tan, grey	adamantin	6	3	massive granular, reticulate, well-formed prisms; fluorescent yellow in long wave ultraviolet light
Anglesite	PbSO <sub>4</sub>	white, colourless, grey, bluish, yellow	vitreous to adamantin	6.3	3–3.5	granular, anhedral to subhedral crystals; commonly fluorescent yellow in ultraviolet light
Pyromorphite	Pb <sub>5</sub> (PO <sub>4</sub> ,AsO <sub>4</sub> ) <sub>3</sub> Cl	green, brown, yellow	resinous to adamantin	6.7–7	4	prismatic or reniform and globular textures
Plumbojarosite	PbFe <sub>6</sub> (SO <sub>4</sub> ) <sub>4</sub> (OH) <sub>12</sub>	golden to dark brown	vitreous to dull	3.6	1.5–2.0	soluble in HCl, earthy, concretionary, encrustations, lumps
Litharge	PbO	red	greasy	9.14–9.3	2	encrustations
Mimetite	Pb <sub>5</sub> (AsO <sub>4</sub> ,PO <sub>4</sub> ) <sub>3</sub> Cl	brown, yellow, tan, brown, white	resinous	7.1–7.3	3.5–4	reniform, globular, sometimes prismatic
<b>Main Fe-bearing minerals</b>						
Goethite	FeO(OH)	dark or rusty brown, black	dull, resinous	4–4.4	3.5–4	earthy, botroidal, stalactitic
Hematite	Fe <sub>2</sub> O <sub>3</sub>	red to nearly black	typically dull	5.2	5	coatings, stains, fracture fillings

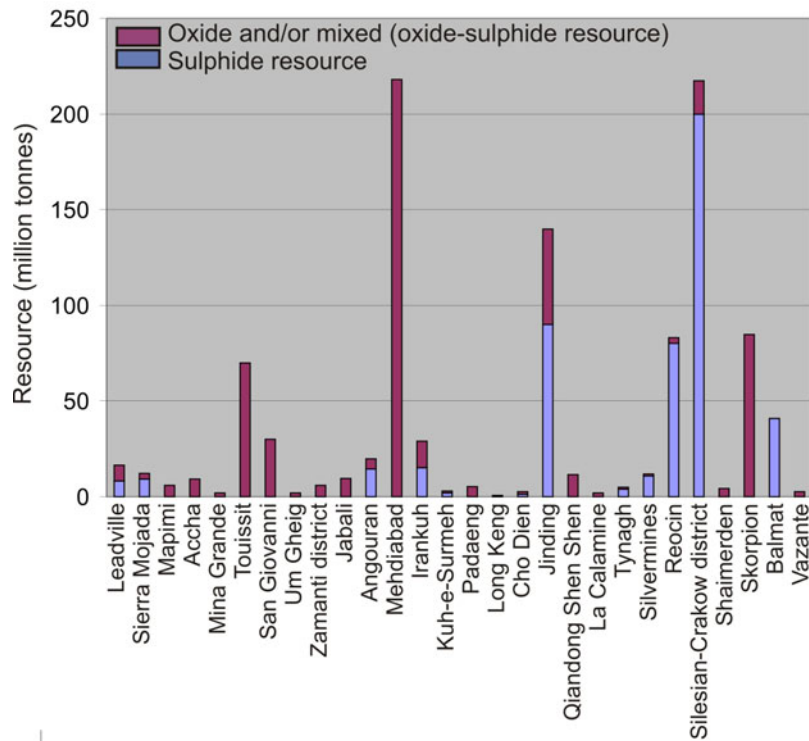


**Figure 2.** Tonnages of selected carbonate-hosted, nonsulphide, base-metal deposits, associated nonoxidized sulphide protore and mixed ores (based on compilation of Hitzman et al., 2003).

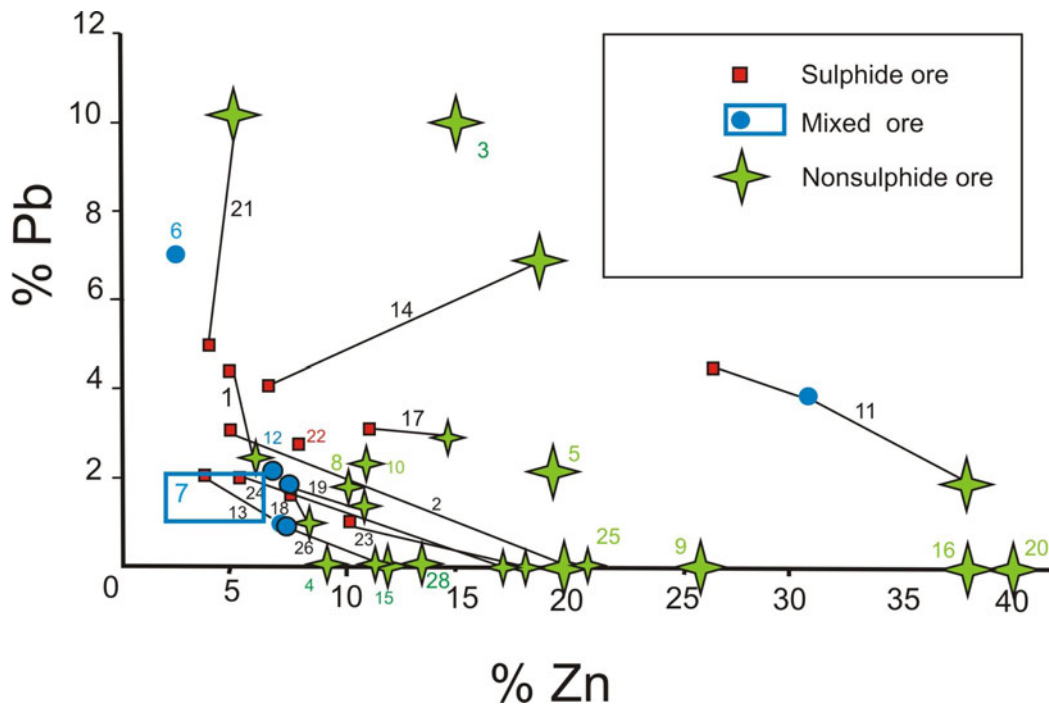


**Figure 3.** Zinc and lead grades of carbonate-hosted, nonsulphide, base-metal (CHNSBM) deposits. Where data are available, Pb and Zn content of genetically related, sulphide protore and mixed (nonsulphide and sulphide) ore are connected by a tie line. In most cases, CHNSBM ore has higher Zn content than related mixed ore and nonoxidized sulphide protore (based on compilation of Hitzman et al., 2003). 1. Leadville (U.S.A.), 2. Sierra Mojada (Mexico), 3. Mapimi (Mexico), 4. Accha (Peru), 5. Mina Grande (Peru), 6. Touissit (Morocco), 7. San Giovanni (Italy), 8. Um Gheig (Egypt), 9. Zamanti district (Turkey), 10. Jabali (Yemen), 11. Augouran (Iran), 12. Mehdiabad (Iran), 13. Irankuh (Iran), 14. Kuh-e-Surmeh (Iran), 15. Padaeng (Thailand), 16. Long Keng (Myanmar), 17. Cho Dien (Vietnam), 18. Jinding (China), 19. Qiangdong Shen Shen (China), 20. La Calamine (Belgium), 21. Tynagh (Ireland), 22. Silvermines (Ireland), 23. Reocin (Spain), 24. Silesian-Crakov district (Poland), 25. Shaimerden (Kazakhstan), 26. Skorpion (Namibia), 27. Balmat (U.S.A.), 28. Vazante (Brazil). All deposits, with the exception of Vazante, are considered supergene in origin.

posits” (Höy, 1982; Nelson, 1991), occur in the Badshot Formation or its equivalent, the Laib Formation (Reeves Member). They are interpreted to be metamorphosed Mississippi Valley-type or Irish-type Pb-Zn deposits (Paradis, 2007, 2008). They range in size from 6 to 10 million tonnes with average grades of 3–4% Zn, 1–2% Pb, 0.4% Cd and traces of Ag (Höy, 1982; Höy and Brown, 2000). They are stratabound and stratiform lens-shaped concentrations of sulphides (sphalerite, galena, pyrite, local pyrrhotite and rare arsenopyrite) in isoclinally folded dolomitized or silicified carbonate layers (Paradis, 2007). Several deposits are past-producers (e.g., Reeves MacDonald, Jersey, HB, Bluebell) and others have seen advanced exploration work (e.g., Duncan, Wigwam), although none are presently in production.

## CARBONATE-HOSTED SULPHIDE DEPOSITS OF THE SALMO CAMP

The Salmo camp comprises numerous carbonate-hosted Zn-Pb deposits. With the exception of Lomond and

Caviar (which are hosted by the Cambrian Nelway Formation), the deposits are hosted by fine-grained, poorly layered or massive dolomite of the Reeves Member, which is texturally distinct from barren, generally medium-grained, well-banded, grey and white or black and white limestone of the same unit. The mineralized dolomite is dark grey, poorly layered and mottled with black flecks, wisps and layers of impurities (Fyles, 1970). The deposits, their dolomitic envelopes, and the limestone hostrock generally lie within secondary isoclinal folds along the limbs of regional anticlinal structures. They form stratiform, tabular and lens-shaped concentrations of pyrite, sphalerite and galena in dolomitized zones. Brecciated zones are common within the more massive sulphide mineralization (Fyles and Hewlett, 1959; Legun, 2000). Some of the deposits are described below. Their description is based on our field investigations (2007, 2008) and descriptions of Fyles and Hewlett (1959), Fyles (1964, 1970), Höy (1982) and Legun (2000).

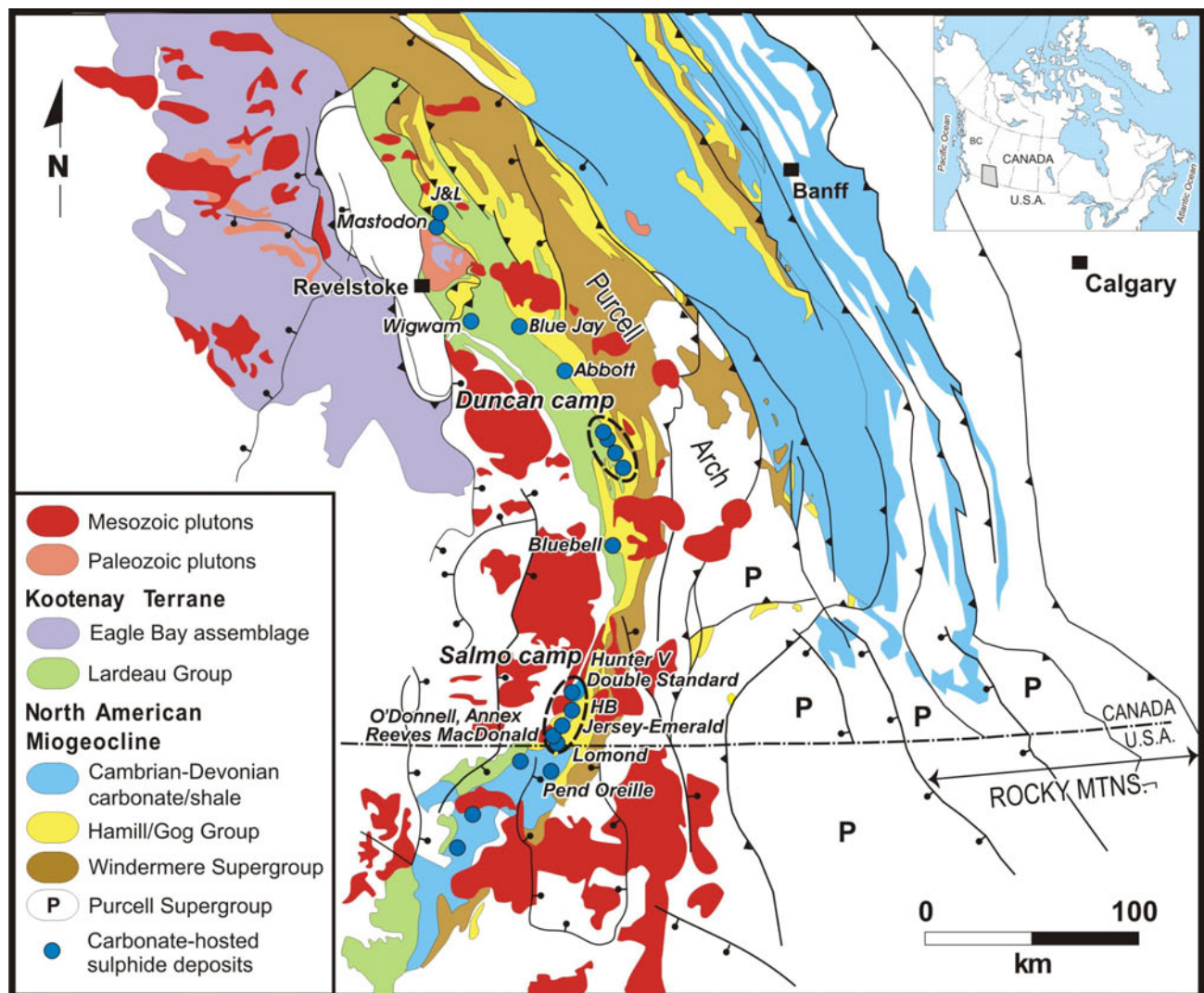


Figure 4. Simplified geological map of southeastern British Columbia showing the Kootenay Arc and location of carbonate-hosted Zn-Pb deposits (modified from Wheeler and McFeely, 1991; Logan and Colpron, 2006; Paradis, 2007).

## CARBONATE-HOSTED NONSULPHIDE DEPOSITS

The near-surface portions of the several previously described carbonate-hosted sulphide deposits are weathered, strongly oxidized and consist, in many cases, of extensive Zn- and Pb-bearing, iron oxide gossans and base-metal-bearing nonsulphide minerals. The weathered zones are partially delimited and were not exploited in the past. The mineralogy and paragenesis of oxidized zones are poorly known but indicative of direct-replacement of sulphides by nonsulphide base-metal-bearing minerals. The main exposure at Lomond is an excellent example of a CHNSBM Fe-rich gossan (Figures 1a, 1b, 5). The Oxide deposit may correspond to the hemimorphite portion of a CHNSBM deposit formed by wallrock-replacement (Figure 1b). There are not enough data available to determine conclusively if the Oxide deposit is of the direct- or wallrock-replacement-type but the dominance of hemimorphite is probably linked to high silica activity (provided by the underlying Reno Formation quartzite) during base metal trapping. In most other occurrences, spatial continuity and/or the close spatial relationships in combination with morphological similarities between sulphide and associated nonsulphide zones suggest direct-replacement CHNSBM mineralization. The evidence for direct-replacement origin is strongest where the transition of nonsulphide to sulphide mineralization with increasing depth is well documented. Detailed descriptions of selected deposits are given below.

### **Lomond Deposit (MINFILE 082FSW018)<sup>4</sup>**

This group of occurrences is located approximately 56 km south of Nelson, BC. Highly oxidized Pb-Zn sulphides are exposed within the middle and upper part of the Middle Cambrian to Early Ordovician Nelway Formation, which consists of cream and grey banded dolomite with discontinuous lenses of darker dolomite and dolomitic siltstone (Fyles and Hewlett, 1959). The main showing (Figure 5) is predominantly goethite. It was mined between 1947 and 1948 and in the 1950s as a source of iron for cement making and a small quantity of hand-sorted galena was shipped to the smelter at Trail, BC. Collapsed remnants of ore bins and rails are visible in Lomond Creek upstream from the main showing.

Two oxidized zones, 1.5 and 3.6 m thick and 3 m apart, are described by Fyles and Hewlett (1959) as conformable to the dolomitic banding but locally discordant. They consist of earthy brown, iron oxide limonite(?) containing harder areas of goethite. Within the soft earthy limonite are occasional anglesite-coated nodules of galena. Transparent to translucent crystals of cerussite (0.5–2 mm long) are locally present. A sample of the main oxidized zone assayed 10.3 g/t Ag, 1.2% Pb and 2.7% Zn (Fyles and Hewlett, 1959). The zone was resampled in 2008 and results of the chemical analyses are pending. Associated showings approximately 450 m to the north appear to be covered by debris slides. They were described as podiform, oxidized sulphide zones a few metres across, spaced along a strike length of 300 m. The Lomond showings may be oxidized analogs of the Yellowhead-type mineralization of the Pend Oreille mine in northeast Washington.

<sup>4</sup>(MINFILE, 2008)

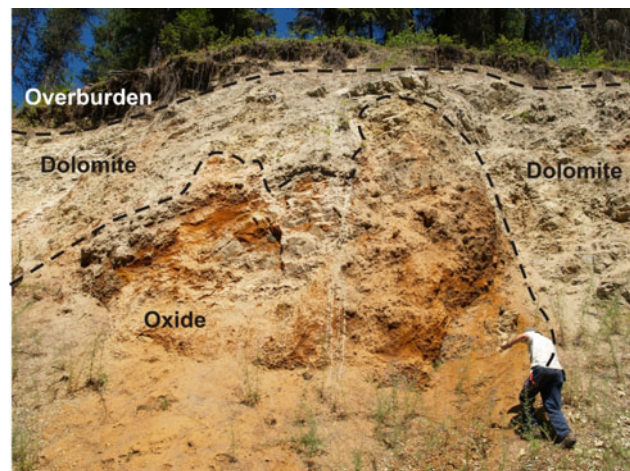


**Figure 5.** The main exposure at the Lomond deposit, southeastern British Columbia; an example of a carbonate-hosted, nonsulphide, base-metal (CHNSBM) deposit (gossan component).

### **Reeves MacDonald (MINFILE 082FSW026), Annex (MINFILE 082FSW219), Red Bird (MINFILE 082FSW024) and Related Deposits**

The Reeves MacDonald deposits are located 56 km south-southwest of the village of Salmo. They include the past-producing deposits of Reeves MacDonald and Annex, and the Red Bird prospect.

Combined production from 1949 to 1971 totalled 5 848 021 t of sulphide ore grading 3.50% Zn and 1.39% Pb. From this ore, 19.9 t of Ag, 203 616 t of Zn, 57 693 t of Pb, 1215 t of Cd and 27.6 t of Cu were recovered (MINFILE 082FSW024, 082FSW026, 082FSW219). Like most carbonate-hosted Zn-Pb deposits in the southern Kootenay Arc, the mineralized zones are enclosed by a dolomitized envelope within the Reeves Member limestone. The sulphide orebodies, their enveloping dolomite and the limestone hostrock are folded and metamorphosed to greenschist facies.

Structure in the area is characterized by nearly east-striking foliation and southwesterly trending fold axes. A series of north-striking faults that dip 25–45° east offset the formations and the mineralized zones (Figure 6).

The Reeves, B.L. (MINFILE 082FSW026) and O'Donnell (MINFILE 082FSW028) deposits are interpreted as faulted segments of the same orebody (Fyles and Hewlett, 1959; Gorzynski, 2001). The Red Bird (MINFILE 082FSW024), Annex (MINFILE 082FSW219), MacDonald (MINFILE 082FSW026), Point (MINFILE 082FSW027) and Prospect (MINFILE 082FSW029) deposits may be related by the style of faulting to the above mineralized zones; they may, however, be separate deposits (Fyles and Hewlett, 1959; G. Klein, pers comm, 2007).

The sulphide bodies are structurally conformable and stratabound. The sulphides form bands, lenses and layers of massive to disseminated material parallel to compositional layering within medium to dark grey dolostone. Layering varies from millimetre-scale to several centimetres in thickness, and is continuous over tens of metres, or discontinuous and highly contorted. Lenses of nonmineralized light grey dolomite interlayered with thin bands of argillite

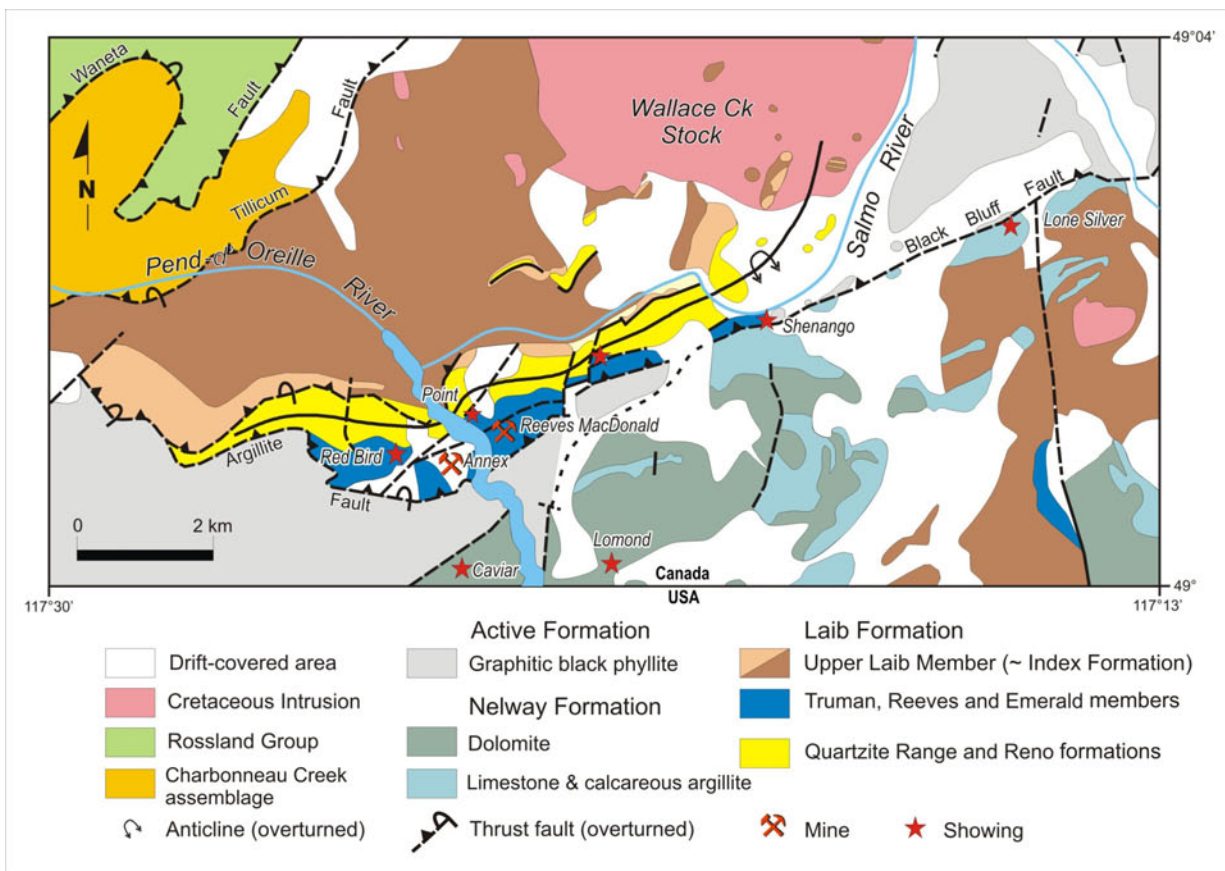


**Figure 6.** Simplified geological map of the Salmo area, southeastern British Columbia (modified from Fyles and Hewlett, 1959).

are common within the ore zones. Sulphides also form a matrix to breccias, which consist of rounded to platy fragments of dolomite, limestone and quartz. The sulphides consist of fine- to medium-grained pyrite, honey-coloured to brown sphalerite, minor galena and traces of chalcopyrite. Copper and cadmium content is typically less than 0.5% and 1 g/t, respectively. Gallium and germanium have been reported in concentrations above background levels.

Only sulphide mineralization was mined and the nonsulphide base-metal-bearing zones, consisting of earthy yellow-brown gossan of limonite(?) and goethite with variable amounts of cerussite, anglesite, smithsonite and hemimorphite, were left behind. According to Höy et al. (1993), the oxidation occurred prior to glaciation and much of the oxidized material was removed by the advancing ice.

Locations and projections of the main mineralized zones to the surface are sketched on Figure 7. The deposits and prospects (Figure 8) are exposed over a distance of approximately 4 km. Some of these mineralized zones, consisting at least in part of nonsulphide base-metal-bearing minerals, are described below.

### MACDONALD ADIT

The portal of the MacDonald adit collapsed before 1954 and is now entirely covered by overburden. Fyles and Hewlett (1959) reported that the adit was driven within “earthy calcareous and limonitic materials containing secondary Pb and Zn minerals”.

### POINT (ZONE Z)

The Point occurrence (zone Z) is located 450 m west of the 1900 level portal of the Reeves MacDonal mine (Figure 8), and most of it is covered by waters of the Pend d'Oreille River. A small faulted section of irregular, tabular masses of limonitic gossan is visible on a roadcut beside the Reeves MacDonal mine road (Figure 9). The Zn-Pb mineralization occurs within irregular, tabular- or pod-shaped envelopes of dolomitized Reeves Member limestone (Fyles and Hewlett, 1959). The deposit consists of two sulphide horizons, each about 6 m thick and separated by 20 m of dolostone. Mineralization consists of bands and lenses of massive and disseminated pyrite, honey-coloured sphalerite and galena. Disseminated, fine-grained, yellow sphalerite and occasional grains of galena also occur in a matrix of brecciated dolomite. A small tonnage of ore, grading 10% zinc was apparently extracted from this zone in the past (Gorzynski, 2001).

### PROSPECT ZONE

The Prospect zone is located in a widespread dolomitized unit informally called the “Prospect dolomite member”. The Prospect dolomite is thought to be a separate carbonate unit from the Reeves Member limestone (G. Klein, pers comm, 2007). It is host to scattered occurrences of disseminated and layered pyrite, sphalerite and traces of galena parallel to a faint layering in the fine-grained, pale grey dolomite. The highest concentrations of sulphides are associated with coarse-grained grey dolomite. The Prospect zone has been tested by two short adits, which exposed irregular and sparse mineralization containing locally 10%

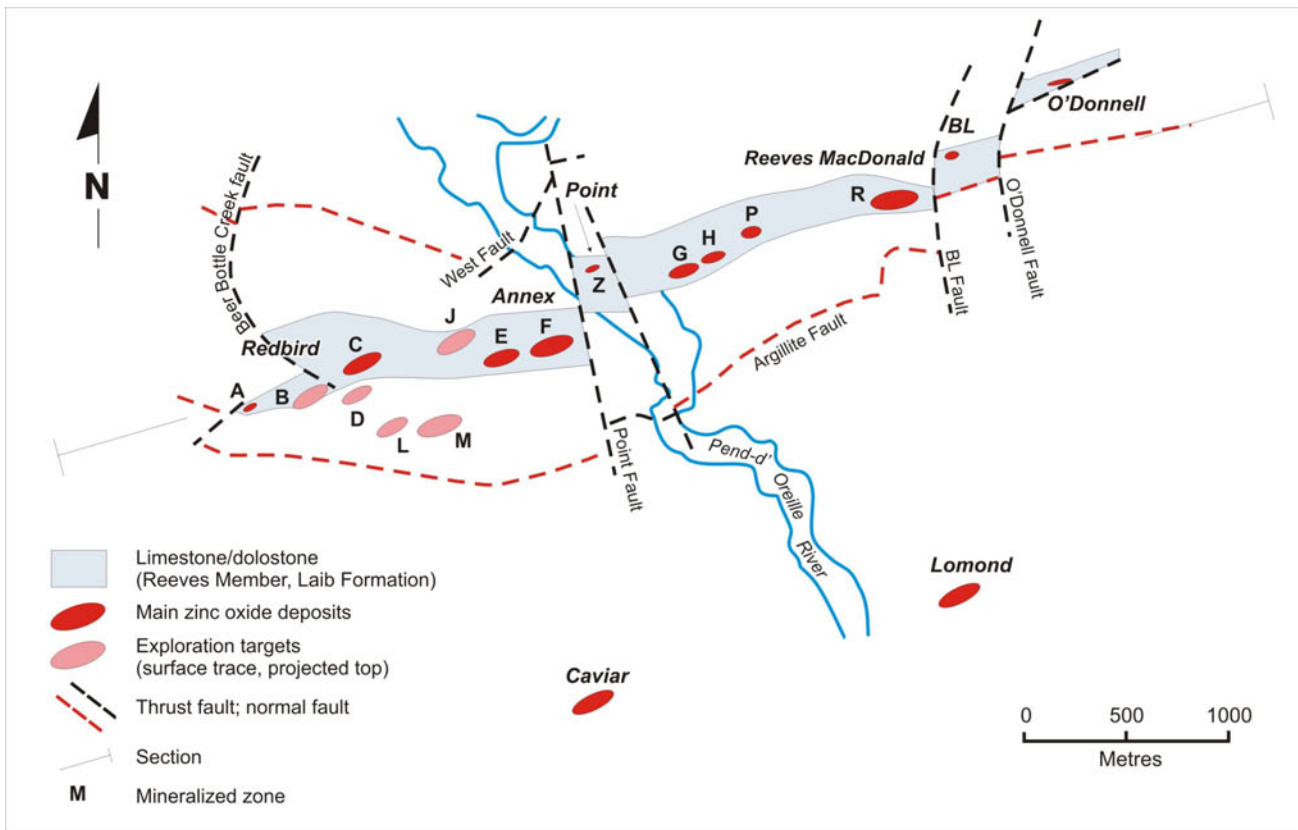


**Figure 7.** Schematic plan view of the main nonsulphide zinc oxide zones within the Reeves Member limestone/dolostone unit of the Laib Formation and the Nelway Formation, southeastern British Columbia (*modified from Redhawk Resources Inc., 2005*).

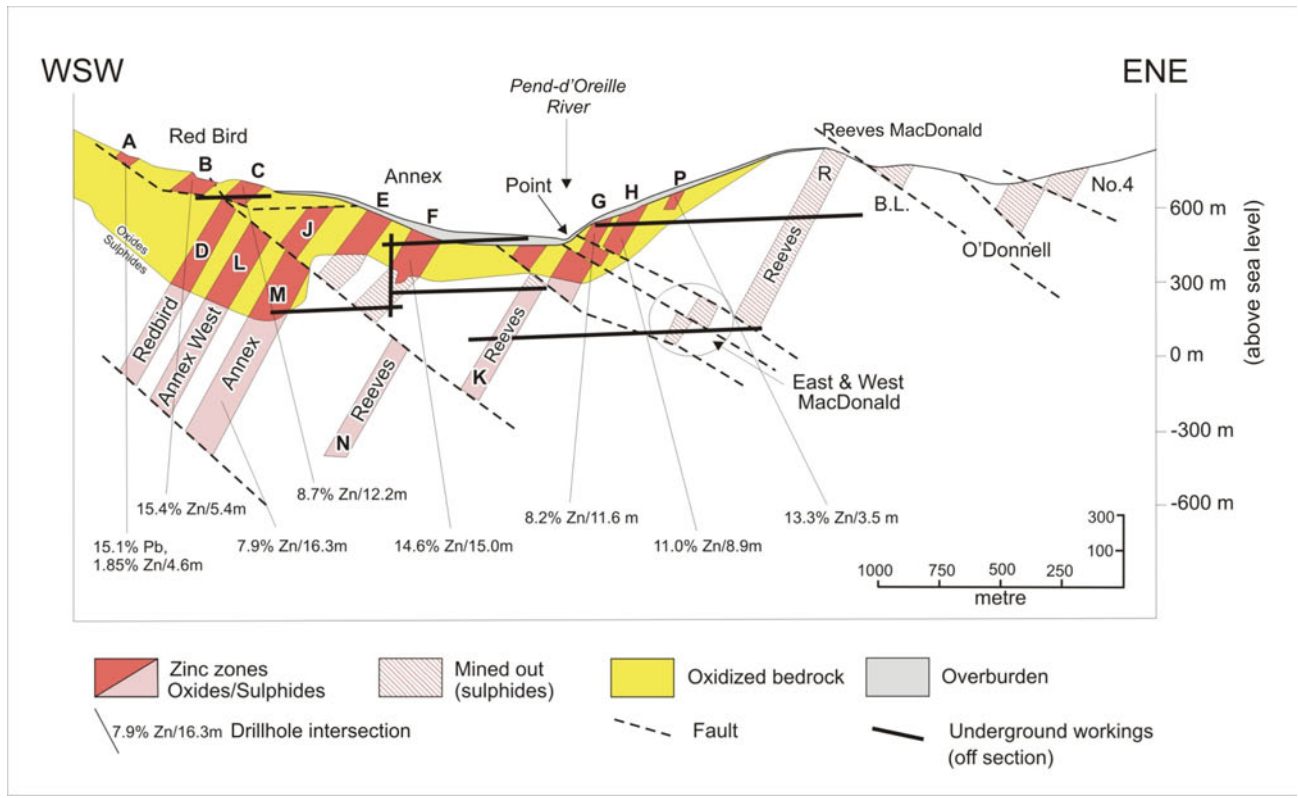


**Figure 8.** Schematic longitudinal east-northeast section (looking north) showing the distinct nonsulphide zinc oxide and sulphide zones. Some of the nonsulphide zones were labelled A to H by ReMac Zinc Corporation (*modified from Addie, 1970; Price, 1987; Gorzynski, 2001*). For location of section see Figure 7.

Pb and 9% Zn over widths of 60 cm (Walker, 1934). Surface trenching has exposed oxidized zones greater than 4 m across (Fyles and Hewlett, 1959).

Redhawk Resources Inc. drilled four holes in the Prospect dolomite member (south of zone C), which intersected 13.7% Zn over 9 m, 8.24% Zn over 4 m and 2.02% Zn over 16.98 m (Klein, 1999).

## ANNEX MINE

The Annex mine (consisting mainly of zones E and F), located on the west side of the Pend-d'Oreille River (Figure 7), operated from 1970 to 1975. It produced 763 314 t of sulphide ore at a recovered grade of 5.59% Zn, 0.93% Pb and 44.61 g/t Ag, most of which came from the E and F zones (Figure 8). Several boreholes drilled from 1986 to 2000 returned significant Zn, Pb and Ag grades within the nonsulphide portions of the Annex mineralization (George Cross News Letter, 1998; Klein, 1998). The last two holes were drilled in 2000 to intersect the upward projection of the sulphide zone. The first hole averaged 9.64% Zn over 21.0 m, with high-grade footwall (18.47% Zn over 3.9 m) and hangingwall (23.75% Zn over 2.3 m) portions and with lower grade dolomitic sections. The second hole averaged 14.62% Zn over 15.0 m without internal dolostone sections. These are the only holes in the area that encountered nonsulphide mineralization below the water table (Gorzynski, 2001). The position of the sulphide-oxide boundary in zone F is known and was established during mining. At both of these holes, drilling also encountered long sections of low-grade mineralization below the main intersections (21.4 m section of dolostone grading 1–2.4% Zn and a 23.4 m section grading 1–5% Zn).

## ZONE G

Zone G is another faulted section of the Annex mine. The first 500 m from the portal of the Reeves 1900 level is in leached limestone with iron oxide zones that were formed by oxidation of the MacDonald sulphide orebody (Fyles and Hewlett, 1959). This oxide zone was further investigated by drilling in 2000 (Gorzynski, 2001). The best intersection was 8.21% Zn, 1.08% Pb and 6.5 g/t Ag over 11.6 m (Gorzynski, 2001). This confirms the presence of base-metal nonsulphide mineralization above the zones encountered in the 1900 level.

## ZONE H

Zone H hosts zinc oxide mineralization. It is interpreted to continue at depth where grab samples of zinc oxides grading 20–25% Zn were collected from underground workings in the early 1970s (G. Klein, pers comm, 2000; Gorzynski, 2001). One of the two holes drilled in 2000 returned 10.98% Zn over 8.9 m, including 14.71% Zn over 5.3 m of true width. A second drillhole located 55 m to the east, returned 6.35% Zn over 4.4 m of true width but the intersection was near surface (Gorzynski, 2001).

## ZONE P

Zone P is a zinc oxide zone discovered by drilling in 2000. A drillhole returned two mineralized intersections, 6.68% Zn over 4.4 m (near the surface) and 13.25% Zn over 3.5 m at depth (Gorzynski, 2001).



**Figure 9.** Limonitic gossan is visible on a roadcut beside the Reeves MacDonald mine road, the Point occurrence (zone Z), southeastern British Columbia.

## Red Bird Prospect

The Red Bird prospect lies south and west of the Pend-d'Oreille River along Red Bird Creek. It includes zones A, B, C and D described below (Figures 7, 8). The main workings include four adits, a shaft and several more recent trenches and roadcuts. All the underground workings are inaccessible. The indicated resource (which predates National Instrument [NI] 43-101) within the Red Bird prospect is reported at 2 177 040 t grading 18.5% Zn, 6.5% Pb and 68.5 g/t Ag (Price, 1987).

## ZONE A

Zone A is located near the old Red Bird no. 4 tunnel. The trenches exposed narrow zones of zinc oxide mineralization in dolostone of the Reeves Member. Gorzynski (2001) reported values of 5.4% Zn over 1.6 m, 6.42% Zn over 1.3 m and 16.11% Zn over 1.5 m.

## BEER BOTTLE ZONE (ZONE B)

The Beer Bottle zone, located approximately 300 m east of zone A (Figures 7, 8), has been traced over a strike length of 110 m. It is truncated to the east by the Beer Bottle Creek fault and remains open to the west (Klein, 1999; Gorzynski, 2001).

The zone has been known since the 1920s and was drilled and retrenched in 1998 and 2000. One of the trenches exposed a section of red-brown limonite intercalated with dolostone (Gorzynski, 2001) and returned 15.00% Zn over 12.8 m. The footwall portion of this zone assayed 22.16% Zn over 6.3 m and the hangingwall portion returned 8.08% Zn over 6.5 m (Gorzynski, 2001). Four other trenches returned disappointing results but one of the roadcuts exposed a 10 m long section interpreted as a collapse breccia (Gorzynski, 2001). According to Gorzynski (2001), the breccia consists of angular dolostone and limestone and rounded clasts of zinc oxide (mainly hemimorphite) varying in size from pebbles to boulders. Five hemimorphite-rich boulders sampled on the property contained 18–32% Zn. Four vertical channel samples taken over the 10 m breccia exposure averaged 17.76% Zn (Gorzynski, 2001).

Based on the above description, this nonsulphide zinc oxide section is very different from other typical nonsulphide mineralization of the Salmo area. Other nonsulphide, karst-related, Zn occurrences are known elsewhere (Hitzman et al., 2003).

### **ZONE C**

Zone C, located 150 m northeast of zone B, is one of the main mineralized zones of the Red Bird prospect exposed at surface. It is interpreted as a down-faulted portion of zone B (Figure 8). Red Bird tunnel no. 1 exposed a nonsulphide section of approximately 140 m in length, including a 75 m long and over 6 m wide zone that has an average grade of 18.55% Zn, 5.97% Pb and 36.7 g/t Ag (Emendorf, 1927; Sorensen, 1942; Gorzynski, 2001). One of the re-excavated roadcuts (60 m in length), located 85 m in elevation above tunnel no. 1, exposed a limonite section that returned 6.93% Zn over 21 m (Gorzynski, 2001). High-grade zones in the footwall and hangingwall of this section assayed 12.30% Zn over 4.4 m and 9.75% Zn over 5.6 m. This zone includes two lenses of low-grade dolostone and a lower grade, iron oxide-rich, central section (3.32% Zn over 11.0 m), which is interpreted as direct-replacement of the pyrite-rich protore.

### **ZONE D**

Zone D was found by deep drilling. One drillhole reported an oxidized intersection of 16.7 m that assayed 7.2% Pb, 8.95% Zn and 23.5 g/t Ag, directly overlying a 1.5 m sulphide-rich dolomite section that assayed 5.64% Zn, 0.38% Pb, 8.8 g/t Ag and 0.06% Cd (Price, 1987). Consequently, the position of this zone (Figure 8) is based entirely on interpretation.

### ***Caviar Showing (MINFILE 082FSW060)***

The Caviar showing consists of two zones located west of the Pend-d'Oreille River and 200 m north of the United States border (Figure 7). These zones consist of lenses and stringers of sphalerite in dolomitic sections of limestone of the Nelway Formation (Fyles and Hewlett, 1959; Gorzynski, 2001). The best of four drillholes returned an intersection of 6.5% Zn over 6 m (Crosby, 1956). The nonsulphide (near surface) portion of the mineralization is believed to be limited to a few metres.

### ***Jersey-Emerald Deposits (MINFILE 082FSW009)***

The Jersey-Emerald property lies approximately 11 km southeast of the village of Salmo. It encompasses the former Jersey and Emerald Zn-Pb mines, and the Emerald, Feeney, Invincible and Dodger tungsten mines. Other deposit types, such as a gold-bismuth zone, SEDEX-type zinc-silver-copper deposits and molybdenum porphyry deposits are also present on this property. Only the Zn-Pb deposits will be considered here.

The historic Jersey Zn-Pb deposit was a small but steady producer from 1906 to 1925. During that period 25 850 t of ore were mined and 705 292 g of Ag, 6 788 936 kg of Pb and 19 771 kg of Zn were recovered. During 1948, when the Emerald tungsten mine was in production, a large tonnage of lead-zinc ore was outlined by drilling at the Jersey Zn-Pb mine. The Jersey Zn-Pb mine operated continuously until 1973. Lead and zinc was pro-

duced from Jersey and Emerald orebodies. Between 1949 and 1973, over 8 million tonnes of ore grading 1.95% Pb and 3.83% Zn were mined and 115 000 t of Pb, 263 000 t of Zn and 21 500 kg of Ag were recovered (MINFILE 082FSW009; Sultan Minerals Inc., 2008).

The Jersey and Emerald Zn-Pb mineralization occurs within a dolomitized zone, near the base of the Reeves Member and varies from 8 to 30 m in thickness. The Truman Member of the Laib Formation forms the mine footwall rocks (Fyles and Hewlett, 1959). It consists of dense, reddish green skarns and a brown argillite hosting tungsten and molybdenum mineralization. Five Pb-Zn dolomite-hosted ore bands, ranging in thickness from 0.3 to 9 m, are recognized within the mine. Sulphide ore consists of fine-grained sphalerite and galena with pyrite, pyrrhotite and minor arsenopyrite. The galena-sphalerite-pyrite-pyrrhotite ores are banded and similar to ores from the HB deposits, except that Pb dominates. Cadmium is associated with low-iron sphalerite and silver with galena. In 1995, during a tungsten exploration program, diamond drilling encountered a second Pb-Zn-bearing dolomite horizon located 55–60 m below the Jersey mine, currently referred to as the Lower Jersey zone (Sultan Minerals Inc., 2008). The widest mineralized intercept was 9 m, and the best single intersection graded 8.1% Zn and 3.8% Pb across 1 m (George Cross News Letter, 1997).

Unlike many of the other carbonate-hosted Pb-Zn deposits in the Salmo area, there is no record of a near-surface oxidation zone. Generally, this agrees with our field observations. The mine is dry and only two of the ten ore zones, B and D, were exposed at surface. Both of these zones are elongated approximately northward and plunge gently south. Only the southern-most and topographically lowest portions of these orebodies outcropped on Iron Mountain. A Fe-rich gossan was noted and sampled at 1394 m of elevation, west of the Emerald Zn-Pb mine portal no. 1. Results of geochemical analyses of this oxide zone are pending.

### ***HB Deposit (MINFILE 082FSW004)***

The HB mine is located 8 km southeast of the village of Salmo. It consists of two distinct zones, the HB and the Garnet deposits. The HB deposit consists of at least five orebodies and the Garnet deposit is a single lens. The mine produced a total of 6 656 101 t of ore between 1912 and 1978. Measured and indicated reserves, published in 1978 (predating NI 43-101) by Canadian Pacific Limited, were 36 287 t grading 0.1% Pb and 4.1% Zn (Anonymous, 1983).

The orebodies, hosted by Reeves Member limestone, are located less than 100 m west of the Argillite fault. Sedimentary rocks in the mine area are folded into a broad synclinorium, and the limestone-dolostone beds hosting the orebodies are on the west limb of this structure. Isoclinal folding is described within the trough of the synclinorium and these folds are affected by crossfolding at the north end of the HB mine and south of the main orebody.

The HB main mineralization consists of three elongated, crudely ellipsoidal orebodies dipping steeply toward the east and plunging 15–20° southward. These steeply dipping orebodies are connected by two gently dipping tabular sulphide breccia bodies, which also plunge 15–20° southward (MINFILE 082FSW004). The steeply dipping orebodies consist of concentrations of discontinuous stringers that have a Pb:Zn ratio of 1:5, whereas the tabular

brecciated mineralized zones have a Pb:Zn ratio of approximately 1:2.5 (MINFILE 082FSW004). The sulphide concentrations within steeply dipping ore zones appear to be parallel to cleavage in the host dolomitic marble (MacDonald, 1973). Sulphide mineralization within the tabular zones appears to follow the bedding.

Sulphide minerals consist predominantly of fine-grained pyrite and subordinate sphalerite, galena and locally minor pyrrhotite. The sulphide mineralization is enveloped by a broad zone of dolomitization, which is bordered along its contact with limestone by a narrow silica-rich zone. Talc and tremolite are reported to be found mainly near the silica-rich zone, suggesting that these minerals formed along the front produced by synmetamorphic element exchange between silica-rich and dolomitic rocks. Alternatively, tremolite and talc may be part of a metasomatic front created by the introduction of silica-bearing fluids into the dolomitic carbonates.

The northern portions of the mineralized zones are exposed at surface and oxidized to a depth of 100 m (Fyles and Hewlett, 1959). Available evidence points to the origin by the direct-replacement process. Nonsulphide minerals include hemimorphite  $\{Zn_4Si_2O_7(OH)_2 \cdot H_2O\}$ , smithsonite  $\{ZnCO_3\}$ , cerussite  $\{PbCO_3\}$  and anglesite  $\{PbSO_4\}$ . Fyles and Hewlett (1959) also mentioned the following phosphates: pyromorphite  $\{Pb_5(PO_4)_3Cl\}$ , hopeite  $\{Zn_4(PO_4)_2(OH)_2 \cdot 3H_2O\}$ , spencerite {an uncommon zinc phosphate;  $Zn_4(PO_4)_2 \cdot 4H_2O$ } and salmoite  $\{Zn_2(PO_4)(OH)\}$ .

### **Oxide Prospect (MINFILE 082FSW022)**

The main showings of the Oxide prospect outcrop to the west of the north-striking Oxide pass, 5.5 km east-southeast of Ymir, BC. The area is underlain by black argillite and slate of the Lower(?) to Middle Ordovician Active Formation, grey limestone of the Reeves Member of the Laib Formation, and micaceous and white quartzite resembling the lower Nevada Member of the Quartzite Range Formation (Fyles and Hewlett, 1959).

The fault zone (up to 9 m wide) consists of crushed and sheared rocks, containing a muddy clay-like gouge about 0.5 m thick (Fyles and Hewlett, 1959; MINFILE 082FSW022). The nonsulphide base-metal-bearing zone at



**Figure 10.** Hemimorphite-bearing material, Oxide deposit, south-eastern British Columbia.

the Oxide adit was reported to be highly oxidized and was exposed along strike for 458 m with a maximum width approaching 9 m. Past drilling and underground development confirmed that the oxidized zone extends more than 180 m in depth. Figure 10 shows the typical exposure in the vicinity of the Oxide fault. The limonitic gossan contains hemimorphite (Figure 11) and parahopeite as the major Zn-bearing minerals (McAllister, 1951). Galena nodules and pyromorphite are the principal Pb-bearing minerals (McAllister, 1951). The highest assay from the adit in 1948 was 15.7% Zn, 1.4% Pb, 0.34 g/t Au and 3.4 g/t Ag (Fyles and Hewlett, 1959). Up to 23% manganese and minor pyritic quartz, with low gold assays, are reported in MINFILE (082FSW022). The International adit, located approximately 830 m to the south of the Oxide adit, intersects an oxide zone up to 7.3 m in width, which is also reported to host nonsulphide Zn-Pb mineralization.

## **DISCUSSION**

The Reeves MacDonald group of deposits represent the best documented examples of CHNSBM deposits in BC. Figure 8 summarizes relationships between the base-metal, nonsulphide mineralization and the sulphide ore within the Reeves MacDonald area. Sulphide zones were oxidized at least up to 450 m below the surface. Several CHNSBM zones are underlain by sulphide mineralization, suggesting that they formed by direct-replacement of sulphide deposits. This is also supported by their mineralogy and Pb and Zn content.

The key controls on the formation of CHNSBM deposits are climate, nature and availability of near-surface protore, lithology, favourable hydrology and the rate of uplift.

Climate and paleoclimate are important factors in the selection of any given area for exploration targeting supergene CHNSBM deposits (Hitzman et al., 2003; Reichert and Borg, 2008). The climate controls the oxidation conditions and the transport of metals. The most favourable conditions for oxidation are achieved in an arid climate, which maximizes the quantity of metals available for transport by supergene solutions. This is done by minimizing biogenic activity within the soil, making more oxygen available for sulphide oxidation and maximizing the



**Figure 11.** Cut through a hemimorphite nodule from Oxide deposit, south-eastern British Columbia, displaying characteristic texture.

quantity of metals that are available for transport by solutions (Reichert and Borg, 2008). Dry climate also favours a low water table, preventing premature dilution of metal-bearing supergene solutions by barren ground water within aquifers and dispersion of the ore-forming metals (Reichert and Borg, 2008). There is no detailed information regarding the paleoclimate in the Salmo area but studies from southern BC indicate that after the last glacial maximum (from 17 000 to 14 000 BP) there was a relatively warm and dry climate around 10 000–7 000 BP (Palmer et al. 2002; Hebda, 2007). This warm dry period may have been ideal for development of CHNSBM deposits.

Areas not affected by glaciation have higher potential to contain preserved, soft, CHNSBM deposits than glaciated ones. The Late Wisconsinan Cordilleran Ice Sheet originated in the Canadian Cordillera and its progression southward was to a large extent controlled by topography (Clague and James, 2002). The last ice sheet started to develop 30 000–25 000 BP and reached its maximum extent 17 000–14 000 BP. Its retreat was accompanied by brief readvances, down wasting and periods of stagnation. According to Clague (1991, Figure 12.1), the Salmo area is located about 100 km north of the maximum southern limit of this ice sheet. The glaciers in the Salmo area may have been thin. Isostatic rebound, which started during the glacial retreat, was probably less in the Salmo area than in areas originally covered by thicker ice.

Sulphide mineralization in the Salmo area is premetamorphic and predeformational (pre-Middle Jurassic). From the field evidence, we know that the sulphide oxidation is post-Middle Jurassic, and may have started before or slightly after the last glacial maximum (17 000–14 000 BP). The relatively warm and dry climate, which prevailed some 10 000–7 000 BP (Palmer et al. 2002; Hebda, 2007), may have been particularly favourable for supergene oxidation of sulphides and formation of CHNSBM deposits in the Salmo area. If this scenario is correct, the formation of CHNSBM deposits coincided with glacial retreat, which also favoured their preservation.

## EXPLORATION CONSIDERATIONS

The selection of grassroots exploration areas involves considering the conditions required or favouring the formation of CHNSBM deposits, such as the presence of known sulphide mineralization containing base-metal-bearing sulphide deposits, favourable climate and/or paleoclimate (which influences the position of the water table and the prevailing oxido-reduction conditions), permissive hydrological characteristics (permeability and porosity of the hostrocks, karsts, and fracture and fault zones), availability of rocks with ability to control the pH of the metal-bearing solutions (carbonates), topography, rate of uplift and glacial history.

Common nonsulphide ore minerals are Zn, Pb and Fe oxides, carbonates, silicates and phosphates (Table 1). With the exception of the Fe-bearing minerals that are common in gossans (Fe-oxyhydroxites, goethite and hematite), these minerals are unfamiliar to today's field geologists. Training in mineralogy, use of a colorimetric field test for zinc ("Zinc Zap"), use of portable X-ray fluorescence (XRF) analyzers and use of heavy mineral surveys (most of the nonsulphide base-metal ore minerals have high densities [Table 1]) will improve the odds for new discovery. Some of the nonsulphide base-metal-bearing minerals may

fluoresce under ultraviolet light (Table 1). Hydrozincite and smithsonite generate distinct short-wave, infrared-spectral responses, therefore under favourable conditions the use of short-wave infrared spectrometry (SWIR) and remote sensing may be justified. Monitoring the water table during an exploration drilling program is essential and obtaining records from water well logs in neighbouring areas may provide useful information. Electronically available results of Regional Geochemical Surveys (available on the MapPlace website; BC Geological Survey, 2008) are useful. Glaciation reduces the chances of preserving the soft CHNSBM deposits. Tracing mineralized glacial erratics back to their source may help to locate such deposits. From a geophysical point of view, nonoxidized sulphide zones containing pyrrhotite will have the best potential to be detected by airborne electromagnetic (EM) surveys. The self-potential (SP) method is ideal to detect zones of active sulphide oxidation, unfortunately the method has a very limited depth of penetration.

Regardless of the intensity of the glacial scouring and erosion, the shape and orientation of the CHNSBM bodies appears to be key to their preservation through the glaciation. Steeply plunging, rod-shaped nonsulphide oxide deposits (such as those of the Reeves MacDonald area), with their smallest dimension exposed at surfaces (Figure 8), enclosed in competent rocks (i.e., dolomitized limestone), have excellent preservation potential. Flat-lying exposed deposits, with the largest dimensions coplanar with erosion surface have lowest survival potential. On the positive side, local, small-scale transportation of nonsulphide ore fragments from steeply plunging CHNSBM bodies is considered beneficial for exploration.

## CONCLUSION

The association of many known CHNSBM zones with underlying massive sulphides in combination with nonsulphide ore characteristics suggests that a large proportion of known CHNSBM mineralized zones in the Salmo area are of the direct-replacement type. Geologists and prospectors look instinctively for red gossan, which is commonly associated with near-surface oxidation of sulphides; however, high-grade Zn, white ores are more difficult to recognize. At least in some cases, massive, nonsulphide white ores were not visually distinguished in the past from the common barren dolostone (Gorzynski, 2001). While the locations of a large proportion of outcropping red ore nonsulphide deposits in the Salmo area are probably already known, it is conceivable that economically significant Zn-rich CHNSBM deposits containing white ore remain to be discovered. There are many genetic factors, such as the timing of the oxidation of sulphides that remain to be better constrained. The Salmo mining camp can be considered an example of economically significant near-surface CHNSBM deposits within a glaciated area. Shape and orientation of a CHNSBM deposit may be the key factor that determines if a given deposit survives glaciation or not.

## ACKNOWLEDGMENTS

The authors extend their appreciation to Art Troup and Ed Lawrence of Sultan Minerals Inc., Lloyd Addie, president of the Chamber of Mines of Eastern BC, and Brian Findlay and Jose Barquet of Dajin Resources Corp. for

sharing their knowledge of the area and permitting us to sample drillcore intersections and surface exposures. Earlier versions of this manuscript benefited from reviews by Tania Demchuk, Philippe Erdmer and Kimberley Bell of the BC Ministry of Energy, Mines and Petroleum Resources. The authors were assisted in the field by Hannah Mills of the University of Alberta, Alan Duffy, a recent graduate from Trinity College, Dublin (Ireland), and Laura Simandl from St. Michaels University School in Victoria. This project is being done under the umbrella of the Cordilleran Targeted Geoscience Initiative Program (TGI-3) of the Geological Survey of Canada, in collaboration with the BC Ministry of Energy, Mines and Petroleum Resources.

## REFERENCES

- Addie, G.G. (1970): The Reeves MacDonald mine, Nelway, British Columbia; in Pb-Zn Deposits in the Kootenay Arc, N.E. Washington and adjacent British Columbia, *State of Washington Department of Natural Resources*, Bulletin 61, pages 79–88.
- Anonymous (1983): Mineral bulletin; *Mines and Resources Canada*, MR 198, page 209.
- BC Geological Survey (2008): MapPlace GIS internet mapping system; *BC Ministry of Energy, Mines and Petroleum Resources*, MapPlace website, URL <<http://www.MapPlace.ca>> [December 16, 2008].
- Brown, R.L., Fyles, J.T., Glover, J.K., Höy, T., Okulitch, A.V., Preto, V.A. and Read, P.B. (1981): Southern Cordillera cross-section—Cranbrook to Kamloops; in *Field Guides to Geology and Mineral Deposits*, *Geological Association of Canada*, pages 335–371.
- Clague, J.J. (1991): Quaternary glaciation and sedimentation; in *Geology of the Cordilleran Orogen in Canada*, Gabrielse, H. and Yorath, C.J., Editors, *Geological Survey of Canada*, Geology of Canada Number 4, pages 419–434.
- Clague, J.J. and James, T.S. (2002): History and isostatic effects of the last ice sheet in southern British Columbia; *Quaternary Science Reviews*, Volume 21, Number 1–3, pages 71–87.
- Colpron, M. and Price, R.A. (1995): Tectonic significance of the Kootenay terrane, southeastern Canadian Cordillera: an alternative model; *Geology*, Volume 23, pages 25–28.
- Corrans, R.D., Gewald, H., Whyte, R.M. and Land, B.N. (1993): The Skorpion SZ secondary zinc deposit, southwestern Namibia; in *Abstracts, Mining Investment in Namibia Conference*, Windhoek, *Namibia Department of Mining and Energy*, pages 46–52.
- Crosby, G.M. (1956). Larch & Caviar crown granted claims; *Day Mines Inc.*, unpublished office memorandum to Henry Day, January 24, 1956, 2 pages.
- Emendorf, W.J. (1927): Report on the property of Red Bird Mining Company; *Red Bird Mining Company*, unpublished company report, 7 pages.
- Fyles, J.T. (1964): Geology of the Duncan Lake area, British Columbia; *BC Ministry of Energy, Mines and Petroleum Resources*, Bulletin 49, 87 pages
- Fyles, J.T. (1970): Geological setting of Pb-Zn deposits in the Kootenay Lake and Salmo areas of British Columbia; in *Pb-Zn Deposits in the Kootenay Arc, N.E. Washington and Adjacent British Columbia*, *BC Ministry of Energy, Mines and Petroleum Resources*, Bulletin 61, pages 41–53.
- Fyles, J.T. and Eastwood, G.P.E. (1962): Geology of the Ferguson area, Lardeau district, British Columbia; *BC Ministry of Energy, Mines and Petroleum Resources*, Bulletin 45, 92 pages.
- Fyles, J.T. and Hewlett, C.G. (1959): Stratigraphy and structure of the Salmo lead-zinc area; *BC Ministry of Energy, Mines and Petroleum Resources*, Bulletin 41, 162 pages.
- George Cross News Letter (1997): Sultan Minerals Inc.—Jersey-Emerald drilling underway; *George Cross News Letter*, Number 27, pages 4–5.
- George Cross News Letter (1998): Redhawk Resources Inc.; *George Cross News Letter*, Number 163, 2 pages.
- Gorzynski, G. (2001): REMAC zinc project, Reeves property and Redbird property—2000 summary report, trenching and drilling program; *Redhawk Resources Inc.*, 47 pages.
- Hebda, R.J. (2007): Biodiversity: geological history in British Columbia; *Biodiversity BC*, Technical Subcommittee for the Report on the Status of Biodiversity in BC, September 7, 2007, 11 pages.
- Heyl, A.V. and Bozion, C.N. (1962): Oxidized zinc deposits of the United States, Part 1, general geology; *United States Geological Survey*, Bulletin 1135-A, 52 pages.
- Hitzman, M.W., Reynolds, N.A., Sangster, D.F., Cameron, R.A. and Carman, C.E. (2003): Classification, genesis, and exploration guides for nonsulfide zinc deposits; *Economic Geology*, Volume 98, Number 4, pages 685–714.
- Höy, T. (1982): Stratigraphic and structural setting of stratabound lead-zinc deposits in southeastern British Columbia; *Canadian Institute of Mining and Metallurgy*, Bulletin 75, pages 114–134.
- Höy, T., Dunne, K.P.E. and Wilton, P. (1993): Massive sulphide and precious metal deposits in southeastern British Columbia; *Geological Association of Canada—Mineralogical Association of Canada*, Annual Meeting, Fieldtrip A7, May 13–16, Edmonton, Alberta.
- Höy, T. and Brown, D. (2000): Introduction to regional stratigraphy and tectonics; Bluebell and Reeves MacDonald; in *Sullivan and Other Zn-Pb deposits, Southeastern BC*, Höy, T., Brown, D. and Lydon, J., Editors, *GeoCanada 2000*, Field Trip Guidebook 17, pages 19–37.
- Klein, G.H. (1998): Red Bird Project 1998—drilling program, Redhawk Resources Inc.; *BC Ministry of Energy, Mines and Petroleum Resources*, Assessment Report 25675, 49 pages.
- Klein, G.H. (1999): 1998 work program, Remac project, Redbird Property; *Redhawk Resources Inc.*, company report, 32 pages.
- Legun, A. (2000): Geology and regional setting of major mineral deposits in the Kootenay district; in *Geology and Regional Setting of Major Mineral Deposits in Southern BC*, Legun, A., Meyers, R.E. and Wilton, H.P., Editors, *Geological Survey of Canada*, 8th IAGOD symposium, Open File 2167, pages 5–27.
- Logan, J.M. and Colpron, M. (2006): Stratigraphy, geochemistry, syngenetic sulphide occurrences and tectonic setting of the lower Paleozoic Lardeau Group, northern Selkirk Mountains, British Columbia; in *Paleozoic Evolution and Metallogeny of Pericratonic Terrane at the Ancient Pacific Margin of North America, Canadian and Alaskan Cordillera*, Colpron, M. and Nelson, J.L., Editors, *Geological Association of Canada*, Special Paper 45, pages 361–382.
- McAllister, A.L. (1951): Ymir map-area, British Columbia; *Geological Survey of Canada*, Paper 51-4.
- MacDonald, A.S. (1973): The Salmo lead-zinc deposits: a study of their deformation and metamorphic features; M.Sc. thesis, University of British Columbia, 223 pages.
- MINFILE (2008): MINFILE BC mineral deposits database; *BC Ministry of Energy, Mines and Petroleum Resources*, URL <<http://www.empr.gov.bc.ca/Mining/Geoscience/MINFILE/Pages/default.aspx>> [December 16, 2008].
- Nelson, J.L. (1991): Carbonate-hosted lead-zinc ( $\pm$  silver, gold) deposits of southeastern British Columbia; in *Ore Deposits*,

- Tectonics and Metallogeny, *BC Ministry of Energy, Mines and Petroleum Resources*, Paper 1991-4, pages 71–88.
- Palmer, S., Walker, I., Heinrichs, M. and Hebda, R. (2002): Postglacial midge community change and Holocene paleotemperature reconstructions near treeline, southern British Columbia (Canada); *Journal of Paleolimnology*, Volume 28, pages 469–490.
- Paradis, S. (2007): Carbonate-hosted Zn-Pb deposits in southern British Columbia—potential for Irish-type deposit; *Geological Survey of Canada*, Current Research 2007-A10, 7 pages.
- Paradis, S. (2008): Kootenay Arc carbonate-hosted Zn-Pb deposits; are they Irish-type or Mississippi Valley-type deposits?; *Geological Association of Canada*, Meeting, Quebec 2008, Program with Abstracts, Volume 33.
- Price, B.J. (1987): Geological summary, Red Bird exploration project; *Golden Eye Minerals Ltd.*, unpublished company report, 18 pages, 15 figures, 4 appendices.
- Read, P.B. and Wheeler, J.O. (1976): Geology of Lardeau W/2 (82K w/2); *Geological Survey of Canada*, Open File Map 432, 1:125 000 scale.
- Redhawk Resources Inc. (2005): The Remac project; *Redhawk Resources Inc.*, URL <<http://www.redhawkresources.com/s/Home.asp>>
- Reichert, J. and Borg, G. (2008): Numerical simulation and geochemical model of supergene carbonate-hosted non-sulphide zinc deposits; *Ore Geology Reviews*, Volume 33, pages 134–151.
- Sangster, D.F. (2003): A special issue devoted to nonsulfide zinc deposits: a new look; *Economic Geology*, Volume 98, Number 4, pages 683–684.
- Sorensen, R.E. (1942): Red Bird mine—sample and geologic map; unpublished company plan map, October 20, 1942, scale 1 in=40 ft.
- Sultan Minerals Inc. (2008): Sultan Minerals Inc. home page; *Sultan Minerals Inc.*, URL <<http://www.sultanminerals.com/s/Home.asp>> [December 2008].
- Titley, S.R. (1993): Characteristics of high-temperature carbonate-hosted massive sulphide ores in the United States, Mexico and Peru; in Mineral Deposit Modeling, Kirkham, R.V., Sinclair, W.D., Thorpe, R.I. and Duke, J.M., Editors, *Geological Association of Canada*, Special Paper 40, pages 585–614.
- Walker, J.F. (1934): Geology and mineral deposits of Salmo map-area, British Columbia; *Geological Survey of Canada*, Memoir 172, 102 pages.
- Wheeler, J.O. and McFeeley, P. (1991): Tectonic assemblage map of the Canadian Cordillera and adjacent parts of the United States of America; *Geological Survey of Canada*, Map 1712A, 1:2 000 000 scale.

# Geochemistry Projects of the British Columbia Geological Survey

by R.E. Lett and J. Doyle

**KEYWORDS:** geochemistry, copper, gold, soils, databases, Spanish Mountain

## INTRODUCTION

Geochemistry traditionally plays a significant role in British Columbia mineral exploration and in the past has been responsible for the discovery of several economically viable deposits. Drainage sediment, soil and rock surveys were among the geochemical techniques first used by mining companies and later by government agencies. Research by the Government of Canada and the need to identify new strategic mineral resources encouraged the federal and provincial governments to start a regional geochemical survey (RGS) over BC in 1976. This survey was a part of a National Geochemical Reconnaissance (NGR) program that now covers much of Canada. Regional stream sediment surveys were subsequently undertaken by the BC Geological Survey (BCGS) and most recently by Geoscience BC, an agency that has also carried out an ambitious program of reanalyzing archived drainage samples for new elements with aqua regia digestion followed by inductively coupled plasma-mass spectrometry (ICP-MS) and instrumental neutron activation analysis (Jackaman, 2008). BCGS geochemistry projects have changed in scope over time from the management of large regional data collections to more focus on research aimed at improving geochemical prospecting methods for minerals. In addition to research, there has also been an emphasis on updating geochemical databases with results from new surveys to make databases continuously useful to the mining community. This paper reports on geochemical research activities and related project work that has been carried out in the past year.

## GEOCHEMICAL DATABASES

### *Regional Geochemical Survey Database*

An atlas of contoured maps showing the spatial variation of As, Au, Cu, Co, Fe, Mn, Mo, Ni, Pb, U and Zn in stream sediment, lake sediment and moss-mat sediments was released in 2008 by Lett et al. (2008). The element values used to create the maps were captured from a Microsoft® Access database that contains location co-ordinates, field records and analyses for over 56 000 stream sediment, lake sediment and moss-mat sediment samples collected at an average density of one sample per 13 km<sup>2</sup>. Updates of information from more detailed drainage and

Geoscience BC regional surveys have produced a version of the database containing records for 59 633 sample sites. Stream sediment, lake sediment and moss-mat sediment sample coverage is shown on Figure 1. Geology codes are included in the most recent database by linking sample sites to the geological polygons of the BC digital geology map published by Massey et al. (2005). One advantage of including stratigraphic and rock-type codes for each sample in the database is that the element data can be easily used for calculating drainage sediment thresholds that more realistically reflect bedrock geology. Another tool for refining the interpretation of drainage sediment geochemistry is a digital catchment basin atlas, like the one created by Cui et al. (2009) for drainage sediment survey sites on Vancouver Island. The atlas has revived an earlier BCGS project by Sibbick (1994) who recalculated geochemical thresholds for drainage sediment samples taken on Vancouver Island based on the predominant rock type within the limits of the stream catchment basin.

### *Till Geochemical Database*

Since 1991, the BCGS and the Geological Survey of Canada (GSC) have analyzed over 5000 drift samples collected across the province. Much of these geochemical data are available to the public in digital form. Ferbey (2008) summarized the spatial coverage of BCGS drift prospecting surveys and Jackaman (2007) compiled BCGS and GSC till geochemical survey data for parts of the BC interior affected by the mountain pine beetle infestation. Lett (2008) created a database of combined BCGS and GSC drift geochemical data from central BC and Vancouver Island with previously unpublished analyses of till samples collected around Mount Milligan (MINFILE 093N 191; MINFILE, 2008). Figure 2 shows the distribution of till sample sites and the outlines of the geochemical survey areas. The analytical methods used to produce the till sample data are instrumental neutron activation analysis (INAA), aqua regia digestion followed by inductively coupled plasma-emission spectroscopy (ICP-ES), ICP-ES with lithium metaborate fusion and loss on ignition (LOI). Not all of the samples have been analyzed by these four techniques. In the database, the till samples have been classified by bedrock geology at the sample site based on published BCGS geology maps (Massey et al., 2005) and also by surficial sediment type (e.g., lodgment till, melt-out till, colluvium) from the descriptions in the source publication for the geochemical data.

## SPANISH MOUNTAIN PROJECT

A geochemical study of the Spanish Mountain Au-deposit rock was initiated in 2008 as a University of Victoria undergraduate thesis project (Figure 3). Gold mineralization at Spanish Mountain is unusual for BC in that the Au

---

*This publication is also available, free of charge, as colour digital files in Adobe Acrobat® PDF format from the BC Ministry of Energy, Mines and Petroleum Resources website at <http://www.empr.gov.bc.ca/Mining/Geoscience/PublicationsCatalogue/Fieldwork/Pages/default.aspx>.*

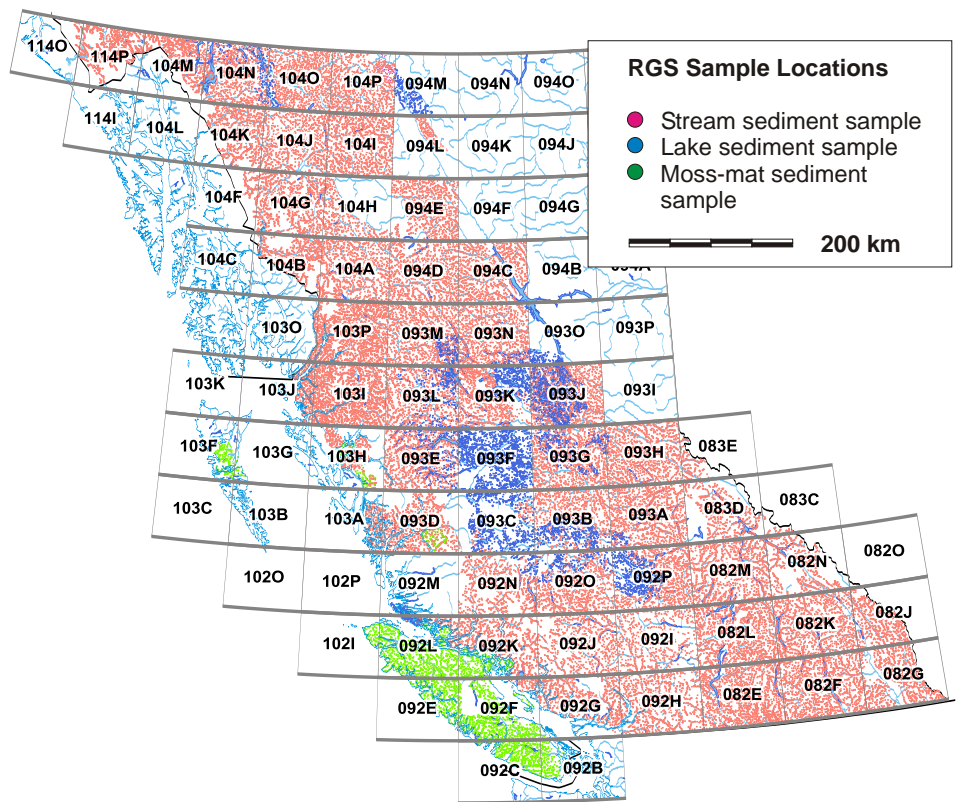


**Figure 1.** Regional Geochemical Survey stream sediment, lake sediment and moss-mat sediment sites in British Columbia.

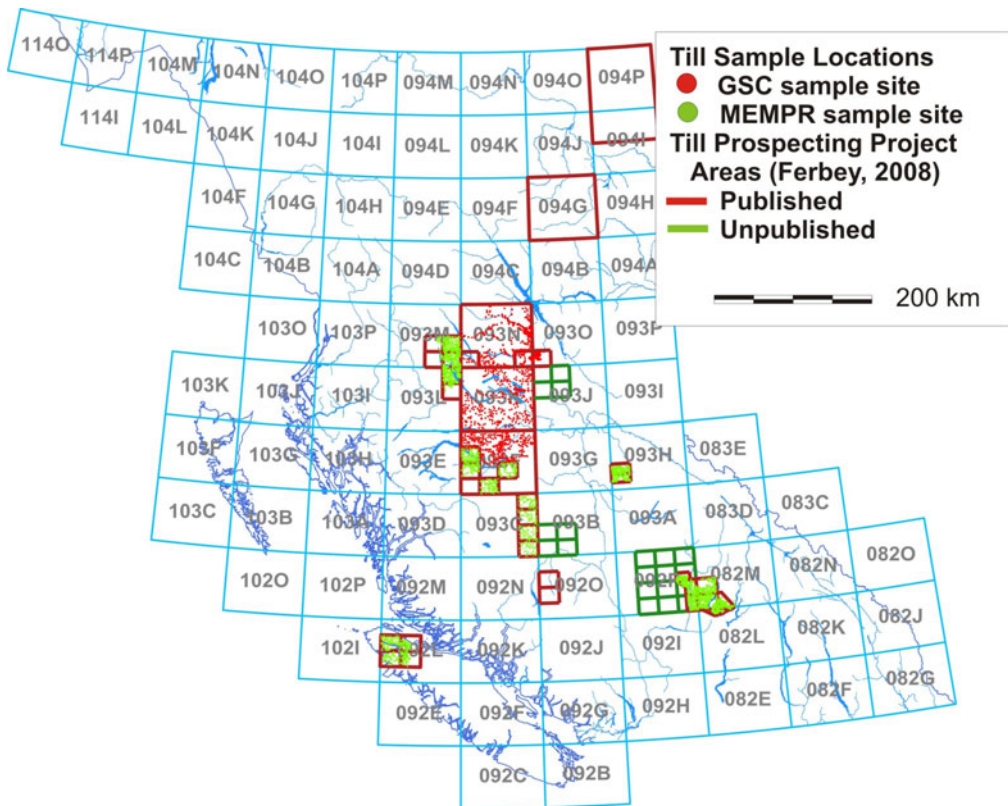


**Figure 2.** Outline of till prospecting survey areas (from Ferbey, 2008) and location of regional till sample sites, British Columbia. Abbreviations: GSC, Geological Survey of Canada; MEMPR, Ministry of Energy, Mines and Petroleum Resources.

is most closely associated with a black argillite unit within a metasedimentary facies of the Quesnel Terrane. The deposit may be orogenic or sedimentary-hosted Au based on a comparison to similar deposits in China, the United States and Russia (Large et al., 2007). At Spanish Mountain, there is extensive Fe-Mg carbonate and sericite alteration, varying Zn, Cu, Sb, Pb, As and Mg concentrations in the bedrock that is associated with the Au mineralization. Among questions that still remain unanswered are the relationship between the carbonate alteration and the Au mineralization. During the summer of 2008, bedrock and diamond-drillcore samples were collected for optical petrography, mineral identification by x-ray diffraction, major oxide, minor and trace-element analysis and laser ablation analysis. The geochemical analysis is largely complete and thin sections have been examined. Project details are documented in Paterson, Lett and Telmer (2009).

## SOIL GEOCHEMICAL ORIENTATION STUDIES

### Background

Preliminary results of detailed geochemical orientation surveys carried out over the Mouse Mountain and Shiko Lake mineral occurrences as well as the Soda Creek area were reported by Lett and Sandwith (2008; Figure 3). The surveys were carried out to establish the optimum soil sampling and analytical techniques to detect porphyry Cu-Au mineralization that is commonly covered by glacially transported overburden. Samples from the major soil horizons (F-H, B, C) were taken from vertical profiles along

traverses crossing each area. The samples were analyzed for elements by several commercial selective extraction methods to determine which combination of soil horizon and analytical method would give the greatest anomaly contrast (signal to noise ratio) for ore indicator and pathfinder elements. Samples for preparation and analysis were taken from the decomposed humus (F-H) horizon just beneath the surface vegetation litter; the upper B-horizon soil just under the eluviated (Ae) horizon (where visible); the lower B-horizon soil close to the transition from the B- to C-horizon soil; and from the C-horizon soil. The C-horizon soil is glacial sediment that is most commonly a till. An additional sample at each profile was collected at a depth of 20–25 cm, independent of the horizon, for Mobile Metal Ion<sup>SM</sup> (MMI) analysis. A typical soil profile is shown in Figure 4.

The methods used to study the soil geochemistry have been previously described by Lett and Sandwith (2008). Here is a brief summary of each analytical method:

Aqua regia digestion followed by ICP-MS analysis of the <0.18 mm fraction of the B-horizon soil sample and the <0.063 mm fraction of the C-horizon soil sample for 37 elements, including Au and Cu, at Acme Analytical Laboratories Ltd. (Vancouver, BC). F-H-horizon soil samples were milled before ICP-MS analysis.

INAA of the <0.18 mm fraction of the B-horizon soil sample and the <0.063 mm fraction of the C-horizon soil sample for 33 elements, including Au, at Activation Laboratories Ltd. (Ancaster, ON).

Enzyme Leach<sup>SM</sup> and Bio Leach<sup>SM</sup> analysis of the <0.18 mm fraction of the B-horizon soil sample for elements including Br and I. Bio Leach<sup>SM</sup> is a proprietary

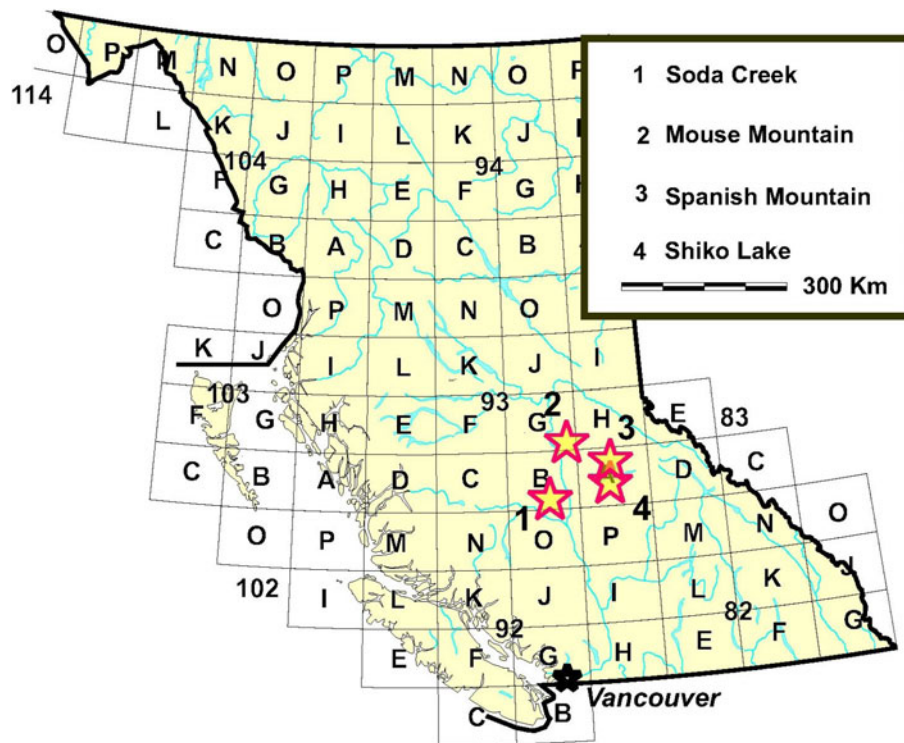


**Figure 3.** The location of the Spanish Mountain project area and geochemical orientation survey areas.

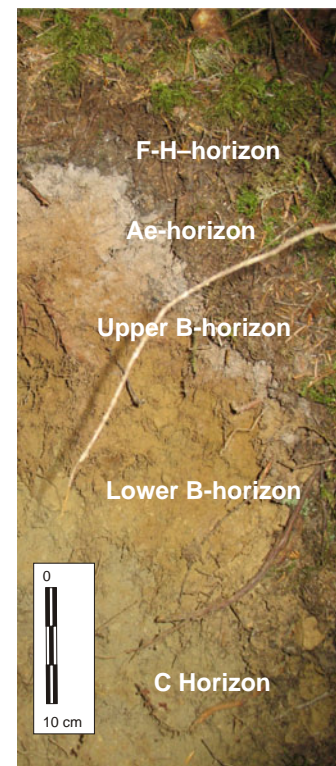


**Figure 4.** A typical soil profile from Mouse Mountain, British Columbia, with the horizons identified.

selective extraction developed by Activation Laboratories Ltd. that utilizes bacterial decomposition of mineral sulphides. The bacteria cell membranes rupture when organisms die leaving a diagnostic organic and inorganic geochemical signature. Bio Leach<sup>SM</sup> dissolves the dead bacterial remnants in the surface soils and detects the geochemical signature of the sulphide minerals (E. Hoffman, pers comm, 2008).

Soil Gas Hydrocarbons<sup>SM</sup> (SGH) analysis for C5–C17 organic compounds that have been absorbed on B-horizon soil samples (Activation Laboratories Ltd.).

MMI analysis, a method described by Mann et al. (1998), of soil samples for metals including Cu, Pb, Zn, Ni, Cd, Au, Ag and Co with a proprietary selective extraction (SGS Minerals Services laboratory, Toronto, ON).

Loss on ignition (LOI) at 500°C of the <0.18 mm fraction of the B-horizon soil samples at Acme Analytical Laboratories Ltd.

Mineral grain identification, Au grain shape (reshaped, modified, pristine) and the number of Au grains in heavy mineral concentrates (specific gravity >3.3) recovered from C-horizon soil samples at Overburden Drilling Management (Nepean, ON).

## Summary of Results

Lett and Sandwith (2008) concluded from an examination of the geochemical data generated mainly by aqua regia digestion–ICP-MS analysis of soil samples from the three orientation survey areas that anomalous Cu and Au with Ag, V and Co in the C- and lower B-horizon soil appeared to be geochemical pathfinders for porphyry Cu–Au mineralization. However, results suggested that the geochemistry of the shallow, upper B-horizon soil is less related to the underlying parent till geochemistry than the C-horizon soil is because of greater modification by various soil-forming and hydromorphic processes. Much of the geochemical data that was unavailable last year has now been assembled allowing a more complete analysis of the information but only the soil geochemical and Au mineral data from the Mouse Mountain and Shiko Lake mineral properties will be reviewed in this paper. A more detailed project report analyzing all of the data will be published in 2009 as a BCGS GeoFile.

Sixty-three elements, loss on ignition and soil pH have been determined by aqua regia digestion–ICP-MS, INAA, MMI, Enzyme Leach<sup>SM</sup> and Bio Leach<sup>SM</sup>. Detection limits for each element by each method are summarized in Table 1. However, only Ag, As, Au, Ba, Co, Cr, La, Mo, Ni, Sb, Sr, U and Zn have been measured by all of the methods and in the case of Cu and Pb there are no INAA results. Bromine and I determined by Enzyme Leach<sup>SM</sup> and Bio Leach<sup>SM</sup> are of particular interest since halogens can migrate relatively easily through thick overburden and cover rock and may be pathfinders for deeply buried, metallic and hydrocarbon deposits. Kendrick et al. (2001) discuss the implication of Br:Cl and I:Cl ratios in fluid inclusions to identifying the source of Cu-porphyry mineralizing fluids. Williams and Gunn (2002) speculate that the presence of elevated halogens in Enzyme Leach<sup>SM</sup> solutions from soil samples collected over Au deposits may reflect the presence of oxidation haloes over deeply buried epithermal Au mineralization. Dunn et al. (2007) studied the variation of

**Table 1.** Elements determined by aqua regia digestion followed by inductively coupled plasma-mass spectrometry (ICP-MS) analysis, instrumental neutron activation analysis (INAA), Enzyme Leach<sup>SM</sup>, Bio Leach<sup>SM</sup> and Mobile Metal Ion<sup>SM</sup> (MMI) analyses with instrumental detection limits. The - indicates that an element was not determined or that all values were below the instrumental detection limit.

Element	ICP-MS (ppm)	INAA (ppm)	MMI <sup>SM</sup> (ppb)	Enzyme Leach <sup>SM</sup> (ppb)	Bio Leach <sup>SM</sup> (ppb)
Ag	2 ppb	5 ppb	1	0.2	0.2
Al	100	-	1	-	-
As	0.1	0.5	10	1	0.5
Au	2 ppb	2 ppb	0.1	0.05	0.05
Ba	0.5	50	10	1	1
Be	-	-	-	2	0.07
Bi	0.02	-	1	0.8	0.1
Br	-	0.5	-	5	5
Ca	100	10000	10	-	-
Cd	0.01	-	1	0.2	0.05
Ce	-	3	5	0.1	0.02
Cl	-	-	-	2	-
Co	0.1	1	5	1	0.1
Cr	0.5	5	100	20	2
Cs	-	1	-	0.1	0.01
Cu	0.01	-	10	3	0.5
Dy	-	-	1	0.1	0.01
Er	-	-	0.5	0.1	0.01
Eu	-	0.2	0.5	0.1	0.01
Fe	100	100	1	-	-
Ga	0.2	-	-	1	0.1
Gd	-	-	1	0.1	0.03
Ge	-	-	-	0.5	0.05
Hf	-	1	-	0.1	0.04
Hg	5 ppb	1 ppb	-	1	0.05
Ho	-	-	-	0.1	0.01
I	-	-	-	2	1
In	-	-	-	0.1	0.1
La	0.5	0.5	1	0.1	0.01
Li	-	-	5	2	0.2
Lu	-	-	-	0.1	0.01
Mg	100	-	1	-	-
Mn	1	-	-	1	0.1
Mo	0.01	1	5	1	2
Nb	-	-	0.5	1	0.2
Nd	-	5	1	0.1	0.03
Ni	0.1	20	5	3	0.2
Pb	0.01	-	10	1	0.1
Pr	-	-	1	0.1	0.01
Pt	-	-	1	1	0.5
Pd	-	-	1	1	0.5
Rb	-	15	5	1	0.1
Ru	-	-	-	1	0.05
Sb	0.02	0.1	1	0.1	0.2
Sc	0.1	0.1	5	100	0.5
Se	0.1	3	-	5	1
Sm	-	0.1	1	0.1	0.03
Sn	-	200	1	0.8	-
Sr	0.5	50	10	1	0.1
Ta	-	0.5	1	0.1	0.01
Tb	-	0.5	1	0.1	0.01
Te	0.02	-	10	1	1
Th	0.1	-	0.5	0.1	0.02
Ti	10	-	3	100	-
Tl	0.02	-	0.5	0.1	0.2
Tm	-	-	-	0.1	0.01
U	0.1	0.5	1	0.1	0.01
V	2	-	-	1	1
W	0.2	1	1	1	0.01
Y	-	-	5	0.5	0.02
Yb	-	0.5	1	0.1	0.02
Zn	0.1	50	20	10	2
Zr	-	-	5	1	0.5

F, Cl, Br and I in soil and vegetation over three mineral properties in central BC. At the Mount Polley porphyry Cu mine, they found that I was the most effective halogen pathfinder for the concealed Cu-Au mineralization. The authors concluded that while further research into methods for halogen analysis in geochemical samples was needed, these elements proved effective tracers for buried mineralization. They also concluded that the halogen signatures varied depending on the style of the mineralization.

Tables 2, 3, 4 and 5 show the mean, median, 95th percentile and maximum value statistics calculated from Au, Ag, Cu and Co soil geochemical data for Mouse Mountain and Shiko Lake. These elements are selected because they are among common geochemical pathfinders for Cu-Au porphyry mineralization. The geochemical data for each area is divided into subsets representing F-H-, upper B-, lower B- and C-horizons. There are no MMI, Enzyme Leach<sup>SM</sup> and Bio Leach<sup>SM</sup> statistics for the F-H- and C-horizons because these selective extractions were only applied to the B-horizon. Mean and percentile values reveal that almost all of the elements are higher in the Shiko Lake data subset compared to the Mouse Mountain data subset and they are all higher in the C-horizon. For example, the mean and 95th percentile Cu values at Shiko Lake increase from the F-H-horizon through the upper B to the lower B to reach a maximum in the C-horizon (Table 4). Geochemical anomaly contrast (the ratio of the maximum element value to the 95th percentile value) for elements measured in selective extractions is generally greater than the contrast for elements determined by aqua regia digestion-ICP-MS. However, contrast is element dependent and extraction dependent. For example, the MMI Au contrast in Shiko Lake soil samples is 6 as compared to 1.3 for Bio Leach<sup>SM</sup> Au whereas the Bio Leach<sup>SM</sup> Cu contrast is 13 as compared to 5 for MMI Cu (Tables 2, 4). One wetland sample from Shiko Lake has been excluded from the statistical analysis because the high Cu and Co contents in the organic-rich material are not typical of the well-drained soil chemistry. Unlike Au, Ag is highest in the F-H-horizon and generally decreases with depth through the B- into the C-horizon. Bio Leach<sup>SM</sup> Ag con-

trast in both areas is greater than MMI Ag contrast and ICP-MS Ag contrast (Table 3). Cobalt soil chemistry is similar to Cu in that the highest values are in the C-horizon and the lowest in the F-H-horizon. Cobalt contrast is similar in both areas for all methods.

A two-sample t-test can be applied to determine if there is a statistical difference at the 0.05 significance level between population means. Population means were determined for samples representing the major soil horizons; samples were analyzed by aqua regia digestion-ICP-MS and INAA. An analysis of variance (F-test) is applied

**Table 2.** Mean, median, 95<sup>th</sup> percentile, maximum values for Au determined by several different analytical methods (aqua regia digestion followed by inductively coupled plasma-mass spectrometry [ICP-MS], Mobile Metal Ion<sup>SM</sup> [MMI], Enzyme Leach<sup>SM</sup> and Bio Leach<sup>SM</sup>). Statistics have been calculated from the analyses of 27 Mouse Mountain and 29 Shiko Lake samples.

Soil Horizon	Mouse Mountain				Shiko Lake			
	ICP-MS	Enzyme		Bio	ICP-MS	Enzyme		Bio
		MMI <sup>SM</sup>	Leach <sup>SM</sup>	Leach <sup>SM</sup>		MMI <sup>SM</sup>	Leach <sup>SM</sup>	Leach <sup>SM</sup>
Au (ppb)	Au (ppb)	Au (ppb)	Au (ppb)	Au (ppb)	Au (ppb)	Au (ppb)	Au (ppb)	
F-H Mean	6.3	-	-	-	5.0	-	-	-
F-H Median	0.3	-	-	-	0.3	-	-	-
F-H 95%ile	8.7	-	-	-	0.8	-	-	-
F-H Max	117.0	-	-	-	143.0	-	-	-
Upper B Mean	1.8	-	0.03	0.03	13.3	-	0.03	0.07
Upper B Median	1.1	-	0.03	0.03	2.9	-	0.03	0.03
Upper B 95%ile	4.6	-	0.09	0.03	49.0	-	0.06	0.20
Upper B Max	12.9	-	0.10	0.05	138.7	-	0.14	0.48
Lower B Mean	3.5	0.2	0.04	0.03	24.0	1.60	0.03	0.08
Lower B Median	2.0	0.2	0.03	0.03	3.6	0.60	0.03	0.03
Lower B 95%ile	13.3	0.6	0.10	0.03	128.6	3.26	0.05	0.21
Lower B Max	24.0	0.7	0.13	0.03	239.1	20.10	0.10	0.27
C Mean	3.1	-	-	-	33.5	-	-	-
C Median	2.6	-	-	-	5.9	-	-	-
C 95%ile	5.7	-	-	-	166.2	-	-	-
C Max	6.8	-	-	-	283.5	-	-	-
C Number	21.0	-	-	-	32.0	-	-	-

**Table 3.** Mean, median, 95<sup>th</sup> percentile, maximum values for Ag determined by several different analytical methods (aqua regia digestion followed by inductively coupled plasma-mass spectrometry [ICP-MS], Mobile Metal Ion<sup>SM</sup> [MMI], Enzyme Leach<sup>SM</sup> and Bio Leach<sup>SM</sup>). Statistics have been calculated from the analyses of 27 Mouse Mountain and 29 Shiko Lake samples.

Soil Horizon	Mouse Mountain				Shiko Lake			
	ICP-MS	Enzyme		Bio	ICP-MS	Enzyme		Bio
		MMI <sup>SM</sup>	Leach <sup>SM</sup>	Leach <sup>SM</sup>		MMI <sup>SM</sup>	Leach <sup>SM</sup>	Leach <sup>SM</sup>
Ag (ppb)	Ag (ppb)	Ag (ppb)	Ag (ppb)	Ag (ppb)	Ag (ppb)	Ag (ppb)	Ag (ppb)	
F-H Mean	234.0	-	-	-	305	-	-	-
F-H Median	187	-	-	-	205	-	-	-
F-H 95%ile	498	-	-	-	855	-	-	-
F-H Max	665	-	-	-	1200	-	-	-
Upper B Mean	114	-	0.10	0.12	163	-	0.1	0.1
Upper B Median	74	-	0.10	0.10	141	-	0.1	0.1
Upper B 95%ile	271	-	0.10	0.10	388	-	0.1	0.1
Upper B Max	578	-	0.10	0.60	700	-	0.1	0.1
Lower B Mean	68	16.3	0.10	0.12	174	32.6	0.1	0.1
Lower B Median	68	13.0	0.10	0.10	128	28.0	0.1	0.1
Lower B 95%ile	132	31.0	0.10	0.21	461	68.6	0.1	0.3
Lower B Max	171	41.0	0.10	0.40	696	74.0	0.1	1.0
C Mean	68	-	-	-	112	-	-	-
C Median	53	-	-	-	85	-	-	-
C 95%ile	155	-	-	-	272	-	-	-
C Max	211	-	-	-	614	-	-	-
C Number	21	-	-	-	32	-	-	-

**Table 4.** Mean, median, 95<sup>th</sup> percentile, maximum values for Cu determined by several different analytical methods (aqua regia digestion followed by inductively coupled plasma-mass spectrometry [ICP-MS], Mobile Metal Ion<sup>SM</sup> [MMI], Enzyme Leach<sup>SM</sup> and Bio Leach<sup>SM</sup>). Statistics have been calculated from the analyses of 27 Mouse Mountain and 29 Shiko Lake samples.

Soil Horizon		Mouse Mountain				Shiko Lake			
		ICP-MS	MMI <sup>SM</sup>	Enzyme Leach <sup>SM</sup>	Bio Leach <sup>SM</sup>	ICP-MS	MMI <sup>SM</sup>	Enzyme Leach <sup>SM</sup>	Bio Leach <sup>SM</sup>
		Cu (ppm)	Cu (ppb)	Cu (ppb)	Cu (ppb)	Cu (ppb)	Cu (ppb)	Cu (ppb)	Cu (ppb)
F-H	Mean	12.6	-	-	-	32.7	-	-	-
F-H	Median	10.9	-	-	-	13.8	-	-	-
F-H	95%ile	24.4	-	-	-	168.7	-	-	-
F-H	Max	29.7	-	-	-	212.0	-	-	-
Upper B	Mean	26.1	-	23.8	341.0	124.6	-	74.0	593.7
Upper B	Median	23.6	-	23.0	348.0	49.6	-	28.5	426.0
Upper B	95%ile	34.5	-	41.0	565.0	329.3	-	249.8	1135.8
Upper B	Max	92.3	-	41.0	680.0	1327.2	-	988.0	2780.0
Lower B	Mean	27.5	377.7	30.9	414.9	105.0	1142.0	46.0	748.0
Lower B	Median	27.0	385.0	28.0	445.0	57.3	660.0	25.0	524.0
Lower B	95%ile	39.9	547.5	52.6	569.6	280.0	1333.0	176.0	222.0
Lower B	Max	49.5	750.0	61.0	595.0	483.0	6070.0	205.0	2830.0
C	Mean	48.8	-	-	-	175.1	-	-	-
C	Median	40.4	-	-	-	84.4	-	-	-
C	95%ile	89.9	-	-	-	631.1	-	-	-
C	Max	123.5	-	-	-	1096.4	-	-	-

**Table 5.** Mean, median, 95<sup>th</sup> percentile, maximum values for Co determined by several different analytical methods (aqua regia digestion followed by inductively coupled plasma-mass spectrometry [ICP-MS], Mobile Metal Ion<sup>SM</sup> [MMI], Enzyme Leach<sup>SM</sup> and Bio Leach<sup>SM</sup>). Statistics have been calculated from the analyses of 27 Mouse Mountain and 29 Shiko Lake samples.

Soil Horizon		Mouse Mountain				Shiko Lake			
		ICP-MS	MMI <sup>SM</sup>	Enzyme Leach <sup>SM</sup>	Bio Leach <sup>SM</sup>	ICP-MS	MMI <sup>SM</sup>	Enzyme Leach <sup>SM</sup>	Bio Leach <sup>SM</sup>
		Co (ppm)	Co (ppb)	Co (ppb)	Co (ppb)	Co (ppb)	Co (ppb)	Co (ppb)	Co (ppb)
F-H	Mean	3.9	-	-	-	5.3	-	-	-
F-H	Median	3.2	-	-	-	3.7	-	-	-
F-H	95%ile	10.2	-	-	-	13.4	-	-	-
F-H	Max	11.2	-	-	-	13.8	-	-	-
Upper B	Mean	9.1	-	19.4	69.1	18.0	-	41.0	73.5
Upper B	Median	8.9	-	13.0	65.9	15.7	-	28.5	49.2
Upper B	95%ile	11.7	-	46	113	25.5	-	68	171.4
Upper B	Max	24.3	-	47	126	77.8	-	276	291
Lower B	Mean	9.2	59.3	21.1	74.2	17.8	72.4	35.5	75.0
Lower B	Median	9.6	43.5	16.5	67.7	17.3	49.5	30.0	61.2
Lower B	95%ile	11.1	158.2	42.6	129.7	27.4	150.2	83.4	218
Lower B	Max	11.9	179	51	155	33.1	175	93	245
C	Mean	11.6	-	-	-	19.6	-	-	-
C	Median	11.2	-	-	-	15.5	-	-	-
C	95%ile	18.4	-	-	-	40.9	-	-	-
C	Max	20	-	-	-	63.5	-	-	-

before the t-test to determine if the data for each horizon has an equal or unequal variance. Once this is determined, the appropriate t-test is used to test the null hypothesis ( $H_0$ ) that there is no significant difference between sample means (Davis, 1973). Figure 5 summarizes the results of the t-test applied to element (Au, Ag, As, Br, Co, Cu, Cr, Hg, Fe, Mn, Mo, Ni, Pb, V, Zn) data for the F-H-horizon compared to element data for the upper B-horizon; element data for the upper B-horizon compared to element data for the lower B-horizon; and element data for the lower B-horizon compared to the element data for the C-horizon. In both areas, there is a significant difference (at the 0.05 significance level) between population means for most elements, except

Au, in the F-H-horizon tested against the upper B-horizon. There is no significant difference for upper B-horizon elements compared to lower B-horizon elements, except for Ag and Zn at Mouse Mountain. However, lower B-horizon elements compared to the C-horizon elements reveal that As, Cu, Cr, Fe, Mn, Ni and V are significantly different for Mouse Mountain samples and Ag, As, Mn, Pb and Zn are significantly different for Shiko Lake samples. The between-horizon element differences for Mouse Mountain compared to Shiko Lake most likely reflect the varying effect of local topography, drainage and climate on soil chemistry. For example, Rose et al. (1979) show that the depth to a Cu-enriched B-horizon soil on the slope of a hill is greater than that on a ridge crest due to increased soil development on the hillside.

A t-test also determined if there were significant differences in the population means of Au, As, Br, Cu, I, Mo, Mn, Pb, V and Zn extracted by Enzyme Leach<sup>SM</sup> and Bio Leach<sup>SM</sup> from upper B-horizon soils compared to lower B-horizon soils in both areas (Figure 5). For the elements determined by Enzyme Leach<sup>SM</sup>, only Zn is significantly different for the upper B- and lower B-horizon soil samples from Shiko Lake but for the elements determined by Bio Leach<sup>SM</sup> there is a significant difference for Mn, Br and I at Shiko Lake and Zn at both sites. Figure 6 summarizes the results of the t-test for elements extracted by MMI compared to those extracted by Bio Leach<sup>SM</sup> from lower B-horizon soil samples. The figure shows that As, Ba and Mo are significantly different at Mouse Mountain and Au, Ba and Pb significantly different at Shiko Lake.

At the Shiko Lake property, several traverses were undertaken by Lett and Sandwith (2008) and Petsel (2006) with soil and soil-overburden samples taken at numerous sites (Figure 7). The bedrock geology at Shiko Lake consists of an early Jurassic intrusive complex emplaced in hornfelsed metasedimentary rocks, volcanoclastic rocks and massive plagioclase-pyroxene basalt. The intrusive stock consists of an older biotite-pyroxene monzodiorite phase and younger potassium-feldspar syenite and alkali-feldspar syenite phases. Near the centre of the stock is medium- to coarse-grained monzonite containing traces of magnetite and sphene. Pyrite and fine-grained, pink,

### ICP-MS and INAA

Soil horizon	Au	Ag	As	Br*	Co	Cu	Cr*	Hg	Fe*	Mn	Mo	Ni	Pb	V	Zn
<b>Mouse Mountain</b>															
F-H – upper B	■	■	■	■	■	■	■	■	■	■	■	■	■	■	■
Upper B – lower B	■	■	■	■	■	■	■	■	■	■	■	■	■	■	■
Lower B – C	■	■	■	■	■	■	■	■	■	■	■	■	■	■	■
<b>Shiko Lake</b>															
F-H – upper B	■	■	■	■	■	■	■	■	■	■	■	■	■	■	■
Upper B – lower B	■	■	■	■	■	■	■	■	■	■	■	■	■	■	■
Lower B – C	■	■	■	■	■	■	■	■	■	■	■	■	■	■	■

Note: \* - results from INAA

### Enzyme Leach<sup>SM</sup>

Mouse Mountain	Au	V	As	Mo	Cu	Zn	Pb	Mn	Br	I
Upper B – lower B	■	■	■	■	■	■	■	■	■	■
<b>Shiko Lake</b>										
Upper B – lower B	■	■	■	■	■	■	■	■	■	■

### Bio Leach<sup>SM</sup>

Mouse Mountain	As	Co	Cu	Mn	Mo	Ni	Pb	V	Zn	Br	I
Upper B – lower B	■	■	■	■	■	■	■	■	■	■	■
<b>Shiko Lake</b>											
Upper B – lower B	■	■	■	■	■	■	■	■	■	■	■

**Figure 5.** Summary of a t-test for the population means of selected elements measured by aqua regia digestion followed by inductively coupled plasma-mass spectrometry (ICP-MS) and instrumental neutron activation analysis (INAA). Comparisons were made between the F-H-horizon and the upper B-horizon, the upper B- and lower B-horizon and the lower B-horizon and the C-horizon. Also shown are results of a t-test for elements measured by Enzyme Leach<sup>SM</sup> and Bio Leach<sup>SM</sup> analysis. Comparisons were made between the upper B-horizon and the lower B-horizon for the two areas. A red square indicates a significant difference at the 0.05 significance level between the means. A blue square indicates no difference. A blank square indicates that there were insufficient values above detection limits for a test to be applied.

### Mobile Metal Ion<sup>SM</sup> and Bio Leach<sup>SM</sup>

Mouse Mountain	Au	As	Ba	Co	Cu	Mo	Ni	Pb	Zn
Lower B-horizon	■	■	■	■	■	■	■	■	■
<b>Shiko Lake</b>									
Lower B-horizon	■	■	■	■	■	■	■	■	■

**Figure 6.** Summary of a t-test for the population means of selected elements in the lower B-horizon. Two different analyses were compared: Mobile Metal Ion<sup>SM</sup> (MMI) and Bio Leach<sup>SM</sup>. A red square indicates a difference at the 0.05 significance level between the means. A blue square indicates no difference. A blank square indicates that there were insufficient values above detection limits for a test to be applied.

quartz-syenite veins and dikes intrude the monzonite forming an intrusive breccia. Chalcopyrite occurs in the matrix of the breccia with bornite and gold in veins or as coarse disseminations, mainly in the youngest quartz syenite. Pervasive, fracture-controlled, potassium alteration and epidote alteration of the volcanoclastic rocks is associated with the Cu mineralization. Potassium and epidote alteration is cut by late-stage, calcite-filled veinlets (Logan and Mihalynuk, 2005). Bedrock is largely covered by sandy till deposited by a northwest ice advance. On the steeper slopes, the till has been mobilized and reworked into colluvium. Humo-ferric podzolic and brunisollic soils have developed on the better drained, sandy till whereas organic and gleysolic soils are common in poorly drained depressions.

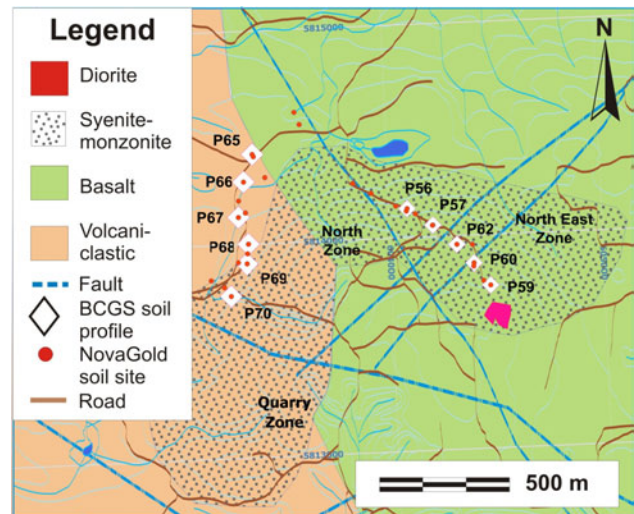


**Figure 7.** The main mineral zones of the Shiko Lake property (after Petsel, 2006) with soil-overburden sampling sites (Petsel, 2006) and soil profile sites (Lett and Sandwith, 2008).

At Shiko Lake, samples were collected at the sites along a 1 km traverse located west of the North Zone (Figure 7). Profiles were created by combining the soil analyses from sites P65 to P70, sampled by Lett and Sandwith (2008), with data reported by Petsel (2006). Petsel submitted overburden samples for fire assay, atomic absorption and aqua regia digestion followed by ICP-ES analyses. Figure 8a shows the results for Cu concentrations determined by aqua regia digestion-ICP-MS. There is a marked Cu anomaly in the C-horizon, it occurs over an interval of 400 m between P65 to P68 reaching a peak value of 405 ppm Cu. The Cu anomaly contrast is greatest for the C-horizon and least for the F-H-horizon. The Cu peak in the C-horizon also has a distinctive asymmetric shape with a steep south-facing slope and a gentler north-facing slope. The Cu profile in the C-horizon has a similar shape and anomaly contrast to the MMI, Enzyme Leach<sup>SM</sup> and Bio Leach<sup>SM</sup> Cu profiles from the lower B-horizon (Figure 8b). Bio Leach<sup>SM</sup> I and Br profiles (Figure 8c) resemble Cu profiles although values for P68 are missing so the sharp peak is absent and the contrast is smaller than the contrast for Cu in the C-horizon. The halogen peak is displaced to the north of the MMI, Enzyme Leach<sup>SM</sup> and Bio Leach<sup>SM</sup> peaks.

Samples from the same traverse were analyzed for Au by aqua regia digestion-ICP-MS. The Au profile for the C-horizon (Figure 9a) reveals an anomaly resembling the Cu profile for the C-horizon (Figure 8a) but with a more symmetrical shape. Again, the Au contrast in the C-horizon is larger than the Au contrast in the B-horizon (no Au was detected in the F-H-horizon soil samples). The larger Au anomaly contrast in the C-horizon may, in part, reflect a higher Au content in the <0.063 mm fraction of the sample compared to the <0.18 mm fraction of the B-horizon soil sample due to less dilution by sand-sized material. Also shown in Figure 9a are the total number of Au grains and pristine Au grains found in the heavy mineral concentrates from the C-horizon samples from sites P65 to P70. A nearby bedrock source for the Cu-Au mineralization would explain the high number of pristine (unweathered) Au grains along with a geochemical Au anomaly in the <0.063 mm fraction of the C-horizon. Figure 9b shows that for the MMI analysis there is a high contrast Au anomaly in

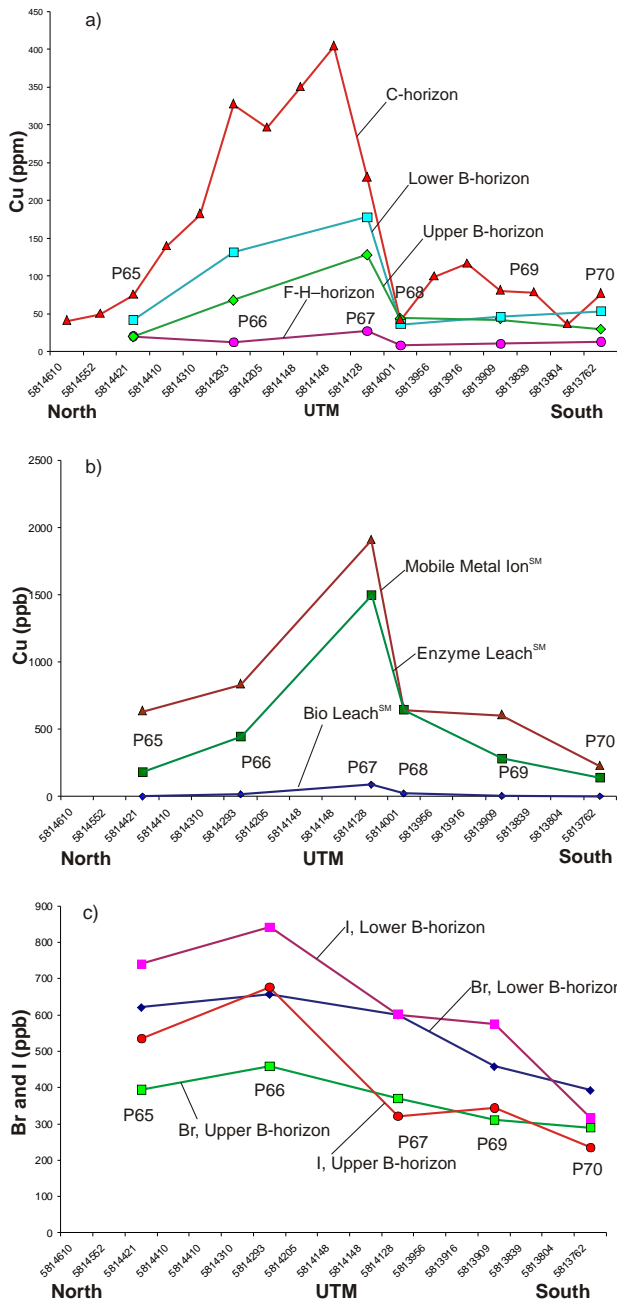


**Figure 8.** Copper profiles along a traverse west of the North Zone, Shiko Lake: **a)** aqua regia digestion followed by inductively coupled plasma-mass spectrometry (ICP-MS) analysis for Cu in the F-H-, upper B-, lower B- and C-horizons; **b)** Mobile Metal Ion<sup>SM</sup> (MMI), Enzyme Leach<sup>SM</sup> and Bio Leach<sup>SM</sup> analyses for Cu in the lower B-horizon; **c)** Bio Leach<sup>SM</sup> analysis for Br and I in the upper B- and lower B-horizons.

the lower B-horizon with a peak at P66 but there is almost no corresponding increase in Au in either the Enzyme Leach<sup>SM</sup> or Bio Leach<sup>SM</sup> analyses over the same interval. The large MMI Au anomaly at P66 corresponds to the C-horizon sample with the greatest number of total and pristine Au grains counted in a heavy mineral concentrate. A smaller MMI Au peak at P69 has a corresponding total and pristine Au grain anomaly but only background levels of

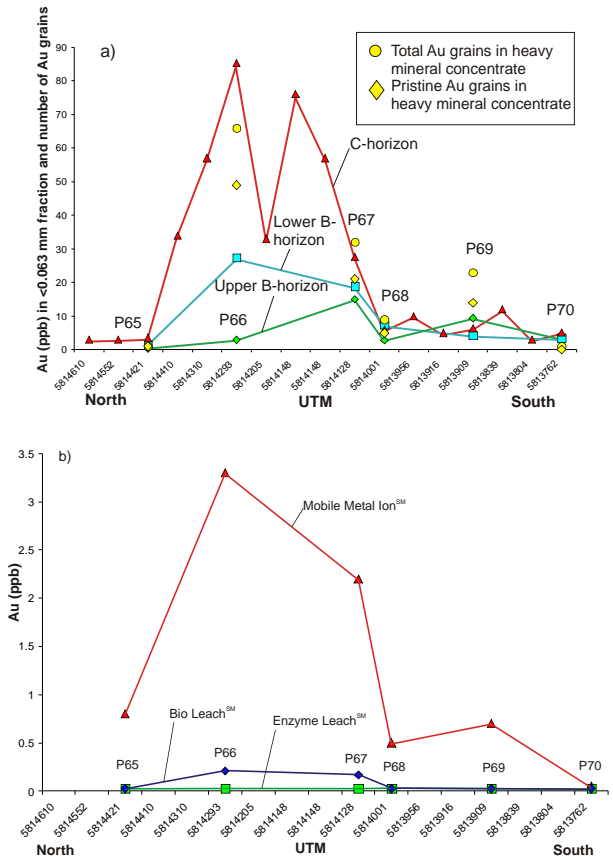


**Figure 9.** Gold profiles along a traverse west of the North Zone, Shiko Lake: **a)** aqua regia digestion followed by inductively coupled plasma-mass spectrometry (ICP-MS) analysis for Au in the F-H-, upper B-, lower B- and C-horizons; **b)** Mobile Metal Ion<sup>SM</sup> (MMI), Enzyme Leach<sup>SM</sup> and Bio Leach<sup>SM</sup> analyses for Au in the lower B-horizon.

Au in the <0.063 mm fraction of the C-horizon sample. Figure 10a shows that the concentration of Co in the soil, determined by aqua regia digestion-ICP-MS, is similar to Cu although the C-horizon Co contrast is smaller and the anomaly shape more symmetrical between P68 and P70 than for Cu in the C-horizon. Selective extraction profiles (Figure 10b) show that the MMI Co and Bio Leach<sup>SM</sup> Co anomaly peaks at P68 are displaced to the south of the C-horizon Co peak. The MMI Co contrast is smaller than the Bio Leach<sup>SM</sup> Co contrast although the anomalies have a similar pattern.

The characteristic down-ice asymmetric shape of the C-horizon Cu anomaly, the abundance of pristine Au grains in the heavy mineral concentrate, Br and I patterns, and the MMI Au contrast suggest a Cu-Au mineral source nearby to the anomaly peak. Although ice flowed from southeast to northwest regionally, the local ice flow could have been deflected by the ridge between the North and Quarry zones so that till may have been deposited by a more north to south ice flow. The source of mineralized rock detected by the geochemistry could therefore be close to the contact between intrusive and volcanoclastic rocks (i.e., near P68 and P69). A nearby diamond-drill hole (SH91-18) intersected fine-grained, moderately hornfelsed siltstone with >5% disseminated pyrite. The drill log records an overburden thickness of 4.6 m (Petsel, 2006).

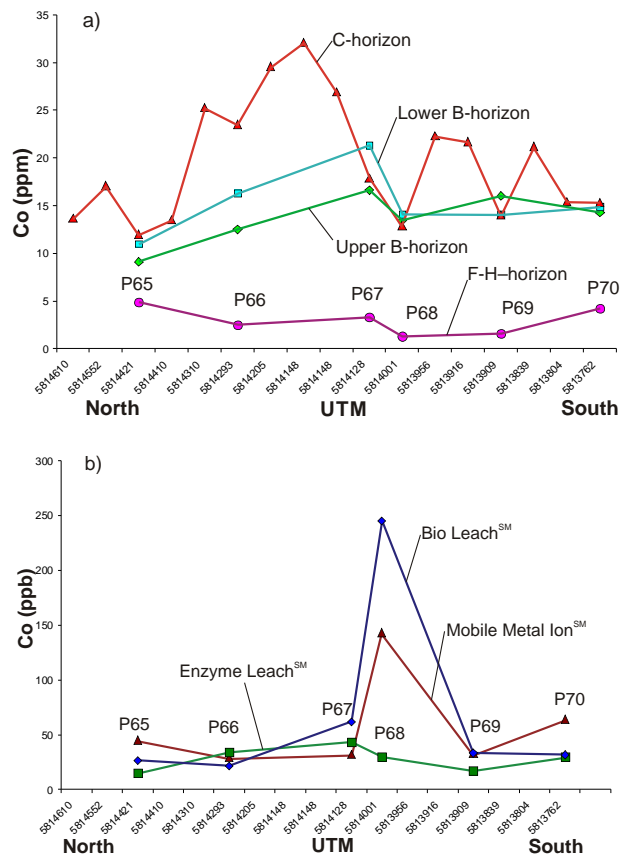


**Figure 10.** Cobalt profiles along a traverse west of the North Zone, Shiko Lake: **a)** aqua regia digestion followed by inductively coupled plasma-mass spectrometry (ICP-MS) analysis for Co in the F-H-, upper B-, lower B- and C-horizons; **b)** Mobile Metal Ion<sup>SM</sup> (MMI), Enzyme Leach<sup>SM</sup> and Bio Leach<sup>SM</sup> analyses for Co in the lower B-horizon.

A second traverse at Shiko Lake extends more than 500 m across the North East mineralized zone. Figure 11a shows Cu concentrations in the F-H-, upper B-, lower B- and C-horizons using data from Lett and Sandwith (2008) combined with the soil-overburden geochemistry reported by Petsel (2006). Copper values were determined by aqua regia digestion-ICP-MS analysis and the pattern is similar to the pattern along the North Zone traverse (Figures 8a, 11a). The Cu in the C-horizon shows the greatest anomaly contrast compared to other horizons and there is an asymmetric Cu peak at P60. Bio Leach<sup>SM</sup> Cu contrast is greater than the MMI Cu contrast and Enzyme Leach<sup>SM</sup> Cu contrast at P60, but there is a secondary MMI Cu anomaly at P56 (Figure 11b). The highest Bio Leach<sup>SM</sup> Br and I values (Figure 11c) occur in the lower B-horizon at P62 suggesting a possible bedrock source for the Cu and Au. The Au pattern in the C-horizon is similar to Cu and there is a sharp Au peak at P60, which is also the site of the greatest number of total and pristine Au grains in the C-horizon heavy mineral concentrate (Figure 12a). A second Au peak at P56 in the lower B-horizon but not the C-horizon has a corresponding marked MMI geochemical anomaly (Figure 12b). The asymmetric shape of the Au and Cu peaks suggests the source to be mineralized material in till, which has been deposited by ice flowing from north to south. Since this is at variance to the regional ice-flow direction, a likely

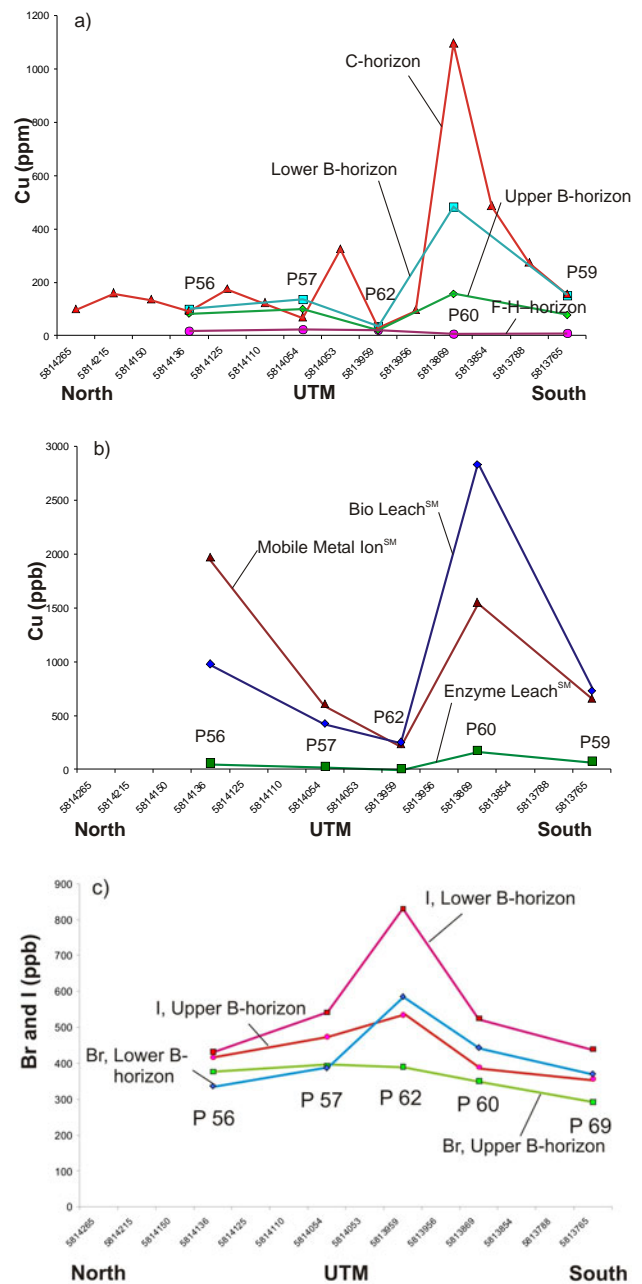


**Figure 11.** Copper profiles along a traverse across the North East Zone, Shiko Lake: **a)** aqua regia digestion followed by inductively coupled plasma-mass spectrometry (ICP-MS) analysis for Cu in the F-H-, upper B-, lower B- and C-horizons; **b)** Mobile Metal Ion<sup>SM</sup> (MMI), Enzyme Leach<sup>SM</sup> and Bio Leach<sup>SM</sup> analyses for Cu in the lower B-horizon; **c)** Bio Leach<sup>SM</sup> analysis for Br and I in the upper B- and lower B-horizons.

explanation is that there are several sources of Au shown by the multiple peaks along the profile.

## CONCLUSIONS

Regional geochemical survey and regional till survey databases have been updated with new information including spatial links of sample locations to bedrock geology.

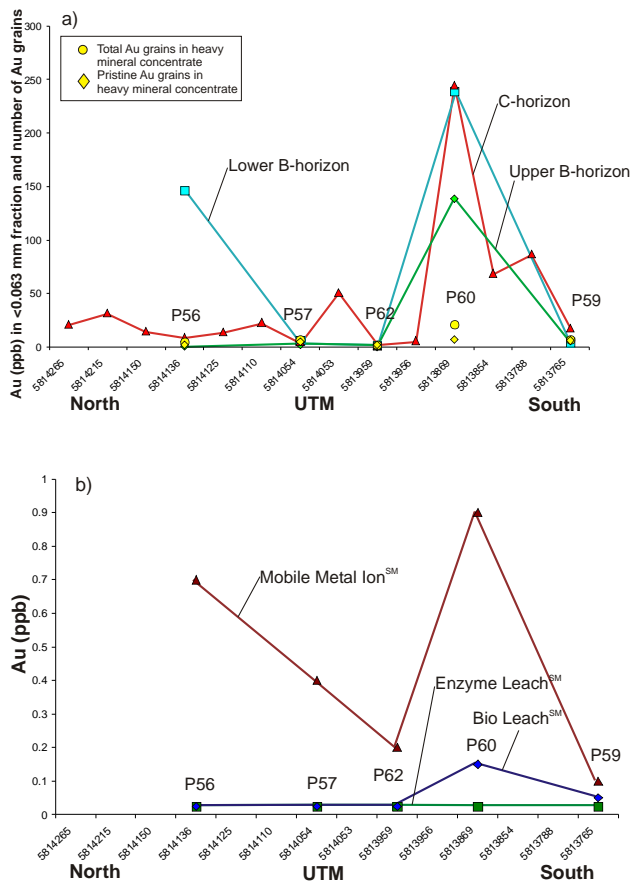


**Figure 12.** Gold profiles along a traverse across the North East Zone, Shiko Lake: **a)** aqua regia digestion followed by inductively coupled plasma-mass spectrometry (ICP-MS) analysis for Au in the F-H-, upper B-, lower B- and C-horizons; **b)** Mobile Metal Ion<sup>SM</sup> (MMI), Enzyme Leach<sup>SM</sup> and Bio Leach<sup>SM</sup> analyses for Au in the lower B-horizon.

Aqua regia digestion–ICP-MS analyses of soil samples from traverses over the Mouse Mountain and Shiko Lake porphyry Cu-Au mineral deposits show that Cu and Au anomaly contrast is greater for the C-horizon compared to the F-H- and B-horizons.

At Shiko Lake, the asymmetric shape of the Cu anomaly in the C-horizon soil and the large number of pristine Au grains in the C-horizon heavy mineral concentrates suggest a nearby mineral source for the soil anomalies. However, local ice-flow direction may be different from the regional direction due to deflection by local bedrock topography and hence the azimuth vector from the bedrock source cannot be determined precisely.

There is very little variation in the element anomalies determined by Enzyme Leach<sup>SM</sup> compared to anomalies determined by other methods. Bio Leach<sup>SM</sup> analysis revealed higher contrast Cu and Co anomalies than the anomalies from MMI analysis. However, for Au the MMI has higher anomaly contrast than the other selective extractions.

In general, Bio Leach<sup>SM</sup> Br and I show similar geochemical patterns to metals although the anomaly peaks appear displaced from the metal peaks.

## ACKNOWLEDGMENTS

Advice from Peter Bernier, President, Richfield Ventures Corp., on the Mouse Mountain property is very much appreciated and Scott Petsel, NovaGold Resources Inc., and Rudi Durfeld are sincerely thanked for providing information and advice about the Shiko Lake property. The Geological Survey of Canada generously funded much of the sample preparation and analysis. A constructive review of this paper by Philippe Erdmer is very much appreciated by the authors.

## REFERENCES

- Cui, Y., Eckstrand, H. and Lett, R.E. (2009): Regional geochemical survey: delineation of catchment basins for sample sites in British Columbia; in *Geological Fieldwork 2008, BC Ministry of Energy, Mines and Petroleum Resources*, Paper 2009-1, pages 231–238.
- Davis, J.C. (1973): *Statistics and data analysis in geology*; John Wiley and Sons, New York, 550 pages.
- Dunn, C.E., Cook, S.J. and Hall, G.E.M. (2007): Halogens in surface exploration geochemistry: evaluation and development of methods for detecting buried mineral deposits; *Geoscience BC*, Report 2007-10, 62 pages.
- Ferbey, T. (2008): Regional to property-scale drift prospecting surveys in British Columbia; *BC Ministry of Energy, Mines and Petroleum Resources*, GeoFile 2008-12.
- Jackaman, W. (2007): Mountain pine beetle infestation area (parts of NTS 082, 092, 093), central British Columbia: Regional Geochemical Data Repository Project; in *Geological Fieldwork 2006, BC Ministry of Energy, Mines and Petroleum Resources*, Paper 2007-1 and *Geoscience BC*, Report 2007-1, pages 307–310.
- Jackaman, W. (2008): Quest Project sample reanalysis digital data release; *Geoscience BC*, Report 2008-3.
- Jackaman, W. and Balfour, J.S. (2008): QUEST Project geochemistry: field surveys and data reanalysis, central British Columbia (parts of NTS 093A, B, G, H, J, K, N, O); in *Geoscience BC Summary of Activities, Geoscience BC*, Report 2008-1, pages 7–10.
- Jackaman, W., Balfour, J.S. and Reichheld, S.A. (2009): QUEST-West Project geochemistry: field survey and data reanalysis, central British Columbia (parts of NTS 093E, F, J, K, L, M, N); in *Geoscience BC Summary of Activities 2008, Geoscience BC*, Report 2009-1, pages 7–14.
- Kendrick, M.A., Burgess, R., Patrick, R.A.D. and Turner, G. (2001): Fluid inclusion noble gas and halogen evidence on the origin of Cu-porphyry mineralizing fluids; *Geochimica et Cosmochimica Acta*, Volume 65, Number 16, pages 2651–2668.
- Large, R.R., Maslennikov, V.V. and Robert, F. (2007): Multistage sedimentary and metamorphic origin of pyrite, gold in the Giant Sukhoi Log deposit, Lena Gold Province, Russia; *Economic Geology*, Volume 102, pages 1233–1267.
- Lett, R.E. (2008): Till geochemical open file; *BC Ministry of Energy, Mines and Petroleum Resources*, GeoFile 2008-13.
- Lett, R.E., Man, E.C. and Mihalynuk, M.G. (2008): Towards a drainage geochemical atlas of British Columbia; in *Geological Fieldwork 2007, BC Ministry of Energy, Mines and Petroleum Resources*, Paper 2008-1, pages 61–68.
- Lett, R.E. and Sandwith, Z. (2008): Geochemical orientation surveys in the Quesnel Terrane between Quesnel and Williams Lake, central British Columbia (NTS 093A, B, G); in *Geological Fieldwork 2007, BC Ministry of Energy, Mines and Petroleum Resources*, Paper 2008-1, pages 49–60.

- Logan, J.M. and Mihalynuk, M.G. (2005): Regional geology and setting of the Cariboo, Bell, Springer and Northeast porphyry Cu-Au zones at Mount Polley, south-central British Columbia; in *Geological Fieldwork 2004, BC Ministry of Energy, Mines and Petroleum Resources*, Paper 2005-1, pages 249–270.
- Mann, A.W., Birrell, R.D., Mann, A.T., Humphreys, D.B. and Perdix, T. (1998): Application of mobile metal ion technique to routine geochemical exploration; *Journal of Geochemical Exploration*, Special Issue on Selective Extractions, Hall, G.E.M and Bonham-Carter, G.F., Editors, Volume 61, pages 87–102.
- Massey, N.W.D., MacIntyre, D.G., Desjardins, P.J. and Cooney, R.T. (2005): Digital geology map of British Columbia; *BC Ministry of Energy, Mines and Petroleum Resources*, GeoFile 2005-1.
- MINFILE (2008): MINFILE BC mineral deposits database; *BC Ministry of Energy, Mines and Petroleum Resources*, URL <<http://www.empr.gov.bc.ca/Mining/Geoscience/MINFILE/Pages/default.aspx>> [December 16, 2008].
- Paterson, K., Lett, R.E. and Telmer, K. (2009): Litho-geochemistry of the Spanish Mountain gold deposit, east-central British Columbia (NTS 093A/11W); in *Geological Fieldwork 2008, BC Ministry of Energy, Mines and Petroleum Resources*, Paper 2009-1, pages 163–168.
- Petsel, S.A. (2006): Rock and soil sampling survey assessment report on the Shiko Lake property; *BC Ministry of Energy, Mines and Petroleum Resources*, Assessment Report 2866, 182 pages.
- Rose, A.W., Hawkes, H.E. and Webb, J.S. (1979): *Geochemistry in mineral exploration*; Academic Press, London, 657 pages.
- Sibbick, S.J. (1994): Preliminary report on the application of catchment basin analysis to regional geochemical survey data, northern Vancouver Island (92L/3, 4, 5 and 6); in *Geological Fieldwork 1993, BC Ministry of Energy, Mines and Petroleum Resources*, Paper 1994-1, pages 111–118.
- Williams, T.M. and Gunn, A.G. (2002): Application of Enzyme Leach<sup>SM</sup> soil analysis for epithermal gold exploration in the Andes of Ecuador; *Applied Geochemistry*, Volume 17, pages 367–385.



# Regional Geochemical Survey: Delineation of Catchment Basins for Sample Sites in British Columbia

by Y. Cui, H. Eckstrand and R.E. Lett

**KEYWORDS:** catchment basins, spatial database, SQL, up-stream query, RDF triples, graph theory, JEQL, dissolve polygons, PostGIS, regional geochemical survey, RGS

## INTRODUCTION

As part of the regional geochemical survey (RGS) program, stream sediment, lake sediment and water samples have been collected from 59 633 locations since 1976, covering approximately 75% of British Columbia (Lett and Doyle, 2009). Geochemical data from the field and multi-element analyses have been compiled and are available to the public. Jackaman and Balfour (2007) recently reported additional chemical analyses performed on RGS archived samples with funding from Geoscience BC.

The geochemical data of the stream sediment samples often reflects the geology and mineralization in the contributing area. As such, a preferred way to visualize the results is to create thematic maps with colour themes or patterns representing element concentrations in upstream catchment basins (Sibbick, 1994).

Catchment basins are recognized as more effective in defining zones of influence for the geochemical results from stream sediment samples (Bonham-Carter and Goodfellow, 1986; Bonham-Carter et al., 1987). Previous studies have linked the catchment basin, stream order and stream gradient to the source of the anomalies detected in stream sediment, especially in small catchment basins with first- and second-order streams (Hawkes, 1976; Sleath and Fletcher, 1982). This link, however, might be weak or even decoupled when the catchment basins are large, the geomorphology is diverse and the hydraulic forces vary significantly across the catchment area (Leggo, 1977; Ryder and Fletcher, 1991; Fletcher, 1997). Bedrock geology, slope, aspect, vegetation, differential weathering of bedrock, rainfall, wildlife and other physical variations in the catchment basins influence the composition of the stream sediment sample and contribute to within-basin variation (Jackaman and Matysek, 1995; Matysek and Jackaman, 1995; Matysek and Jackaman, 1996).

In BC, preliminary catchment basins were delineated for 290 RGS samples (Sibbick, 1994) covering part of northern Vancouver Island (NTS 092L/03, 04, 05 and 06). These were based on 1:100 000 scale topographic maps that were photo reduced from the 1:50 000 scale NTS maps. Catchment basins were defined as the topographic heights

of land that separate stream drainages. Catchment basins were delineated by hand tracing the heights of land (represented by contours) onto a Mylar overlay. The resulting polygons were then digitized at 1:100 000 scale and each polygon labelled to correspond to its RGS sample number. Following a similar method, 3 906 catchment basins were delineated for RGS samples located in 1:250 000 scale NTS map areas 103I, 103J, 103O and 103P (Jackaman and Matysek, 1995; Matysek and Jackaman, 1995; Matysek and Jackaman, 1996).

The previous work demonstrated a new way of disseminating geochemical survey results for stream sediment and water samples. There are, however, shortfalls in the catchment basin methodology and outcome due to the limitation and availability of hydrographic data and spatial technology, including that

- there is no province-wide coverage of catchment basins for the RGS sample sites; only less than 8% of the RGS sites have been delineated and published since 1994;

- the previous delineation process was labour intensive and very time consuming;

- manual catchment-basin delineation has the potential to introduce inconsistency in the results;

- heights of land were not available for every drainage within a catchment basin, impossible to query a given catchment basin at a finer granularity; and

- the 1:100 000 scale topographic base used for the delineation was generated from 1:50 000 scale topographic maps and lacks resolution and detail.

The main focus of the project described in this paper is to develop a fully automated process to yield highly reliable catchment basins for a number of reasons:

- A repeatable algorithm generates consistent catchment basins.

- Delineating catchment basins is possible after corrections or adjustments are made to the sample locations, when new sample sites are available or when new and more detailed topographic maps are available.

- Refining catchment basins with criteria provided by users is possible.

- A processing environment based on open standards or solutions implemented with open standards (such as those by Open Geospatial Consortium and the International Organization for Standardization) ensures its interoperability with lasting relevance in the foreseeable future.

- Rapid processing of province-wide sample sites is possible, and processing of a small group of sites and returning results in real time over a web service is achievable.

---

*This publication is also available, free of charge, as colour digital files in Adobe Acrobat® PDF format from the BC Ministry of Energy, Mines and Petroleum Resources website at <http://www.empr.gov.bc.ca/Mining/Geoscience/PublicationsCatalogue/Fieldwork/Pages/default.aspx>.*

The most current and detailed BC Provincial Terrain Resource Information Management (TRIM) watersheds with fully connected stream networks are used as the topographic base in the delineation of catchment basins for stream sediment and water sample sites.

## DESCRIPTIONS OF INPUT DATA

### *Regional Geochemical Survey Data*

The RGS data include 59 633 sample locations, field observations and analytical results for up to 40 metals for water, stream and lake sediment samples collected over a period of 30 years. Sample sites are plotted on 1:50 000 scale NTS maps and co-ordinates are estimated or measured. The 1:50 000 scale NTS maps are based on the NAD27 datum and have not been updated since publication.

Of the RGS sample locations, 51 639 are stream sediment and water sample sites. Stream sediment and water samples are collected mostly above the confluences for first- or second-order drainages.

### *Watersheds and Stream Network Data*

Watersheds and stream networks are the topographic drainage base that is used for the delineation of RGS catchment basins. For this delineation exercise, we used a version of the watersheds and stream networks produced in June 2008 by the BC Integrated Land Management Bureau (ILMB). In total, there are 3 241 667 watershed polygons and 4 910 953 stream network edges. The data are derived from the 1:20 000 scale TRIM topographic base and are considered as one of the provincial standard hydrographic datasets with fully connected stream networks and well-formed watershed polygons. Stream data collected through TRIM II and updates from the TRIM data exchange program were not included in the stream networks.

Stream networks have full connectivity by adding 'skeleton' network edges or connectors through water bodies such as lakes, rivers and canals digitized as polygons, in addition to the TRIM hydrographic features, including construction lines for polygon closures or connections.

The watersheds were delineated as polygonal units from height-of-land boundaries generated from the TRIM digital elevation model (DEM) and TRIM hydrographic data. The watershed units are fine-grained; however, they are not subdivided as left drainage and right drainage to a stream network edge. The notion of 0-order drainages is problematic for upstream queries if sample sites are located in those watersheds.

Nongeometric attributes for both watersheds and stream networks include names for hydrographic features, drainage order and magnitude, cross referencing of hydrographic features between data based on 1:20 000 scale TRIM and NTS 1:50 000 scale maps, and hierarchical keys. Modified Strahler drainage order and magnitude (Strahler, 1952) were generated, including the notion of 0-order drainage for small watershed units along river banks or lakes that do not have drainage edges. The notion of hierarchical keys was introduced to provide the ability to carry out upstream and downstream queries in a nonspatial manner. The hierarchical keys were computed as the proportional distance along a stream where a child stream flows

into its parent. The hierarchical keys are available in both the watersheds and stream networks.

## METHODS

### *Computing Environment*

All the data processing and analyses were carried out in a 32-bit development environment configured for a number of object-relational databases with spatial extension, including PostgreSQL/PostGIS and Microsoft SQL Server® 2008. Extraction, transformation and loading (ETL) tools include FME from Safe Software, JTS and JEQL (Davis, 2008a, b). The main visualization environment and earlier prototyping were carried out using Manifold® System version 8. Results are stored in a database and were converted by JEQL to KML format for visualization using Google™ Earth.

Additional testing of upstream queries was carried out in a 64-bit environment configured with AllegroGraph RDF Triple Store (Franz, 2008), with stream edges as RDF (Resource Description Framework) triples.

The main programming interfaces are VBscript® in Manifold, SQL for Microsoft SQL Server and PostGIS, PL/pgSQL in PostGIS, Java in AllegroGraph and Perl for batch processing.

A high-level view of the system architecture for this processing environment is depicted in Figure 1. Each of the components consists of a subsystem.

This environment is configured with spatial databases and software components that have either implemented the Open Geospatial Consortium (OGC) Simple Features Specification for SQL (SFS; Open Geospatial Consortium, 1999) or are interoperable at a more primitive and practical level. A major effort was made to ensure the simplicity and consistency in the data model across different subsystems. This practice saves time as data are readily transferable between different subsystems to the environment where performance is optimal. Compliance with OGC SFS has the benefit of implementing the same sets of binary predicates and spatial functions, resulting in the development of applications usable in different subsystems either directly or with minimum modification.

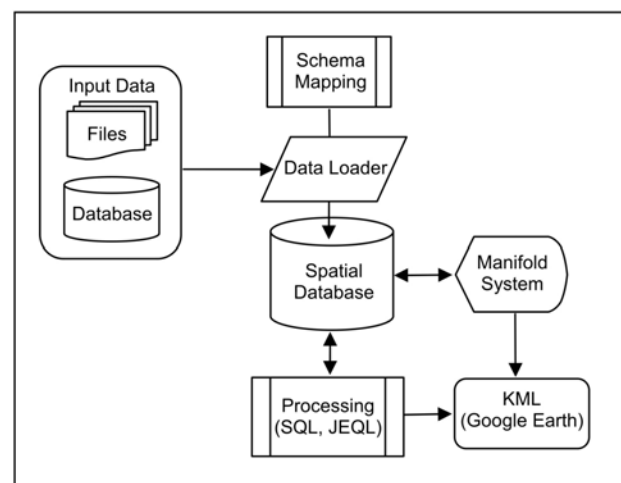


**Figure 1.** High-level view of system architecture for the upstream processing environment.

The streamlined processes are outlined in Figure 2, with more detailed descriptions in the following three sections.

### Data Loading

Before the data are loaded into the spatial database, effort is invested into simplifying data models for the input datasets. The practicality and consistency of data models across different subsystems ensure the interoperability of applications and data in a more meaningful way. Results are achieved through a level of data modelling and automated schema mapping.

Data loading is carried out in batch mode through FME, Manifold and, in earlier tests, through Shape2SQL by SharpGIS (Nielsen, 2008).

When data are loaded into a spatial database, a process is used to validate the geometries against the OGC Simple Features Specifications. The syntax for Microsoft SQL Server is of the form:

```
UPDATE [topobase].[dbo].[watersheds_poly]
SET GEOM=GEOM.MakeValid();
```

This process automatically converts invalid geometries into valid OGC SFS-type geometries. This step is crucial as the spatial operation using the data can fail if the geometries are not compliant to the OGC standard.

A spatial index is created for every table with geometry. Additional indices are created depending on the query.

For RGS sample sites, a query is used to create a new table with stream sediment and water sample sites only.

### Upstream Query

The upstream query is the process used to search and collect all the upstream watersheds. It consists of the following stages:

The first stage is to find watershed polygons that contain RGS stream sediment and water sample sites. These polygons are called 'root' watersheds (Figure 3). A SQL statement to do this would look like:

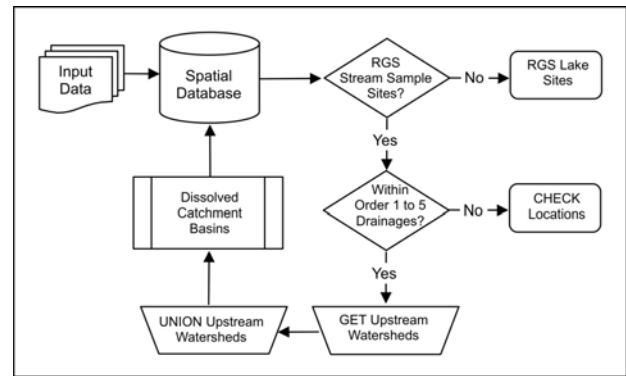


Figure 2. Simplified processing flow diagram.

```
SELECT b.master_id, a.watershed_id INTO
rgs_stream_rootwatershed
```

```
FROM watershed_poly a,
rgs_stream_sites_sp b
```

```
WHERE ST_CONTAINS(a.geom, b.geom);
```

The catchment basins could include a small downstream area below the sample sites by using 'root' watersheds. If the sample sites are close to the confluences, the downstream areas should be small and insignificant. A refinement on this methodology could eliminate all the downstream areas.

In the second stage, root watersheds, or the equivalent of root stream edges, are used to query and collect the upstream watershed polygons or stream edges. Three methods were proposed. In the first method, the hierarchical keys were used to search the upstream watersheds or stream edges in a nonspatial query. As discussed in the next section of this paper, this is a time-consuming query if the dataset is large.

In the second method, a graph theory (e.g., Bondy and Murty, 1976) approach was used. The basic concept is to use stream networks as edges to form RDF triples as specified by Resource Description Framework (W3C, 2000, 2004), such as:

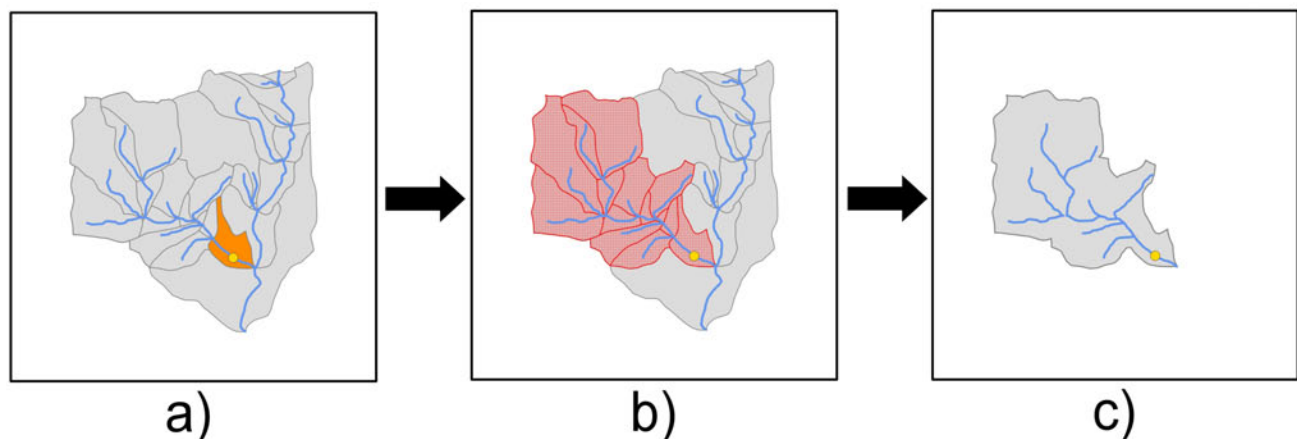


Figure 3. Catchment basin delineation stages depicted with examples: **a)** locate root watershed (highlighted in orange) for a sample site (yellow dot), **b)** retrieve all upstream watersheds (highlighted in red) and **c)** dissolve the upstream watersheds as the catchment basin for the sample site.

```
edge_a, "is upstream of", edge_b
```

Endpoints of stream networks are extracted out of the PostGIS database and are used to extract stream edges and identify their topological relationship through a spatial query such as:

```
SELECT rt.cwb_edgeid, up.cwb_edgeid AS
upedgeid, (rt.the_geom) AS the_geom

INTO bc_upedges_2_sp

FROM all_edge_endpoints rt,
all_edge_startpoints up

WHERE (ST_intersects(up.the_geom,
rt.the_geom)) AND (rt.cwb_edgeid
up.cwb_edgeid);
```

The stream edge triples are loaded into an RDF Triple Store in AllegroGraph, a database and application framework developed by Franz (2008). Upstream query is performed on the stream edge triples through query APIs (application programming interfaces) such as SPARQL (the proposed W3C query language) and Prolog with custom code in Common Lisp. A visual representation of the stream graph edges is shown in Figure 4.

A third method is recursive queries using a common table expression (CTE). It uses the same stream edge triples as the input data loaded into a relational database.

### Dissolving Upstream Watersheds

In the last step of the process, the upstream watershed polygons are dissolved for each of the RGS stream sediment and water sample sites.

Dissolving polygons remains one of the most challenging tasks in improving performance. Open standards-based solutions usually implement one of the OGC predicates called 'UNION' to combine or dissolve polygons. The spatial databases tested in our study take considerable time to dissolve a relatively small number of polygons. For the data size in this study, it is not practical to run such a query. Alternative methods within spatial databases were tested, such as the UnionAggregate functions in Microsoft SQL Server along with the PostGIS Analysis Tool (Martinez-Llario et al., 2008) but none provided a significant performance improvement.

A more practical approach is to use JEQL, with the idea of a Cascaded Union function, to dissolve the polygons outside the spatial database in batch mode (Davis, 2008a, b). The JEQL interface uses JTS as the spatial processing engine and can interface with Microsoft SQL Server and PostGIS.

## DISCUSSION OF RESULTS

### Data Loading Performance

Initially, data loading takes approximately 70 minutes for 4.9 million stream edges and less than two hours for 3.2 million watershed polygons, using a single process from a desktop workstation. Spatial indexing takes approximately a quarter of the load time. Load time can be improved by launching multiple data-loading processes from different workstations.

### Locations of RGS Stream Sample Sites

The query to locate root watersheds for the RGS stream sediment and water sample sites reveals that 94% are located within watersheds with drainage orders from 1 to 5, and a small portion are located in watersheds with drainage orders from 6 to 10 (Table 1, Figure 5). There are 228 sites located in drainage order 0 watersheds and another 36 sites that are not contained in any watershed.

The RGS samples sites located in root watersheds with drainage orders from 1 to 5 are used for the next steps in upstream queries.

The RGS sample sites within drainage order 0 or not within any watersheds are separated into another table to verify their locations.

There are cases where the RGS stream sample sites fall in watersheds with drainage order 0 and the watersheds appear to be skinny in shape and not adequately subdivided along river and lake banks (Figure 6). Upstream queries on such a root watershed could return a very large catchment basin (e.g., over half a million upstream watersheds).

The sample sites not within any watersheds are all located offshore, but within a short distance of the sea coastline, which is likely due to resolution differences between the 1:50 000 scale maps and 1:20 000 scale maps. These sample sites will be identified in a separate study with streams in the original 1:50 000 scale NTS maps in digital copy. With an existing cross-referencing between the 1:50 000 scale hydrographic features and the more detailed 1:20 000 scale TRIM streams, the RGS sample streams will be matched or linked to TRIM streams and the RGS sample sites transferred or snapped to the TRIM streams.

The RGS sample sites within watersheds with a drainage order above 5 could include large upstream areas that are meaningless when the entire catchment basin is delin-

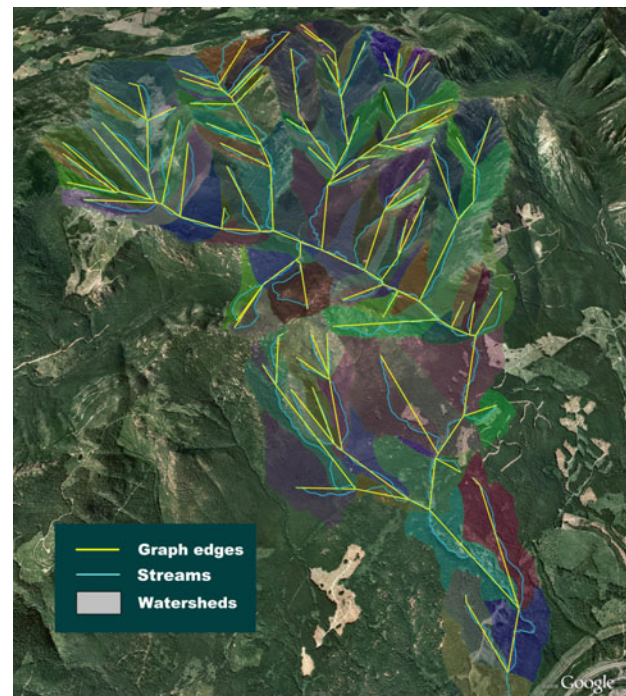


Figure 4. Visual representation of upstream graph shown on Google Earth (Google, 2008).

**Table 1.** Summary of RGS stream sediment and water sample sites and drainage orders (note: 36 sites are not contained in any watershed).

Stream Order	Number of RGS Sites	Percentage
0	228	0.44%
1	6544	12.68%
2	11736	22.74%
3	16034	31.07%
4	10148	19.67%
5	4291	8.32%
6	1550	3.00%
7	610	1.18%
8	233	0.45%
9	191	0.37%
10	38	0.07%

eated. In this study, these sample sites (less than 5% of the total) were filtered out for dissolving watershed polygons.

### Upstream Watersheds

The query on searching and collecting upstream watersheds for the RGS stream sediment and water sample sites was carried out in PostGIS and tested in Microsoft SQL Server. The query initially returned greater than 47 million polygons in 20 hours, averaging one million upstream watershed polygons in 2.3 hours. The sample sites within drainage order 0 or above 5 forms only 5% of the RGS stream sample sites, but 87% of the upstream watersheds are associated with them. The highest RGS site has over 500 000 upstream watersheds. These sample sites are filtered out for further processing because the sites need to be validated and an overly large catchment basin is perhaps not useful. This study processed the remaining 5.8 million upstream watersheds for 51 639 stream sediment and water

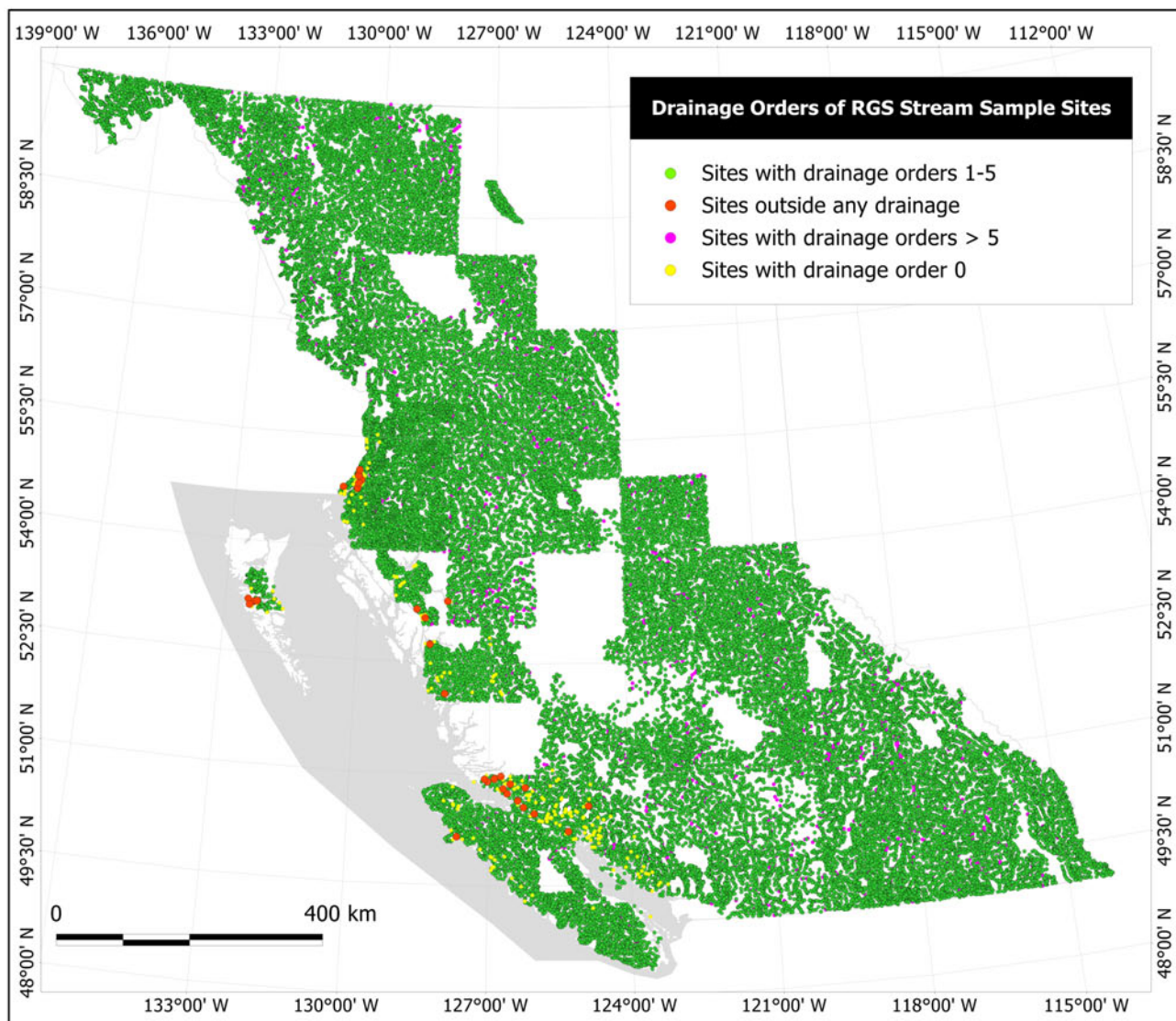


**Figure 5.** Drainage orders of RGS stream sites.

sample sites that fall mostly within watersheds with drainage order from 1 to 5.

In a separate test, the AllegroGraph RDFStore™ was used to traverse the edge trees and retrieve 1 000 000 upstream edges in only 6 seconds (not including the time to write results). Traversal of edge trees happens at basically computer memory speed. While it is recognized that this is not a fair comparison, the performance numbers nevertheless are interesting enough to warrant further investigation of graph-theory-based technology such as AllegroGraph for the improvement of upstream queries, in addition to its emerging spatial-temporal reasoning capabilities in applications such as building knowledge base with RDF triples (Aasman, 2008a, b) and mapping mineral potential.

The performance from recursive CTE is also impressive. They are capable of retrieving over 1 000 000 upstream edges in less than 50 seconds in a relational database, including the time to group and write output.

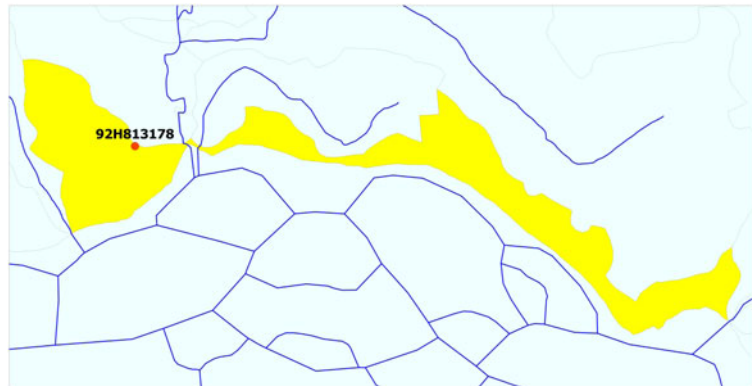


**Figure 6.** Example of an RGS stream sample located in a 0-order watershed adjacent to a river. Note the skinny shape of the watershed is highlighted.

### Results on Delineating Catchment Basins

In total, 5.7 million polygons were successfully dissolved into 51 639 catchment basins in 3 hours by JEQL interfacing into PostGIS, in a batch mode with RGS sample sites divided into groups of 1 000 sample sites. Since the

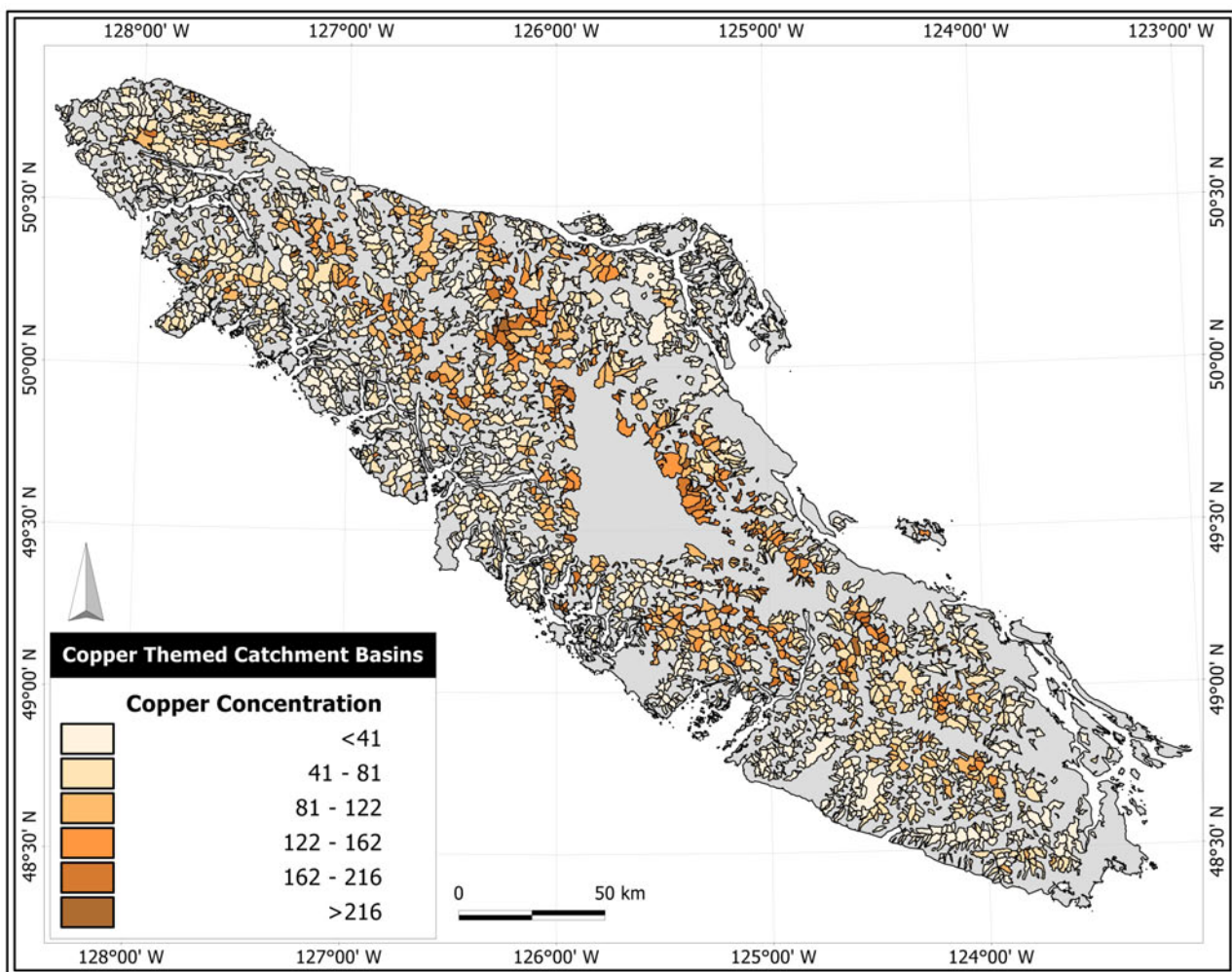


**Figure 7.** Example of catchment basins themed with copper concentrations for RGS sediment samples on Vancouver Island.

processing is carried out on desktop workstations outside the database, multiple processes could be launched simultaneously from different desktop workstations to significantly improve performance, which is being further tested.

In an earlier development, polygons were dissolved with VBScript in Manifold with results shown in Figure 7. In small batch testing, both PostGIS and Microsoft SQL Server were capable of dissolving up to 30 000 polygons within 30 minutes. When all 5.7 million polygons were submitted for dissolving, the query ran for up to six days without returning any results.

### Known Issues

The catchment basins were delineated for RGS stream sediment and water sample sites that were considered to be reasonably correct. Fewer than 5% of the sites were not processed due to their locations either outside any watershed or within watersheds with a drainage order 0 or above 5. If these errors are eliminated, it should take less than two days to reprocess all the RGS stream sediment and water sample data.

Even after filtering out the RGS sample sites within watersheds with drainage order 0 or above 5, some sample sites still have relatively large catchment basin areas. A new version of catchment basins should be delineated with limited upstream reaches, such as within an arbitrary cut-off distance.

Watersheds with drainage order 0 are still an issue. A legitimate sample site located within this type of watershed will invalidate upstream query results.

The hydrographic base does not have the notion of left and right drainages for a given stream edge, limiting the possibility of further refinement of catchment basins with finer granularity using criteria such as slope or geology to compare results on the left drainage versus the right drainage.

### CONCLUSIONS

A fully automated process was developed for the delineation of catchment basins (also known as an upstream query). It was applied for the delineation of catchment basins for the RGS stream sediment and water sample sites. The results will be released once data quality has been verified and aberrant locations for a small number of sample sites are addressed.

Object-relational databases with spatial extension have reasonable performance in data storage and simple queries, but are not fast enough for intense processing or complex spatial or nonspatial queries. Java application-based solutions outperform spatial databases by a wide margin in intense processing. Graph-theory-based methods also potentially open the door for other applications in geoscience.

This processing is facilitated in an interoperable system environment configured with spatial databases and Java applications that are implemented with open standards-based geometry data type, binary predicate and spatial functions.

### ACKNOWLEDGMENTS

Mitch Mihalyuk inspired us to attempt this project with a demonstration of the Surface Tools from Manifold Systems. Refractions Research Inc. and GeoBC kindly provided the TRIM hydrographic data. We sincerely thank Martin Davis for developing JEQL and extending its capability for this work. David Skea from GeoBC co-ordinated the upstream query with RDF Triple Store and Steve Haflich prototyped the query testing in AllegroGraph at Franz Inc., Oakland, California. We also thank Pat Desjardins, Philippe Erdmer and Larry Jones for reviewing the text and Tania Demchuk for providing editorial logistics.

### REFERENCES

- Aasman, J. (2008a): Unification of geospatial reasoning, temporal logic, & social network analysis in event-based systems; *in* Proceedings of the Second International Conference on Distributed Event-based Systems, Rome, Italy, *Association for Computing Machinery*, Volume 332, pages 139–145.
- Aasman, J. (2008b) Unification of geospatial reasoning, temporal logic, & social network analysis in a Semantic Web 3.0 database; Franz Inc., unpublished manuscript distributed during *GeoWeb 2008 Conference*, Vancouver, Canada, 7 pages.
- Bondy, J.A. and Murty, U.S.R. (1976): Graph Theory with Applications; *Elsevier Science Publishing Co., Inc.*, 264 pages.
- Bonham-Carter, G.F. and Goodfellow, W.D. (1986): Background correction to stream geochemical data using digitized drainage and geological maps: application to Selwyn Basin, Yukon and Northwest Territories; *Journal of Geochemical Exploration*, Volume 25, pages 139–155.
- Bonham-Carter, G.F., Rogers, P.J. and Ellwood, D.J. (1987): Catchment basin analysis applied to surficial geochemical data, Cobequid Highlands, Nova Scotia; *Journal of Geochemical Exploration*, Volume 29, pages 259–278.
- Davis, M. (2008a): JTS Topology Suite: user guide, Javadoc for the JTS API, and History of JTS and GEOS; URL <<http://tsusiatsoftware.net/jts/main.html>> [December 2008].
- Davis, M. (2008b): JEQL Extended Query Language: user guide, standard library reference, and technical specifications; URL <<http://tsusiatsoftware.net/jeql/main.html>> [December 2008].
- Fletcher, W.K. (1997): Stream sediment geochemistry in today's exploration world; *in* Proceedings of Exploration 97: Fourth Decennial International Conference on Mineral Exploration, A.G. Gubins, Editor, pages 249–260.
- Franz, Inc. (2008): AllegroGraph 3.1; URL <<http://agraph.franz.com/allegrograph>> [December 2008].
- Google Inc. (2008): Google Earth, <<http://earth.google.com>> [December 2008].
- Hawkes, H.E. (1976): The downstream dilution of stream sediment anomalies; *Journal of Geochemical Exploration*, Volume 6, pages 345–358.
- Jackaman, W. and Balfour, J.S. (2007): QUEST project geochemistry: field surveys and data re-analysis (parts of NTS 093A, B, G, H, J, K, N, O), central British Columbia; *in* Geological Fieldwork 2006, *Geoscience BC*, Report 2007-1, pages 311–314.
- Jackaman, W. and Matysek, P.F. (1995): British Columbia Regional Geochemical Survey – Nass River (NTS 103O/P); *BC Ministry of Energy, Mines and Petroleum Resources*, BC RGS 43.
- Leggo, M.D. (1977): Contrasting geochemical expression of copper mineralization at Namosi, Fiji; *Journal of Geochemical Exploration*, Volume 8, pages 431–456.

- Lett, R.E. and Doyle, J. (2009): Geochemistry projects of the British Columbia Geological Survey; in *Geological Fieldwork 2008, BC Ministry of Energy, Mines and Petroleum Resources*, Paper 2009-1, pages 219–230.
- Matysek, P.F. and Jackaman, W. (1995): British Columbia Regional Geochemical Survey – Prince Rupert/Terrace (NTS 103I/J); *BC Ministry of Energy, Mines and Petroleum Resources*, BC RGS 42.
- Matysek, P. and Jackaman, W. (1996): B.C. regional geochemical survey anomaly recognition, an example using catchment basin analysis (103I, 103J); in *Geological Fieldwork 1995, BC Ministry of Energy, Mines and Petroleum Resources*, Paper 1996-1, pages 185–190.
- Martinez-Llario, J., Weber-Jahnke, J.H. and Coll, E. (2008): Improving dissolve spatial operations in a simple feature model; *Advances in Engineering Software*, in press, doi:10.1010/j.advengsoft.2008.03.014.
- Nielsen, M. (2008): SQL spatial tools; URL <<http://www.sharpgis.net>> [December 2008].
- Open Geospatial Consortium, Inc. (1999): OpenGIS Simple Features Specification for SQL, Revision 1.1; *OpenGIS Project Document 99-049*, Release May 5, 1999, 78 pages.
- Ryder, J.M. and Fletcher, W.K. (1991): Exploration geochemistry – sediment supply to Harris Creek (82L/2); in *Geological Fieldwork 1990, BC Ministry of Energy, Mines and Petroleum Resources*, Paper 1991-1, pages 301–306.
- Sibbick, S.J. (1994): Preliminary report on the application of catchment basin analysis to regional geochemical survey data, northern Vancouver Island (NTS 92L/03,04,05 and 06); in *Geological Fieldwork 1993, BC Ministry of Energy Mines and Petroleum Resources*, Paper 1994-1, pages 111–117.
- Sleath, A.W. and Fletcher, W.K. (1982): Geochemical dispersion in a glacier melt-water stream, Purcell Mountains, B.C.; in *Prospecting in Areas of Glaciated Terrain 1982*, Canadian Institute Mining Metallurgy, pages 195–203.
- Strahler, A.N. (1952): Hypsometric (area altitude) analysis of erosional topography; *Geological Society of America Bulletin*, Volume 63, pages 1117–1142.
- W3C (2000): Resource Description Framework (RDF) schema specification 1.0; *W3C Candidate Recommendation*, 27 March 2000, URL <<http://www.w3.org/RDF>> [December 2008].
- W3C (2004): RDF Vocabulary Description Language 1.0: RDF schema; *W3C Recommendation*, 10 February 2004, URL <<http://www.w3.org/RDF>> [December 2008].